

# RNA Recognition by Fluoro Aromatic Substituted Nucleic Acid Analogues



Dissertation  
zur Erlangung des Doktorgrades  
der Naturwissenschaften

vorgelegt dem Fachbereich  
Chemische und Pharmazeutische Wissenschaften  
der Johann Wolfgang Goethe-Universität  
in Frankfurt am Main

von  
**Aleksandra Živković**  
aus  
Niš, Yugoslavia

Frankfurt am Main  
März 2005

I do not think there is any thrill that can go through the human heart like that felt by the inventor as he sees some creation of the brain unfolding to success....Such emotions make a man forget food, sleep, friends, love, everything.

**Nikola Tesla**, 1856-1943, inventor, electrical engineer and scientist

## Acknowledgments

I would like to express my gratitude to **Prof. Dr. J. W. Engels** for his invaluable supervision, guidance in every progress of project, discussions, review of my thesis manuscript and especially for his kindness and patience.

I owe my warm gratitude to **Astrid Klöpffer, Jelena Božilović, Jörg Parsch** and **Martina Adams** for review of my thesis manuscript and useful discussions about thesis.

I express my thanks to **Dalibor Odadzić** for translation of summary into German.

My sincere thanks also go to:

- **Dr. Zimmerman** and his coworkers for NMR measurements
- **Dr. J. W. Bats** for crystallographic data
- **Dr. G. Dürner** and his coworkers for preparative HPLC-separations of nucleosides
- **Beate Conrady** for nice collaboration while performing oligonucleotide synthesis and HPLC separations of oligonucleotides
- **Hannelore Brill** and **Ilona Priess** for MALDI and ESI measurements
- **Marianne Christof** for elementary analysis

I express my sincere thanks to all members of **AK Engels** for creating a nice working atmosphere. I also want to express my thanks to our secretary **Mrs. Eva Rheinberger** for her help.

Thanks to many friends for support and friendship: **Jelena Božilović, Astrid Klöpffer, Katharina Strube** and **Dalibor Odadzić** etc.

I would like here to thank all other people whose name has not been mentioned here, who gave me a lot of support and courage in my work.

This list would not be complete without the big appreciations to my parents and my brother for their continued support, encouragement and love.

# Table of Contents

<b>1</b>	<b>Introduction.....</b>	<b>1</b>
<b>2</b>	<b>Molecular Design of Life.....</b>	<b>7</b>
2.1	Structure and Function of Nucleic Acids .....	7
2.2	DNA Structures.....	10
2.3	RNA Structures .....	13
2.4	Stability of a Double Helix .....	16
2.4.1	Hydrogen Bonds .....	16
2.4.2	Base Stacking .....	17
2.4.3	Solvation.....	19
2.5	Universal Bases.....	21
<b>3</b>	<b>Organic Fluorine.....</b>	<b>25</b>
3.1	Fluorine- Properties and Hydrogen Bonding Ability .....	25
3.1.1	Crystal Structures of Fluoro Benzenes.....	27
3.2	Fluorine in Nucleic Acids.....	30
3.2.1	Fluoro Modifications on Sugar Moiety.....	31
3.2.1.1	C 2'- Fluoro Nucleosides .....	31
3.2.1.2	C3'-Fluoro Nucleosides .....	32
3.2.1.3	C4'-Fluoro Nucleosides .....	33
3.2.1.4	C5'-Fluoro Nucleosides .....	33
3.2.2	Fluoro Modification on Phosphate Group.....	34
3.2.2.1	Fluoro Phosphonates .....	34
3.2.2.1.1	Fluoro Alkyl Phosphonates .....	34
3.2.3	Fluoro Modifications on Nucleobases.....	36
3.2.3.1	Fluoro Modified Pyrimidines .....	36
3.2.3.2	Fluoro Modified Purines .....	37
3.2.3.3	Fluoro Modified Nucleobase Analogues.....	37
<b>4</b>	<b>Overview.....</b>	<b>39</b>
<b>5</b>	<b>Chemical Synthesis.....</b>	<b>43</b>

5.1	Modified Nucleobases Containing Fluorine.....	43
5.2	Fluorobenzimidazoles .....	46
5.3	Benzimidazole, Fluoro-benzimidazole and Trifluoromethyl- benzimidazole Nucleosides.....	49
5.3.1	Glycosilation.....	49
5.3.2	Deprotection.....	53
5.4	C-Nucleosides .....	54
5.4.1	$\gamma$ -Lactone .....	54
5.4.2	Benzene, Fluoro- and Chloro Benzene-Nucleosides.....	56
5.4.2.1	C-Glycosilation and Dehydroxylation .....	56
5.4.2.2	Debenzylation.....	60
5.5	Protection of Nucleosides for Solid Phase RNA Synthesis.....	61
5.5.1	Dimethoxytrinitration Reaction.....	61
5.5.2	Protection of 2'-OH Group .....	62
5.5.3	Phosphitilation.....	63
5.6	Abasic Site.....	64
5.7	Overview on Synthesis.....	66
5.8	Partition Coefficients and HPLC Retention Times.....	71
5.8.1	Partition Coefficients.....	71
5.8.2	HPLC-Retention Times .....	72
6	Crystallography.....	75
6.1	What do we Learn from Crystals?.....	75
6.2	Theoretical Background.....	75
6.2.1	Lattice Planes and Bragg's Law .....	76
6.3	Crystal Structure of Fluorine-modified and Chlorine-modified Benzene Nucleosides .....	78
6.4	Crystal Structure of 5'-O-(4,4'-dimethoxytriphenylmethyl)-2'-O- <i>tert.</i> - butyldimethylsilyl-1'-deoxy-1'-(4,6-difluoro-1-N-benzimidazolyl)- $\beta$ -D- ribofuranose .....	83

7	Oligonucleotides .....	87
7.1	Synthesis of Oligonucleotides .....	87
7.1.1	Phosphoramidite method .....	87
7.2	Synthesised Oligonucleotides .....	90
7.3	Purification of Oligonucleotides .....	91
7.4	Characterizations of Oligonucleotides .....	93
8	Spectroscopic Measurements of Oligonucleotides .....	99
8.1	UV-Spectroscopic Measurements .....	99
8.1.1	Calculations from UV- Melting Curves .....	101
8.1.1.1	Determination of the Melting Point .....	101
8.1.1.2	Determination of Thermodynamical Data .....	104
8.1.1.2.1	Van't Hoff Plot .....	104
8.1.2	Results of the UV-Melting Curves .....	106
8.1.3	Enthalpy-Entropy Compensation .....	124
8.2	CD Spectroscopic Measurements .....	126
8.2.1	CD-Spectroscopy .....	126
8.2.2	Results of CD-Spectroscopy .....	129
9	Summary .....	133
9	Zusammenfassung .....	141
10	Experimental Part .....	149
10.1	Main Methods .....	149
10.1.1	Chromatography .....	149
10.1.2	Spectroscopy .....	150
10.1.3	Mass spectrometry .....	151
10.1.4	Elementary Analysis .....	151
10.1.5	Melting Point Determination .....	151
10.2	List of Chemical Reagents .....	151
10.2.1	For the synthesis of oligonucleotides .....	155
10.3	The Buffer solutions .....	156

10.4	List of Synthesised Compounds .....	156
10.5	Synthesis, spectral data and other characteristics of synthesised compounds .....	162
10.6	Synthesis of Oligonucleotides.....	295
10.7	Purification and Analytics of Oligonucleotides.....	295
10.7.1	HPLC-purification.....	295
10.7.2	The amounts of synthesised oligonucleotides.....	296
10.7.3	The Extinction coefficient of Oligonucleotides.....	296
10.8	UV-Melting Curves .....	297
10.9	CD-Spectroscopy of Oligonucleotides.....	298
10.10	Determination of Partition Coefficient.....	298
10.11	Determination of HPLC Retention Times.....	299
11	References.....	301
12	Attachment.....	323
12.1	Crystal Data of Crystalized Compounds .....	323
12.1.1	Crystal data of 1'-deoxy-1'-(2,4,6-trifluorophenyl)- $\beta$ -D- ribofuranose .....	323
12.1.2	Crystall data of 1'-deoxy-1'-(2,4,5-trifluorophenyl)- $\beta$ -D- ribofuranose .....	331
12.1.3	Crystal data of 1'-deoxy-1'-(4-chlorophenyl)- $\beta$ -D-ribofuranose..	338
12.1.4	Crystal data of 5'-O- (4,4'-Dimethoxytriphenylmethyl) -2'-O-tert.- butyldimethylsilyl-1'-deoxy-1'- (4,6-difluoro-1-N-benzimidazolyl) - $\beta$ -D- ribofuranose 106 at -123 C.....	346
12.2	Abbreviations.....	359
	<i>Curriculum vitae</i> .....	363
	Publications .....	365

# 1 Introduction

Nucleic acids are the memory of all the information of life of every plant and living beings in general. Deoxyribonucleic acids (DNA) consist of long double-stranded chains of nucleotides. The nucleotides themselves consist of a sugar moiety (ribose for ribonucleic acid (RNA) and 2'-deoxyribose for DNA), a phosphate group and a nucleobase. Generally only four nucleobases can be found in natural DNA and RNA. There are guanine, cytosine, adenine and thymine in DNA, and uracil instead of thymine in RNA. These double stranded DNA strands are held together by highly specific hydrogen bonds between the nucleobases. The base pairs are guanine-cytosine and adenine-thymine (*Figure 1.1*), and their ratio was first defined by Chargaff (Chargaff, 1951).

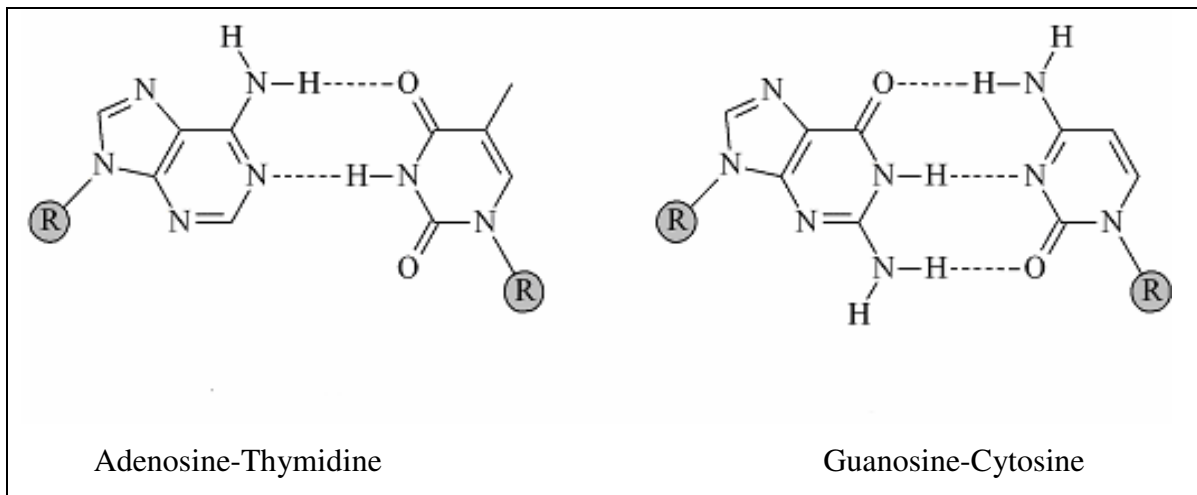


*Figure 1.1. Watson –Crick base pairs R=2'-deoxyribose (Watson & Crick, 1953)*

The information saved in the DNA must be translated into proteins. Therefore the DNA must be first transcribed into messenger RNA (mRNA), which leaves the nucleus. The mRNA will be translated into proteins at the ribosomes (Watson & Crick, 1953a).



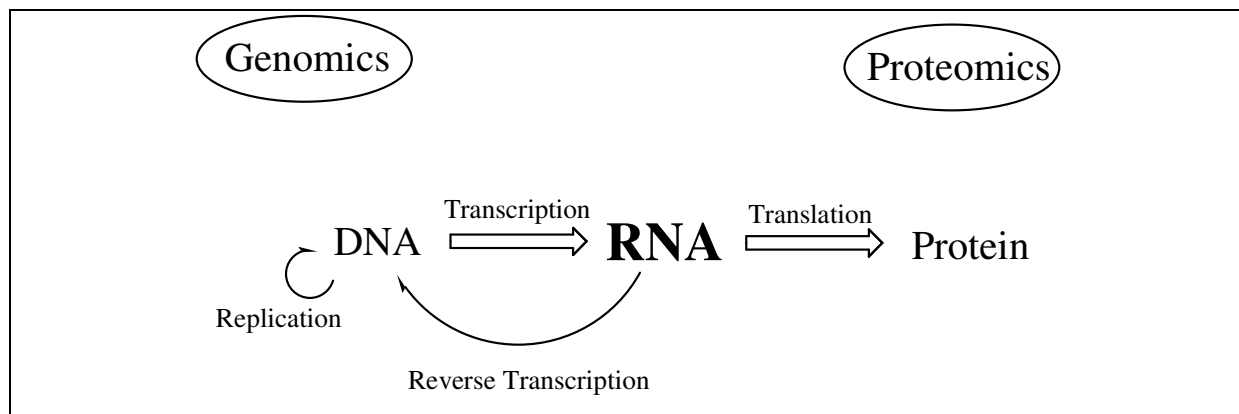


Figure 1.2. Central dogma of molecular biology

All these processes are possible points of attack of nucleic acid drugs. Targeting at the RNA level is an economical approach to address non-drugable proteins and targets that have failed to give leads, as it can build on biological knowledge gathered over years (Zaman *et al.*, 2003). Several different concepts or mechanisms of action of nucleic acid drugs are now under investigation. The most important are: antisense concept, the triple helix concept, the RNA interference (RNAi) concept and ribozymes as drugs (Figure 1.3).

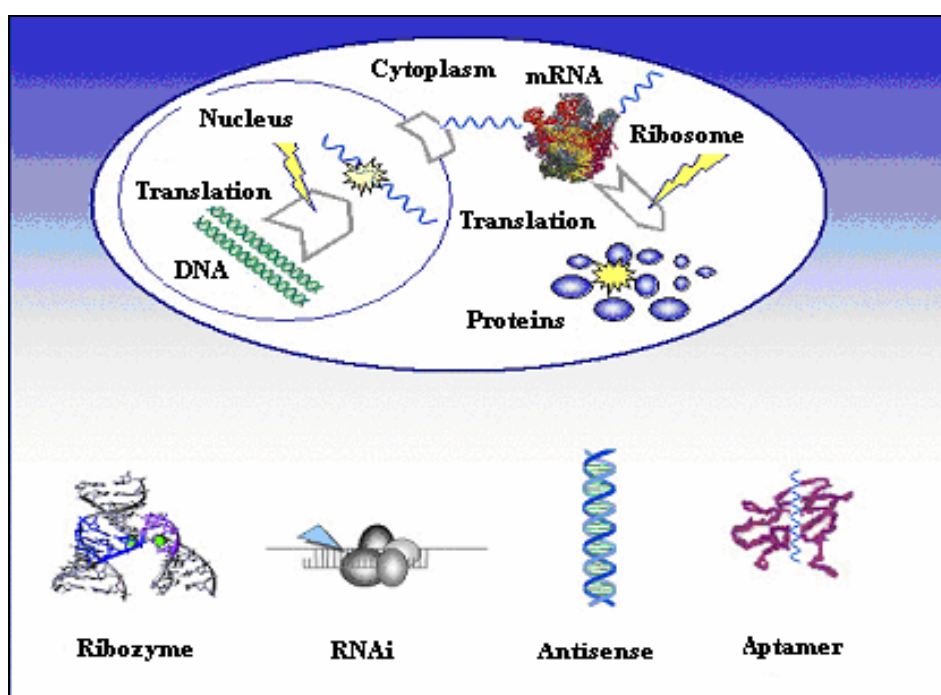


Figure 1.3. Oligonucleotide interference (Engels & Parsch, 2004)

The **antisense concept** follows the most important way of action to modulate the transfer of genetic information to proteins. Antisense oligonucleotides can be classified in to main classes on the bases of their mechanism of action: RNase H dependant oligos, which induce the degradation of mRNA by RNase H, and steric blocking oligonucleotides, which

physically prevent or inhibit the splicing or the translation. In original concept, the antisense method for the sequence-specific inhibition of gene expression was quite simply steric blockage of translation by binding of oligonucleotide to the mRNA target. However, it is now generally accepted that mode of action is more complicated. Even some of antisense-oligonucleotides act by this mechanism, the most commonly used antisense-oligonucleotides act by degradation of RNA target by Rnase H in the hybrid formed upon annealing of the antisense-oligonucleotide. The phosphothioate analogues played a crucial role in this development (Engels & Eckstein, 2003; Zamenick *et al.*, 1978; Stephenson *et al.*, 1978):

The **triplex concept** is one possibility to regulate gene expression *in vivo*. In this concept the third nucleic acid strand should hybridise with the DNA double helix in the nucleus and inhibit translation of the DNA to the corresponding RNA (Engels & Eckstein, 2003; Batey *et al.*, 199; Gewirß *et al.*, 1998).

**Ribozymes** are catalytically competent RNAs that occur either in nature or have been obtained by *in vitro* selection. The most popular are hammerhead (*figure 1.4*) and hairpin ribozyme. They have been applied for the inhibition of gene expression on the RNA level. They catalyse mostly ligation and cleavage reactions. Their principle of action is based on sense-antisense principle. The fundamental difference between classical antisense method and that of RNA ribozyme is that ribozymes have the inherent catalytic power to cleave the target RNA rather than to have to rely on cellular proteins for this step (Engels & Eckstein, 2003; Klöpffer, 2004);

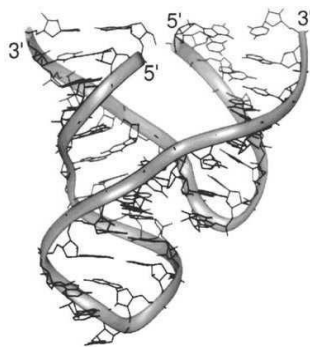


*Figure 1.4 X-ray structure of an Hammerhead ribozyme*

**RNA interference** (RNAi) is a recently detected approach for targeting mRNA and is also called posttranscriptional gene silencing. That is the process by which double-stranded RNA in the way shown in *figure 1.5* destroys mRNA and thus silence further transcription from a specific gene.

Chemical variation of natural oligonucleotide structures is necessary to render these compounds useful in biological systems. For a good nucleic acid drug we need to take care about the following characteristics: modifications must be sufficiently stable against serum nucleases in serum within cells, they should enter various organs of the body and be able to penetrate cellular membranes to reach their site of action and they must form stable Watson-Crick or Hoogsteen complexes with complementary sequences under physiological conditions.

There are different possibilities for modifications: they could be on the sugar or on the base. There are also completely backbone-modified nucleic acids like polypeptide nucleic chains (PNAs) or locked nucleic acids (LNAs). Unmodified oligonucleotides are widely used as tools in molecular biology. However, in cellular and animal experiments it was observed that oligonucleotides with a natural phosphodiester internucleoside linkage are degraded in serum within few hours, mainly by the action of fast cleaving 3'-exonucleases that are accompanied by slower cleaving endonucleases (Tuschl, 2003; Schwarz *et al.*, 2003; Hannon *et al.*, 2002).

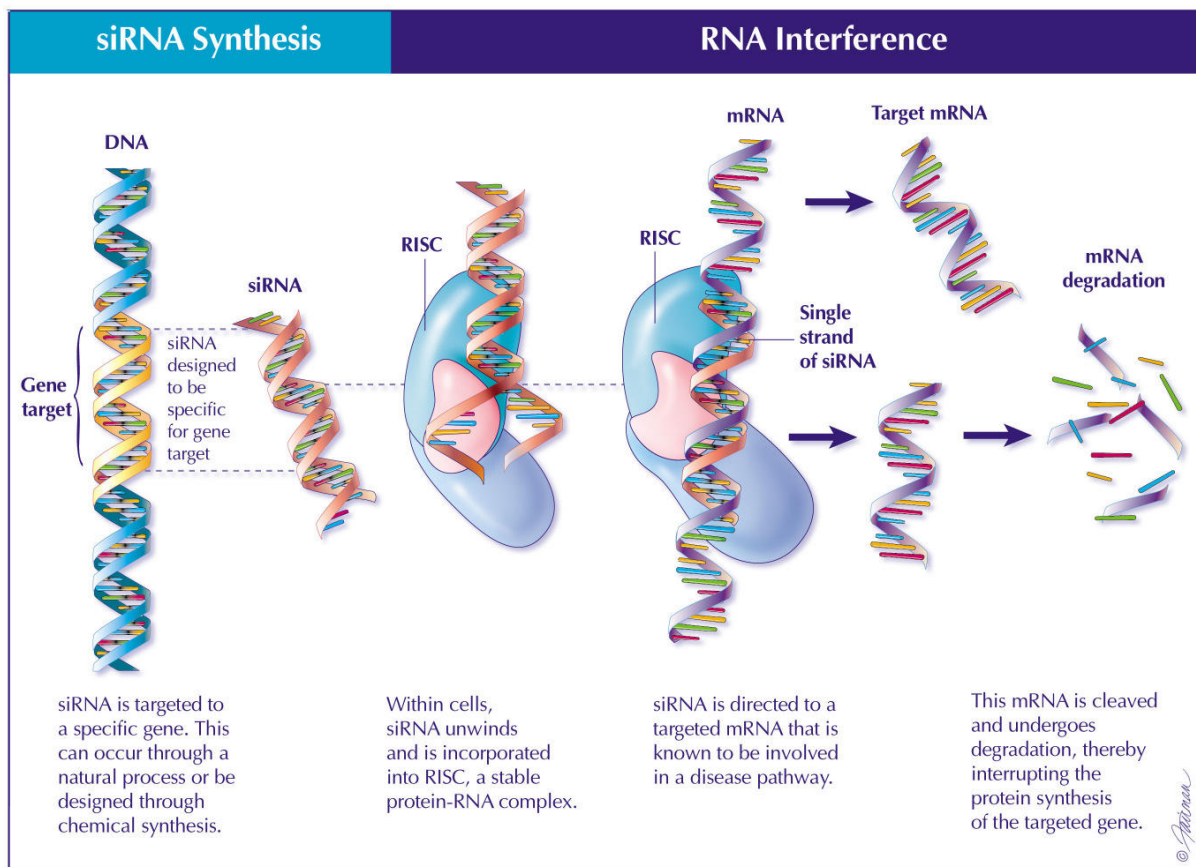


Figure 1.5. RNAi mechanism (www.alnylam.com)

So, in general the nucleic acid synthesis opens up broad possibilities for future progress in modern medicine. We still learn a lot about nucleic acids and the synthesis of new nucleic acid analogues is in the field one of the main tools.



# 1 Molecular Design of Life

## 1.1 Structure and Function of Nucleic Acids

Nucleic acids appear in nature in two different forms as DNA (2'deoxyribonucleic acid) and RNA (ribonucleic acid). DNA is a polymer of deoxyribonucleotide units and RNA is a polymer of ribonucleotide units. A nucleotide consists of a nitrogenous base, a sugar and one or more phosphate groups. The sugar in DNA is deoxyribose and in RNA the sugar is ribose.

The nitrogenous base is a derivative of purine or pyrimidine. The C-1 atom of ribose or deoxyribose is bonded to N-1 of a pyrimidine or N-9 of a purine. The configuration of this N-glycosidic linkage is  $\beta$  (the base lies above the plane of the sugar ring). The nucleobase might have two main orientations concerning sugar and glycosidic C1-N bond. This position is defined with torsion angle  $\chi$  (by purines O4'-C1'-N9-C4 and by pyrimidines: O4'-C1'-N9-C2 (*figure 2.1*) (IUPAC, 1983). By natural nucleosides *anti* conformation is favourable, but an exception are purines in Z-DNA.

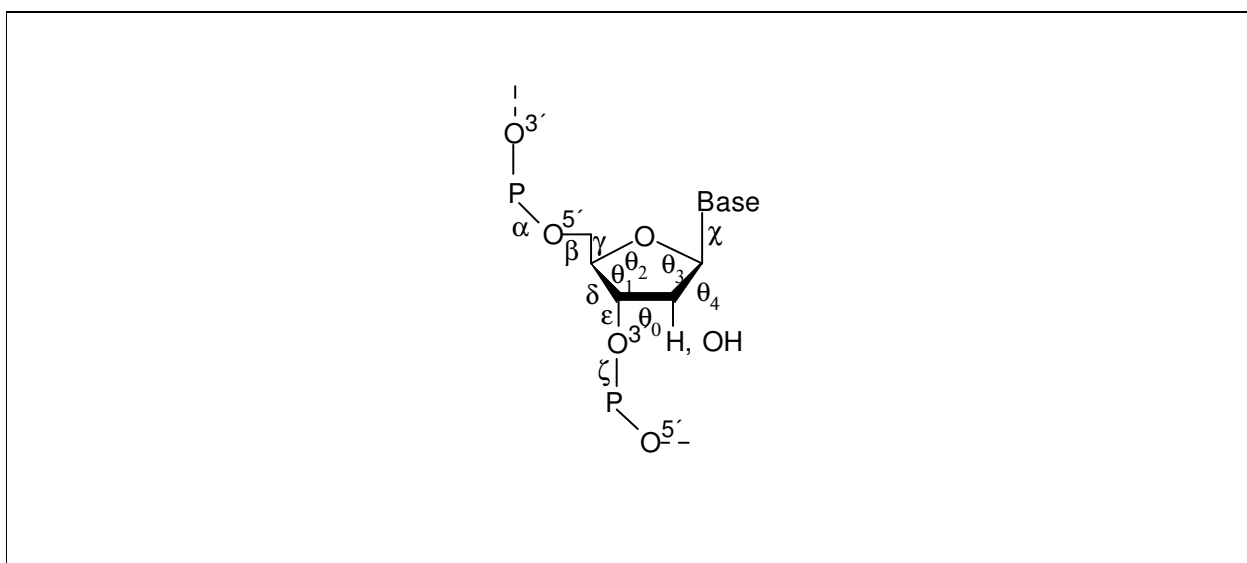
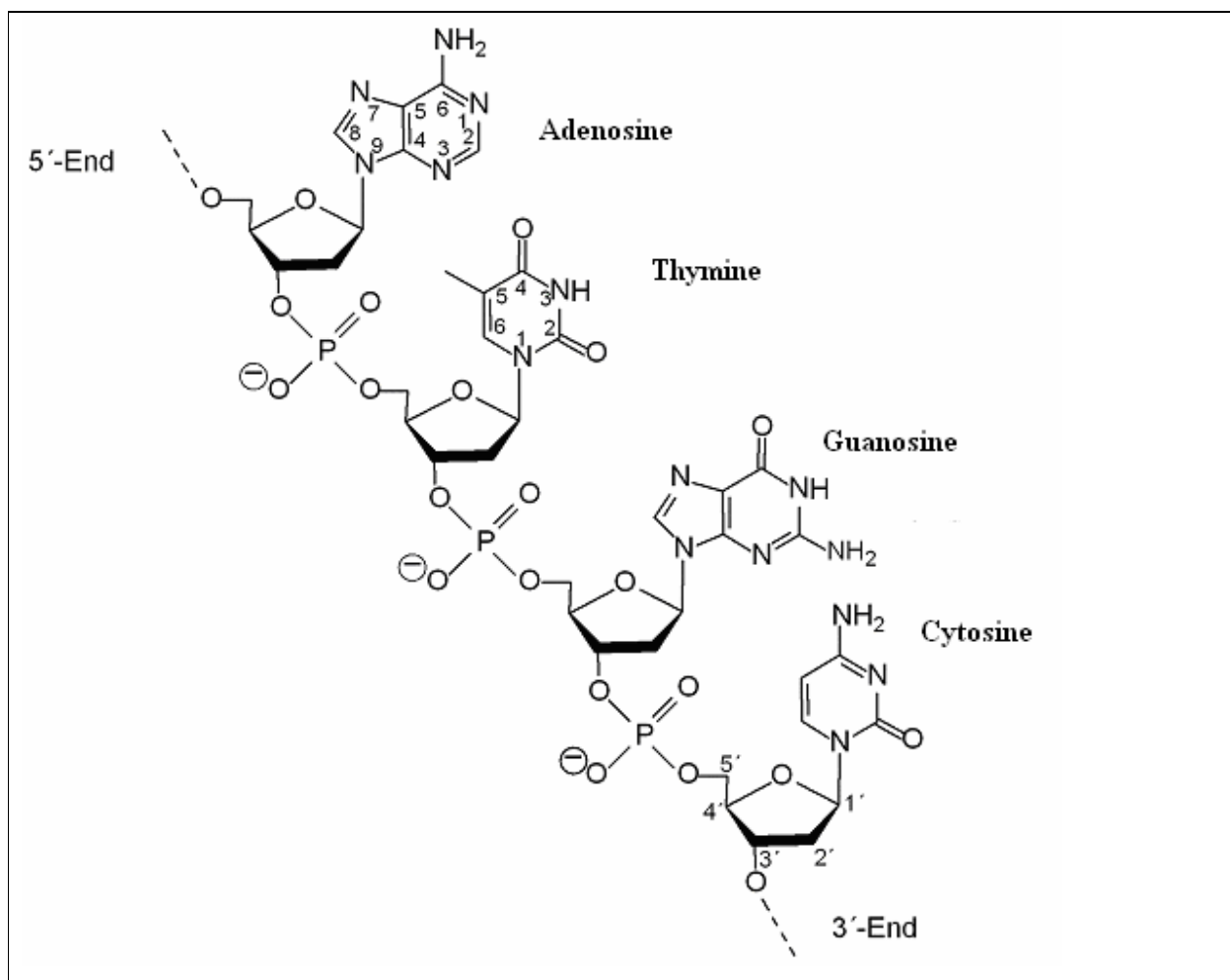


Figure 2.1. Torsion angle at nucleotides (Blackburn & Gait, 1996)

Purines in DNA are adenine (A) and guanine (G) and pyrimidines are thymine (T) and cytosine (C). In RNA only thymine is exchanged with uracil (U).

The four nucleosides that exist in DNA are deoxyadenosine, deoxyguanosine, deoxythymidine and deoxycytidine. In RNA they are called: adenosine, guanosine, uridine and cytidine. Nucleotides are phosphor esters of nucleosides. A DNA chain is shown in *figure 2.2*.



*Figure 2.2. DNA structure with numbering of the bases*

Phosphate groups are charged negatively and that explains their good water solubility. The nucleobases can have different tautomeric forms. Existing tautomers are keto-enol and also amino-imino-tautomers. Spectroscopic investigations have shown that all five natural bases exist as amino- and keto- tautomers in a rate >99.99%

DNA consists of two helical polynucleotide chains that are coiled around a common axis. The chains run in opposite directions. The purine and pyrimidine bases are on the inside of the helix

where as the phosphate and sugar units are on the outside. The planes of the bases are perpendicular to the helix axis. The planes of the sugars are nearly at right angles to those of the bases. The two chains are held together by hydrogen bonds between pairs of bases. So known Watson-Crick-pairs are adenine and thymine and guanine is paired with cytosine. The double helix is also stabilized through  $\pi$ - $\pi$  interactions in-between the bases of the same chain. As a consequence of non-diametric positions of glycosidic bonds exist major and minor grooves. Except this B-DNA form that was established by Watson and Crick there are also some other forms and structures that DNA forms in nature (chapter 2.4).

Conformation of the sugar unit has a big influence on the DNA structure because the furanose ring is not planar. It can form E-conformation (envelope) or T-conformation (twist). In envelope conformation four atoms of the furanose ring are in one plane and the fifth is 0,5 Å above or under that plane. In the twist conformation three atoms are in one plane, one of two other atoms is under that plane while the other one is above. Atoms that are above that plane are called *endo* and the ones under the plane are *exo* (figure 2.3).

The sugar of the DNA is in C2'-*endo* (S) conformation and in RNA is usually favourable C3'-*endo* conformation.

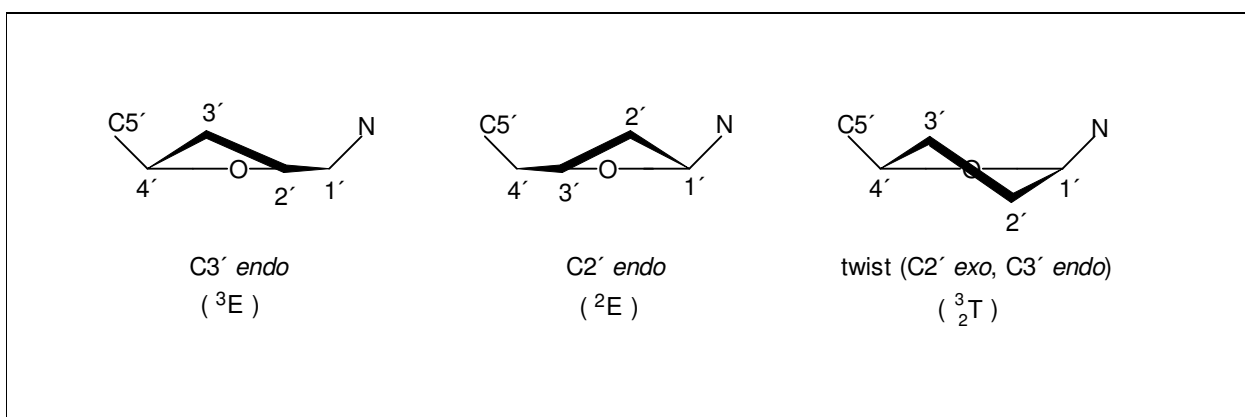
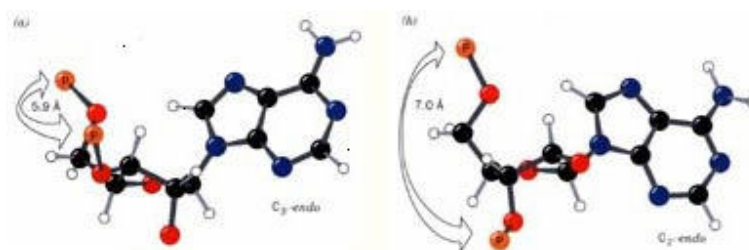


*Figure 2.3. Conformations of the furanose ring*



## 2.2 DNA Structures

The structures of DNA double helices exist in different conformational types. The most important are A-DNA, B-DNA and Z-DNA.

The helix axis is located in the major groove side of the base pairs in A-DNA form. Base pairs are tilted towards helix axis in A-DNA.

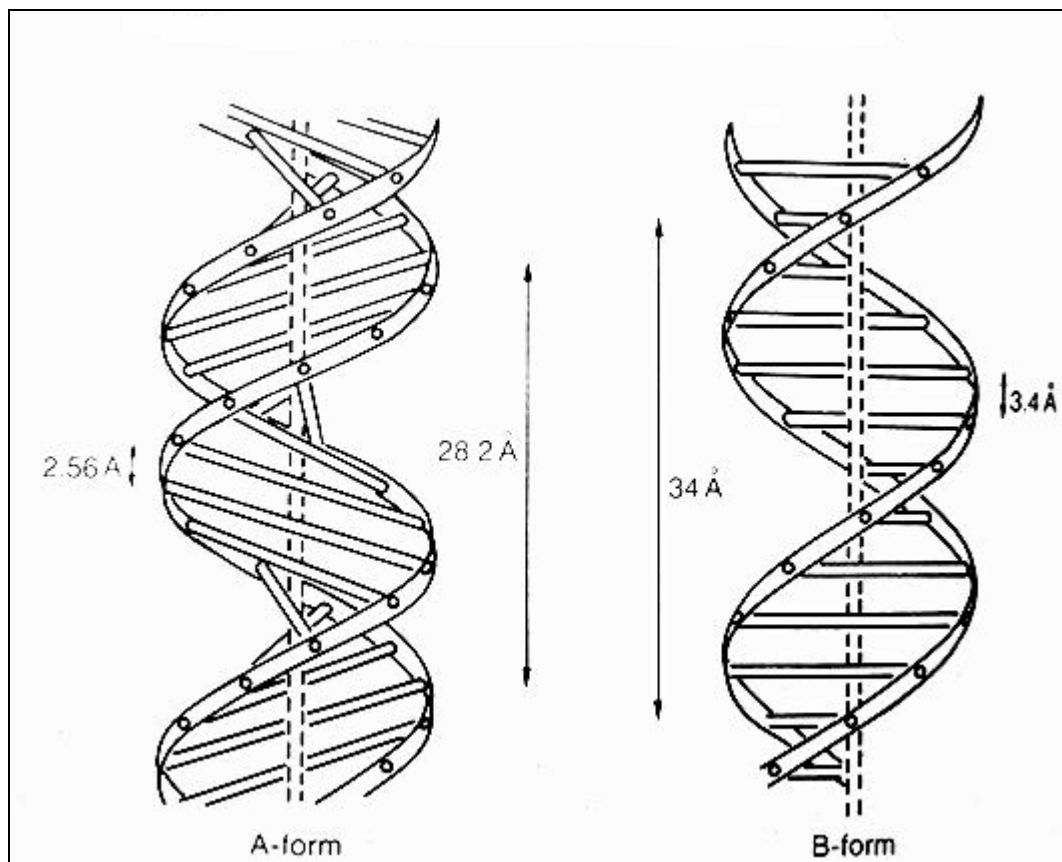


Figure 2.4. A and B forms of DNA double helix

The radius of the helix is 2,55 nm and the height pro base pair is 0,23 nm. In the right-handedness helix the glycosidic linkage is always *anti*. 11 base pairs build one turn of the helix. The special characteristics of A-DNA are strong slope (inclination) of the base pair towards the helix axis. The major groove is narrow and deep; the minor groove is wide and plane. The sugar conformation is C3'-*endo*. The orientation of the C1'-N-glycosidic linkage is characterized by torsion angle  $\chi$  of  $-160^\circ$  (Saenger, 1984; Stryer, 1991).

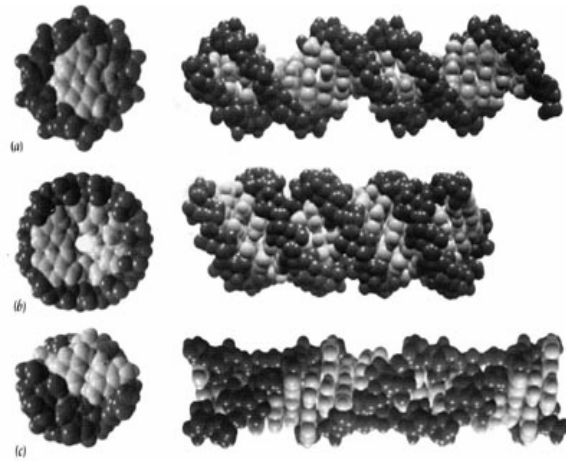


Figure 2.5. Different forms of DNA a) B-DNA form b) A-DNA form c) Z-DNA form

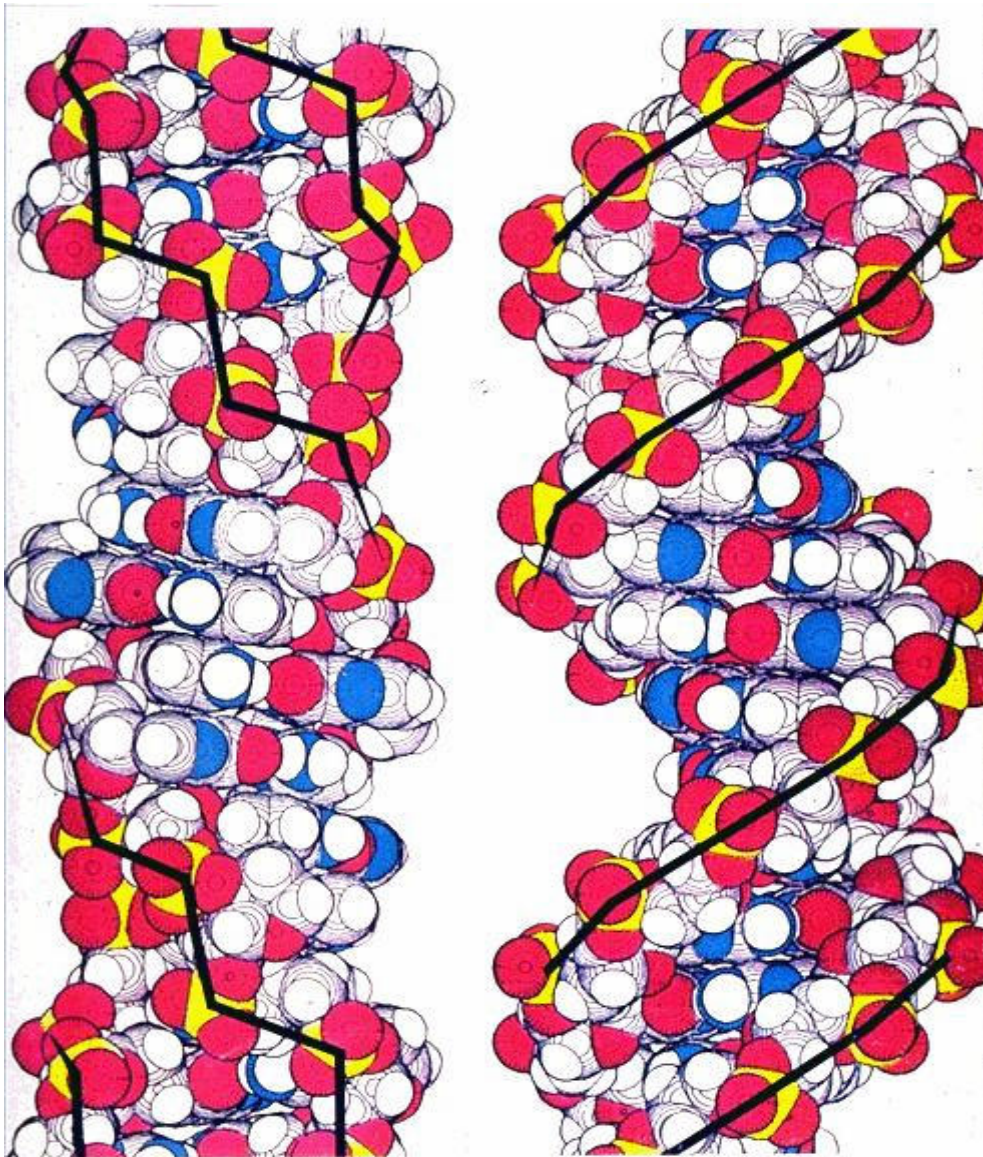


Figure 2.6. Z and B forms of DNA helix

The radius of the B-DNA helix is 2,37 nm; the height per base pair is 0,34 nm. The helix is right-handed with *anti* conformation of the glycosidic linkage. The number of base pairs per turn is 10. The major groove is wide and deep while the minor groove is deep but narrow. The sugar conformation is C2'-*endo*. The orientation of the C1'-N-glycosidic linkage has a torsion angle  $\chi$  of  $-120^\circ$ .

Opposite to A-DNA and B-DNA (*figure 2.5*) that are right-handed the Z-DNA (*figure 2.6*) is left-handed. The sugar phosphate backbone is zigzagged and the repeat unit is a dinucleotide. The radius of the Z-DNA helix is 1,84 nm. The height per base pair is 0,38 nm. 12 base pairs make one full turn of the helix. The pyrimidine bases have *anti* conformation to the glycosidic linkage. The major groove is plane and the minor groove is narrow and deep.

For better comparison data of all three types are given in *figure 2.7*.

	A DNA	B DNA	Z DNA
HANDEDNESS	RIGHT	RIGHT	LEFT
HELICAL TWIST (DEGREES)			
MEAN AND STANDARD DEVIATION	33.1 ± 5.9	35.9 ± 4.3	G-C: -51.3 ± 1.6 C-G: -8.5 ± 1.1
OBSERVED RANGE	16.1 to 44.1	27.7 to 42.0	
BASE PAIRS PER TURN	10.9	10.0	12.0
HELIX RISE PER BASE PAIR (ANGSTROM UNITS)	2.92 ± .39	3.36 ± .42	G-C: 3.52 ± .22 C-G: 4.13 ± .18
BASE INCLINATION (DEGREES)	13.0 ± 1.9	-2.0 ± 4.6	8.8 ± .7
PROPELLER TWIST (DEGREES)	15.4 ± 6.2	11.7 ± 4.8	4.4 ± 2.8
BASE ROLL (DEGREES)	5.9 ± 4.7	-1.0 ± 5.5	3.4 ± 2.1

*Figure 2.7. Comparison of A-DNA, B-DNA and Z-DNA*

Beside hydrogen bonds of the Watson-Crick base pairs there are more factors that have influence on the structure and stability of nucleic acids. The most important are: hydration of helix and base stacking effects. More explanations on this subject can be found in the subchapter 2.4.

## 2.3 RNA Structures

Inside the cells, there are three major types of RNA: messenger RNA (mRNA), transfer RNA (tRNA) and ribosomal RNA (rRNA). There are a number of other types of RNA as well, including small nuclear RNA (snRNA), the 4.5S signal recognition particle (SRP) RNA etc. Novel species of RNA continue to be identified.

Although RNA molecules are linear polymers, they fold back on themselves to make intricate secondary and tertiary structures that are essential for them to perform their biological roles.

RNA double helix has always A-form. A characteristic structural feature of A family of double helices of nucleic acids is the 3'-*endo*-conformation of the sugar. Insofar as helical RNA is concerned, such a conformation of the ribose seems to be the only possible one and, consequently, transition A-B for this class of nucleic acids is forbidden. The fact that the ribose can not change from C3'-*endo*- into C2'-*endo*-conformation is caused by the contacts between the hydroxyl group at C2' and other atoms (primarily oxygen in the phosphor diester bond). Its major groove is deep and narrow while the minor groove is shallow and wide. As a result, in contrast to DNA, the main site of interaction with ligands in double-stranded RNA is its minor groove. Secondary structures of RNA are internal loops, hairpin loops bulges and junctions (figure 2.8)

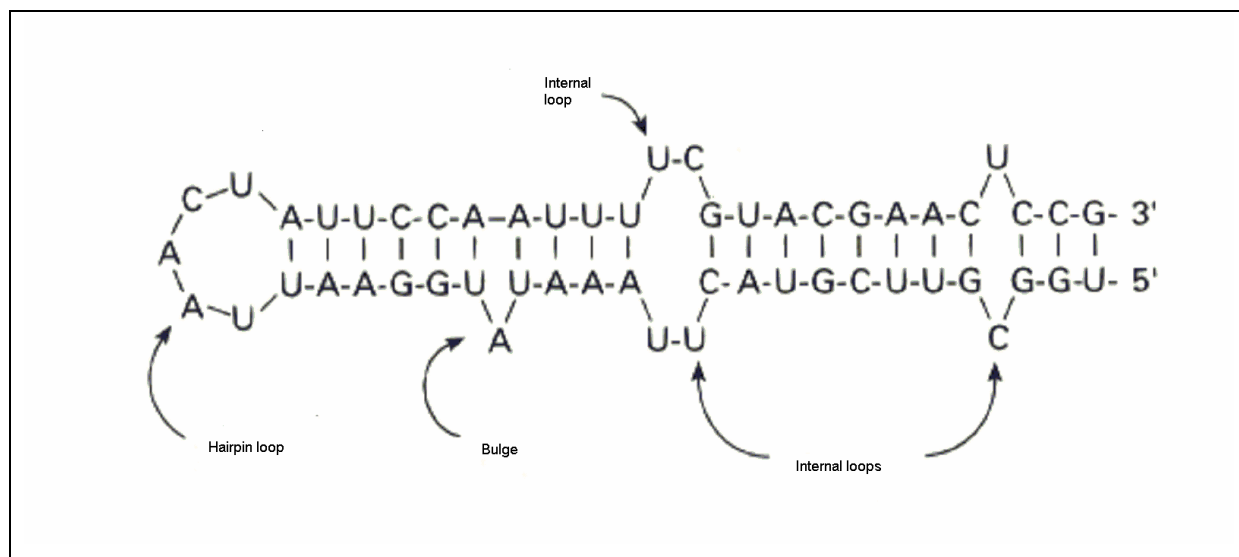
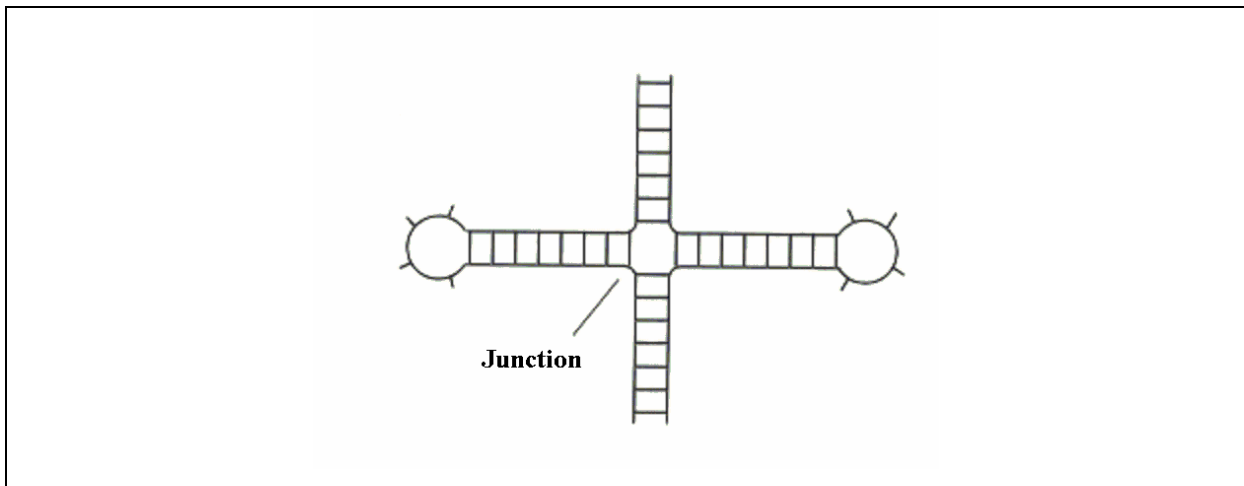


Figure 2.8. RNA secondary structures

**Hairpin loops** (figure 2.8) are elements invariably present in the secondary structure of any single stranded RNA. There is every reason to assert that stability of hairpin loops is determined by stacking interactions and hydrogen bonding within the loops. Analysis of the

thermodynamic stability of many synthetic hairpins has shown that the most stable structures are those with loops of four or five nucleotides especially the UUCG tetraloop is very stable. The **bulges** (*figure 2.8*) are short single stranded parts, non-paired, where the complete complementary chain is involved in pairing. The bulges can have only one nucleotide but can also have more. These internal sequences are usually rich with purines. They are also considered as potentially functional sites. Very little is known about larger bulges. There is a reason to believe that they are destabilizing RNA in greater extent than single base bulges.

**Internal loops** (*figure 2.8*) arise whenever bases that are not complementary in the Watson-Crick sense find themselves opposite each other in a double stranded segment of RNA. Therefore, the stability of an internal loop will depend on whether the bases in the opposite strands become paired as well as on the degree to which such pairing disturbs the geometry of the helix. The least disturbance in the double helix is caused by formation of the G-U pair from the mismatches.



*Figure 2.9. RNA secondary structure-a junction*

Next known secondary RNA structure is **junction**. In the junction more helical parts meet at one point (*figure 2.9*). The big junctions vary from four to five helices that are meeting at a point.

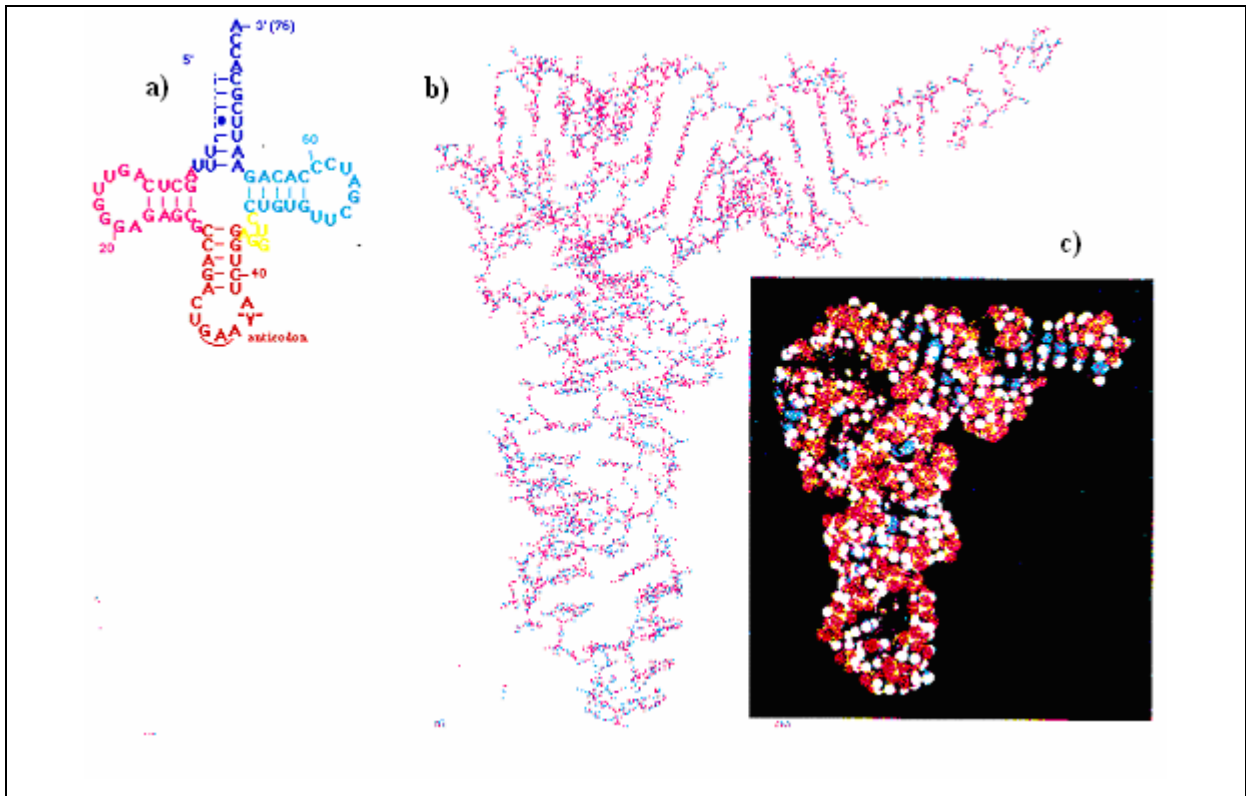


Figure 2.10. a) Secondary structure of one of tRNA-clover-leaf model b) three dimensional tertiary structure of tRNA (Blackburn&Gait, 1996) c) space filling model

Beside secondary structures RNA builds also tertiary structures. The tertiary RNA structures are stabilised with hydrogen bonds and base stacking. *Figure 2.10* shows secondary structure of tRNA and in part b) shows the real three-dimensional structure of t-RNA (Blakburn&Gait, 1996). The defined tertiary structure of RNA molecules is important for their function.

## 2.4 Stability of a Double Helix

### 2.4.1 Hydrogen Bonds

Hydrogen bonds can be formed between uncharged molecules as well as between charged ones. In a hydrogen bond, two atoms share one hydrogen atom. The atom to which hydrogen is more tightly linked is called hydrogen bond donor, whereas the other atom is a hydrogen bond acceptor. The acceptor has a partial negative charge that attracts the hydrogen atom. In fact, a hydrogen bond can be considered as an intermediate in the transfer of proton from an acid to a base. It is reminiscent of a *ménage a trois*.

The hydrogen bond donors in biological systems are usually oxygen or nitrogen. The acceptor is either oxygen or nitrogen. The length of hydrogen bonds differs from 2,63Å (O-H...O) to 3,10 Å (N-H ...N) and the energy from 3 to 7 kcal/mol. Hydrogen bonds are stronger than van der Waals bonds but weaker than covalent bonds. The length of a hydrogen bond is between that of a covalent bond and van der Waals bond. The important feature of a hydrogen bond is that they are highly directional. The strongest hydrogen bonds are those in which donor, hydrogen and acceptor atoms are collinear. (Stryer, 1991)

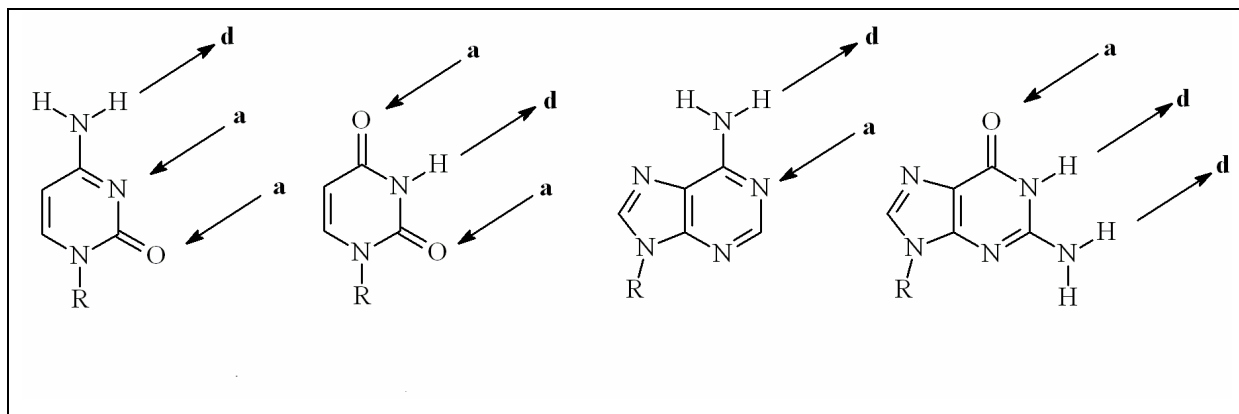


Figure 2.11. Donors and acceptors in hydrogen bonds in natural nucleosides

*R=ribose or 2'-deoxyribose*

The distance between donor and acceptor in one hydrogen bond is between 2,8 and 2,95 Å. The donor and acceptor atoms in building Watson Crick base pairs are shown in *figure 2.11*. Beside Watson-Crick base pairs there are Hoogsteen base pairs (Hoogsten, 1959). In Hoogsteen base pair hydrogen bonds are built between the Watson-Crick side of pyrimidine

and the opposite side of purine (Hoogsteen side). In the double helix they are not of any importance. On the other hand there are also Wobble base pairs. The bases in there are opposite one another but just a bit moved so that it is again possible to have donor and acceptor in one line again. Examples are uridine-guanosine and uridine-inosine Wobble base pairs (*figure 2.12*).

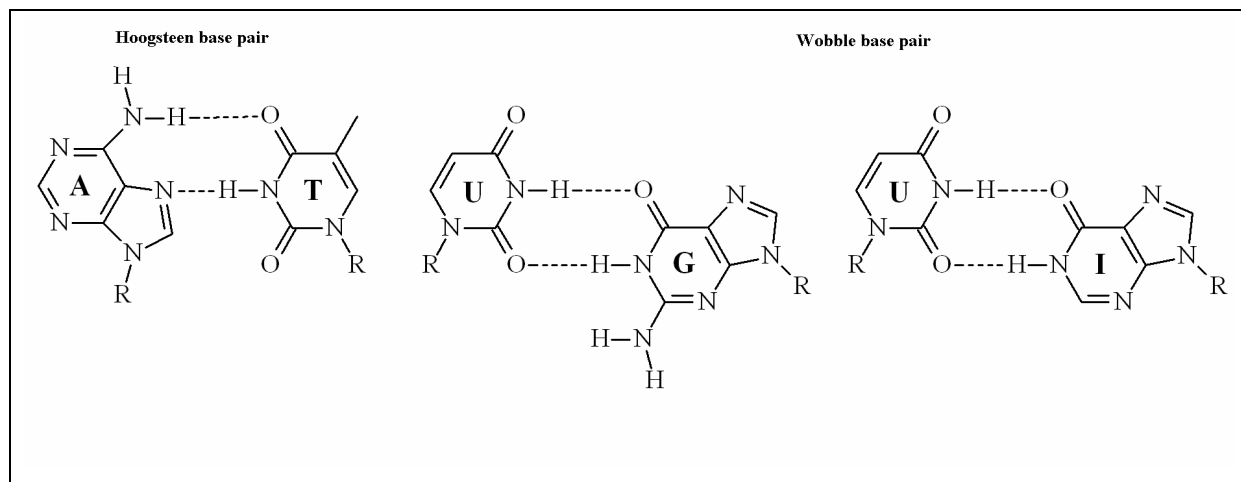


Figure 2.12. Hoogsteen and Wobble base pairs

## 2.4.2 Base Stacking

Besides hydrogen bonding base stacking is one of the most important stabilizing effects in the double helix. Among the most significant aromatic-aromatic interactions are those found in nucleic acids (Guckian *et al.*, 1996). The base stacking are the  $\pi$ - $\pi$  interactions between bases of the same chain and is crucial for the stabilization of these structures. Stacking interactions play an essential role in mRNA-cap recognition by proteins (Castellano *et al.*, 2003). The nucleobases are not exactly one over another because that is not possible from the structural characteristics. How much they are moved depends on the type (A, B or Z) and sequence. Also modifications affect the neighbouring nucleobases. *Figure 2.13* shows different possibilities of orientation and positioning of two neighbouring bases (Cambridge DNA Nomenclature; Dickerson *et al.*, 1989).

Hunter (Hunter, 1993) has recognized four energetically principles, for base stacking in DNA and those are:

1. van der Waals forces (vary with  $r^{-6}$ )



2. Electrostatic forces between partial atom charges (atom-atom; vary with  $r^{-1}$ )
3. Electrostatic forces between  $\pi$  electron density above and under the plane of the nucleobase (atom- $\pi\sigma$ ; vary with  $r^{-4}$ )
4. Electrostatic forces between  $\pi$  electron density and charged atoms (atom- $\pi\sigma$ ; vary with  $r^{-4}$ )

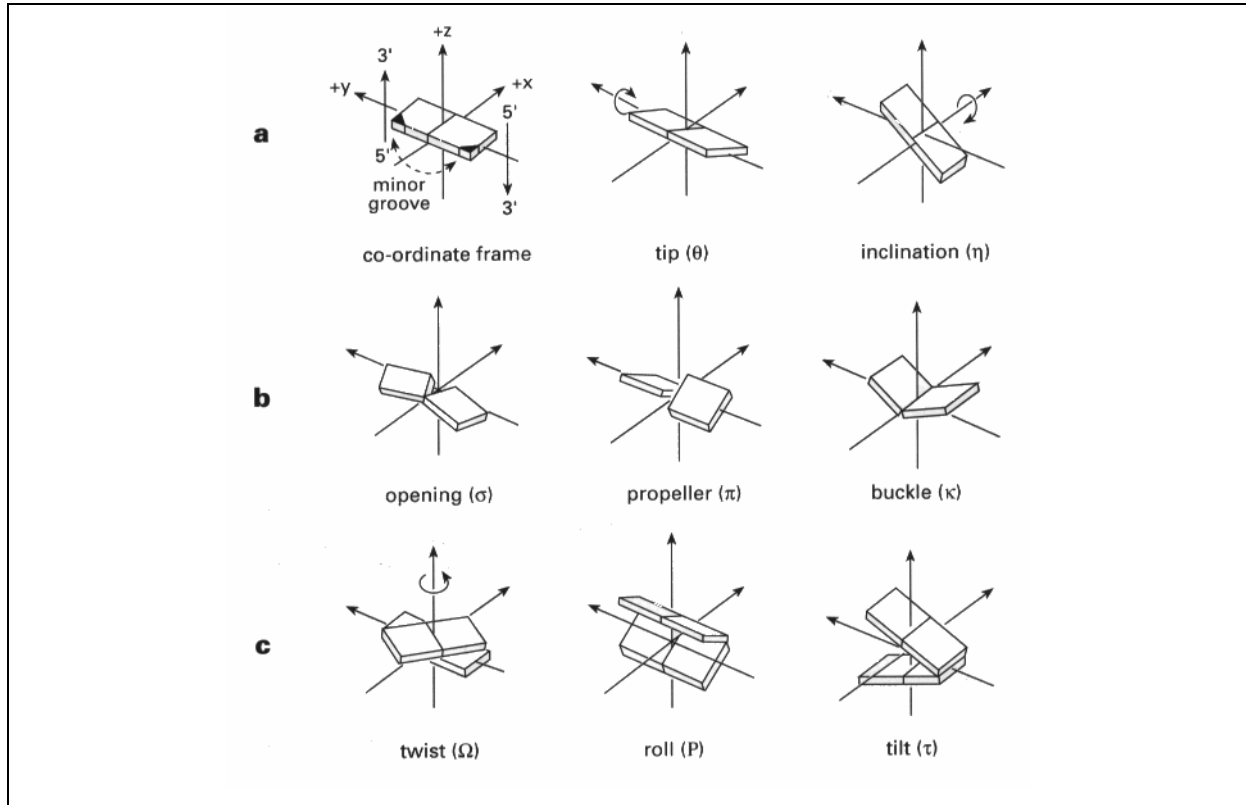


Figure 2.13. Possible positions of pairing nucleosides (Blackburn&Gait, 1996)

Studies about associations of nucleobases and nucleosides in water solutions show that the process of base stacking is reversible and has a constant value of free enthalpy for every step. Enthalpies are additive and not cooperative values. The strength of base stacking is different for purines and pyrimidines. The base stacking between two purines is stronger than between a purine and a pyrimidine and that one is also stronger than stacking between two pyrimidines. (Saenger, 1984). Base stacking keeps one chain of RNA in helical structure (Haasnoot&Altona, 1979).

To separate stacking from hydrogen bonding usually used method for determination of thermodynamical stacking parameters is placing the wanted base in so called “dangling” position (without a pairing partner). The resulting stabilisation of the duplex can be measured by denaturising experiments. The results of such investigations show that not only the surface

area is responsible for good stacking but also substituents are of great importance. The results also indicated that the natural bases are not particularly effective for stacking, at least in global comparison with aromatic structures. Evolution may not favour the bases, which stack too strongly, since helix unwinding is requirement for DNA replication (Guckian *et al.*, 1996). These results were interpreted as indicating that hydrophobic interactions provide the greatest contribution to stacking interaction. The plot of polarizability versus stacking energy appears to show a rough qualitative correlation between increasing polarizability and increasing stacking ability.

**Quadrupole-quadrupole** interactions were also proposed to be important for electron-poor rings such as 4-nitroindole. Rosemayer and Seela have also shown that the polarizability of the dangling base correlates with stability of the duplex better than hydrophobicity (Rosemayer & Seela, 2002). A general difficulty with interpreting the results from dangling-base studies is that geometry of interaction in these systems typically is not known (Waters, 2002). The greater difference (of opposite sign) of quadrupole moments of two compounds greater is the attractive interaction in-between them (Castellano *et al.*, 2003).

The example, which shows how significant quadrupole-quadrupole interactions are, is the structure of 1:1 mixture of benzene: hexafluorobenzene. Those two compounds have large quadrupole moments, but of opposite sign, and the mixture has higher melting point than both pure benzene and pure hexafluorobenzene (Ladig, 1991; Williams, 1993; Castellano *et al.*, 2003).

The current known data suggest that a quadrupolar effect may be a significant factor in stacking, particularly with no natural bases having strong electron-donating or –withdrawing groups (Guckian *et al.*, 2000).

### 2.4.3 Solvation

Water solvates nucleic acids in nature. Water is however not only a medium that keeps nucleic acids in solution it is also important for stabilizing secondary and tertiary structures (Edelhoch&Osborne, 1976). The level of hydration of DNA plays also an important role for the secondary structure of DNA. High hydration is characteristic for B-DNA form and low hydration is characteristic for A-DNA.

The hydration of macromolecules is expressed with  $\Gamma$ .  $\Gamma$  is the number of water molecules per mol of nucleotide. The secondary structure depends also on  $\Gamma$ . This value is in direct connection with the water activity  $a_w$ , which can be adjusted by addition of salt. At and above

complete hydration, B-DNA prevails. It changes to some other conformations if the hydration is reduced, to an attainable minimum of 3.6 water molecules per nucleotide. If water is added in excess, the sample swells but remains in B-DNA form. The effect of ions on  $a_w$  is determined through ion strength and depends mostly on the nature of ions.

Experiments with DNA have shown that the DNA double helix is strongly solvated. The hydration of DNA is not homogeneous. It can be described in terms of two shells, as suggested by sedimentation equilibrium studies and gravimetric and infrared spectroscopic investigations. These experiments indicate that the structure of the primary hydration shell is not ice-like. It is impermeable to ions and consists of 11-12 water molecules per nucleotide. These water molecules can be grouped in three classes with decreasing binding affinity for phosphate, phosphodiester plus sugar oxygen atoms and functional groups of bases.

The *primary hydration shell* is different from bulk water. Of the 20 water molecules per nucleotide, only 11-12 are directly bound to DNA. They form a shell, which is impermeable to cations and does not freeze into an ice-like state. These water molecules are observed in crystal structure analyses and are hydrogen-bonded to DNA oxygen and nitrogen atoms.

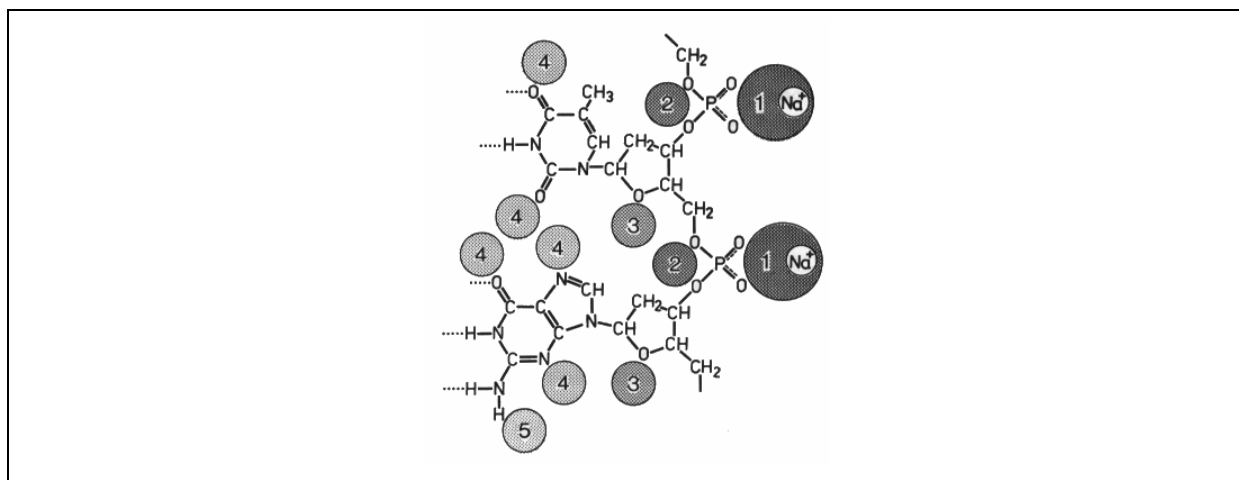


Figure 2.14. Hydration regions in B-DNA

The *secondary hydration shell* is permeable to cations. At subzero temperatures, it crystallizes in the form of ice and therefore resembles bulk water (Saenger, 1984).

## 2.5 Universal Bases

A universal base analogue forms 'base pairs' with each of four natural bases with little discrimination between them. A number of such analogues have been prepared and their applications as biochemical tools were investigated. Most of those bases are hydrophobic, aromatic bases, which stabilise duplex (DNA or RNA) by stacking interactions (Loakes, 2001). The desirable requirements for a universal base have been defined (Loakes *et al.*, 1997). They should:

- Pair with all the natural bases equally when opposite them in an oligonucleotide duplex
- Form a duplex which primes oligonucleotide synthesis by a polymerase
- Direct incorporation of the 5'-triphosphate of each of the natural nucleosides opposite when copied by a polymerase
- Be a substrate for polymerase as the 5'-triphosphate
- Be recognised by intracellular enzymes such that DNA containing them may be cloned.

At present no analogue has been shown to fulfil all these requirements and it may be that no single analogue does it. However, each of analogues prepared so far has set of properties that enable their use or some of these purposes.

There are no universal nucleobases that fulfil all conditions. There are only nucleosides that fulfil some of those conditions (Loakes, 2001). Here we are going to show some of them.

The first universal base analogue was 3-nitropyrrole (1, *figure 2.15*), described by Bergstrom and co-workers (Bergstrom *et al.*, 1995). The design of this analogue was aimed at maximising base stacking interactions; the presence of nitro group enhances stacking by polarisation of the  $\pi$ -aromatic system of the pyrrole ring. Compound 1 was shown to behave indiscriminately in base pairing with four natural bases, there was significant destabilisation of duplexes containing it. It was concluded that the pyrrole ring does not stack as well as expected and the design of future analogues should aim at replacing the nitro group by less bulky substituents. A related analogue is 5-nitroindole (2). This analogue has been shown to be less destabilising and is not discriminating towards the natural bases. A large number of non-hydrogen bonding base analogues has been investigated, though mainly in hybridisation applications. These include 4-nitrobenzimidazole (3) analogue that behaves indiscriminately towards the natural bases but is more destabilising than 2. Similar preferences show 4-aminobenzimidazole (4).

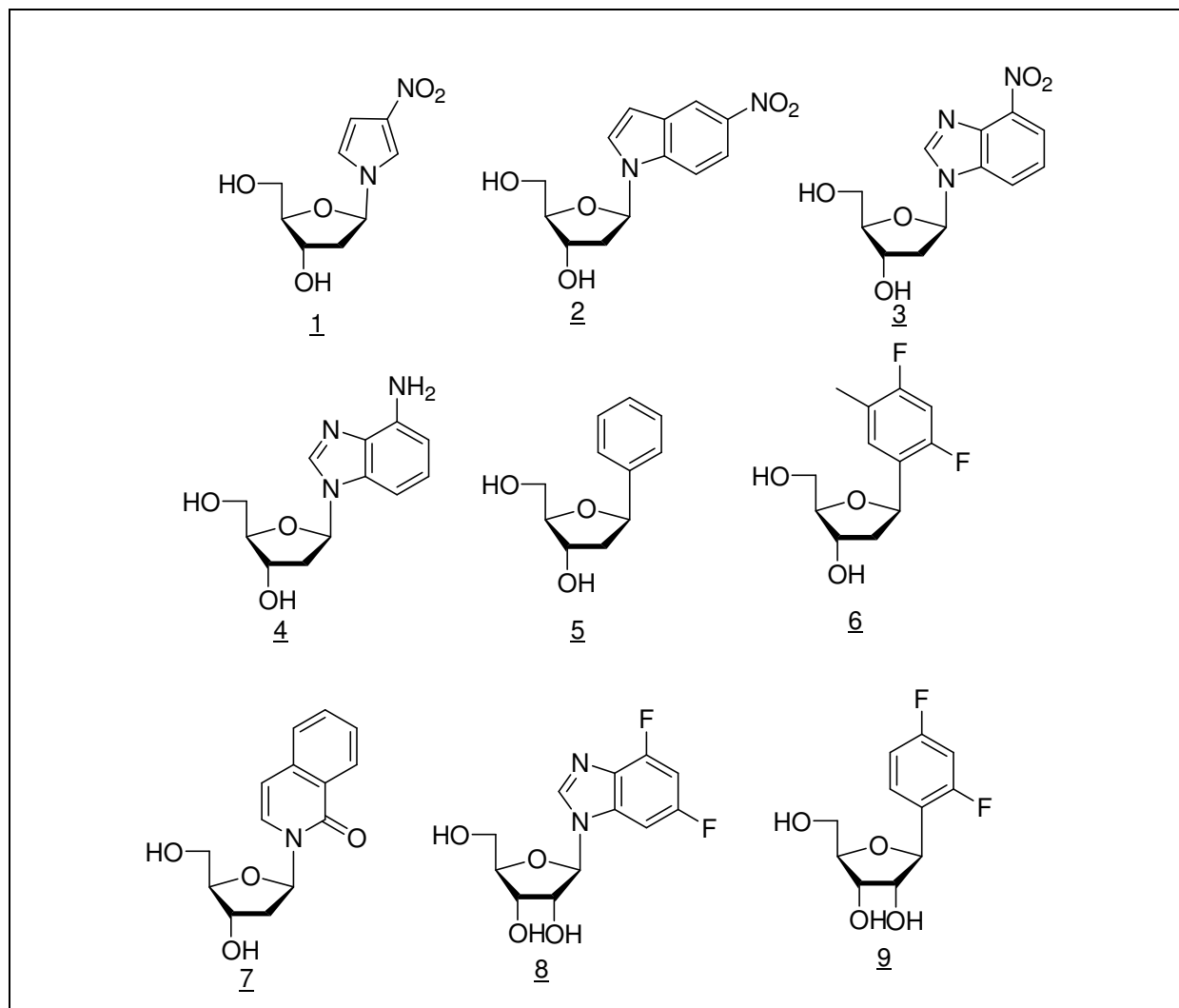


Figure 2.15. Universal nucleobases

One of the earliest analogues to be investigated was phenyl-C-ribonucleoside (5). These earlier findings of Millican *et al.* showed that phenyl-C-ribonucleoside is quite destabilising and it was essentially the same as an abasic site. Thus, the presence of phenyl ring offers little to no contribution to stacking interactions. Nevertheless, those analogues show little discrimination towards pairing with each of the natural bases. Compound 6 stacks more strongly than it is expected from surface area alone (Schweitzer *et al.*, 1994). These results show that surface area is not the only factor affecting stacking affinity, but increased hydrophobicity must also in some way enhance the stabilisation of oligonucleotides containing such analogues. Compound 7 directs the insertion of natural triphosphates by Klenow fragment with a 4-fold lower variation in efficiency and, at high dNTP concentration, full length DNA is synthesised. Compounds 8 and 9 give with all natural bases base pairs with almost the same stability (Parsch, 2002). The triphosphates of both compounds were

incorporated by RNA polymerase (Kloepffer, 2004). Some more details of those two compounds are going to be given further in this dissertation.

There is a little known about RNA universal bases and behaviour of bases is different in A- and B- helix.

Universal Nucleobase	Reduction of the stability $\Delta T_m$ [°C]	Difference in $T_m$ when pairing with A, C, G and U [°C]
<u>1</u>	8-11	3
<u>2</u>	4-7	3
<u>6</u>	14-19	5
<u>7</u>	3-5	2
<u>8</u>	9-10	1
<u>9</u>	10-10,5	0,5

*Figure 2.16. Influence of the universal nucleobases on the melting point of RNA duplexes*



## 3 Organic Fluorine

### 3.1 Fluorine- Properties and Hydrogen Bonding Ability

Special properties of fluorine are as follows:

- High electro negativity
- Relatively small size
- Very low polarizability
- Tightly bound, three non-bonding electron pairs
- Excellent overlap between F 2s and 2p with corresponding orbitals of other second period elements

Fluorination usually but not always increases lipophilicity but on the other hand aromatic fluorination always increases lipophilicity. Also, fluorination always increases hydrogen bond acidity. Perfluoroalkyl groups are always electron withdrawing. Fluorination also increases the steric size of alkyl groups. (Smart, 1994; Smart, 2001)

The van der Waals radii of fluorine (1.47 Å) can be compared to that of hydrogen (1.20 Å) or oxygen (1.57 Å) and it emerges that fluorine has a close isosteric relationship to oxygen. To be a successful hydroxyl mimic in bioorganic chemistry the fluorine atom must replace the hydrogen bond acceptor ability of the hydroxyl oxygen (Sein et al., 2000).

Pauling discussed the strong hydrogen bond in hydrofluoric acid (HF)<sub>n</sub> and the very strong one in the hydrogendifluoride ion [HF<sub>2</sub>]<sup>-</sup> and concluded that the proton in the latter should lie in a single minimum potential well or in a double minimum potential with a very small barrier ( Pauling, 1960).

Theoretical calculations variously estimate the strength of an F...H bond to be between 2 and 3.2 kcal mol<sup>-1</sup>. This can be compared to an O...H hydrogen bond, which is typically between 5-10 kcal mol<sup>-1</sup>. Thus the greater electro negativity and lower polarisability of fluorine over oxygen suppresses its electrostatic influence and renders it a poorer



hydrogen bond acceptor. There is also a significant increase in short contacts to C ( $sp^3$ )-F over C ( $sp^2$ ) bound fluorine atoms (Figure 3.1). A further intensive search of CSD (Cambridge Structural Database), confirmed that organic fluorine hardly ever accepts hydrogen bonds, that is, it does so only in the absence of a better acceptor.

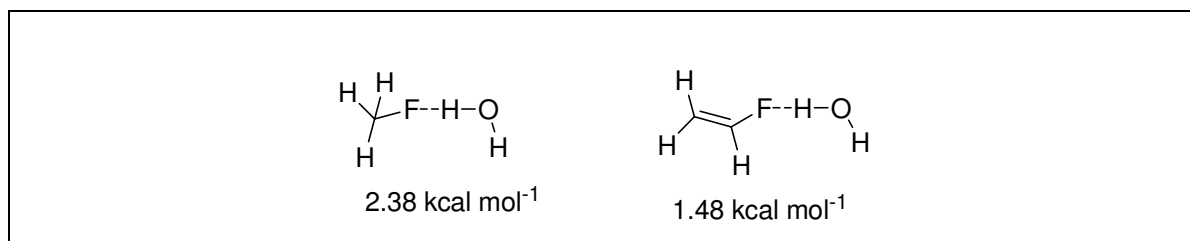


Figure 3.1. The F...H bond is stronger to a C ( $sp^3$ ) rather than a C ( $sp^2$ )-F acceptor (Howard *et al.*, 1996)

This observation implies that aliphatic fluorine atoms are better hydrogen bond acceptors than olefinic or aromatic fluorine atoms. A clear conclusion from this data is that vinyl (and aryl) fluorines are less effective than aliphatic fluorines as hydrogen bond acceptors. However if the hydrogen bond donor can find stabilization with an alternative acceptor to fluorine then it will do this and adversely influence the binding interaction (Howard *et al.*, 1996).

Despite the larger van der Waals radii for fluorine over hydrogen, the experimental evidence suggests that, in general terms, the substitution of a single fluorine for a hydrogen atom introduces only small steric and geometric perturbations relative to the hydrocarbon counterpart. However it is generally appreciated that the methyl and trifluoromethyl groups bear very little steric resemblance. A comparison of the molar volumes of a series of related compounds with various substituents, and with a  $CF_3$  group, reveals a size closer to an isopropyl than a methyl group (O'Hagan *et al.*, 1997). Fluorination increases the strength of C-C single bonds but weakens the strength of C=C double bonds (Dunitz&Taylor, 1997; Dunitz, 2005).

It has become a common practise in bioorganic chemistry to replace a hydrogen atom or a hydroxyl group for fluorine to generate a fluorinated enzyme substrate analogue, which may act as substrate or inhibitor in a given enzymatic process. The rationale for such a strategy is that the size of fluorine atom is intermediate between that of hydrogen and oxygen. The substitution of hydrogen by fluorine is one of the most commonly employed monovalent isosteric replacements. Not so commonly used, but supported by Grimm's hydride displacement law, are exchanges of  $-NH_2$ ,  $-OH$  and  $-CH_3$  groups with fluorine. (Patani & LaVoie, 1996).

### 3.1.1 Crystal Structures of Fluoro Benzenes

Hydrogen bonding, the master key of molecular recognition, is the most reliable design element in crystal engineering (Thalladi *et al.*, 1998). On the other hand very little is known about hydrogen bonds that involve fluorine. Hydrogen bonds of the C-H...X-C type has been increasingly implicated in the stabilization of crystal structures. The C-H group is known to be a hydrogen bond donor, and C-H...O, C-H...N and C-H...Cl hydrogen bonds have been used in crystal engineering. This raises the question to the existence and nature of the C-H...F-C hydrogen bonds.

Thalladi was investigating crystal structures of fluorobenzenes. All of those crystal structures involve C-H...F-C hydrogen bonds of approximately 2.4 Å. To clear up the nature of those interactions the structures of fluoro benzenes were compared to structures of: pyridinium fluoride (Boenigk & Mootz, 1998), pyridine-N-oxide (Ulku *et al.*, 1971) and benzonitrile (Fauvet *et al.*, 1978). Those structures are stabilized with C-H...F, C-H...O- and C-H...N-interactions. However, there are similarities in between them and crystal structures of fluoro benzenes (Figure 3.2).

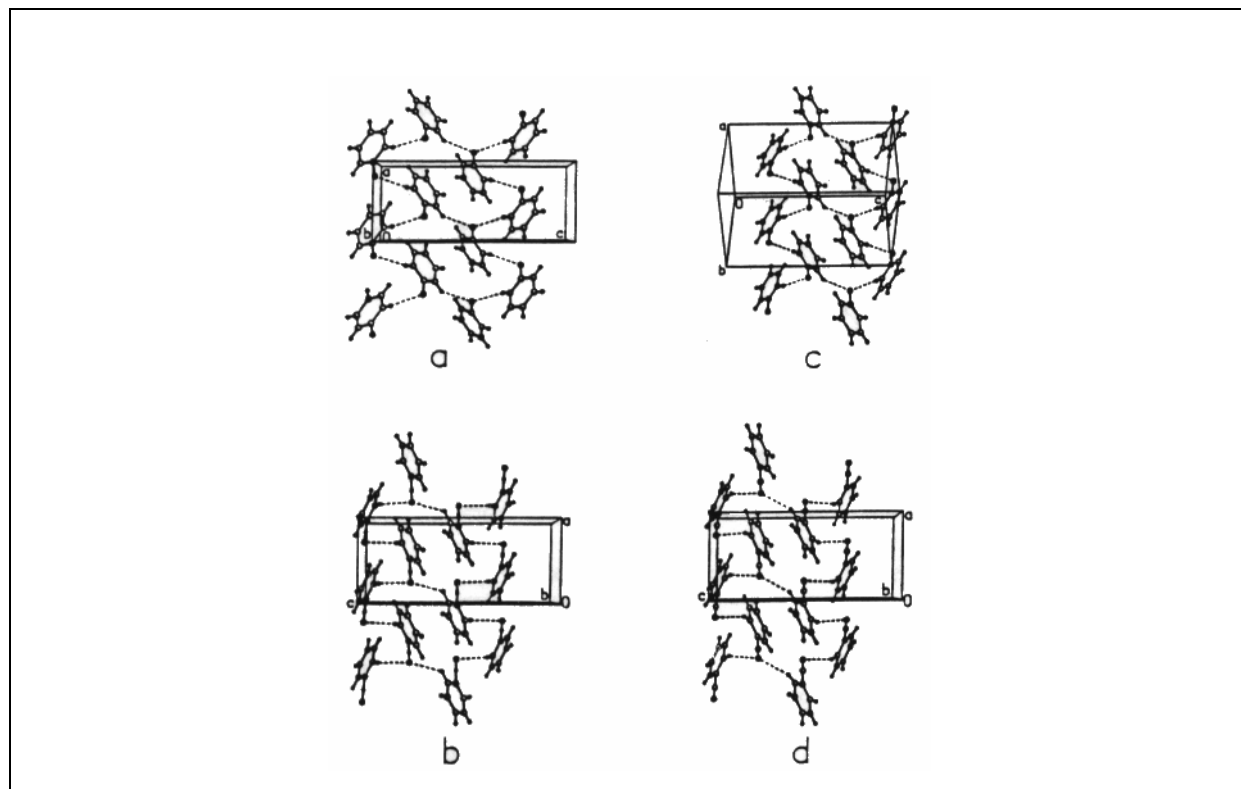
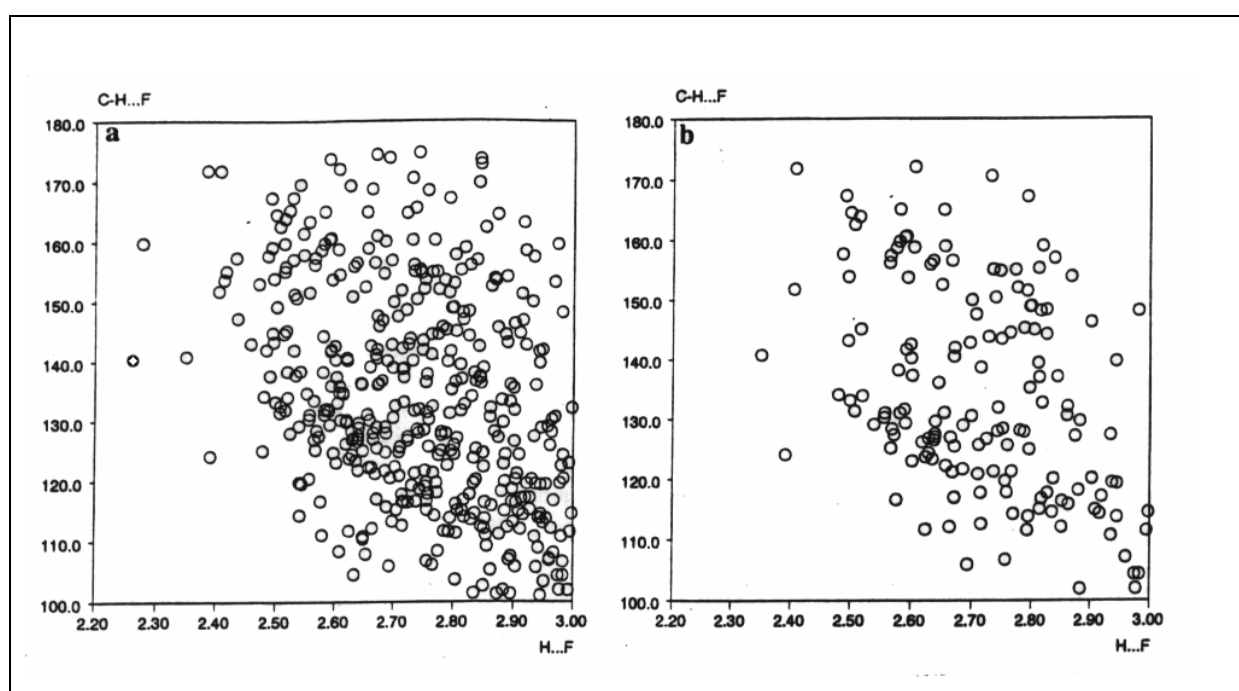


Figure 3.2. Crystal structures of: a) fluoro benzene, b) pyridinium fluoride, c) pyridine-N-oxide and d) benzonitrile (Thalladi *et al.*, 1998)

The structural similarity at this very fine level, that is, at the level of individual interactions, between fluoro benzenes on the one hand and other mentioned structures on the other, indicates that the nature and character of the structure-determining intermolecular interactions in these four structures are identical. Therefore, it has been shown that C-H...F interactions can be as important as C-H...O and C-H...N hydrogen bonds in stabilizing specific crystal structures. Fluorine would form rather C-H...F-C interactions than F...F contacts, whereas the heavier halogens seem to prefer the formation of halogen halogen interactions. In *Figure 3.3*, scatter plots of H...F distances versus C-H...F angles for C-H...F interactions are shown and there can be seen differences in distances when the C atom is  $sp$  or  $sp^2$  hybridised.



*Figure 3.3. a) C-H...F-C distances (433 examples); b) C ( $sp^2$ )-H...F-C ( $sp^2$ ) distances (155 examples (Thalladi et al., 1998)*

Crystal structures of fluorobenzenes show that only when carbon acidity is enhanced and only in absence of competing acceptors the hydrogen bonding accepting ability of organic fluorine revealed (Desiraju, 2002).

Very recently by Lancaster and co workers were reported intra- and inter-molecular C-H...F-C and N-H...F-C hydrogen bonds in secondary amine adducts of  $B(C_6F_5)_3$  with H...F distance of 2.10 Å. Evidence that the N-H...F-C interactions exist in solution is provided by  $^{19}F$  NMR spectroscopy. The large C-H...F angle of  $151^\circ$  and the short F...H distance places it within the shortest C-H...F-C hydrogen bonds (Mountford et al., 2003).

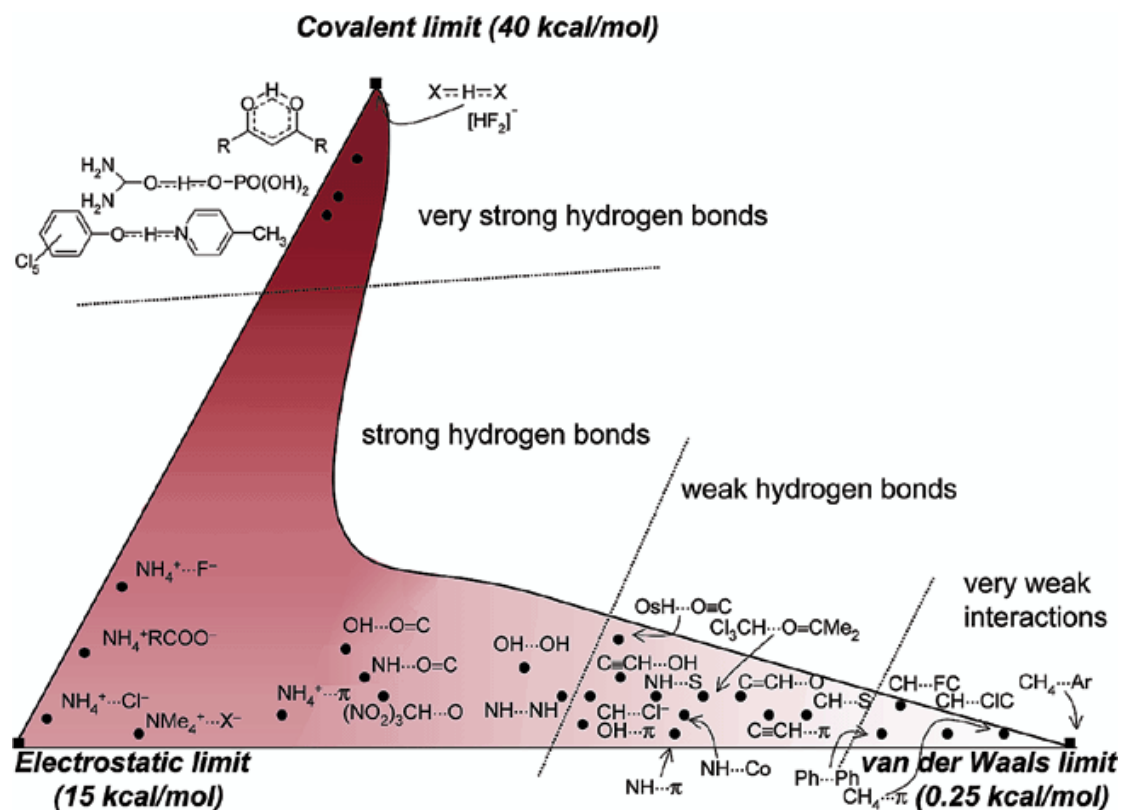
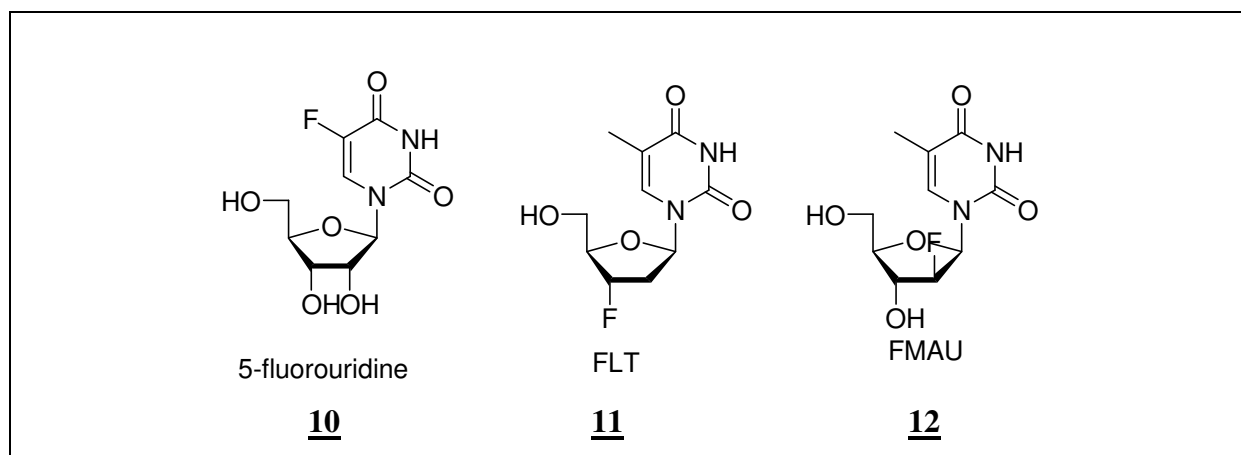


Figure 3.4. The hydrogen bridge. The composite nature of the interaction is highlighted by the three extreme situations of widely differing energies. The sketch is not strictly quantitative but the colouring attempts to provide a visual scale of energies. This figure serves as a rough guide to the balance of electrostatics, van der Waals nature, and covalency in any X-H...A interaction. For the weak interactions, the covalent character is very small and may be interpreted as charge transfer. A van der Waals interaction is considered to have dispersive and repulsive components. (Desiraju, 2002)

### 3.2 Fluorine in Nucleic Acids

Fluorine substituted analogues of nucleic acids are known for antiviral and antitumor activity. 5-Fluorouridine **10**, FLT **11** (3'-fluoro-2',3'-dideoxythymidine) (Etzold *et al.*, 1971) and FMAU **12** (2'-fluoro-5-methyl-1- $\beta$ -arabinofuranosyluracil) (Watanabe *et al.*, 1979) compounds with potential antiviral activity, are shown in *figure 3.5*. There are a lot of substances at a time that are under investigation for their biochemical activity.



*Figure 3.5. Fluorinated Nucleic Acids with potential antiviral activity*

Fluorine substitution is not generally detrimental for binding, however the high electronegativity of fluorine can have dramatic mechanistic consequences, which can lead to mechanistic deviations and enzyme inhibition. (O'Hagan *et al.*, 1997).

Significant role in bioactivity of those compounds plays fluorine because of its high electronegativity and polarity (Bergstrom & Swartling, 1988). Fluorine is also a mimic for hydrogen and also is in the pool of hydrogen bond acceptors (Pankiewitch, 2000).

In the next parts some different fluoro modifications of nucleic acids will be shown. Basically there are three different kinds: fluorine on the sugar moiety, on phosphate or on the base of the nucleoside.

### 3.2.1 Fluoro Modifications on Sugar Moiety

Fluoro atoms on the ribose of nucleosides can be seen on the C atom from C 2' to C 5'. The most of the known compounds have F on the C 2' atom but also not rare are the nucleosides, which have F on C 3' or C 5' carbon. On the other hand the nucleic acids analogues with fluorine on C 4' atom are very rare.

#### 3.2.1.1 C 2'- Fluoro Nucleosides

There are two main scientific reasons why C 2' fluoro analogue are interesting. One is their significant biological activity and the other that the fluorine takes the role of the 2' OH group in nucleic acids.

The effect of the fluorine atom on the conformation of ribose is intensively under investigation since this is very important as for binding of oligonucleotides to enzymes as for activity. Roentgen structure analysis shows that there are two main conformations of the ribose. They are: C 2'-*endo* form in B-DNA and C 3'-*endo* form in A-DNA. NMR investigations have shown that the conformation is more dependant on electronegativity of the substituent than on its size or ability to build hydrogen bonds ( Ikehara, 1984; Uesugi *et al.*, 1983; Cheng *et al.*, 1983). As example we can take 2'-fluoro-deoxyadenosine which has 67% in C3'-*endo* conformation where 2'-iodine-2'-deoxyadenosine and 2'-deoxy adenosine have only 19% and 7% C 3'-*endo* conformation. ( Uesugi *et al.*, 1979)

The synthesis of 2' –fluoronucleosides can be done in three different ways:

- Direct fluorination of the protected nucleosides
- Fluorination of the protected sugar, and than nucleoside synthesis
- The synthesis of the fluorinated sugar from the beginning compound containing fluorine, and than nucleoside synthesis

The mostly used method today is fluorination of protected nucleosides. The often used reagents for fluorination are: hydro fluoride (HF) and its complexes (f.e. HF\*pyridine), potassium fluoride (KF), potassium hydrogen difluoride (KHF<sub>2</sub>), diethylaminosulphur trifluoride (DAST) and tris-(dimethylamino)-sulphur-(trimethylsilyl)-difluoride (TASF).

The most common nucleosides that belong to this group are: 2'-fluoro-5-methyl-1-β-D-arabinofuranosylcytosine **13** (FIAC) and 2'-fluoro-5-iodine-1-β-D-arabinofuranosyluracil **14** (FIAU) (*Figure 3.6*). They are active and selective inhibitors for herpes simplex virus type I

and type II etc. (Watanabe *et al.*, 1983; Watanabe *et al.*, 1984). Their triphosphates are incorporated in virus DNA with viral polymerases. (Harada *et al.*, 1987).

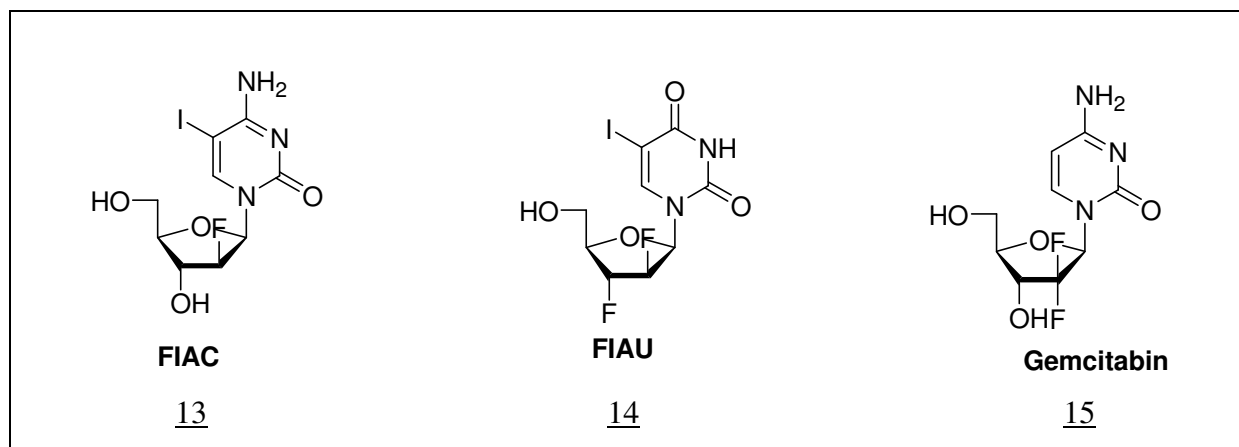


Figure 3.6. Antiviral 2'-fluoro nucleosides

There are also fluorinated nucleosides with two fluorines on the C-2' atom. Good known is 2'-deoxy-2',2'-difluoroguanosine **15** (Gemcitabin) (Figure 3.5.). The hydrochloride of the gemcitabin is used as a medicine in a lot of countries under the name Gezar. Gemcitabin shows a complicated mechanism of inhibiting DNA and also RNA synthesis through inhibition of ribonucleotide reductase (Schmid *et al.*, 2005). Gandhi showed that 2'-deoxy-2',2'-difluoroguanosine is similar to gemcitabin (Gandhi *et al.*, 1995).

### 3.2.1.2 C3'-Fluoro Nucleosides

The 3'-fluoro substitution of the ribose has almost the same effect as the 2'-fluoro substitution. NMR investigations show, that 2'-fluoro-2-deoxyuridine is 78 % in C 2'-*endo* conformation where 3'-fluoro-2',3'-dideoxyuridine adopts with 88% C 3'-*endo* conformation (Joecks *et al.*, 1983). The commonly known representative of this group is 3'-fluoro-2',3'-dideoxythymidine **11** (FLT, Figure 3.1.).

In 1988 it was discovered that FLT has a strong activity against HIV. After investigation it was shown that the activity of FLT is greater than that of the AZT ( Balzarini *et al.*, 1988.). Unfortunately, it has also higher cytotoxicity.

3'-Fluoronucleosides are active as 5'-triphosphates as strong inhibitors of DNA polymerases, for example the ones from *Micrococcus luteus*, *Streptomyces hygroscopicus* (Waehnert&Langen, 1979) or E.coli DNA polymerase I (Chidgeavadze *et al.*, 1985).

### 3.2.1.3 C4'-Fluoro Nucleosides

Antibiotic nucleocidine **16** (figure 3.7.), from the group of C4'-fluoronucleosides, exists as a natural compound. Nucleocidine was isolated in 1957 and synthesised in 1976 by Moffat for the first time (Jenkins *et al.*, 1976).

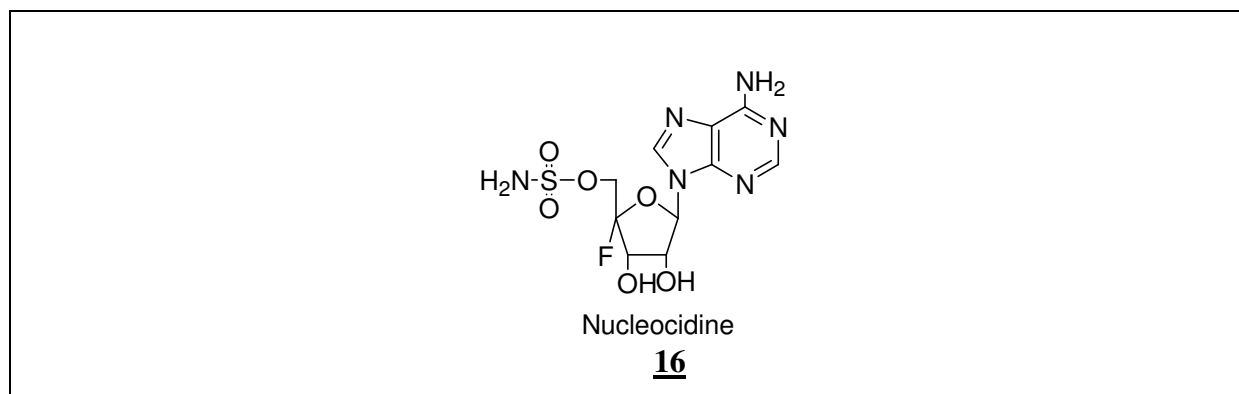


Figure 3.7. Antibiotic with C 4'-fluoro atom

The compounds that belong to this group don't have only instead of hydrogen or hydroxyl group a fluoro atom in C4' position to differ from C2' and C3' fluorinated nucleosides, but also other functional groups. By Nucleocidine that is a sulphonamide group.

### 3.2.1.4 C5'-Fluoro Nucleosides

The last group containing fluorine on the sugar moiety is the group of C5'-fluoronucleosides. Different 5'-fluoronucleosides were synthesised to observe their activity. The synthesis of those nucleosides starts with glycosilation of 1-O-acetyl-2,3-di-O-benzoyl-5-deoxy-5-fluoro- $\alpha,\beta$ -D-ribofuranose and nucleobase. The direct fluorination of C5' is also possible.

Synthetic improvement was to exchange the 5'-hydroxyl group with a CF<sub>2</sub>-group for the synthesis of difluoromethylene phosphonate nucleotide **17** (Figure 3.8.). With introduction of difluoromethylene group into the nucleoside we get -CH<sub>2</sub>-CF<sub>2</sub>-P- bond, which is a good mimic for natural -CH<sub>2</sub>-O-P-. This exchange should mean that the CF<sub>2</sub>-P bond cannot be hydrolysed under physiological conditions. Those molecules are under investigation (Harada *et al.*, 1987).



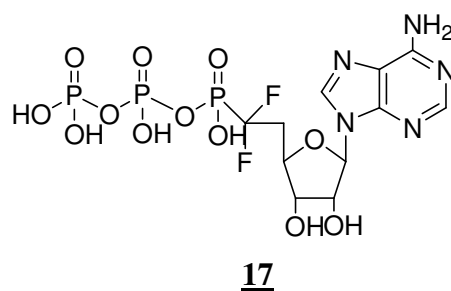


Figure 3.8. 5'-Deoxy-5'-difluoromethyl-adenosine-triphosphate **17**

### 3.2.2 Fluoro Modification on Phosphate Group

There are two possibilities to modify phosphate group of a nucleoside with fluorine. When we exchange one hydroxyl group of the phosphate with fluorine we become fluorophosphonate. When we exchange hydroxyl group with  $\text{CF}_2$  or CHF group we get fluoro alkyl phosphonate.

#### 3.2.2.1 Fluoro Phosphonates

Fluoro phosphonate analogues of nucleosides were synthesised to investigate the role of the phosphate group in enzyme studies. When a hydroxyl group of one phosphate is exchanged with fluorine than the nucleotide has only one negative charge. Than there is a possibility to investigate the influence of charges on enzyme-substrate bond. The other phosphonate modifications (methyl phosphonates) are not recommended for this because the introduction of methyl group makes the molecule bigger and the steric factor is than also important. Because of the high electronegativity, fluorine has also another important influences on the phosphate group. The  $\text{pK}_a$  becomes smaller with fluorination. As a consequence of this for example  $\text{Mg}^{2+}$  ions bind stronger to phosphate group ( Vogel&Bridger, 1982).

##### 3.2.2.1.1 Fluoro Alkyl Phosphonates

Phosphate esters and phosphate anhydrides belong to important groups in living organisms. Transfer and exchange of phosphate groups are essential biochemical reactions. In those molecules methylene or fluoromethylene groups exchange hydrogen atoms. It was shown that the  $\text{CH}_2$  group is the best isosteric exchange of a hydrogen atom in phosphonates. Blackburn

has shown that fluoro alkyl phosphonates are better analogues than methylene phosphonates (Blackburn, 1981).

The synthesis of fluoromethylene-modified triphosphates **18** (Figure 3.9) is performed over pyrophosphate.

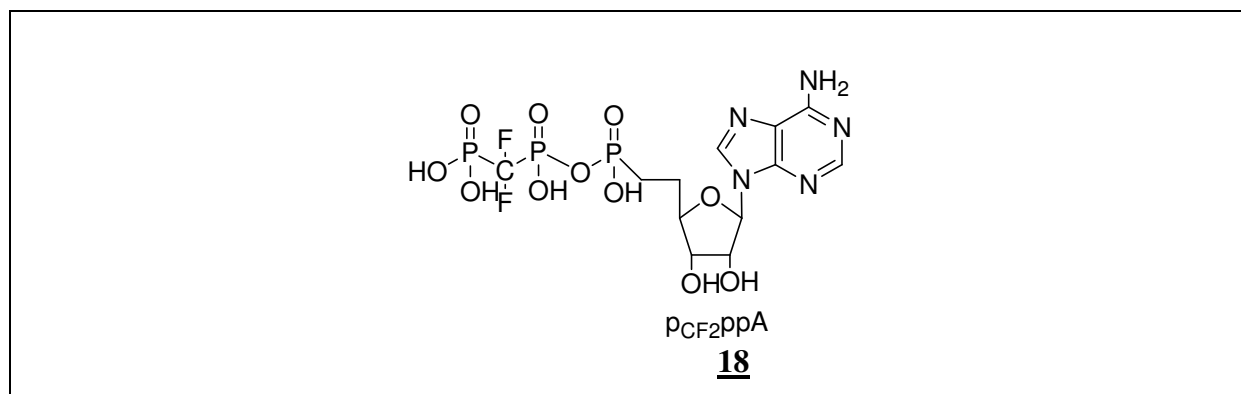


Figure 3.9. Difluoro methylene adenosine-triphosphate **18**

The investigations of  $\beta$ ,  $\gamma$ -difluoromethylene-triphosphates have shown that those compounds have biological activity as the  $\beta$ , $\gamma$ -methylene-triphosphates but smaller than natural phosphates. Experiments with pCF<sub>2</sub>ppA **18** (Figure 3.9.) have shown that pCF<sub>2</sub>ppA is a good inhibitor for some enzymes and a good substrate for the other ones (Blackburn *et al.*, 1986).

### 3.2.3 Fluoro Modifications on Nucleobases

There are three main groups of fluoro-modified nucleobases. They are modified pyrimidines, purines and fluoro modified nucleobases similar to either purine or pyrimidine nucleobases.

#### 3.2.3.1 Fluoro Modified Pyrimidines

Fluoro substituted pyrimidine nucleosides, as for example 5-fluoro-2'-deoxy uridine (FdU) **19** or trifluoromethyl-2'-deoxy uridine **20** ( $F_3CdU$ ) are used as therapeutic compounds (*Figure 3.10*).

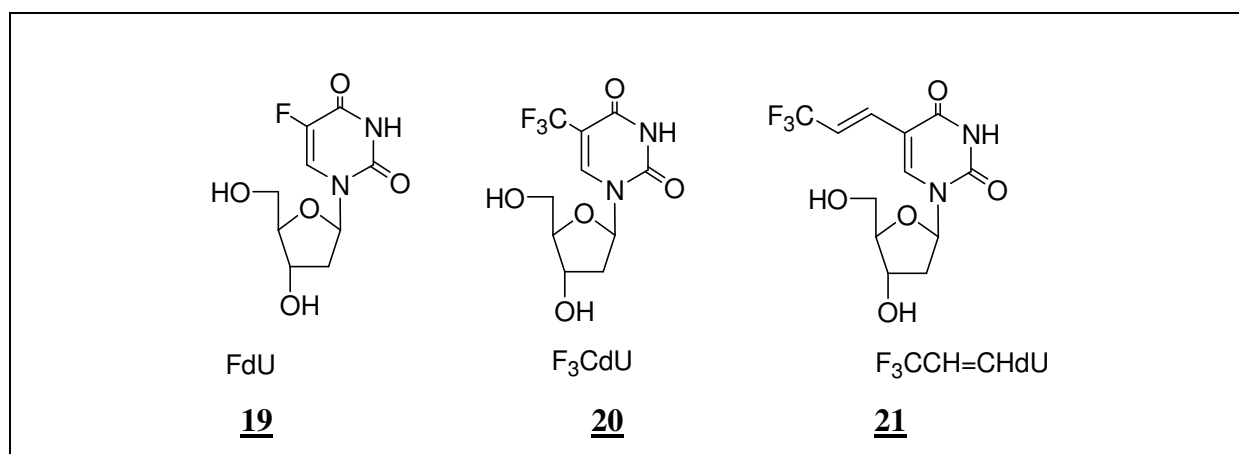


*Figure 3.10. Fluoro modified pyrimidine nucleobases*

New studies consider more pharmacokinetics and the influence of fluorine on the structure and activity and less synthetic methods.

Fluorination on the 5 position is done in reaction with  $F_2$  or  $CF_3OF$  in water as a solvent. The fluorination is not simple. The  $CF_3$  group is introduced in the reaction of trifluoromethyl iodide with 5-iodo-pyrimidine in the presence of copper (Kobayashi *et al.*, 1977), and for longer alkyl chains another strategy is developed. Primary, position 5 is methylated and brominated (Matulic-Adamic *et al.*, 1986). Then fluoro compounds are added with different alkyl chains.

In the last years compounds with longer alkyl chains are becoming the main point of interest since those compounds have a great activity against herpes viruses. It is important that those compounds are more selective against herpes viruses than classical antiherpes medicines (for example FdU **19** and  $F_3CdU$  **20**, *Figure 3.10.*) (Bergstrom *et al.*, 1984). However, it is also shown that not only fluoro substitution is responsible for selectivity (some compounds are

inactive even if they contain fluorine). The introduction of single fluorine in an alkyl side chain on nucleobasis is basically improving antiviral activity.

### 3.2.3.2 Fluoro Modified Purines

Only a few of the fluorinated purines are published. 2-Fluoro adenosine (2FA) **22** and 6-fluoro nebularine **23** (6FN) are shown in the *figure 3.11*. They were synthesised in the late 60s (Hashzimie *et al.*, 1968).

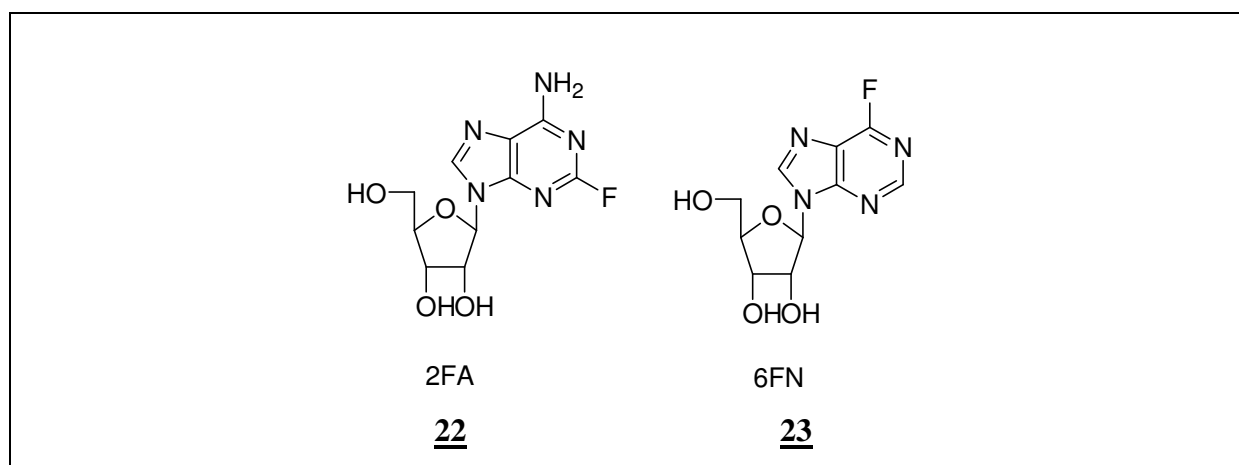


*Figure 3.11. Fluoro modified purines*

There are no significant results for antiviral effects of those compounds.

### 3.2.3.3 Fluoro Modified Nucleobase Analogues

Two groups of fluoro modified nucleobase analogues exist. The first ones are developed with chemical reactions on natural nucleobases and the second are similar in some points to nucleobases.

In *Figure 3.12*, we can see two examples of nucleobases that are synthesised from natural nucleobases. Molecule **24** (*Figure 3.12*) is synthesised from uridine and chloro fluoro carben in the presence of silver. However, this molecule shows no significant biological activity (Thieller *et al.*, 1977). If 4-O-trimethylsilyl thymidine reacts with difluorocarbene the compound **25** (*Figure 3.12*) is obtained (Pein & Cech, 1985). That one shows antiviral activity against herpes simplex viruses of type 1.

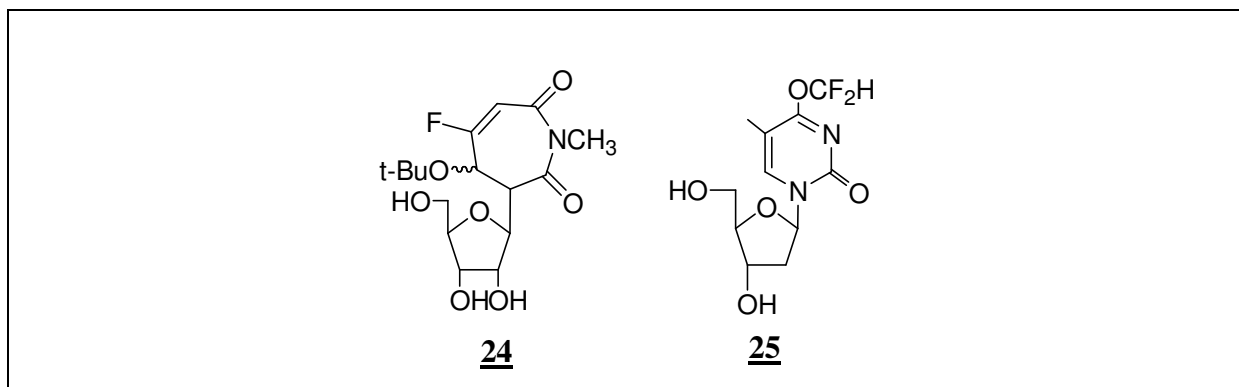


Figure 3.12. Fluoro modified bases synthesised from natural nucleobases

In *Figure 3.13*, there are three different modified nucleobases that are synthesised. The fluoropyridine **26** is tested in mice against leukaemia (McNamara&Cook, 1987). Compound **27** was synthesised by Matulic-Adamic and Beigelman and incorporated in ribozyme to investigate their influence on enzyme activity ( Matulic-Adamic&Beigelman, 1997).

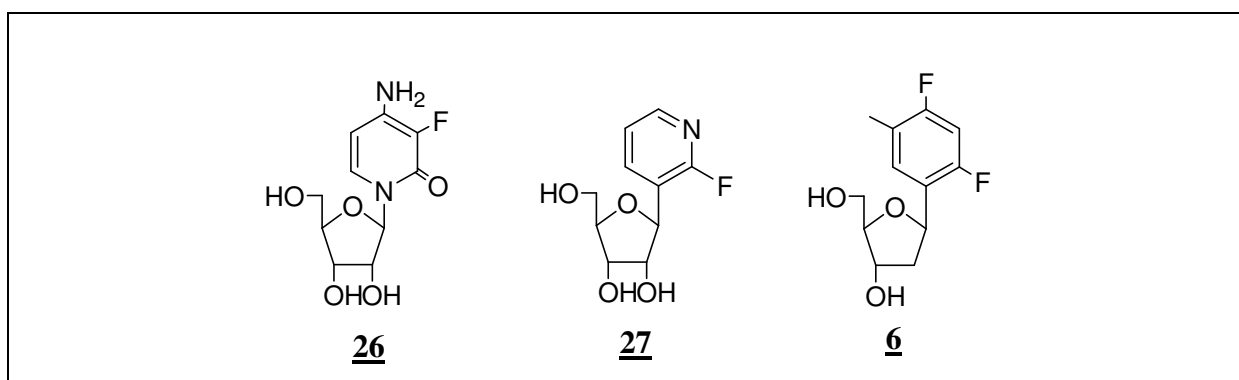


Figure 3.13. Fluoro modified nucleobases

The difluorotoluene **6** (*Figure 3.13*) was synthesised as an isostere of thymine (Schweitzer&Kool, 1994). It was used for investigation of hydrogen bonds in the DNA double helix. Because of its similarity to thymine it is mostly incorporated against adenine (Moran *et al.*, 1997).

## 4 Overview

Chemically modified bases are frequently used to stabilize nucleic acids, to study the driving forces for nucleic acid structure formation and to tune DNA and RNA hybridization conditions. In particular, fluorobenzene and fluorobenzimidazole base analogues can act as universal bases able to pair with any natural base and to stabilize RNA duplex formation.

The noncovalent interactions affecting the thermodynamic stability of natural and modified RNA have been topics of broad interest in recent years. The effects of sterics, stacking, hydrogen bonding, and minor-groove solvation have been considered as contributing factors. Probably the dominant stabilizing factors in helical RNA are base stacking and hydrogen bonding. In order to probe the physical factors that contribute to the stability of this stacking in water, we wanted to measure melting data of short RNA oligomers, both naturally and nonnaturally substituted. Understanding these issues could allow better design of modified RNAs, but relatively little experimental information is available on such electrostatic factors. Quadrupolar interactions have also been documented in specialized cases; for example, benzene is capable of electrostatic interactions with molecules containing a positive charge, as demonstrated by well-documented cation- $\pi$  interactions, even in aqueous systems. By contrast, perfluorobenzene, with its opposite quadrupolar sign, can stack well (in low polarity environments) with electron-rich aromatic rings.

We now describe a series of fluorinated aromatic nucleoside analogues having a wide range of dipole and quadrupole moments and also substituents of different size and positions (*figure 4.1.*). We wanted to study the stacking thermodynamics of these compounds in short synthetic RNA duplexes, with all four neighbouring nucleobases. We also wanted to show examine how different substitution pattern influences stability of modified oligonucleotides.

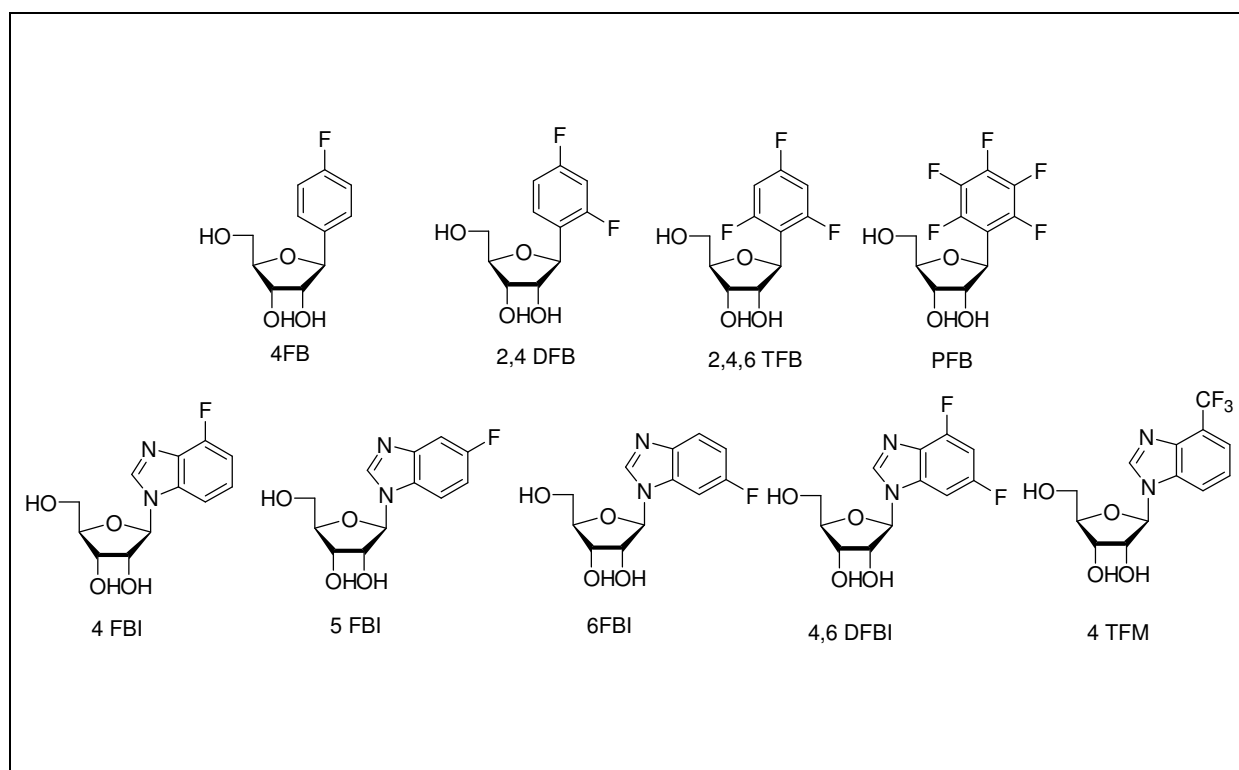


Figure 4.1. Synthesized fluoro-modified bases

2,4 DFB and 4,6 DFBI are isosters for natural bases and have been shown (Parsch & Engels, 1999; Parsch & Engels, 2000) to be universal. In addition we decided to synthesise different benzene modifications with different number (1, 2, 3 and 5) and positions of fluorine atoms. We wanted to synthesise a series of fluorobenzimidazole modifications and also a modification with trifluoromethyl group (4 TFM). All of those modifications we synthesised aimed at a better understanding of base stacking and H bonding ability of ‘organic’ fluorine, which although discussed at great length, is complex and remains considerably less well understood. We wanted to underline favourable characteristics for better base stacking abilities in one series of compounds specially substituents and their arrangement. Fluorine substitution may be critical for stacking and RNA pairing pattern as fluorine affects dipole moment and polarizability of nucleobases. We also wanted to examine self-pairing of those bases.

Interesting issue in these studies would have been also the possibility of forming C-F...H-C bridges in double helix of RNA. Interactions were ‘‘organic fluorine’’ accepts hydrogen bonds are less examined and up to discussions in scientific committee.

Therefore we wanted to crystallise our nucleosides and allow crystal engineering to help us to predict behaviour and pairing pattern of those bases in RNA.

For the oligonucleotides studies we wanted to use UV and CD –spectroscopy in defined 12mer sequences shown in figure 4.2. Those sequences were used in our group by Parsch (Parsch & Engels, 1999) and would give us the ability to compare our results.

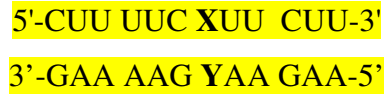


*Figure 4.2. The sequences for spectroscopic investigation of RNA ( X and Y are for modifications)*

The results shed light on the importance and origins of electrostatic interactions in DNA base stacking, and reveal some previously unrecognised structural and electrostatic effects that will be useful in future molecular designs.





## 5 Chemical Synthesis

### 5.1 Modified Nucleobases Containing Fluorine

We wanted to synthesise different modified nucleobases containing fluorine that don't build hydrogen bonds with adenosine, guanidine, cytidine or uridine. Therefore we wanted to choose molecules that don't contain N or O. Some of the molecules that we synthesised are isosteric to natural nucleobases (*Figure 5.1*).

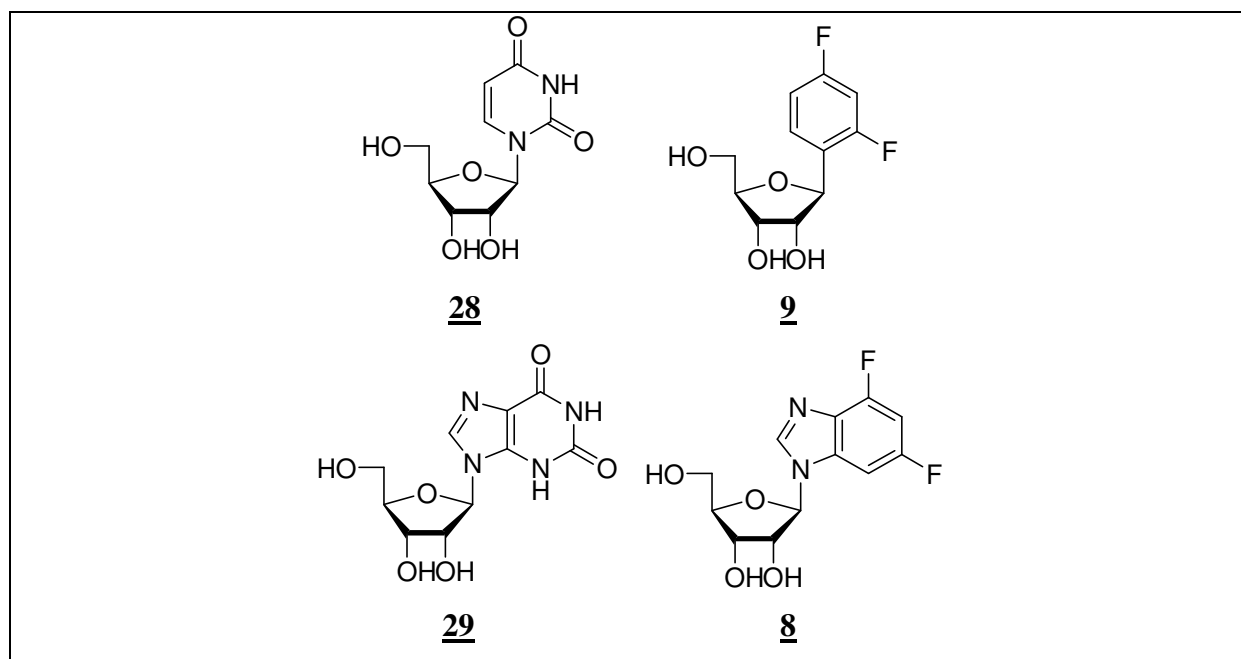
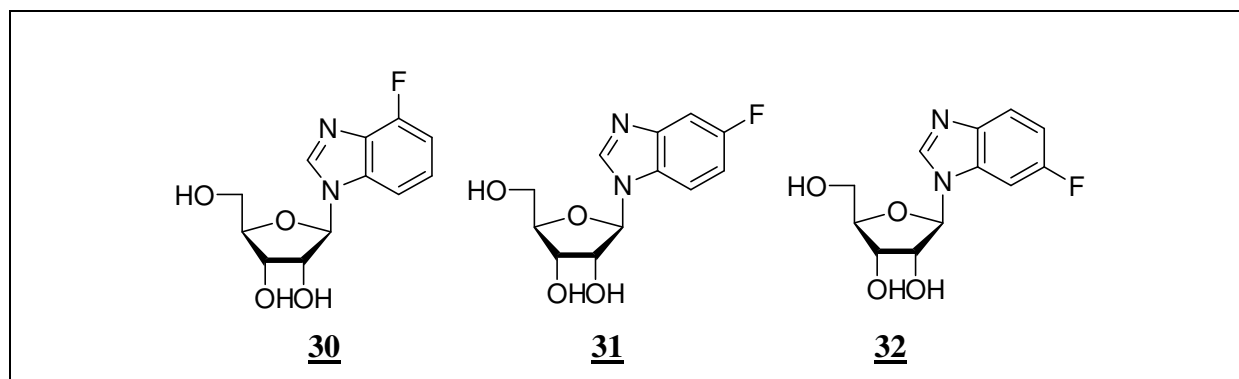


Figure 5.1. Comparison of natural nucleosides with fluoro-modified ones

1'-deoxy-1'-(2,4-difluorophenyl)-β-D-ribofuranose **9** is isosteric to natural uridine **28** and 1'-deoxy-1'-(4,6-difluoro-1-N-benzimidazolyl)-β-D-ribofuranose **8** is isosteric to natural xantine **29**. Both of them have no nitrogen or oxygen atoms that could be involved in hydrogen bonding. As it is already mentioned fluorine is a very good mimic for hydrogen and oxygen

atom (Parsch&Engels, 2000). Additionally we synthesised also different fluoro modified benzimidazoles to observe how the position of the fluorine atom influences oligonucleotide characteristics (*Figure 5.2.*).



*Figure 5.2. Synthesised fluoro- modified benzimidazoles*

We also decided to synthesise a series of the trifluoromethyl-modified benzimidazoles (*Figure 5.3.*). As F is a good isosteric exchange for hydrogen and the methyl group we decided to try how the exchange of hydrogen atoms with fluorines in the methyl group will influence the stability of oligonucleotides.

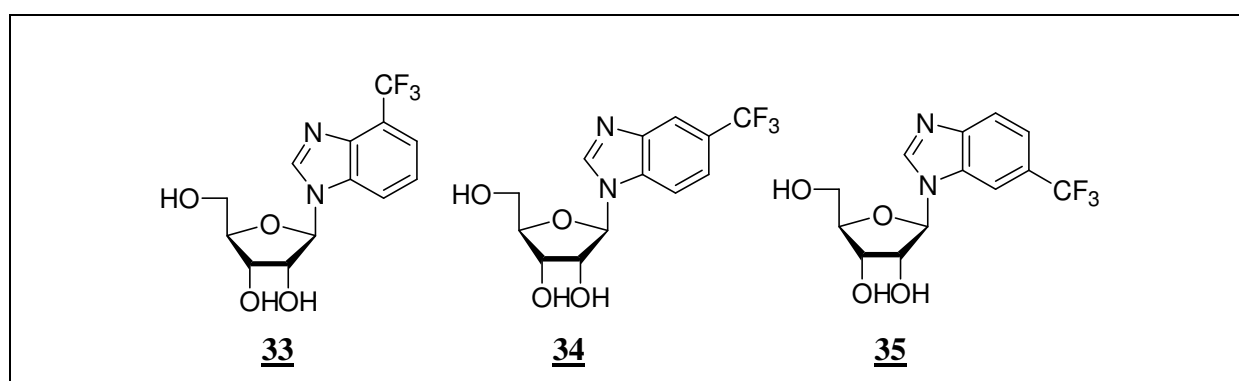


*Figure 5.3. Synthesised trifluoromethyl- modified nucleosides*

We were aware that the size of trifluoromethyl group resembles more to isopropyl group than to that of methyl group, but if the size wouldn't have been deciding point than we would have improved F as acceptor for C-F...H-C hydrogen bonding.

We also synthesised a series of fluoro-modified benzenes, which differ not only in number of fluorine atoms but also in their positions (*Figure 5.4.*).

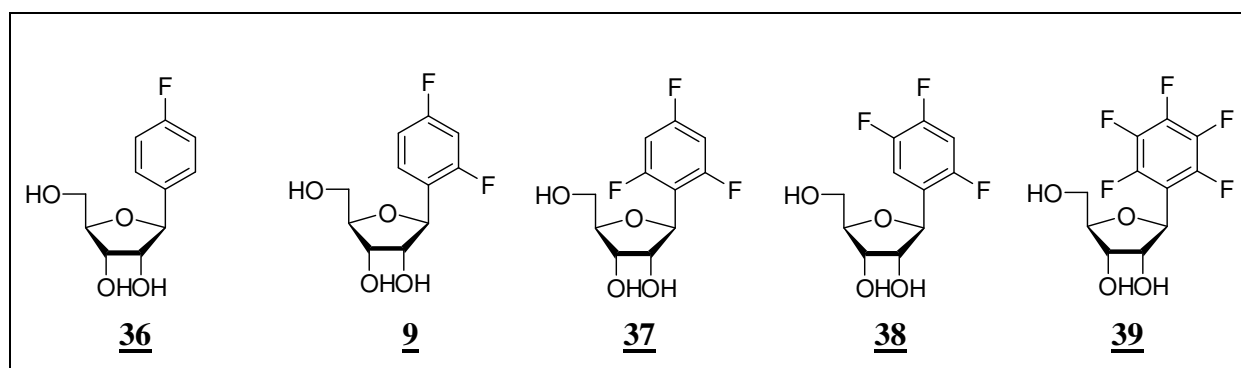


*Figure 5.4. Fluoro modified benzenes*

With an increasing number of fluorine atoms we are increasing the acidity of the hydrogen atoms that could be involved in hydrogen bonding. We also have one modification that has no hydrogen atoms on the base to observe differences in thermodynamical measurements. The mono-fluoro-benzene modifications with all possible different positions for fluorine were synthesised previously in our group and the ones with best characteristics were resynthesised. These were incorporated in oligonucleotides to measure thermodynamical parameters when paired with different new modifications (Parsch&Engels, 2000).

In order to observe the influence of fluorine and trifluoromethyl group on stability of RNA duplexes we synthesized 1'-deoxy-1'-benzimidazolyl- $\beta$ -D-ribofuranose **40** and 1'-deoxy-1'-phenyl-  $\beta$ -D-ribofuranose **41**. We also synthesised an abasic site **42** (1-deoxy-D-ribofuranose) for use in the investigating of stacking effects (*Figure 5.5.*).

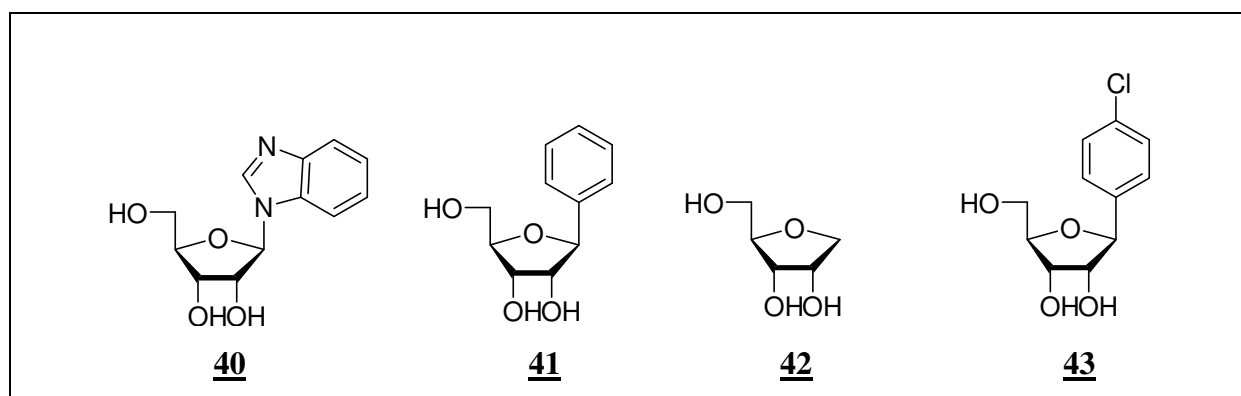


*Figure 5.5. Modified nucleobases without fluorine*

We also synthesised one modification containing a chlorine atom (1'-deoxy-1'-(4-chlorophenyl)-  $\beta$ -D-ribofuranose **43**) to compare the crystal structures of fluoro benzenes with this structure (*Figure 5.5.*).

## 5.2 Fluorobenzimidazoles

The synthesis of **54** 4-fluorobenzimidazole and **51** 4,6-difluorobenzimidazole starts from the corresponding fluoro acetanilides. The first reaction to be done is the nitration of the fluoro acetanilides. Because of different reactivity, different reaction conditions were required. The more active 2,4-difluoro acetanilide was treated with a mixture of 65% nitric acid, sulphuric acid and acetic acid over 90 min. at 40-50°C (Finger *et al.*, 1951) (Figure 5.7). To nitrate the less reactive 4-fluoro acetanilide we used 100% nitric acid, acetic acid anhydride and acetic acid. The reaction time is than 48 h and is significantly longer than for difluoroacetanilide **47**. From difluoroacetanilide **47** we got 96% yield of 2,4-difluoro-6-nitro-acetanilide **48**. The nitration of 2-fluoro acetanilide gave two products (isomers): 2-fluoro-4-nitro acetanilide **45** and 2-fluoro-6-nitro-acetanilide **46** in ratio 1:1 (Figure 5.6). Separation of those two isomers was done on the basis of different solubility in Witt-Utermann solution (Witt & Utermann, 1906; Wepster & Verkade, 1949). This solution consists of 50 % water solution of potassium hydroxide, 4 parts of water and one part of ethanol. Adding ice-cold Witt-Utermann solution separated the isomer mixture. The solution dissolves *o*-nitro acetanilide but not *p*-nitro acetanilide. After filtration we separated the isomers and obtain pure 2-fluoro-6-nitro acetanilide **46**.

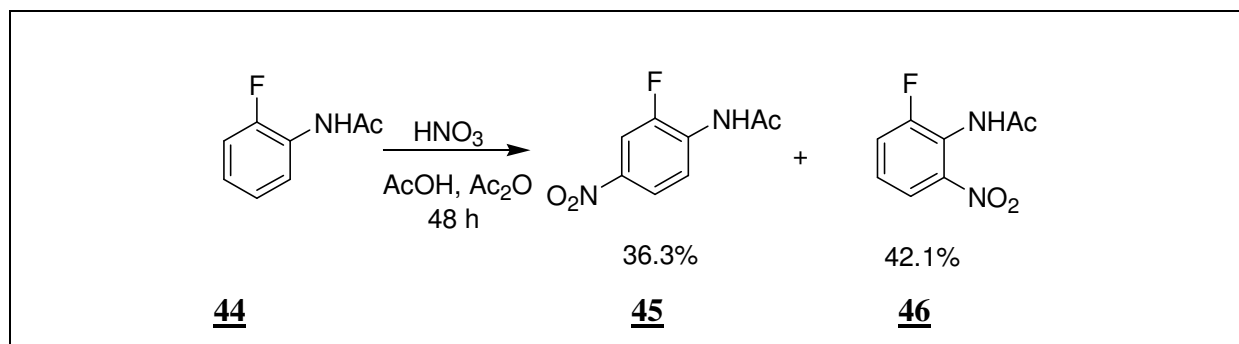


Figure 5.6. Nitration of 2-fluoro-6-nitro acetanilide

Deprotection of the amino group was done for both compounds with acid. 2-Fluoro-6-nitro acetanilide **46** reacted over 3 h with 3 M HCl and gave 2-fluoro-6-nitro aniline **52** in a yield of 89%. Because of the higher solubility of 2,4-difluoro-6-nitro aniline **49** in water the corresponding acetanilide **48** was deprotected in conc. sulphuric acid. To precipitate **49** the reaction mixture was poured into ice water, filtered on vacuum and washed with cold water.

**49** is quite soluble in water and this procedure makes the yield of this reaction lower (Finger *et al.*, 1951).

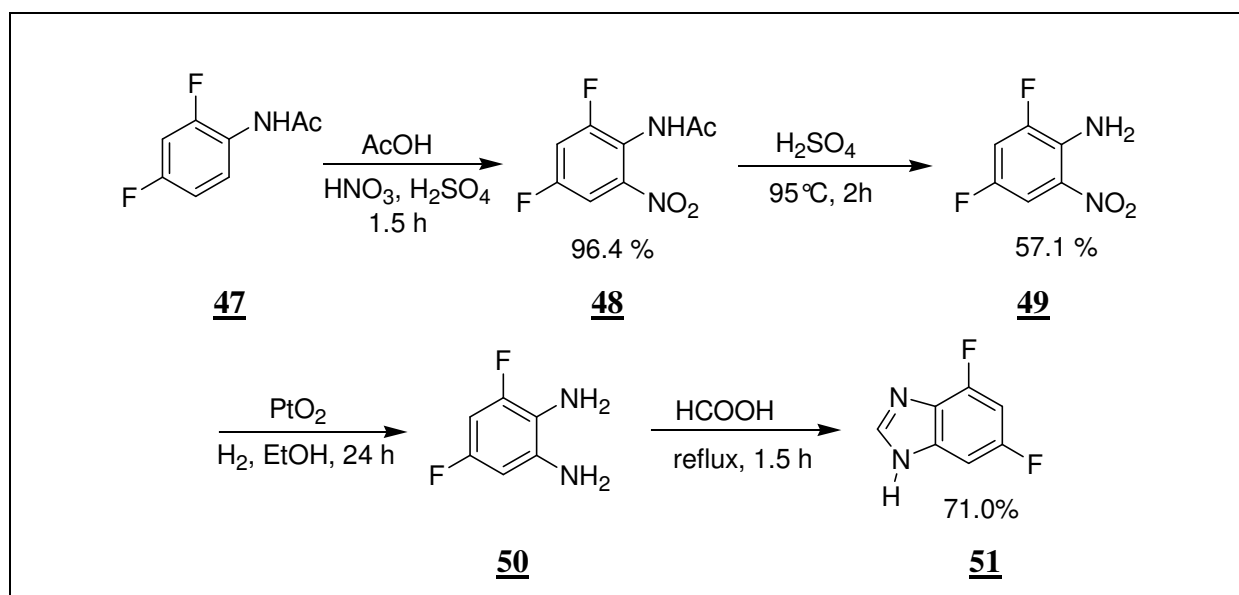


Figure 5.7. Schema for the synthesis of 4,6-difluorobenzimidazole

The reduction of the nitro group to an amino group was done by a metal catalysed reaction under hydrogen (Montgomery & Hewson, 1965). Therefore the nitro compounds were dissolved in ethanol, catalyst was added and the reaction performed in hydrogen atmosphere. The reaction was vigorously stirred to get the biggest possible contact surface of the catalyst. The reaction is accomplished when the solution is not yellow any more from nitro compound (TLC control). The reaction was also done using Pd as a catalyst, but there the reaction times vary greatly and in the experimental part is the experiment with highest yield. Times vary from 2 to 36 h. After the reaction was complete the catalyst was filtered over celite and the left reaction mixture was evaporated to dryness. Both phenylene diamines **50** and **53** were immediately used for the next reaction.

The synthesis of the corresponding imidazoles were done from **50** and **53** refluxing them with formic acid for 1,5 h and 2 h respectively (Kirk & Cohen, 1969). Then the formic acid was evaporated and the product was dried. Both 4-fluoro benzimidazole **54** and 4,6-difluoro benzimidazole **51** were obtained as colourless solids. Since on TLC and in NMR only small impurities could be seen and the solubility of both compounds in eluents was very small we used both compounds without further purifications for the next reactions ( Parsch, Doctor thesis, 2001).

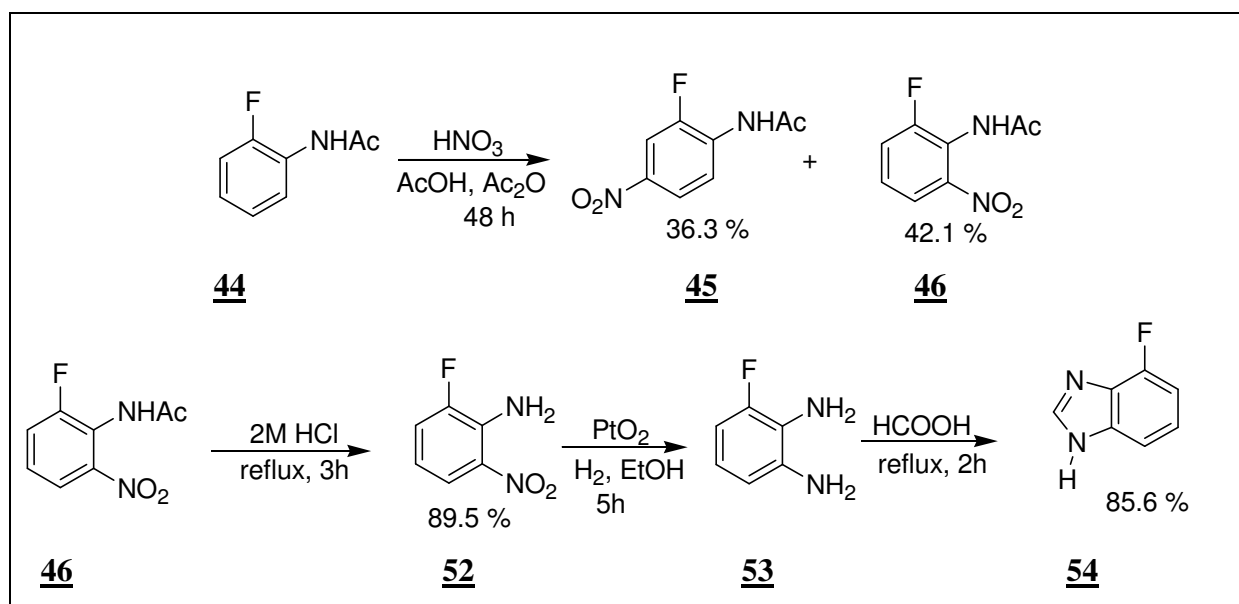


Figure 5.8. Scheme for synthesis of 4-fluoro benzimidazole

Synthesis of 4-trifluoromethyl imidazole **61** was done as shown in figure 5.9. and the procedures are rather similar to those already described.

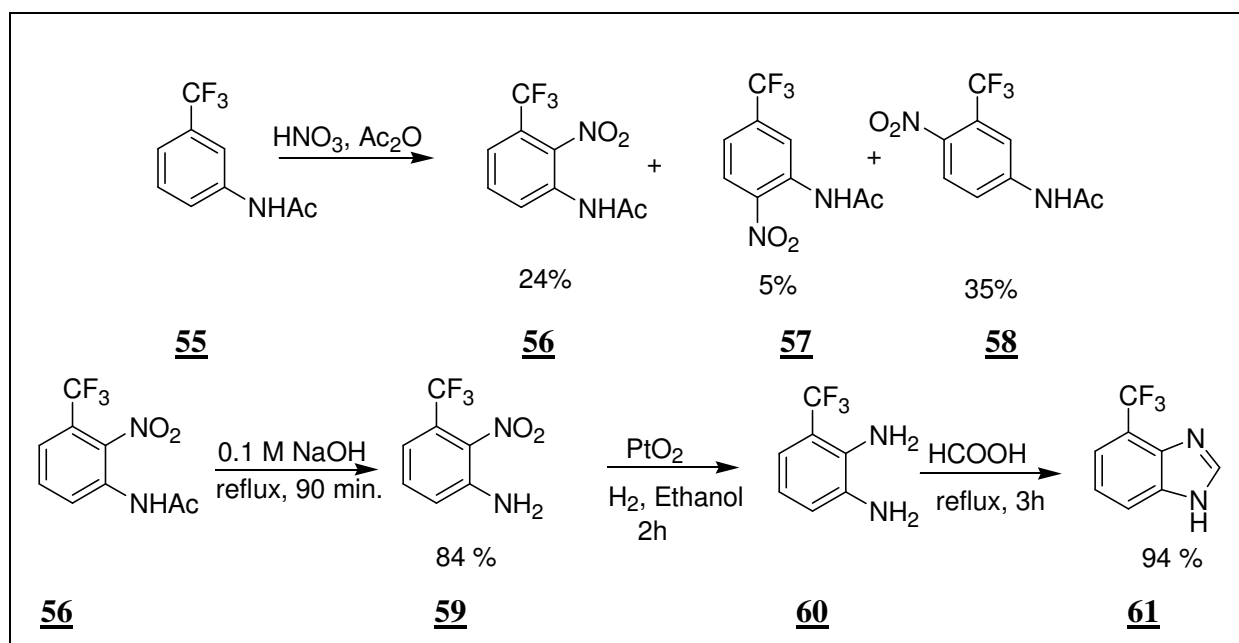


Figure 5.9. Scheme of the synthesis of 4-trifluoromethyl benzimidazole

3-trifluoromethyl acetamide **55** was nitrated with a mixture of equal parts of 100% nitric acid and acetic anhydride over 4h. 2-nitro-3-trifluoro acetanilide **56** precipitates as white solid and two other isomers **57** and **58** stay in solution. They were extracted with methylene chloride, separated by FC and characterized. The white precipitate **56** was filtered, dried and used for the next reaction (Pouterman & Girardet, 1947).

5-trifluoromethylbenzimidazole **63** was synthesized from 4-trifluoromethyl phenylene diamine **62** after refluxing with formic acid for 3h with a yield of 90 %. The product was purified by FC. The same procedure was used for the synthesis of 5-fluorobenzimidazole **65** (Figure 5.10).

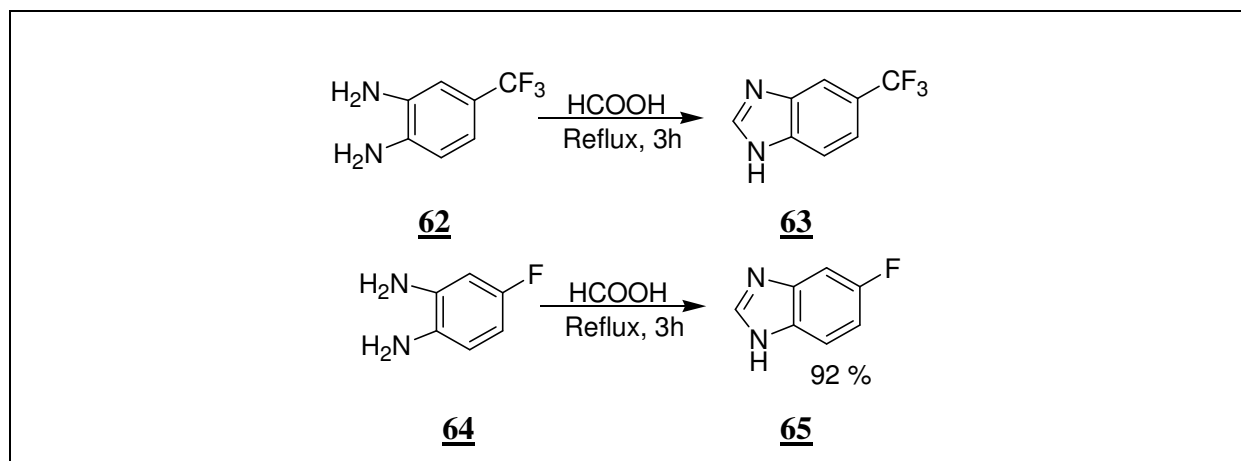


Figure 5.10. Synthesis of 5-trifluoromethylbenzimidazole **63** and 5-fluorobenzimidazole **65**

### 5.3 Benzimidazole, Fluoro-benzimidazole and Trifluoromethylbenzimidazole Nucleosides

#### 5.3.1 Glycosilation

The glycosilation of all benzimidazole nucleosides was done with 1,2,3,5-tetra-O-acetyl- $\beta$ -D-ribofuranose **69** after the procedure of Vorbrüggen (Vorbrüggen & Höfle, 1981). The mechanism of the reaction is given in Figure 5.11. using the example of 4-trifluoromethyl benzimidazole **61**. In this compound in solution the H atom is migrating from N1 to N3 and also the compound **66** exists. The equilibrium of this reaction is on the side of the N1 isomer. This equilibrium is influenced with the number and kind of substituents on the benzene aromatic ring. The Silyl-Hilbert-Johnson reaction begins with silylation of the N-H function with N,O-bis-(trimethylsilyl)-acetamide (BSA). Because of the existence of both isomers, N1 and N3, we get also two silylated products.



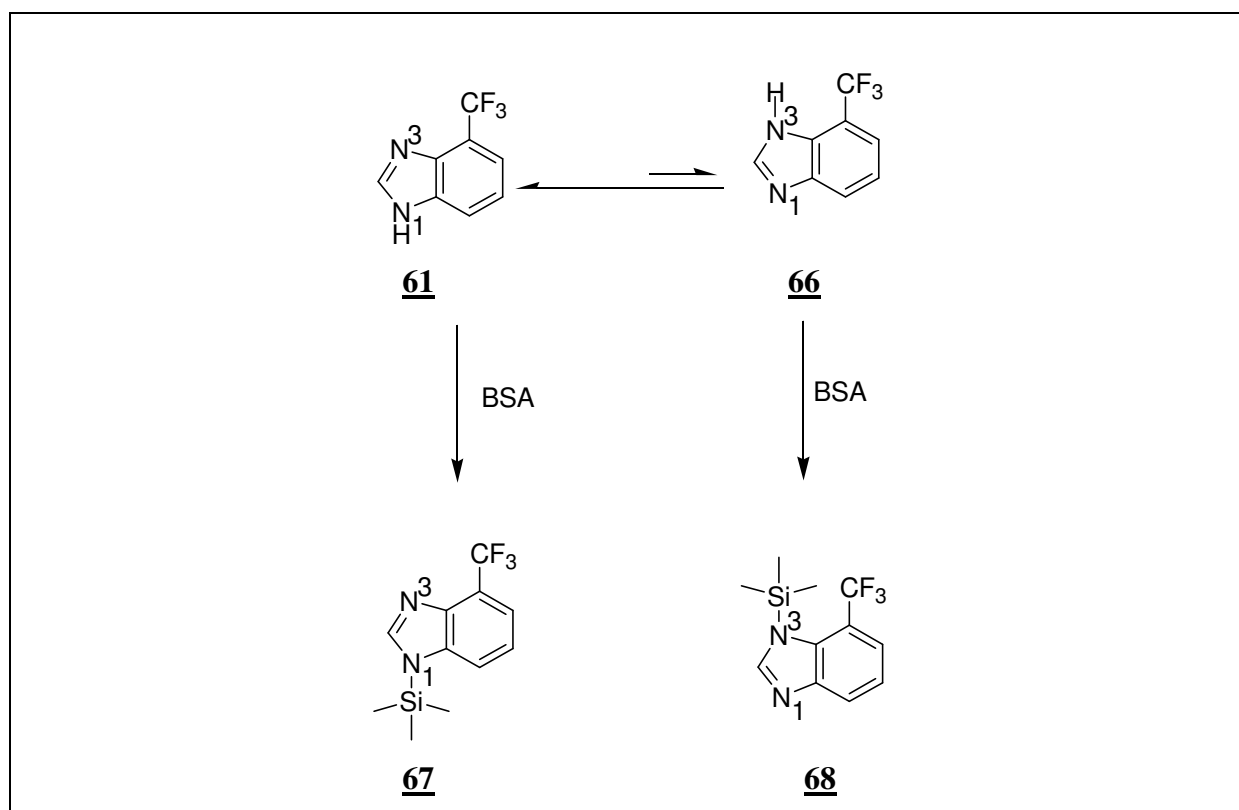


Figure 5.11. Possible silylations of 4-trifluoromethyl imidazole  
BSA=N,O-bis-(trimethylsilyl)-acetamide

In the mean time 1,2,3,5-tetra-O-acetyl  $\beta$ -D-ribofuranose **69** is set up with Lewis acid, trimethylsilyltrifluoromethane sulphonate (TMSOTf). Then the sugar builds a cation **70** through an intramolecular attack of the 2-acetyl group on C1 position and at the same time the acetyl group leaves (Figure 5.12). The C1-acetyl group leaves the reaction as trimethylsilylacetate ester. Therefore five membered ring, in  $\alpha$  position of the sugar ring, is formed. When the sugar cation is added to the silylated base solution, this nucleophile attacks the sugar-cation on C1. The attack can only be on the  $\beta$  side of the sugar ring. After the attack on the five membered ring, which is formed with an intramolecular reaction of the C2-acetyl group, the ring is again opened and a nucleobase is covalently bonded to the sugar ring.

The big advantage of this reaction is that only  $\beta$ -nucleoside can be formed. Because of the existence of two silylated isomers of nucleobase **67** and **68** we get two regioisomers anyway. The reaction of **67** with sugar-cation **70** gives the N1-isomer 2',3',5'-tri-O-acetyl-1'-deoxy-1'-(4-trifluoromethyl-1-N-benzimidazolyl)- $\beta$ -D-ribofuranose **71** and the reaction of **70** with **68** gives the N3 isomer 2',3',5'-tri-O-acetyl-1'-deoxy-1'-(4-trifluoromethyl-3-N-benzimidazolyl)- $\beta$ -D-ribofuranose **72**. The ratio of the obtained isomers is the same as the

ratio of 4-trifluoromethyl imidazole isomers **61** and **66** in solution. For 4-trifluoromethyl benzimidazole the ratio is 10:1.

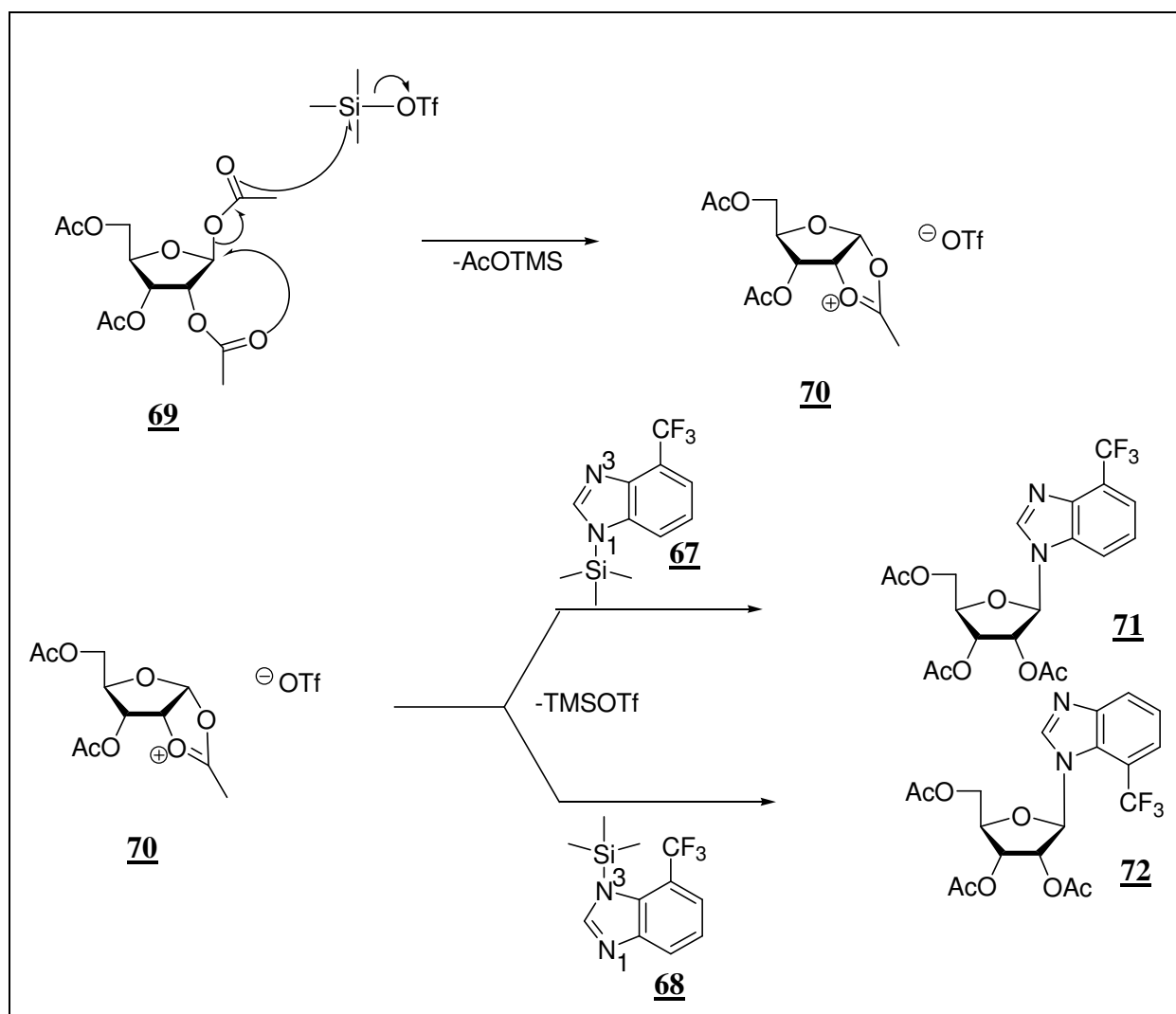


Figure 5.12. Glycosylation reaction

Under the reaction conditions only  $\beta$ -nucleosides can be formed, but there are N1 and N3 isomers to be separated and identified. Therefore we measured ROESY-NMR spectra. The difference in between those two isomers can be seen in *figure 5.13*. and for the N1 (a) isomer there is a ROE-signal in between the H7 proton of the base and the H1' proton of the sugar moiety. As expected (*figure 5.13,b*) for the N3 isomer there is no ROE-signal in between those two protons.

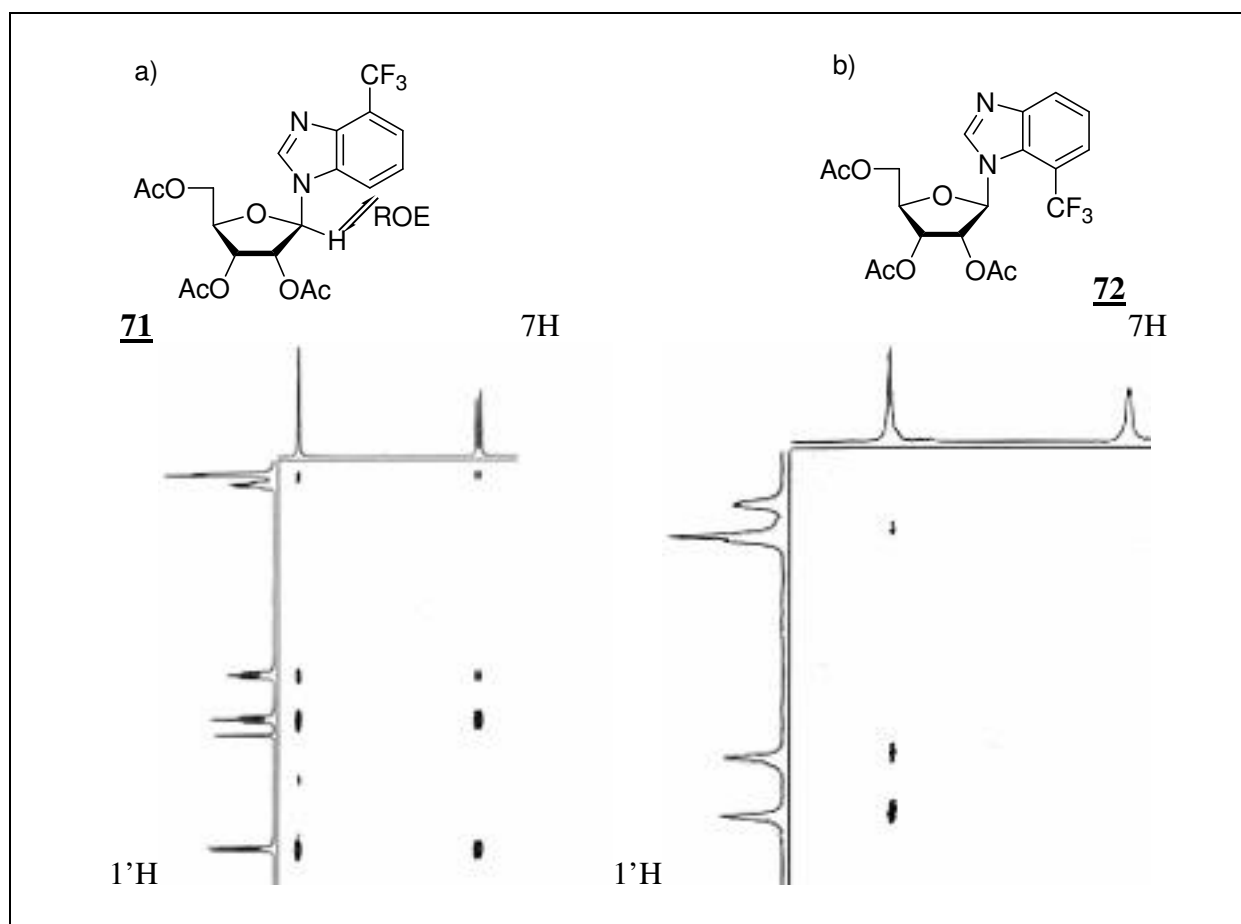


Figure 5.13. Part from 400MHz ROESY-NMR-spectra of 2',3',5'-tri-O-acetyl-1'-deoxy-1'-(4-trifluoromethyl-1-N-benzimidazolyl)- $\beta$ -D-ribofuranose **71** and 2',3',5'-tri-O-acetyl-1'-deoxy-1'-(4-trifluoromethyl-3-N-benzimidazolyl)- $\beta$ -D-ribofuranose **72**

While glycosylating benzimidazole with 1,2,3,5-tetra-O-acetyl- $\beta$ -D-ribofuranose **69** we did not become N1-N3 isomers, because those two positions do not differ. However, there is another side product of the silylated benzimidazole, that is the twice silylated product **75** (figure 5.14.). When we add this mixture to the Hilbert-Johnson-reaction and we add the sugar cation to silylated benzimidazole we get a mixture of wanted product 2',3',5'-tri-O-acetyl-1'-deoxy- $\beta$ -D-ribofuranose **77** and **76**, a side product with two sugar moieties and one benzimidazole.

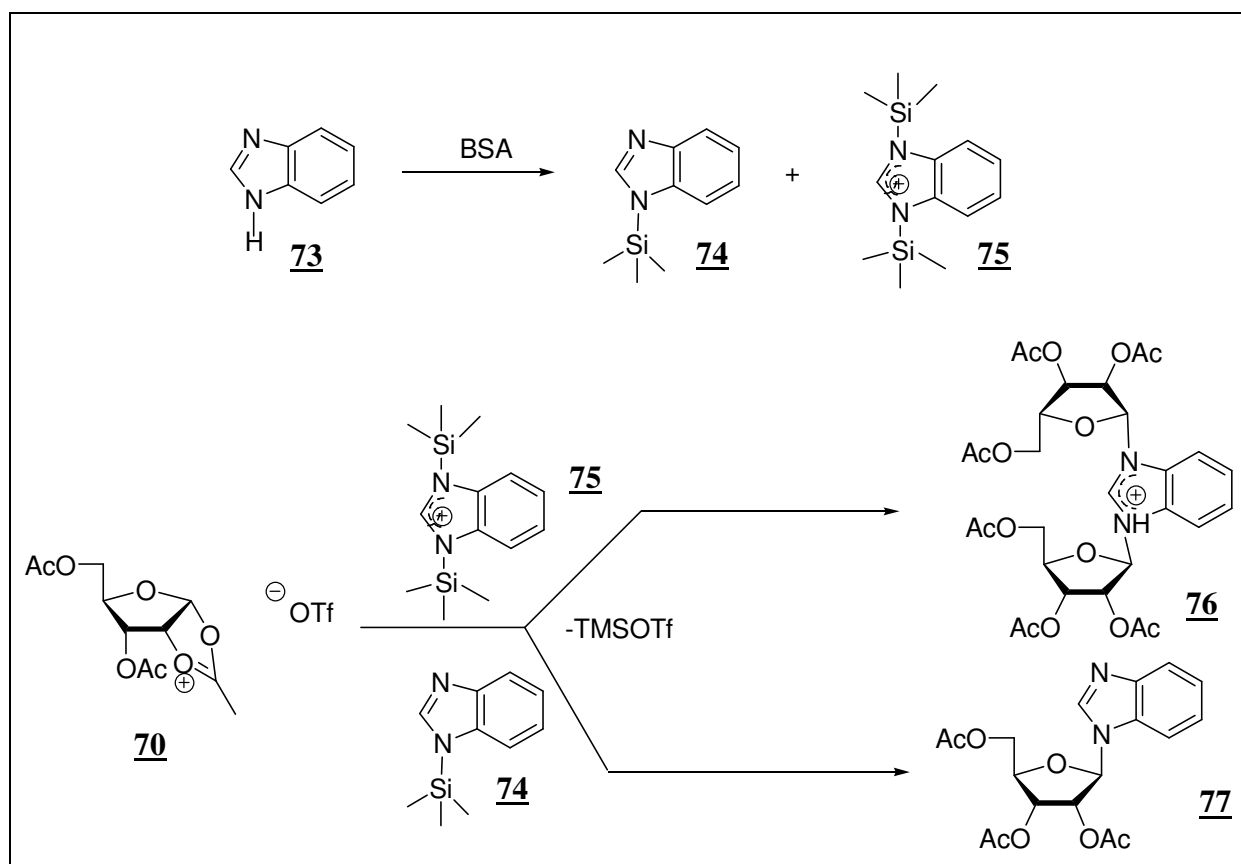


Figure 5.14. Glycosylation reaction of 1,2,3,5-tetra-O-acetyl-β-D-ribofuranose **69** with benzimidazole **73**

### 5.3.2 Deprotection

There are two common methods for the deprotection of acetylated nucleosides. The first one is using a methanolic ammonia solution (Nielson *et al.*, 1971) and the second one is with sodium methoxide in methanol (Wolfrom & McWain, 1965). We decided to use the second method because of shorter reaction times (instead of 20 h for the first method the reaction is finished after 90 minutes) and high yields. All yields are over 90 %.

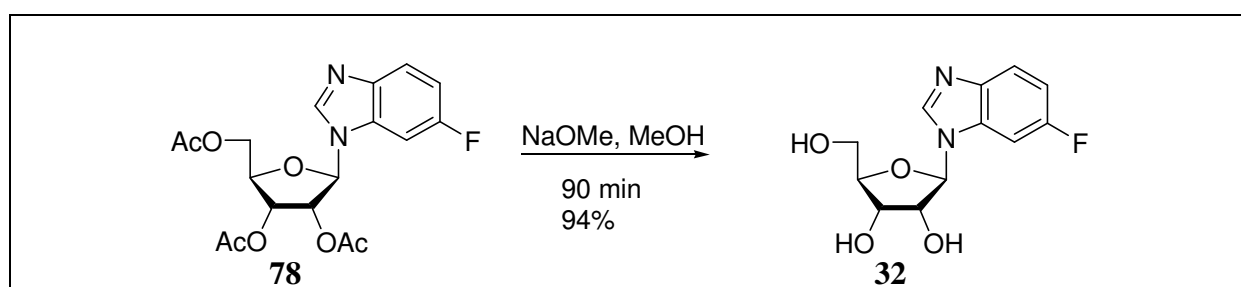


Figure 5.15. Deacetylation

## 5.4 C-Nucleosides

### 5.4.1 $\gamma$ -Lactone

For the synthesis of C-nucleosides we used the protected  $\gamma$ -Lactone **83**. However, the protecting groups on  $\gamma$ -lactone have to be stable under the conditions of glycosilation and dehydroxylation. The reaction conditions of the glycosilation are strong basic (n-BuLi or t-BuLi) where for dehydroxylation conditions are strong acidic ( $\text{BF}_3 \cdot \text{Et}_2\text{O}$ ). Furthermore that the protecting groups, have to be removed after the glycosilation to become unprotected nucleoside for further synthesis. Those were our reasons to choose benzyl groups for protection (Engels & Parsch, 2001). The synthetic pathway for the synthesis of  $\gamma$ -lactone is shown in *figure 5.16*.

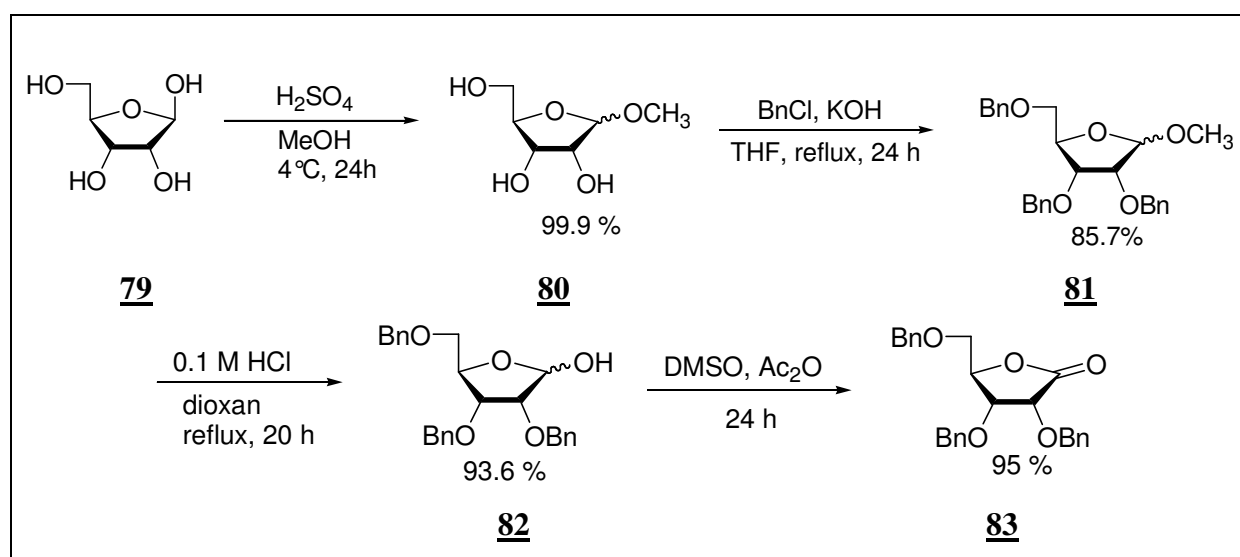


Figure 5.16 .  $\gamma$ -Lactone synthesis

The synthesis of  $\gamma$ -lactone begins with methylation of D-ribose **79** on the anomeric hydroxyl group. D-ribose is a natural product and cheap starting material for this reaction. Methylation of the anomeric hydroxyl group is done in methanol with a catalytical amount of sulphuric acid at  $4^\circ\text{C}$  (Heath *et al.*, 1983). The low reaction temperature is needed for the selectivity of this reaction. Sulphuric acid does not only catalyse the methylation but also the epimerisation of methyl-D-ribofuranose. During this reaction the furanose ring of ribose can be opened and closed again. The reaction lasts 24 hours to give a quantitative yield of methyl-D-ribofuranose **81**. The ratio of  $\beta$ - and  $\alpha$ - isomers is usually around 3:1. The epimers were not separated after

the reaction because they can be both used in further synthesis to give  $\gamma$ -lactone **83**. Benzylation of both epimers was done with benzyl chloride and potassium hydroxide in tetrahydrofurane (Barker & Fletcher, 1961). Potassium hydroxide was used as a powder for the reaction. We used a large excess of the benzyl chloride for this reaction. Wanted product, 1-methyl-2,3,5-tri-O-benzyl-ribofuranose **81**, was obtained in 85.7 % of yield after purification.

In the next step the anomeric hydroxyl group was again deprotected. Therefore, 1-methyl-2,3,5-tri-O-benzyl-ribofuranose **81** was dissolved in dioxane, 0.1M HCl was added and the mixture was refluxed. After 20 h we got our product, 2,3,5-tri-O-benzyl-ribofuranose **82**, with 93.6 % yield (Barker & Fletcher, 1961).

The last step in synthesis of  $\gamma$ -lactone was oxidation of both epimers (Timpe *et al.*, 1975). The oxidation was done with dimethyl sulphoxide (DMSO) and acetic acid anhydride. This oxidation is called Pfitzner-Moffatt-oxidation (Pfitzner & Moffatt, 1965), which was modified by Goldman (Albright & Goldman, 1967). The reaction was performed 24 hours at room temperature. After extraction of reaction mixture with methylene stirred and FC purification  $\gamma$ -lactone **83** was obtained in 95 % yield.

## 5.4.2 Benzene, Fluoro- and Chloro Benzene-Nucleosides

In this part we are going to describe the synthesis of seven different benzene and fluoro-benzene-nucleosides. Six of them were synthesised as phosphoramidites and used for RNA synthesis, and 1'-deoxy-1'-(4-chlorophenyl)- $\beta$ -D-ribofuranose **43** was only recrystallised and its structure is given in another chapter (chapter 6-Crystal structures).

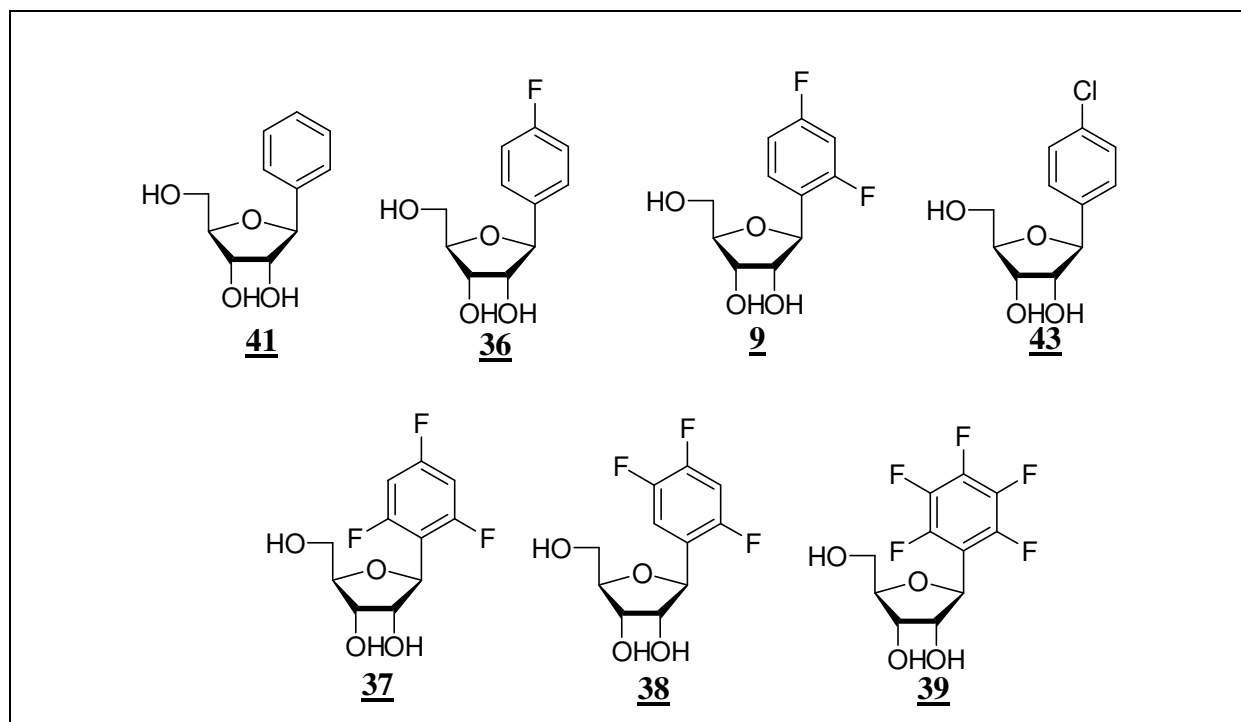
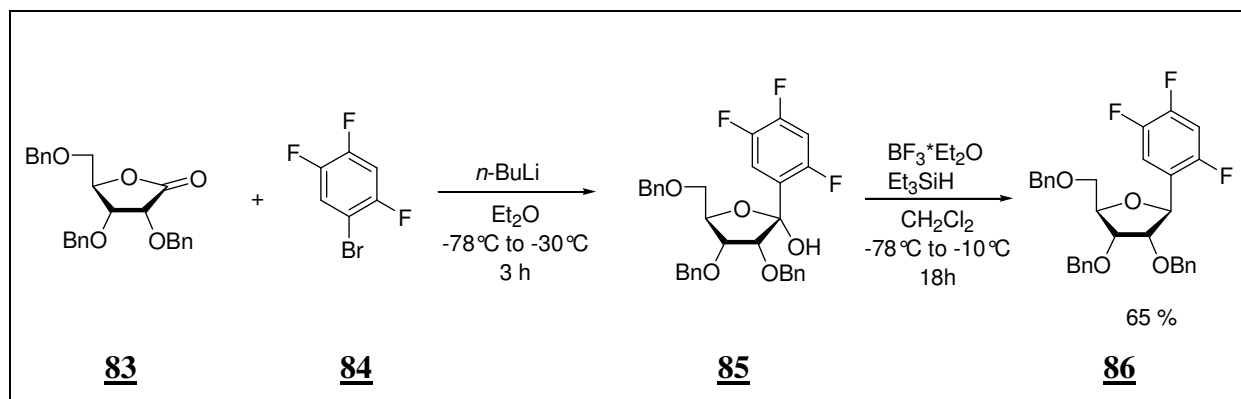


Figure 5.17. Synthesised C-nucleosides

### 5.4.2.1 C-Glycosilation and Dehydroxylation

The synthesis of all C-nucleosides has the same mechanism (Krohn *et al.*, 1992). As reagents we used bromo-fluoro-benzenes, bromo-benzene or fluoro-benzenes in the reaction with 2,3,5-tri-O-benzyl-ribo- $\gamma$ -lactone **83**. In *figure 5.18*, the synthesis of 2',3',5'-tri-O-benzyl-1'-deoxy-1'-(2,4,5-trifluoro phenyl)- $\beta$ -D-ribofuranose **86** is shown. For this reaction 2,4,5-trifluoro bromo benzene **84** was dissolved in diethyl ether and cooled to  $-78^{\circ}\text{C}$ , with acetone/liquid nitrogen mixture. Then n-BuLi in hexane was slowly added. While adding n-BuLi bromine on bromo-fluoro-benzene is being exchanged with Li. Afterwards  $\gamma$ -lactone **83** dissolved in diethyl ether is added. The bromine-lithium exchange allows nucleophilic attack of fluorobenzene on  $\gamma$ -lactone **83**. The nucleophilic attack is on the si-side of the lactone and

therefore we get fluoro-benzene only in  $\beta$ -position on the sugar (*figure 5.18.*). The obtained lactol **85** was immediately worked up and set up in the dehydroxylation reaction (Kraus *et al.*, 1988; Krohn *et al.*, 1992).



*Figure 5.18. C-glycosilation and dehydroxylation*

The dehydroxylation reaction is done with boron trifluoride-etherate and triethylsilane in methylene chloride at  $-78^{\circ}\text{C}$ . In this reaction boron trifluoride attacks the hydroxyl group of the lactol **85** and it cleaves from the molecule. The intermediate cation **87**, is stabilised with acid (Brückner *et al.*, 1988). Triethylsilane is a hydride donor in this reaction. The H atom attacks the *re*-side of the sugar, because of the anomeric effect, and leaves benzene in  $\beta$ -position. Even though transition cation is planar we become only  $\beta$ -nucleoside as a product (*figure 5.19*).

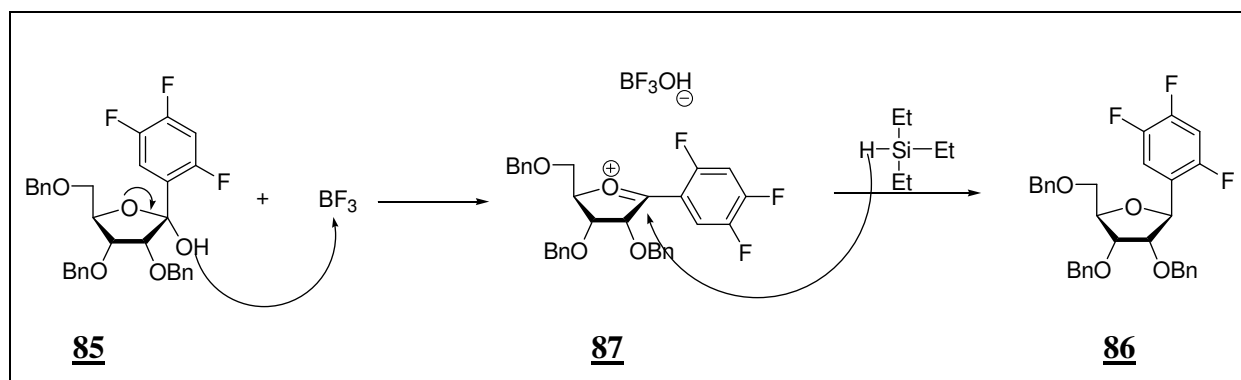


*Figure 5.19. Dehydroxylation with  $\text{BF}_3$*

The syntheses of the monofluoro benzene modification **36**, mono-chloro- **43** and benzene nucleoside **41** were done in tetrahydrofuran and all other syntheses were done in ether. The reason for that is that in tetrahydrofuran not only the bromine-lithium exchange can take



place but also the (acidic) hydrogen –lithium exchange (Coe et al., 1990; Bridges et.al, 1990; Schirley et al., 1968; Haidic et al.,1967). In ether as a solvent we became higher yields of the wanted products ( *Figure 5.20*).

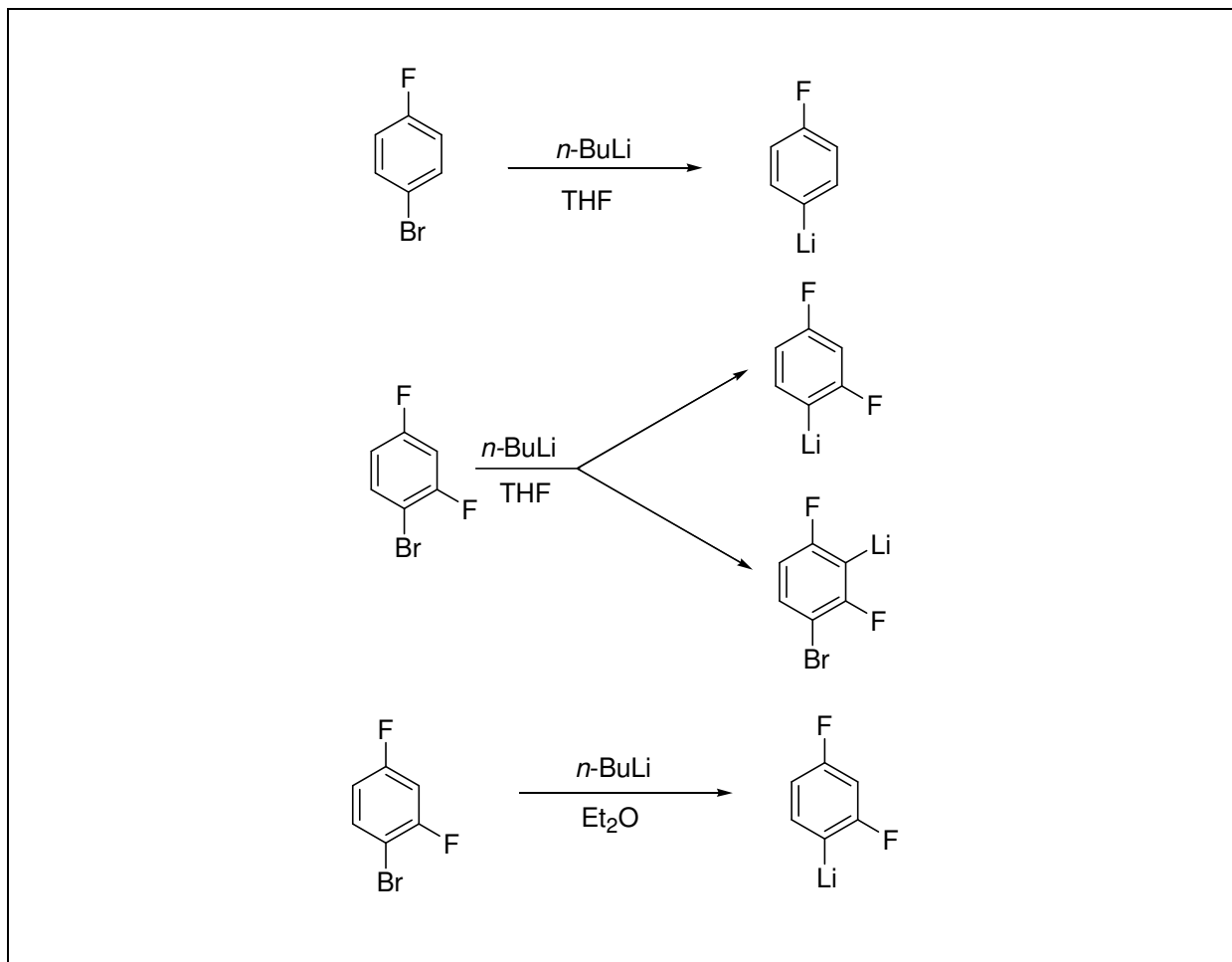


*Figure 5.20.: Influence of the solvent on the reaction of  $n\text{-BuLi}$  and fluoro benzenes*

Reactions of 2,3,5-trifluorobromobenzene with different solvents and lithiated bases gave very poor yields. Therefore we performed the reaction of 1,3,5-trifluorobenzene **88** with  $t\text{-BuLi}$  in  $n\text{-pentane}$ . In this reaction we obtained the wanted product in 55 % yield (*figure 5.21.*). The enhanced metalating abilities of  $t\text{-BuLi}$  vs.  $n\text{-BuLi}$  has been attributed to a greater tendency of the less stable  $t\text{-butyl}$  anion to donate an electron to an aromatic system and to give more stable  $t\text{-butyl}$  radical. It was shown that there is little steric requirement difference in metalation of aromatic systems with  $t\text{-BuLi}$  vs.  $n\text{-BuLi}$ . However the rate of alkylation is  $t\text{-butyl} > \text{sec-butyl} > n\text{-butyl}$ , but usually for alkylation products higher concentrations of alkyllithium compounds are required (Howells *et al.*, 1974; Adamson *et al.*, 1996). An overview over the glycosilation reactions is given in *figure 5.22*.

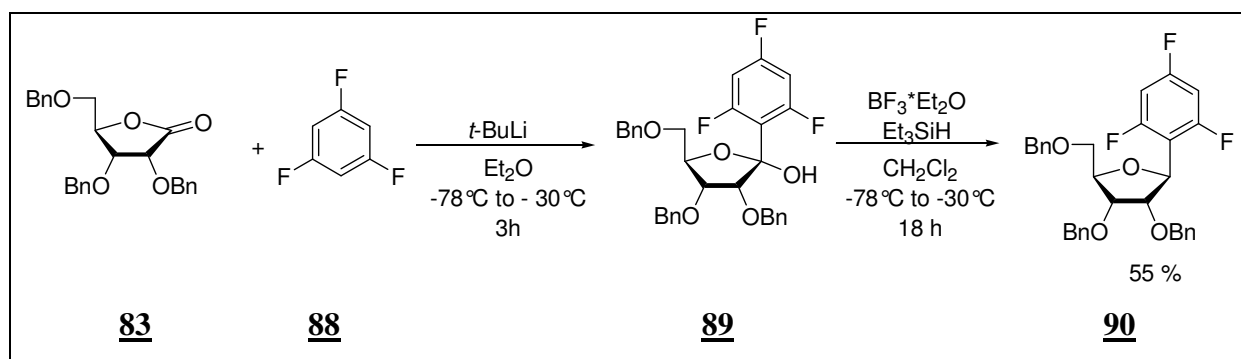


Figure 5.21. Synthesis of 2,3,5-tri-O-benzyl-1'-deoxy-1'-(2,3,5-trifluoro phenyl)- $\beta$ -D-ribofuranose **90**

It is important to stress at this point that in the reactions described in experimental part no aryne formation was observed (Gilman et al., 1957).

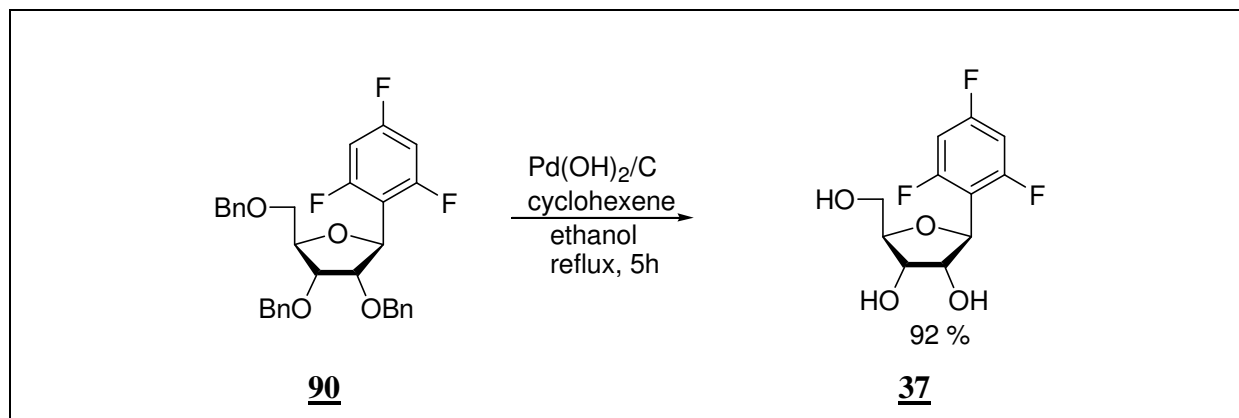
Reagent	Base	Solvent	Yield of wanted product
4-fluoro-bromo benzene	<i>n</i> -BuLi	THF	75.8 % <sup>1</sup>
4-chloro-bromo benzene	<i>n</i> -BuLi	THF	73 % <sup>1</sup>
2,4-difluorobromo benzene	<i>n</i> -BuLi	Et <sub>2</sub> O	84.6 % <sup>1</sup>
1,3,5-trifluorobenzene	<i>t</i> -BuLi	Et <sub>2</sub> O	55 % <sup>1</sup>
2,4,6-trifluorobromo benzene	<i>n</i> -BuLi	Et <sub>2</sub> O	32 %
1,3,5-trifluorobenzene	<i>n</i> -BuLi	Et <sub>2</sub> O	10 %
1,3,5-trifluorobenzene	<i>n</i> -BuLi	THF	7 %
2,4,5-trifluorobromo benzene	<i>n</i> -BuLi	Et <sub>2</sub> O	65 % <sup>1</sup>
Bromo benzene	<i>n</i> -BuLi	THF	74.7 % <sup>1</sup>
Pentafluorobromo benzene	<i>n</i> -BuLi	Et <sub>2</sub> O	50 % <sup>1</sup>
Pentafluorobromo benzene	<i>t</i> -BuLi	Et <sub>2</sub> O	10 %
Pentafluorobromo benzene	<i>n</i> -BuLi	THF	12 %

Figure 5.22. Yields on C-glycosilation reactions of the synthesised C-nucleosides under different conditions; <sup>1</sup>-reactions described in experimental part

### 5.4.2.2 Debenzylation

The debenzylation of the protected nucleosides was done with palladium hydroxide on carbon and cyclohexene (Hanessian *et al.*, 1981). As a catalyst Pearlmans catalyst, 20 % palladium hydroxide on carbon was used (Pearlman, 1967). In this reaction cyclohexene is a hydrogen donor. An example is given in *figure 5.23*.

Yields for all synthesised compounds were over 90%.



*Figure 5.23. Debenzylation of 2',3',5'-tri-O-benzyl-1'-deoxy-1'-(2,3,5-trifluoro phenyl)-β-D-ribofuranose **84***

Debenzylation of 2',3',5'-tri-O-benzyl-1'-deoxy-1'-phenyl -β-D-ribofuranose **91** under these conditions doesn't lead to the wanted product, 1'-deoxy-1'-phenyl -β-D-ribofuranose **41**, but to 1-deoxy-1-phenyl-D-ribitol **92** (Parsch, 2001). Wanted product, 1'-deoxy-1'-phenyl -β-D-ribofuranose **41**, was obtained in reaction with boron tribromide (Krohn *et al.*, 1992)(*figure 5.24*).

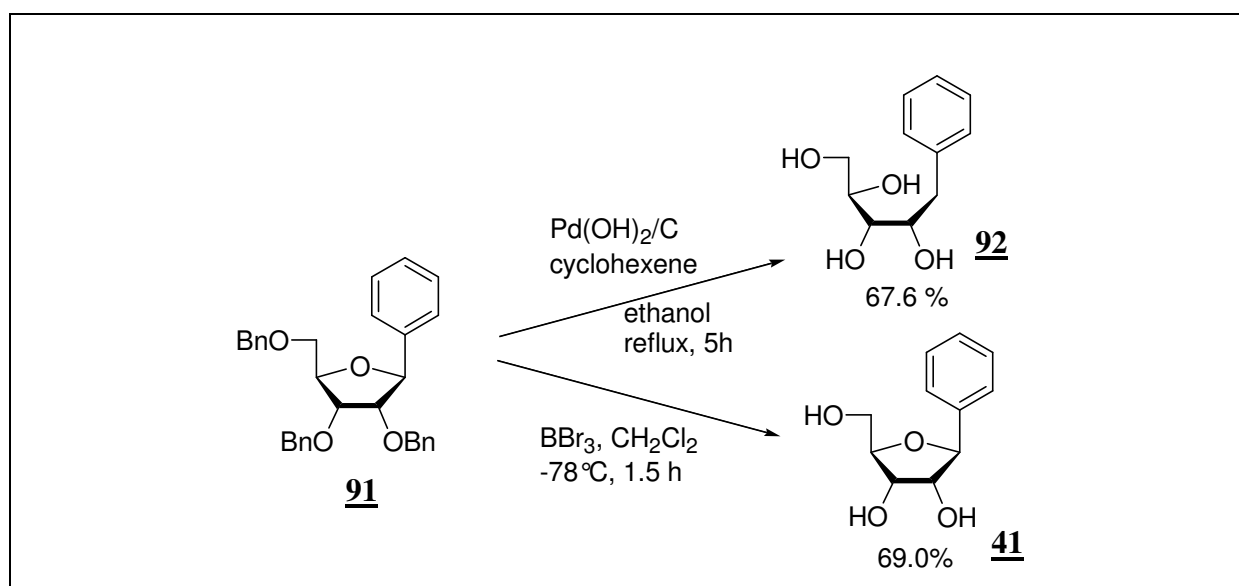


*Figure 5.24. Debenzylation of 2',3',5'-tri-O-benzyl-1'-deoxy-1'-phenyl -β-D-ribofuranose **91***

## 5.5 Protection of Nucleosides for Solid Phase RNA Synthesis

For RNA synthesis sequential formation of phosphodiester group between the 3'OH group and the 5'OH group has to be performed. We have to install a temporary protecting group either at 3'OH or 5'OH, which has to cleave in every step during the synthesis. Today it is most common to protect the 5'OH group with DMTr group, which is cleaved in an E1-type mechanism with acid. For RNA synthesis we also need a protecting group for the 2'OH group and therefore we used TBDMS group.

### 5.5.1 Dimethoxytritylation Reaction

For the 5'-OH group of phosphoramidites as protecting group the dimethoxytriphenylmethyl-protecting group was used (Smith *et al.*, 1962; Schaller *et al.*, 1963). Triphenylmethyl- and monomethoxytriphenylmethyl- (MMTr) protecting groups are also used for phosphoramidites. The advantage of DMTr-protecting group is that it can be easily cleaved with trichloro acetic acid (TCA) and absorbs at the 498 nm after cleavage on the DNA-/RNA-synthesizer. That allows to observe and calculate yields of each coupling step on the synthesizer (Fisher & Caruthers, 1983). For this reaction we dissolve nucleoside in pyridine and triethylamine. Triethyl amine is a base that supports the reaction. The dimethoxytriphenyl methyl-group has a high selectivity for primary 5'-OH group. Using 1,2 equivalents of DMTrCl we don't get any 2'-OH or 3'-OH product.

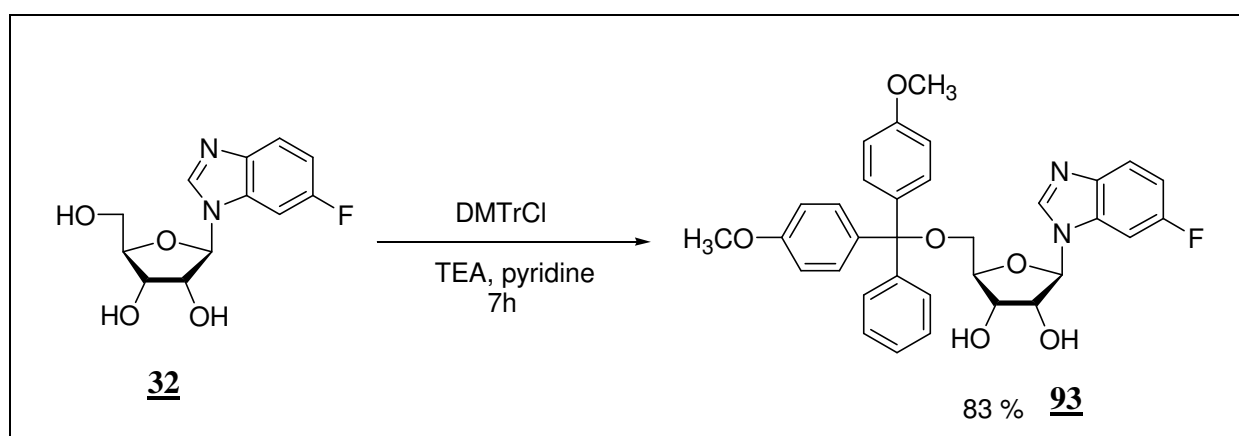


Figure 5.25. Dimethoxytritylation

The reactivity of the nucleosides varies. For example in the reaction of 1'-deoxy-(5-fluoro-3-*N*-benzimidazolyl)- $\beta$ -D-ribofuranose **32** we get the tritilated product in 83 % over 7h and in reaction of 1'-deoxy-(4-trifluoromethyl-1-*N*-benzimidazolyl)-  $\beta$ -D-ribofuranose **33** (figure 5.25.) we get 68 % over 20 h. An explanation would be the size of the trifluoromethyl group makes the reaction slower. Fluoro-benzene modifications were usually protected over shorter time and with higher yields than fluoro-benzimidazoles.

### 5.5.2 Protection of 2'-OH Group

For RNA synthesis we need a protecting group at the 2'-OH group. For this, either the TBDMS-protecting group or TOM-protecting group are in use, which are cleaved with fluoride after RNA synthesis (Stawinski *et al.*, 1988; Gasparutto *et al.*, 1992; Westman & Strömberg, 1994). Recently the ACE- (acethoxyethoxy-) protecting group is developed, whose easy cleavage and high purity of the oligonucleotides are main advantages (Scaringe *et al.*, 2004). We used the TBDMS-protecting group because in our hands it gave better results than the TOM-protecting group and it is cheaper (Ogilvie *et al.*, 1974; Ogilvie *et al.*, 1978; Pitsch, 1999). The problem with the TBDMS group is that in reaction we get two regioisomers as products, 2' and 3' protected OH groups (Hakimelaki *et al.*, 1981; Hakimelaki *et al.*, 1981) and the group also migrates from one position to another (Jones & Reese, 1979). Using silver nitrate in the reaction we got more of 2'-protected nucleoside (Hakimelahi *et al.*, 1981; Hakimelahi *et al.*, 1982).

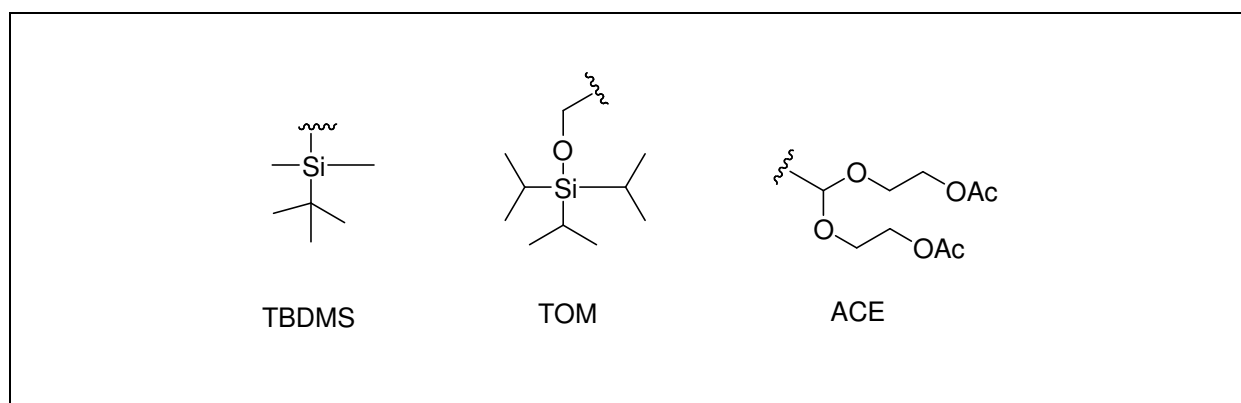
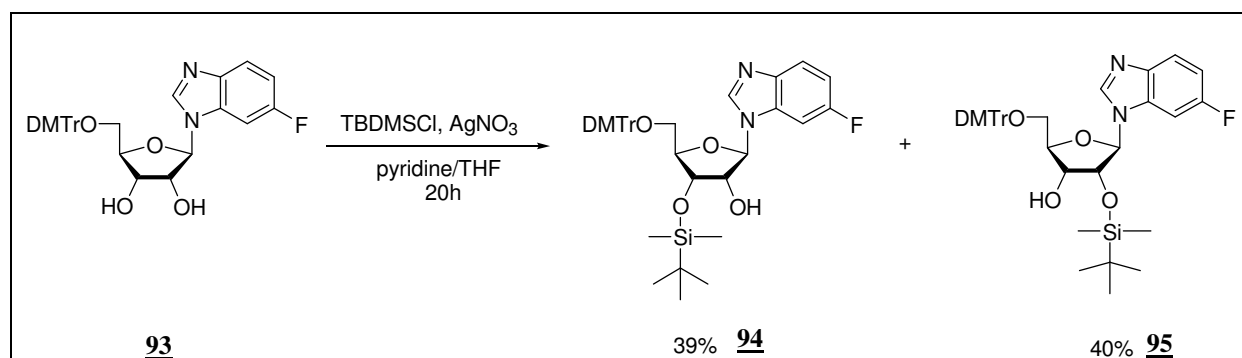


Figure 5.26. RNA protecting groups in common use today TBDMS-, TOM- and ACE-

The reaction time was 20 h for all our modifications (an example is given in *Figure 5.27.* ).

The main problem in isolating the wanted 2'-protected nucleoside is migration of the TBDMS-group and that influences the yields of the wanted isomers. Since in polar solvents (*Figure 5.28.*) this migration is greater we avoided using them and therefore most of the 2'-protected nucleosides were isolated by means of preparative HPLC.

The isomers were identified with  $^1\text{H}$ ,  $^1\text{H}$ -COSY-NMR measurements.



*Figure 5.27. Protection with the TBDMS-group*

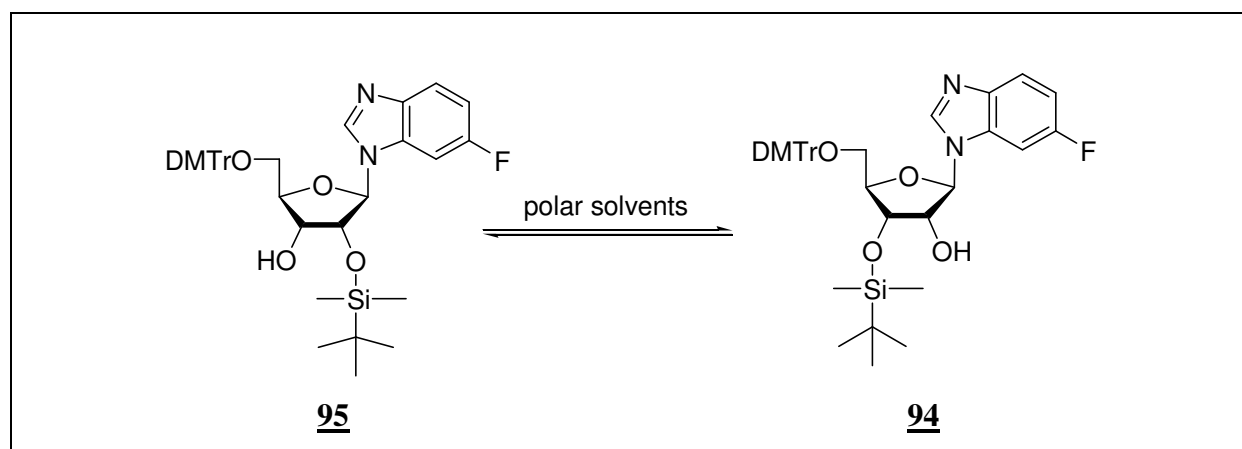


*Figure 5.28. Migration of the TBDMS-group in polar solvents*

### 5.5.3 Phosphitilation

To avoid migration of the TBDMS-protecting group in the synthesis of phosphoramidites instead of *N,N*-diisopropylethyl amine (DIPEA) sym.-collidine was used as a base. As a catalyst *N*-methylimidazole was used.

In this reaction a very high dryness of the reagents is important. As a solvent acetonitrile was used. The nucleoside was dissolved in acetonitrile and sym.-collidine and *N*-methyl imidazole

were added. Then the reaction mixture was cooled to 0°C and cyanoethyl-diisopropylchlorophosphoramidite **96** (Sinha *et al.*, 1983) was added. The reaction mixture was left 15 min. at 0°C and then left 25-60 minutes at room temperature (an example is shown in *figure 5.29*) (Parsch & Engels, 2000).

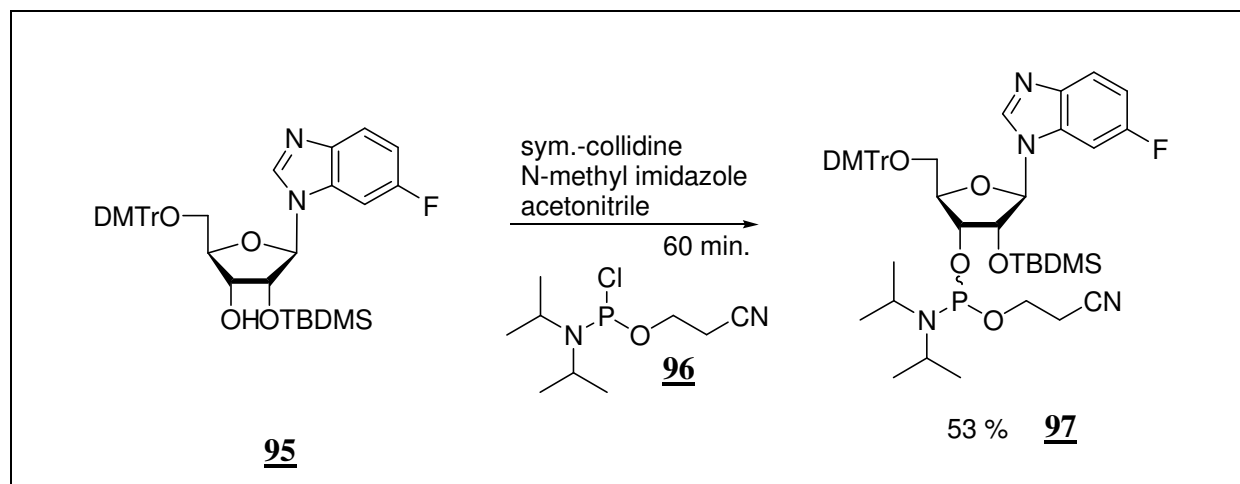


Figure 5.29. Synthesis of phosphoramidite for solid phase synthesis of RNA

The purification was done as fast as possible. First the reaction mixture was extracted with methylene chloride three times and then the collected organic layers were extracted with 0.01M citric acid to remove sym.-collidine. This concentration of the citric acid in this solution is important because it is high enough to remove sym.-collidine but low enough not to cleave DMTr-protecting group.

The synthesis of phosphoramidite of benzene modification was done in 1996 by Matulic-Adamic and coworkers (Matulic-Adamic *et al.*, 1996; Matulic-Adamic *et al.*, 1996a).

## 5.6 Abasic Site

For the investigation of base stacking we had to synthesise an abasic site for comparison. An abasic site has no nucleobase on the sugar.

The synthesis of the abasic site amidite **102** for solid phase synthesis of RNA begins with 2,3,5-tri-O-benzyl-ribofuranose **82**. 2,3,5-tri-O-benzyl ribofuranose **82** is synthesised from D-ribose and is the third step in the synthesis of 2,3,5-tri-O-benzyl-ribo- $\gamma$ -lactone **83**. To get the abasic building block the hydroxyl group on C1 has to be removed. Therefore **82** was dissolved in acetonitrile and boron trifluoride-etherate and triethylsilane were added (Purdy

*et al.*, 1994). After 1,5 h the reaction was finished. The product, 2,3,5-tri-O-benzyl-1-deoxy-D-ribofuranose **98**, was obtained in 88.4 % yield.

The next step was to deprotect the benzyl groups and therefore we dissolved **98** in ethanol and cyclohexene and we added palladium hydroxide (20 %) on carbon. ( Hanessian *et al.*, 1981). After work up we obtained the wanted product **42** in 95.3 % yield (Engels & Parsch, 1999).

The following steps to synthesise the corresponding amidite are shown in in *figure 5.30* and details are described in the experimental part.

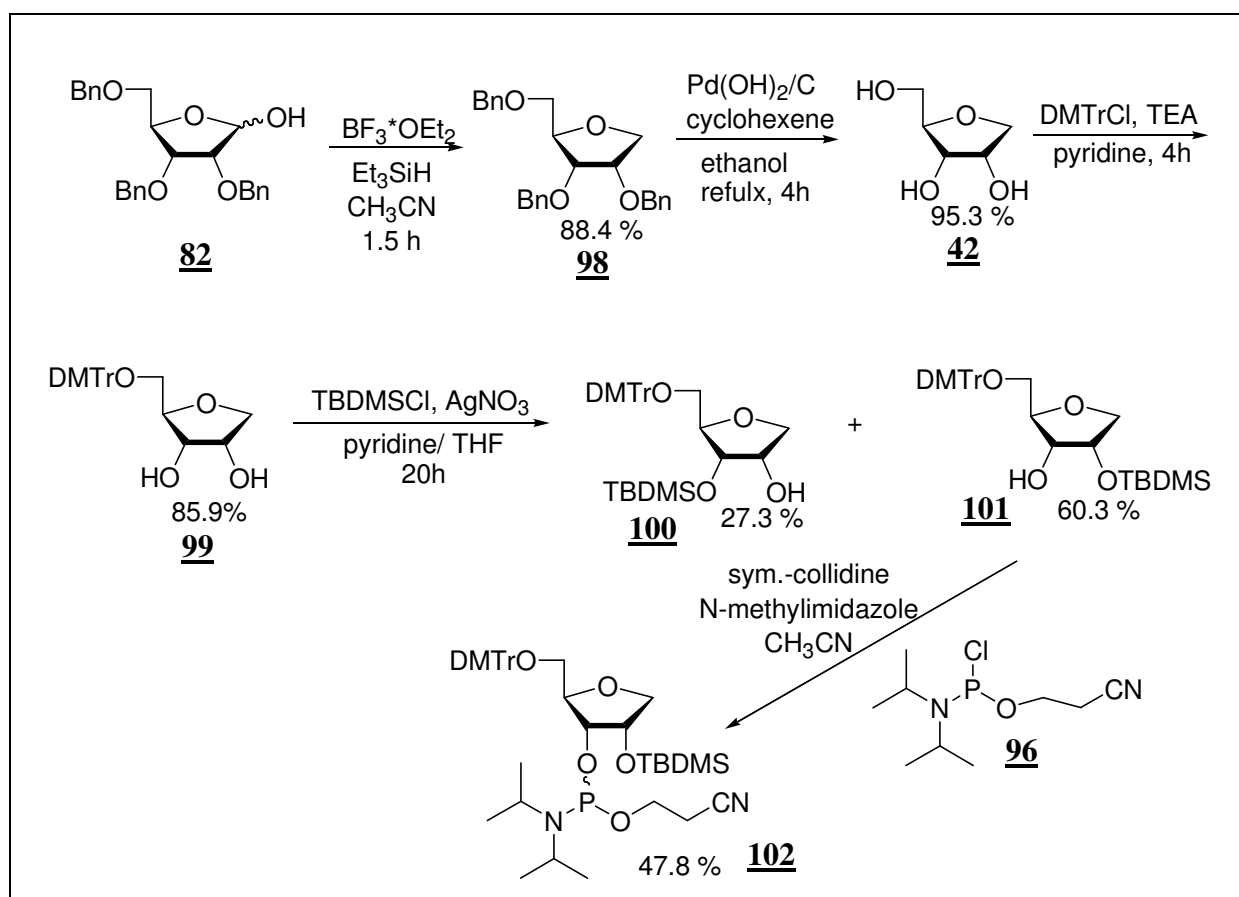


Figure 5.30. Synthesis of the abasic building block for RNA synthesis



## 5.7 Overview on Synthesis

In figures 5.31, 5.32, 5.33, 5.34 and 5.35. are overviews on the all syntheses given (yields and other precise information on experiments are given in the experimental part).

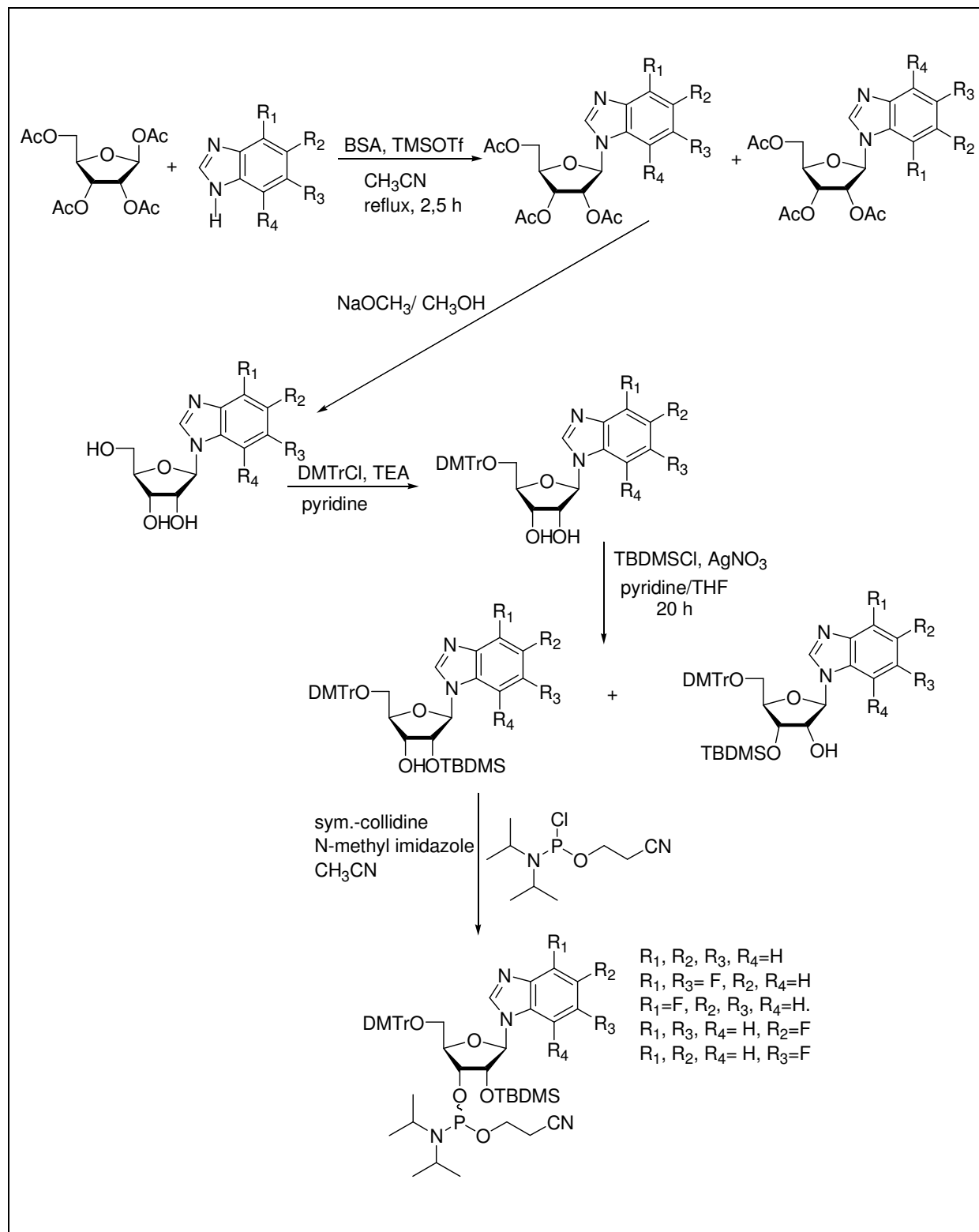


Figure 5.31. Overview of fluoro- benzimidazole syntheses

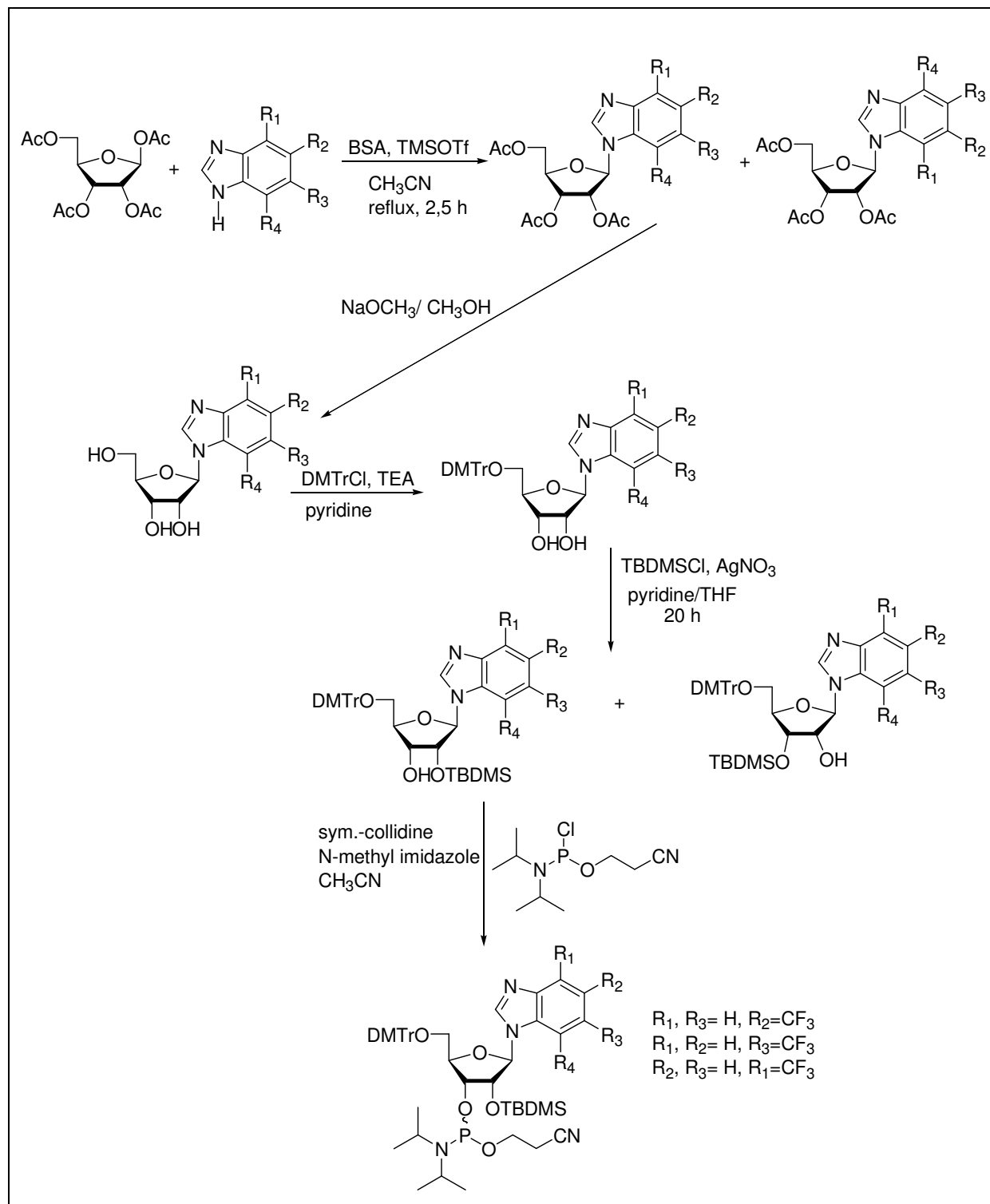


Figure 5.32.: Overview of trifluoromethyl-benzimidazole synthesis

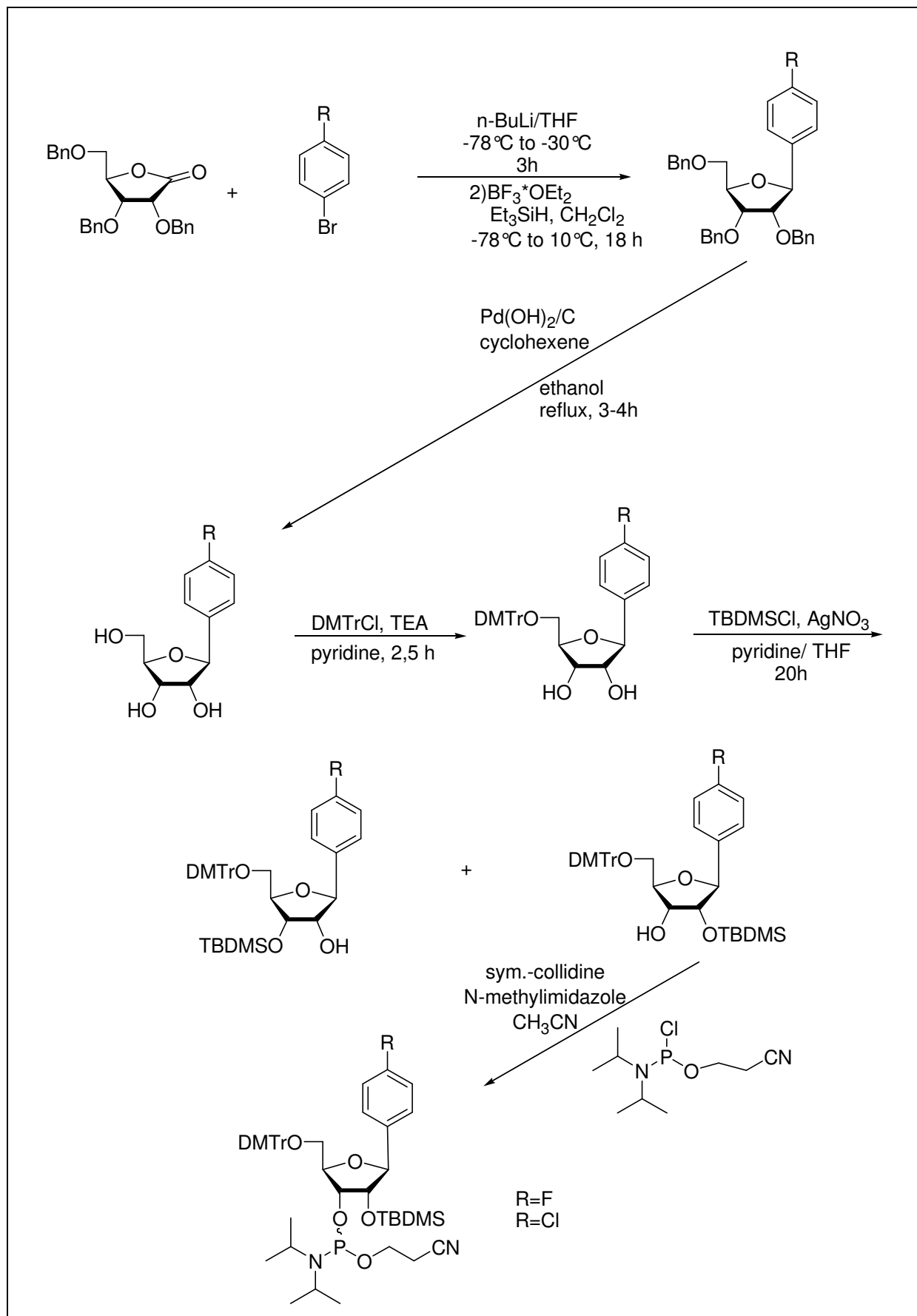


Figure 5.33. Overview on 4-fluoro- and 4-chloro-benzene nucleosides for RNA synthesis

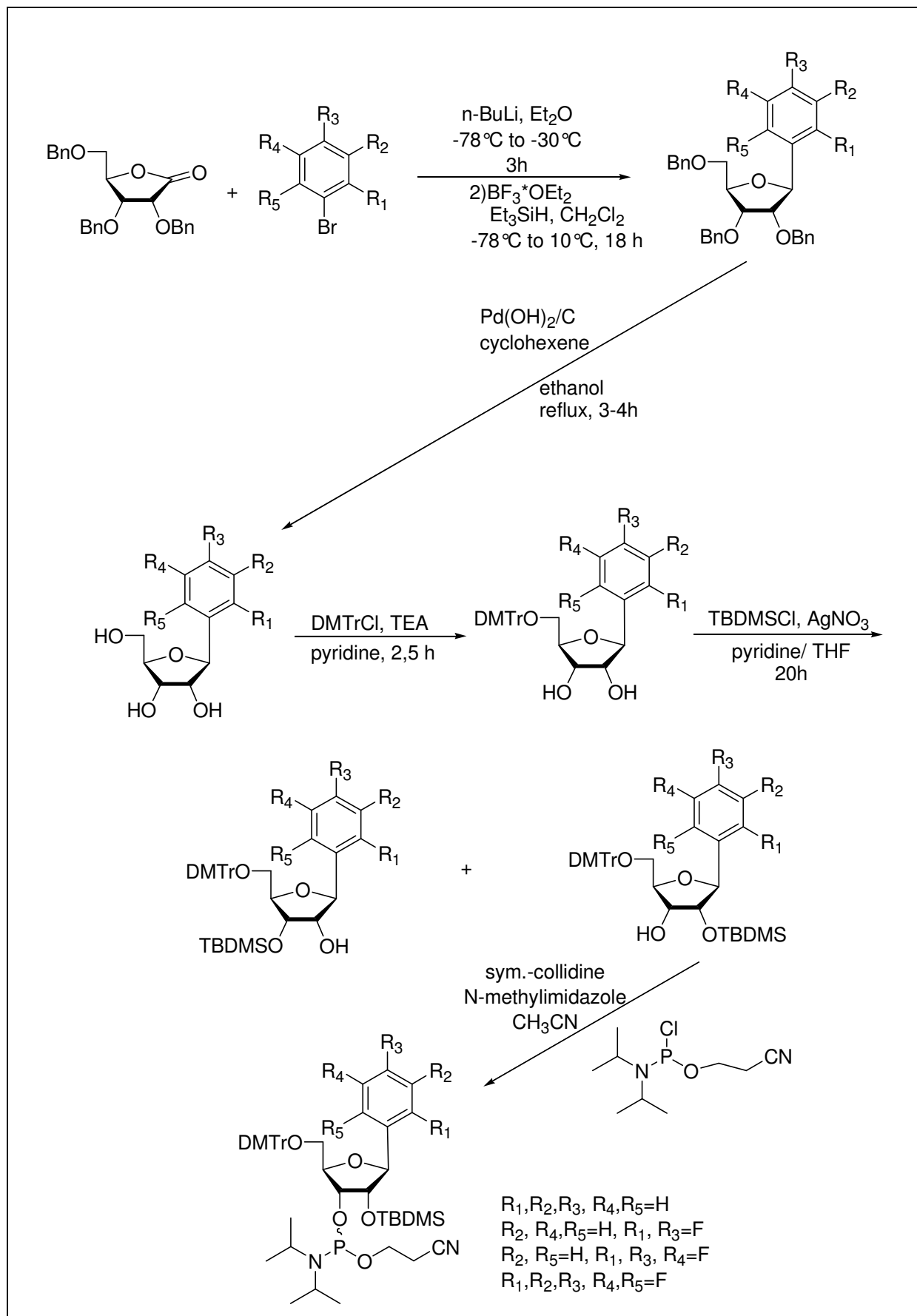


Figure 5.34. Overview of fluoro benzene synthesis in Et<sub>2</sub>O

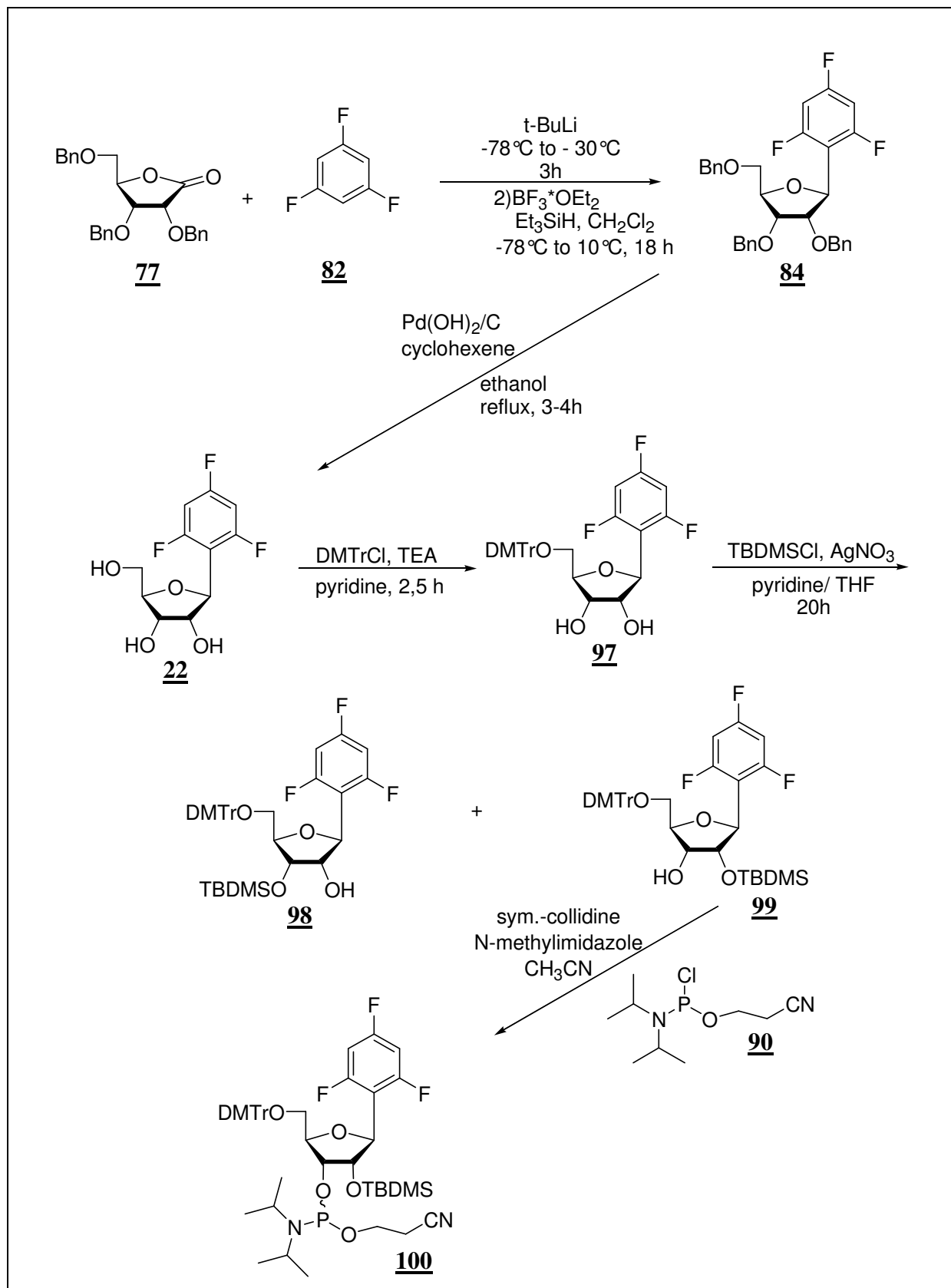


Figure 5.35. Overview over 2,4,6-trifluoro-benzene modification synthesis for RNA solid phase synthesis with *t*-BLLi, Et<sub>2</sub>O

## 5.8 Partition Coefficients and HPLC Retention Times

From all synthesised modified nucleosides partition coefficients and HPLC retention times were determined. We used unprotected nucleosides for determinations.

### 5.8.1 Partition Coefficients

Octanol/water partition coefficients are measure of the lipophilicity of molecules and therefore are in correlation with penetration across biological membranes (Csizmadia *et al.*, 1997). Octanol-water partition coefficient,  $\log P$ , is defined as the ratio of the equilibrium concentration of a solute in octanol to that in water. More lipophilic molecules have bigger values for partition coefficient. Investigation of lipophilicity of molecules is of great importance in drug research. This is the main reason why programmes for predicting partition coefficients are designed (Haeberlein & Brinc, 1993).

Unprotected nucleosides were dissolved in water in concentrations that correspond to extinction between 0,8 and 1,2. Than, 2ml of 1-octanol and 2ml of these solutions were 10 minutes strongly mixed. The probes were than 10 minutes centrifuged at 10 000 U/min. The phases were carefully separated and extinctions of both phases were measured. From the measured values partition coefficient was calculated using following equation [5-1]:

$$[5-1] \quad \log P = E_{\text{octanol}} / E_{\text{water}}$$

where  $E_{\text{octanol}}$  is measured extinction of octanol phase and  $E_{\text{water}}$  is measured extinction of water phase. Measured partition coefficients are shown in figure 5.36.

Measure partition coefficients  $\log P$  were between 0,149 and 5,884. As expected smallest value we have for non-substituted imidazol and the biggest for trifluoromethyl substituted imidazoles. From our data it is also clear that aromatic fluorination always increases lipophilicity as perfluorination also does ( Smart, 2001). It also can be noticed that position of fluorines is important (look at the data for 2,4,6 TFB and 2,4,5 TFB) as previously showed by Parsh for monofluorinated derivatives (Parsch, 2000). For both derivatives that have bis-*ortho* substitution (PFB and 2,4,6 TFB) values for  $\log P$  are lower than expected.

Nucleoside	Partition Coefficient (log <i>P</i> )
<b>I</b>	0,149
<b>4 FBI</b>	1,789
<b>5 FBI</b>	1,802
<b>6 FBI</b>	1,799
<b>4,6 DFBI</b>	4,240
<b>4 TFM</b>	6,762
<b>5 TFM</b>	6,757
<b>6 TFM</b>	6,688
<b>B</b>	1,050
<b>4 FB</b>	1,497
<b>2,4 DFB</b>	1,695
<b>2,4,6 TFB</b>	1,398
<b>2,4,5 TFB</b>	1,825
<b>PFB</b>	2,156

Figure 5.36. Partition coefficients of nucleosides

## 5.8.2 HPLC-Retention Times

Another method for investigating lipophilicity of compounds is the determination of HPLC retention time ( Balzarini *et al.*, 1989). Substances that have longer retention times on reverse phase HPLC column are more lipophilic (Lien *et al.*, 1991). Hydrophilic substances are eluted very fast from those columns.

We used RP-18 (5 $\mu$ m) column from Merck company (LiChrospher EcoCART 125-3, Nr. 647318). Acetonitrile in 5% concentration in water was used as eluent. The flow was 0,6ml/min.

Retention times are given in *figure 5.37*. Measured retention times vary from 10 to 62 minutes.

As already is seen from partition coefficient more lipophilic are trifluoromethyl modifications (TFM). Those are followed by 4,6 DFBI modification. Benzene modifications are in generally less lipophilic and their retention times are from 10,1 (for B) to 17,8 (for PFB).

Nucleoside	Retention time (min)
<b>I</b>	16,4
<b>4 FBI</b>	16,8
<b>5 FBI</b>	17,0
<b>6 FBI</b>	17,4
<b>4,6 DFBI</b>	24,6
<b>4 TFM</b>	62,3
<b>5 TFM</b>	61,9
<b>6 TFM</b>	63,0
<b>B</b>	10,1
<b>4 FB</b>	14,9
<b>2,4 DFB</b>	13,6
<b>2,4,6 TFB</b>	14,0
<b>2,4,5 TFB</b>	15,8
<b>PFB</b>	17,0

*Figure 5.36. HPLC Retention times of nucleosides*

Data given in figure 5.37. correlate very well with values obtained for partition coefficients.





## 6 Crystallography

### 6.1 What do we Learn from Crystals?

A crystal is an ordered supramolecular system and according to Dunitz “ a supermolecule par excellence” ( Dunitz, 1996). X-Ray crystallography provides accurate information on the structures of molecular complexes and the nature of the nonbonded interaction between the binding partners in the solid state. The technique has become the central one in molecular recognition studies.

All databases containing information on crystal structures are growing at exponential rate, and have been vaults for finding information on chemical interactions: they have been the bases for extensive investigations of classical H bonds in the past and more recently have been used to explore weaker H bonds such as C-H...O, C-H...N, C-H...Cl and nowadays more and more often mentioned C-H...F hydrogen bond. Directionality, energetics, distance relative to van der Waals radii, and bond length are useful criteria for classifying H bonds. In this context C-H/  $\pi$  interaction has been defined as hydrogen bond.

Parallels can be drawn between molecular recognition events that occur within model systems in the liquid phase and those that define the supramolecular nature of a molecular network in the solid state. Crystal structures of benzene and different fluoro-benzenes follow herringbone pattern (edge-to-face) so we wanted to see if our nucleosides would allow the same pattern or a different one ( Castellano *et al.*, 2003).

### 6.2 Theoretical Background

X-Ray crystallography is a standard technique for solving crystal structures. Its basic theory was developed soon after x-rays were discovered more than a century ago. However, over the

years it has gone through continual development in data collection instrumentation and data reduction methods. Today X-ray crystallography is widely used in material science and structure determination. For crystallography the proper wavelength is  $10^{-8}$  cm (Strähle, 1990). X-rays are produced generally by either x-ray tubes or synchrotron radiation. In a x-ray tube, which is the primary x-ray source used in laboratory x-ray instruments, x-rays are generated when a focused electron beam accelerated across a high voltage field bombards a stationary or rotating solid target. As electrons collide with atoms in the target and slow down, a continuous spectrum of x-rays are emitted, which are termed Bremsstrahlung radiation. The high-energy electrons also eject inner shell electrons in atoms through the ionisation process. When a free electron fills the shell, an x-ray photon with an energy characteristic of the target material is emitted. Common targets used in x-ray tubes include Cu and Mo, which emit 8 keV and 14 keV x-rays with corresponding wavelengths of 1.54 Å and 0.8 Å, respectively. (The energy  $E$  of a x-ray photon and its wavelength is related by the equation  $E = hc/\lambda$ , where  $h$  is Planck's constant and  $c$  the speed of light). In recent years synchrotron facilities have become widely used as preferred sources for x-ray diffraction measurements. Synchrotron radiation is emitted by electrons or positrons travelling at near light speed in a circular storage ring. These powerful sources, which are thousands to millions of times more intense than laboratory x-ray tubes, have become indispensable tools for a wide range of structural investigations and brought advances in numerous fields of science and technology.

### 6.2.1 Lattice Planes and Bragg's Law

X-rays primarily interact with electrons in atoms. When x-ray photons collide with electrons, some photons from the incident beam will be deflected away from the direction where they originally travelled, much like billiard balls bouncing off one another. If the wavelength of these scattered x-rays does not change (meaning that x-ray photons did not lose any energy), the process is called elastic scattering (Thompson Scattering) in that only *momentum* has been transferred in the scattering process. *These are the x-rays that we measure in diffraction experiments, as the scattered x-rays carry information about the electron distribution in materials.* On the other hand, in the inelastic scattering process (Compton Scattering), x-rays

transfer some of their energy to the electrons and the scattered x-rays will have different wavelength than the incident x-rays.

Diffracted waves from different atoms can interfere with each other and the resultant intensity distribution is strongly modulated by this interaction. If the atoms are arranged in a periodic fashion, as in crystals, the diffracted waves will consist of sharp interference maxima (peaks) with the same symmetry as in the distribution of atoms. Measuring the diffraction pattern therefore allows us to deduce the distribution of atoms in a material.

The peaks in an x-ray diffraction pattern are directly related to the atomic distances. Let us consider an incident x-ray beam interacting with the atoms arranged in a periodic manner as shown in 2 dimensions in the following illustrations. The atoms, represented as green spheres in the graph, can be viewed as forming different sets of planes in the crystal (coloured lines in the graph on the left). For a given set of lattice plane with an inter-plane distance of  $d$ , the condition for a diffraction (peak) to occur can be simply written as

$$2d\sin\theta = n\lambda$$

which is known as the Bragg's law, after W.L. Bragg, who first proposed it (Bragg & Bragg, 1913). In the equation,  $\lambda$  is the wavelength of the x-ray,  $\theta$  the scattering angle, and  $n$  an integer representing the order of the diffraction peak. The Bragg's Law is one of most important laws used for interpreting x-ray diffraction data.

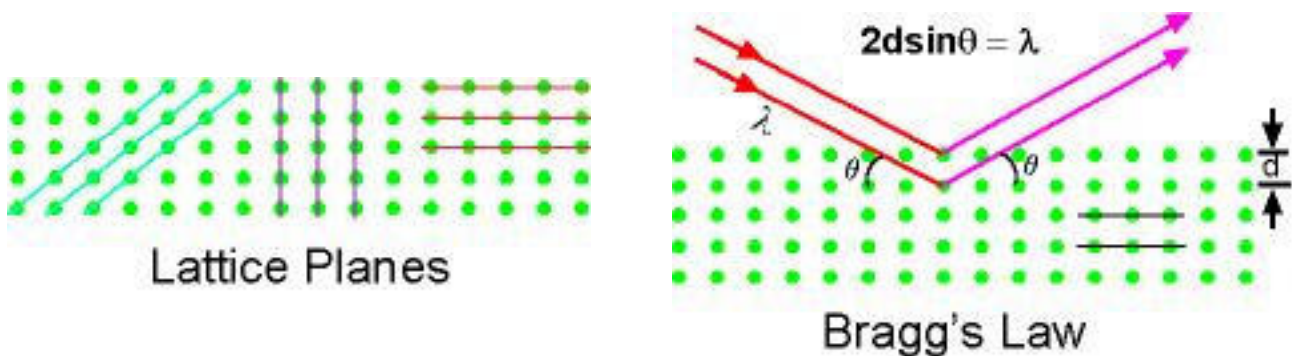


*Figure 6.1. Lattice planes(left) and Bragg's Law(right)*

### 6.3 Crystal Structure of Fluorine-modified and Chlorine-modified Benzene Nucleosides

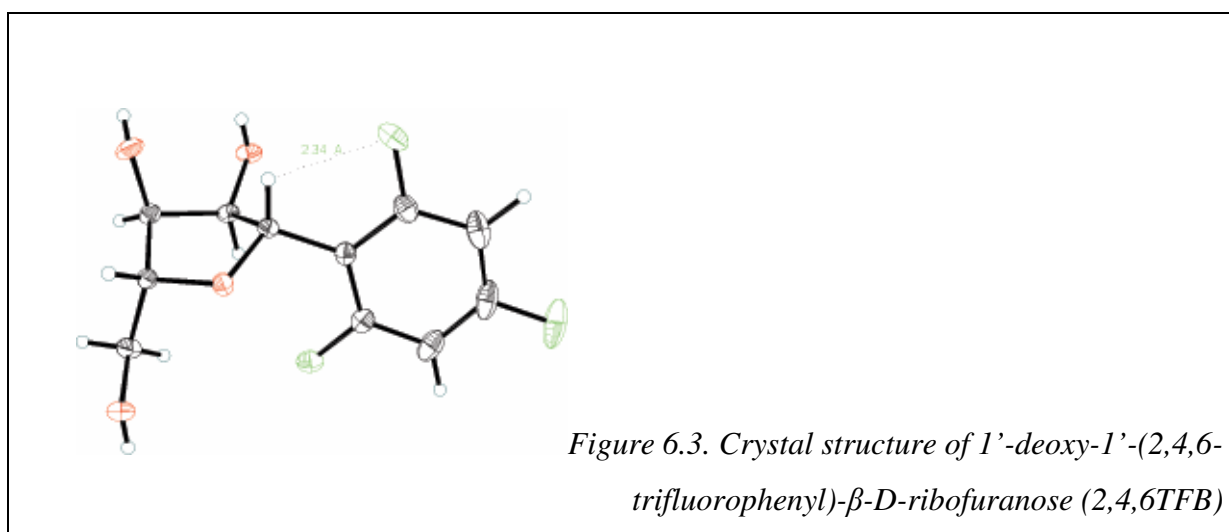
In this work all fluorine modified benzene nucleosides were crystallized (2,4,6 TFB, 2,4,5 TFB and also 4 ClB). Crystal structures of 4FB and 2,4 DFB were done in our group and published previously ( Bats *et al.*, 1999).

Nucleoside	Crystallized from...	Temperature (°C)	Crystal system	Space Group	Sugar Conformation
Benzene ( <b>B</b> )	Toluol/ethylacetate	-18	monoclinic	P 2 <sub>1</sub>	C2' <i>endo</i>
4-Fluoro-benzene ( <b>4FB</b> )	methanol	20	orthorhombic	P 2 <sub>1</sub> 2 <sub>1</sub> 2 <sub>1</sub>	C1' <i>exo</i> C2' <i>endo</i>
4-Fluoro-benzene ( <b>4FB</b> )	methanol	4	orthorhombic	P 2 <sub>1</sub> 2 <sub>1</sub> 2 <sub>1</sub>	Between C2' <i>endo</i> and C2' <i>endo</i> C3' <i>exo</i>
4-Fluoro-benzene ( <b>4FB</b> )	water	20	monoclinic	C 2	Between C2' <i>endo</i> and C1' <i>exo</i> C2' <i>endo</i>
2,4-difluoro-benzene ( <b>2,4DFB</b> )	water	20	monoclinic	C 2	C2' <i>exo</i> C3' <i>endo</i>
2,4,6-trifluorobenzene ( <b>2,4,6 TFB</b> )	methanol	4	orthorhombic	P22121	C2' <i>endo</i>
2,4,5-trifluorobenzene ( <b>2,4,5 TFB</b> )	methanol	4	monoclinic	C2	C2' <i>endo</i>
4-chloro-benzene- ( <b>4ClB</b> )	water	4	orthorhombic	P22121	Between C2' <i>endo</i> and C3' <i>exo</i>

Figure 6.2. Crystal data of C-nucleosides

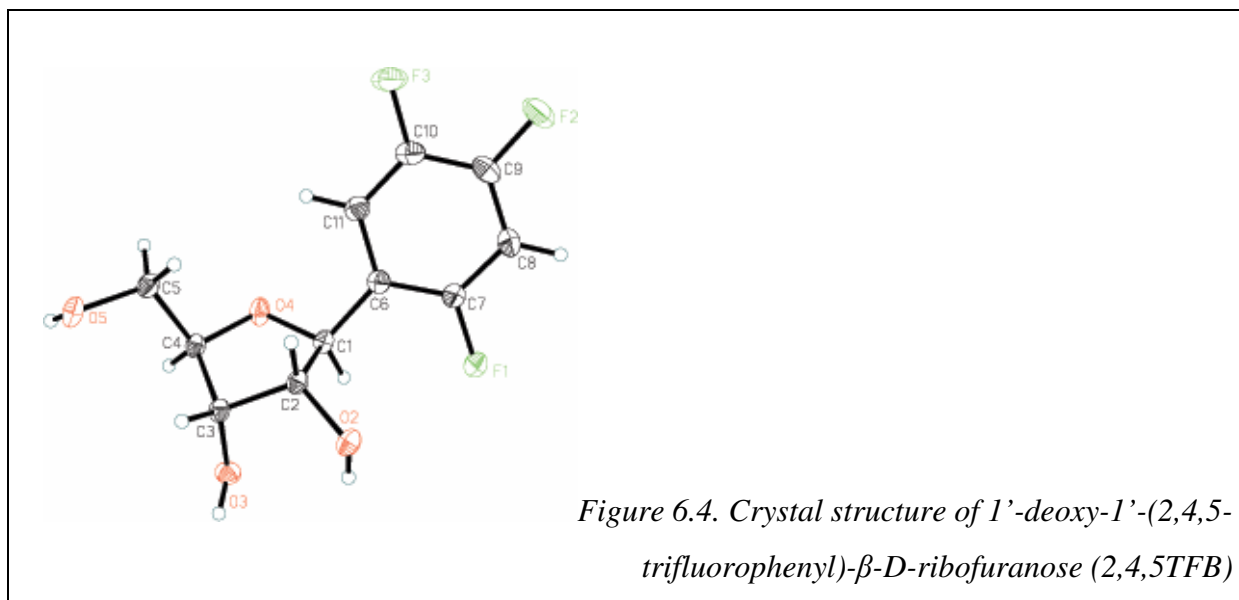
Crystal structure of B, 1'-deoxy-1'-phenyl- $\beta$ -D-ribofuranose was published from Matulic-Adamic and co workers and is used for comparison here (Matulic-Adamic *et al.*,1996). Crystals were obtained either from water or from methanol. Complete tables with results are given in the attachment. In *figure 6.2* are crystallographic data of C-nucleosides given.

All crystals crystallised in either orthorhombic or monoclinic crystal group. The five-membered furanose ring of 1'-deoxy-1'-(2,4,6-trifluorophenyl)- $\beta$ -D-ribofuranose (2,4,6 TFB) has approximately a C2'-*endo*-envelope conformation. The hydroxyl group attached to C2' is in an equatorial position, the hydroxyl group attached to C3' is in a pseudo-axial position and the phenyl group attached to C1' is in a pseudo-equatorial position with respect to the furanose ring. The trifluorophenyl group adopts a position with an almost syn-periplanar orientation of the C11-F3 bond and the C1-H1 bond. The intramolecular H1...F3 distance of 2.34 Å is slightly shorter than the van der Waals contact distance. The phenyl group shows a small deviation from planarity: substituent atoms C1 and F1 deviate 0.11 Å in opposite directions from the phenyl plane. This deviation from planarity may result from a steric interaction between atoms F1 and O4. The observed F1...O4 distance of 2.819 Å is slightly shorter than the van der Waals contact distance. The ribofuranose groups are connected by intermolecular O-H...O hydrogen bonds to a two-dimensional network parallel to the a,b - plane. These molecular layers are connected in the c - direction by an intermolecular C-H...O interaction with a H...O distance of 2.48 Å and two intermolecular C-H...F interactions (involving the para-F atom) with H...F distances of 2.54 and 2.63Å(*figure6.3.*).



The crystal structure of 1'-deoxy-1'-(2,4,5-trifluorophenyl)- $\beta$ -D-ribofuranose (2,4,5 TFB) is isomorphous with the structure of 1'-deoxy-1'-(2-fluorophenyl)- $\beta$ -D-ribofuranose (Bats *et al.* 1999). The five-membered furanose ring approximately has a C2-*endo*-envelope

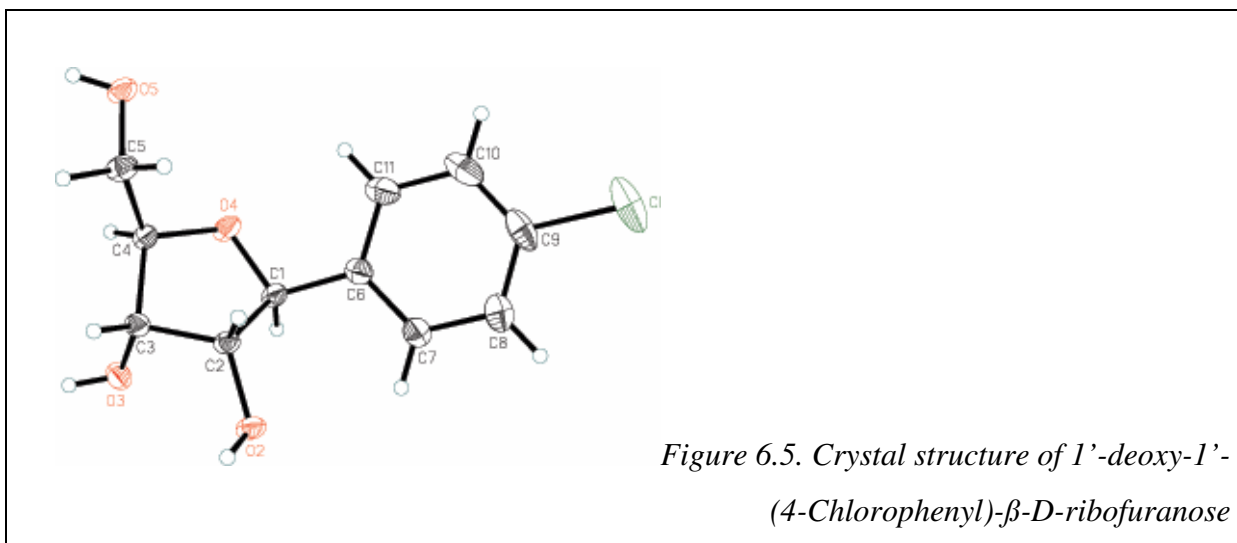
conformation. The phenyl group attached to C1 and the hydroxyl group attached to C2' are in pseudo-equatorial positions, the hydroxyl group attached to C3' is in a pseudo-axial position with respect to the furanose ring. The phenyl group is planar within experimental uncertainty. The ribofuranose groups are connected by intermolecular O-H...O hydrogen bonds to a two-dimensional network parallel to the a,b - plane. The molecules are further stabilized in the a,b -direction by a number of weak C-H...F interactions (involving F1 and F3) with H...F distances between 2.60 and 2.75 Å. Neighbouring molecules are connected in the b - direction by a rather short intermolecular C-H...O interaction with a H...O distance of 2.32 Å. No significant intermolecular interactions are observed in the crystallographic c - direction: the shortest intermolecular C8-H8...F2 interactions have a H...F distance of 2.90 Å which is too long to be significant. Surprisingly the C-H... $\pi$  (phenyl) interaction which was observed in the isomorphous 2-fluoro-phenyl compound is replaced in the title compound by an intermolecular C10-F3...C9 interaction with a F...C distance of 3.05 Å, which is slightly shorter than the van der Waals contact distance. The nature of this interaction is unclear. Similar C-H...C interactions with F...C distances between 2.96 and 3.15 Å are found in the crystal structure of hexafluorobenzene (Boden *et al.*,1973; Bertolucci *et al.*, 1974).



The crystal structure of the 1'-deoxy-1'-(4-Chlorophenyl)-β-D-ribofuranose compound is isomorphous with the crystal structure of one of the two modifications of 1'-deoxy-1'-(4-fluorophenyl)-β-D-ribofuranose reported by Bats, Parsch and Engels (Bats *et al.*,2000).The ribofuranose ring has a conformation which is intermediate between a C2'-endo,C3'-exo twist and a C2'-endo envelope. The conformation of the molecule is rather similar to the

conformation observed in 1'-deoxy-1'-(4-fluorophenyl)- $\beta$ -D-ribofuranose (Bats *et al.*, 1999) and the conformation observed in 1'-deoxy-1'-phenyl- $\beta$ -D-ribofuranose Matulic-Adamic and coworkers (Matulic-Adamic *et al.*, 1996). The phenyl group attached to C1' and the hydroxyl group attached to C2' are in pseudo-equatorial positions, the hydroxyl group attached to C3' and the methanol group attached to C4' are in a pseudo-axial positions with respect to the five-membered ring. The shortest intramolecular contact distance is 2.43 Å between O4 and H11. The crystal packing shows three intermolecular hydrogen bonds.

In this way each molecule is connected by hydrogen bonding to six different neighboring molecules leading to a two-dimensional network in the a,b - direction. The bonding in the c - direction consists of weak intermolecular C8-H8...Cl interactions with a H...Cl distance of 2.74 Å and a C-H-Cl angle of 150°. A search of the Cambridge Data Base for structures containing intermolecular C(phenyl)-Cl...H-C(phenyl) interactions with a Cl...H distance shorter than 2.8 Å revealed 149 possible crystal structures. Intermolecular C-H...Cl contacts with a H...Cl distance of 2.78 Å, very similar to those in the title compound, occur in the crystal structure of N-(4-chlorophenyl)-mannopyranosylamine (Ojala *et al.*, 2000).



Important in our crystal structures is the fact which was also established by Parsch & Engels (Parsch & Engels, 1999), that in crystal structures of our fluoro-benzenes F...H hydrogen bond, which is important for crystal packing of those compounds, can be recognized. The Cl...H bond is already very developed for investigating the crystal structures and we can conclude here that that bond has the same nature as the F...H bond because of the similarity in structures of 1'-deoxy-1'-(4-fluorophenyl)- $\beta$ -D-ribofuranose and 1'-deoxy-1'-(4-chlorophenyl)- $\beta$ -D-ribofuranose (*figure 6.6.*).



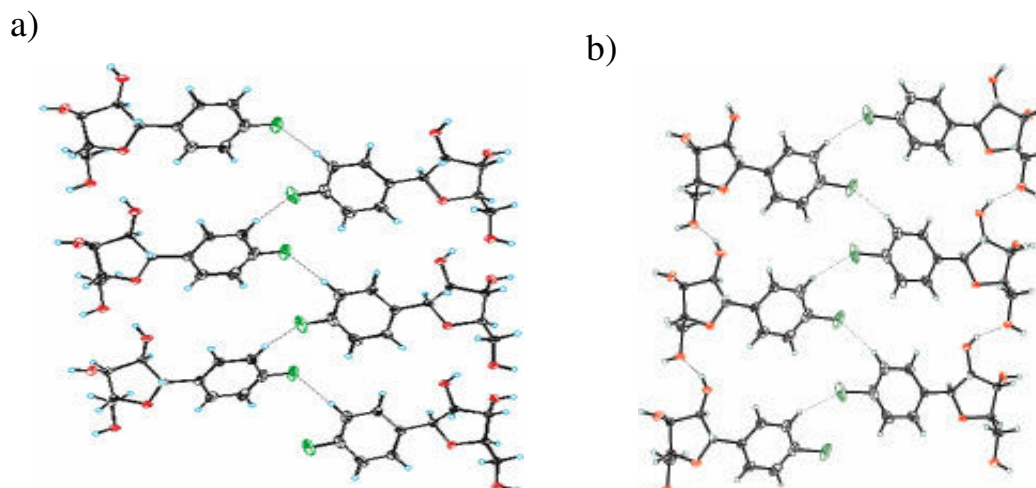


Figure 6.6. Crystal packing of 1'-deoxy-1'-(4-fluorophenyl)-β-D-ribofuranose (a) and 1'-deoxy-1'-(4-chlorophenyl)-β-D-ribofuranose (b)

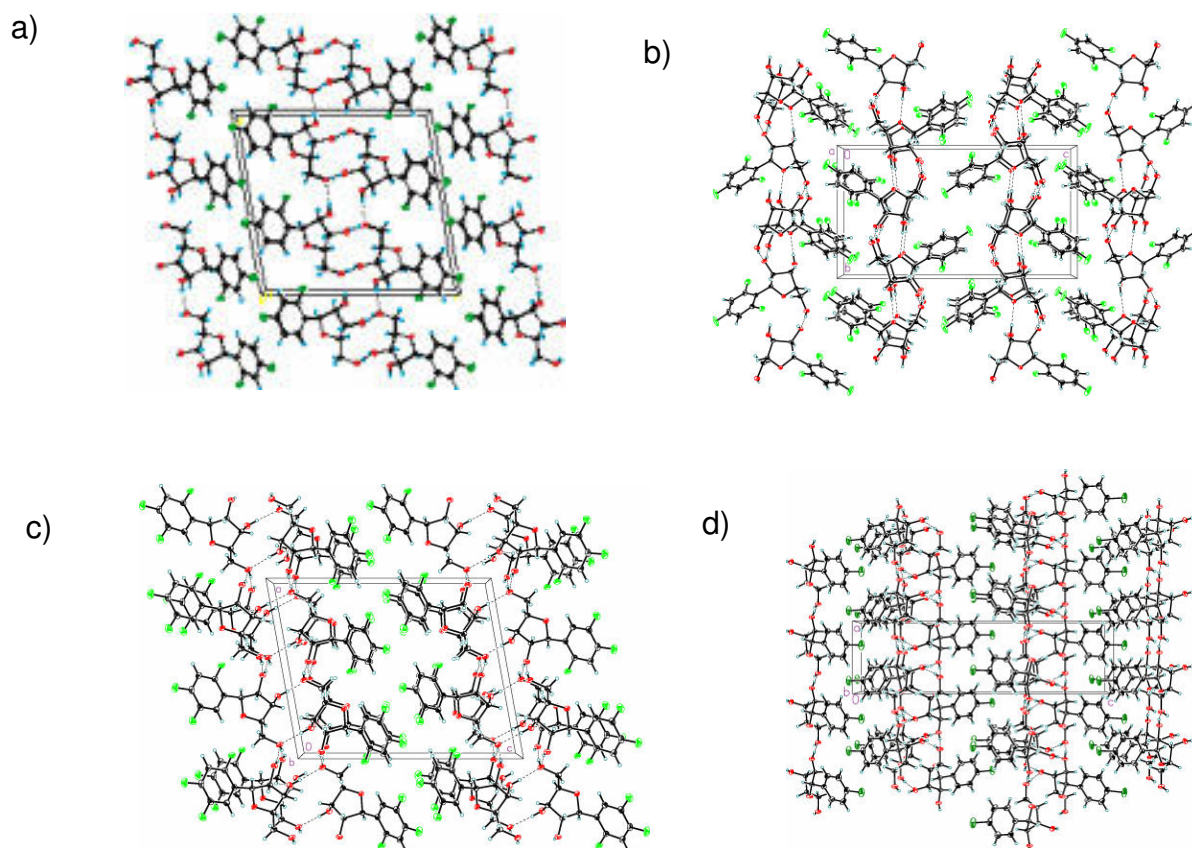


Figure 6.7. Crystal packing of: a) 1'-deoxy-1'-(2,4-difluorophenyl)-β-D-ribofuranose b) 1'-deoxy-1'-(2,4,6-trifluorophenyl)-β-D-ribofuranose c) 1'- deoxy-1'-(2,4,5-trifluorophenyl)-β-D-ribofuranose d) 1'-deoxy-1'-(4-chlorophenyl)-β-D-ribofuranose

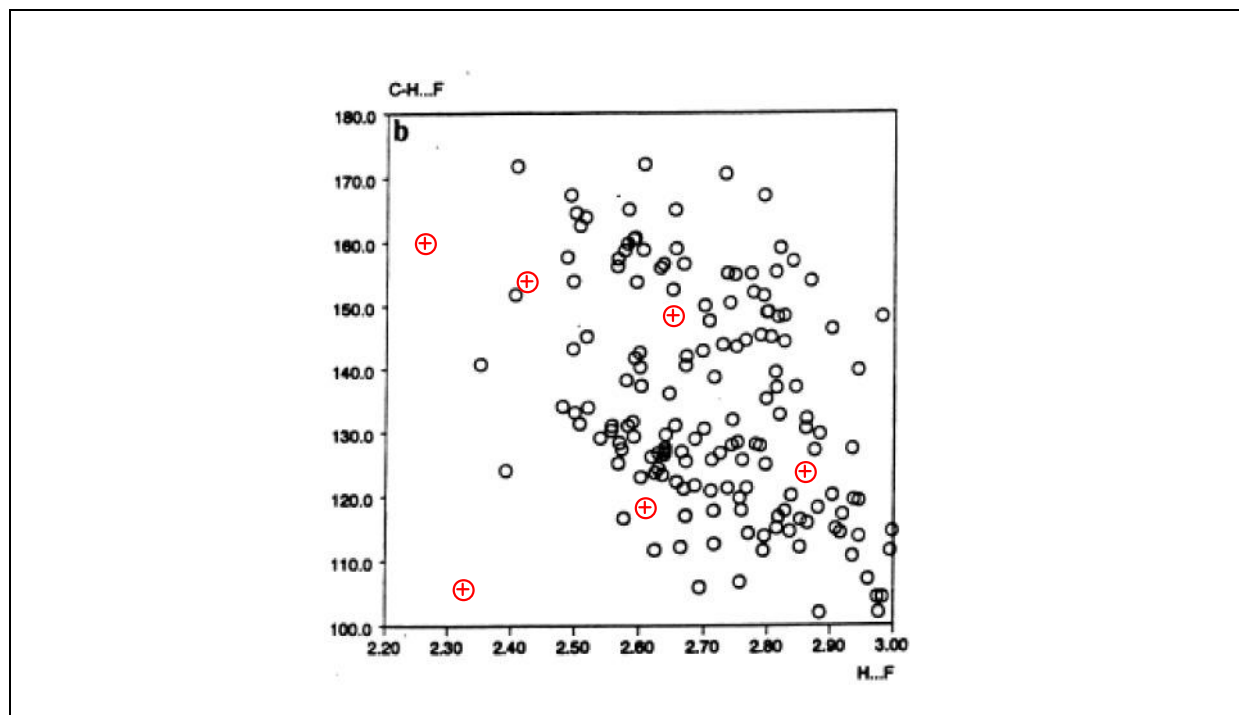


Figure 6.8.  $F\dots H$  distances and angle of hydrogen bonds of  $C_{sp^2}\text{-}F\dots H\text{-}C_{sp^2}$  (Thalladi et al., 1998) filled with distances found and mentioned in this work (red circles) (Parsch, 2000)

#### 6.4 Crystal Structure of 5'-O-(4,4'-dimethoxytriphenylmethyl)-2'-O-tert.-butyldimethylsilyl-1'-deoxy-1'-(4,6-difluoro-1-N-benzimidazolyl)- $\beta$ -D-ribofuranose

Unfortunately, we couldn't crystallize any of our fluoro-benzimidazole modifications. However, one of our derivatives, while preparing phosphoramidite (TBDMS protected derivative), crystallized after HPLC separation from the mixture isopropanol:hexane. The properties of the crystal structure of the title compound were the following:

The five-membered furanose ring has a twisted O4-endo, C1-exo conformation. The C1-N1, C2-O2 and C4-C5 bonds are in pseudo-equatorial positions, the C3-O3 bond is in a bisecting position with respect to the furanose ring. A different conformation (C2-endo) has been reported for the related 2-chloro-( $\beta$ -D-ribofuranosyl)-benzimidazole (Sprang & Sundaralingam, 1973). The bond distances in the ribofuranosyl group are very similar in the title compound and in the 2-chloro-( $\beta$ -D-ribofuranosyl)-benzimidazole structure, with rather short O4-C1 and C4-C5 bonds and a long O4-C4 bond. The benzimidazole group adopts a syn orientation about the glycosyl bond with a torsion angle O4-C1-N1-C12 of 62.5°. The

benzimidazole group is planar (mean deviation from the plane: 0.008 Å). The orientation about the exocyclic C4-C5 bond is +sc (gauche,gauche). The shortest intramolecular contacts are O5...H3 2.40 Å, O5...H32 2.42 Å and O5...H35 2.41 Å. The angles between the planes of the three phenyl groups attached to C19 are 64.5°, 74.5° and 85.2°. The molecules are connected by intermolecular hydrogen bonds between the hydroxyl group and the imidazole group to chains running in the crystallographic b-direction, which also corresponds to the long macroscopic dimension of the crystal. The hydrogen bonded chains are also stabilized by intermolecular C3-H3...F1 contacts with an H...F distance of 2.43 Å and a C-H..F angle of 150°. The crystal packing also shows an additional intermolecular C-H...O contact and three intermolecular C-H... $\pi$ (phenyl) contacts.

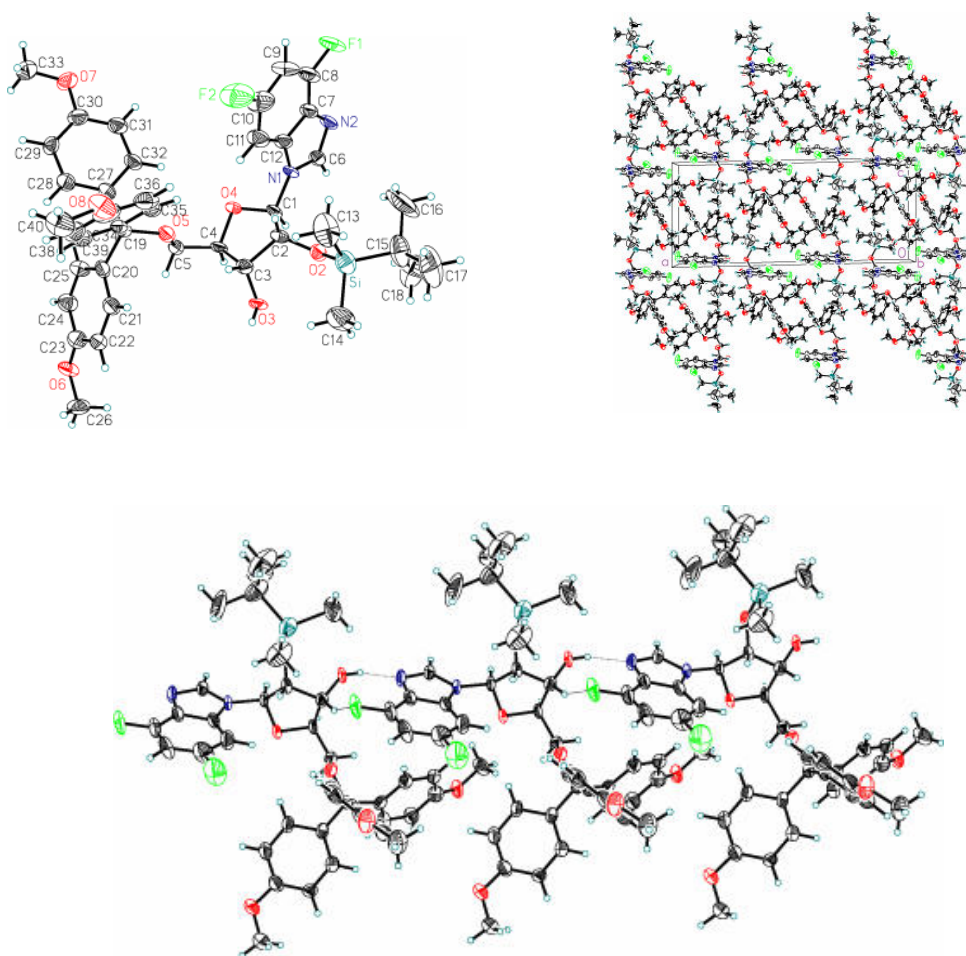


Figure 6.9. Crystal Structure of 5'-O-(4,4'-dimethoxytriphenylmethyl)-2'-O-tert.-butyldimethylsilyl-1'-deoxy-1'-(4,6-difluoro-1-N-benzimidazolyl)- $\beta$ -D-ribofuranose

As one can see from figure 6.9. this crystal structure is also stabilized with F...H hydrogen bonds which are also one of the shortest hydrogen F..H bonds known( similar to that in 4-

fluorobenzimidazole modification). We represented this distance, as all distances F...H for fluoro-benzene modifications, in a graph to compare this one with other known F...H distances.

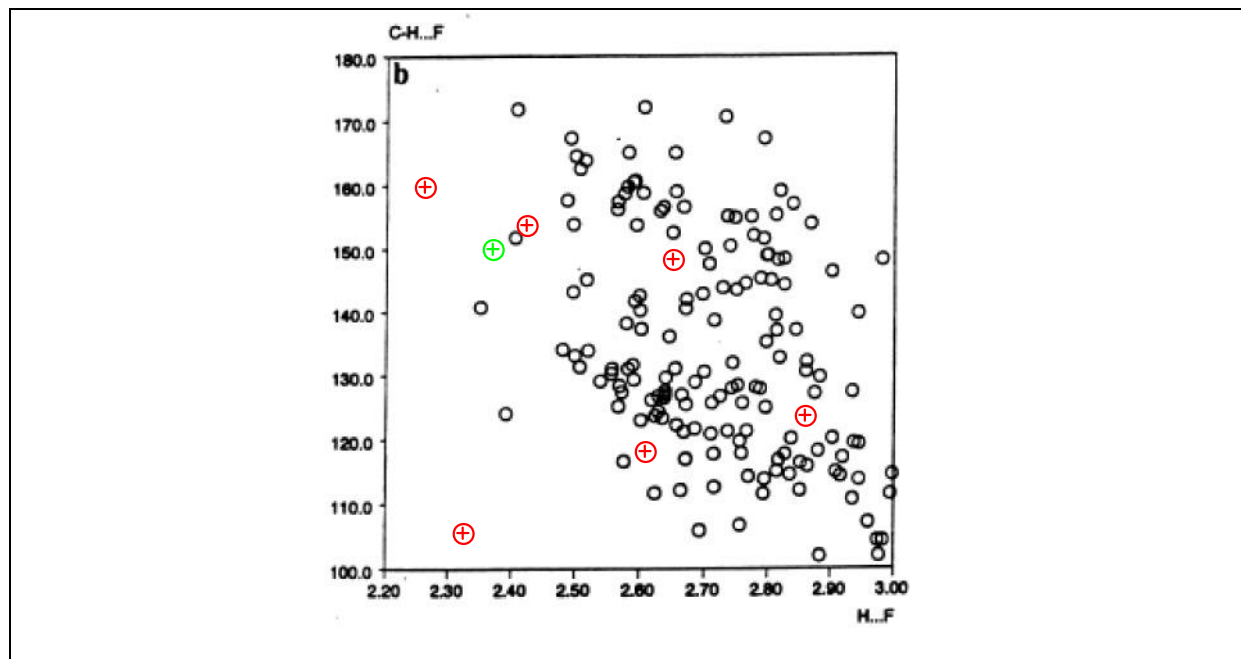


Figure 6.10.  $F\dots H$  distances and angle of hydrogen bonds of  $C_{sp^2}\text{-}F\dots H\text{-}C_{sp^2}$  (Thalladi et al., 1998) fulfilled with distances found and mentioned in this work (Parsch, 2000)-green for title compound, red for fluoro benzene modifications



# 7 Oligonucleotides

## 7.1 Synthesis of Oligonucleotides

Oligonucleotides are long-chain molecules built from nucleotides. The reaction conditions differ slightly for DNA- and RNA- synthesis. By RNA- synthesis coupling times are longer and in the synthesis of nucleotides the 2'-position has to be protected. The connection of the building blocks (nucleotides) is from 3' to 5' direction.

In the 70s Letsinger developed solid phase synthesis of oligonucleotides (Letsinger *et al.*, 1975; Letsinger *et al.*, 1976) on the base of solid phase synthesis of polipeptides (Merrifield, 1963). Solid phase synthesis of oligonucleotides has great advantages over the synthesis in solution. Oligonucleotide synthesis lasts significantly shorter and there is no need to purify products after every synthesis step. The synthesis process is automated.

Nucleotides for the synthesis have to be protected at free OH and NH<sub>2</sub> groups, to avoid side products in the synthesis. Known automatic methods are: phosphodiester method, phosphotriester method (Narang *et al.*, 1980), H-phosphonate method (Garegg *et al.*, 1986), today mostly used is phosphoramidite method (Beaucage & Caruthers, 1981; Sinha *et al.*, 1983; Eckstein, 1991).

### 7.1.1 Phosphoramidite method

The most important method for synthesising oligonucleotides, using automatic solid phase synthesis, is the phosphoramidite method (phosphite-triester-method) (Beaucage & Caruthers, 1981; Sinha *et al.*, 1983; McBride & Caruthers, 1983; Gait, 1984; Caruthers, 1985; Caruthers *et al.*, 1987; Eckstein, 1991; Beaucage & Iyer, 1992; Beaucage & Iyer, 1993). In the coupling, one protected nucleoside is activated with an activator (usually 1H-tetrazole) reacts with 5'-

OH group of the next nucleoside. After every step the oxidation of phosphitetriester is done (Figure 7.1. ). Activation with 1H-tetrazole gives from phosphoamidite a reactive species, which doesn't make any known side products.

The synthesis cycles of the phospho-amidite-solid phase method is given in figure 7.2. . As starting nucleoside the 5'-dimethoxytrityle protected nucleoside can be used, which is bound to the solid phase over 3'-hydroxyl group with a spacer (usually succinate linker).

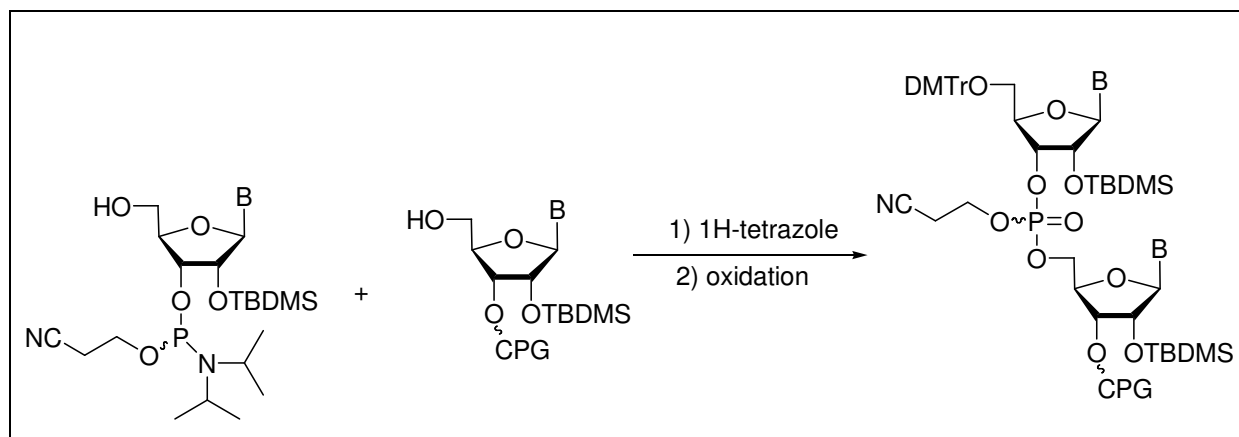


Figure 7.1. Phosphoramidite method

In most cases solid phase support is made from glass balls, with defined pore size, known as controlled pore glass (CPG). Steps of the oligonucleotide synthesis are the following:

- Deprotection of 5'-dimethoxytrityle group with 3% trichloro acetic acid in methylene chloride
- Activation of the amidite with 1H-tetrazole in acetonitrile
- Coupling
- Protection of the unreacted 5'-OH group with acetic anhydride/2,6-lutidine/THF and 1-methylimidazole in THF, known as "capping"
- Oxidation of the phosphite to phosphate with iodine in water/pyridine/THF

After complete synthesis the separation from the solid phase support is done with conc. ammonia solution.

After every synthetic step washing with acetonitrile is done. Exocyclic amino groups on the nucleobases are protected with acyl protecting groups like benzoyl (for A and C), isobutyryl (for G). Sometimes the tac protecting group (tac= tert. Butylphenoxyacetyl), which main advantage is fast deprotection (3 h), is also used. Those protecting groups are deprotected together with cleavage from the solid phase support, over night at 55°C in ammonia solution.

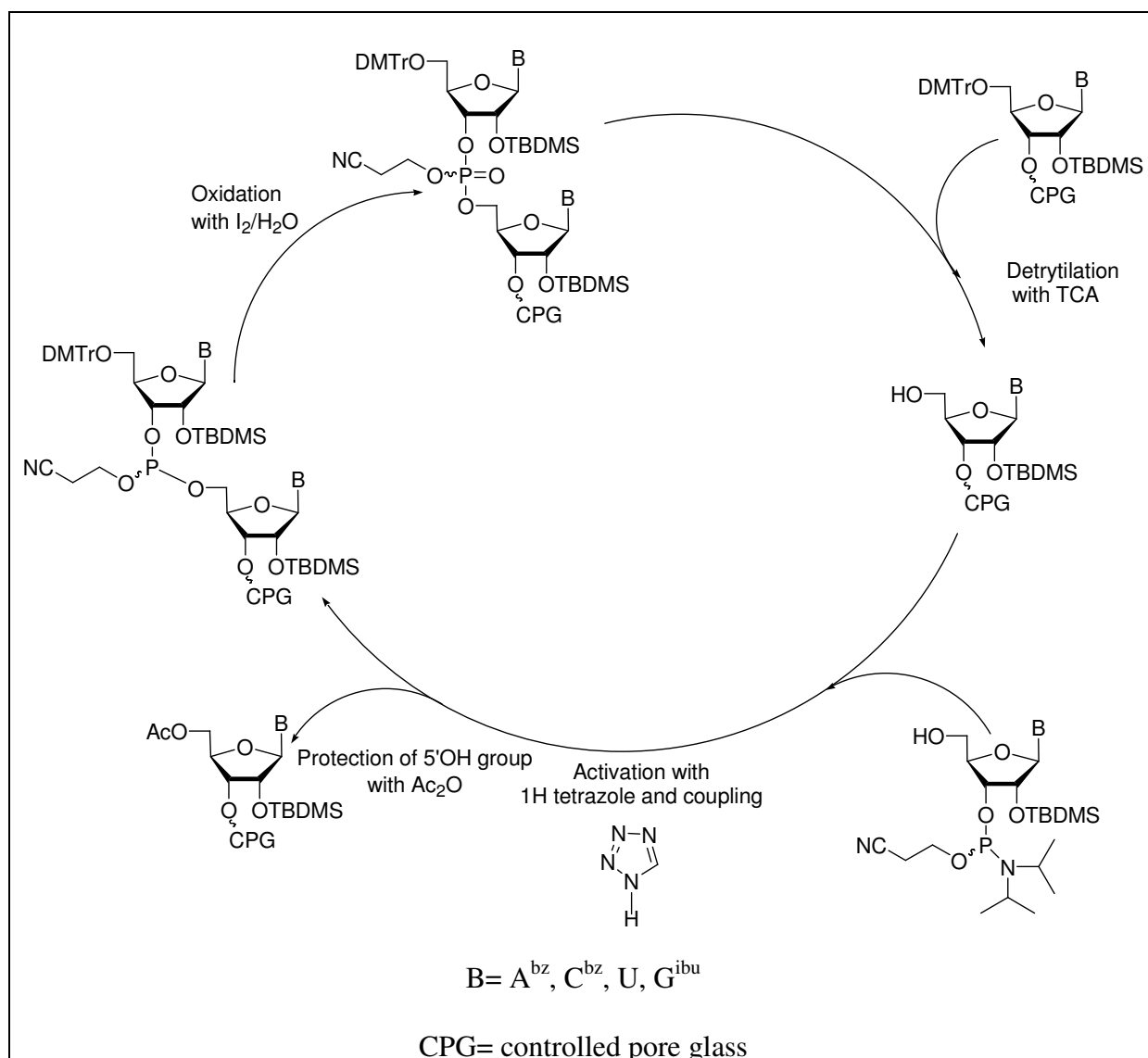


Figure 7.2. Synthesis of RNA using phosphoramidite chemistry

The mechanism of 1H-tetrazole catalysis is not yet completely explained. It is however thought that tetrazole reacts as acid and protonates the nucleoside at phosphor or nitrogen. The resulting cation reacts with a second tetrazole molecule to make tetrazolide. This is the reactive species, which reacts with 5'-OH-group on the support (Dahl *et al.*, 1987). <sup>31</sup>P NMR investigations of Berner confirmed this mechanism (Berner *et al.*, 1989).



## 7.2 Synthesised Oligonucleotides

All oligonucleotides synthesised in this work were synthesised with the phosphoramidite method on 1  $\mu$ mol synthesis on PerSeptive Biosystems (Modell Expedite 8905). We used columns from PerSeptive Biosystems with CPG support. All the used chemicals and reagents are given in chapter 11. Standard coupling time of 10 minutes was used for all modified and unmodified nucleotides. Final dimethoxytrityle group was cleaved on all oligonucleotides. All nucleotides incorporated in the RNA are shown in *figure 7.3* .

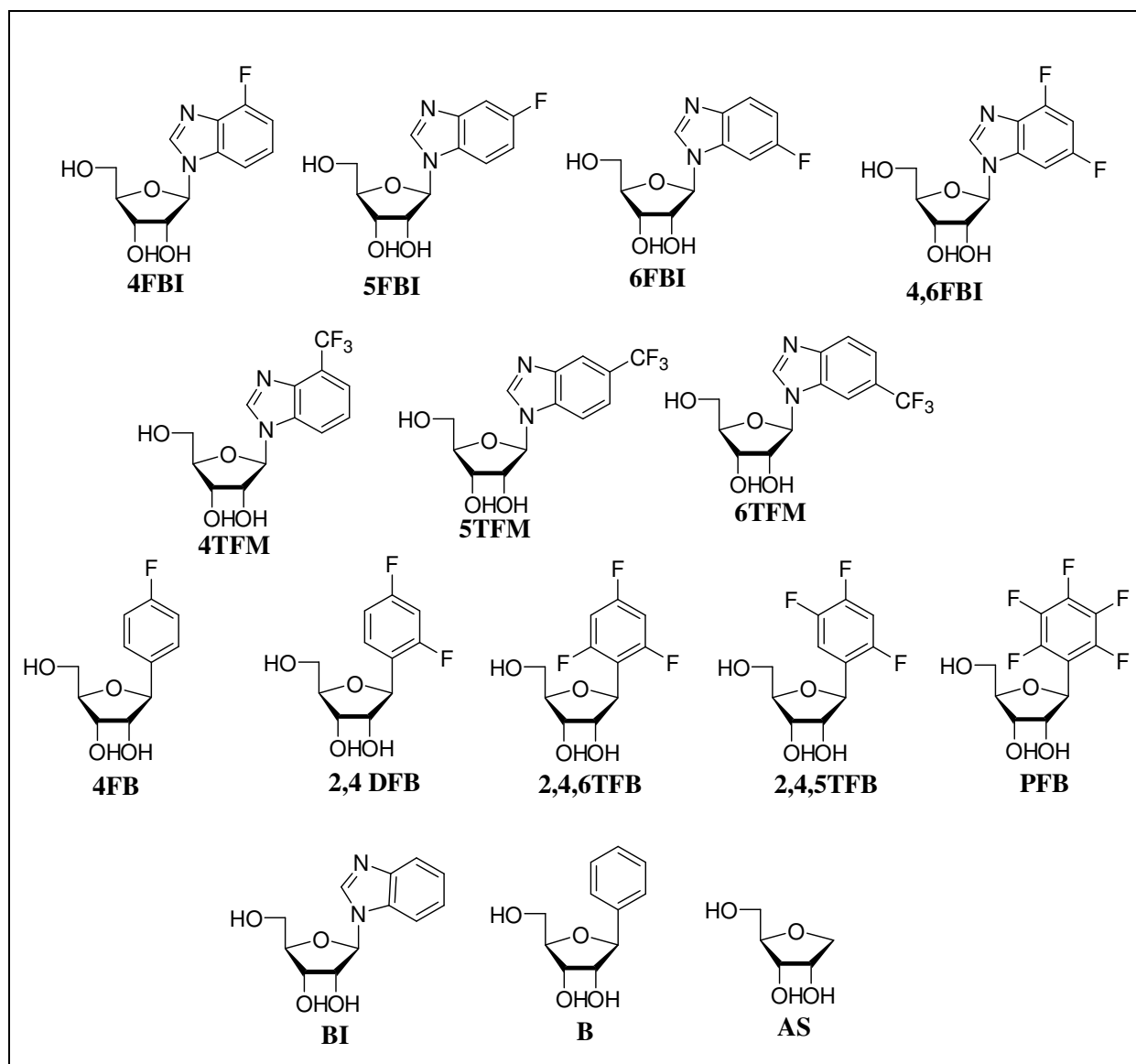


*Figure 7.3. Incorporated nucleosides in RNA and their abbreviations*

The nucleotides synthesised in this work were incorporated in A-rich strands and U-rich strands. Modifications were incorporated in the middle and paired with each other and natural nucleotides to measure T<sub>m</sub> values and other thermodynamical parameters. In *figure 7.4*, synthesised modified RNA oligonucleotides are given.

'Name''	Sequence	'Name''	Sequence
<b>S1</b>	5'-CUU UUC UUU CUU-3'	<b>S20</b>	5'-AAG AAG GAA AAG-3'
<b>S2</b>	5'-CUU UUC CUU CUU-3'	<b>S21</b>	5'-AAG AAU GAA AAG-3'
<b>S3</b>	5'-CUU UUC AUU CUU-3'	<b>S22</b>	5'-AAG AAA GAA AAG-3'
<b>S4</b>	5'-CUU UUC GUU CUU-3'	<b>S23</b>	5'-AAG AAC GAA AAG-3'
<b>S5</b>	5'-CUU UUC <b>4FBUU</b> CUU-3'	<b>S24</b>	5'-AAG AA <b>4FBI</b> GAA AAG-3'
<b>S6</b>	5'-CUU UUC <b>2,4DFBUU</b> CUU-3'	<b>S25</b>	5'-AAG AA <b>5FBI</b> GAA AAG-3'
<b>S7</b>	5'-CUU UUC <b>2,4,6TFBUU</b> CUU-3'	<b>S26</b>	5'-AAG AA <b>6FBI</b> GAA AAG-3'
<b>S8</b>	5'-CUU UUC <b>2,4,5TFBUU</b> CUU-3'	<b>S27</b>	5'-AAG AA <b>4,6DFBI</b> GAA AAG-3'
<b>S9</b>	5'-CUU UUC <b>PFBUU</b> CUU-3'	<b>S28</b>	5'-AAG AA <b>4TFM</b> GAA AAG-3'
<b>S10</b>	5'-CUU UUC <b>BUU</b> CUU-3'	<b>S29</b>	5'-AAG AA <b>5TFM</b> GAA AAG-3'
<b>S11</b>	5'-CUU UUC <b>ASUU</b> CUU-3'	<b>S30</b>	5'-AAG AA <b>6TFM</b> GAA AAG-3'
<b>S12</b>	5'-CUU UUC <b>4FBIUU</b> CUU-3'	<b>S31</b>	5'-AAG A <b>ABI</b> GAA AAG-3'
<b>S13</b>	5'-CUU UUC <b>5FBIUU</b> CUU-3'	<b>S32</b>	5'-AAG A <b>AB</b> GAA AAG-3'
<b>S14</b>	5'-CUU UUC <b>6FBIUU</b> CUU-3'	<b>S33</b>	5'-AAG AA <b>AS</b> GAA AAG-3'
<b>S15</b>	5'-CUU UUC <b>4,6DFBIUU</b> CUU-3'	<b>S34</b>	5'-AAG AA <b>4FB</b> GAA AAG-3'
<b>S16</b>	5'-CUU UUC <b>4TFMUU</b> CUU-3'	<b>S35</b>	5'-AAG AA <b>2,4DFB</b> GAA AAG-3'
<b>S17</b>	5'-CUU UUC <b>5TFMUU</b> CUU-3'	<b>S36</b>	5'-AAG AA <b>2,4,6TFB</b> GAA AAG-3'
<b>S18</b>	5'-CUU UUC <b>6TFMUU</b> CUU-3'	<b>S37</b>	5'-AAG AA <b>2,4,5TFB</b> GAA AAG-3'
<b>S19</b>	5'-CUU UUC <b>BIUU</b> CUU-3'	<b>S38</b>	5'-AAG A <b>APFB</b> GAA AAG-3'

*Figure 7.4. Synthesised RNA oligonucleotides*

### 7.3 Purification of Oligonucleotides

Purification of oligonucleotides was done with ion-exchange-HPLC. This method gives the highest level of purity of wanted oligonucleotides. The ion exchange HPLC is standard method for short RNA sequences.

The ion exchange HPLC separates according to charge differences. Main principle of this effective method leans on forces between negative charges of oligonucleotide and stationary phase immobilised cationic groups. Bound oligonucleotides are then eluted with rising

gradient of salt (rising ion strength) where the wanted nucleotide is the last one. Therefore there is a lot of salt and oligonucleotides have to be desalted. For that are used: gel filtration and dialysis. We used gel filtration. The main principle for separation in this method is diffusion of molecules of the probes in the pores of stationary phase. Polymer separating material as for example Sephadex G25, has small pores, in which diffused molecules of salt stay while the large oligonucleotide molecules stay in pores and are eluted. For desalting in this work commercial columns packed with Sephadex G25 are used.

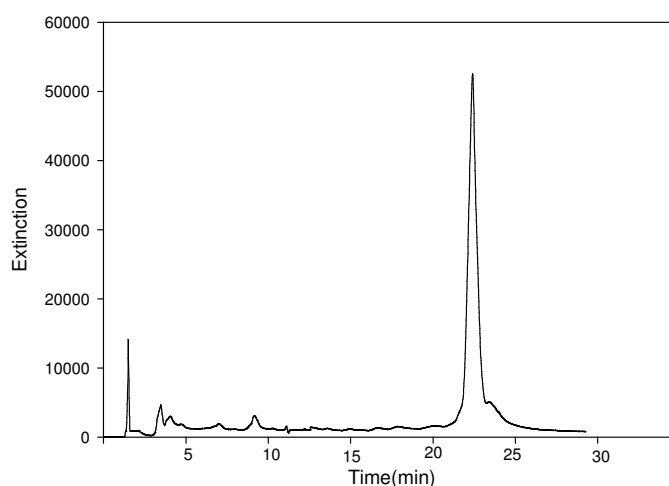


Figure 7.5. HPLC diagram from S 29

Figure 7.5. shows as an example a HPLC diagram from strain S 29 . It is easy to recognise the main signal around 20 minutes of clean 12-mer oligonucleotide. Other signals belong to shorter sequences. Details of HPLC separations are described in the experimental part (chapter 11).

After purification and desalting the amounts of synthesised oligonucleotides were measured using UV-spectroscopy. Therefore the extinction of the probe was measured at 260 nm. Measured optical density (OD) is used for calculating the concentration of the probes using Lambert-Beer equation ( Chapter 11). The calculation of extinction coefficients is given in chapter 10. For the synthesised oligonucleotides extinction coefficients are given in figure 7.10 .

## 7.4 Characterizations of Oligonucleotides

Even though retention times of oligonucleotides give an idea of their length all synthesised oligonucleotides were characterized by mass measurements. However, mass measurements tell us also if all protecting groups are cleaved completely. For the mass measurements there are two methods: electron spray-ionisation-(ESI) and matrix- assisted laser desorption/ionization (MALDI). Both methods could be used. In this work all oligonucleotides were characterized by MALDI. As ESI was used for characterization of phosphoramidite modification synthesis we will represent it here shortly, also.

- Electron spray-ionisation-mass spectrometry (ESI)

That is a special form of ionisation under atmospheric pressure. The phenomena of electro spray has been known for hundreds years (Chapman, 1937), but is not until the early parts of the 20th century that its significance to science was fully understood. Some 30 years later, the pioneering experiments by Malcom Dole *et al* (Dole *et al.*, 1968; Dole *et al.*, 1970) demonstrated the use of electro spray to ionise intact chemical species and the technique of electro spray ionisation (ESI) was invented. The ESI source has undergone continued development since the earliest examples, but the general arrangement has remained basically the same - see *figure 7.6*. The analyte is introduced to the source in solution either from a syringe pump or as the eluent flow from liquid chromatography. Flow rates are typically of the order of  $1\mu\text{l min}^{-1}$ . The analyte solution flow passes through the electro spray needle that has a high potential difference (with respect to the counter electrode) applied to it (typically in the range from 2.5 to 4 kV). This forces the spraying of charged droplets from the needle with a surface charge of the same polarity to the charge on the needle. The droplets are repelled from the needle towards the source-sampling cone on the counter electrode (shown in blue). As the droplets traverse the space between the needle tip and the cone and solvent evaporation occurs. As the solvent evaporation occurs, the droplet shrinks until it reaches the point that the surface tension can no longer sustain the charge (the Rayleigh limit) at which point a "Coulombic explosion" occurs and the droplet is ripped apart. This produces smaller droplets that can repeat the process as well as naked charged analyte molecules. These charged analyte molecules (they are not strictly ions) could be singly or multiply charged. This is a very soft method of ionisation as very little residual energy is retained by the analyte upon ionisation. This is why ESI-MS is such an important technique in biological studies where the analyst often requires that non-covalent molecule-protein or protein-protein interactions are representatively transferred into the gas-phase. The major disadvantage of the technique is

that very little (usually no) fragmentation is produced. For structural elucidation studies, this leads to the requirement for tandem mass spectrometry where the analyte molecules can be fragmented. One of the main problems with the mass spectral analysis of proteins (and other macromolecules) has always been that their masses fall outside the mass ranges of most mass spectrometers. A problem that also occurs is presence of salts, especially sodium salts. In this way products with negatively charged phosphorus backbone are build and process of ionisation is disturbed. A possible solution to this problem is exchange of sodium with ammonium ion, which through ammonium acetate precipitation can be removed (Stults & Masters, 1991).

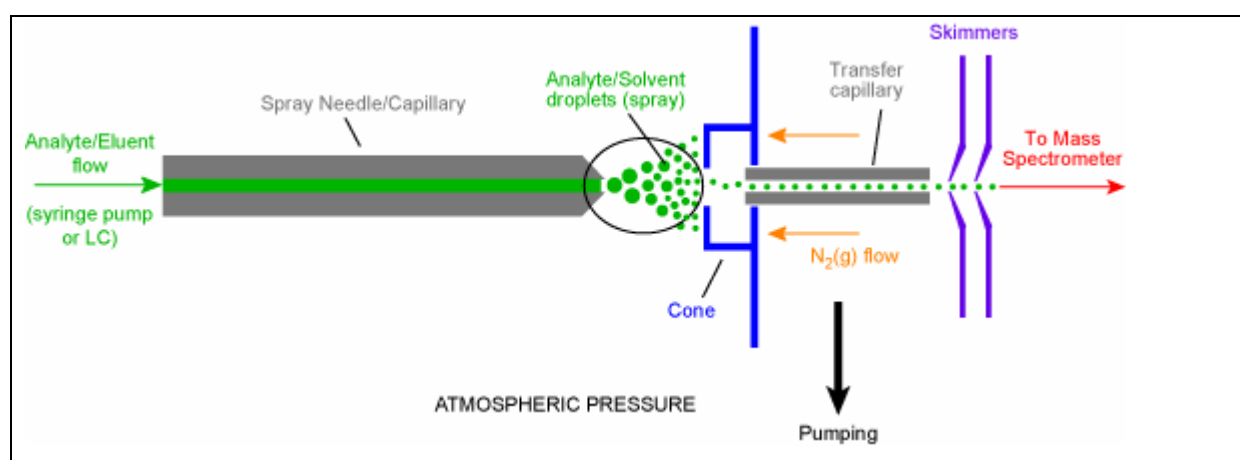


Figure 7.6. A schematic of an ESI source (picture-University of Bristol)

- Matrix assisted desorption/ionisation mass spectrometry (MALDI)

Matrix-assisted laser desorption/ionization mass spectrometry (MALDI-MS) has been responsible for solving many problems in structural biology. It was discovered by Karas and Hillenkamp (Karas and Hillenkamp, 1988) and Tanaka (Tanaka *et al.*, 1988). Mass analysis is now used routinely to confirm proper expression and processing of proteins, and to locate and identify post-translational modifications. Innovative advances in instrumentation have led to higher mass resolution and mass accuracy. New sample preparation methods are likewise yielding higher sensitivity plus greater tolerance for buffer components that have in the past-suppressed signals at higher concentrations. Advancements in the technique have also led to new or improved applications in many areas, including peptide sequencing and the identification of proteins by database searching with peptide masses. Instruments with lower cost, smaller size, and higher performance are making mass measurements available to an

increasing number of laboratories. MALDI-MS is poised to continue to improve in performance and in its usefulness for current and new applications.

To explain, we'll walk through the MALDI process to see just how it takes place. First of all, we take our probe, and we dissolve it in a solvent (water). We also add a special ingredient. The special ingredient is a compound like *trans*-cinnamic acid or 2,5-dihydroxybenzoic acid. It varies from polymer to polymer, but the important thing is that our special ingredient has to absorb ultraviolet light. Usually we put about  $10^4$  times more of our UV absorber than polymer. Once all this is mixed together, the sample is placed in an airtight chamber, on the tip of the *sample probe* (take a look at the picture below in *figure 7.7.*). With a vacuum pump we then suck all the air out of the chamber, or at least very close to all of it. When we do this the solvent evaporates, and we're left with layer of our UV-absorbing compound, with a little bit of our polymer in it. In fancy words, we like to say that the polymer is now dispersed in a *matrix* of the UV-absorbing compound. That's why we call it *matrix*-assisted laser desorption/ionization mass spectrometry.

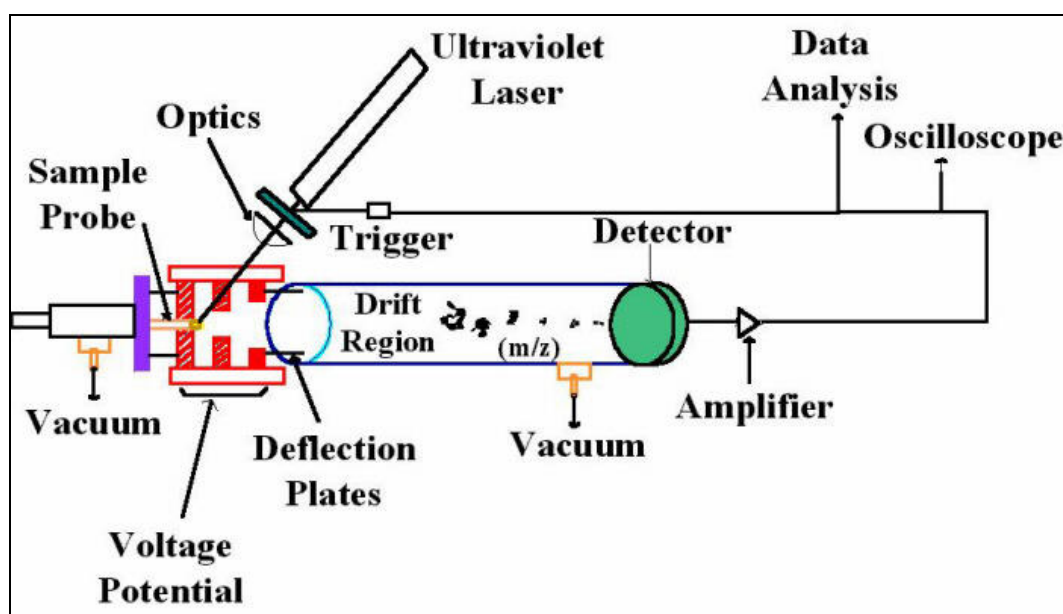


Figure 7.7. A diagram of a MALDI apparatus

Usually an ultraviolet laser is used in the 330-360 nm range ( Karas & Hillenkamp, 1988; Tanaka *et al*, 1988; Bahr *et al*, 1994; Fitzgerald & Smith, 1995; Piels *et al.*,1993; Kirpekar *et al.*, 1994). MALDI is in comparison with ESI less sensitive to the existence of salt in probes. RNA oligonucleotides show higher stability in MALDI measurements than DNA oligonucleotides (Lehmann, 1996).

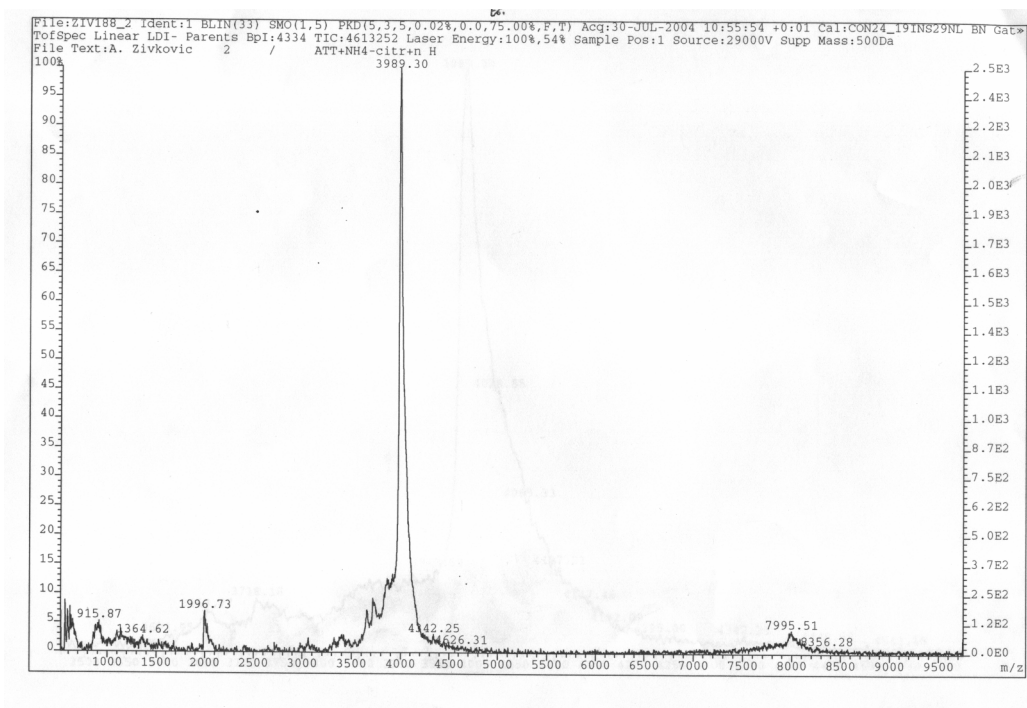


Figure 7.8. MALDI-spectra of oligonucleotide S 28 (incorporated 4TFM in G,A-reachsequence)

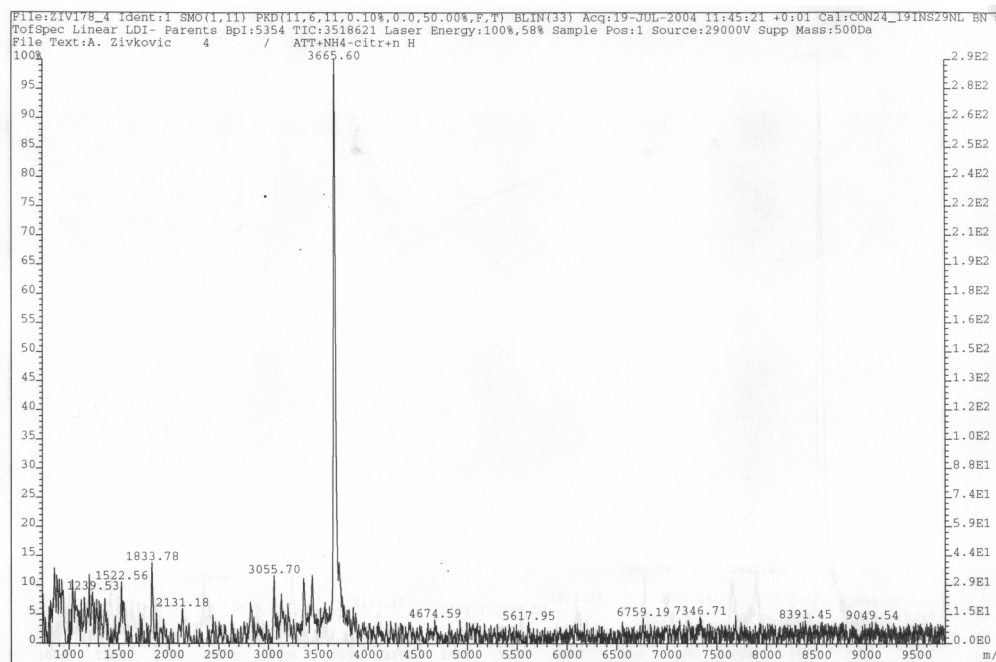


Figure 7.9. MALDI-spectra of modified oligonucleotide S 9(PFB incorporated in C,U-reach sequence)

In figures 7.8. and 7.9. two MALDI-spectra of unmodified two modified oligonucleotides, one with fluoro-benzene modification and the other with trifluoromethyl benzimidazole modification are shown.

"Name"	Sequence	Calculated mass [Da]	Measured mass [Da]	Extinction coeff. (260 nm)
S1	5'-CUU UUC UUU CUU-3'	3609.07	3610.54	110.28
S2	5'-CUU UUC CUU CUU-3'	3608.12	3609.1	99
S3	5'-CUU UUC AUU CUU-3'	3632.15	3633.15	104.08
S4	5'-CUU UUC GUU CUU-3'	3648.15	3650.1	102.3
S5	5'-CUU UUC <b>4FBUU</b> CUU-3'	3593.07	3614.56	110.26
S6	5'-CUU UUC <b>2,4DFBUU</b> CUU-3'	3611.07	3634.4	110.26
S7	5'-CUU UUC <b>2,4,6TFBUU</b> CUU-3'	3629.07	3630.14	110.26
S8	5'-CUU UUC <b>2,4,5TFBUU</b> CUU-3'	3629.07	3630.15	110.26
S9	5'-CUU UUC <b>PFBUU</b> CUU-3'	3665.07	3665.60	110.26
S10	5'-CUU UUC <b>BUU</b> CUU-3'	3575.08	3595.46	110.26
S11	5'-CUU UUC <b>ASUU</b> CUU-3'	3499	3514.24	100.25
S12	5'-CUU UUC <b>4FBIUU</b> CUU-3'	3633.11	3634.23	104.08
S13	5'-CUU UUC <b>5FBIUU</b> CUU-3'	3633.11	3632.81	104.08
S14	5'-CUU UUC <b>6FBIUU</b> CUU-3'	3633.11	3656.11	104.08
S15	5'-CUU UUC <b>4,6DFBIUU</b> CUU-3'	3651.11	3652.1	104.08
S16	5'-CUU UUC <b>4TFMUU</b> CUU-3'	3685.11	3687.01	104.08
S17	5'-CUU UUC <b>5TFMUU</b> CUU-3'	3685.11	3686.21	104.08
S18	5'-CUU UUC <b>6TFMUU</b> CUU-3'	3685.11	3709.23	104.08
S19	5'-CUU UUC <b>IUU</b> CUU-3'	3615.11	3615.1	104.08
S20	5'-AAG AAG GAA AAG-3'	3952.55	3952.69	143.92
S21	5'-AAG AAU GAA AAG-3'	3913.51	3959.28	142.51
S22	5'-AAG AAA GAA AAG-3'	3936.52	3964.32	145.18
S23	5'-AAG AAC GAA AAG-3'	3912.5	3911.45	140.16
S24	5'-AAG AA <b>4FBI</b> GAA AAG-3'	3937.52	3954.62	145.18
S25	5'-AAG AA <b>5FBI</b> GAA AAG-3'	3937.52	3938.5	145.18
S26	5'-AAG AA <b>6FBI</b> GAA AAG-3'	3937.52	3941	145.18
S27	5'-AAG AA <b>4,6DFBI</b> GAA AAG-3'	3955.52	3978.79	145.18
S28	5'-AAG AA <b>4TFM</b> GAA AAG-3'	3989.6	3989.05	145.18
S29	5'-AAG AA <b>5TFM</b> GAA AAG-3'	3989.6	4008.9	145.18
S30	5'-AAG AA <b>6TFM</b> GAA AAG-3'	3989.6	3984.82	145.18
S31	5'-AAG AAI GAA AAG-3'	3919.54	3919.43	142.51
S32	5'-AAG AAB GAA AAG-3'	3879.49	3881.4	145.18
S33	5'-AAG AAAS GAA AAG-3'	3803.41	3804.24	133.2
S34	5'-AAG AA <b>4FB</b> GAA AAG-3'	3897.51	3920.6	142.51
S35	5'-AAG AA <b>2,4DFB</b> GAA AAG-3'	3915.51	3936.78	142.51
S36	5'-AAG AA <b>2,4,6TFB</b> GAA AAG-3'	3933.51	3934	142.51
S37	5'-AAG AA <b>2,4,5TFB</b> GAA AAG-3'	3933.51	3936.51	142.51
S38	5'-AAG AAP <b>FB</b> GAA AAG-3'	3969.51	3968.9	142.51

Figure 7.10. Overview over synthesised oligonucleotides, their calculated and found masses and also their extinction coefficients



In *figure 7.10*. calculated and measured masses by MALDI and extinction coefficients of those oligonucleotides are shown. For all synthesised oligonucleotides measured masses were in good accordance with calculated ones and therefore we can conclude that the wanted oligonucleotides were synthesised in the wanted sequence.

## 8 Spectroscopic Measurements of Oligonucleotides

### 8.1 UV-Spectroscopic Measurements

Employing UV spectroscopic measurements, the melting points of nucleic acids duplexes could be measured. The melting point of a duplex is the temperature at which exactly half of the molecules of one sample are still in a duplex. The other half of the molecules is at this temperature already melted and is single stranded in the sample. By UV measurements we use the characteristic that absorbance of the sample that contains a duplex and a single stranded sample is changed.

The change of absorbance is the reason of temperature dependence of UV-Spectroscopy. Through rising of the temperature the duplex is melted and pairing of bases, of heterocycles of nucleotides is disturbed, absorbance is also changed. While changing from duplex structure (high order) to single stranded structure the absorbance is rising. This is known as hyperchromicity. The melting point is not only dependent on the length and sequence of the duplex. It also depends on the salt concentration and pH value of the solution in which the sample is measured. With higher salt concentrations the melting point rises. We measured all the melting curves with phosphate puffer with 140 mM NaCl at pH 7.00. First we measured unmodified sequences of 12mer and one of those with the middle base pair of 2,4,5 TFB: 2,4 DFB is shown in the *figure 8.1.*, and has melting point of 33.2°C.

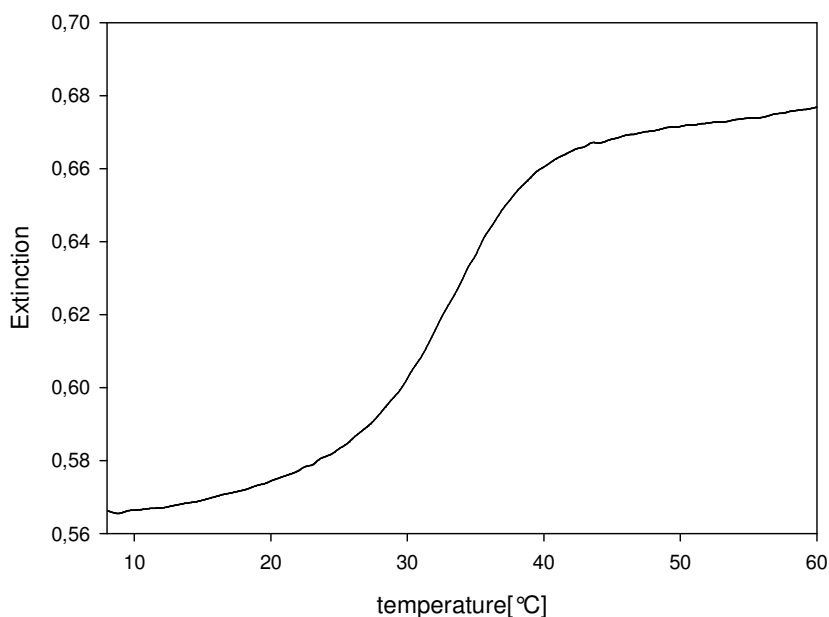


Figure 8.1. UV melting curve of S8 and S35 RNA duplex (2,4,5TFB-2,4DFB middle base pair)

The change of absorbance depends on the wavelength. The maximum for the A-T base pair is on 260 nm and for the G-C base pair is on 276 nm (Figure). The optimal value of wavelength for UV measurement is between those two values. Most samples were measured at 260 nm and 274 nm. Characteristic of the melting of nucleic acids is the cooperativity of the process (Saenger, 1984) that means that a nucleotide has an influence on the conformation of the neighbouring nucleoside. When one base pair is separated the hydrogen bonds of the neighbouring base pair are quickly broken. The structure of double helix is then ruined and we get non-paired single strands. The breaking down of double helices usually begins from one end of a helix and is moving fast through the helix. The consequence of this "cooperativity" is that the small oligonucleotides exist only either as duplexes or as single strands.

The UV- and CD-spectroscopy was our choice for determination of  $T_m$  values because of its easiness, the small amounts of substances and the reproducibility.

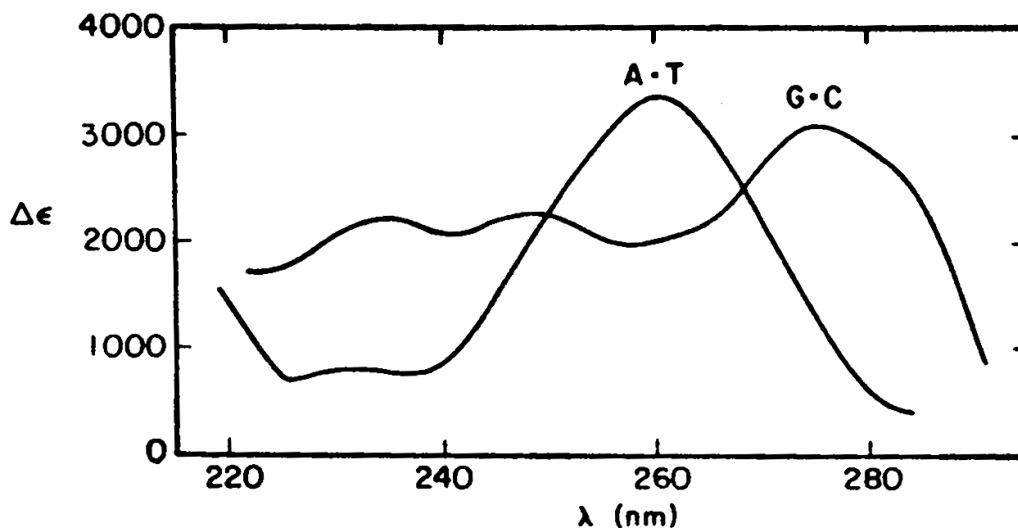


Figure 8.2. Wavelength dependence of the absorbance coefficient ( $\epsilon$ ) of CG- and AT-base pairs in DNA ( Felsenfeld & Hirschman, 1965)

In principle, the higher  $T_m$  value is the higher stability of the structure. From the melting curves we were also able to calculate other thermodynamic parameters  $\Delta H^\circ$ ,  $\Delta S^\circ$  and  $\Delta G^\circ$ . It is important to stress at this point that the calculated data only have value when we consider as existing the model "all-or-none".

Measuring the UV melting curves with the heating rate  $0.2^\circ\text{C}$  and  $0.5^\circ\text{C}$  did not show any differences in thermodynamical calculations and parameters so we measured all the curves with the heating rate of  $0.5^\circ\text{C}$ .

## 8.1.1 Calculations from UV- Melting Curves

### 8.1.1.1 Determination of the Melting Point

The UV-melting curves were measured using a UV-/VIS-spectrophotometer Cary from Varian company. As buffer we used phosphate buffer 140 mM NaCl, 10 mM  $\text{Na}_2\text{HPO}_4$  and 10 mM  $\text{NaH}_2\text{PO}_4$  with pH value of 7.00.

For measuring, we added from both samples of oligonucleotides the amount that makes a concentration of  $2\ \mu\text{M}$  in sample vial. The measurement of UV melting curve was done at 260 and 274 nm with a heating rate of  $0.5^\circ\text{C}/\text{min}$ . Details for measurements are given in chapter 10.

For the calculations from the melting curves it is important to know whether the sequences are self-complementary or not. The sequences that we used were not self complementary.

For the thermodynamical analysis the melting curve of a duplex (absorbance as the function of temperature) (*figure 8.1*) is transformed in the dependence of  $\alpha$ , which equals the fraction of single strands in the duplex state, as the function of temperature. (Markey & Breslauer, 1987). For this purpose we observe the melting process considering the model “all-or-none” as the existing one. This model considers that there is no transition state in-between ordered and disordered state. For the transformation from  $OD=f(T)$  to  $\alpha=f(T)$  the correction of the base line has to be done (after and before "melting") (*figure 8.3*). This takes in to the calculations the temperature dependence of absorbance. The correction of the base line has a linear relation to temperature and could be expressed with the following equations:

$$[8-1] \quad OD_d = m_d \cdot T + b_d$$

$$[8-2] \quad OD_u = m_u \cdot T + b_u$$

where OD is absorbance, m is slope, T is temperature, b is X-axis intercept, **d**-is down base line and **u** is upper base line.

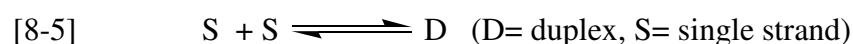
When any of the base lines is too short the error of determination of  $T_m$  value is greater. In this case the thermodynamical analysis of the curve is not possible because a bad correction of the base line is one of the biggest mistakes in determination (Puglisi & Tinoco, 1989).

As the measured absorbance is direct measure of the number of base pairs we can transform  $OD = f(T)$  curve into the  $\alpha = f(T)$  curve, where  $\alpha$  is fraction of single strands in a duplex state. The melting temperature is defined as a value of temperature at which exactly half molecules is in the duplex and the other half is denatured, where is also  $\alpha(T_m) = 0,5$ .

$$[8-3] \quad \alpha = [\text{oligonucleotide in duplex}] / [\text{all present oligonucleotides}]$$

$$[8-4] \quad \alpha = \{ [OD_0] - [OD(T)] \} / \{ [OD_0] - [OD_d] \}$$

For association of not self-complementary sequence in a double helix is valid:



and

$$[8-6] \quad K = [D] / [S]^2$$

The concentrations of both present single strands in the equilibrium constant  $K$  are equal and when we exchange that to express  $\alpha$

$$[8-7] \quad \{(1-\alpha) \cdot c_t/n\} \cdot \{(1-\alpha) \cdot c_t/n\} \rightleftharpoons \alpha \cdot c_t/n$$

and

$$[8-8] \quad K = \{\alpha \cdot c_t/n\} / \{(1-\alpha) \cdot c_t/n\} \cdot \{(1-\alpha) \cdot c_t/n\}$$

the general expression for the corresponding equilibrium constant, in terms of  $\alpha$  and  $n$ , is

$$[8-9] \quad K = \{\alpha \cdot c_t/n\} / \{(1-\alpha) \cdot (c_t/n)\}^n$$

where  $c_t$  is the strand concentration = [strand 1] + [strand 2] and  $n$  is the molecularity of the reaction. Reformulation of the previous equation gives us:

$$[8-10] \quad K = \alpha / \{(1-\alpha)^n \cdot (c_t/n)^{(n-1)}\}$$

For  $K$  at  $T = T_m$   $\alpha = 0,5$  and then:

$$[8-11] \quad K_{T=T_m} = 0,5 / \{(0,5)^n \cdot (c_t/n)^{(n-1)}\} = 1 / (c_t/2n)^{(n-1)}$$

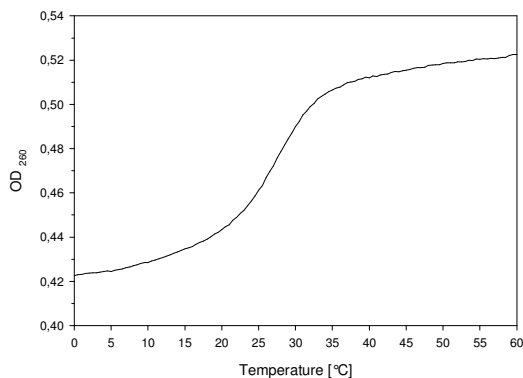
The last [8-11] equation gives a possibility to calculate  $K$  at the melting point of the reaction of association of not self-complementary sequences. In the case of bimolecular reaction ( $n=2$ ) and equation [8-11] is simpler:

$$[8-12] \quad K_{T=T_m} = 1 / (c_t/4) = 4 / c_t$$

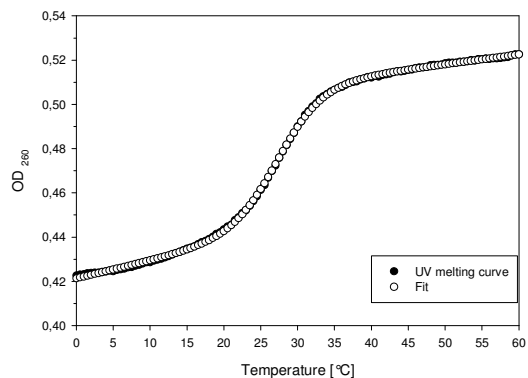
This means that the equilibrium constant  $K$  at  $T_m$  of bimolecular reactions is the function of the total concentration of single strands.

**S6** : 5'-CUU UUC 2,4DFBUU CUU-3' and **S22**: 5'-AAG AAA GAA AAG-3'

a) UV Melting curve



b) UV Melting curve-fit



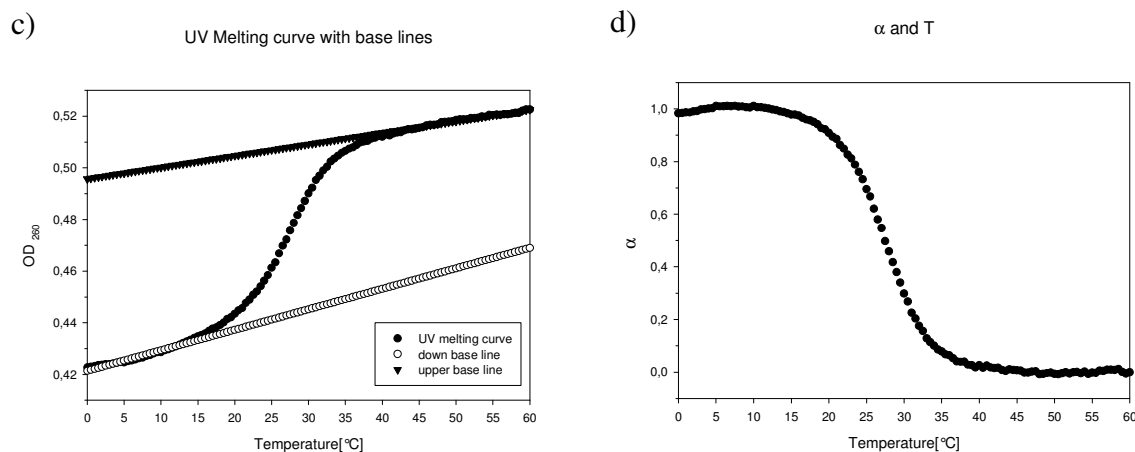


Figure 8.3. a) UV-melting curve of double helix b) Fitting of melting curve, c) melting curve with down and upper base line, d) transformed curve  $\alpha = f(T)$

### 8.1.1.2 Determination of Thermodynamical Data

In this part it will be explained how we calculated other thermodynamically parameters from spectroscopic measurements.

When the molecularity of the reaction is known, the thermodynamical parameters could be calculated using different approaches. The method that we used is the known van't Hoff method from  $R \ln K$  as the function of  $1/T$ . The other possibility results out from numerical differentiation of  $\alpha$  at the point when  $T=T_m$ , expressing  $1/T_m$  in terms of  $\ln c_i$  and curve fitting with help of algorithms.

#### 8.1.1.2.1 Van't Hoff Plot

Values for the equilibrium constants  $K$  can be calculated with equation [8-10] and could be calculated for the value of two for molecularity. Only the points that have  $0,15 \leq \alpha \leq 0,85$  are considered for the van't Hoff calculation because the values for  $K$  in between these values are most precise. Equation [8-13] gives the connection between  $\Delta G^0$  and  $K$  :

$$[8-13] \quad \Delta G^0 = -RT \ln K$$

With rearrangement of the basic equation:

[8-14] 
$$\Delta G^0 = \Delta H^0 - T\Delta S^0$$

to:

[8-15] 
$$\Delta S^0 = (\Delta H^0 - \Delta G^0) / T$$

and exchange in equation [8-15] gives:

[8-16] 
$$\Delta S^0 = (\Delta H^0 + RT \ln K) / T$$

simple rearrangement gives following equation:

[8-17] 
$$R \ln K = -\Delta H^0 \cdot 1/T + \Delta S^0$$

Determination of  $R \ln K$  to  $1/T$  gives  $-\Delta H^0$  as slope and  $\Delta S^0$  as X-axis intercept. An example is shown in *figure 8.4*. When  $\Delta H^0$  doesn't depend on temperature than the graph should be a straight line. A not linear graph could have several reasons: temperature dependence of  $\Delta H^0$ , bad correction of base line or the model "all-or-none" is not a suitable model.

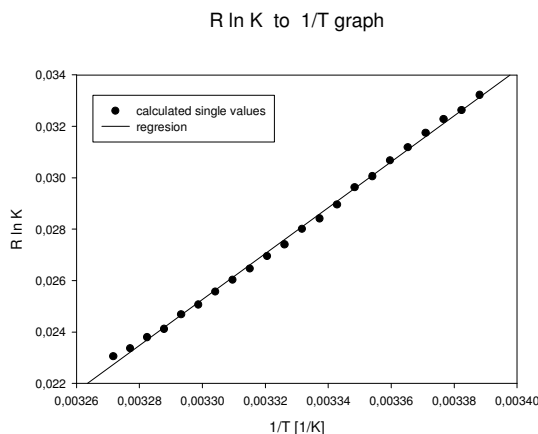


*Figure 8.4. R ln K to 1/T graph ( $r^2=0,998$ )*



### 8.1.2 Results of the UV-Melting Curves

Melting curves of RNA-duplexes were measured and the melting points ( $T_m$ ) were calculated using van't Hoff plot. Given values are for the dissociation reaction. We measured always RNA 12mers. The position of the modification was not changed.  $T_m$  values mentioned in the next chapters are on the 12mers if it is not stressed differently. The abbreviations for the modifications are given in *figure 8.5.* and are used every time the bases are mentioned in discussion.

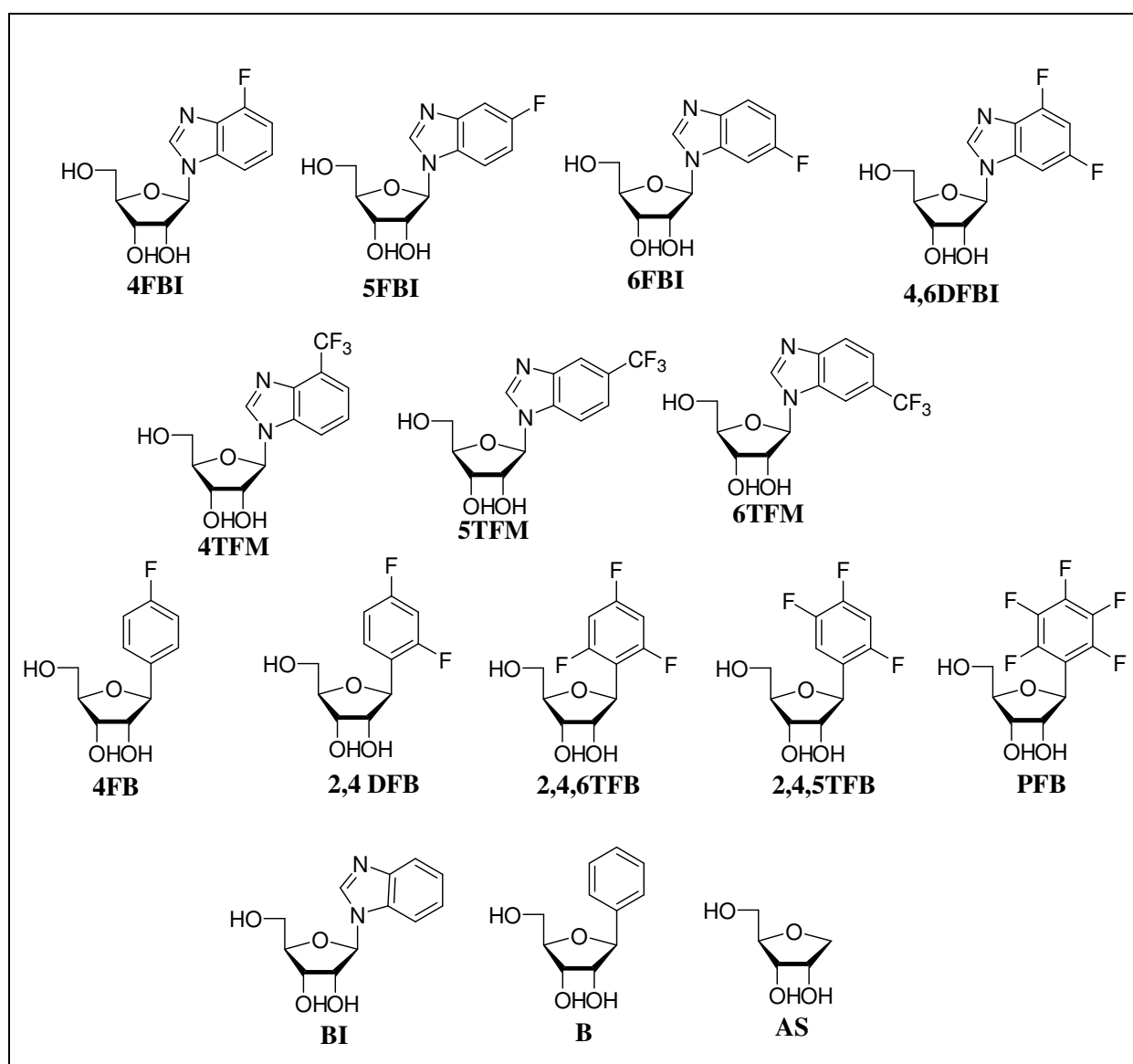
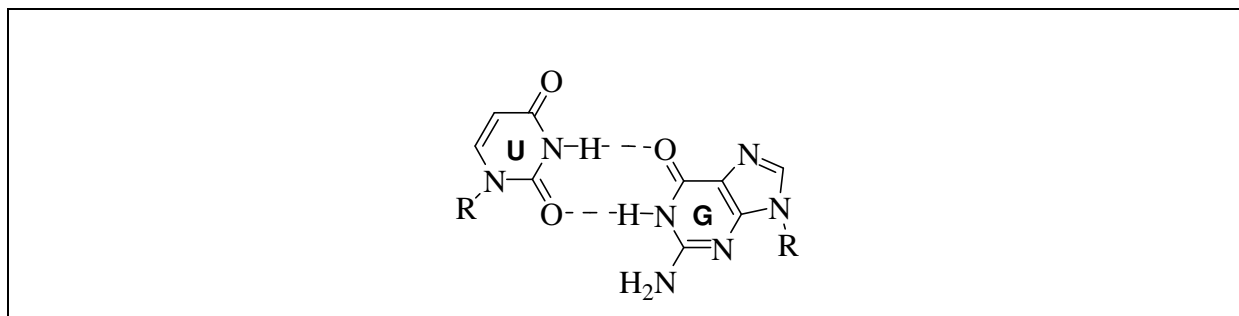


Figure 8.5. Abbreviations for synthesised nucleobases

First measurements were done on unmodified RNA chains. Uridine was paired with all natural bases. Natural U-A base pair did not build the most stable base pair but U-G did (so called Wobble base pair). In Wobble base pair the bases are slightly moved a side, so that donors and acceptors are in good positions for hydrogen bonding (*Figure 8.6*).



*Figure 8.6. Wobble base pair-(uridine-guanosine)*

Both other duplexes U-C and U-U are significantly less stable. In both RNA duplexes containing those two base pairs there aren't hydrogen bonds in between them and that makes those duplexes around 7.5°C or 2.1 kcalmol<sup>-1</sup> less stable (*figure 8.10.*).

Next measurements were done with fluoro-benzene and benzene nucleosides (*figure 8.10*).

The electrostatics vary widely over the series of benzene-nucleoside, with the phenyl nucleoside showing a negative potential at the center of the flat aromatic face, and the pentafluorinated case having a strongly positive potential. Thus the quadrupoles are gradually inverted over this series. By comparison natural bases are not so strongly polarized in the quadrupole sense and their quadrupole moments are close to zero. In this series of fluorobenzenes also could be seen a broad range of dipole moments though the dipole orientations are quite similar over the series (*figure 8.7.*).

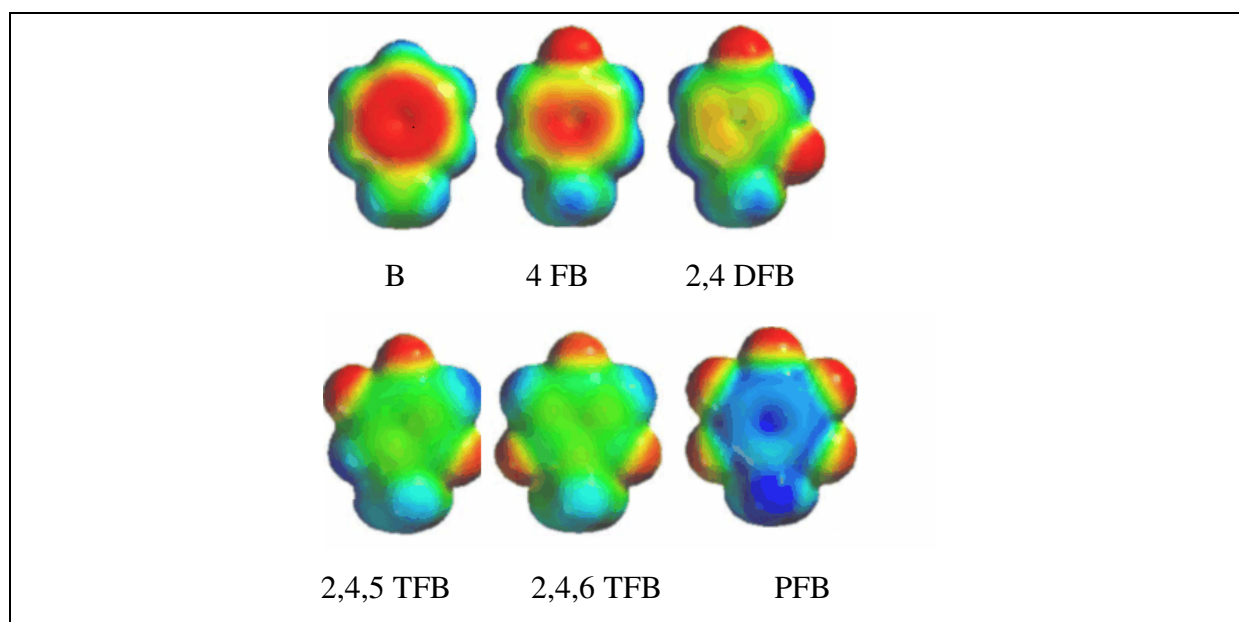


Figure 8.7. Calculated electrostatic surface potentials of six progressively fluorinated aromatic base analogues, with an attached methyl group to approximate effect of ribose (red shows negative potential and blue-positive)( Lai et al., 2003)

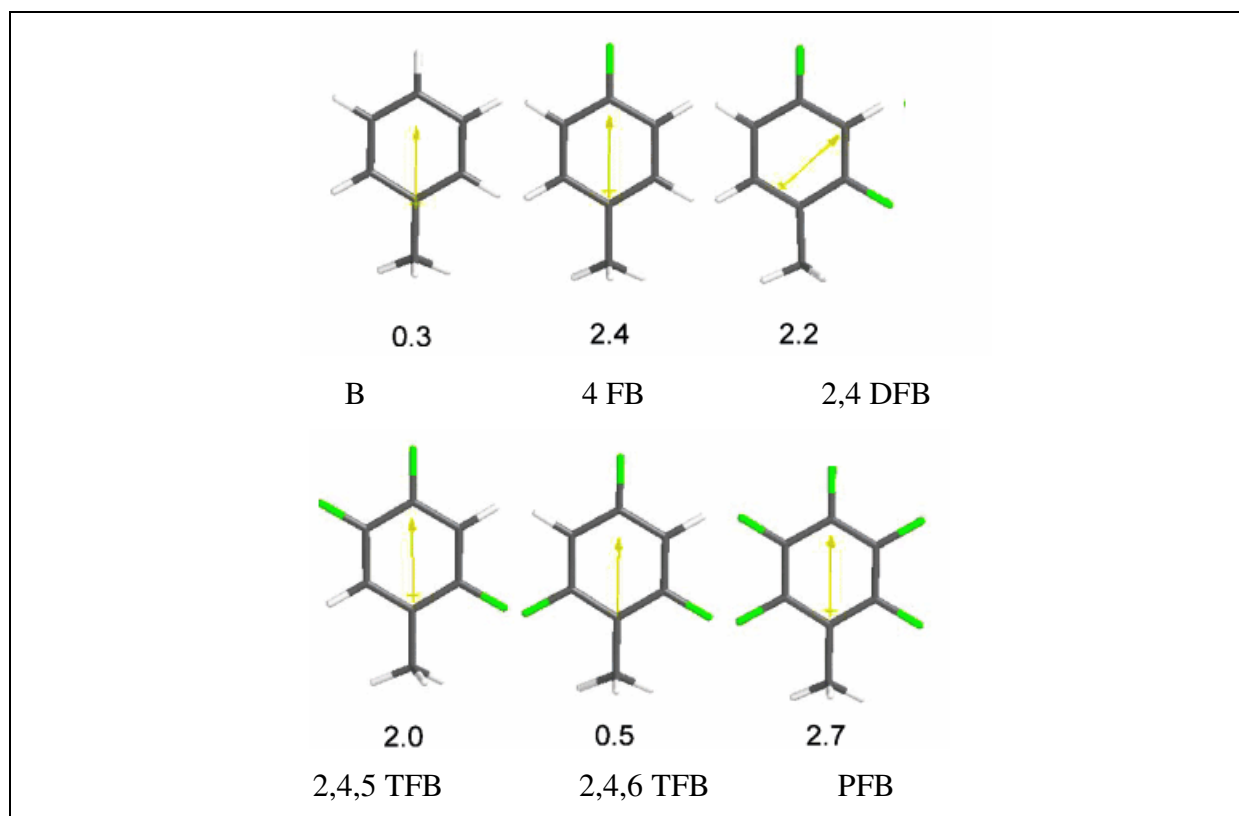
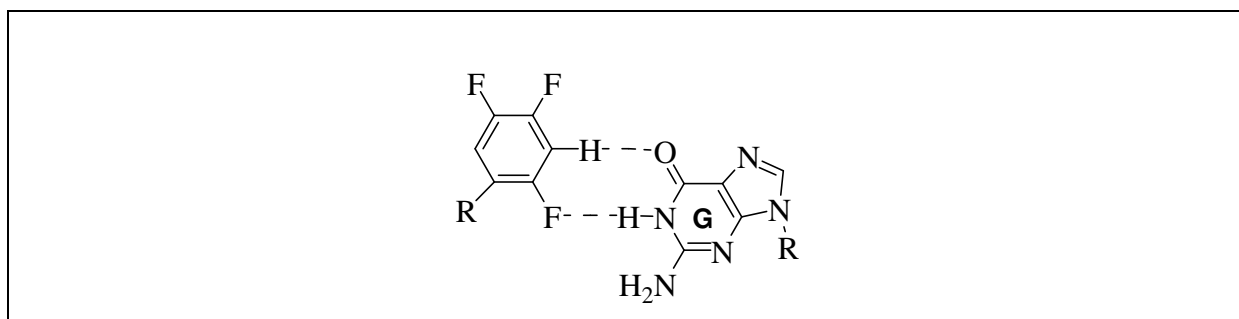


Figure 8.8. Calculated dipole moments (debye) of aromatic fluorinated base analogues; dipole orientations are shown with yellow arrows, fluorine atoms are in green. Electrostatics was calculated with Spartan'02 (wavefunct. Incl) employing AM1 Hamiltonian (Lai et al., 2003)

When B is incorporated in RNA against A there is 14.8°C destabilization comparing to A-U base pair. That can be explained with the absence of hydrogen bonds and less solvation. With fluoro-modified benzenes the destabilizing effect is smaller.  $T_m$  values for 2,4 DFB are lower up to 10.5°C. The difference for pairing of 4FB with natural bases is bigger and is more destabilizing than 2,4 DFB. All synthesised fluoro-benzene modifications, except 2,4 DFB, differ between natural bases. For two trifluoro-benzene modifications (2,4,6 TFB and 2,4,5 TFB) there are great differences in pairing and that tells us that not only the number but also the positions of fluorines are important. The surface area of those two compounds is very similar and also their polarisability (Makochkannwa *et al.*, 2004), their dipole moments (1,3,5-trifluorobenzene has dipole moment of zero) and their quadrupole moments differ significantly. In *figure 8.10*. one can see that 2,4,5 TFB builds 5-6°C more stable base pairs than 2,4,6 TFB. On the one side 2,4,5 TFB is almost as good as 2,4 DFB on the other 2,4,6 TFB is as bad as the benzene modification itself. Therefore we think that position 5 of the benzene ring is not of great importance for base pairing but the 2 and 6 positions, first positions next to the glycosidic linkage) are significant for base pairing pattern of benzenes. When 2,4,5 TFB is incorporated against natural bases can be noticed that stability slanders in order G>U>>C>A what suggests that 2,4,5 TFB might be able to form Wobble base pair with G (*figure 8.9*).



*Figure 8.9. Assumed Wobble base-pare (2,4,5 TFB-guanosine)*

PFB modification also differs between natural bases. The stabilities of PFB-natural base (A, C, G and U) base pairs are around 13°C lower than natural base pairs. The deciding points for low stability are: steric reasons and all five positions exchanged with fluorine.

DFB is a universal base, developed in our group (Parsch & Engels, 2001) that is less stable than natural bases but doesn't differ between A, C, G and U. In *figure 8.10*. one can see differences in the pairing of natural bases with fluoro-benzene nucleosides.

<b>1<sup>st</sup> Base</b>	<b>2<sup>nd</sup> Base</b>	<b>T<sub>m</sub> (°C)</b>	<b>ΔH° (kcal/mol)</b>	<b>TΔS° (kcal/mol) T = 298 K</b>	<b>ΔG°(kcal/mol)</b>
<b>U</b>	<b>A</b>	37.8	87.8	75.9	11.9
	<b>C</b>	30.4	84.5	74.8	9.7
	<b>G</b>	38.6	8.	71.1	11.9
	<b>U</b>	30.1	89.5	79.8	9.7
<b>4FB</b>	<b>A</b>	23.8	81.6	73.7	7.9
	<b>C</b>	24.1	83	75	8
	<b>G</b>	24.2	80.2	72.2	8
	<b>U</b>	25.6	85.8	77.4	8.4
<b>2,4 DFB</b>	<b>A</b>	27.4	88.6	79.6	9
	<b>C</b>	27.3	84.8	75.9	8.9
	<b>G</b>	27.6	83.6	74.6	9
	<b>U</b>	27.9	91.2	82.1	9.1
<b>2,4,6 TFB</b>	<b>A</b>	23.3	81.2	73.4	7.8
	<b>C</b>	20.6	82	74.9	7.1
	<b>G</b>	22.8	70.2	62.5	7.7
	<b>U</b>	22.9	77.9	70	7.9
<b>2,4,5 TFB</b>	<b>A</b>	25.6	71.5	63.1	8.4
	<b>C</b>	26.7	83.2	74.4	8.8
	<b>G</b>	28.7	83.8	74.5	9.3
	<b>U</b>	27.5	74.7	65.8	8.9
<b>PFB</b>	<b>A</b>	22.9	69.7	62	7.7
	<b>C</b>	21.7	68.9	61.7	7.2
	<b>G</b>	23	69.8	62.1	7.7
	<b>U</b>	23.1	69.4	61.9	7.5
<b>B</b>	<b>A</b>	23	80.5	72.8	7.7
	<b>C</b>	22.6	84.4	76.8	7.6
	<b>G</b>	23.5	69.8	61.9	7.9
	<b>U</b>	23.1	73.3	65.6	7.7

Figure 8.10. Pairing of fluoro-benzene modifications with natural bases  
 Uncertainty of the given values:  $T_m = \pm 0.5^\circ\text{C}$ ;  $\Delta H^\circ = \pm 5\%$ ;  $\Delta G^\circ = \pm 2\%$

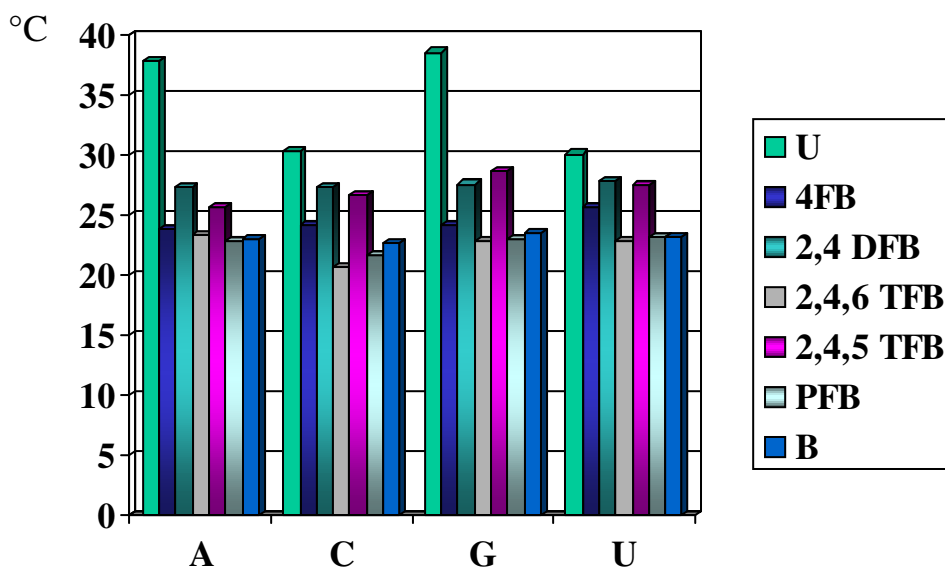


Figure 8.11. Graphical overview of  $T_m$  values of base pairs of fluoro-benzimidazole modifications and natural bases

However, base stacking is a complicated and not completely explained interaction that consists of number of interactions such as: electrostatic (dipole-dipole and dipole-induced dipole) interactions, dispersion (momentary dipole- induced dipole) effects, solvation effects, stacking surface area, polarizability (that does not depend only on the size of the molecule but also on its shape and geometry overlap with the neighbouring base pair) and shape (Guckian *et al.*, 2000). The plots of those factors did not show qualitative correlation, at least within the bigger series of compounds so it is very complicated to define the factor responsible for the different stacking abilities of modified fluorobenzenes since the superposition of all factors is in theory very complicated (Guckian *et al.*, 2000). It is known in physical chemistry that electron-withdrawing substituents are increasing the magnitude of quadrupole-moment and that they do especially if *ortho*- positioned (Rashkin *et al.*, 2002; Goodman *et al.*, 2001). Therefore we can conclude that in this series of fluorobenzenes positions of fluorines have influence on base pairing pattern in RNA oligonucleotides as expected from the quadrupole moments of those compounds and their polarizability. Another factor that leads to destabilization are electrostatic repulsions between fluorines and  $\pi$ -cloud of non-fluorinated phenyl system (this is obvious on the example of PFB modification) (Reichenbacher *et al.*, 2005).

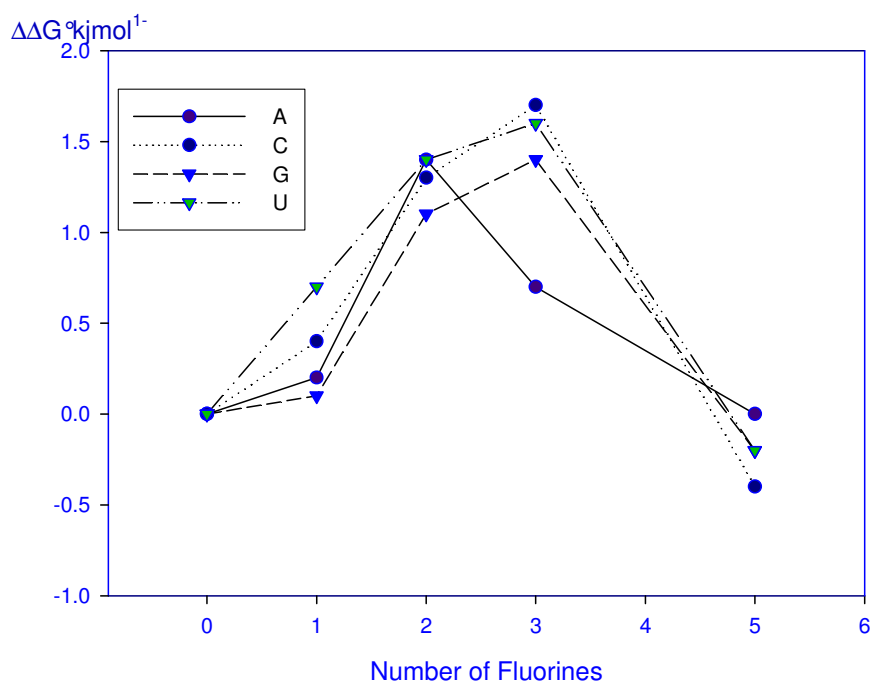


Figure 8.12. Plot showing trends in stacking free energies as a function of the number of fluorine substituents (2,4,6 TFB is omitted here)-compared with benzene

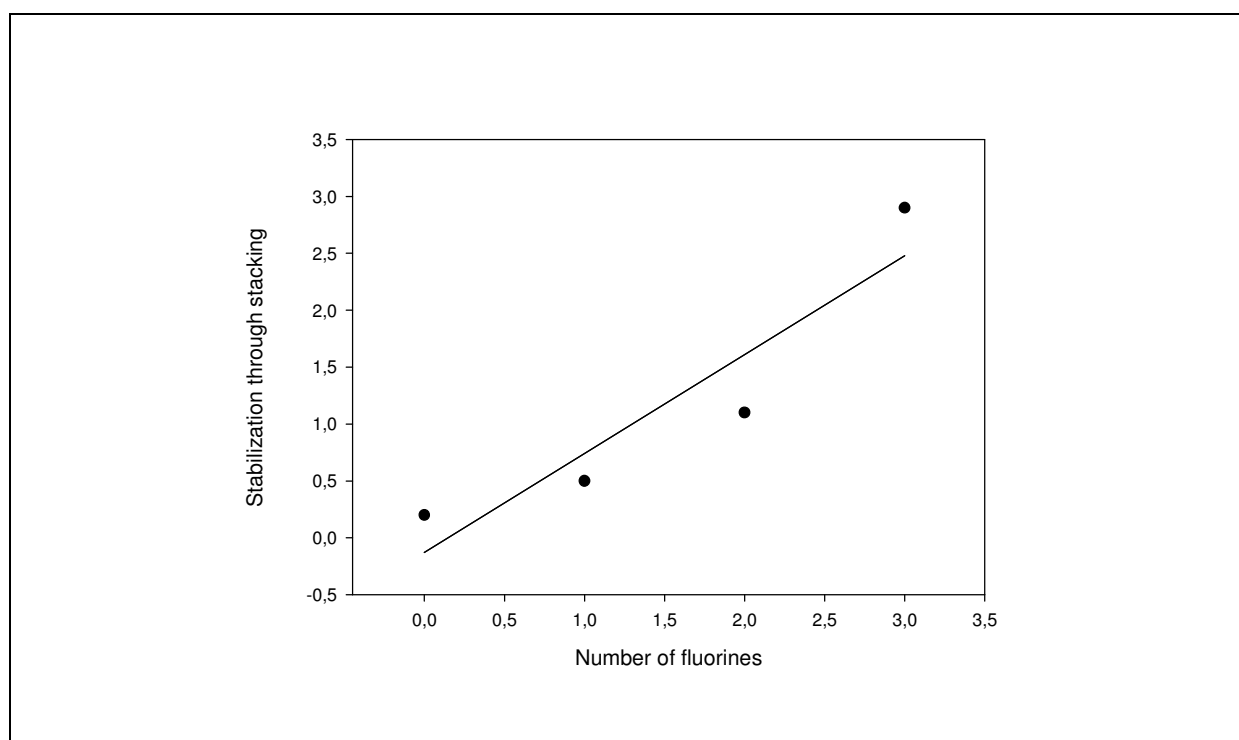
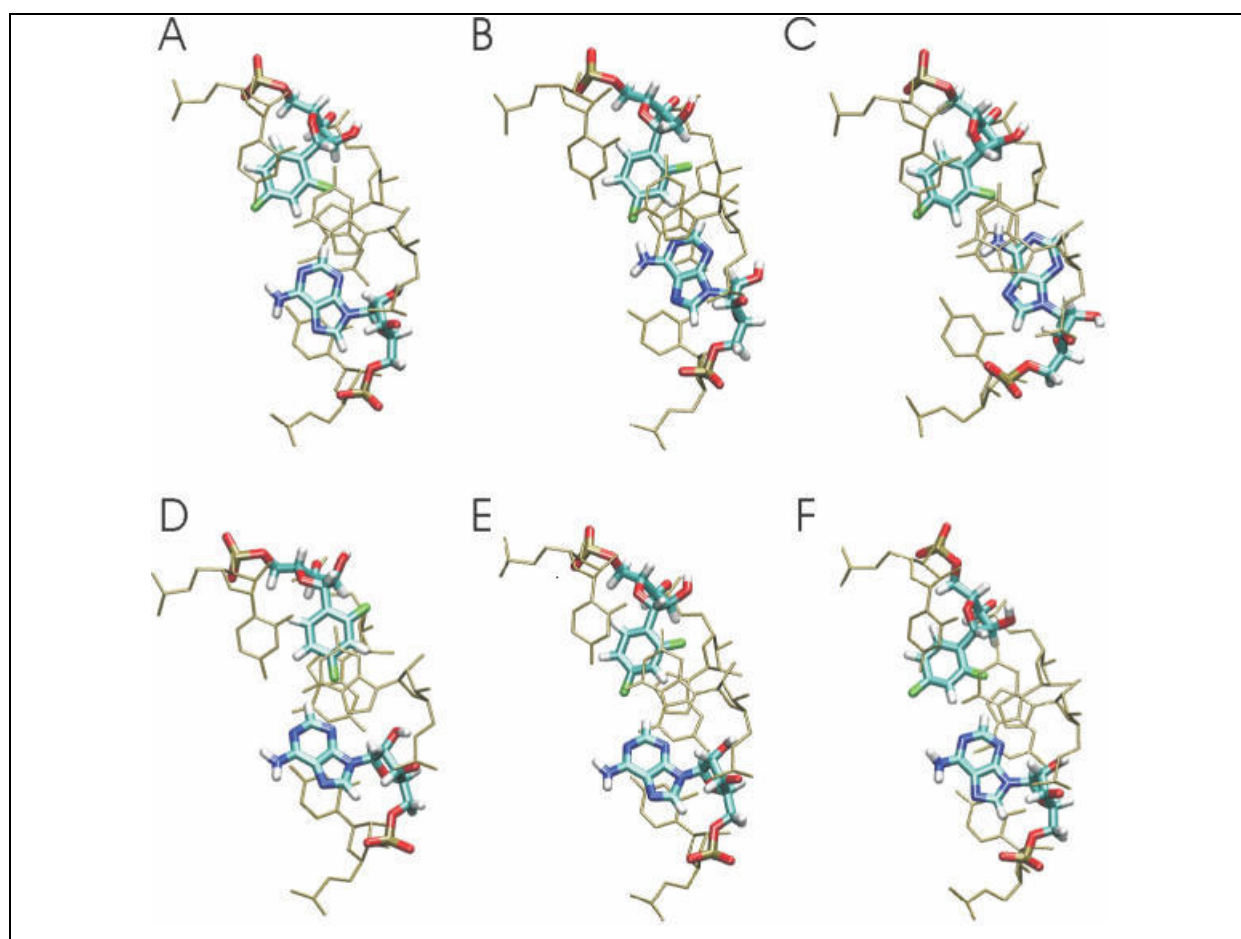


Figure 8.13. Test of possible linear relationship between stacking free energies and number of fluorine substituents (bis-ortho effects are omitted)-  $y = 0.87x - 0.13$

In addition, with 2,4 DFB modification was done a study aimed at characterizing the influence of 2,4 DFB and a phenyl base analogue (B) opposite to an adenine base on the flexibility of RNA (Zacharias & Engels, 2004). In this study no stable ‘base-paired’ geometry was found for the base analogue: adenine pairs, which explains in part universal base character of these analogues. Instead the conformational fluctuations of the base analogues lead to enhanced accessibility of the bases in major and minor grooves of the helix compared with a regular base pair.

The simulations indicate that the 2,4 DFB can only form weak transiently stable ‘‘ hydrogen bonds’’ to the opposing base in the RNA duplex. This result offers an explanation for the experimental observation that 2,4 DFB is a universal base and the stabilization effect of the helix is primarily due to the stacking effects. Any stable hydrogen bonding is likely to interfere with the characteristics of a universal base (Zacharias & Engels, 2004).



*Figure 8.14. Conformational snapshots (A-2,4 DFB) observed during the simulation of the RNA with a central A-2,4 DFB base pair. The view is along the helical axis of the RNA. For clarity, only the central base pair (thick lines) and the neighbouring base pairs (thin lines) are shown (Zacharias & Engels, 2004)*



In the next table (figure 8.15.) results for pairing benzimidazole modifications with natural bases are shown.

<b>1<sup>st</sup> Base</b>	<b>2<sup>nd</sup> Base</b>	<b>T<sub>m</sub> (°C)</b>	<b>ΔH° (kcal/mol)</b>	<b>TΔS° (kcal/mol) T = 298 K</b>	<b>ΔG°(kcal/mol)</b>
<b>4 FBI</b>	<b>A</b>	28	86.7	77.6	9.1
	<b>C</b>	27.5	81.8	72.9	8.9
	<b>G</b>	28.7	84.1	74.8	9.3
	<b>U</b>	28.5	85.8	76.6	9.2
<b>5 FBI</b>	<b>A</b>	28.9	85.7	76.6	9.1
	<b>C</b>	31	89	79.8	9.2
	<b>G</b>	31.7	88.7	79.4	9.3
	<b>U</b>	28.2	86.4	77.5	8.9
<b>6 FBI</b>	<b>A</b>	34	53.6	46.1	7.5
	<b>C</b>	31.3	56.2	46.1	10.1
	<b>G</b>	32.4	86.1	75.8	10.3
	<b>U</b>	28.6	85.2	75.9	9.3
<b>4,6 DFBI</b>	<b>A</b>	28.4	81.4	72.2	9.2
	<b>C</b>	28.7	81.5	72.3	9.2
	<b>G</b>	29.4	84.8	75.3	9.5
	<b>U</b>	29.3	85.3	75.8	9.5
<b>4 TFM</b>	<b>A</b>	30.1	81.1	70.1	11
	<b>C</b>	27.4	82	72.1	9.9
	<b>G</b>	29.2	81.2	71.5	9.7
	<b>U</b>	25.1	80.3	72	9.3
<b>5 TFM</b>	<b>A</b>	30.2	52.1	43	9.1
	<b>C</b>	28.1	55	46.2	8.8
	<b>G</b>	29.3	48	39.3	8.7
	<b>U</b>	24.1	70.2	62.1	8.1
<b>6 TFM</b>	<b>A</b>	30.1	53	42.1	10.9
	<b>C</b>	28	79.8	70.9	8.9
	<b>G</b>	27.1	79.8	70.2	9.6
	<b>U</b>	24.8	73.3	64.9	8.2
<b>BI</b>	<b>A</b>	28.7	81	71.8	9.2
	<b>C</b>	25.6	82.3	73.8	8.5
	<b>G</b>	28.9	97.4	88	9.4
	<b>U</b>	29.1	73.1	63.8	9.3

Figure 8.15. Pairing of benzimidazole nucleosides with natural bases  
Uncertainty of the given values:  $T_m = \pm 0.5^\circ\text{C}$ ;  $\Delta H^\circ = \pm 5\%$ ;  $\Delta G^\circ = \pm 2\%$

It is obvious that they all destabilize the double helix in almost the same range. The least destabilizing was 6FBI and it still did differ in between natural bases. On the other hand 2,4 DFBI and 4FBI are universal (Parsch & Engels, 2001). The existence of either fluorine or the trifluoromethyl group made only minor differences comparing to benzimidazole BI (no substituents). In the pairing of AS (abasic site) with modified nucleosides one can see that all base pairs are more stable than AS-natural base pairs. Therefore we can conclude that the enhanced stacking of fluorinated nucleosides leads to a smaller loss of stabilisation.

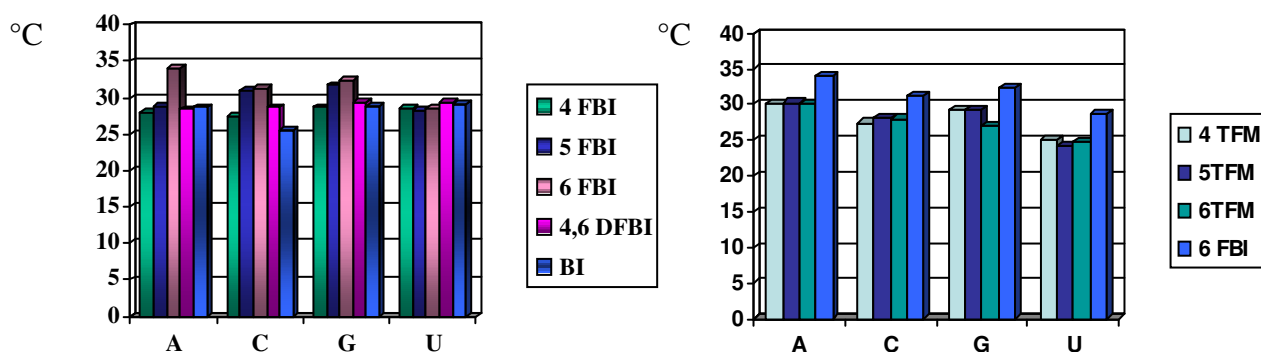
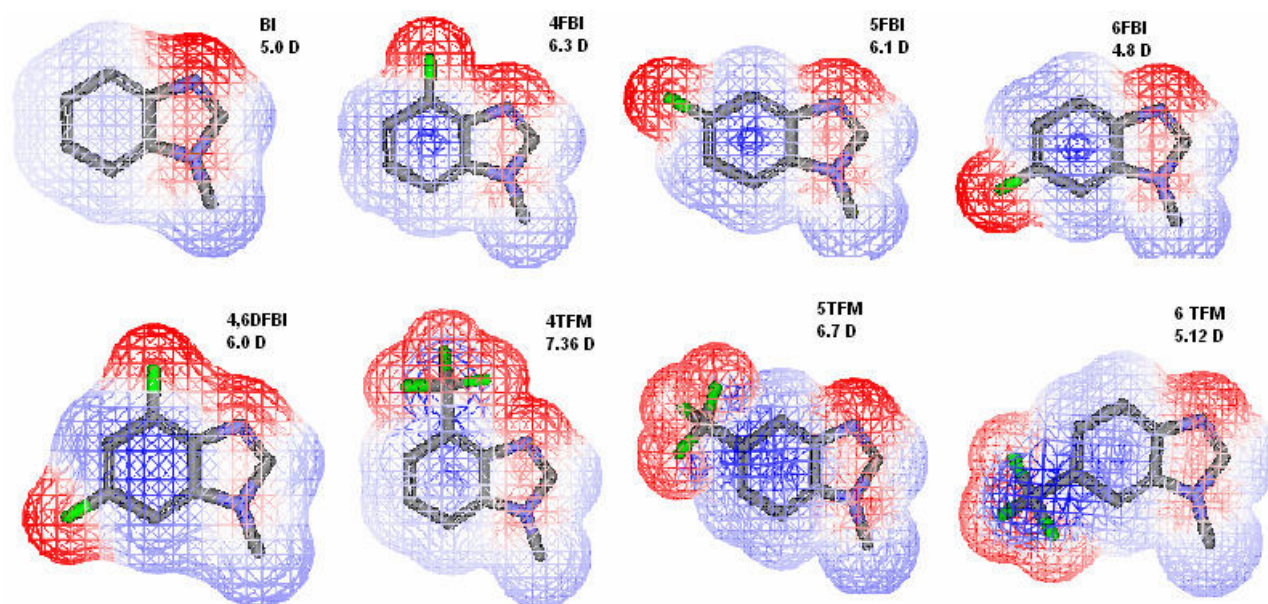


Figure 8.16. Graphical overview of  $T_m$  values of base pairs of fluoro-benzimidazole modifications and natural bases

In this series of substituted benzimidazoles there is hardly a difference in between the substituted and non-substituted analogue (figure 8.17.). In figure 8.17. one can see that imidazole ring has the largest influence on charge distribution in the benzimidazoles and that influence of the substituents is very small. Also dipole moments do not vary in this series so widely as in series of fluorobenzenes.

Knowing that in the series of bigger molecules (larger surface area) the influence on the quadrupole moment is smaller in magnitude very small differences in  $T_m$ -values can be easily explained. For example the position of trifluoromethyl group is of no importance for the magnitude of quadrupole moment of those compounds (Rashkin *et al.*, 2002) and our results with any of TFM modifications hardly differ. However the great loss of stability is also due to hydrophobic effect, size of trifluoromethyl group suggested to be 2.5 times larger than methyl group (Seebach, 1990) and results for 6-trifluoromethyl purine (Veliz *et al.*, 2001) indicate that this nucleotide does not form base pair in duplex RNA and already exists in flipped out

conformation. In *figure 8.16*, one can see pairing of natural bases with benzimidazole modifications.



*Figure 8.17. Calculated electrostatic surfaces potentials and dipole moments of fluorinated benzimidazole analogues with an attached methyl group to approximate effect of ribose*

In addition, all benzimidazole compounds that we synthesised were used for investigation of DNA polymerase  $\alpha$ , Klenow fragment (DNA polymerase I) and primase ( Moore *et al.*, 2004; Kinckaid *et al.*, 2005). All of triphosphates were incorporated, however after incorporation all used compounds were not efficiently elongated. Where as pol  $\alpha$  and Klenow fragment exhibited minimal discrimination against 5- and 6- regioisomers, they discriminated much more effectively against the 4- and 7-regioisomers. All of the compounds inhibited primase activity with remarkably similar potency. Changing the shape and size of compounds was not an important issue (Kinckaid *et al.*, 2005).

When the abasic building block is pairing with A and G,  $T_m$  values are 20,6°C and 20,9°C respectively, and for C and U those values are 18,6°C and 18,2 °C respectively. This dramatic loss of stability can be explained in loosing hydrogen bonding ability (AS has no base) and disturbed stacking in the middle of the oligonucleotide (*figure 8.18*). Both forces are responsible for the double helix stability. Interestingly in *figure 8.18*, one can see that 2,4,5 TFB and 4,6 DFBI stack equally good even one would think that due to it's larger stacking area 4,6 DFBI would stack better. Addition of fluorine in position 5 of benzene ring adds as much stacking energy as imidazole ring.

1. Base	2.Base	T <sub>m</sub> (°C)	ΔH° (kcal/mol)	TΔS° (kcal/mol) T = 298 K	ΔG°(kcal/mol)
AS	A	20.6	67.2	60	7.2
	C	18.6	51.3	44.6	6.7
	G	20.9	65.1	57.8	7.3
	U	18.2	58.9	52.3	6.6
	4 FB	20.9	81.9	74.8	7.1
	2,4 DFB	22.6	59.7	52	7.7
	2,4,6 TFB	19.8	66.5	59.7	6.8
	2,4,5 TFB	26.4	83.7	75.1	8.6
	PFB	19.6	80.3	73.2	7.1
	B	19.5	78.3	72	6.8
	4 FBI	25.3	58.1	49.8	8.3
	5 FBI	25.4	60	51.7	8.3
	6 FBI	26.6	58.5	50.1	8.4
	4,6 DFBI	26.3	55.1	44.6	8.5
	4 TFM	28.3	66.6	57.5	9.1
	5 TFM	28.4	70.8	61.8	9
	6 TFM	28.7	70.1	60.8	9.3
I	26.2	110.9	102.4	8.5	

Figure 8.18. Abasic site (AS) paired with natural and modified nucleosides  
 Uncertainty of the given values: T<sub>m</sub>=±0.5°C; ΔH°=±5%; ΔG°=±2%

Modified base pairs have lower melting points than natural ones but besides TFM modifications they all had higher melting points than pairs of modified and natural bases.

By exchanging of the first nucleobase in a natural base pair with modification there is a loss of stability because of loosing hydrogen bonding ability but also rising stability caused by stronger stacking. Because of the higher negative effect T<sub>m</sub> values of those pairs are sinking. When the second base is exchanged with modification there is no further destabilizing effect and T<sub>m</sub> values are rising (no loosing of hydrogen bonding).

In the case of the TFM modifications the situation seems to be more complicated since those base pairs are less stable when they have a modification on the other side than pairing with natural bases. Our educated guess would be that since we know that the size of trifluoromethyl group is more like isopropyl than the methyl group, some other negative effects are involved when there are modifications on the other side.

1 <sup>st</sup> Base	2 <sup>nd</sup> Base	T <sub>m</sub> (°C)	$\Delta H^\circ$ (kcal/mol)	T $\Delta S^\circ$ (kcal/mol) T = 298 K	$\Delta G^\circ$ (kcal/mol)
<b>4 FB</b>	<b>4 FBI</b>	30.6	82.2	72.4	9.8
	<b>5 FBI</b>	30.1	82	72.3	9.7
	<b>6FBI</b>	30.4	82.2	72.4	9.8
	<b>4,6 DFBI</b>	31.3	85	75	10
	<b>4 TFM</b>	25.1	81.3	73.4	7.9
	<b>5 TFM</b>	25.2	82.6	74.5	8.1
	<b>6 TFM</b>	25	81.7	73.8	7.9
<b>4,6 DFBI</b>	<b>4 FBI</b>	33.5	88.1	77.4	10.7
	<b>5 FBI</b>	33.2	89.2	78.8	10.4
	<b>6FBI</b>	33.6	84.9	74.1	10.8
	<b>4,6 DFBI</b>	34.6	94.4	83.2	11.2
	<b>4 TFM</b>	25.1	75.1	66.6	8.5
	<b>5 TFM</b>	26.5	77.2	68.6	8.6
	<b>6 TFM</b>	26.1	98.2	89.2	9
<b>2,4,6 TFB</b>	<b>4 FBI</b>	29.6	84.9	75.5	9.4
	<b>5 FBI</b>	28.1	83.9	75.2	8.7
	<b>6FBI</b>	28.2	96.7	87.4	9.3
	<b>4,6 DFBI</b>	29.1	80.1	70.7	9.4
	<b>4 TFM</b>	24.1	64	56.5	7.5
	<b>5 TFM</b>	25	83.5	75.2	8.3
	<b>6 TFM</b>	24.8	83.9	74.9	9
<b>2,4,5 TFB</b>	<b>4 FBI</b>	32.9	73.1	63	10.1
	<b>5 FBI</b>	31	72.1	62.4	9.7
	<b>6FBI</b>	34.7	96.7	85.3	11.4
	<b>4,6 DFBI</b>	33.5	76.7	66.3	10.4
	<b>4 TFM</b>	26	79.1	70	9.1
	<b>5 TFM</b>	26.1	86.9	78.4	8.5
	<b>6 TFM</b>	26.8	110.6	101.7	8.9
<b>PFB</b>	<b>4 FBI</b>	23.2	88.8	80.6	8.2
	<b>5 FBI</b>	23.5	89.2	81	8.2
	<b>6FBI</b>	23.5	91.1	82.8	8.3
	<b>4,6 DFBI</b>	24.5	91.3	82.5	8.8
	<b>4 TFM</b>	20.1	73.1	65.4	7.7
	<b>5 TFM</b>	21.2	74.1	66.2	7.9
	<b>6 TFM</b>	22.1	80.5	72.8	7.7
<b>I</b>	<b>B</b>	28.9	67.1	58	9.1

Figure 8.19. Pairing of fluoro- modified benzenes with fluoro- modified benzimidazols  
 Uncertainty of the given values:  $T_m = \pm 0.5^\circ\text{C}$ ;  $\Delta H^\circ = \pm 5\%$ ;  $\Delta G^\circ = \pm 2\%$

In an unmodified RNA, the nucleobases in oligonucleotides are surrounded with water molecules, which build hydrogen bonds with nucleobases. When they form a double helix, hydrogen bonds are lost and new ones are built to the opposite nucleobases. When a natural nucleobase is pairing with a modified it is different. In single stranded RNA the modified base is bad or not solvated but the natural one is. When building a base pair of those two compounds the hydrogen bonds of natural one are lost but no other are built. In the sum that makes higher negative effect on the stability on the new double helix. When building a base pair from both modified nucleobases both fluorinated bases are badly or not solvated and therefore there is no decrease in stability as result of loosing solvation (figure 8.20).

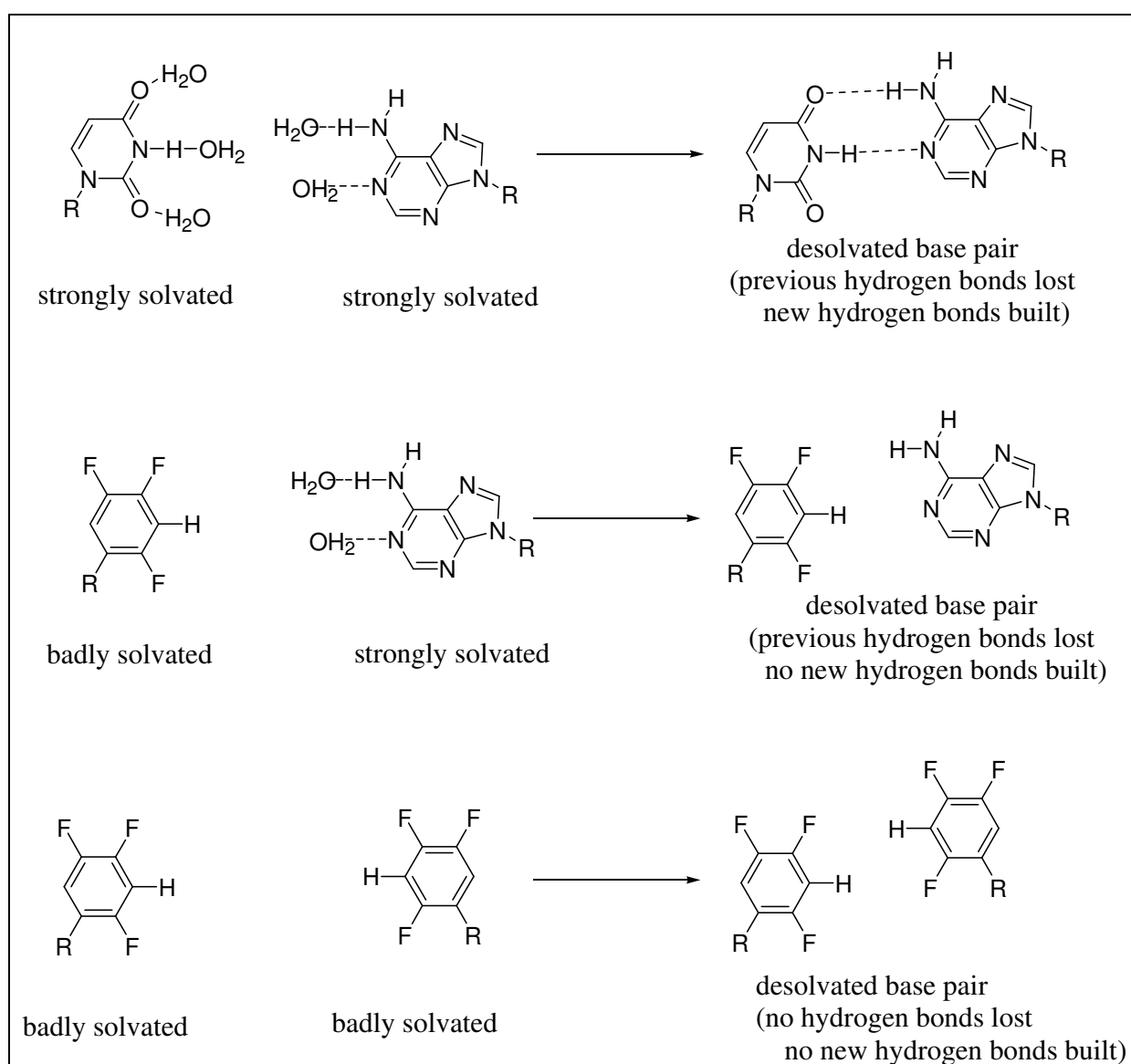


Figure 8.20. Solvation of natural and modified bases

1. Base	2.Base	$T_m$ (°C)	$\Delta H^\circ$ (kcal/mol)	$T\Delta S^\circ$ (kcal/mol) T = 298 K	$\Delta G^\circ$ (kcal/mol)
4 FB	4FB	27,3	80,4	71,5	8,9
2,4 DFB	2,4 DFB	32,5	82,4	72,2	10,2
2,4,6 TFB	2,4,6 TFB	29,1	87,1	77,7	9,4
2,4,5 TFB	2,4,5 TFB	35,8	99,7	87,9	11,8
PFB	PFB	25	79,8	72,1	7,7

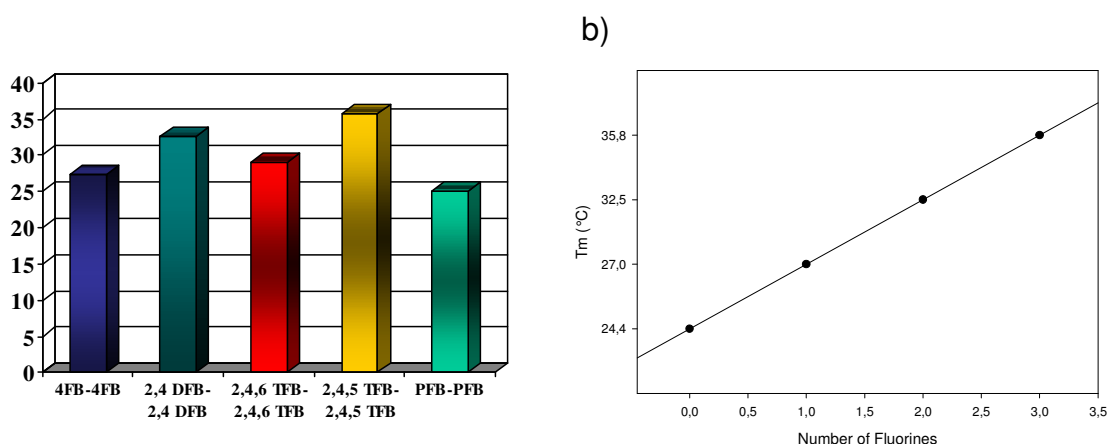


Figure 8.21. Pairing of flour-benzene modifications in-between two same bases b) linear dependence between  $T_m$  values and number of fluorines (if bis-ortho cases are omitted)

Uncertainty of the given values:  $T_m = \pm 0.5^\circ\text{C}$ ;  $\Delta H^\circ = \pm 5\%$ ;  $\Delta G^\circ = \pm 2\%$

From the presented data one can see that with fluorine substitution in this self-pairs (number of fluorines, but also their orientation (mentioned bis-ortho effect) change the stability of double RNA helix. That is in contrast from Romesberg and co-workers, who investigated self pairing (but with different fluorine substitution) of fluorobenzenes in DNA and concluded that once fluorine is in helix it's position is not important (Henry *et al.*, 2004).

From the measured melting points of the base pairs one can calculate values for solvation and the stacking ability of all synthesised modifications. We will explain the calculation on the example of 2,4,5 TFB. The values for other modifications were calculated in the same manner.

Number	Base pair	T <sub>m</sub> (°C)	ΔG° (kcalmol <sup>-1</sup> )
1	AS-U	18.2	6.6
2	U-U	30.1	9.7
3	U-2,4,5 TFB	27.5	8.9
4	2,4,5 TFB-2,4,5 TFB	35.8	11.8
5	2,4,5 TFB-AS	26.4	9.4

Figure 8.22. Calculating stacking and solvation thermodynamical data for 2,4,5 TFB modification

Uncertainty of the given values: T<sub>m</sub>=±0.5°C; ΔH°=±5%; ΔG°=±2%

For calculating solvation and stacking for 2,4,5 TFB the values given in figure 8.22. were used. For the calculations we used values for following base pairs: abasic site and U (1), U-U base pair (2), U and 2,4,5 TFB (3), 2,4,5 TFB-2,4,5 TFB pair(4) and 2,4,5 TFB-AS (5). The different stacking ability of 2,4,5 TFB base one can calculate in comparison to U from difference between (5) and (1). Exchange of U with 2,4,5 TFB rises the T<sub>m</sub> for 8.2 °C. This rise of T<sub>m</sub> corresponds to rise in stability of 2.9 kcalmol<sup>-1</sup>. With this exchange there is no need to take care about solvation effects because both bases are paired with abasic site that has no base and therefore cannot be solvated. There is also no loss of hydrogen bonding and therefore no negative effect of solvation on the stability of the double helix.

The influence of the solvation on the stability of the double helix with incorporated 2,4,5 TFB nucleoside can be calculated comparing values for (3) and (2). When one exchanges a base pair from two U with U-2,4,5 TFB base pair, the melting point sinks for 2.6°C (corresponds to 0.8 kcalmol<sup>-1</sup>). The destabilizing effect through solvation is 2.6°C+ 8.2°C=10.8°C altogether which corresponds to 3.7 kcalmol<sup>-1</sup>.

The calculated value can be checked through comparing (3) and (4) in figure 8.22. When second U is exchanged with 2,4,5 TFB no other destabilisation through solvation effects take place. Because of enhanced stacking the T<sub>m</sub> of 2,4,5 TFB-2,4,5 TFB should rise for 8.2°C (2.9 kcalmol<sup>-1</sup>) comparing to 2,4,5 TFB-U base pair. The expected melting point is therefore 35.7°C and free enthalpy 11.7 kcalmol<sup>-1</sup>. The measured values are 35.8°C and 11.8 kcalmol<sup>-1</sup> and in excellent agreement with calculated ones.



Nucleoside	Stabilizing through stacking	Destabilizing through solvation
4 FB	2.7°C; 0.5 kcalmol <sup>-1</sup>	-7.2°C; -1.8 kcalmol <sup>-1</sup>
2,4 DFB	4.4°C; 1.1 kcalmol <sup>-1</sup>	-6.6°C; -1.7 kcalmol <sup>-1</sup>
2,4,5 TFB	8.2°C; 2.9 kcalmol <sup>-1</sup>	-10.8°C; -3.7 kcalmol <sup>-1</sup>
2,4,6 TFB	1.6°C; 0.2 kcalmol <sup>-1</sup>	-8.8°C; -2.1 kcalmol <sup>-1</sup>
PFB	1.4°C; 0.2 kcalmol <sup>-1</sup>	-8.4°C; -2.2 kcalmol <sup>-1</sup>
B	1.3°C; 0.2 kcalmol <sup>-1</sup>	-8.3°C; -2.2 kcalmol <sup>-1</sup>
4 FBI	4.4°C; 1.0 kcalmol <sup>-1</sup>	-6.3°C; -1.6 kcalmol <sup>-1</sup>
5 FBI	4.5°C; 1.1 kcalmol <sup>-1</sup>	-6.4°C; -1.8 kcalmol <sup>-1</sup>
6 FBI	5.7°C; 1.3 kcalmol <sup>-1</sup>	-6.9°C; -1.7 kcalmol <sup>-1</sup>
4,6 DFBI	5.4°C; 1.2 kcalmol <sup>-1</sup>	-6.5°C; -1.5 kcalmol <sup>-1</sup>
4 TFM	7.4 °C; 1.8 kcalmol <sup>-1</sup>	-14.0°C; -3.3 kcalmol <sup>-1</sup>
5 TFM	7.5 °C; 1.7 kcalmol <sup>-1</sup>	-13.5°C; -3.3 kcalmol <sup>-1</sup>
6 TFM	7.8 °C; 2.0 kcalmol <sup>-1</sup>	-14.0°C; -3.1 kcalmol <sup>-1</sup>
I	5.3°C; 1.2 kcalmol <sup>-1</sup>	-6.3°C; -1.7 kcalmol <sup>-1</sup>

Figure 8.23. Calculated thermodynamical parameters for stacking and solvation for synthesised modifications

Figure 8.23. shows the calculated values for the solvation and the stacking of all synthesised bases and their influence on stability of double helix. Values for the benzene nucleosides were calculated comparing to U and for benzimidazole modifications to G.

All modifications raise stability of double helix through base stacking but destabilize it because of the solvation. By TFM modifications there are additional destabilizing effects when they are paired with fluorinated bases. We think that for that the size of CF<sub>3</sub> group and the presence of great number of negatively charged fluorine atoms towards one another are responsible. That destabilizes double helix further more. Surprisingly there is a big difference to notice between 2,4,5 TFB and 2,4,6 TFB. While 2,4,5 TFB stabilizes double helix with 8.2°C for 2,4,6 TFB that value is only 1.6°C. The difference in destabilization through solvation is not so dramatically, -10.8°C for 2,4,5 TFB and -8.8 °C for 2,4,6 TFB. That shows that not only the number but also the orientation of fluorine atoms influences the double helix stability.

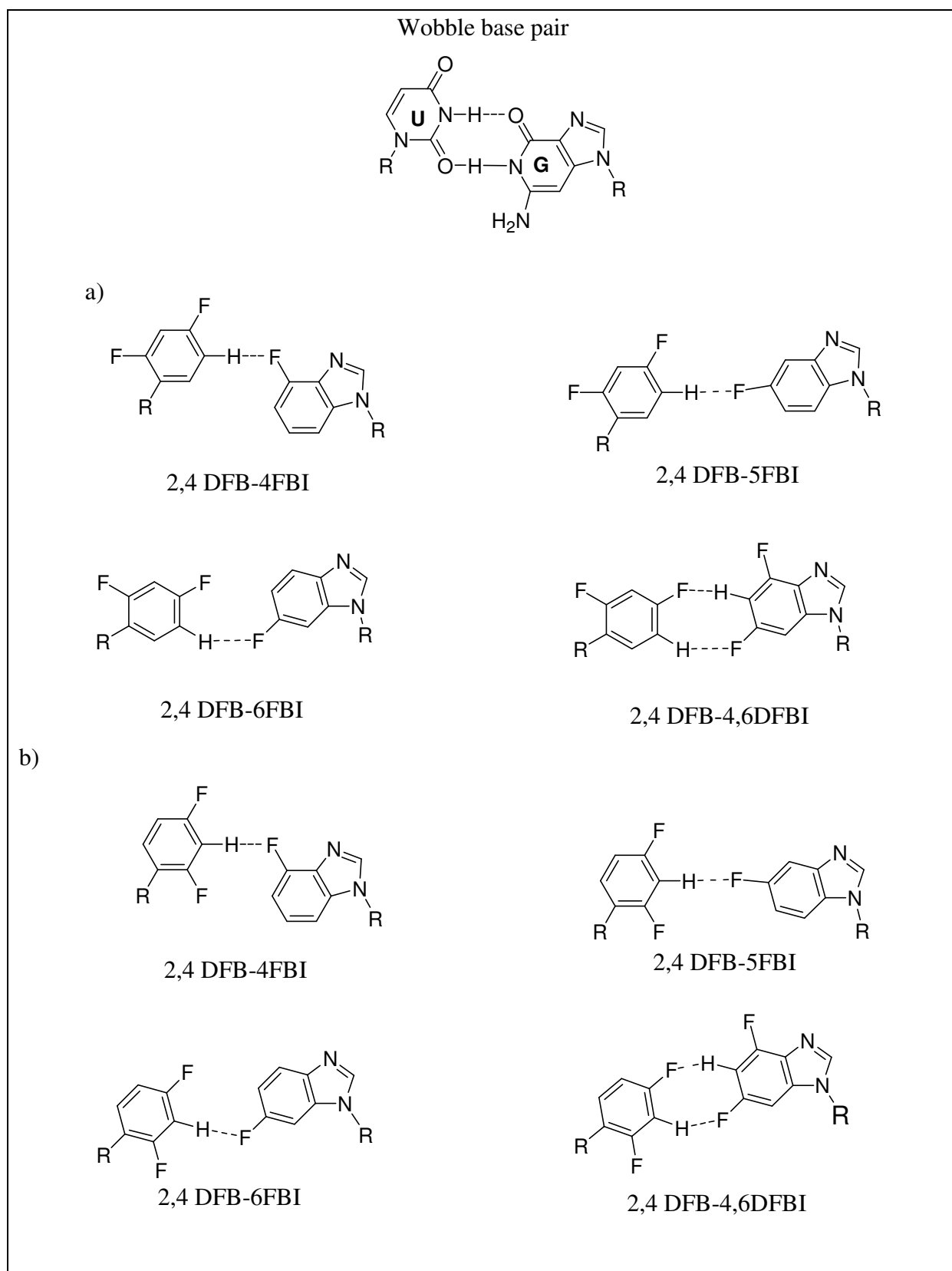


Figure 8.24. Wobble base pair and modified base pairs stabilized with C-F...H-C bonding (a and b are two possible orientations of modified bases in base pairs)

A base pair from U and 6FBI, in a 12mer RNA sequence, has a melting point of 28.5°C and a free enthalpy  $\Delta G^\circ$  of 9.3 kcalmol<sup>-1</sup>. If U is replaced with 2,4 DFB the  $T_m$  value should rise for 4.4°C (1.1 kcalmol<sup>-1</sup>). Therefore the melting point of the RNA duplex, with central base pair 6FBI-2,4DFB, should have melting point of 33.0°C and free enthalpy  $\Delta G^\circ$  of 10.4 kcalmol<sup>-1</sup>. Measured melting point is however 33.6°C with free enthalpy  $\Delta G^\circ$  of 10.8 kcalmol<sup>-1</sup>, that means 0.6°C and 0.4 kcalmol<sup>-1</sup> higher than expected. The same is for base pairs with 2,4 DFB on the one side and 4FBI (Parsch & Engels, 2000) and 5 FBI on the other side. If the same calculation is made for 2,4 DFB and 4,6DFBI we get difference from 0.9°C and 0.6 kcalmol<sup>-1</sup> (Parsch & Engels, 2000). In all four base pairs there are stabilizing forces and for those fluorine is of main importance. These weak interactions can be assigned as the C-F...H-C hydrogen bonding, which is already known to be present in crystal structures (chapter 6). For stabilization of 0.4 kcalmol<sup>-1</sup> in 4FBI-2,4DFB, 5FBI-2,4DFB and 6FBI-2,4DFB one C-F...H-C hydrogen bond is responsible while by 4,6DFBI-2,4DFB two hydrogen bonds of the same time are responsible for difference of 0.6 kcalmol<sup>-1</sup>. Slight movement of nucleobases like in Wobble base pairs, allows forming of C-F...H-C hydrogen bond.

### 8.1.3 Enthalpy-Entropy Compensation

The phenomenon of entropy-enthalpy compensation, an empirical observation that in many chemical processes the change in enthalpy is partially compensated by a corresponding change in entropy, resulting in a smaller net free energy change, has been widely documented (Searle & Williams, 1993; Gallicchio *et al.*, 1998).

The enthalpy change measures a change in the strength of the interactions between molecules while entropy change measures a change in the order of the system. It is more difficult, however, to interpret free energy changes. Invariably, in fact, the analysis of free energy changes must involve the analysis of the relative importance of the corresponding enthalpy and entropy changes. Following equations are expressing these facts mathematically (Chen & Russu, 2004).

$$[8-18] \quad \Delta G_{\text{helix}} = \Delta G_r + \Delta G_h + \Delta G_{s+} + \Delta G_{\text{hb}}$$

$$[8-19] \quad \Delta H_{\text{helix}} = \Delta H_r + \Delta H_h + \Delta H_{s+} + \Delta H_{\text{hb}}$$

$$[8-20] \quad \Delta S_{\text{helix}} = \Delta S_r + \Delta S_h + \Delta S_{s+} + \Delta S_{\text{hb}}$$

r-internal rotations, h-hydrophobic interactions, s-stacking interactions, hb-hydrogen bonding.

Factorisation of experimental free energies for helix formation in terms of approximate contributions from the restriction of rotations, hydrophobic interactions, electrostatic interactions due to base stacking, and contributions from hydrogen bonding, and estimate the adverse free energy cost per rotor (mainly entropy) of ordering the phosphate backbone is expressed with equations [8-18], [8-19] and [8-20].

The phenomenon of enthalpy-entropy compensation agrees with our intuition that a stronger interaction between molecules will also result in a reduction of the entropy. Correspondingly, weaker molecular interactions as also higher extent of free rotation will produce a looser molecular association and an increase of entropy.

The thermodynamics of self association (stacking) of free bases and nucleotides, intramolecular stacking in dinucleotides, nearest-neighbour base pair stacking interactions in duplex DNA and RNA, and the formation of hairpin loops illustrate enthalpy-entropy compensations. Large stacking exothermicities are associated with large negative entropy changes that ensure that  $\Delta G$  is small, permitting readily reversible associations in solution.

There are also exceptions of this enthalpy-entropy compensations (Gallicchio *et al.*, 1998) but *Figure 8.25*. shows the correlation between enthalpy and entropy changes for all our modified RNA duplexes. The correlation coefficient of our measurements is 0.990, which is an ideal value.

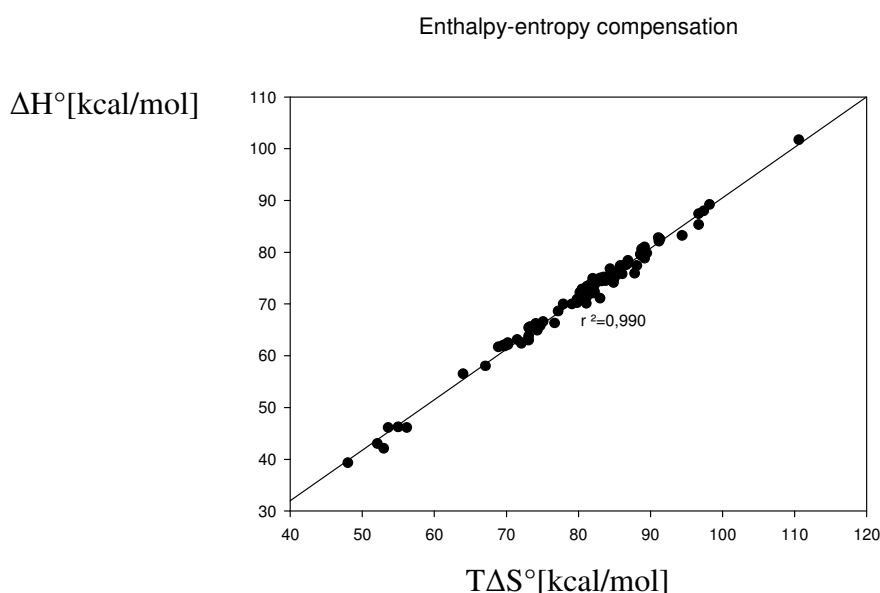


*Figure 8.25. Enthalpy-entropy compensation of all synthesised RNA duplexes*

## 8.2 CD Spectroscopic Measurements

### 8.2.1 CD-Spectroscopy

CD-spectroscopy (circular dichroism spectroscopy) is a method, which uses chirality of molecules for measurements. The beginning point for those measurements is that chiral molecules differently interact with right and left polarized light.

Plane polarized light  $E$  can be resolved into two components  $R$  and  $L$ . As long as the intensities and phases of two circularly polarized components remain the same, their resultant will lie in the plane and oscillate in magnitude. If the right circularly polarized component is less intense (absorbed more) than the left circularly polarized component, the electric vector of the light follows an elliptical path corresponding to elliptically polarized light. (figure 8.26).

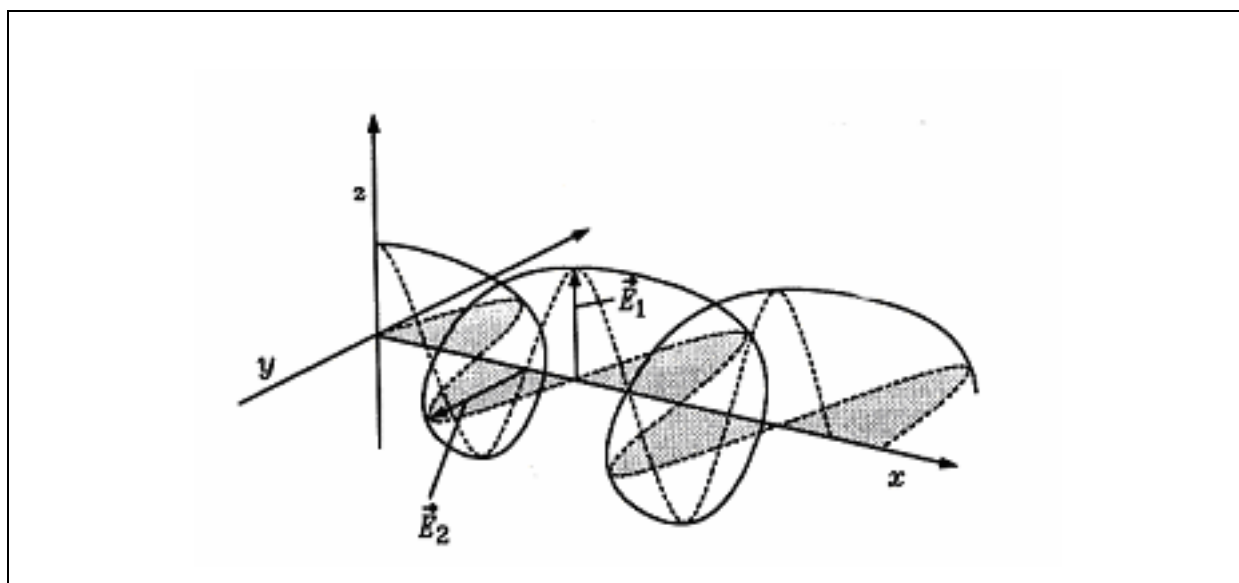


Figure 8.26.: Circular polarized light (Winter & Noll, 1998)

CD-spectroscopy leans on the fact that extinction coefficients for right and left polarized light,  $\epsilon_r$  and  $\epsilon_l$  are different. The difference in absorption can have positive or negative value.

$$[8-21] \quad \Delta\epsilon = \epsilon_L - \epsilon_R$$

In CD-spectroscopy we measure, however, not  $\Delta\epsilon$  but the ellipticity  $\Theta$ . Ellipticity is another effect that circular dichroism causes. When coming into the sample  $I_{0L} = I_{0R}$  but when leaving the sample those intensities are different. If we design than a sum vector it oscillates no more

along the line and describes an ellipse. The originally linearly polarized light is becoming elliptically polarized ( Berova *et al.*, 2000).

$$[8-22] \quad \tan \Theta_{\lambda} = (I_R - I_L) / (I_R + I_L)$$

$I_R$  and  $I_L$  are intensities of right and left polarized light. The ellipticity itself does not depend on wavelength. For quantitative and standardized description we refer to Lambert-Beer's law. With exchange of [8-23] in Lambert-Beer's equation:

$$[8-23] \quad A = \log (I_0/I) = l \cdot c_m \cdot d$$

we get:

$$[8-24] \quad \Theta_{\lambda} = \ln 10 \cdot (180^{\circ} / 4\pi) \cdot (\epsilon_L - \epsilon_R) \cdot c_m \cdot d$$

After we get specific ellipticity  $[\Theta]_{\lambda}$ :

$$[8-25] \quad [\Theta]_{\lambda} = \Theta_{\lambda} / c_m \cdot d$$

Specific ellipticity  $[\Theta]_{\lambda}$  has as unit:  $\text{grad} \cdot \text{cm}^2 \cdot \text{dmol}^{-1}$  ( $c_m = \text{g} \cdot \text{cm}^{-3}$ ,  $d = \text{dm}$ ). Molar ellipticity therefore is:

$$[8-26] \quad \Theta_M]_{\lambda} = [\Theta]_{\lambda} \cdot M / 100$$

$M$  is molecular mass in  $\text{g/mol}$ . For faster calculation of extinction coefficients from molar ellipticity, when we calculate in all constants we get:

$$[8-27] \quad \Theta_M]_{\lambda} = 3298 \cdot \Delta\epsilon$$

In CD spectra ellipticity as function of wavelength is measured. By CD measurements we get positive and negative values. Typical values for ellipticity are around  $10^5 \text{ Grad} \cdot \text{cm}^2 \cdot \text{dmol}^{-1}$ . The CD spectroscopy is very useful for the investigations of biomacromolecules. It is also often used for investigating the structure of nucleic acids. In nucleic acids the sugar molecule is responsible for chirality, as bases have a plane of symmetry. CD spectra, however, gives no defined structure information but only helps to complete picture formed using other structural methods. The intensities and positions of absorption bands can be only discussed in comparison with known structures.

We have to be very careful in comparing two CD-spectra of different sequences. This method also has some advantages like: sensitivity on structure change, not destructive method, simple

measurements and small amounts of oligonucleotides for the measurements (Gray *et al.*, 1992).

The first CD measurements in DNA were done in 1963 by Brahms (Brahms, 1963). The differences in CD-spectra of RNA and DNA were widely studied in the following years (Brahms, 1964; Brahms, 1965; Brahms & Mommaerts, 1964; Bush & Brahms, 1967; Brahms *et al.*, 1967) Figure 8.27 shows CD spectra of A-DNA and B-DNA. The change of structure gives big changes in CD spectra. The CD of B-DNA has maximum at 282 nm and minimum at 245 nm. One more maximum is at 220 nm. At 258 nm the ellipticity changes from positive to negative value and at 282 nm again to positive values. On the other hand main characteristics of A-DNA are: long wavelength band centred around 260 nm, a fairly intense negative band around 210 nm, and a very intense positive CD at about 190 nm. This CD spectrum is quite similar to CD of natural RNAs that normally exist only in A form. CD measurements done in this work were measure on a JASCO J-710 spectrometer with thermostate. For the CD measurements same samples as for UV-spectroscopy were used. Details are given in experimental part (chapter 10).

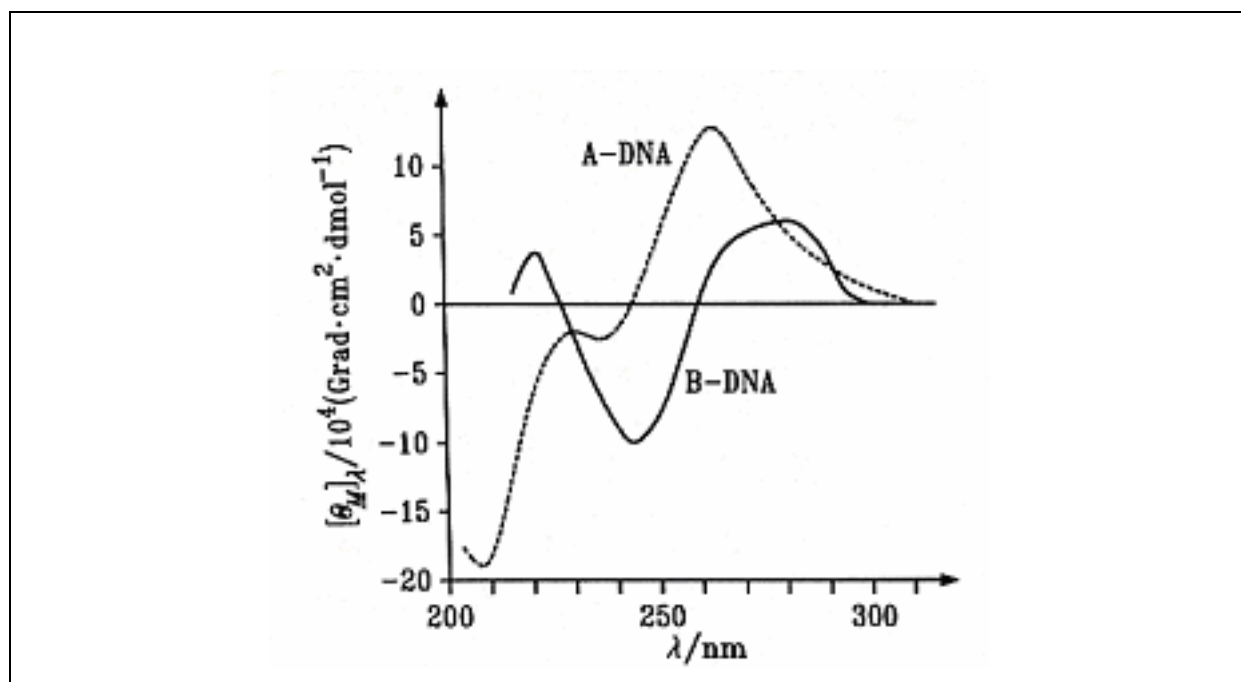
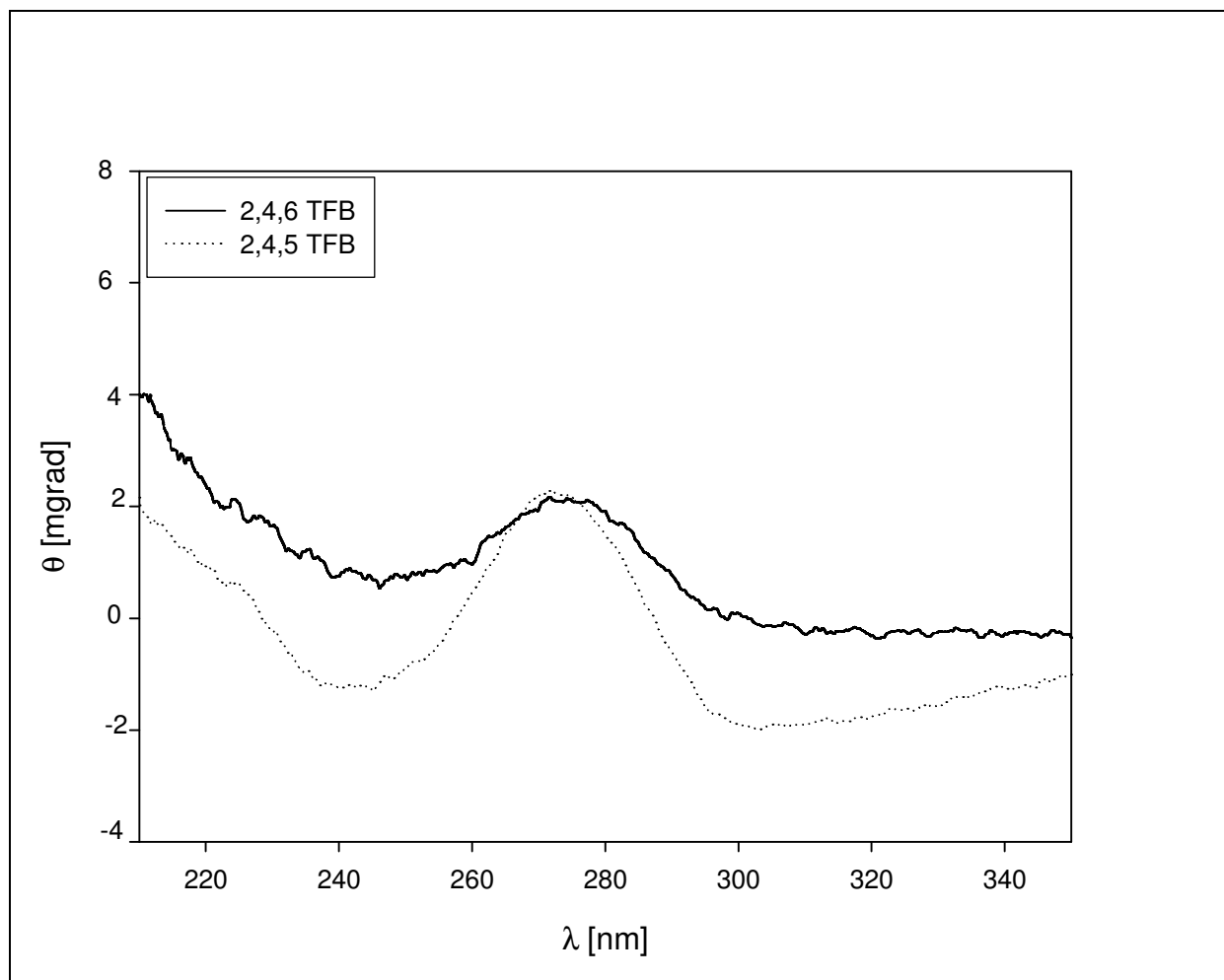


Figure 8. 27. CD-spectra of A-DNA and B-DNA (Winter & Noll, 1998)

## 8.2.2 Results of CD-Spectroscopy

CD-spectroscopic measurements were done on single strands of RNA and also RNA duplexes. Some examples are given in *figures 8.28-33*. The measurements were done on different temperatures. In *figure 8.28* are given CD of single strands at 10°C of S 7 and S 8 . Those CDs have maximum at 265-270 nm and no defined structure can be seen.



*Figure 8.28. CD of single stranded RNA S 7 (2,4,6 TFB) and S8 ( 2,4,5 TFB)*

The investigations of RNA duplexes (*figure 8.29* , *figure 8.30.*, *figure 8.31* and *figure 8.32* ) All of those duplexes show A-DNA structure and modified structures do not differ from unmodified ones. When stabilities of duplexes are lower the intensity is from 210 to 270 nm, also smaller.



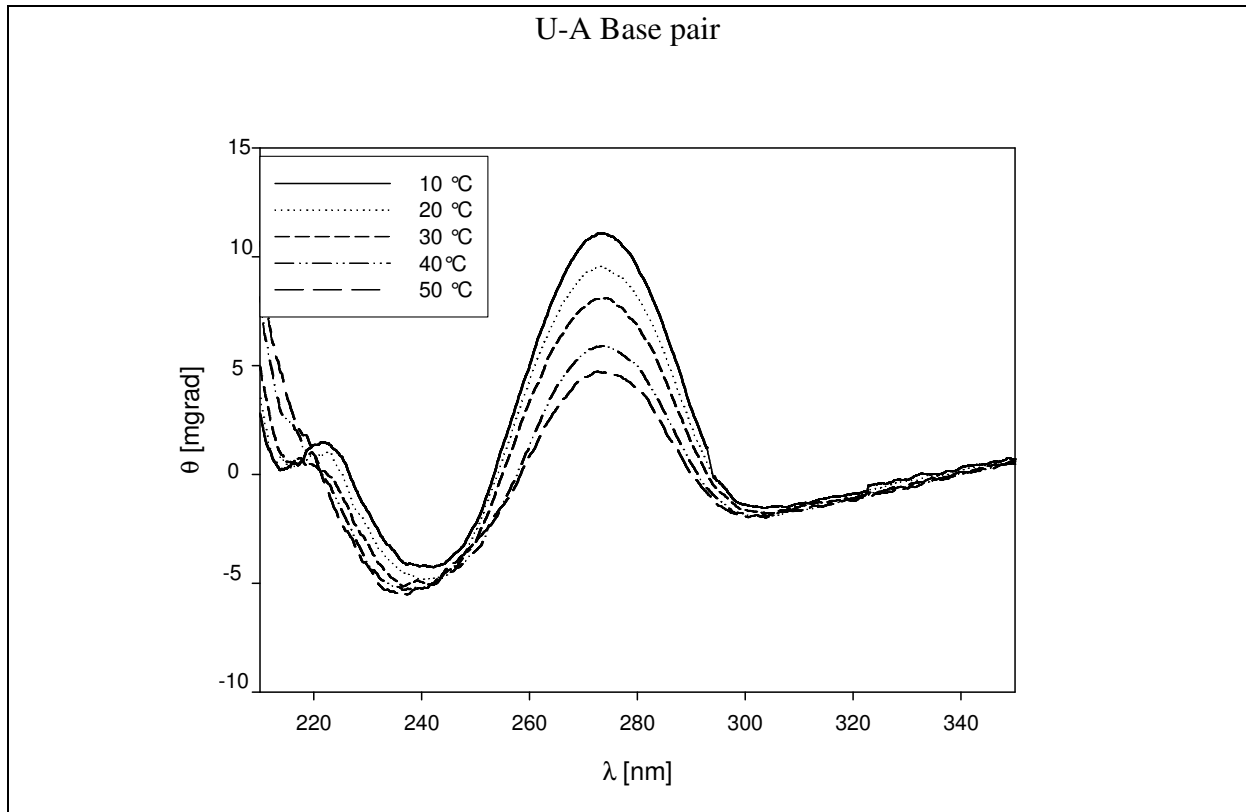


Figure 8.29. CD of RNA unmodified duplex ( S 1 and S 22 )

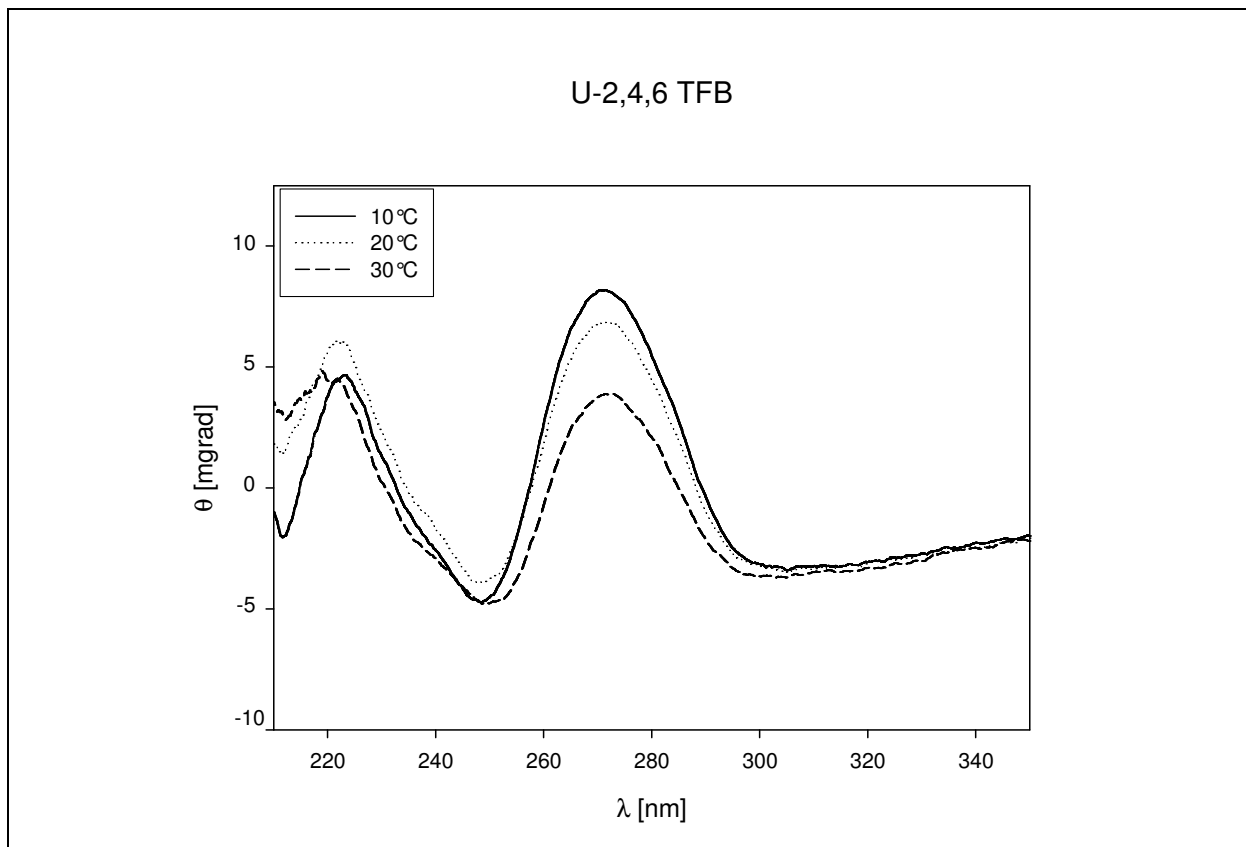


Figure 8.30. CD of RNA duplex of S1 and S36

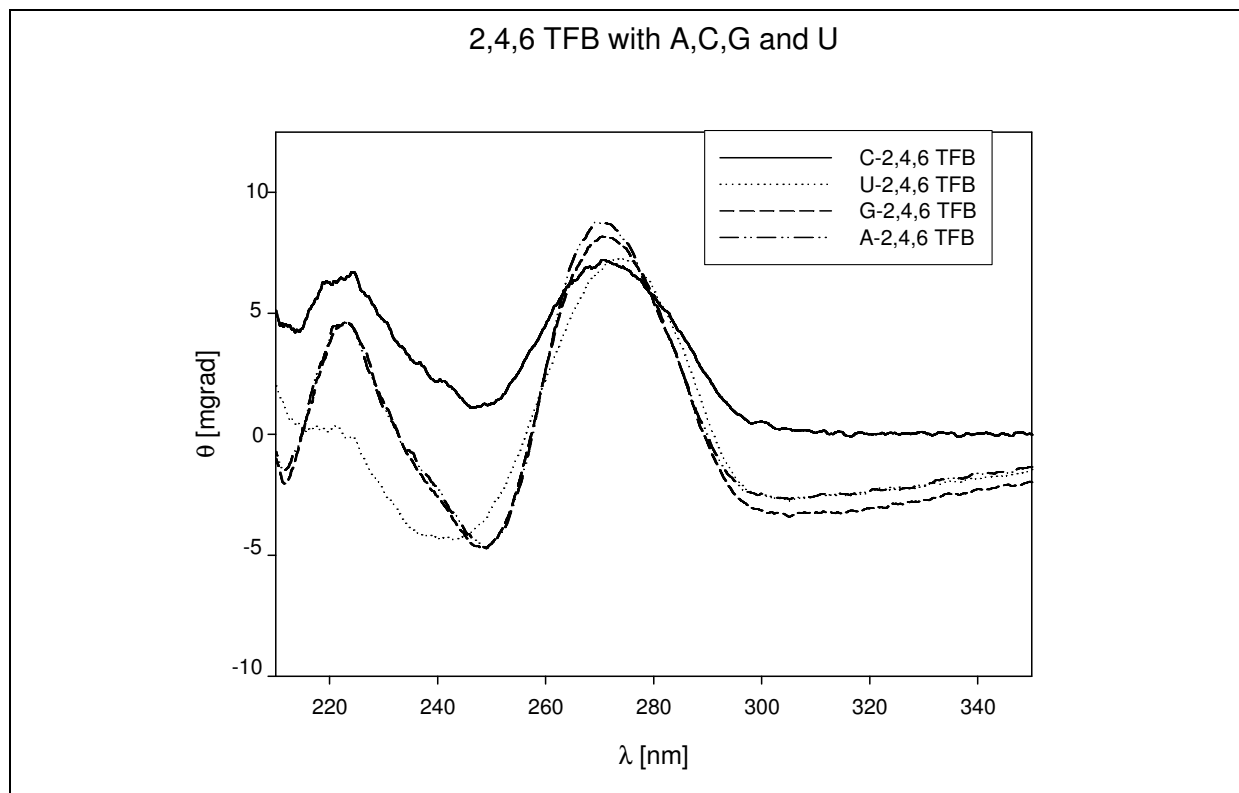


Figure 8.31.: CD spectrum of RNA duplex which at middle positions has 2,4,6 TFB paired with natural bases at 10°C, 20 °C and 30°C

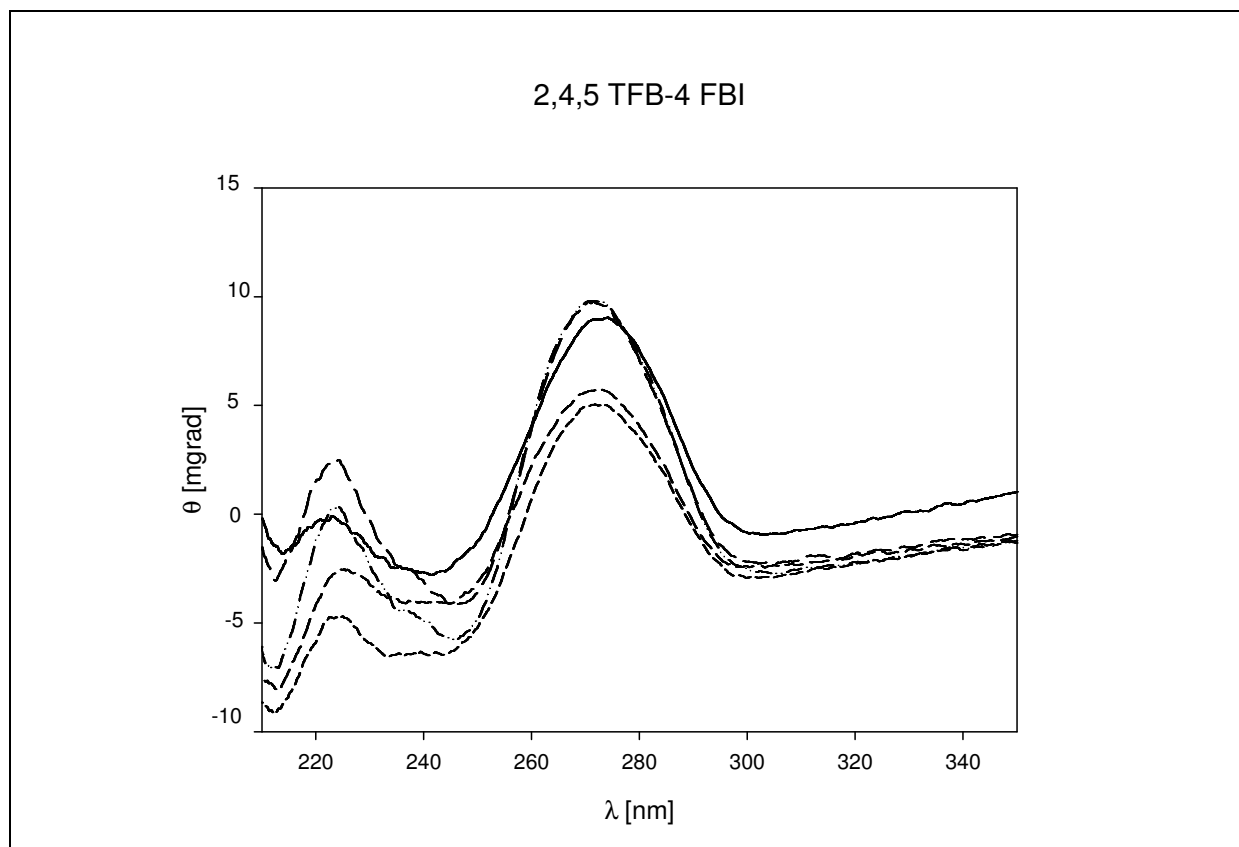


Figure 8.32. RNA duplexes at 10°C containing 2,4,5 TFB as middle base in C,U-rich sequence and A,C, G, U and 4 FBI in A,G-rich sequence

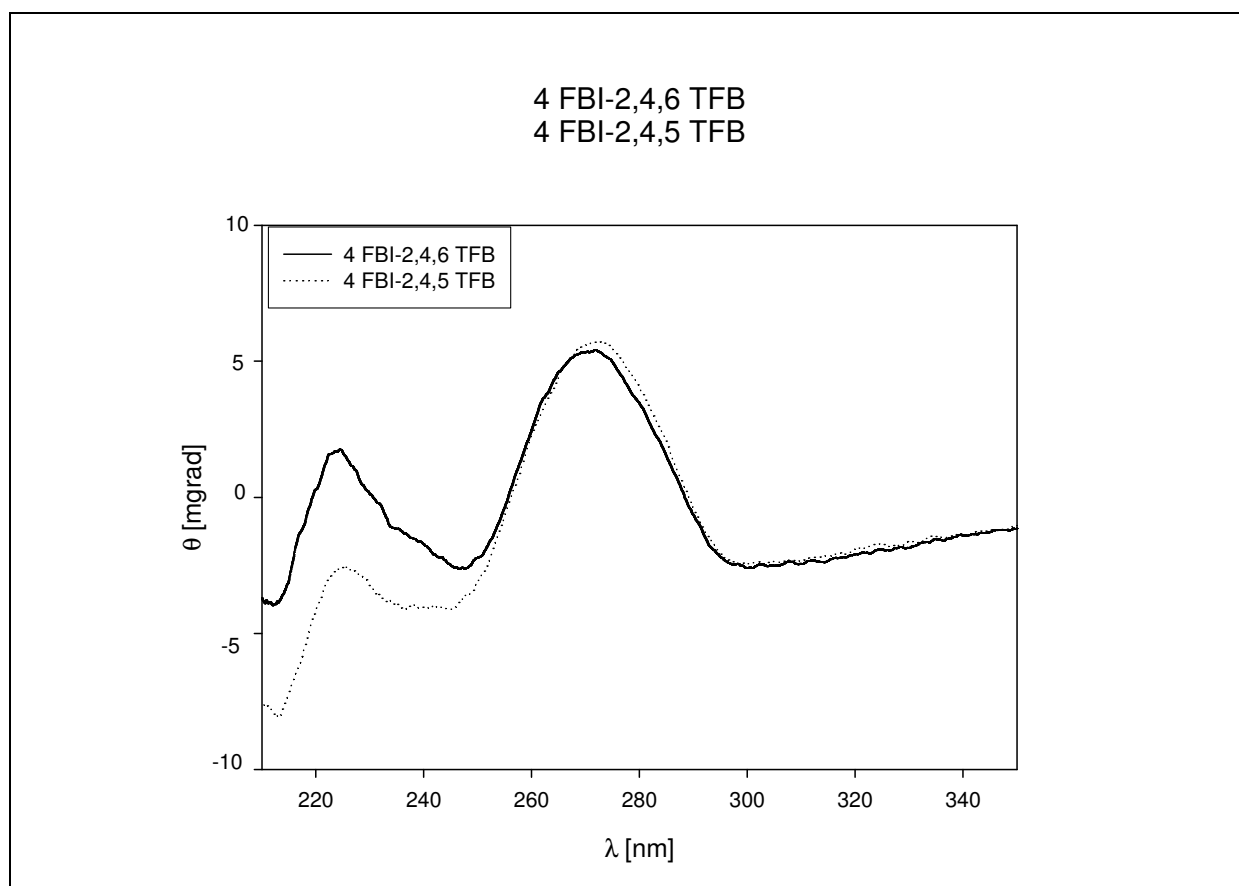


Figure 8.33. CD of RNA duplexes containing 2,4,5 TFB-4 FBI (S8+S24) and 2,4,6 TFB-4FBI (S7+S24) as middle base pairs

From all figures (8.28-8.33) can be seen that RNA duplexes with one and two modifications do not differ from unmodified ones. There from we can conclude that incorporation of our modifications has no influence on RNA structure, even our CDs have minor differences compared to ideal one but in our hands it was also the case with unmodified RNA duplexes (figure 8.29) (Clark *et al.*, 1997; Wörner *et al.*, 1999).

## 9 Summary

This work presents synthesis of the following fluorobenzene- and fluorobenzimidazole-nucleosides.

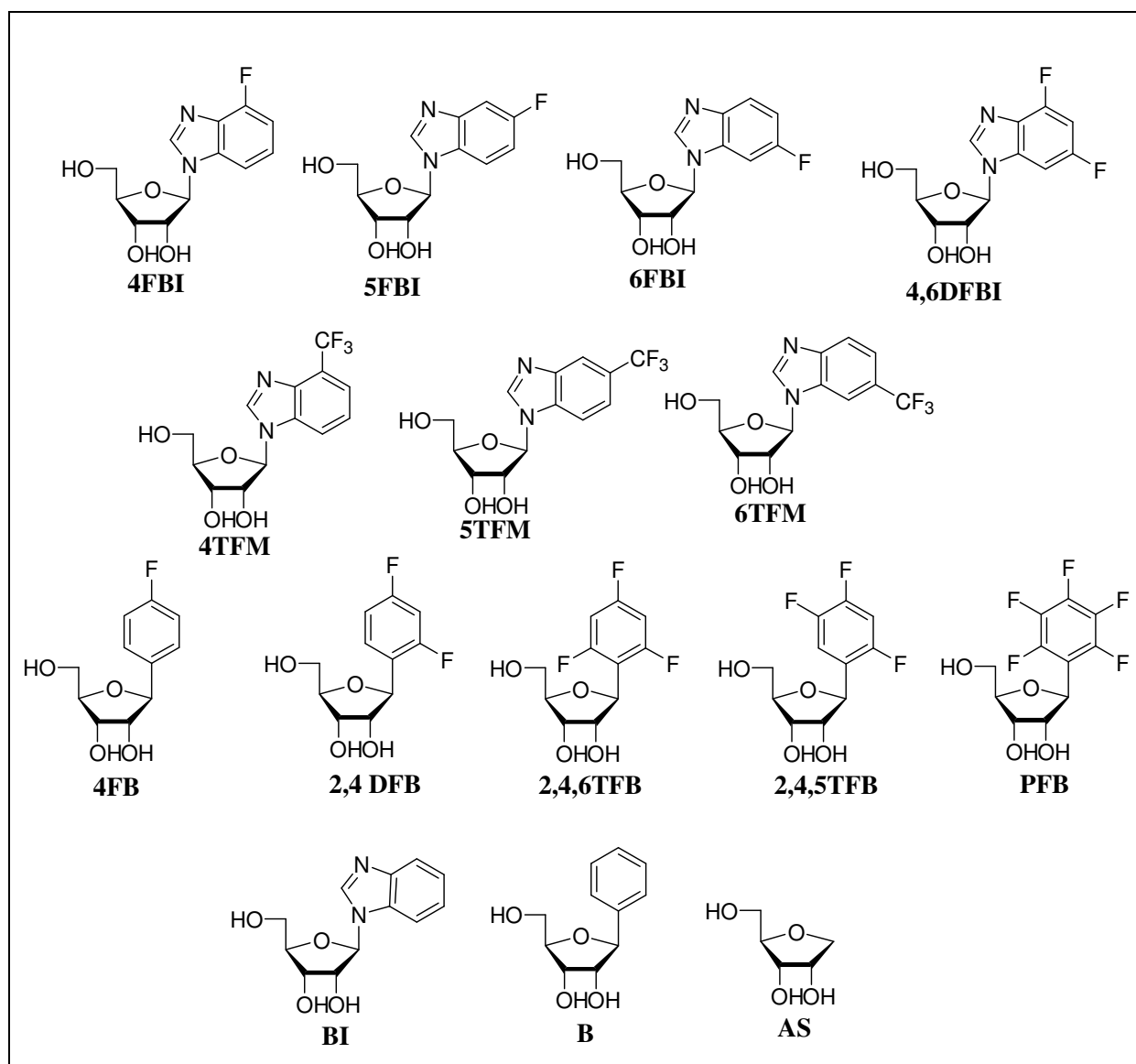


Figure 9.1. Synthesised modified bases and their abbreviations

All modifications shown in *figure 9.1.* were synthesised as phosphoramidites and incorporated in RNA oligonucleotides. In all cases ribose moiety is constant but the ``base` groups vary in the extent and orientation of fluorine substitution, from zero (as for B and BI) to 5 (for PFB).

1'-deoxy-1'(4,6-difluoro-1-N-benzimidazolyl)-  $\beta$ -D-ribofuranose (2,4 DFBI) is an isoster of natural xantine and 1'-deoxy-1'-(2,4-difluorophenyl)-  $\beta$ -D-ribofuranose (2,4 DFB) is isoster for uracil.

Fluorobenzimidazoles were synthesised from corresponding fluoroacetanilides. Trifluoromethylbenzimidazole nucleosides were from diamines synthesised (except 4TFM which was synthesised from corresponding trifluoromethylacetanilide). Glycosilation was done by Silyl-Hilbert-Johnson reaction and followed by deacetylation with sodium methanolate in methanol. For glycosilation of C-nucleosides we used 2,3,5-tri-O-benzyl-ribo- $\gamma$ -lactone. It was synthesised in a four-step procedure. After glycosilation (with n-BuLi or t-BuLi) with corresponding fluorobromobenzenes (or fluoro benzenes) nucleoside was deprotected with palladium hydroxide on carbon and with cyclohexene. The exception was AS, that was deprotected with bortribromide. Abasic site (AS) was obtained after dehydroxylation and deprotection of 2,3,5-tri-O-benzyl-ribofuranose.

From the crystal structures of fluorobenzonucleosides obtained, from water or methanol, we got data on their structures. In no crystal packing was seen a herringbone structure characteristic for fluorobenzenes themselves. The molecules have their hydrophilic part (ribose) and lipophilic part (base). The sugar parts are bonded with hydrogen bonds but for orientation of the molecules fluorine atoms are responsible. Short  $C_{sp}^2-F...H-C_{sp}^2$  distances were found in all crystal structures. In the bis-*ortho*-substituted trifluorobenzene modification (2,4,5 TFB) was found also one intermolecular distance of the type  $C_{sp}^2-F...H-C_{sp}^2$  from 2.34Å.

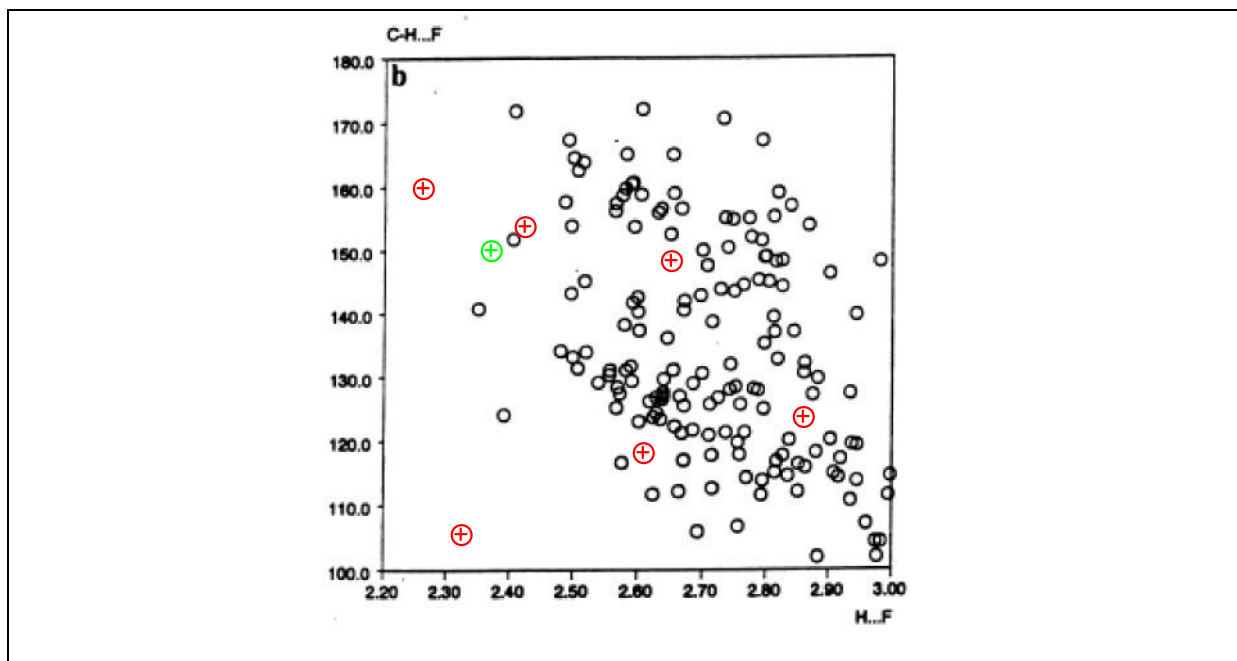


Figure 9.2. :  $F\dots H$  distances and angles of hydrogen bonds of  $C_{sp^2}-F\dots H-C_{sp^2}$  (Thalladi et al., 1998) filled with distances found and mentioned in this work (Parsch, 2000)-green for title compound, red for fluoro benzene modifications

We investigated also lipophilicity of synthesised nucleosides. Therefore we determined octanol-water partition coefficient and HPLC-retention times of nucleosides. All fluorinated nucleosides have significantly higher lipophilicity than non-fluorinated ones.

The unprotected nucleosides were incorporated in RNA as phosphoamidites by standard methods. Migration ability of TBDMS group in the 3'-direction did not allow high yields of 2'-TBDMS protected nucleosides. Obtained phosphoamidites were incorporated in RNA on the synthesiser by means of phosphoamidite chemistry. We synthesised 12mer RNA strands to investigate oligonucleotides with UV- and CD-spectroscopy. From the obtained melting curves we determined melting points and thermodynamical data.

The electrostatics vary widely over the series of benzene-nucleosides, with the phenyl nucleoside showing a negative potential at the centre of the flat aromatic face, and the penta fluorinated case having a strongly positive potential. Thus the quadrupoles are gradually inverted over this series. By comparison natural bases are not so strongly polarized in the quadrupole sense) and the quadrupole moments are close to zero. In this series also could be seen a broad range of dipole moments though the dipole orientations are quite similar over the series.

2,4,5 TFB builds 5-6°C more stable base pairs than 2,4,6 TFB. On one hand 2,4,5 TFB is almost as good as 2,4 DFB (not so “universal”) on the other hand 2,4,6 TFB is as bad as the benzene modification itself. Therefore we think that position 5 of the benzene ring is not of great importance for base pairing but the 2 and 6 positions (bis-*ortho*), first positions next to the glycosidic linkage) are significant for base pairing pattern of benzenes. Both PFB and 2,4,6 TFB are almost as poorly stabilizing as benzene itself (*figure 9.3*).

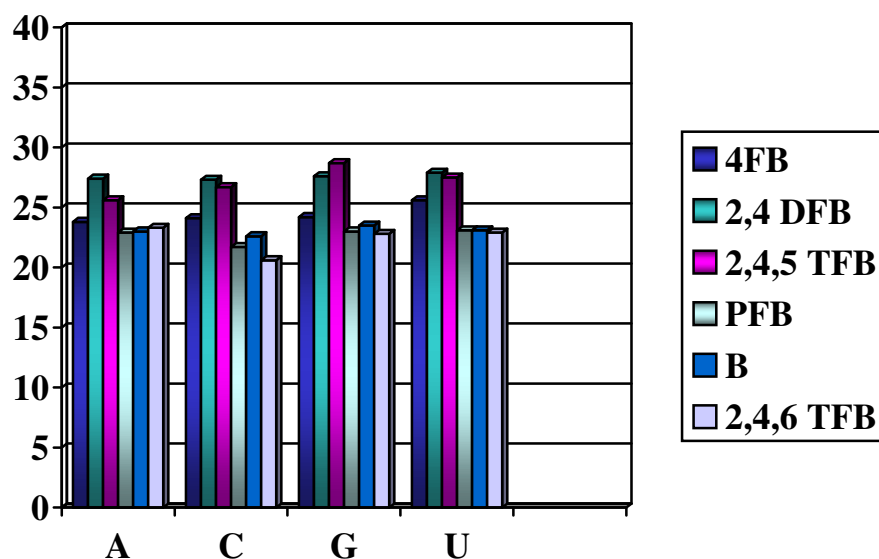


Figure 9.3. Graphical overview of  $T_m$  values of base pairs of fluoro-benzene modifications and natural bases

Therefore we can conclude here for this series that:

- Though fluorine is a very small substituent it can alter glycosidic orientation preferences in nucleosides, presumably by steric interactions with neighbouring bonds and substituents
- Bis-*ortho* substitution was very poor in stabilization and there is a great change in stability when a fluorine atom is ‘moved’ from *ortho* to *meta* position ( see results for 2,4,5 TFB and 2,4,6 TFB). This could be due to a sterically induced twist in the glycosidic bond and/or in the sugar. This would also explain large magnitude of instability of oligonucleotides containing PFB. These bis-ortho substituted bases are certainly to be avoided in the future design of nucleobases.
- On the example of PFB one can see that electrostatic repulsions between fluorines and  $\pi$ -cloud of non-fluorinated compound lead to additional destabilization of double helix RNA structure.

- When natural bases are involved in pairing with non-natural fluorinated bases quadrupole effect and dipole moment are small or nonexistent. However with to non-natural stacking partners (stronger polarized than natural bases) they might exhibit quadropolar stabilization or destabilization in water.

If we move now further, to the fluorinated benzimidazoles one can notice that there is a very small difference, if any, compared to benzimidazole (*figure 9.4.*).

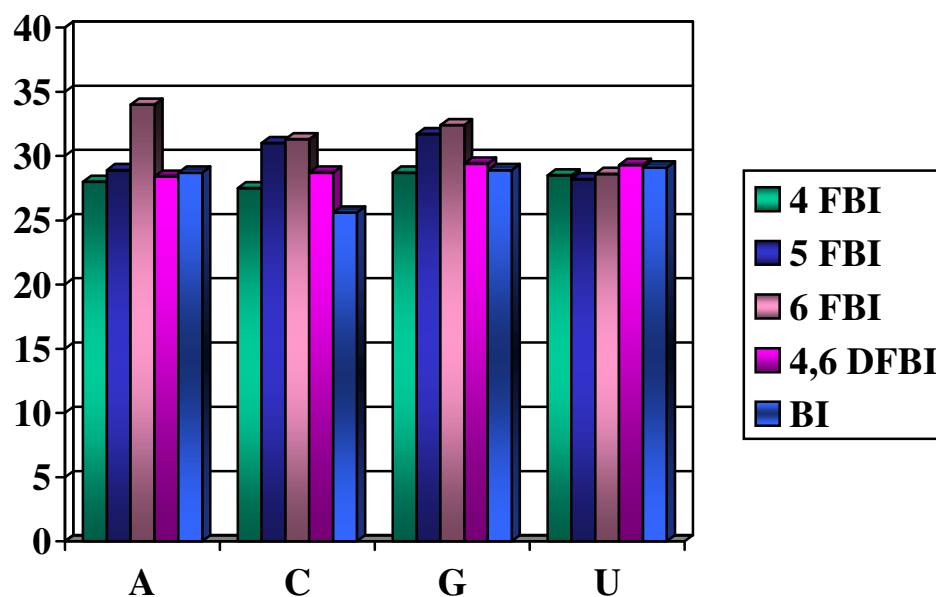


*Figure 9.4: Graphical overviews of Tm values of base pairs of fluoro-benzimidazole modifications and natural bases*

Here we can conclude the following:

- In benzimidazole modifications containing **fluorine** atom in different positions there is almost no difference compared to non-substituted imidazole (*figure 9.4.*)
- When there is in a base trifluoromethyl group the destabilization of duplex is of large magnitude (due to the large size of trifluoromethyl group and it's probable orientation in RNA duplex, we assume it is flipped out because results show clearly that stability of RNA duplex is higher when opposite TFM modification is an abasic site than any other base (*figure 9.5*))
- In general, that would mean that when the surface areas for stacking are larger (than in benzenes for example) the influence of constituents is almost of no importance. Only



when too large constituents are present the level of destabilization is larger (as for trifluoromethyl group)

- One can also notice that between the trifluoromethyl isomers (4 TFM, 5 TFM and 6 TFM) there is almost no difference in stability which is in accordance with the fact that position of trifluoromethyl group has no larger influence on polarizability, polarity or quadrupole moments of such compounds (figure 9.5)

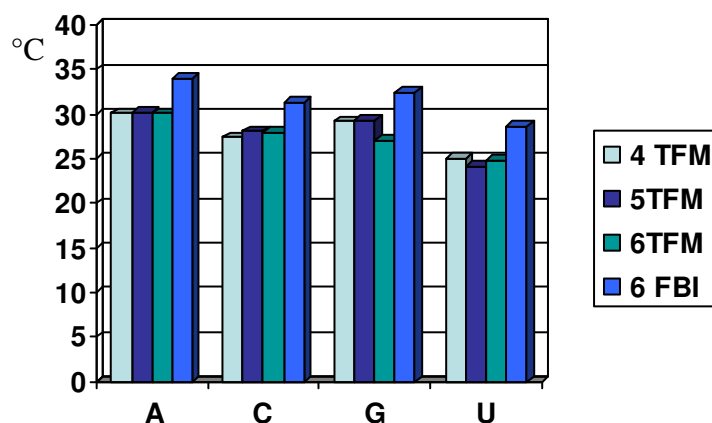
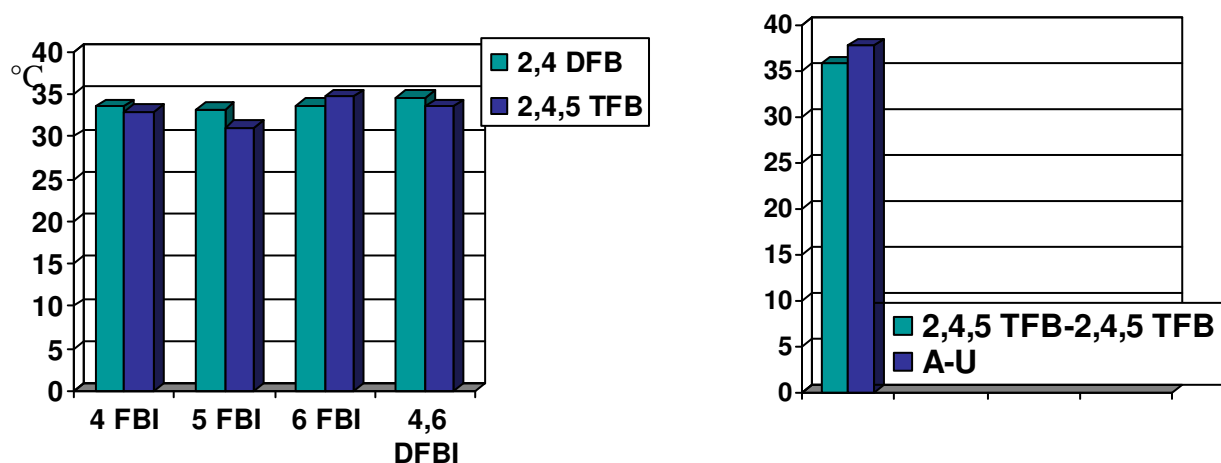


Figure 9.5. Graphical overviews of T<sub>m</sub> values of base pairs of trifluoromethyl-benzimidazole modifications and natural bases compared to 6FBI modification



	4FBI	5FBI	6FBI	4,6 DFBI
<b>2,4 DFB</b>	33.5°C	33.2°C	33.6°C	34.6°C
<b>2,4,5 TFB</b>	32.9°C	31°C	34.7°C	33.5°C

Figure 9.6. Most stable modified base pairs (values are shown in table)

If we compare than the non-natural base pairs we can say that most stable base pair from the ones we investigated is self-pair from 2,4,5 TFB which has T<sub>m</sub> value of 35.8 °C and the natural A-U base pair (in defined sequence) has T<sub>m</sub> of 37.8°C. From the base pairs formed in-

between benzene and benzimidazole modifications the most stable are the ones that are formed from 2,4 DFB and 2,4,5 TFB on the one side and 4 FBI, 5 FBI, 6 FBI and 4,6 DFBI on the other. Equally stable and the most stable are those two: 2,4 DFB -4,6 DFBI and 6 FBI-2,4,5 TFB (*figure 9.6.*).

In addition we found some additional stabilization forces (see chapter 8) with in following base pairs: 2,4 DFB on the one side and 4 FBI, 5 FBI, 6 FBI and 4,6 DFBI on the other side. The stabilization for the first three base pairs is 0.6°C and 0.4 kcalmol<sup>-1</sup> and for the 2,4 DFB-4,6 DFBI this stabilization is 0.9°C and 0.6 kcal mol<sup>-1</sup>. We assume that fluorine is very important for those stabilization forces and this interaction can be assigned as C-F...H-C hydrogen bonding, which is already known to be present in crystal structures. For stabilization of 0.4 kcalmol<sup>-1</sup> in 4 FBI-2,4 DFB, 5 FBI-2,4 DFB and 6 FBI-2,4 DFB one C-F...H-C hydrogen bridge is responsible while by 4,6 DFBI-2,4 DFB two hydrogen bonds are responsible for difference of 0.6 kcalmol<sup>-1</sup>. Slight movement of nucleobases, like in Wobble base pairs, allows forming of C-F...H-C hydrogen bond.

This work opens a few interesting further tasks in synthesis and investigation of modified nucleic acid analogues. An ‘unusual hydrogen bond’ as assumed is forming we would like to investigate employing NMR measurements of RNA oligonucleotides. In addition one can study stable 2,4,5 TFB-2,4,5 TFB base pair and it’s characteristics and also try to design ‘better’ modifications (more stable ones) than benzimidazoles (substituted indols etc.). Design of four-fluorinated (with one *ortho* position without fluorine) benzene nucleoside would be also an interesting task to check if that value corresponds our calculations ( $T_m$  value of this self-pair should than be 40°C-*figure 8.19*).



## 9 Zusammenfassung

Im Rahmen dieser Arbeit wurden folgende Fluorbenzol- und Fluorbenzimidazol-Nucleoside synthetisiert.

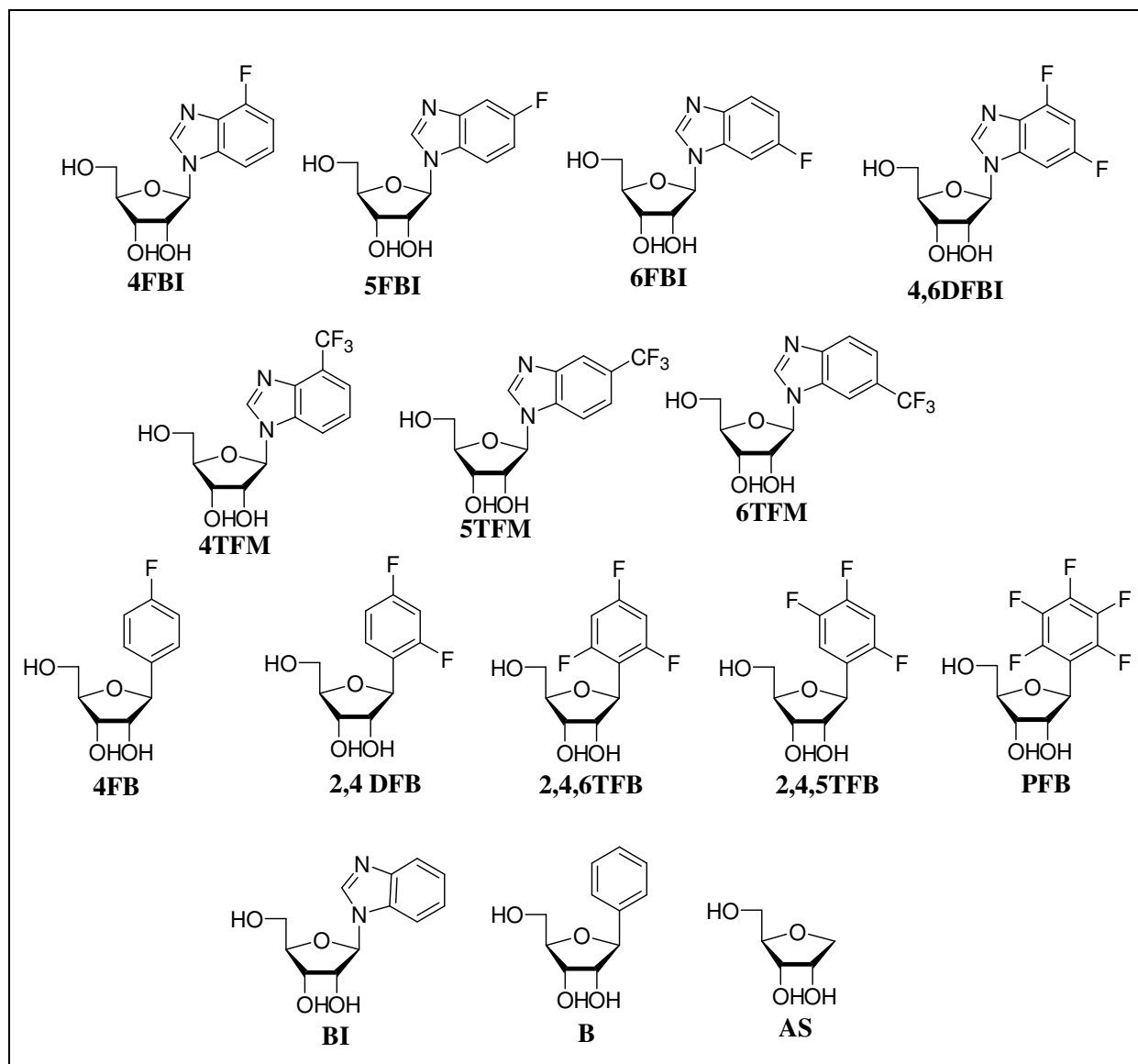


Abbildung 9.1. Synthetisierte Nucleoside

Alle Modifikationen die in Abbildung 9.1. dargestellt sind wurden synthetisiert und als Phosphoramidite in RNA Oligonucleotide eingebaut. Um den Einfluss der Fluorsubstitution untersuchen zu können wurden verschiedene Nucleobasen synthetisiert, ohne Fluor Substituenten (B, BI) bis zu fünf (PFB). 1'-Desoxy-1'(4,6-difluoro-1-N-benzimidazolyl)- $\beta$ -D-ribofuranose (4,6 DFBI) ist isoster zu natürlichem Xanthin und 1'-Desoxy-1'-(2,4-difluorophenyl)- $\beta$ -D-ribofuranose (2,4 DFB) zu Uracil.

Die Fluorobenzimidazole wurden ausgehend von den entsprechenden Fluoracetaniliden dargestellt. Die Trifluoromethylbenzimidazole wurden den entsprechenden von Diaminen dargestellt (nur 4 TFM von Trifluoromethylacetanilid). Die Glykosylierung erfolgte nach Silyl-Hilbert-Johnson Reaktion mit anschließender Deacetylierung der Hydroxylfunktionen mit Natriummethanolat in Methanol. Für die Glycosylierung der C-Nucleoside wurde 2,3,5-Tri-O-benzyl-ribo- $\gamma$ -lacton benötigt. Dies wurde über vier Stufen aus D-Ribose dargestellt. Nach der C-Glycosylierung (mit n-BuLi oder t-BuLi) mit dem entsprechenden Fluorobrombenzol wurde das Nucleosid mit Palladiumhydroxid auf Kohle und Cyclohexen in einer Transfer-Katalyse geschützt. Die Ausnahme bildete AS, das mit Bortribromid geschützt wurde. Der abasische Baustein (AS) wurde aus 2,3,5-Tri-O-benzyl-ribofuranose durch Dehydroxylierung und anschließende Entschützung gewonnen.

Von den Fluorobenzol-Nucleosiden gelang es Kristalle aus Wasser oder Methanol zu erhalten und röntgenkristallographisch zu untersuchen. Die Kristallpackungen zeigten eine sehr interessante Anordnung der Moleküle. Alle Fluor-Benzol Nucleoside zeigten nicht die für aromatische Systeme normale Fischgräten-Struktur, sondern eine Anordnung, in der sich die Moleküle gegenüberliegen. Kurze  $C_{sp^2}-F...H-C_{sp^2}$  Abstände wurden in allen Kristallstrukturen gefunden. In den bis-ortho-substituierten Trifluorobenzol-modifikation (2,4,6 TFB) wurde ein intermolekularer Abstand von 2,34 Å gefunden.

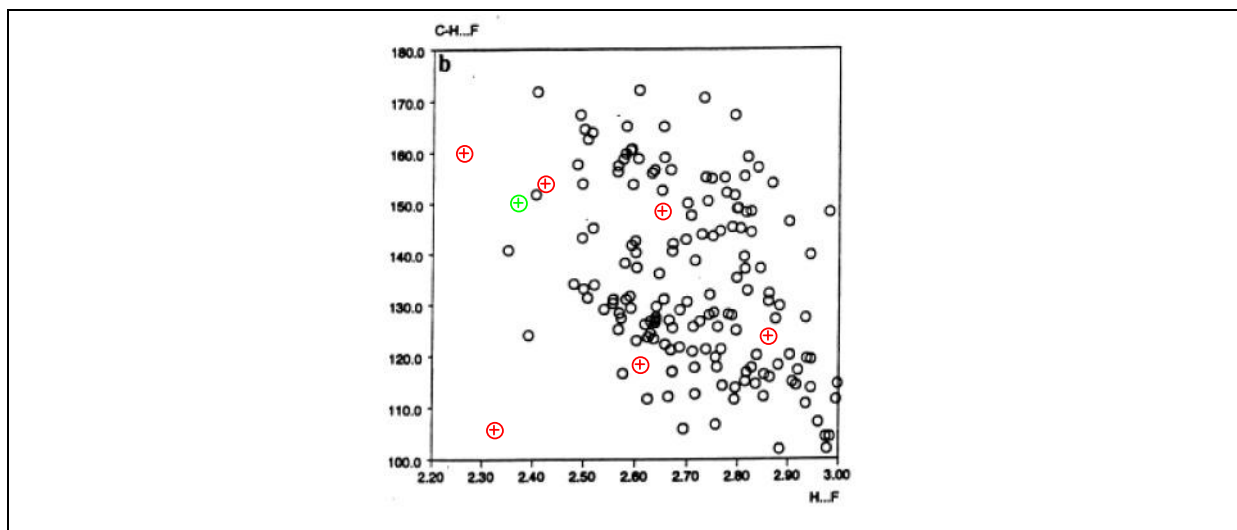


Abb. 9.2. :  $F\dots H$  Abstände und Winkel von Wasserstoffbrücken des Typs  $C_{sp^2}\text{-F}\dots\text{H-C}_{sp^2}$  (Thalladi et al., 1998) ergänzt mit den in dieser Arbeit gefundenen Werten (rote Kreise-fluorobenzole, grüner Kreis Fluorbenzimidazol)

Die Nucleoside wurden auf ihre Lipophilie hin untersucht. Zu diesem Zweck wurden Octanol-Wasser Verteilungskoeffizienten und HPLC-Retentionzeiten der Nucleoside gemessen. Die fluorierten Nucleoside zeigten im Gegensatz zu den nichtfluorierten Nucleosiden eine deutlich größere Lipophilie.

Die entschützten Nucleoside wurden nach Standardmethoden für RNA Bausteine in ihre Phosphoramidite überführt. Dabei stellte sich heraus, dass durch eine starke Wanderungstendenz der TBDMS-Gruppe in Richtung 3'-Hydroxylfunktion bei allen fluormodifizierten Nucleosiden das gewünschte 2'-geschützte Isomer nur in niedrigen Ausbeuten erhalten werden konnte.

Die erhaltenen Phosphoramiditbausteine wurden mittels der Phosphoramiditmethode an einem Syntheseautomaten in Ribonukleinsäure (RNA) eingebaut. Dazu wurden RNA Stränge aus zwölf Nucleotiden mit einer Modifikation in der Mitte synthetisiert und aufgereingt. Um festzustellen, ob die erhaltenen 12mer RNA Duplexe bilden, wurde mittels UV- und CD-Spektroskopie untersucht. Aus den erhaltenen Schmelzkurven wurden die Schmelzpunkte bestimmt und die thermodynamischen Daten errechnet.

Die elektrostatischen Wechselwirkungen variieren über eine Serie von Benzol-Nucleosiden (B), mit einem Phenyl-Nucleosid das ein negatives Potential in Zentrum des Aromaten zeigt und dem pentafluorierten-Nucleosid (PFB) das dort stark positives Potential hat. Beim Vergleich sind die natürlichen Basen nicht so stark polarisiert und die Quadrupol Momente sind fast Null.

2,4,5 TFB bildet 5-6°C stabilere Basenpaare als 2,4,6 TFB. Einerseits ist 2,4,5 TFB so gut wie 2,4 DFB (nicht so "universell") andererseits ist 2,4,6 TFB so schlecht wie die Benzol Modifikationen (B). Aufgrund dessen liegt die Vermutung nahe, dass die Position 5 des Benzols für die Basenpaarung nicht essentiell ist. Die Positionen 2 und 6 hingegen sind für die Basenpaarung essentiell. Die ersten Positionen in nächster Nähe zur glykosidischen Bindung sind signifikant für die Basenpaarung des Benzols. Die Modifikationen PFB und 2,4,6 TFB haben dieselben  $T_m$  - Werte wie die Benzolmodifikationen ( Abb.9.3 ).

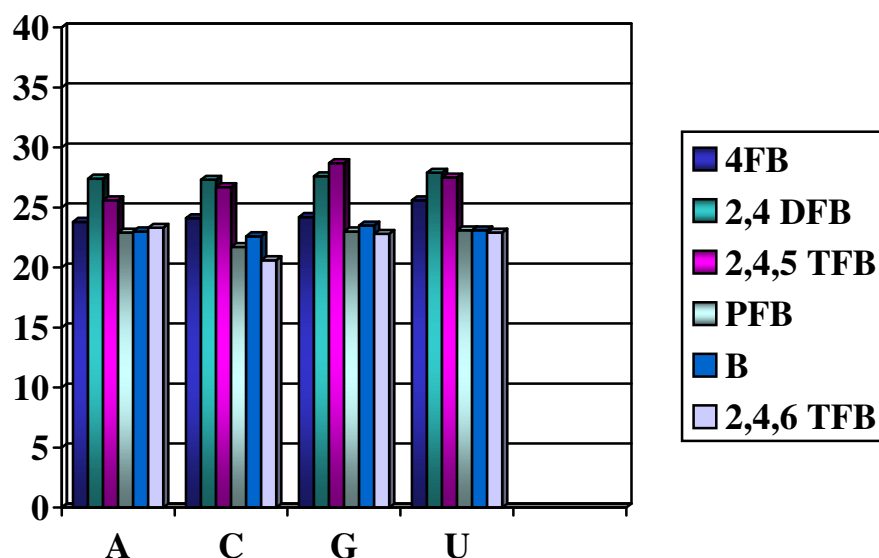


Abb. 9.3.: Graphische Darstellung der  $T_m$  Werte von Fluorbenzol-mit Natürlichen Basen

Somit können wir für diese Serie festhalten:

- Obwohl die Fluorsubstituenten klein sind können sie die glykosidische Orientierung beeinflussen. Dies liegt höchstwahrscheinlich an der sterischen Wechselwirkung mit benachbarten Bindungen und Substituenten.
- Die bis-ortho Substitution bewirkt keine gute Stabilisierung. Die Substitution eines Fluors in meta anstatt in der ortho-Stellung bewirkte einen großen Unterschied in der Stabilität( 2,4,5 TFB und 2,4,6 TFB). Der Grund dafür ist der sterisch induzierte Twist in der glykosidischen Bindung und/oder in der Ribose. Dies wäre ebenfalls eine Erklärung für die große Destabilisierung in PFB modifizierten Oligonukleotiden. Diese bis-ortho substituierten Basen sollten in zukünftigem Design von Nukleobasen nicht verwendet werden.

- Am Beispiel des PFB wurde ersichtlich, dass elektrostatische Repulsionen zwischen Fluor und dem delokalisierten  $\pi$ -System von nichtfluorierten Komponenten zu einer wachsenden Destabilisierung der Doppelhelix RNA führen.
- Bei der Basenpaarung von natürlichen Nukleobasen mit nicht-natürlichen fluorierten Basen wurde ersichtlich, dass der Quadrupol Effekt sowie das Dipolmoment sehr klein bzw. nicht vorhanden sind. Zwei nicht-natürliche Stacking Partner, die stärker polarisiert sind als natürliche Nukleobasen, können zu einer quadrularen Stabilisierung oder Destabilisierung in Wasser führen.

Bei der Betrachtung der fluorierten Benzimidazole wird ersichtlich, dass es nur einen kleinen Unterschied zu Benzimidazolen gibt. (Abb. 9.4.).

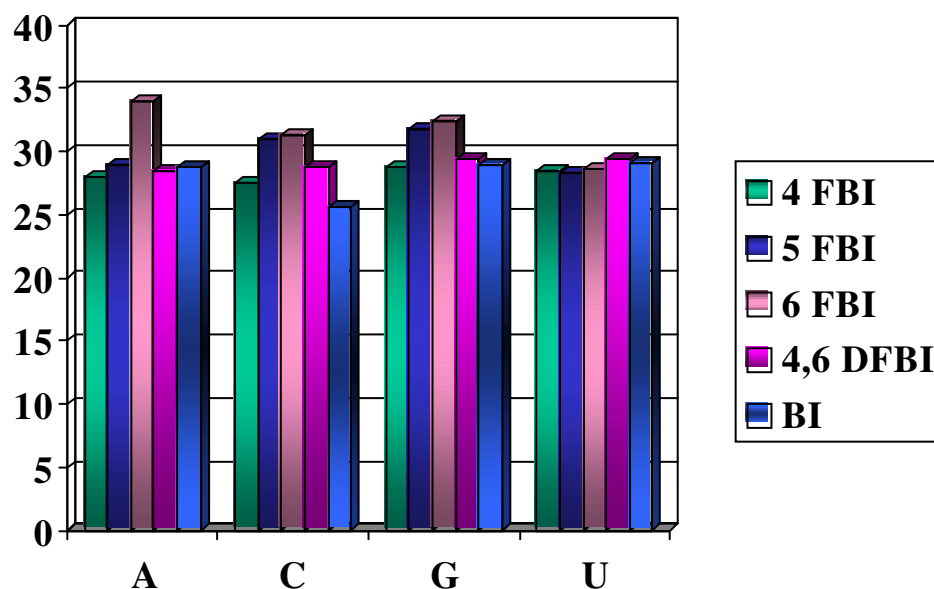


Abb. 9.4: Graphische Darstellung der  $T_m$  Werte von den Fluorbenzimidazol-Natürlichen Basenpaaren

Folgende lässt sich zusammenfassen:

- In Benzimidazol Modifikationen die Fluor-Atome in verschiedenen Positionen enthalten ist fast kein Unterschied im Vergleich i nicht-substituierten Benzimidazolen (Abb. 9.4.)
- Beim Vorhandensein einertrifluoromethylgruppe ist die Destabilisierung groß, aufgrund der großen Trifluormethylgruppe und der wahrscheinlichen Orientierung im RNA Duplex ( DieVermutung liegt nahe, dass diese Base sich außerhalb des Duplexes befindet ) (Abb. 9.5).



- Allgemein würde das bedeuten, dass für größere  $\pi$ -Stacking Systeme ( z.B. größer als Benzol) der Einfluss der Substituenten von geringerer Wichtigkeit ist. Nur beim Vorhandensein sehr großer Substituenten ist die Destabilisierung größer.
- Es wurde ersichtlich, dass zwischen den Trifluor Isomeren ( 4TFM, 5TFM, 6TFM ) es keinen Unterschied in der Stabilität gibt. Die Position der Trifluormethylgruppe hat keinen bedeutenden Einfluss auf die Polarisierbarkeit, Polarität oder das Quadrupol Moment (Abb. 9.5).

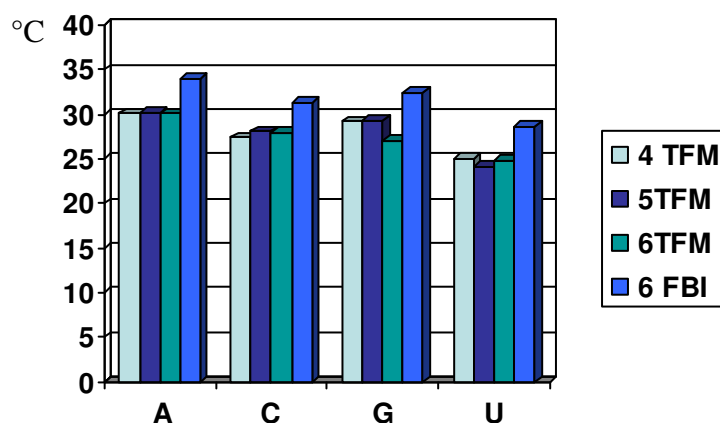
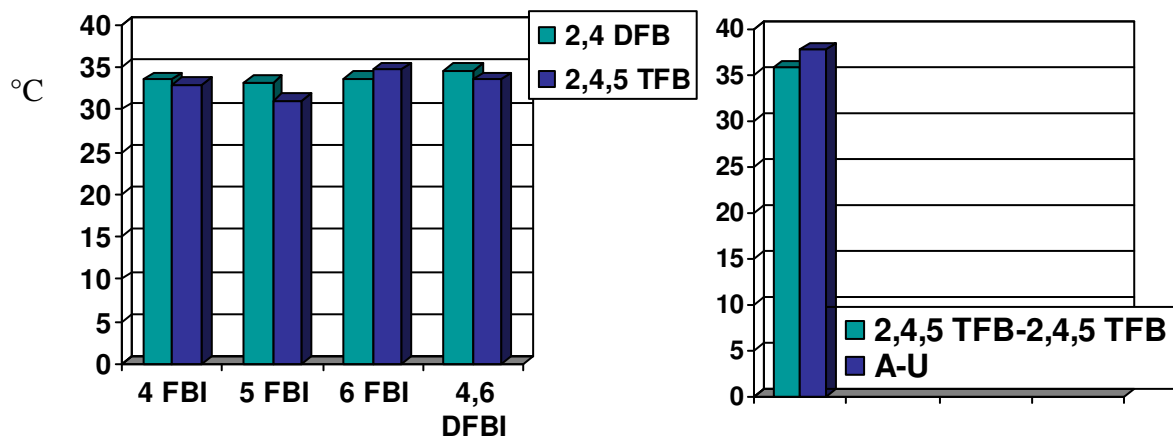


Abb. 9.5: Graphische Darstellung der Tm Werte der Trifluoromethylbenzimidazol-Natürliche Basenpaare im Vergleich zu 6FBI-Natürlichen Basenpaaren



	4FBI	5FBI	6FBI	4,6 DFBI
<b>2,4 DFB</b>	33,5°C	33,2°C	33,6°C	34,6°C
<b>2,4,5 TFB</b>	32,9°C	31°C	34,7°C	33,5°C

Abb. 9.6.: Graphische Darstellung der Tm Werte von den Modifizierten Basenpaaren

Beim Vergleich von nicht-natürlichen Basenpaaren sind die stabilsten Basenpaare von 2,4,5, TFB mit einem Tm von 35,8°C und das natürliche Basenpaar A-U mit einem Tm von 37,8°C.

Die stabilsten Basenpaare zwischen Benzol und Benzimidazol Modifikationen sind die zwischen 2,4 PFB und 2,4,5 TFB auf der einen Seite und 4FBI, 5 FBI, 6 FBI auf der anderen Seite. Die stabilsten sind : 2,4 DFB – 4,6 DFBI sowie 6 FBI – 2,4,5 TFB (Abb. 9.6).

Im Falle der 2,4 DFB- 4 FBI, 2,4 DFB-5 FBI, 2,4 DFB-6 FBI und 2,4 DFB-4,6 DFBI Basenpaare sind die gemessenen Werte allerdings um 0,6°C (0,4kcal/mol) bzw. 0,9°C (0,6 kcal/mol) höher als die errechneten. Da sich diese Basenpaare von dem Benzimidazol(I)-Benzol (B) nur durch die Fluoroatome unterscheiden, muss die Stabilisierung der RNA Duplexe durch Wechselwirkungen des Fluors zustande kommen. Bei dieser Wechselwirkung zwischen zwei modifizierten Nucleobasen könnte es sich um F...H Wasserstoffbrücken handeln, wie sie auch schon in Kristallen von Nucleosiden nachgewiesen werden konnten.

Als Ausblick für zukünftige Arbeiten auf diesem Gebiet ausgehend von den in dieser Arbeit erhaltenen Ergebnisse werden folgende Untersuchungen angeregt:

Diese Arbeit eröffnet ein interessantes Aufgabenfeld für die Synthese von modifizierten Nukleinsäureanaloga. Die von uns vermutete unübliche Wasserstoffbrückenbindung wurde bestätigt und wird in nächster Zeit mittels NMR-Messungen von RNA Oligonukleotiden verifiziert. Des weiteren könnte man die Stabilität der 2,4,5 TFB-2,4,5 TFB Basenpaare und ihre Charakteristiken untersuchen. Die Synthese von verbesserten Modifikationen, d.h. stabilere als die der Benzimidazole sowie die Synthese von vierfach fluorierten ( ortho Position ohne Fluor) Benzol Nucleosiden und die anschließende Untersuchung der Schmelzpunkte sind ebenfalls lohnende Aufgabenstellungen für anstehende Arbeiten.



# 10 Experimental Part

## 10.1 Main Methods

### 10.1.1 Chromatography

For the chromatography (TLC, pTLC and FC) the following solvents were used:

- Acetonitrile; p.a.
- Ethyl acetate; technical quality, dried over calcium chloride and distilled
- *n*-Hexane; technical quality, distilled under normal pressure
- Isopropanol; technical quality, distilled under normal pressure
- Methanol; technical quality, distilled under normal pressure over CaCO<sub>3</sub>
- Methylene chloride; technical quality, dried over calcium chloride and distilled
- Water; distilled

#### Thin Layer Chromatography (TLC)

For the analytical TLC silica gel 60 on the aluminum plates with fluorescence indicator was used (Merck Nr. 5554; 0,2 nm), that were cut to 2-5 × 10 cm dimensions. The eluent way is around 8-9 cm. UV-active substances were detected with UV-lamp by 254 nm. TLC with UV-inactive substances (sugar moieties) were put in reagent that consists of: 10% acetic acid, 5% anisaldehyde and 5% of conc. sulphuric acid in 75 % of water and 25 % ethanol and then warmed up to around 300°C (heating gun). Then the compounds are coloured black.

The dimethoxytrityle group could be detected with vapour of conc. HCl (orange colour).

### **Preparative Thin Layer Chromatography**

For the preparative thin layer chromatography was used chromatotron (company Harrison Research (Model 7924 T)). As the separating material was used silica gel (Merck 60 PF<sub>254</sub>, Nr. 7749), that was put on the glass plate (radius 20 cm) in the density of 1,2 or 4 mm. The detection was performed with the wavelength of 254 nm.

### **Preparative Column Chromatography (Flash-Chromatography, FC)**

The FC (Still at al., 1978) was performed with silica gel 60 (40-63  $\mu\text{m}$ , Merck Nr. 9385) The columns of different size and radius were used for separations.

### **High Performance Liquid Chromatography (HPLC)**

The HPLC separations of oligonucleotides were done on the JASCO machine. Details are described in the chapter 7.

## **10.1.2 Spectroscopy**

### **NMR-Spectroscopy**

The NMR spectra were recorded on the following machines: AM 250, WH 270, AMX 400 and AMX 800 from Bruker company. As solvents were used: DMSO-d<sub>6</sub> with  $\delta = 2,49$  ppm and CDCl<sub>3</sub> with  $\delta = 7,27$  ppm for the <sup>1</sup>H-NMR-Spectra; DMSO-d<sub>6</sub> with  $\delta = 39,5$  ppm and CDCl<sub>3</sub> with  $\delta = 77,0$  ppm for the <sup>13</sup>C-NMR-Spectra. For the <sup>19</sup>F-NMR-Spektra in DMSO-d<sub>6</sub> as standard CCl<sub>3</sub>F  $\delta = -162,9$  ppm was used. All spectra were measured at 300K.

### **UV/VIS-Spectroscopy**

The UV-Spectra were measured on a UV-Spectral photometer from Varian Company (Model Cary 1).

### **IR-Spectroscopy**

The IR Spectra were recorded on an IR-Spectrometer from Perkin Elmer ( 1600 Series FTIR).

### 10.1.3 Mass spectrometry

The mass spectra were measured on the machines from the companies VG Analytical and VG Biotec (today: Micromass). For the electron spray-ionisation (ESI) was used VG Platform II with Quadrupol Analysator. Spectra with matrix support laser desorption/ ionisation (MALDI) were measured on VG Tofspec.

### 10.1.4 Elementary Analysis

The elementary analysis was done on the machine of the company Foss-Heraeus (CHN-O-Rapid).

### 10.1.5 Melting Point Determination

The melting points were measured on an apparatus according to Tottoli from company Büchi (Model Büchi 510). The values are given as measured.

## 10.2 List of Chemical Reagents

Acetic acid;  $C_2H_4O_2$  [60,05]; Riedel-de Haën Nr. 33209,  $\geq 99,8 \%$ , Bp. 117-118°C,  $d = 1,049$

Acetic acid anhydride;  $C_4H_6O_3$  [102,09]; Fluka Nr. 45830, puriss. p.a., Bp. 138-140°C,  
 $d = 1,08$

Acetonitrile;  $C_2H_3N$  [41,05]; Roth Nr. 8825.2, 99,5 %, for HPLC, Bp. 81-82°C,  $d = 0,78$

Acetonitrile;  $C_2H_3N$  [41,05]; Fluka Nr. 00695, puriss.,  $\geq 99,5 \%$ , absolute, over molecular  
sieve  $H_2O \leq 0,01 \%$ , Bp. 82°C,  $d = 0,782$

Acetonitrile;  $C_2H_3N$  [41,05]; Fluka Nr. 00709, puriss.  $\geq 99,5 \%$ , absolute, over molecular  
sieve  $H_2O \leq 0,001 \%$ , Bp. 82°C,  $d = 0,782$  (for the synthesis of phosphoramidites)

Amberlite IRA 93; Fluka Nr. 06441, freebase

Ammonium hydroxide;  $NH_4OH$  [35,05]; Merck Nr. 1.05426, 32 %,  $d = 0,88$

Ammonium chloride;  $NH_4Cl$  [53,49]; Fluka Nr. 09702, purum p.a.,  $\geq 99 \%$

Argon; Quality 4.8

Benzimidazole;  $C_7H_6N_2$  [118,14]; Fluka Nr. 12250, purum,  $\geq 98 \%$ , Mp. 171-173°C

Benzene;  $C_6H_6$  [78,12]; Fluka Nr. 12552, puriss. p.a., Bp. 80°C,  $d = 0,879$

Benzyl chloride;  $C_7H_7Cl$  [126,59]; Fluka Nr. 13280, purum,  $\geq 99 \%$ ,  $d = 1,10$

- N,O*-Bis-(trimethylsilyl)-acetamide;  $C_8H_{21}NOSi_2$  [203,43]; Fluka Nr. 15241, Bp.<sup>(35 mm)</sup> 71-73°C,  $d = 0,832$
- Borontribromide; 1 M solution in methylene chloride;  $BBr_3$  [250,54]; Fluka Nr. 15692; purum,  $d = 1,46$
- Borontrifluoride-Ethyletherat;  $BF_3 \cdot C_4H_{10}O$  [141,93]; Fluka Nr. 15719, purum, acid free, Bp. 128°C,  $d = 1,13$
- Bromobenzene;  $C_6H_5Br$  [157,02]; Fluka Nr. 16350, puriss.,  $\geq 99,5 \%$ , Sdp. 154-155°C,  $d = 1,494$
- 1-Bromo-2,4-difluorobenzene;  $C_6H_3BrF_2$  [192,99]; Lancaster Nr. 0930,  $\geq 98 \%$ , Bp.<sup>(20 mm)</sup> 53-54°C,  $d = 1,708$
- 1-Bromo-2-fluorobenzene;  $C_6H_4BrF$  [175,01]; Lancaster Nr. 2374, 99 %, Bp. 155-157°C,  $d = 1,611$
- 1-Bromo-3-fluorobenzene;  $C_6H_4BrF$  [175,01]; Lancaster Nr. 6478, 99 %, Bp.<sup>(80 mm)</sup> 77-79°C,  $d = 1,594$
- 1-Bromo-4-fluorobenzene;  $C_6H_4BrF$  [175,01]; Lancaster Nr. 3391, 99 %, Bp. 152-155°C,  $d = 1,604$
- 1-Bromo-2,4,6-trifluorobenzene;  $C_6H_2BrF_3$  [210,98]; Lancaster Nr. 2134, 98 %, Bp. 140-141°C,  $d = 1,790$
- 1-Butanol;  $C_4H_{10}O$  [74,12]; Fluka Nr. 19430, purum,  $\geq 98 \%$ , Bp. 116-118°C,  $d = 0,81$
- tert.*-Butyldimethyl chlorosilane (TBDMSCl); 1 M solution in THF;  $C_6H_{15}ClSi$  [150,73]; Fluka Nr. 19904, purum,  $d = 0,886$
- n*-Butyllithium; 1,6 M solution in *n*-hexane;  $C_4H_9Li$  [64,09]; Aldrich Nr. 18,617-1,  $d = 0,68$
- Celite-Filtergel; Fluka Nr. 22139
- Citric acid monohydrate;  $C_6H_8O_7 \cdot H_2O$  [210,1]; Fluka 27490, puriss, p.a.;
- Chloroforme- $d_1$ ;  $CDCl_3$  [120,37]; Deutero GmbH, 99,8 Atom % D, stabilisiert mit Silber
- Chrometrioxyde;  $CrO_3$  [99,99]; Fluka Nr. 27083, purum p.a.
- sym.*-Collidine = 2,4,6-Trimethylpyridine;  $C_8H_{11}N$  [121,18]; Fluka Nr. 27690, puriss. p.a.,  $\geq 99 \%$ , Bp. 170-172°C,  $d = 0,914$
- Cyclohexene;  $C_6H_{10}$  [82,15]; Fluka Nr. 29240, purum,  $\geq 99 \%$ , stabilised with ~0,01 % 2,6-Di-*tert.*-butyl-*p*-kresol, Bp. 81-84°C,  $d = 0,81$
- Deuterium oxide;  $D_2O$ ; Deutero GmbH, 99,9 Atom % D
- Dibutyltin dichloride;  $C_8H_{18}Cl_2Sn$  [303,83]; Fluka Nr. 34920, pract.  $\approx 97 \%$
- 1,2-Dichlorethane = Ethylene chloride;  $C_2H_4Cl_2$  [98,96]; Fluka Nr. 03527, puriss., absolute, over molecular sieve  $\geq 99,5 \%$ ,  $H_2O < 0,005 \%$ , Bp. 84°C,  $d = 1,253$

- Diethyl ether;  $C_4H_{10}O$  [74,12]; Fluka Nr. 31685, puriss.,  $\geq 99,5 \%$ , over molecular sieve, stabilised with 2,6-Di-*tert.*-butyl-*p*-kresol, Bp. 35-36°C,  $d = 0,713$
- Diethyl pyrocarbonate (DEPC);  $C_6H_{10}O_5$  [162,14]; Fluka Nr. 32490, purum,  $\geq 97 \%$ , Bp. 160-163°C,  $d = 1,12$
- 2,4-Difluoroacetanilide;  $C_8H_7F_2NO$  [171,15]; Lancaster Nr. 14152, Mp. 122-124°C
- Diisopropylazodicarboxilate (DIAD);  $C_8H_{14}N_2O_4$  [202,21]; Fluka Nr. 11626, pract.  $\approx 95 \%$ , Bp.<sup>(0,25 mm)</sup> 75-77°C,  $d = 1,044$
- Diisopropylamine;  $C_6H_{15}N$  [101,19]; Aldrich Nr. 47,122-4,  $\geq 99,5 \%$ ,  $d = 0,722$
- Diisopropylethylamine (Hünigs Base, DIPEA);  $C_8H_{19}N$  [129,25]; Aldrich Nr. D12,580-6, 99 %, Mp. 127°C,  $d = 0,742$
- 4,4'-Dimethoxytriphenylmethylechloride = 4,4'-Dimethoxytritylechloride (DMTrCl);  $C_{21}H_{19}ClO_2$  [338,83]; Merck Nr. 818616,  $> 99 \%$ , Mp. 120-123°C
- N,N*-Dimethyl formamide (DMF);  $C_3H_7NO$  [73,10]; Fluka Nr. 40248, puriss.,  $> 99,5 \%$ , over molecular sieve,  $H_2O \leq 0,01 \%$ , Bp. 153-155°C,  $d = 0,948$
- Dimethyl sulphoxide (DMSO);  $C_2H_6OS$  [78,13]; Fluka Nr. 41648, puriss., absolute, over molecular sieve,  $H_2O \leq 0,01 \%$ , Mp. 190-192°C,  $d = 1,100$
- Dimethyl sulphoxide- $d_6$  (DMSO- $d_6$ );  $C_2D_6OS$  [84,13]; Groupe C. E Saclay, 99,8 Atom % D
- Disodium hydrogen phosphate Dodecahydrat;  $Na_2HPO_4 \cdot 12H_2O$  [358,14]; Fluka Nr. 71650, puriss. p.a., crystallized
- 1,4 Dioxane;  $C_4H_8O_2$  [88,11]; Riedel-de Haën Nr. 33147, p.a.  $\geq 99,5 \%$
- 1,4 Dioxane;  $C_4H_8O_2$  [88,11]; Fluka Nr. 42510, puriss., absolute, over molecular sieve,  $\geq 99,5 \%$ , Mp. 100-102°C,  $d = 1,034$
- Ethanol;  $C_2H_6O$  [46,07]; Riedel-de Haën Nr. 32205, p.a.
- 2-Fluoro acetanilide;  $C_8H_8FNO$  [153,16]; Lancaster Nr. 1201,  $\geq 98 \%$ , Mp. 75-77°C
- p*-Formaldehyde;  $(CH_2O)_x$  [30,03]<sub>x</sub>; Riedel-de Haën Nr. 16005, puriss., 95-100 %
- Formic acid;  $CH_2O_2$  [46,03]; Merck Nr. 2541884, 98-100 %,  $d = 1,22$
- n*-Hexan;  $C_6H_{14}$  [86,17]; Fluka Nr. 52766, puriss., absolute, over molecular sieve,  $H_2O \leq 0,01 \%$ , Bp. 69°C,  $d = 0,659$
- 3-Hydroxypropionitrile = 2-Cyanoethanol;  $C_3H_5NO$  [71,08]; Fluka Nr. 56270, puriss.,  $\geq 99 \%$ , Bp. 106-108°C,  $d = 1,045$
- Imidazole;  $C_3H_4N_2$  [68,08]; Fluka Nr. 56760, puriss. p.a.,  $\geq 99,5 \%$
- Potassium hydroxide; KOH [56,11]; Fluka Nr. 60370, puriss. p.a.,  $\geq 86 \%$
- Potassium hydroxide; KOH [56,11]; Fluka Nr. 60380, purum, pulver,  $\geq 85 \%$



Lithium chloride; LiCl [42,39]; Fluka Nr. 62480, purum p.a.

Magnesium sulphate; MgSO<sub>4</sub> [120,37]; Riedel-de Haën Nr. 13143, dry

Methanol; CH<sub>4</sub>O [32,04]; Riedel-de Haën Nr. 32213, > 99,8 %, max. 0,05 % H<sub>2</sub>O, Bp. 64-65°C, d = 0,792

Methanol; CH<sub>4</sub>O [32,04]; Fluka Nr. 65542, puriss., > 99,5 %, over molecular sieve, H<sub>2</sub>O ≤ 100 ppm, Bp. 64-65°C, d = 0,79

Methylene chloride = Dichlormethan; CH<sub>2</sub>Cl<sub>2</sub> [84,93]; Fluka Nr. 66749; puriss., > 99,5 %, over molecular sieve, H<sub>2</sub>O ≤ 50 ppm, Bp. 40°C, d = 1,325

1-Methylimidazole; C<sub>4</sub>H<sub>6</sub>N<sub>2</sub> [82,11]; Fluka Nr. 67560, puriss., ≥ 99 %, Bp. 195-197°C, d = 1,033

1-Methyl-2-pyrrolidinon; C<sub>5</sub>H<sub>9</sub>NO [99,13]; Aldrich Nr. 27,045-8, > 99 %, for HPLC, Bp.<sup>(10 mm)</sup> 81-82°C, d = 1,028

Molecular sieve 3 Å; Fluka Nr. 69831

*p*-Nitrophenylethanol; C<sub>8</sub>H<sub>9</sub>NO<sub>3</sub> [167,16]; Aldrich Nr. 18,346-6, 99 %, Bp. 62-64°C

1-Octanol; C<sub>8</sub>H<sub>18</sub>O [130,23]; Fluka Nr. 74848, for UV-Spectroscopy, ≥ 99,5 %, d = 0,82

Sodium carbonate; Na<sub>2</sub>CO<sub>3</sub> [105,99]; Merck Nr. 106395, mind. 99,5 %, dry

Sodium chloride; NaCl [58,44]; Merck Nr. 1540, > 99,5 %

Sodium dihydrogenphosphate Dihydrat; NaH<sub>2</sub>PO<sub>4</sub>\*2H<sub>2</sub>O [156,01]; Fluka Nr. 71500, purum

Sodium hydrogen carbonate; NaHCO<sub>3</sub> [84,01]; Fluka Nr. 71630, purum, > 98 %

Sodium hydroxide; NaOH [40,00]; Grüssing Nr. 12155, 99 %

Palladium on carbon; Pd/C; ABCR Nr. PD-7150, ≈ 10 % Palladium

Palladium hydroxide on carbon (Pearlman's catalyst); Fluka Nr. 76063, puriss., ≈ 20 %

#### Palladium

Phosphorpentoxide; P<sub>2</sub>O<sub>5</sub> [141,94]; Riedel-de Haën Nr. 04113, 98,5 %

Phosphortrichloride; PCl<sub>3</sub> [137,33]; Riedel-de Haën Nr. 04603, ≥ 99 %, d = 1,57

Platinum dioxide; PtO<sub>2</sub> [227,09]; ABCR Nr. PT-5227, 99,9 %, 82 % Platinum

Pyridine; C<sub>5</sub>H<sub>5</sub>N [79,10]; Grüssing Nr. 13057, > 99,5 %, Bp. 115°C, d = 0,978, was at least 2h CaH<sub>2</sub> under reflux and than distilled

Pyridine; C<sub>5</sub>H<sub>5</sub>N [79,10]; Fluka Nr. 82704, puriss., > 99,8 %, H<sub>2</sub>O < 50 ppm, over molecular sieve, Bp. 116°C, d = 0,983

*β*-D-Ribofuranose; C<sub>5</sub>H<sub>10</sub>O<sub>5</sub> [150,13]; Aldrich Nr. R175-7, 98 %

Nitric acid; HNO<sub>3</sub> [63,01]; Merck Nr. 1.00456; p.a., 65 %, d = 1,40

Nitric acid, fuming; HNO<sub>3</sub> [63,01]; Merck Nr. 1.00455; p.a., 100 %, d = 1,52

Hydrochloric acid; HCl [36,46]; Riedel-de Haën Nr. 30721, p.a., 37 %

Sulphuric acid; H<sub>2</sub>SO<sub>4</sub> [98,07]; Merck Nr. 100731, 95-97 %, Bp. 330°C, d = 1,84

Silver nitrate; AgNO<sub>3</sub> [169,88]; Fluka Nr. 85228, puriss. p.a., ≥ 99,5 %

Nitrogen; N<sub>2</sub> [28,01]; Quality 99,9 %,

Sulphuryl chloride; SO<sub>2</sub>Cl<sub>2</sub> [134,97]; Aldrich Nr. 15,776-7, 97 %, Bp. 68-70°C, d = 1,680

Tetrahydrofuran; C<sub>4</sub>H<sub>8</sub>O [72,11]; Fluka Nr. 87371, puriss., absolute, over molecular sieve, ≥ 99,5 %

1,2,3,5 Tetra-*O*-acetyl-β-D-ribofuranose = β-D-Ribofuranose-1,2,3,5-tetraacetat; C<sub>13</sub>H<sub>18</sub>O<sub>9</sub> [318,28]; Aldrich Nr. 15,902-6, 98 %, Mp. 81-83°C

Toluol; C<sub>7</sub>H<sub>8</sub> [92,14]; Fluka Nr. 89682, purum, ≥ 99 %, Bp. 110-112°C, d = 0,866

Triethylamine (TEA); C<sub>6</sub>H<sub>15</sub>N [101,19]; Fluka Nr. 90340, puriss. p.a., > 99,5 %, Bp. 88-89°C, d = 0,726

Triethylamine trihydrofluoride; C<sub>6</sub>H<sub>15</sub>N\*3HF [161,21]; Aldrich Nr. 34,464-8, 98 %, d = 0,989

Triethylsilane; C<sub>6</sub>H<sub>16</sub>Si [116,28]; Fluka Nr. 90550, purum, > 97 %, Bp. 105-110°C, d = 0,732

Triisopropylchlorsilane; C<sub>9</sub>H<sub>21</sub>ClSi [192,81]; Aldrich Nr. 24,172-5, 97 %, Bp.<sup>(739 mm)</sup> 198°C, d = 0,901

Trimethylsilyltrifluormethane sulfonate, TMSTf C<sub>4</sub>H<sub>9</sub>F<sub>3</sub>O<sub>3</sub>SSi [222,26]; Fluka Nr. 91741, purum, ≥ 98 %, Bp.<sup>(11 mm)</sup> 39-40°C, d = 1,225

Hydrogen; H<sub>2</sub> [2,01];

### 10.2.1 For the synthesis of oligonucleotides

Acetonitrile; for DNA-synthesis, PerSeptive Biosystems

Acetonitrile; amidite diluent, PerSeptive Biosystems

Capping Reagent, PerSeptive Biosystems

Columns with CPG-material, PerSeptive Biosystems

Deblock-Mix, PerSeptive Biosystems

Oxidizer, PerSeptive Biosystems

Phosphoramidite, PerSeptive Biosystems

Sephadex PD10 Columns with G25 material, Amersham Pharmacia Biotech

### 10.3 The Buffer solutions

a) For the ion-exchange HPLC:

Buffer A: DEPC-water with LiOH, pH 8,0 adjusted

Buffer B: As buffer A and 42,39 g (1 mol) of lithium chloride

b) For recording of UV-melting curves and CD-spectra

For recording UV-melting curves and the CD-spectra of oligonucleotides the following buffer system was prepared: 140 mM Sodium chloride (2,04 g NaCl), 10 mM disodium hydrogen phosphate dodecahydrate (895 mg Na<sub>2</sub>HPO<sub>4</sub>\*12H<sub>2</sub>O) and 10 mM sodium dihydrogen phosphate dihydrate (390 mg NaH<sub>2</sub>PO<sub>4</sub>\*2H<sub>2</sub>O). After filling water up to 250 ml the pH of the buffer was adjusted to 7 using hydrochloric acid (0,1 N). In this way prepared buffer was then worked up with diethyl pyrocarbonate (DEPC). For that 0,1 % solution was prepared, left over night and autoclaved at the end 30 minutes.

### 10.4 List of Synthesised Compounds

2,4-Difluoro-6-nitroacetanilide (*N*-(2,4-Difluoro-*r*-nitro-phenyl)-acetanilide) **48**

2,4-Difluoro-6-nitroaniline **49**

4,6-Difluorobenzimidazole **51**

2', 3', 5'-Tri-*O*-acetyl-1'-deoxy-1'-(4,6-difluoro-1-*N*-benzimidazolyl)-β-D-ribofuranose **103**

2', 3', 5'-Tri-*O*-acetyl-1'-deoxy-1'-(4,6-difluoro-3-*N*-benzimidazolyl)-β-D-ribofuranose **104**

1'-Deoxy-1'-(4,6-difluoro-1-*N*-benzimidazolyl)-β-D-ribofuranose **8**

1'-Deoxy-5'-*O*-(4,4'-dimethoxytriphenylmethyl)-1'-(4,6-difluoro-1-*N*-benzimidazolyl)-β-D-ribofuranose **105**

5'-*O*-(4,4'-Dimethoxytriphenylmethyl)-2'-*O*-*tert*-butyldimethylsilyl-1'-deoxy-1'-(4,6-difluoro-1-*N*-benzimidazolyl)-β-D-ribofuranose **106**

5'-*O*-(4,4'-Dimethoxytriphenylmethyl)-3'-*O*-*tert*-butyldimethylsilyl-1'-deoxy-1'-(4,6-difluoro-1-*N*-benzimidazolyl)-β-D-ribofuranose **107**

3'-*O*-(2-Cyanethoxydiisopropylphosphin)-1'-deoxy-5'-*O*-(4,4'-dimethoxy-triphenylmethyl)-1'-(4,6-difluoro-1-*N*-benzimidazolyl)-2'-*O*-(*tert*-butyl-dimethylsilyl)-β-D-ribofuranose **108**

2-Fluoro-6-nitroacetanilide **46**

2-Fluoro-4-nitroacetanilide **45**

2-Fluoro-6-nitroaniline **52**

4-Fluorobenzimidazole **54**

- 2', 3', 5'-Tri-*O*-acetyl-1'-deoxy-1'-(4-fluoro-1-*N*-benzimidazolyl)- $\beta$ -D-ribofuranose **109**
- 2', 3', 5'-Tri-*O*-acetyl-1'-deoxy-1'-(4-fluoro-3-*N*-benzimidazolyl)- $\beta$ -D-ribofuranose **110**
- 1'-Deoxy-1'-(4-fluoro-1-*N*-benzimidazolyl)- $\beta$ -D-ribofuranose **30**
- 1'-Deoxy-5'-*O*-(4,4'-dimethoxytriphenylmethyl)-1'-(4-fluoro-1-*N*-benzimidazolyl)- $\beta$ -D-ribofuranose **111**
- 5'-*O*-(4,4'-Dimethoxytriphenylmethyl)-2'-*O*-*tert.*-butyldimethylsilyl-1'-deoxy-1'-(4-fluoro-1-*N*-benzimidazolyl)- $\beta$ -D-ribofuranose **112**
- 5'-*O*-(4,4'-Dimethoxytriphenylmethyl)-3'-*O*-*tert.*-butyldimethylsilyl-1'-deoxy-1'-(4-fluoro-1-*N*-benzimidazolyl)- $\beta$ -D-ribofuranose **113**
- 3'-*O*-(2-Cyanethoxydiisopropylphosphin)-1'-deoxy-5'-*O*-(4,4'-dimethoxy-triphenylmethyl)-1'-(4-fluoro-1-*N*-benzimidazolyl)-2'-*O*-*tert.*-butyldimethyl-silyl- $\beta$ -D-ribofuranose **114**
- 5-fluoro-1H-benzimidazole **65**
- 2', 3', 5'-Tri-*O*-acetyl-1'-deoxy-1'-(4-fluoro-1-*N*-benzimidazolyl)- $\beta$ -D-ribofuranose **115**
- 2', 3', 5'-Tri-*O*-acetyl-1'-deoxy-1'-(5-fluoro-3-*N*-benzimidazolyl)- $\beta$ -D-ribofuranose **78**
- 1'-Deoxy-1'-(5-fluoro-1-*N*-benzimidazolyl)- $\beta$ -D-ribofuranose **31**
- 1'-Deoxy-5'-*O*-(4,4'-dimethoxytriphenylmethyl)-1'-(5-fluoro-1-*N*-benzimidazolyl)- $\beta$ -D-ribofuranose **116**
- 5'-*O*-(4,4'-Dimethoxytriphenylmethyl)-2'-*O*-*tert.*-butyldimethylsilyl-1'-deoxy-1'-(5-fluoro-1-*N*-benzimidazolyl)- $\beta$ -D-ribofuranose **117**
- 5'-*O*-(4,4'-Dimethoxytriphenylmethyl)-3'-*O*-*tert.*-butyldimethylsilyl-1'-deoxy-1'-(5-fluoro-1-*N*-benzimidazolyl)- $\beta$ -D-ribofuranose **118**
- 3'-*O*-(2-Cyanethoxydiisopropylphosphin)-1'-deoxy-5'-*O*-(4,4'-dimethoxy-triphenylmethyl)-1'-(5-fluoro-1-*N*-benzimidazolyl)-2'-*O*-*tert.*-butyldimethyl-silyl- $\beta$ -D-ribofuranose **119**
- 1'-Deoxy-1'-(5-fluoro-3-*N*-benzimidazolyl)- $\beta$ -D-ribofuranose **32**
- 1'-Deoxy-5'-*O*-(4,4'-dimethoxytriphenylmethyl)-1'-(5-fluoro-3-*N*-benzimidazolyl)- $\beta$ -D-ribofuranose **93**
- 5'-*O*-(4,4'-Dimethoxytriphenylmethyl)-2'-*O*-*tert.*-butyldimethylsilyl-1'-deoxy-1'-(5-fluoro-1-*N*-benzimidazolyl)- $\beta$ -D-ribofuranose **95**
- 5'-*O*-(4,4'-Dimethoxytriphenylmethyl)-3'-*O*-*tert.*-butyldimethylsilyl-1'-deoxy-1'-(5-fluoro-3-*N*-benzimidazolyl)- $\beta$ -D-ribofuranose **94**
- 3'-*O*-(2-Cyanethoxydiisopropylphosphin)-1'-deoxy-5'-*O*-(4,4'-dimethoxy-triphenylmethyl)-1'-(5-fluoro-3-*N*-benzimidazolyl)-2'-*O*-*tert.*-butyldimethyl-silyl- $\beta$ -D-ribofuranose **97**
- 2',3',5'-Tri-*O*-acetyl-1'-deoxy-1'-benzimidazolyl- $\beta$ -D-ribofuranose **77**
- 1'-Deoxy-1'-benzimidazolyl- $\beta$ -D-ribofuranose **40**

- 1'-Deoxy-5'-*O*-(4,4'-dimethoxytriphenylmethyl)-1'-benzimidazolyl-β-D-ribofuranose **120**
- 5'-*O*-(4,4'-Dimethoxytriphenylmethyl)-2'-*O*-*tert.*-butyldimethylsilyl-1'-deoxy-1'-benzimidazolyl-β-D-ribofuranose **121**
- 5'-*O*-(4,4'-Dimethoxytriphenylmethyl)-3'-*O*-*tert.*-butyldimethylsilyl-1'-deoxy-1'-benzimidazolyl-β-D-ribofuranose **122**
- 3'-*O*-(2-Cyanethoxydiisopropylphosphin)-1'-deoxy-5'-*O*-(4,4'-dimethoxy-triphenylmethyl)-1'-benzimidazolyl-2'-*O*-(*tert.*-butyldimethylsilyl)-β-D-ribofuranose **123**
- N*-(2-nitro-3-trifluoromethyl-phenyl) acetamide **56**
- 2-Nitro-3-trifluoromethyl-phenylamine **59**
- 4-Trifluoromethyl-1H-benzoimidazole **61**
- 2',3,5'-Tri-*O*-acetyl-1'-deoxy-1'-(4-trifluoromethyl-1-*N*-benzoimidazole-1-yl)-β-D-ribofuranose **71**
- 2',3',5'-Tri-*O*-acetyl-1'-deoxy-1'-(4-trifluoromethyl-3-*N*-benzoimidazole-1-yl)-β-D-ribofuranose **72**
- 1'-Deoxy-1'-(4-trifluoromethyl-1-*N*-benzoimidazole-1-yl)-β-D-ribofuranose **33**
- 1'-Deoxy-1'-(4-trifluoromethyl-3-*N*-benzoimidazole-1-yl)-β-D-ribofuranose **124**
- 1'-Deoxy-5'-*O*-(4,4'-dimethoxytriphenylmethyl)-1'-(4,6-difluor-1-*N*-benzimidazolyl)-β-D-ribofuranose **125**
- 5'-*O*-(4,4'-Dimethoxytriphenylmethyl)-2'-*O*-*tert.*-butyldimethylsilyl-1'-deoxy-1'-(4-trifluoromethyl-1-*N*-benzimidazolyl)-β-D-ribofuranose **126**
- 5'-*O*-(4,4'-Dimethoxytriphenylmethyl)-3'-*O*-*tert.*-butyldimethylsilyl-1'-deoxy-1'-(4-trifluoromethyl-1-*N*-benzimidazolyl)-β-D-ribofuranose **127**
- 3'-*O*-(2-Cyanethoxydiisopropylphosphin)-1'-deoxy-5'-*O*-(4,4'-dimethoxy-triphenylmethyl)-1'-(4,6-difluor-1-*N*-benzimidazolyl)-2'-*O*-(*tert.*-butyl-dimethylsilyl)-β-D-ribofuranose **128**
- 5-Trifluoromethyl-1H-benzoimidazole **63**
- 2',3',5'-Tri-*O*-acetyl-1'-deoxy-1'-(5-trifluoromethyl-1-*N*-benzoimidazole-1-yl)-β-D-ribofuranose **129**
- 1'-deoxy-1'-(5-trifluoromethyl-1-*N*-benzoimidazole-1-yl)-β-D-ribofuranose **34**
- 1'-Deoxy-5'-*O*-(4,4'-dimethoxytriphenylmethyl)-1'-(5-trifluoromethyl-1-*N*-benzimidazolyl)-β-D-ribofuranose **130**
- 5'-*O*-(4,4'-Dimethoxytriphenylmethyl)-2'-*O*-*tert.*-butyldimethylsilyl-1'-deoxy-1'-(5-trifluoromethyl-1-*N*-benzimidazolyl)-β-D-ribofuranose **131**
- 5'-*O*-(4,4'-Dimethoxytriphenylmethyl)-3'-*O*-*tert.*-butyldimethylsilyl-1'-deoxy-1'-(5-trifluoromethyl-1-*N*-benzimidazolyl)-β-D-ribofuranose **132**

- 3'-*O*-(2-Cyanoethoxydiisopropylphosphin)-1'-deoxy-5'-*O*-(4,4'-dimethoxy-triphenylmethyl)-1'-(5-trifluoromethyl-1-*N*-benzimidazolyl)-2'-*O*-(*tert.*-butyl-dimethylsilyl)-β-D-ribofuranose **133**
- 2',3',5'-Tri-*O*-acetyl-1'-deoxy-1'-(5-trifluoromethyl-3-*N*-benzimidazole-1-yl)-β-D-ribofuranose **134**
- 1'-deoxy-1'-(5-trifluoromethyl-3-*N*-benzimidazole-1-yl)-β-D-ribofuranose **35**
- 1'-Deoxy -5'-*O*-(4,4'-dimethoxytriphenylmethyl)-1'-(5-trifluoromethyl-3-*N*-benzimidazolyl)-β-D-ribofuranose **135**
- 5'-*O*-(4,4'-Dimethoxytriphenylmethyl)-2'-*O*-*tert.*-butyldimethylsilyl-1'-deoxy-1'-(5-trifluoromethyl-3-*N*-benzimidazolyl)-β-D-ribofuranose **136**
- 5'-*O*-(4,4'-Dimethoxytriphenylmethyl)-3'-*O*-*tert.*-butyldimethylsilyl-1'-deoxy-1'-(5-trifluoromethyl-3-*N*-benzimidazolyl)-β-D-ribofuranose **137**
- 3'-*O*-(2-Cyanoethoxydiisopropylphosphin)-1'-deoxy-5'-*O*-(4,4'-dimethoxy-triphenylmethyl)-1'-(5-trifluoromethyl-3-*N*-benzimidazolyl)-2'-*O*-(*tert.*-butyl-dimethylsilyl)-β-D-ribofuranose **138**
- 1-Methyl-ribofuranose **80**
- 1-Methyl-2,3,5-tri-*O*-benzyl-ribofuranose **81**
- 2,3,5-Tri-*O*-benzyl-ribofuranose **82**
- 2,3,5-Tri-*O*-benzyl-ribo-γ-lacton **83**
- 2',3',5'-Tri-*O*-benzyl-1'-deoxy-1'-(2,4-difluorophenyl)-β-D-ribofuranose **139**
- 1'-Deoxy-1'-(2,4-difluorophenyl)-β-D-ribofuranose **9**
- 5'-*O*-(4,4'-Dimethoxytriphenylmethyl)-1'-deoxy-1'-(2,4-difluorophenyl)-β-D-ribofuranose **140**
- 5'-*O*-(4,4'-Dimethoxytriphenylmethyl)-2'-*O*-*tert.*-butyldimethylsilyl-1'-deoxy-1'-(2,4-difluorophenyl)-β-D-ribofuranose **141**
- 5'-*O*-(4,4'-Dimethoxytriphenylmethyl)-3'-*O*-*tert.*-butyldimethylsilyl-1'-deoxy-1'-(2,4-difluorophenyl)-β-D-ribofuranose **142**
- 3'-*O*-(2-Cyanoethoxydiisopropylphosphin)-1'-deoxy-5'-*O*-(4,4'-dimethoxy-triphenylmethyl)-1'-(2,4-difluorophenyl)-2'-*O*-*tert.*-butyldimethylsilyl-β-D-ribofuranose **143**
- 2',3',5'-Tri-*O*-benzyl-1'-deoxy-1'-(4-fluorophenyl)-β-D-ribofuranose **144**
- 1'-Deoxy-1'-(4-fluorophenyl)-β-D-ribofuranose **36**
- 5'-*O*-(4,4'-Dimethoxytriphenylmethyl)-1'-deoxy-1'-(4-fluorophenyl)-β-D-ribofuranose **145**
- 5'-*O*-(4,4'-Dimethoxytriphenylmethyl)-2'-*O*-*tert.*-butyldimethylsilyl-1'-deoxy-1'-(4-fluorophenyl)-β-D-ribofuranose **146**

- 5'-O-(4,4'-Dimethoxytriphenylmethyl)-3'-O-*tert.*-butyldimethylsilyl-1'-deoxy-1'-(4-fluorophenyl)- β -D-ribofuranose **147**
- 3'-O-(2-Cyanethoxydiisopropylphosphin)-1'-deoxy-5'-O-(4,4'-dimethoxy-triphenylmethyl)-1'-(4-fluorophenyl)-2'-O-*tert.*-butyldimethylsilyl- β -D-ribofuranose **148**
- 2',3',5'-Tri-*O*-benzyl-1'-deoxy-1'-(2,4,6-triifluorophenyl)- β -D-ribofuranose **90**
- 1'-Desoxy-1'-(2,4,6-trifluorophenyl)- β -D-ribofuranose **37**
- 5'-O-(4,4'-Dimethoxytriphenylmethyl)-1'-deoxy-1'-(2,4,6-trifluorophenyl)-β-D-ribofuranose **149**
- 5'-O-(4,4'-Dimethoxytriphenylmethyl)-2'-O-*tert.*-butyldimethylsilyl-1'-deoxy-1'-(2,4,6-trifluorophenyl)- β -D-ribofuranose **150**
- 5'-O-(4,4'-Dimethoxytriphenylmethyl)-3'-*tert.*-butyldimethylsilyl-1'-deoxy-1'-(2,4,6-trifluorophenyl)- β -D-ribofuranose **151**
- 3'-O-(2-Cyanethoxydiisopropylphosphin)-1'-deoxy-5'-O-(4,4'-dimethoxy-triphenylmethyl)-1'-(2,4,6-trifluorophenyl)-2'-O-*tert.*-butyldimethylsilyl- β -D-ribofuranose **152**
- 2',3',5'-Tri-*O*-benzyl-1'-deoxy-1'-(2,4,5-triifluorophenyl)- β -D-ribofuranose **86**
- 1'-Deoxy-1'-(2,4,5-trifluorophenyl)- β -D-ribofuranose **38**
- 5'-O-(4,4'-Dimethoxytriphenylmethyl)-1'-deoxy-1'-(2,4,5-trifluorophenyl)-β-D-ribofuranose **153**
- 5'-O-(4,4'-Dimethoxytriphenylmethyl)-2'-O-*tert.*-butyldimethylsilyl-1'-deoxy-1'-(2,4,5-trifluorophenyl)- β -D-ribofuranose **154**
- 5'-O-(4,4'-Dimethoxytriphenylmethyl)-3'-*tert.*-butyldimethylsilyl-1'-deoxy-1'-(2,4,5-trifluorophenyl)- β -D-ribofuranose **155**
- 3'-O-(2-Cyanethoxydiisopropylphosphin)-1'-deoxy-5'-O-(4,4'-dimethoxy-triphenylmethyl)-1'-Deoxy-1'-(2,4,5-trifluorophenyl)-2'-O-*tert.*-butyldimethylsilyl- β -D-ribofuranose **156**
- 2,3,5-Tri-*O*-benzyl-1-deoxy- D-ribofuranose **98**
- 1-Deoxy-D-ribofuranose **42**
- 5-*O*-(4,4'-Dimethoxytriphenylmethyl)-1-deoxy-D-ribofuranose **99**
- 5-*O*-(4,4'-Dimethoxytriphenylmethyl)-2-*O*-*tert.*-butyldimethylsilyl-1-deoxy-β-D-ribofuranose **101**
- 5-*O*-(4,4'-Dimethoxytriphenylmethyl)-3-*O*-*tert.*-butyldimethylsilyl-1-deoxy-β-D-ribofuranose **100**
- 3-*O*-(2-Cyanethoxydiisopropylphosphin)-1-deoxy-5-*O*-(4,4'-dimethoxy-triphenylmethyl)-2-*O*-*tert.*-butyldimethylsilyl- β -D-ribofuranose **102**
- 2-Cyanethoxy-dichlorphosphin **157**

2-Cyanethyldiisopropylchlorphosphoramidit **96**

2',3',5'-Tri-*O*-benzyl-1'-deoxy-1'-phenyl-  $\beta$  -D-ribofuranose **91**

1'-Deoxy-1'-phenyl-  $\beta$  -D-ribofuranose **41**

5'-*O*-(4,4'-Dimethoxytriphenylmethyl)- 1'-deoxy-1'-phenyl-  $\beta$  -D-ribofuranose **158**

5'-*O*-(4,4'-Dimethoxytriphenylmethyl)-2'-*O*-*tert.*-butyldimethylsilyl-1'-deoxy-1'-phenyl-  $\beta$  -  
D-ribofuranose **159**

5'-*O*-(4,4'-Dimethoxytriphenylmethyl)-3'-*O*-*tert.*-butyldimethylsilyl-1'-deoxy-1'-phenyl-  $\beta$  -  
D-ribofuranose **160**

3'-*O*-(2-Cyanethoxydiisopropyl-phosphin)-1'-deoxy-5'-*O*-(4,4'-dimethoxy-triphenylmethyl)-  
1'-phenyl-2'-*O*-*tert.*-butyldimethylsilyl-  $\beta$  -D-ribofuranose **161**

2',3',5'-Tri-*O*-benzyl-1'-deoxy-1'-pentafluorophenyl-  $\beta$  -D-ribofuranose **162**

1'-Deoxy-1'-pentafluorophenyl-  $\beta$  -D-ribofuranose **39**

5'-*O*- (4,4'-Dimethoxytriphenylmethyl)- 1'-deoxy-1'-pentafluorophenyl-  $\beta$  -D-ribofuranose  
**163**

5'-*O*-(4,4'-Dimethoxytriphenylmethyl)-2'-*O*-*tert.*-butyldimethylsilyl-1'-deoxy-1'-  
pentafluorophenyl-  $\beta$  -D-ribofuranose **164**

5'-*O*-(4,4'-Dimethoxytriphenylmethyl)-3'-*tert.*-butyldimethylsilyl-1'-deoxy-1'-  
pentafluorophenyl-  $\beta$  -D-ribofuranose **165**

3'-*O*-(2-Cyanethoxydiisopropylphosphin)-1'-deoxy-5'-*O*-(4,4'-dimethoxy-triphenylmethyl)-  
1'-pentafluorophenyl-2'-*O*-*tert.*-butyldimethylsilyl-  $\beta$  -D-ribofuranose **166**

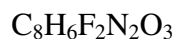
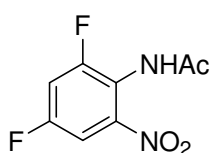
2',3',5'-Tri-*O*-benzyl-1'-deoxy-1'-(4-chlorophenyl)-  $\beta$  -D-ribofuranose **167**

1'-Deoxy-1'-(4-chlorophenyl)-  $\beta$  -D-ribofuranose **43**



## 10.5 Synthesis, spectral data and other characteristics of synthesised compounds

### 2,4-Difluoro-6-nitroacetanilide 48



216.14 g/mol

7.8 g (39.4 mmol) 2,4-Difluoro acetanilide were dissolved in a mixture of 9 ml conc.  $\text{H}_2\text{SO}_4$  and 3.1 ml  $\text{CH}_3\text{COOH}$ . Slowly, a mixture of 3.1 ml conc.  $\text{H}_2\text{SO}_4$  and 3.1 ml conc.  $\text{HNO}_3$  was added, taking care that the temperature stays below  $40^\circ\text{C}$ . At the end the mixture was stirred for 90 minutes at  $45^\circ\text{C}$ . The reaction mixture was poured in 25 ml of icewater and stirred over 30 minutes (cooled in icebath for full recrystallization). Yellow precipitate was filtered in vacuum, washed with icewater and dried.

Yield: 9.55 g (96.4 %)

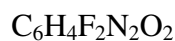
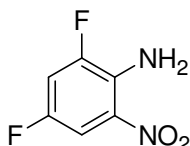
$^1\text{H-NMR}$ :  $\delta$  [ppm] (270 MHz,  $\text{DMSO-}d_6$ )  
 10.20 (s, 1H, NH); 7.85 (m, 2H, 3H, 5H); 2.05 (s, 3H,  $\text{CH}_3$ )

IR (KBr): 1119.8  $\text{cm}^{-1}$  C-F  
 1547.7  $\text{cm}^{-1}$   $\text{NO}_2$   
 1676.6  $\text{cm}^{-1}$  C=O  
 3237.4  $\text{cm}^{-1}$ ; 3181.8  $\text{cm}^{-1}$  N-H

Melting point:  $135^\circ\text{C}$

ESI(+): m/z 216.7 ( $[\text{M}+\text{H}]^+$ )

**2,4-Difluoro-6-nitroaniline 49**



174.1 g/mol

9.5 g (44 mmol) 2,4-Difluoro-6-nitroacetanilide **48** were dissolved in 9 ml conc.  $H_2SO_4$  and stirred over 2 h at  $95^\circ C$ . At the end the reaction mixture was poured into the ice and cooled 30 min. in ice bath, for full recrystallization of the product. Yellow precipitate was filtered in vacuum, washed with ice-water and dried. The crude product was recrystallised from ethanol.

Yield: 4.37 g (57.1 %)

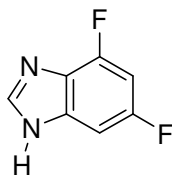
$^1H$ -NMR:  $\delta$  [ppm] (270 MHz,  $DMSO-d_6$ )  
7.65 (m, 2H, 3H, 5H); 7.20 (s br, 2H,  $NH_2$ )

IR (KBr):  $1127.6\text{ cm}^{-1}$  C-F  
 $1531.7\text{ cm}^{-1}$   $NO_2$   
 $3495.0\text{ cm}^{-1}$ ;  $3376.5\text{ cm}^{-1}$  N-H

Melting point.:  $85 - 86^\circ C$

ESI(-): m/z 172.8 ([M-H]<sup>-</sup>)

## 4,6-Difluorbenzimidazole 51



154.11 g/mol

13 g (74.7 mmol) 2,4-Difluoro-6-nitroaniline 49 were dissolved in 200 ml abs. ethanol and 700 mg (3.1 mmol) PtO<sub>2</sub> were added. The reaction mixture was stirred 24 h in H<sub>2</sub> atmosphere at room temperature. The catalyst was filtered over celite and the reaction mixture evaporated to dryness. The left dark coloured oil was dissolved immediately in 200ml HCOOH and refluxed 1.5 h. At the end HCOOH was evaporated under reduced pressure and the product dried on the oil pump. For further reactions the product was used without further purification. For analytical purposes a part of the product was sublimed and the white product was obtained.

Yield: 8.17 g (71.0 %)

<sup>1</sup>H-NMR: δ [ppm] (250 MHz, DMSO-*d*<sub>6</sub>)  
 12.87 (s, 1H, NH); 8.28 (s, 1H, 2H); 7.25 (dd, J = 1.9 Hz, J = 8.8 Hz, 1H, 7H);  
 7.03 (dt, J = 2.1 Hz, J = 10.6 Hz, 1H, 5H)

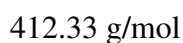
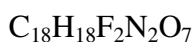
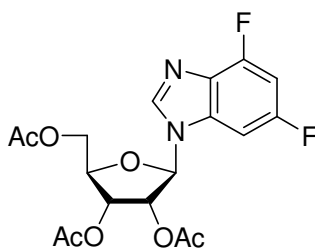
IR (KBr): 1115.7 cm<sup>-1</sup> C-F  
 3073.6 cm<sup>-1</sup> N-H

Melting point.: 233 – 234 °C

ESI(+): m/z 154.8 ([M+H]<sup>+</sup>)

El. Analysis:	Counted:	C: 54.55 %	H: 2.62 %	N: 18.18 %
	Found:	C: 54.30 %	H: 2.90 %	N: 17.98 %

**2', 3', 5'-Tri-*O*-acetyl-1'-deoxy-1'-(4,6-difluoro-1-*N*-benzimidazolyl)- $\beta$ -D-ribofuranose 103**



3.1 g (20 mmol) 4,6-Difluorobenzimidazole **51** were suspended in 80 ml abs. acetonitrile and 7.4 ml (30 mmol) *N,O*-Bis-(trimethylsilyl)-acetamide were added. The reaction mixture was refluxed for 15 min. After cooling to room temperature 6.4 g (20 mmol) 1,2,3,5-tetra-*O*-acetyl- $\beta$ -D-ribofuranose in 35 ml abs. acetonitrile and 4.5 ml (25 mmol) trimethylsilyltrifluoro sulphonate (TMSOTf) were added. The reaction mixture was then refluxed 2.5 hours and cooled to room temperature. After cooling the reaction mixture was treated with 10 ml 5%  $\text{NaHCO}_3$ -solution and extracted with methylene chloride three times. The combined organic phases were dried over  $\text{MgSO}_4$  and evaporated to dryness. The product was purified by means of FC with methylene chloride/methanol 98:2. The product was obtained as white foam.

Yield: 5.6 g (67.8 %)

TLC:  $R_f = 0.49$  ( $\text{CH}_2\text{Cl}_2/\text{MeOH}$  95:5)

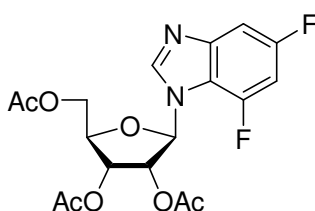
$^1\text{H-NMR}$ :  $\delta$  [ppm] (250 MHz,  $\text{DMSO-}d_6$ )  
 8.56 (s, 1H, 2H); 7.57 (dd,  $J = 9.0$  Hz,  $J = 2.1$  Hz, 1H, 7H); 7.19 (dt,  $J = 10.5$  Hz,  $J = 2.0$  Hz, 1H, 5H); 6.33 (d,  $J = 6.1$  Hz, 1H, 1'H); 5.64 (t,  $J = 6.3$  Hz, 1H, 2'H); 5.43 (dd,  $J = 6.3$  Hz,  $J = 4.3$  Hz, 1H, 3'H); 4.40 (m, 3H, 4'H, 5'H); 2.14 (s, 3H,  $\text{CH}_3$ -acetyl); 2.08 (s, 3H,  $\text{CH}_3$ -acetyl); 2.04 (s, 3H,  $\text{CH}_3$ -acetyl)

$^{13}\text{C-NMR}$ :  $\delta$  [ppm] (63.9 MHz,  $\text{DMSO-}d_6$ )  
 170.00 (C=O); 169.52 (C=O); 169.26 (C=O); 158.48 (C4); 152.67 (C6); 143.67 (C2); 134.67 (C9); 128.94 (C8); 98.32 (C5); 95.09 (C7); 86.43 (C1')

79.57 (C4'); 71.69 (C3'); 69.43 (C2'); 62.95 (C5'); 20.48 (CH<sub>3</sub>-acetyl); 20.38 (CH<sub>3</sub>-acetyl); 20.18 (CH<sub>3</sub>-acetyl)

ESI (+): m/z 413.0 ([M+H]<sup>+</sup>);

**2',3',5'-Tri-*O*-acetyl-1'-deoxy-1'-(4,6-difluoro-3-*N*-benzimidazolyl)-β-D-ribofuranose 104**



C<sub>18</sub>H<sub>18</sub>F<sub>2</sub>N<sub>2</sub>O<sub>7</sub>

412.33 g/mol

2',3',5'-Tri-*O*-acetyl-1'-deoxy-1'-(4,6-difluoro-3-*N*-benzimidazolyl)-β-D-ribofuranose 104 was obtained as a side product in preparing 2',3',5'-Tri-*O*-acetyl-1'-deoxy-1'-(4,6-difluoro-1-*N*-benzimidazolyl)-β-D-ribofuranose 103.

Yield: 0.94 g (11.4 %)

TLC: R<sub>f</sub> = 0.42 (CH<sub>2</sub>Cl<sub>2</sub>/MeOH 95:5)

<sup>1</sup>H-NMR: δ [ppm] (250 MHz, DMSO-*d*<sub>6</sub>)

8.63 (s, 1H, 2H); 7.45 (dd, J = 9.1 Hz, J = 2.1 Hz, 1H, 7H); 7.30 (dt, J = 10.8 Hz, J = 2.2 Hz, 1H, 5H); 6.28 (d, J = 5.8 Hz, 1H, 1'H); 5.63 (t, J = 6.2 Hz, 1H, 2'H); 5.39 (Ψt, J = 5.1 Hz, 1H, 3'H); 4.40 (m, 2H, 5'H); 4.24 (m, 1H, 4'H); 2.11 (s, 3H, CH<sub>3</sub>-acetyl); 2.05 (s, 3H, CH<sub>3</sub>-acetyl); 2.03 (s, 3H, CH<sub>3</sub>-acetyl)

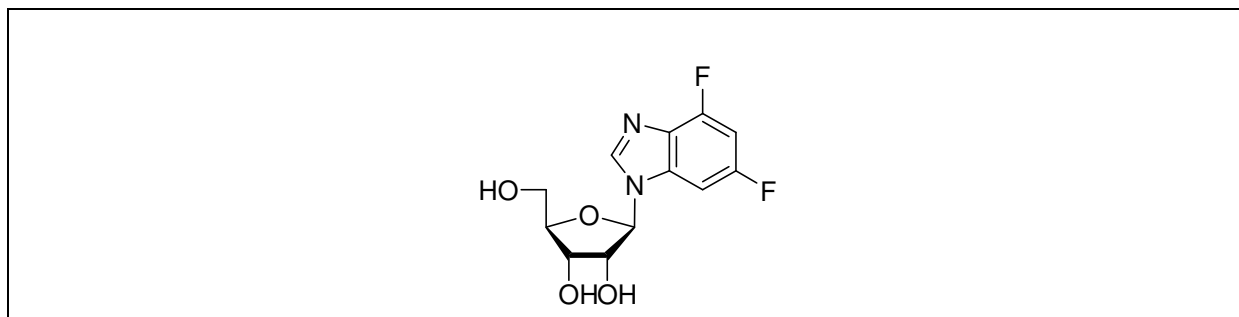
<sup>13</sup>C-NMR: δ [ppm] (63.9 MHz, DMSO-*d*<sub>6</sub>)

170.41 (C=O); 169.82 (C=O); 169.57 (C=O); 158.35 (C4); 147.89 (C6); 146.99 (C9); 145.56 (C2); 117.66 (C8); 102.63 (C5); 100.25 (C7); 87.81

(C1'); 79.57 (C4'); 73.57 (C3'); 69.62 (C2'); 63.00 (C5'); 20.83 (CH<sub>3</sub>-acetyl);  
20.71 (CH<sub>3</sub>-acetyl); 20.51 (CH<sub>3</sub>-acetyl)

ESI (+): m/z 413.0 ([M+H]<sup>+</sup>);

**1'-Deoxy-1'-(4,6-difluoro-1-N-benzimidazolyl)-β-D-ribofuranose 8**



C<sub>12</sub>H<sub>12</sub>F<sub>2</sub>N<sub>2</sub>O<sub>4</sub>

286.23 g/mol

5.59 g (13.5 mmol) 2',3',5'-Tri-*O*-acetyl-1'-deoxy-1'-(4,6-difluoro-1-*N*-benzimidazolyl)-β-*D*-ribofuranose **103** were dissolved in 50 ml of methanol and 370 μl of MeONa/MeOH (5.4M, Fluka) were added at RT and the reaction was TLC controlled. After 60 min the reaction was complete and neutralised with DOWEX 50, filtered and evaporated. The product was obtained as white foam.

Yield: 3.66 g (94.2 %)

TLC: R<sub>f</sub> = 0.64 (CH<sub>2</sub>Cl<sub>2</sub>/MeOH 4:1)

<sup>1</sup>H-NMR: δ [ppm] (250 MHz, DMSO-*d*<sub>6</sub>)

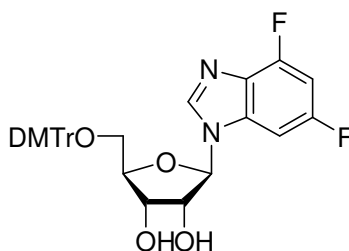
8.52 (s, 1H, 2H); 7.65 (dd, J = 9.1 Hz, J = 2.2 Hz, 1H, 7H); 7.13 (dt, J = 2.2 Hz, J = 10.5 Hz, 1H, 5H); 5.87 (d, J = 6.4 Hz, 1H, 1'H); 5.51 (d, J = 6.5 Hz, 1H, 2'-OH); 5.25 (d, J = 4.6 Hz, 3'-OH); 5.22 (t, J = 5.0 Hz, 1H, 5'-OH); 4.34 (q, J = 6.3 Hz, 1H, 2'H); 4.12 (m, 1H, 3'H); 4.00 (q, J = 3.1 Hz, 1H, 4'H); 3.66 (m, 2H, 5'H)

$^{13}\text{C}$ -NMR:  $\delta$  [ppm] (63.9 MHz,  $\text{DMSO-}d_6$ )  
 158.13 (C4); 152.53 (C6); 143.70 (C2); 134.95 (C9); 129.01 (d,  $J = 17.7$  Hz, C8); 97.66 (C5); 95.43 (C7); 89.07 (C1'); 85.83 (C4'); 73.63 (C2'); 70.04 (C3'); 61.08 (C5')

$^{19}\text{F}$ -NMR:  $\delta$  [ppm] (254.2 MHz,  $\text{DMSO-}d_6$ )  
 -116.40 (m, 1F, 6F); -125.25 (m, 1F, 4F)

ESI(-):  $m/z$  285.1 ( $[\text{M-H}]^-$ );

**1'-Deoxy-5'-O-(4,4'-dimethoxytriphenylmethyl)-1'-(4,6-difluoro-1-N-benzimidazolyl)- $\beta$ -D-ribofuranose 105**



$\text{C}_{33}\text{H}_{30}\text{F}_2\text{N}_2\text{O}_6$

588.62 g/mol

640 mg (2.2 mmol) 1'-Deoxy-1'-(4,6-difluoro-1-N-benzimidazolyl)- $\beta$ -D-ribofuranose **8** were dissolved in 10 ml abs. pyridine and 0.47 ml (3.3 mmol) triethylamine and 0.91 g (2.6 mmol) 4,4'-Dimethoxytriphenylmethyl chloride were added. The reaction mixture was stirred under argon at RT 20 h. The reaction was stopped by adding 3 ml of methanol and a saturated water solution of  $\text{NaHCO}_3$ . It was extracted with methylene chloride three times, organic phases were collected and dried over  $\text{MgSO}_4$  and evaporated to dryness. The product was co-evaporated with toluene twice. Further purification was done by FC with methylene chloride/methanol 95:5, as eluent. The product was obtained as yellow foam.

Yield: 980 mg (74.8 %)

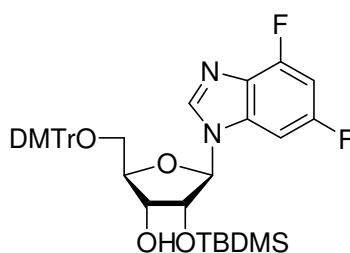
TLC:  $R_f = 0.52$  ( $\text{CH}_2\text{Cl}_2/\text{MeOH}$  95:5)

$^1\text{H-NMR}$ :  $\delta$  [ppm] (270 MHz,  $\text{DMSO-}d_6$ )  
 8.43 (s, 1H, 2H); 7.47 (dd,  $J = 8.8$  Hz,  $J = 1.9$  Hz, 1H, 7H); 7.35 – 6.81 (m, 14H,  $\text{H}_{\text{ar}}$ , 5H); 5.93 (d,  $J = 5.1$  Hz, 1H, 1'H); 5.69 (d,  $J = 5.9$  Hz, 1H, 2'-OH); 5.30 (d,  $J = 5.5$  Hz, 1H, 3'-OH); 4.49 (q,  $J = 5.5$  Hz, 1H, 2'H); 4.21 (q,  $J = 5.2$  Hz, 1H, 3'H); 4.12 (m, 1H, 4'H); 3.72 (s, 6H,  $\text{OCH}_3$ ); 3.23 (m, 2H, 5'H)

$^{13}\text{C-NMR}$ :  $\delta$  [ppm] (67.9 MHz,  $\text{DMSO-}d_6$ )  
 158.22 (C4); 158.04 (DMTr); 152.57 (C6); 146.82 (C2); 144.69 (DMTr); 135.36 (DMTr); 135.31 (DMTr); 135.13 (C9); 129.05 (DMTr); 128.94 (C8); 127.75 (DMTr); 127.59 (DMTr); 126.66 (DMTr); 113.11 (DMTr); 97.83 (C5); 95.17 (C7); 89.09 (C1'); 85.62 (DMTr); 83.50 (C4'); 73.26 (C2'); 69.90 (C3'); 63.40 (C5'); 54.95 ( $\text{OCH}_3$ )

ESI (-):  $m/z$  587.4 ( $[\text{M-H}]^-$ );

**5'-O-(4,4'-Dimethoxytriphenylmethyl)-2'-O-*tert.*-butyldimethylsilyl-1'-deoxy-1'-(4,6-difluoro-1-*N*-benzimidazolyl)- $\beta$ -D-ribofuranose 106**



$\text{C}_{39}\text{H}_{44}\text{F}_2\text{N}_2\text{O}_6\text{Si}$

702.84 g/mol

2.53 g (4.3 mmol) 5'-O-(4,4'-Dimethoxytriphenylmethyl)-1'-deoxy-1'- $\beta$ -D-(4,6-difluoro-benzimidazolyl)-ribofuranose 105 were dissolved in 40 ml of a 1:1 mixture of THF/Pyridine and with 900 mg (5.3 mmol)  $\text{AgNO}_3$  and 6.2 ml (6.2 mmol) 1 M *tert.*-butyldimethylsilyl chloride-solution in THF were added. The reaction mixture was stirred for 20 hours in the dark at RT under argon. Adding 10 ml of saturated water  $\text{NaHCO}_3$ -solution stopped the



reaction. Left AgCl was filtered over celite and filtrate was extracted with methylene chloride three times. Collected organic phases were dried over MgSO<sub>4</sub> and evaporated to dryness. Crude product was co-evaporated with toluene twice. Further purification of the product was done by HPLC (*MN Nucleoprep 100-20* of *Macherey-Nagel*, *n*-hexane/isopropyl acetate 3:2). The product (*slow-Isomer*) was obtained as a white foam.

Yield: 970 mg (32.1 %)

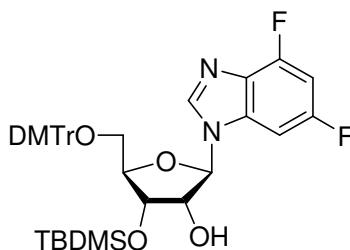
TLC: R<sub>f</sub> = 0.55 (CH<sub>2</sub>Cl<sub>2</sub>/MeOH 99:1)

<sup>1</sup>H-NMR: δ [ppm] (400 MHz, DMSO-*d*<sub>6</sub>)  
8.47 (s, 1H, 2H); 7.47 (dd, J = 8.9 Hz, J = 2.0 Hz, 1H, 7H); 7.39 – 6.84 (m, 13H, H<sub>ar</sub>); 7.12 (dt, J = 8.5 Hz, J = 2.0 Hz, 1H, 5H); 5.97 (d, J = 6.3 Hz, 1H, 1'H); 5.24 (d, J = 5.5 Hz, 1H, 3'-OH); 4.59 (t, J = 5.8 Hz, 1H, 2'H); 4.19 (m, 1H, 3'H); 4.14 (m, 1H, 4'H); 3.73 (s, 6H, OCH<sub>3</sub>); 3.31 (m, 2H, 5'H); 0.72 (s, 9H, C(CH<sub>3</sub>)<sub>3</sub>); -0.08 (s, 3H, SiCH<sub>3</sub>); -0.24 (s, 3H, SiCH<sub>3</sub>)

<sup>13</sup>C-NMR: δ [ppm] (100.6 MHz, DMSO-*d*<sub>6</sub>)  
158.08 (C4); 158.02 (DMTr); 152.58 (C6); 144.63 (DMTr); 143.52 (C2); 135.10 (DMTr); 135.05 (DMTr); 134.45 (C9); 129.64 (DMTr); 128.95 (C8); 127.67 (DMTr); 127.43 (DMTr); 126.64 (DMTr); 113.07 (DMTr); 97.91 (C5); 95.31 (d, J = 32.6 Hz, C7); 88.56 (C1'); 85.72 (DMTr); 84.23 (C4'); 74.59 (C2'); 69.67 (C3'); 63.28 (C5'); 54.88 (OCH<sub>3</sub>); 25.31 (SiC(CH<sub>3</sub>)<sub>3</sub>); 17.61 (SiC(CH<sub>3</sub>)<sub>3</sub>); -5.16 (SiCH<sub>3</sub>); -5.76 (SiCH<sub>3</sub>)

ESI (-): m/z 701.5 ([M-H]<sup>-</sup>);

**5'-O-(4,4'-Dimethoxytriphenylmethyl)-3'-O-tert.-butyldimethylsilyl-1'-deoxy-1'-(4,6-difluoro-1-N-benzimidazolyl)- $\beta$ -D-ribofuranose 107**



$C_{39}H_{44}F_2N_2O_6Si$

702.84 g/mol

5'-O-(4,4'-Dimethoxytriphenylmethyl)-3'-O-tert.-butyldimethylsilyl-1'-deoxy-1'-(4,6-difluoro-1-N-benzimidazolyl)- $\beta$ -D-ribofuranose 107 was obtained as a side product (*fast-Isomer*) in synthesizing 5'-O-(4,4'-Dimethoxytriphenylmethyl)-2'-O-tert.-butyldimethylsilyl-1'-deoxy-1'-(4,6-difluoro-1-N-benzimidazolyl)- $\beta$ -D-ribofuranose 106.

Yield: 1.55 g (51.3 %)

TLC:  $R_f = 0.55$  ( $CH_2Cl_2/MeOH$  99:1)

$^1H$ -NMR:  $\delta$  [ppm] (400 MHz,  $DMSO-d_6$ )

8.47 (s, 1H, 2H); 7.48 (dd,  $J = 8.7$  Hz,  $J = 2.0$  Hz, 1H, 7H); 7.36 – 6.82 (m, 14H, 5H,  $H_{ar}$ ); 5.90 (d,  $J = 5.6$  Hz, 1H, 1'H); 5.53 (d,  $J = 6.4$  Hz, 1H, 2'-OH); 4.50 (q,  $J = 5.8$  Hz, 1H, 2'H); 4.32 (t,  $J = 4.7$  Hz, 1H, 3'H); 4.07 (q,  $J = 4.0$  Hz, 1H, 4'H); 3.72 (s, 6H,  $OCH_3$ ); 3.26 (m, 2H, 5'H); 0.81 (s, 9H,  $SiC(CH_3)_3$ ); 0.06 ( $SiCH_3$ ); -0.01 ( $SiCH_3$ )

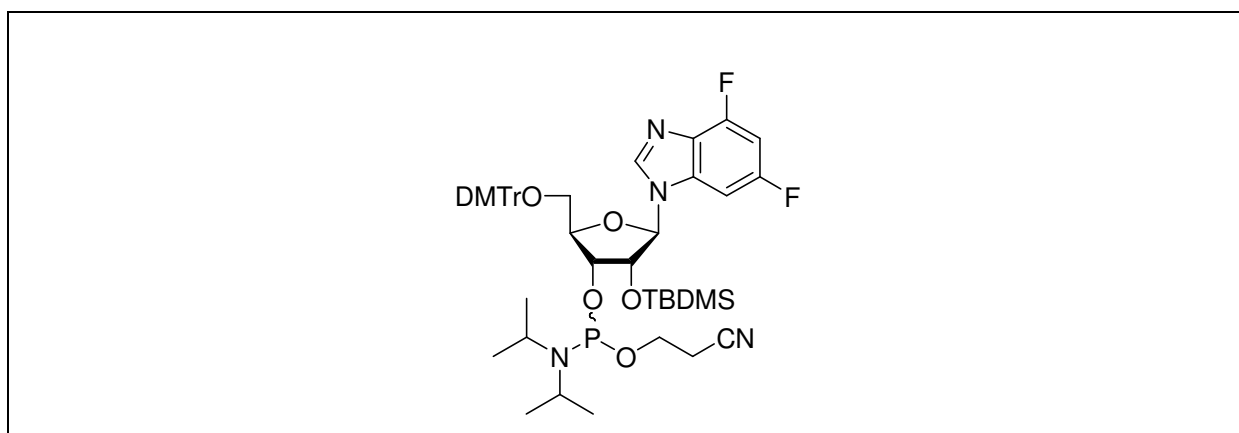
$^{13}C$ -NMR:  $\delta$  [ppm] (100.6 MHz,  $DMSO-d_6$ )

158.20 (C4); 158.11 (DMTr); 152.59 (C6); 144.55 (DMTr); 143.32 (C2); 135.22 (DMTr); 135.19 (DMTr); 134.86 (C9); 129.64 (DMTr); 129.04 (C8); 127.77 (DMTr); 127.57 (DMTr); 126.72 (DMTr); 113.13 (DMTr); 97.87 (C5); 95.40 (C7); 89.11 (C1'); 85.86 (DMTr); 84.00 (C4'); 72.71 (C2'); 71.65 (C3')

62.87 (C5'); 54.97 (OCH<sub>3</sub>); 25.69 (SiC(CH<sub>3</sub>)<sub>3</sub>); 17.93 (SiC(CH<sub>3</sub>)<sub>3</sub>); -4.53 (SiCH<sub>3</sub>); -5.19 (SiCH<sub>3</sub>)

ESI (-): m/z 701.5 ([M-H]<sup>-</sup>);

**3'-O- (2-Cyanoethoxydiisopropylphosphin) -1'-deoxy-5'-O- (4,4'-dimethoxy-triphenylmethyl) -1' - (4,6-difluoro-1-N-benzimidazolyl) -2'-O- (tert.-butyl-dimethylsilyl) -β-D-ribofuranose 108**



C<sub>48</sub>H<sub>61</sub>F<sub>2</sub>N<sub>4</sub>O<sub>7</sub>PSi

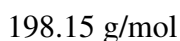
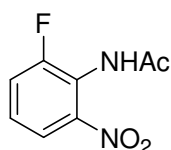
903.04 g/mol

200 mg (0.29 mmol) 5'-O-(4,4'-Dimethoxytriphenylmethyl)-2'-O-tert.-butyldimethylsilyl-1'-deoxy-1'-(4,6-difluoro-1-N-benzimidazolyl)-β-D-ribofuranose 106 were dissolved in 10 ml abs. acetonitrile and 380 μl (2.9 mmol) *sym.* collidine and 12 μl (0.15 mmol) 1-methylimidazole were added. The reaction mixture was cooled in an icebath to 0°C and 96 μl (0.43 mmol) 2-cyanoethoxydiisopropylchlorophosphoramidite 96 were added. The reaction was stirred for 15 min. at 0°C and 25 min. at RT. The reaction was stopped by adding 10 ml of 0.01 M citric acid and extracted with methylene chloride three times. Collected organic phases were washed with 0.01 M citric acid twice, dried over MgSO<sub>4</sub> and evaporated to dryness. Purification was done by FC with methylene chloride/methanol 99:1 as eluent. The product (mixture of two diastereomers) was obtained as white foam.

Yield: 200 mg (80.0%)

- TLC:  $R_f = 0.65$  ( $\text{CH}_2\text{Cl}_2/\text{MeOH}$  98:2)
- $^1\text{H-NMR}$ :  $\delta$  [ppm] (270 MHz,  $\text{CDCl}_3$ )  
 8.12, 8.11 (s, 2H, 2H); 7.46 – 6.73 (m, 30 H,  $\text{H}_{\text{ar}}$ , 5H, 7H); 5.85, 5.78 (d,  $J = 7.6$  Hz,  $J = 7.2$  Hz, 2H, 1'H); 4.67 (m, 2H, 2'H); 4.41 (m, 2H, 3'H); 4.32 (m, 2H, 4'H); 3.79, 3.78 (s, 12H,  $\text{OCH}_3$ ); 3.52 (m, 8H, 5'H,  $\text{CH}_2\text{CN}$ ); 2.67 (m, 4H,  $\text{OCH}_2$ ); 1.19 (m, 12H,  $\text{CH}(\text{CH}_3)_2$ ); 0.82, 0.76 (s, 18H,  $\text{SiC}(\text{CH}_3)_3$ ); -0.09, -0.10, -0.32, -0.34 (s, 12H,  $\text{SiCH}_3$ )
- $^{31}\text{P-NMR}$ :  $\delta$  [ppm] (162 MHz,  $\text{CDCl}_3$ )  
 152.62 and 149.33 (Ratio 1: 2.75)
- ESI(+):  $m/z$  903.6 ( $[\text{M}+\text{H}]^+$ );

### 2-Fluoro-6-nitroacetanilide 46



20.8 g (135.8 mmol) 2-Fluoroacetanilide were dissolved in 18.4 ml (166 mmol) acetic anhydride and 13.8 ml (219 mmol) acetic acid. The reaction mixture was cooled to  $-5^\circ\text{C}$  and a mixture from 7.4 ml conc.  $\text{HNO}_3$  and 11.5 ml (182 mmol)  $\text{CH}_3\text{COOH}$  was added over 10 minutes. While warming up to room temperature over 2 hours yellow crystals precipitated. The reaction mixture was left at room temperature for two days. Afterwards reaction mixture was poured in 200 ml of icewater and for two hours cooled in icebath. The yellow precipitate was filtered on vacuum, washed with icewater and dried. In crude product 90 ml of Witt-Utermann-solution were added to the crude product and stirred for 3 minutes. The solution was filtered and washed with 30 ml Witt-Utermann-solution twice and with 60 ml of icewater once. The filtrate was neutralised with  $\text{CH}_3\text{COOH}$ , 2 hours in icebath crystallized filtered and dried. The product was crystallized from ethanol and obtained as crème solid.

Yield: 11.34 g (42.1 %)

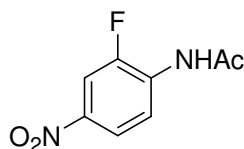
<sup>1</sup>H-NMR: δ [ppm] (250 MHz, DMSO-*d*<sub>6</sub>)  
 7.79 (d, J = 8.2 Hz, 1H, 5H); 7.69 (dt, J = 1.3 Hz, J = 8.4 Hz, 1H, 4H); 7.48 (m, 1H, 3H); 2.08 (s, 3H, CH<sub>3</sub>)

IR (KBr): 1184.5 cm<sup>-1</sup> C-F  
 1539.1 cm<sup>-1</sup> NO<sub>2</sub>  
 1674.7 cm<sup>-1</sup> C=O  
 3285.0 cm<sup>-1</sup> N-H

Melting point.: 171 - 174°C

El. Analysis:      Counted:      C: 48.49 %      H: 3.56 %      N: 14.14 %  
                          Found:      C: 48.28 %      H: 3.78 %      N: 13.96 %

### 2-Fluoro-4-nitroacetanilide **45**



C<sub>8</sub>H<sub>7</sub>FN<sub>2</sub>O<sub>3</sub>  
 198.15 g/mol

2-Fluoro-4-nitroacetanilide **45** was obtained as a side product in the preparation of 2-Fluoro-6-nitroacetanilide **46** while separating isomers with Witt-Utermann-solution 2-Fluoro-4-nitroacetanilide **45** does not dissolve and stays on the filter. After drying it was crystallized from ethanol. The product was obtained as crème solid.

Yield: 9.77 g (36.3 %)

<sup>1</sup>H-NMR: δ [ppm] (250 MHz, DMSO-*d*<sub>6</sub>)  
 8.41 (dd, J = 9.1 Hz, J = 7.8 Hz, 1H, 3H); 8.12 (m, 2H, 5H, 6H); 2.19 (s, 3H, CH<sub>3</sub>)

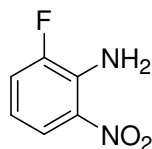
IR (KBr): 1162.3 cm<sup>-1</sup> C-F

1559.9 cm<sup>-1</sup> NO<sub>2</sub>  
 1688.3 cm<sup>-1</sup> C=O  
 3266.1 cm<sup>-1</sup>; 3218.5 cm<sup>-1</sup> N-H

Melting point.: 204°C

El. Analysis:      Counted:      C: 48.49 %    H: 3.56 %    N: 14.14 %  
                          Found:      C: 48.61 %    H: 3.31 %    N: 14.07 %

### 2-Fluoro-6-nitroaniline 52



C<sub>6</sub>H<sub>5</sub>FN<sub>2</sub>O<sub>2</sub>  
 156.11 g/mol

12 g (60.5 mmol) 2-Fluoro-6-nitroacetanilide **46** were dissolved in 60 ml 2 N HCl and refluxed for 3 hours. After cooling to room temperature the reaction mixture was neutralised with a saturated water solution of NaHCO<sub>3</sub> and for 30 minutes cooled in icebath. The yellow to black precipitate was filtered on vacuum, washed with water and dried. The product was obtained as yellow solid.

Yield: 8.46 g (89.5 %)

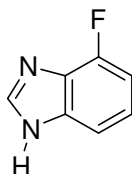
<sup>1</sup>H-NMR: δ [ppm] (270 MHz, DMSO-*d*<sub>6</sub>)  
 7.83 (d, J = 8.9 Hz, 1H, 5H); 7.44 (dt, J = 1.0 Hz, J = 7.9 Hz, 1H, 4H); 7.24 (s br, 2H, NH<sub>2</sub>); 6.62 (m, 1H, 3H)

IR (KBr): 1164.3 cm<sup>-1</sup> C-F  
 1532.9 cm<sup>-1</sup> NO<sub>2</sub>  
 3490.7 cm<sup>-1</sup>; 3368.7 cm<sup>-1</sup> N-H

Melting point: 75 - 76°C

El. Analysis:	Counted:	C: 46.16 %	H: 3.23 %	N: 17.95 %
	Found:	C: 46.16 %	H: 3.14 %	N: 17.90 %

### 4-Fluorobenzimidazole 54



136.12 g/mol

4.59 g (29.4 mmol) 2-Fluoro-6-nitroaniline 52 were dissolved in 100 ml abs. ethanol and 300 mg (1.3 mmol) PtO<sub>2</sub> were added. The reaction mixture was stirred for 5 hours (TLC control) in hydrogen atmosphere. The catalyst was filtered over celite and the filtrate evaporated to dryness under reduced pressure. The left dark brown oil (53-diamine) was immediately dissolved in 100 ml of HCOOH and refluxed for 90 minutes. Afterwards HCOOH was evaporated and the product purified by FC with methylene chloride/methanol 9:1 as eluent. The product was obtained as dark brown solid.

Yield: 3.43 g (85.6 %)

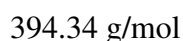
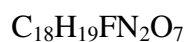
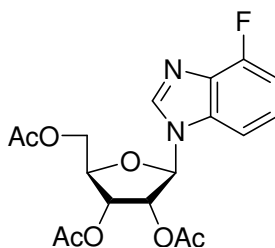
<sup>1</sup>H-NMR: δ [ppm] (270 MHz, DMSO-*d*<sub>6</sub>)  
 12.86 (s, 1H, NH); 8.29 (s, 1H, 2H); 7.40 (d, J = 8.0 Hz, 1H, 7H); 7.16 (m, 1H, 6H); 6.98 (m, 1H, 5H)

IR (KBr): 1169.0 cm<sup>-1</sup> C-F  
 3200 - 3000 cm<sup>-1</sup> N-H

Melting point.: 185 - 187°C

El. Analysis:	Counted:	C: 61.76 %	H: 3.67 %	N: 20.58 %
	Found:	C: 61.69 %	H: 3.92 %	N: 20.50 %

**2',3',5'-Tri-*O*-acetyl-1'-deoxy-1'-(4-fluoro-1-*N*-benzimidazolyl)- $\beta$ -D-ribofuranose 109**



4.8 g (35.3 mmol) 4-Fluorobenzimidazole 54 were suspended in 120 ml abs. acetonitrile and 11.1 ml (45 mmol) *N, O*-Bis- (trimethylsilyl)-acetamide were added. The reaction mixture was refluxed for 15 min. After cooling to room temperature 9.6 g (30 mmol) 1,2,3,5-Tetra-*O*-acetyl- $\beta$ -D-ribofuranose in 50 ml abs. acetonitrile and 6.7 ml (37 mmol) trimethylsilyltrifluoro sulphonate (TMSOTf) were added. The reaction mixture was then refluxed for 2.5 h and cooled to room temperature. After cooling the reaction mixture was treated with 20 ml of 5% NaHCO<sub>3</sub>-solution and extracted with methylene chloride three times. The collected organic phases were dried over MgSO<sub>4</sub> and evaporated to dryness. The product was purified by means of FC with methylene chloride/methanol 98:2 and obtained as a white foam.

Yield: 9.1 g (64.3 %)

TLC:  $R_f = 0.41$  (CH<sub>2</sub>Cl<sub>2</sub>/MeOH 98:2)

<sup>1</sup>H-NMR:  $\delta$  [ppm] (250 MHz, DMSO-*d*<sub>6</sub>)

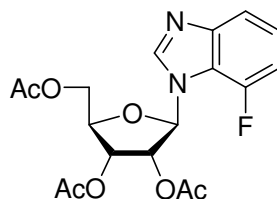
8.54 (s, 1H, 2H); 7.60 (d,  $J = 7.8$  Hz, 1H, 7H); 7.30 (dt,  $J = 4.9$  Hz,  $J = 8.1$  Hz, 1H, 6H); 7.10 (dd,  $J = 7.8$  Hz,  $J = 11.0$  Hz, 1H, 5H); 6.34 (d,  $J = 6.2$  Hz, 1H, 1'H); 5.66 (t,  $J = 6.3$  Hz, 1H, 2'H); 5.43 (dd,  $J = 4.6$  Hz,  $J = 6.3$  Hz, 1H, 3'H); 4.42 (m, 1H, 4'H); 4.37 (m, 2H, 5'H); 2.13 (s, 3H, CH<sub>3</sub>-acetyl); 2.07 (s, 3H, CH<sub>3</sub>-acetyl); 2.03 (s, 3H, CH<sub>3</sub>-acetyl)



$^{13}\text{C}$ -NMR:  $\delta$  [ppm] (62.9 MHz, DMSO- $d_6$ )  
 170.01 (C=O acetyl); 169.52 (C=O acetyl); 169.22 (C=O acetyl); 143.04 (C2);  
 135.37 (C6); 132.24 (C5); 123.94 (C8); 108.02 (C9); 107.87 (C7); 86.47 (C1');  
 79.47 (C4'); 71.75 (C2'); 69.53 (C3'); 62.94 (C5'); 20.50 (CH<sub>3</sub>-acetyl); 20.36  
 (CH<sub>3</sub>-acetyl); 20.15 (CH<sub>3</sub>-acetyl)

ESI (+): m/z 395.1 ([M+H]<sup>+</sup>);

**2',3',5'-Tri-*O*-acetyl-1'-deoxy-1'-(4-fluoro-3-*N*-benzimidazolyl)- $\beta$ -D-ribofuranose 110**



$\text{C}_{18}\text{H}_{19}\text{FN}_2\text{O}_7$

394.34 g/mol

2',3',5'-Tri-*O*-acetyl-1'-deoxy-1'-(4-fluoro-3-*N*-benzimidazolyl)- $\beta$ -D-ribofuranose 110 is obtained as a side product in the synthesis of 2',3',5'-Tri-*O*-acetyl-1'-deoxy-1'-(4-fluoro-1-*N*-benzimidazolyl)- $\beta$ -D-ribofuranose 109.

Yield: 1.14 g (8.1 %)

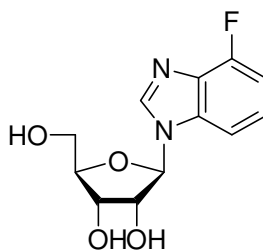
TLC:  $R_f$  = 0.35 (CH<sub>2</sub>Cl<sub>2</sub>/MeOH 98:2)

$^1\text{H}$ -NMR:  $\delta$  [ppm] (400 MHz, DMSO- $d_6$ )  
 8.58 (s, 1H, 2H); 7.56 (d,  $J$  = 7.9 Hz, 1H, 7H); 7.26 (m, 1H, 6H); 7.19 (m, 1H, 5H); 6.31 (d,  $J$  = 5.9 Hz, 1H, 1'H); 5.66 (t,  $J$  = 6.2 Hz, 1H, 2'H); 5.40 (m, 1H, 3'H); 4.38 (m, 2H, 4'H, 5'H); 4.26 (m, 1H, 5'H); 2.12 (s, 3H, CH<sub>3</sub>-acetyl); 2.05 (s, 3H, CH<sub>3</sub>-acetyl); 2.03 (s, 3H, CH<sub>3</sub>-acetyl)

<sup>13</sup>C-NMR: δ [ppm] (62.9 MHz, DMSO-*d*<sub>6</sub>)  
 170.01 (C=O acetyl); 169.43 (C=O acetyl); 169.17 (C=O acetyl); 148.24 (C4);  
 147.17 (C8); 143.58 (C2); 123.07 (C6); 120.24 (C9); 116.33 (C7); 109.55  
 (C5); 87.34 (C1'); 79.10 (C4'); 72.61 (C2'); 69.27 (C3'); 62.64 (C5'); 20.41  
 (CH<sub>3</sub>-acetyl); 20.29 (CH<sub>3</sub>-acetyl); 20.08 (CH<sub>3</sub>-acetyl)

ESI(+): m/z 395.1 ([M+H]<sup>+</sup>);

**1'-Deoxy-1'-(4-fluoro-1-*N*-benzimidazolyl)-β-D-ribofuranose 30**



C<sub>12</sub>H<sub>13</sub>FN<sub>2</sub>O<sub>4</sub>

268.23 g/mol

5.46 g (13.8 mmol) 2',3',5'-Tri-*O*-acetyl-1'-deoxy-1'-(4-fluoro-1-*N*-benzimidazolyl)-β-D-ribofuranose 109 were dissolved in 50 ml of methanol and 370 μl of MeONa/MeOH ( 5.4M, Fluka) were added at RT and the reaction TLC controlled. After 60 min the reaction was complete, neutralised with DOWEX 50, filtered and evaporated. The product was obtained as white foam and purified by FC with methylene chloride/methanol 4:1 as eluent.

Yield: 3.58 g (96.4 %)

TLC: R<sub>f</sub> = 0.42 (CH<sub>2</sub>Cl<sub>2</sub>/MeOH 4:1)

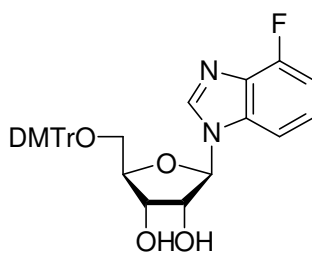
<sup>1</sup>H-NMR: δ [ppm] (250 MHz, DMSO-*d*<sub>6</sub>)  
 8.51 (s, 1H, 2H); 7.60 (d, J = 8.2 Hz, 1H, 7H); 7.26 (dt, J = 5.0 Hz, J = 8.0 Hz, 1H, 6H); 7.06 (dd, J = 8.0 Hz, J = 11.0 Hz, 1H, 5H); 5.89 (d, J = 6.2 Hz, 1H 1'H); 5.51 (d, J = 6.4 Hz, 1H, 2'-OH); 5.23 (d, J = 4.7 Hz, 1H, 3'-OH); 5.14 (t, J = 5.2 Hz, 1H, 5'-OH); 4.36 (q, J = 5.9 Hz, 1H, 2'H); 4.13 (m, 1H, 3'H); 3.99 (q, J = 3.4 Hz, 1H, 4'H); 3.64 (m, 2H, 5'H)

<sup>13</sup>C-NMR: δ [ppm] (67.9 MHz, DMSO-*d*<sub>6</sub>)  
 142.81 (C2); 136.04 (C6); 132.46 (C5); 123.28 (C8); 108.05 (C7); 107.37 (C9); 88.89 (C1'); 85.62 (C4'); 73.77 (C2'); 70.04 (C3'); 61.13 (C5')

<sup>19</sup>F-NMR: δ [ppm] (254.2 MHz, DMSO-*d*<sub>6</sub>)  
 -128.92 (m, 1F, 4F)

ESI(-): m/z 267.1 ([M-H]<sup>-</sup>);

**1'-Deoxy -5'-O-(4,4'-dimethoxytriphenylmethyl)-1'-(4-fluoro-1-N-benzimidazolyl)-β-D-ribofuranose 111**



C<sub>33</sub>H<sub>31</sub>FN<sub>2</sub>O<sub>6</sub>

570.59 g/mol

1.08 g (4.0 mmol) 1'-Deoxy-1'-(4-fluoro-1-N-benzimidazolyl)-β-D-ribofuranose **30** were dissolved in 20 ml abs. pyridine and 0.74 ml (6.0 mmol) triethylamine and 1.44 g (4.3 mmol) 4,4'-dimethoxytriphenylmethyl chloride were added. The reaction mixture was stirred under argon at RT for 6.5 h. The reaction was stopped by adding 5 ml of methanol and saturated water solution of NaHCO<sub>3</sub>. It was extracted with methylene chloride three times, organic phases were collected, dried over MgSO<sub>4</sub> and evaporated to dryness. The product was co-

evaporated with toluene twice. Further purification was done by FC with methylene chloride/methanol 95:5 as eluent. The product was obtained as yellow foam.

Yield: 2.04 g (89.1 %)

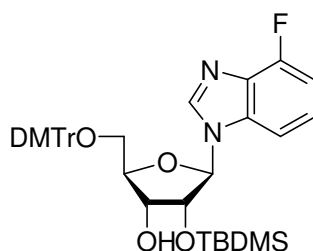
TLC:  $R_f = 0.40$  ( $\text{CH}_2\text{Cl}_2/\text{MeOH}$  9:1)

$^1\text{H-NMR}$ :  $\delta$  [ppm] (250 MHz,  $\text{DMSO-}d_6$ )  
 8.42 (s, 1H, 2H); 7.54 (d,  $J = 9.0$  Hz, 1H, 7H); 7.39 – 6.81 (m, 13H,  $\text{H}_{\text{ar}}$ ); 7.07 (m, 2H, 5H, 6H); 5.94 (d,  $J = 5.4$  Hz, 1H, 1'H); 5.66 (d,  $J = 6.0$  Hz, 1H, 2'-OH); 5.30 (d,  $J = 5.5$  Hz, 1H, 3'-OH); 4.52 (q,  $J = 5.6$  Hz, 1H, 2'H); 4.23 (q,  $J = 5.1$  Hz, 1H, 3'H); 4.13 (m, 1H, 4'H); 3.71 (s, 6H,  $\text{OCH}_3$ ); 3.24 (m, 2H, 5'H)

$^{13}\text{C-NMR}$ :  $\delta$  [ppm] (67.9 MHz,  $\text{DMSO-}d_6$ )  
 158.12 (DMTr); 153.34 (C4); 144.76 (DMTr); 142.65 (C2); 135.88 (C6); 135.42 (DMTr); 135.30 (DMTr); 132.29 (C5); 129.75 (DMTr); 127.86 (DMTr); 127.73 (DMTr); 126.75 (DMTr); 123.33 (C8); 113.20 (DMTr); 108.38 (C7); 107.62 (C9); 89.18 (C1'); 85.72 (DMTr); 83.53 (C4'); 73.25 (C2'); 70.10 (C3'); 63.59 (C5'); 55.05 ( $\text{OCH}_3$ )

ESI(-):  $m/z$  569.4 ( $[\text{M-H}]^-$ );

**5'-O-(4,4'-Dimethoxytriphenylmethyl)-2'-O-tert.-butyldimethylsilyl-1'-deoxy-1'-(4-fluoro-1-N-benzimidazolyl)- $\beta$ -D-ribofuranose 112**



$\text{C}_{39}\text{H}_{45}\text{FN}_2\text{O}_6\text{Si}$

684.85 g/mol

2.52 g (4.4 mmol) 5'-O-(4,4'-Dimethoxytriphenylmethyl)-1'-deoxy-1'- $\beta$ -D-(4-fluoro-1-N-benzimidazolyl)-ribofuranose 111 were dissolved in 40 ml of a 1:1 mixture THF/pyridine

and 900 mg (5.3 mmol) AgNO<sub>3</sub> and 6.2 ml (6.2 mmol) 1 M *tert.*-butyldimethylsilyl chloride-solution in THF were added. The reaction mixture was stirred for 20 hours at RT under argon. The reaction was stopped by adding 10 ml of saturated water NaHCO<sub>3</sub>-solution. Left AgCl was filtered over celite and the filtrate was extracted with methylene chloride three times. Collected organic phases were dried over MgSO<sub>4</sub> and evaporated to dryness. The crude product was co-evaporated with toluene twice. Further purification of the product was done by HPLC (*MN Nucleoprep 100-20* of *Macherey-Nagel*, *n*-hexan/dioxan 5:2). The product (*fast-Isomer*) was obtained as white foam.

Yield: 1.23 g (40.7 %)

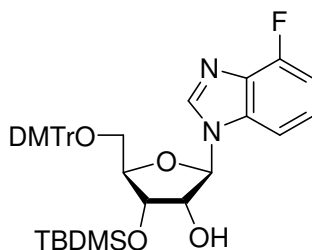
TLC: R<sub>f</sub> = 0.26 (*n*-hexan/ethyl acetate 4:1)

<sup>1</sup>H-NMR: δ [ppm] (270 MHz, DMSO-*d*<sub>6</sub>)  
 8.45 (s, 1H, 2H); 7.57 (d, J = 7.6 Hz, 1H, 7H); 7.41 – 6.83 (m, 13H, H<sub>ar</sub>); 6.98 (m, 2H, 5H, 6H); 5.97 (d, J = 6.3 Hz, 1H, 1'H); 5.26 (d, J = 5.3 Hz, 1H, 3'-OH); 4.60 (q, J = 6.0 Hz, 1H, 2'H); 4.35 (m, 1H, 3'H); 4.09 (m, 1H, 4'H); 3.72 (s, 6H, OCH<sub>3</sub>); 3.30 (m, 2H, 5'H); 0.82 (s, 9H, SiC(CH<sub>3</sub>)<sub>3</sub>); 0.07 (s, 3H, SiCH<sub>3</sub>); 0.02 (s, 3H, SiCH<sub>3</sub>)

<sup>13</sup>C-NMR: δ [ppm] (67.9 MHz, DMSO-*d*<sub>6</sub>)  
 158.10 (DMTr); 153.27 (C4); 144.47 (DMTr); 142.78 (C2); 135.63 (C6); 135.21 (DMTr); 135.14 (DMTr); 132.28 (C5); 129.62 (DMTr); 127.74 (DMTr); 127.60 (DMTr); 126.69 (DMTr); 123.15 (C8); 113.13 (DMTr); 108.36 (C7); 107.52 (C9); 89.07 (C1'); 85.85 (DMTr); 83.95 (C4'); 72.64 (C2'); 71.81 (C3'); 62.99 (C5'); 54.98 (OCH<sub>3</sub>); 25.67 (SiC(CH<sub>3</sub>)<sub>3</sub>); 17.90 (SiC(CH<sub>3</sub>)<sub>3</sub>); -4.56 (SiCH<sub>3</sub>); -5.19 (SiCH<sub>3</sub>)

ESI(+): m/z 685.5 ([M+H]<sup>+</sup>);

**5'-O-(4,4'-Dimethoxytriphenylmethyl)-3'-O-*tert.*-butyldimethylsilyl-1'-deoxy-1'-(4-fluoro-1-N-benzimidazolyl)- $\beta$ -D-ribofuranose 113**



$C_{39}H_{45}FN_2O_6Si$

684.85 g/mol

5'-O-(4,4'-Dimethoxytriphenylmethyl)-3'-O-*tert.*-butyldimethylsilyl-1'-deoxy-1'-(4-fluoro-1-N-benzimidazolyl)- $\beta$ -D-ribofuranose 113 was obtained as a side product slow-*Isomer* in synthesizing 5'-O-(4,4'-Dimethoxytriphenylmethyl)-2'-O-*tert.*-butyldimethylsilyl-1'-deoxy-1'-(4-fluoro-1-N-benzimidazolyl)- $\beta$ -D-ribofuranose 112.

Yield: 1.48 g (49.0 %)

TLC:  $R_f = 0.26$  (*n*-hexan/ethyl acetate 4:1)

$^1H$ -NMR:  $\delta$  [ppm] (270 MHz, DMSO- $d_6$ )

8.46 (s, 1H, 2H); 7.56 (d,  $J = 9.0$  Hz, 1H, 7H); 7.38 – 6.82 (m, 13H,  $H_{ar}$ ); 7.07 (m, 2H, 5H, 6H); 5.92 (d,  $J = 5.9$  Hz, 1H, 1'H); 5.53 (d,  $J = 6.5$  Hz, 1H, 2'-OH); 4.51 (q,  $J = 6.0$  Hz, 1H, 2'H); 4.35 (m, 1H, 3'H); 4.09 (m, 1H, 4'H); 3.72 (s, 6H, OCH<sub>3</sub>); 3.30 (m, 2H, 5'H); 0.82 (s, 9H, SiC(CH<sub>3</sub>)<sub>3</sub>); 0.07 (s, 3H, SiCH<sub>3</sub>); 0.02 (s, 3H, SiCH<sub>3</sub>)

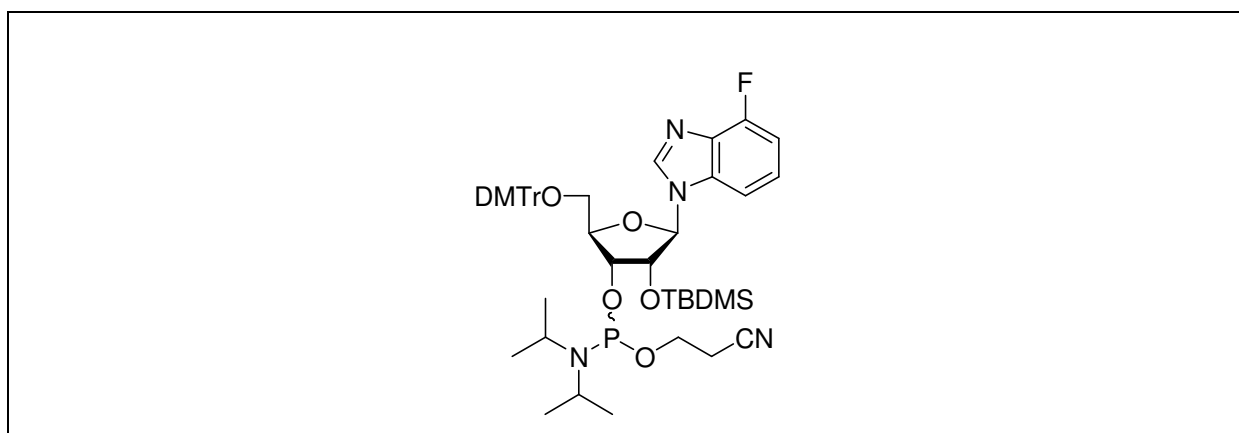
$^{13}C$ -NMR:  $\delta$  [ppm] (67.9 MHz, DMSO- $d_6$ )

158.10 (DMTr); 153.27 (C4); 144.47 (DMTr); 142.78 (C2); 135.63 (C6); 135.21 (DMTr); 135.14 (DMTr); 132.28 (C5); 129.62 (DMTr); 127.74 (DMTr); 127.60 (DMTr); 126.69 (DMTr); 123.15 (C8); 113.13 (DMTr); 108.36 (C7); 107.52 (C9); 89.07 (C1'); 85.85 (DMTr); 83.95 (C4'); 72.64

(C2'); 71.81 (C3'); 62.99 (C5'); 54.98 (OCH<sub>3</sub>); 25.67 (SiC(CH<sub>3</sub>)<sub>3</sub>); 17.90 (SiC(CH<sub>3</sub>)<sub>3</sub>); -4.56 (SiCH<sub>3</sub>); -5.19 (SiCH<sub>3</sub>)

ESI(+): m/z 685.5 ([M+H]<sup>+</sup>);

**3'-O-(2-Cyanethoxydiisopropylphosphin)-1'-deoxy-5'-O-(4,4'-dimethoxy-triphenylmethyl)-1'-(4-fluoro-1-N-benzimidazolyl)-2'-O-tert.-butyldimethylsilyl-β-D-ribofuranose 114**



C<sub>48</sub>H<sub>62</sub>FN<sub>4</sub>O<sub>7</sub>PSi

885.05 g/mol

200 mg (0.29 mmol) 5'-O-(4,4'-Dimethoxytriphenylmethyl)-2'-O-tert.-butyldimethylsilyl-1'-deoxy-1'-(4-fluoro-1-N-benzimidazolyl)-β-D-ribofuranose 112 were dissolved in 10 ml abs. acetonitrile and 380 μl (2.9 mmol) *sym.* collidine and 12 μl (0.15 mmol) 1-methylimidazole were added. The reaction mixture was cooled in an icebath to 0°C and 96 μl (0.43 mmol) 2-cyanethyldiisopropylchlorophosphoramidit 96 were added. The reaction mixture was stirred at 0°C for 15min and for 45 min. at RT. The reaction was stopped by adding of 10 ml of 0.01 M citric acid and extracted with methylene chloride three times. Collected organic phases were washed twice with 0.01 M citric acid, dried over MgSO<sub>4</sub> and evaporated to dryness. Purification was done by FC with methylene chloride/methanol 99:1 as eluent. The product (mixture of two diastereomers) was obtained as white foam.

Yield: 135 mg (52.3 %)

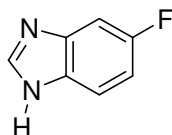
TLC: R<sub>f</sub> = 0.33; 0.41 (CH<sub>2</sub>Cl<sub>2</sub>/MeOH 99:1)

<sup>1</sup>H-NMR: δ [ppm] (400 MHz, CDCl<sub>3</sub>)  
 8.12, 8.08 (s, 2H, 2H); 7.49 – 6.81 (m, 32H, H<sub>ar</sub>, 5H, 6H, 7H); 5.92, 5.84 (d, J = 7.7 Hz, J = 5.8 Hz, 2H, 1'H); 4.75 (m, 2H, 2'H); 4.40 (m, 2H, 3'H); 4.32 (m, 2H, 4'H); 3.80, 3.79 (s, 12H, OCH<sub>3</sub>); 3.48 (m, 4H, 5'H); 2.66 (m, 4H, OCH<sub>2</sub>), 1.20 (m, 12H, CH (CH<sub>3</sub>)<sub>2</sub>); 0.75 (s, 18H, SiC(CH<sub>3</sub>)<sub>3</sub>); -0.12 (s, 6H, SiCH<sub>3</sub>); -0.38 (s, 6H, SiCH<sub>3</sub>)

<sup>31</sup>P-NMR: δ [ppm] (162 MHz, CDCl<sub>3</sub>)  
 152.49 and 149.32 (ratio 1: 2.7)

ESI (+): m/z 885.8 ([M+H]<sup>+</sup>);

### 5-fluoro-1H-benzimidazole 65



C<sub>7</sub>H<sub>5</sub>FN<sub>2</sub>

136.12 g/mol

3,4-diamino benzofluoride (4g, 32 mmol) was heated for 3h under reflux with 100ml of 90% HCOOH. HCOOH was then evaporated and the crude product purified by FC (CH<sub>2</sub>Cl<sub>2</sub>/MeOH, 9:1).

Yield: 4 g (92 %);

TLC: R<sub>f</sub>=0.55 (CH<sub>2</sub>Cl<sub>2</sub>/MeOH, 9:1):

<sup>1</sup>H NMR: δ [ppm] (250MHz, DMSO- *d*<sub>6</sub>)  
 12.87 (s,1H, NH), 8.23 (s,1H, 2H), 7.57 (m, 1H, 4H), 7.33 (m,1H, 7H), 7.03 (m,1H, 6H);

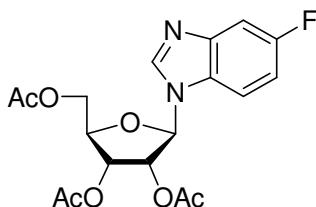
<sup>13</sup>C NMR : δ [ppm] (60.9 MHz, DMSO-*d*<sub>6</sub>):  
 142.05 (C2), 140.50, 138.10, 121.10, 119.10, 119.70, 119.20 (*arom C*);

El. Analysis:	Counted:	C: 61.76 %	H: 3.67 %	N: 20.58 %
	Found:	C: 61.71 %	H: 3.96 %	N: 20.65 %



ESI-MS: 136.7 ( $[M+H]^+$ );

**2',3',5'-Tri-*O*-acetyl-1'-deoxy-1'-(5-fluoro-1-*N*-benzimidazolyl)- $\beta$ -D-ribofuranose 115**



$C_{18}H_{19}FN_2O_7$

394.34 g/mol

7.9 g (58 mmol) 5-fluorobenzimidazole **65** were suspended in 200 ml abs. acetonitrile and 18.25 ml (74 mmol) *N, O*-Bis-(trimethylsilyl)-acetamide were added. The reaction mixture was refluxed for 15 min. After cooling to room temperature 18.9 g (59 mmol) 1,2,3,5-Tetra-*O*-acetyl- $\beta$ -D-ribofuranose in 90 ml abs. acetonitrile and 11.00 ml (60.8 mmol) trimethylsilyltrifluoro sulphonate (TMSOTf) were added. The reaction mixture was refluxed for 2.5 h and cooled to room temperature. After cooling the reaction mixture was treated with 40 ml 5%  $NaHCO_3$ -solution and extracted with methylene chloride three times. Combined organic phases were dried over  $MgSO_4$  and evaporated to dryness. The product was purified by means of FC with methylene chloride/methanol 99:1 and obtained as white foam.

Yield: 9.6 g (42 %)

TLC:  $R_f = 0.39$  ( $CH_2Cl_2/MeOH$  98:2)

$^1H$ -NMR:  $\delta$  [ppm] (250 MHz,  $DMSO-d_6$ )

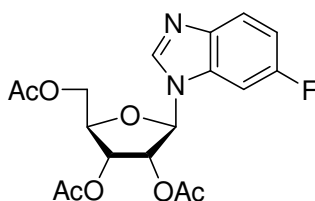
8.56 (s, 1H, 2H); 7.78 (m, 1H, 7H); 7.53 (m, 1H, 4H); 7.22 (m, 1H, 5H); 6.33 (d,  $J = 6.32$  Hz, 1H, 1'H); 5.65 (m, 1H, 2'H); 5.53 (m, 1H, 3'H); 4.42 (m, 1H, 4'H); 4.37 (m, 2H, 5'H); 2.14 (s, 3H,  $CH_3$ -acetyl); 2.04 (s, 3H,  $CH_3$ -acetyl); 2.03 (s, 3H,  $CH_3$ -acetyl)

$^{13}C$ -NMR:  $\delta$  [ppm] (62.9 MHz,  $DMSO-d_6$ )

170.01 (C=O acetyl); 169.52 (C=O acetyl); 169.22 (C=O acetyl); 143.04 (C2);  
135.37 (C6); 132.24 (C4); 123.94 (C8); 108.02 (C9); 107.87 (C7); 86.47 (C1');  
79.47 (C4'); 71.75 (C2'); 69.53 (C3'); 62.94 (C5'); 20.50 (CH<sub>3</sub>-acetyl); 20.36  
(CH<sub>3</sub>-acetyl); 20.15 (CH<sub>3</sub>-acetyl)

ESI (+): m/z 395.1 ([M+H]<sup>+</sup>);

**2', 3', 5'-Tri-*O*-acetyl-1'-deoxy-1'-(5-fluoro-3-*N*-benzimidazolyl)-β-D-  
ribofuranose 78**



C<sub>18</sub>H<sub>19</sub>FN<sub>2</sub>O<sub>7</sub>

394.34 g/mol

2',3',5'-Tri-*O*-acetyl-1'-deoxy-1'-(5-fluoro-3-*N*-benzimidazolyl)-β-D-ribofuranose 78 is obtained as second product in the synthesis of 2',3',5'-Tri-*O*-acetyl-1'-deoxy-1'-(5-fluoro-1-*N*-benzimidazolyl)-β-D-ribofuranose 115.

Yield: 8.7 g (38 %)

TLC: R<sub>f</sub> = 0.35 (CH<sub>2</sub>Cl<sub>2</sub>/MeOH 98:2)

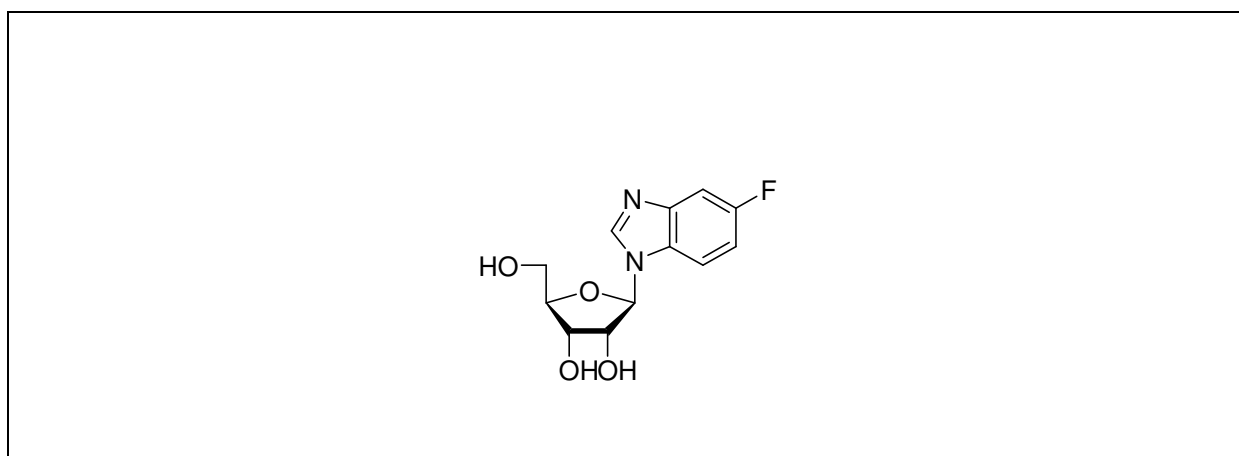
<sup>1</sup>H-NMR: δ [ppm] (400 MHz, DMSO-*d*<sub>6</sub>)  
8.58 (s, 1H, 2H); 7.74 (m, 1H, 7H); 7.65 (m, 1H, 4H); 7.15 (m, 1H, 6H); 6.31  
(d, J = 6.7 Hz, 1H, 1'H); 5.64 (m, 1H, 2'H); 5.42 (m, 1H, 3'H); 4.46 (m, 1H,  
4'H); 4.38 (m, 2H, 5'H); 2.18 (s, 3H, CH<sub>3</sub>-acetyl); 2.09 (s, 3H, CH<sub>3</sub>-acetyl);  
2.02 (s, 3H, CH<sub>3</sub>-acetyl)

<sup>13</sup>C-NMR: δ [ppm] (62.9 MHz, DMSO-*d*<sub>6</sub>)

170.01 (C=O acetyl); 169.43 (C=O acetyl); 169.17 (C=O acetyl); 148.24 (C4);  
 147.17 (C8); 143.58 (C2); 123.07 (C6); 120.24 (C9); 116.33 (C7); 109.55  
 (C5); 87.34 (C1'); 79.10 (C4'); 72.61 (C2'); 69.27 (C3'); 62.64 (C5'); 20.41  
 (CH<sub>3</sub>-acetyl); 20.29 (CH<sub>3</sub>-acetyl); 20.08 (CH<sub>3</sub>-acetyl)

ESI(+): m/z 395.1 ([M+H]<sup>+</sup>);

### 1'-Deoxy-1'-(5-fluoro-1-N-benzimidazolyl)-β-D-ribofuranose 31



C<sub>12</sub>H<sub>13</sub>FN<sub>2</sub>O<sub>4</sub>

268.23 g/mol

2.86 g (7.25 mmol) 2',3',5'-Tri-*O*-acetyl-1'-deoxy-1'-(5-fluoro-1-*N*-benzimidazolyl)-β-D-ribofuranose **115** were dissolved in 25 ml of methanol and 190 μl of MeONa/MeOH (5.4M, Fluka) were added at RT and the reaction TLC controlled. After 90 min the reaction was complete than neutralised with DOWEX 50, filtered and evaporated. The roduct was obtained as white foam and purified by FC with methylene chloride/methanol 4:1 as eluent.

Yield: 1.9 g (96 %)

TLC: R<sub>f</sub> = 0.42 (CH<sub>2</sub>Cl<sub>2</sub>/MeOH 4:1)

<sup>1</sup>H-NMR: δ [ppm] (400 MHz, DMSO-*d*<sub>6</sub>)

8.51 (s, 1H, 2H); 7.78 (m, 1H, 7H); 7.48 (m, 1H, 4H); 7.13 (m, 1H, 6H); 5.86 (d, J = 8.0 Hz, 1H 1'H); 5.45 (d, J = 7.8 Hz, 1H, 2'-OH); 5.19 (d, J = 5.7 Hz,

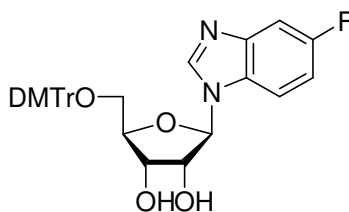
1H, 3'-OH); 5.11 (t, J = 8.2 Hz, 1H, 5'-OH); 4.35 (m, 1H, 2'H); 4.11 (m, 1H, 3'H); 3.98 (m, 1H, 4'H); 3.64 (m, 2H, 5'H)

<sup>13</sup>C-NMR: δ [ppm] (67.9 MHz, DMSO-*d*<sub>6</sub>)  
142.81 (C2); 136.04 (C6); 132.46 (C4); 123.28 (C8); 108.05 (C7); 107.37 (C9); 88.89 (C1'); 85.62 (C4'); 73.77 (C2'); 70.04 (C3'); 61.13 (C5')

<sup>19</sup>F-NMR: δ [ppm] (254.2 MHz, DMSO-*d*<sub>6</sub>)  
-128.90 (m, 1F, 5F)

ESI(-): m/z 267.1 ([M-H]<sup>-</sup>);

**1'-Deoxy -5'-O-(4,4'-dimethoxytriphenylmethyl)-1'-(5-fluoro-1-N-benzimidazolyl)-β-D-ribofuranose 116**



C<sub>33</sub>H<sub>31</sub>FN<sub>2</sub>O<sub>6</sub>

570.59 g/mol

1.00 g (3.73 mmol) 1'-Deoxy-1'-(5-fluoro-1-N-benzimidazolyl)-β-D-ribofuranose **31** was dissolved in 20 ml abs. pyridine and 0.76 ml (6.0 mmol) triethylamine and 1.44 g (4.3 mmol) 4,4'-dimethoxytriphenylmethyl chloride were added. The reaction mixture was stirred under argon at RT for 6.5 hours. The reaction was stopped by adding 5 ml of methanol and saturated water solution of NaHCO<sub>3</sub>. It was extracted with methylene chloride three times, organic phases were collected, dried over MgSO<sub>4</sub> and evaporated to dryness. The product was co-evaporated with toluene twice. Further purification was done by FC with methylene chloride/methanol 95:5 as eluent. The product was obtained as yellow foam.

Yield: 1.97 g (86 %)

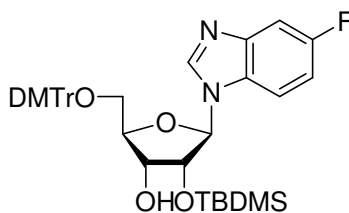
TLC:  $R_f = 0.30$  ( $\text{CH}_2\text{Cl}_2/\text{MeOH}$  95:5)

$^1\text{H-NMR}$ :  $\delta$  [ppm] (400 MHz,  $\text{DMSO-}d_6$ )  
 8.42 (s, 1H, 2H); 7.70 (m, 1H, 7H); 7.39 – 6.81 (m, 13H,  $\text{H}_{\text{ar}}$ ); 7.07 (m, 2H, 4H, 6H); 5.94 (d,  $J = 5.4$  Hz, 1H, 1'H); 5.66 (d,  $J = 6.0$  Hz, 1H, 2'-OH); 5.30 (d,  $J = 5.4$  Hz, 1H, 3'-OH); 4.52 (m, 1H, 2'H); 4.23 (m, 1H, 3'H); 4.13 (m, 1H, 4'H); 3.74 (s, 6H,  $\text{OCH}_3$ ); 3.23 (m, 2H, 5'H)

$^{13}\text{C-NMR}$ :  $\delta$  [ppm] (67.9 MHz,  $\text{DMSO-}d_6$ )  
 158.10 (DMTr); 154.34 (C5); 144.78 (DMTr); 142.65 (C2); 135.88 (C6); 135.42 (DMTr); 135.34 (DMTr); 132.39 (C4); 129.75 (DMTr); 127.86 (DMTr); 127.73 (DMTr); 126.75 (DMTr); 123.33 (C8); 113.20 (DMTr); 108.38 (C7); 107.62 (C9); 89.18 (C1'); 85.72 (DMTr); 83.53 (C4'); 73.25 (C2'); 70.10 (C3'); 63.59 (C5'); 55.05 ( $\text{OCH}_3$ )

ESI(-):  $m/z$  569.4 ( $[\text{M-H}]^-$ );

**5'-O-(4,4'-Dimethoxytriphenylmethyl)-2'-O-*tert.*-butyldimethylsilyl-1'-deoxy-1'-(5-fluoro-1-*N*-benzimidazolyl)- $\beta$ -D-ribofuranose 117**



$\text{C}_{39}\text{H}_{45}\text{FN}_2\text{O}_6\text{Si}$

684.85 g/mol

1.26 g (2.2 mmol) 5'-O-(4,4'-Dimethoxytriphenylmethyl)-1'-deoxy-1'- $\beta$ -D-(5-fluoro-1-*N*-benzimidazolyl)-ribofuranose 116 were dissolved in 20 ml of a 1:1 mixture of THF/pyridine and 450 mg (2.6 mmol)  $\text{AgNO}_3$  and 3.1 ml (3.1 mmol) 1 M *tert.*-butyldimethylsilyl chloride-solution in THF were added. The reaction mixture was stirred at RT under argon for 20 hours. The reaction was stopped by adding 10 ml of saturated water  $\text{NaHCO}_3$ -solution. Left  $\text{AgCl}$

was filtered over celite and the filtrate was extracted with methylene chloride three times. Collected organic phases were dried over MgSO<sub>4</sub> and evaporated to dryness. The crude product was co-evaporated with toluene twice. Further purification of the product was done by HPLC (*MN Nucleoprep 100-20* of *Macherey-Nagel*, *n*-hexan/dioxan 5:2). The product (*fast-Isomer*) was obtained as white foam.

Yield: 0.60 g (40 %)

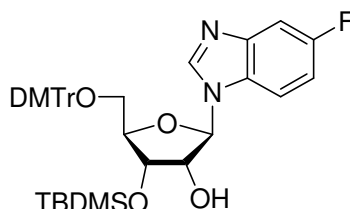
TLC: R<sub>f</sub> = 0.26 (*n*-hexan/ethyl acetate 4:1)

<sup>1</sup>H-NMR: δ [ppm] (400 MHz, DMSO-*d*<sub>6</sub>)  
 8.46 (s, 1H, 2H); 7.57 (m, 1H, 7H); 7.41 – 6.83 (m, 13H, H<sub>ar</sub>); 6.98 (m, 2H, 4H, 6H); 5.87 (d, J = 6.7 Hz, 1H, 3'OH); 5.26 (d, J = 5.3 Hz, 1H, 1'H); 4.60 (m, 1H, 2'H); 4.35 (m, 1H, 3'H); 4.09 (m, 1H, 4'H); 3.78 (s, 6H, OCH<sub>3</sub>); 3.30 (m, 2H, 5'H); 0.86 (s, 9H, SiC(CH<sub>3</sub>)<sub>3</sub>); 0.09 (s, 3H, SiCH<sub>3</sub>); 0.01 (s, 3H, SiCH<sub>3</sub>)

<sup>13</sup>C-NMR: δ [ppm] (67.9 MHz, DMSO-*d*<sub>6</sub>)  
 158.10 (DMTr); 154.27 (C5); 144.47 (DMTr); 142.78 (C2); 135.63 (C6); 135.31 (DMTr); 135.14 (DMTr); 132.28 (C4); 129.62 (DMTr); 127.74 (DMTr); 127.60 (DMTr); 126.69 (DMTr); 125.15 (C8); 113.13 (DMTr); 108.36 (C7); 107.52 (C9); 89.27 (C1'); 85.95 (DMTr); 83.95 (C4'); 72.64 (C2'); 71.87 (C3'); 63.00 (C5'); 54.98 (OCH<sub>3</sub>); 25.67 (SiC(CH<sub>3</sub>)<sub>3</sub>); 17.90 (SiC(CH<sub>3</sub>)<sub>3</sub>); -4.56 (SiCH<sub>3</sub>); -5.19 (SiCH<sub>3</sub>)

ESI(+): m/z 685.8 ([M+H]<sup>+</sup>);

**5'-O-(4,4'-Dimethoxytriphenylmethyl)-3'-O-*tert.*-butyldimethylsilyl-1'-deoxy-1'-(5-fluoro-1-*N*-benzimidazolyl)- $\beta$ -D-ribofuranose 118**



$C_{39}H_{45}FN_2O_6Si$

684.85 g/mol

5'-O-(4,4'-Dimethoxytriphenylmethyl)-3'-O-*tert.*-butyldimethylsilyl-1'-deoxy-1'-(5-fluoro-1-*N*-benzimidazolyl)- $\beta$ -D-ribofuranose 118 was obtained as a side product (slow-*Isomer*) in the synthesis of 5'-O-(4,4'-Dimethoxytriphenylmethyl)-2'-O-*tert.*-butyldimethylsilyl-1'-deoxy-1'-(5-fluoro-1-*N*-benzimidazolyl)- $\beta$ -D-ribofuranose 117.

Yield: 0.58 g (39.0 %)

TLC:  $R_f = 0.26$  (*n*-Hexan/Ethylacetat 4:1)

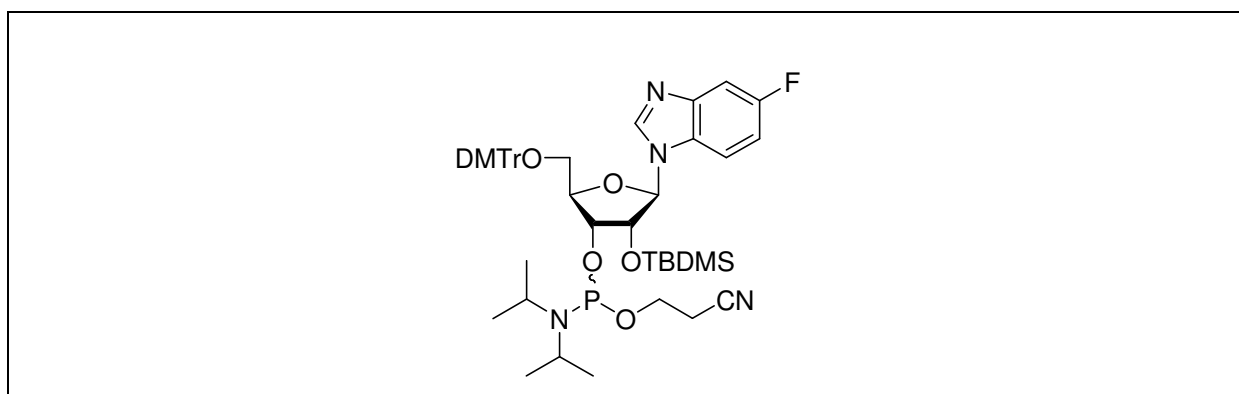
$^1H$ -NMR:  $\delta$  [ppm] (400 MHz, DMSO- $d_6$ )  
 8.46 (s, 1H, 2H); 7.56 (m, 1H, 7H); 7.38 – 6.82 (m, 13H,  $H_{ar}$ ); 7.07 (m, 2H, 4H, 7H); 5.91 (d,  $J = 5.9$  Hz, 1H, 1'H); 5.53 (d,  $J = 6.5$  Hz, 1H, 2'-OH); 4.51 (m, 1H, 2'H); 4.35 (m, 1H, 3'H); 4.09 (m, 1H, 4'H); 3.72 (s, 6H, OCH<sub>3</sub>); 3.30 (m, 2H, 5'H); 0.82 (s, 9H, SiC(CH<sub>3</sub>)<sub>3</sub>); 0.08 (s, 3H, SiCH<sub>3</sub>); 0.01 (s, 3H, SiCH<sub>3</sub>)

$^{13}C$ -NMR:  $\delta$  [ppm] (67,9 MHz, DMSO- $d_6$ )  
 158.10 (DMTr); 17.90 (SiC(CH<sub>3</sub>)<sub>3</sub>); 154.27 (C5); 144.47 (DMTr); 142.78 (C2); 135.63 (C6); 135.31 (DMTr); 135.14 (DMTr); 132.28 (C4); 129.62 (DMTr); 127.74 (DMTr); 127.60 (DMTr); 126.69 (DMTr); 125.15 (C8); 113.13 (DMTr); 108.36 (C7); 107.52 (C9); 89.27 (C1'); 85.95 (DMTr); 83.95

(C4'); 72.64 (C2'); 71.87 (C3'); 63.00(C5'); 54.98 (OCH<sub>3</sub>) ; -4.56 (SiCH<sub>3</sub>); -5.19 (SiCH<sub>3</sub>)

ESI(+): m/z 685.5 ([M+H]<sup>+</sup>);

**3'-O-(2-Cyanethoxydiisopropylphosphin)-1'-deoxy-5'-O-(4,4'-dimethoxy-triphenylmethyl)-1'-(5-fluoro-1-N-benzimidazolyl)-2'-O-tert.-butyldimethylsilyl-β-D-ribofuranose 119**



C<sub>48</sub>H<sub>62</sub>FN<sub>4</sub>O<sub>7</sub>PSi

885,05 g/mol

200 mg (0.29 mmol) 5'-O-(4,4'-Dimethoxytriphenylmethyl)-2'-O-tert.-butyldimethylsilyl-1'-deoxy-1'-(5-fluoro-1-N-benzimidazolyl)-β-D-ribofuranose 117 were dissolved in 10 ml abs. acetonitrile and 380 μl (2.9 mmol) *sym.* collidine and 12 μl (0.15 mmol) 1-methylimidazole were added. The reaction mixture was cooled in an icebath to 0°C and 96 μl (0.43 mmol) 2-cyanethyldiisopropylchlorophosphoramidite 96 were added. The reaction was stirred for 15min. at 0°C and 45 min. at RT. The reaction was stopped by adding 10ml of 0.01 M citric acid and extracted with methylene chloride three times. The combined organic phases were washed with 0.01 M citric acid twice, dried over MgSO<sub>4</sub> and evaporated to dryness. Purification was done by FC with methylene chloride/methanol 99:1, as eluent. The product (mixture of two diastereomers) was obtained as white foam.

Yield: 135 mg (52.3 %)

TLC: R<sub>f</sub> = 0.33; 0.41 (CH<sub>2</sub>Cl<sub>2</sub>/MeOH 99:1)

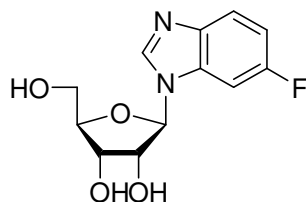


$^1\text{H-NMR}$ :  $\delta$  [ppm] (400 MHz,  $\text{CDCl}_3$ )  
 8.12, 8.08 (s, 2H, 2H); 7.49 – 6.81 (m, 32H,  $\text{H}_{\text{ar}}$ , 4H, 6H, 7H); 5.92, 5.84 (d,  $J$  = 5.9,  $J$  = 5.8 Hz, 2H, 1'H); 4.75 (m, 2H, 2'H); 4.40 (m, 2H, 3'H); 4.32 (m, 2H, 4'H); 3.80, 3.79 (s, 12H,  $\text{OCH}_3$ ); 3.48 (m, 4H, 5'H); 2.66 (m, 4H,  $\text{OCH}_2$ ), 1.20 (m, 12H,  $\text{CH}(\text{CH}_3)_2$ ); 0.75 (s, 18H,  $\text{SiC}(\text{CH}_3)_3$ );  $-0.12$  (s, 6H,  $\text{SiCH}_3$ );  $-0.38$  (s, 6H,  $\text{SiCH}_3$ )

$^{31}\text{P-NMR}$ :  $\delta$  [ppm] (162 MHz,  $\text{CDCl}_3$ )  
 153.12 and 149.92 (ratio 1 : 4)

ESI(+):  $m/z$  885.8 ( $[\text{M}+\text{H}]^+$ );

**1'-Deoxy-1'-(5-fluor-3-N-benzimidazolyl)- $\beta$ -D-ribofuranose 32**



$\text{C}_{12}\text{H}_{13}\text{FN}_2\text{O}_4$

268.23 g/mol

1.50 g (3.8 mmol) 2',3',5'-Tri-*O*-acetyl-1'-deoxy-1'-(5-fluor-3-*N*-benzimidazolyl)- $\beta$ -D-ribofuranose **78** were dissolved in 25 ml methanol and 190  $\mu\text{l}$  MeONa/MeOH (5.4M, Fluka) were added at RT and the reaction was TLC controlled. After 90 min reaction was complete than neutralised with DOWEX 50, filtered and evaporated. The product was obtained as white foam and purified by FC with methylene chloride/methanol 4:1 as eluent.

Yield: 0.96 g (94 %)

TLC:  $R_f$  = 0.41 ( $\text{CH}_2\text{Cl}_2/\text{MeOH}$  4:1)

$^1\text{H-NMR}$ :  $\delta$  [ppm] (400 MHz,  $\text{DMSO-}d_6$ )

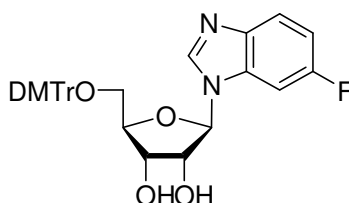
8.47 (s, 1H, 2H); 7.88 (m, 1H, 4H); 7.68 (m, 1H, 7H); 7.13 (m, 1H, 6H); 5.85 (d, J = 7.5 Hz, 1H 1'H); 5.42 (d, J = 7.6 Hz, 1H, 2'-OH); 5.19 (d, J = 4.56 Hz, 1H, 3'-OH); 5.11 (t, J = 5.04 Hz, 1H, 5'-OH); 4.35 (m, 1H, 2'H); 4.11 (m, 1H, 3'H); 3.98 (m, 1H, 4'H); 3.65 (m, 2H, 5'H)

<sup>13</sup>C-NMR: δ [ppm] (67,9 MHz, DMSO-*d*<sub>6</sub>)  
 142.81 (C2); 136.04 (C6); 132.46 (C4); 123.28 (C8); 108.05 (C7); 107.37 (C9); 88.89 (C1'); 85.62 (C4'); 73.77 (C2'); 70.04 (C3'); 61.13 (C5')

<sup>19</sup>F-NMR: δ [ppm] (254,2 MHz, DMSO-*d*<sub>6</sub>)  
 -128.90 (m, 1F, 5F)

ESI(-): m/z 267,1 ([M-H]<sup>-</sup>);

**1'-Deoxy -5'-O-(4,4'-dimethoxytriphenylmethyl)-1'-(5-fluor-3-N-benzimidazolyl)-β-D-ribofuranose 93**



C<sub>33</sub>H<sub>31</sub>FN<sub>2</sub>O<sub>6</sub>

570.59 g/mol

0.95 g (3.54 mmol) 1'-Deoxy-1'-(5-fluoro-3-N-benzimidazolyl)-β-D-ribofuranose **32** were dissolved in 20 ml abs. pyridine and 0.66 ml (5.31 mmol) triethylamine and 1.27 g (3.81 mmol) 4,4'-dimethoxytriphenylmethyl chloride were added. The reaction mixture was stirred under argon at RT for 7 hours. The reaction was stopped by adding of 5 ml of methanol and saturated water solution of NaHCO<sub>3</sub>. It was extracted with methylene chloride three times, organic phases were collected, dried over MgSO<sub>4</sub> and evaporated to dryness. The product was co-evaporated with toluene twice. Further purification was done by FC with methylene chloride/methanol 95:5 as eluent. The product was obtained as yellow foam.

Yield: 1.7 g (83 %)

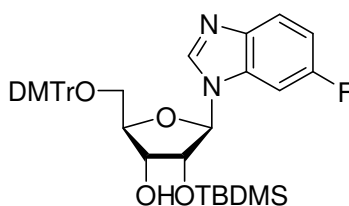
TLC:  $R_f = 0.32$  ( $\text{CH}_2\text{Cl}_2/\text{MeOH}$  95:5)

$^1\text{H-NMR}$ :  $\delta$  [ppm] (400 MHz,  $\text{DMSO-}d_6$ )  
 8.41 (s, 1H, 2H); 7.70 (m, 1H, 7H); 7.49 – 6.86 (m, 13H,  $\text{H}_{\text{ar}}$ ); 7.17 (m, 2H, 4H, 6H); 5.96 (d,  $J = 5.7$  Hz, 1H, 1'H); 5.68 (d,  $J = 6.0$  Hz, 1H, 2'-OH); 5.32 (d,  $J = 5.4$  Hz, 1H, 3'-OH); 4.52 (m, 1H, 2'H); 4.25 (m, 1H, 3'H); 4.10 (m, 1H, 4'H); 3.76 (s, 6H,  $\text{OCH}_3$ ); 3.23 (m, 2H, 5'H)

$^{13}\text{C-NMR}$ :  $\delta$  [ppm] (67.9 MHz,  $\text{DMSO-}d_6$ )  
 158.10 (DMTr); 154.34 (C5); 144.78 (DMTr); 142.65 (C2); 135.88 (C6); 135.42 (DMTr); 135.34 (DMTr); 132.39 (C4); 129.75 (DMTr); 127.86 (DMTr); 127.73 (DMTr); 126.75 (DMTr); 123.33 (C8); 113.20 (DMTr); 108.38 (C7); 107.62 (C9); 89.18 (C1'); 85.72 (DMTr); 83.53 (C4'); 73.25 (C2'); 70.10 (C3'); 63.59 (C5'); 55.05 ( $\text{OCH}_3$ )

ESI(-):  $m/z$  569.4 ( $[\text{M-H}]^-$ );

**5'-O-(4,4'-Dimethoxytriphenylmethyl)-2'-O-tert.-butyldimethylsilyl-1'-deoxy-1'-(5-fluoro-3-N-benzimidazolyl)- $\beta$ -D-ribofuranose 95**



$\text{C}_{39}\text{H}_{45}\text{FN}_2\text{O}_6\text{Si}$

684.85 g/mol

1.8 g (3.15 mmol) 5'-O-(4,4'-Dimethoxytriphenylmethyl)-1'-deoxy-1'- $\beta$ -D-(5-fluoro-3-N-benzimidazolyl)-ribofuranose 93 were dissolved in 20 ml 1:1 of a mixture of THF/pyridine and with 650 mg (3.8 mmol)  $\text{AgNO}_3$  and 4.40 ml (4.40 mmol) 1 M *tert.*-butyldimethylsilylchloride-solution in THF were added. The reaction mixture was stirred for 20 hours at RT under argon. The reaction was stopped by adding 10ml of saturated water

NaHCO<sub>3</sub>-solution. Left AgCl was filtered over celite and the filtrate was extracted with methylenchloride three times. Combined organic phases were dried over MgSO<sub>4</sub> and evaporated to dryness. The crude product was co-evaporated with toluene twice. Further purification of product was done by HPLC (MN Nucleoprep 100-20 of Macherey-Nagel, n-hexan/dioxan 10:5). The product (*fast-Isomer*) was obtained as white foam.

Yield: 0.84 g (39 %)

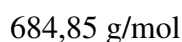
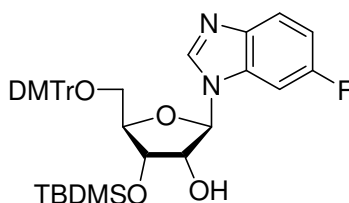
TLC: R<sub>f</sub> = 0.26 (n-hexan/ethyl acetate 4:1)

<sup>1</sup>H-NMR: δ [ppm] (400 MHz, DMSO-*d*<sub>6</sub>)  
8.40 (s, 1H, 2H); 7.68 (m, 1H, 7H); 7.54 (m, 1H, 6H); 7.41 – 6.83 (m, 14H, H<sub>ar</sub>, 4H); 5.94 (d, J = 5.36 Hz, 1H, 3'OH); 5.19 (d, J = 5.52 Hz, 1H, 1'H); 4.58 (dd, J=6.3 Hz, 1H, 2'H); 4.20 (m, 2H, 4'H, 3'H); 3.73 (s, 6H, OCH<sub>3</sub>); 3.30 (m, 2H, 5'H); 0.71 (s, 9H, SiC(CH<sub>3</sub>)<sub>3</sub>); -0.10 (s, 3H, SiCH<sub>3</sub>); -0.26 (s, 3H, SiCH<sub>3</sub>)

<sup>13</sup>C-NMR: δ [ppm] (67.9 MHz, DMSO-*d*<sub>6</sub>)  
158.50 (DMTr); 154.37 (C5); 144.67 (DMTr); 142.98 (C2); 136.63 (C6); 135.31 (DMTr); 135.14 (DMTr); 133.28 (C4); 129.62 (DMTr); 128.74 (DMTr); 127.60 (DMTr); 126.69 (DMTr); 125.15 (C8); 114.13 (DMTr); 108.36 (C7); 107.52 (C9); 89.17 (C1'); 85.95 (DMTr); 84.95 (C4'); 73.64 (C2'); 71.87 (C3'); 63.00 (C5'); 54.98 (OCH<sub>3</sub>); 25.67 (SiC(CH<sub>3</sub>)<sub>3</sub>); 17.90 (SiC(CH<sub>3</sub>)<sub>3</sub>); -4.59 (SiCH<sub>3</sub>); -5.21 (SiCH<sub>3</sub>)

ESI(+): m/z 685.8 ([M+H]<sup>+</sup>);

**5'-O-(4,4'-Dimethoxytriphenylmethyl)-3'-O-*tert.*-butyldimethylsilyl-1'-deoxy-1'-(5-fluoro-3-*N*-benzimidazolyl)- $\beta$ -D-ribofuranose 94**



5'-O-(4,4'-Dimethoxytriphenylmethyl)-3'-O-*tert.*-butyldimethylsilyl-1'-deoxy-1'-(5-fluoro-3-*N*-benzimidazolyl)- $\beta$ -D-ribofuranose 94 was obtained as a side product slow-*Isomer*) in the synthesis of 5'-O-(4,4'-Dimethoxytriphenylmethyl)-2'-O-*tert.*-butyldimethylsilyl-1'-deoxy-1'-(5-fluoro-3-*N*-benzimidazolyl)- $\beta$ -D-ribofuranose 95.

Yield: 0.80 g (37.0 %)

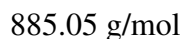
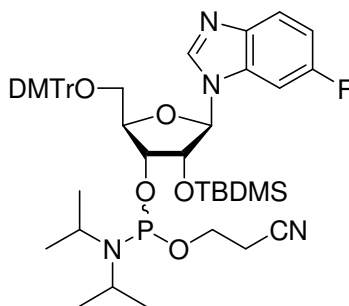
TLC:  $R_f = 0.26$  (*n*-Hexan/Ethylacetat 4:1)

$^1\text{H-NMR}$ :  $\delta$  [ppm] (400 MHz, DMSO- $d_6$ )  
 8.42 (s, 1H, 2H); 7.69 (dd, 1H, 7H); 7.56 (m, 1H, 6H); 7.38 – 6.82 (m, 14H,  $H_{ar}$ , 4H); 5.88 (d,  $J = 5.9$  Hz, 1H, 1'H); 5.49 (d,  $J = 6.5$  Hz, 1H, 2'-OH); 4.5 (m, 1H, 2'H); 4.35 (m, 1H, 3'H); 4.09 (m, 1H, 4'H); 3.72 (s, 6H, OCH<sub>3</sub>); 3.30 (m, 2H, 5'H); 0.82 (s, 9H, SiC(CH<sub>3</sub>)<sub>3</sub>); 0.06 (s, 3H, SiCH<sub>3</sub>); 0.005 (s, 3H, SiCH<sub>3</sub>)

$^{13}\text{C-NMR}$ :  $\delta$  [ppm] (67.9 MHz, DMSO- $d_6$ )  
 158.10 (DMTr); 154.27 (C5); 144.47 (DMTr); 142.78 (C2); 135.63 (C6); 135.31 (DMTr); 135.14 (DMTr); 132.28 (C4); 129.62 (DMTr); 127.74 (DMTr); 127.60 (DMTr); 126.69 (DMTr); 125.15 (C8); 113.13 (DMTr); 108.36 (C7); 107.52 (C9); 89.27 (C1'); 85.95 (DMTr); 83.95 (C4'); 72.64 (C2'); 71.87 (C3'); 63.00 (C5'); 54.98 (OCH<sub>3</sub>); -4.56 (SiCH<sub>3</sub>); -5.19 (SiCH<sub>3</sub>)

ESI(+):  $m/z$  685.5 ([M+H]<sup>+</sup>);

**3'-O-(2-Cyanethoxydiisopropylphosphin)-1'-deoxy-5'-O-(4,4'-dimethoxy-triphenylmethyl)-1'-(5-fluor-3-N-benzimidazolyl)-2'-O-tert.-butyldimethylsilyl- $\beta$ -D-ribofuranose 97**



200 mg (0.29 mmol) 5'-O-(4,4'-Dimethoxytriphenylmethyl)-2'-O-tert.-butyldimethylsilyl-1'-desoxy-1'-(5-fluor-3-N-benzimidazolyl)- $\beta$ -D-ribofuranose 95 were dissolved in 10 ml abs. acetonitrile and 380  $\mu\text{l}$  (2.9 mmol) *sym.* collidine and 12  $\mu\text{l}$  (0.15 mmol) 1-methylimidazole were added. The reaction mixture was cooled in an icebath to 0°C and 96  $\mu\text{l}$  (0.43 mmol) 2-cyanethyldiisopropylchlorphosphoramidit 96 were added. The reaction was stirred for 15min. at 0°C and 45 min. at RT. The reaction was stopped by adding 10ml of 0.01 M citric acid and extracted with methylenchloride three times. Combined organic phases were washed with 0.01 M citric acid twice, dried over  $\text{MgSO}_4$  and evaporated to dryness. Purification was done by FC with methylene chloride/methanol 99:1, as eluent. The product ( mixture of two diastereomers) was obtained as white foam.

Yield: 150 mg (58 %)

TLC:  $R_f = 0.34; 0.41$  ( $\text{CH}_2\text{Cl}_2/\text{MeOH}$  99:1)

$^1\text{H-NMR}$ :  $\delta$  [ppm] (400 MHz,  $\text{CDCl}_3$ )

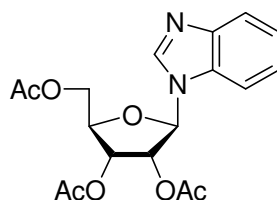
8.12, 8.08 (s, 2H, 2H); 7.49 – 6.81 (m, 32H,  $H_{ar}$ , 4H, 6H, 7H); 5.92, 5.84 (d, J = 5.9, J = 5.8 Hz, 2H, 1'H); 4.75 (m, 2H, 2'H); 4.40 (m, 2H, 3'H); 4.32 (m, 2H, 4'H); 3.80, 3.79 (s, 12H,  $\text{OCH}_3$ ); 3.48 (m, 4H, 5'H); 2.66 (m, 4H,  $\text{OCH}_2$ ),

1.20 (m, 12H, CH(CH<sub>3</sub>)<sub>2</sub>); 0.75 (s, 18H, SiC(CH<sub>3</sub>)<sub>3</sub>); -0.02 (s, 6H, SiCH<sub>3</sub>);  
-0.12 (s, 6H, SiCH<sub>3</sub>)

<sup>31</sup>P-NMR: δ [ppm] (162 MHz, CDCl<sub>3</sub>)  
154.22 and 151.92 (ratio 1 : 3.5)

ESI(+): m/z 885.8 ([M+H]<sup>+</sup>);

### 2',3',5'-Tri-*O*-acetyl-1'-deoxy-1'-*N*-benzimidazolyl-β-D-ribofuranose 77



C<sub>18</sub>H<sub>20</sub>N<sub>2</sub>O<sub>7</sub>

376.35 g/mol

5.2 g (44.0 mmol) benzimidazole were suspended in 80 ml abs. acetonitrile and 10.75 ml (44 mmol) *N,O*-Bis-(trimethylsilyl)-acetamide were added. The reaction mixture was refluxed for 15 min. After cooling to room temperature 7.0 g (22 mmol) 1,2,3,5-Tetra-*O*-acetyl-β-D-ribofuranose in 50 ml abs. acetonitrile and 5.0 ml (27.6 mmol) trimethylsilyltrifluorosulfonate (TMSOTf) were added. The reaction mixture was refluxed for 2,5 hours and cooled to room temperature. After cooling the reaction mixture was treated with 10 ml 5% NaHCO<sub>3</sub>-solution and extracted with methylene chloride three times. Combined organic phases were dried over MgSO<sub>4</sub> and evaporated to dryness. The product was purified by means of FC with methylene chloride/methanol 98:2. The product was obtained as white foam.

Yield: 4.57 g (55.3 %)

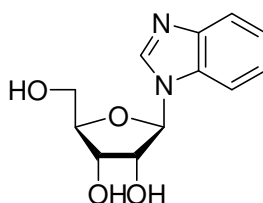
TLC: R<sub>f</sub> = 0.43 (CH<sub>2</sub>Cl<sub>2</sub>/MeOH 95:5)

<sup>1</sup>H-NMR: δ [ppm] (400 MHz, DMSO-*d*<sub>6</sub>)  
 8.49 (s, 1H, 2H); 7.73 (m, 2H, H<sub>ar</sub>); 7.29 (m, 2H, H<sub>ar</sub>); 6.32 (d, J = 6.4 Hz, 1H, 1'H); 5.68 (t, J = 6.3 Hz, 1H, 2'H); 5.43 (dd, J = 4.6 Hz, 1H, 3'H); 4.41 (m, 1H, 4'H); 4.37 (m, 2H, 5'H); 2.13 (s, 3H, CH<sub>3</sub>-acetyl); 2.08 (s, 3H, CH<sub>3</sub>-acetyl); 2.03 (s, 3H, CH<sub>3</sub>-acetyl)

<sup>13</sup>C-NMR: δ [ppm] (100.6 MHz, DMSO-*d*<sub>6</sub>)  
 169.55 (C=O); 169.06 (C=O); 168.76 (C=O); 143.36 (C2); 142.36 (C<sub>ar</sub>); 131.93 (C<sub>ar</sub>); 122.65 (C<sub>ar</sub>); 119.06 (C<sub>ar</sub>); 110.85 (C<sub>ar</sub>); 85.76 (C1'); 78.11 (C4'); 71.10 (C2'); 69.09 (C3'); 62.53 (C5'); 20.04 (CH<sub>3</sub>-acetyl); 19.90 (CH<sub>3</sub>-acetyl); 19.69 (CH<sub>3</sub>-acetyl)

ESI(+): m/z 377.2 ([M+H]<sup>+</sup>);

**1'-Deoxy-1'-N-benzimidazolyl-β-D-ribofuranose 40**



C<sub>12</sub>H<sub>14</sub>N<sub>2</sub>O<sub>4</sub>  
 250.24 g/mol

2.98 g (7.9 mmol) 2',3',5'-Tri-*O*-acetyl-1'-deoxy-1'-benzimidazolyl-β-D-ribofuranose 77 were dissolved in 25 ml of methanol and 175 μl of MeONa/MeOH ( 5.4 M, Fluka) were added at RT and the reaction was TLC controlled. After 60 min the reaction was complete neutralised with DOWEX 50, filtered and evaporated. The product was obtained as white foam and used without further purification.

Yield: 1.90 g (95.1 %)  
 TLC: R<sub>f</sub> = 0.53 (CH<sub>2</sub>Cl<sub>2</sub>/MeOH 4:1)

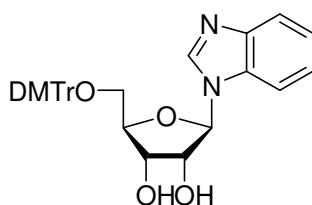


$^1\text{H-NMR}$ :  $\delta$  [ppm] (250 MHz,  $\text{DMSO-}d_6$ )  
 8.45 (s, 1H, 2H); 7.70 (m, 2H,  $\text{H}_{\text{ar}}$ ); 7.24 (m, 2H,  $\text{H}_{\text{ar}}$ ); 5.86 (d,  $J = 6.2$  Hz, 1H, 1'H); 5.46 (d,  $J = 6.5$  Hz, 1H, 2'-OH); 5.21 (d,  $J = 4.8$  Hz, 1H, 3'-OH); 5.10 (t,  $J = 5.2$  Hz, 1H, 5'-OH); 4.36 (q,  $J = 5.3$  Hz, 1H, 2'H); 4.12 (m, 1H, 3'H); 3.96 (q,  $J = 3.4$  Hz, 1H, 4'H); 3.63 (m, 2H, 5'H)

$^{13}\text{C-NMR}$ :  $\delta$  [ppm] (62.9 MHz,  $\text{DMSO-}d_6$ )  
 143.82 ( $\text{C}_2$ ); 142.42 ( $\text{C}_{\text{ar}}$ ); 132.98 ( $\text{C}_{\text{ar}}$ ); 122.62 ( $\text{C}_{\text{ar}}$ ); 122.02 ( $\text{C}_{\text{ar}}$ ); 119.54 ( $\text{C}_{\text{ar}}$ ); 111.54 ( $\text{C}_{\text{ar}}$ ); 88.64 ( $\text{C}1'$ ); 85.43 ( $\text{C}4'$ ); 73.58 ( $\text{C}2'$ ); 70.13 ( $\text{C}3'$ ); 61.26 ( $\text{C}5'$ )

ESI(+):  $m/z$  251.1 ( $[\text{M}+\text{H}]^+$ );

**5'-O-(4,4'-Dimethoxytriphenylmethyl) -1'-deoxy -1'-N-benzimidazolyl- $\beta$ -D-ribofuranose 120**



$\text{C}_{33}\text{H}_{32}\text{N}_2\text{O}_6$

552.59 g/mol

2.73 mg (10.9  $\mu\text{mol}$ ) 1'-Deoxy-1'-N-benzimidazolyl- $\beta$ -D-ribofuranose **40** were dissolved in 100 ml abs. pyridine and 5.17 g (15.4  $\mu\text{mol}$ ) 4,4'-dimethoxytriphenylmethylchloride were added. The reaction mixture was stirred under argon at RT for 4h. The reaction was stopped by adding of 10 ml of methanol and saturated water solution of  $\text{NaHCO}_3$ . It was extracted with methylene chloride three times; organic phases were collected and dried over  $\text{MgSO}_4$  and than evaporated to dryness. The product was co evaporated with toluol twice. Further

purification was done by FC with methylene chloride/methanol 95:5, as eluent. The product was obtained as yellow foam.

Yield: 4.43 g (73.5 %)

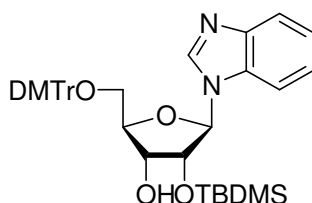
TLC:  $R_f = 0.68$  ( $\text{CH}_2\text{Cl}_2/\text{MeOH}$  9:1)

$^1\text{H-NMR}$ :  $\delta$  [ppm] (250 MHz,  $\text{DMSO-}d_6$ )  
8.35 (s, 1H, 2H); 7.68 (m, 2H,  $\text{H}_{\text{ar}}$ ); 7.38 – 6.81 (m, 15H,  $\text{H}_{\text{ar}}$ ); 5.91 (d,  $J = 5.5$  Hz, 1H, 1'H); 5.59 (d,  $J = 6.1$  Hz, 1H, 2'-OH); 5.27 (d,  $J = 5.4$  Hz, 1H, 3'-OH); 4.36 (q,  $J = 5.7$  Hz, 1H, 2'H); 4.19 (q,  $J = 5.2$  Hz, 1H, 3'H); 4.10 (q,  $J = 5.2$  Hz, 1H, 4'H); 3.73 (s, 6H,  $\text{OCH}_3$ ); 3.23 (m, 2H, 5'H)

$^{13}\text{C-NMR}$ :  $\delta$  [ppm] (62.9 MHz,  $\text{DMSO-}d_6$ )  
158.08 (DMTr); 144.78 (DMTr); 143.94 ( $\text{C}_2$ ); 142.24 ( $\text{C}_{\text{ar}}$ ); 135.42 (DMTr); 135.33 (DMTr); 132.84 ( $\text{C}_{\text{ar}}$ ); 129.77 (DMTr); 127.84 (DMTr); 127.71 (DMTr); 126.71 (DMTr); 122.57 ( $\text{C}_{\text{ar}}$ ); 122.13 ( $\text{C}_{\text{ar}}$ ); 119.65 ( $\text{C}_{\text{ar}}$ ); 113.19 (DMTr); 111.75 ( $\text{C}_{\text{ar}}$ ); 88.95 ( $\text{C}1'$ ); 85.68 (DMTr); 83.33 ( $\text{C}4'$ ); 73.07 ( $\text{C}2'$ ); 70.12 ( $\text{C}3'$ ); 63.70 ( $\text{C}5'$ ); 55.02 ( $\text{OCH}_3$ )

ESI (+):  $m/z$  553.4 ( $[\text{M}+\text{H}]^+$ );

**5'-O-(4,4'-Dimethoxytriphenylmethyl)-2'-O-*tert.*-butyldimethylsilyl-1'-deoxy-1'-N-benzimidazolyl- $\beta$ -D-ribofuranose 121**



$C_{39}H_{46}N_2O_6Si$

666.85 g/mol

0.95 g (1.7 mmol) 5'-O-(4,4'-Dimethoxytriphenylmethyl)-1'-deoxy-1'-N-benzimidazolyl-ribofuranose 120 were dissolved in 20 ml of a 1:1 mixture of THF/pyridine and with 380 mg (5.3 mmol)  $AgNO_3$  and 2.2 ml (2.2 mmol) 1 M *tert.*-Butyldimethylsilylchloride-solution in THF. The reaction mixture was stirred at RT under argon for 24 hours. Adding 10 ml of saturated water  $NaHCO_3$ -solution stopped the reaction. Left  $AgCl$  was filtered over celite and filtrate was extracted with methylene chloride three times. Combined organic phases were dried over  $MgSO_4$  and evaporated to dryness. The crude product was co-evaporated with toluene twice. Further purification of the product was done by FC using methylene chloride/isopropanol 98:2 as eluent. The product was obtained as white foam.

Yield: 310 mg (27.2 %)

TLC:  $R_f = 0.35$  ( $CH_2Cl_2/iPrOH$  98:2)

$^1H$ -NMR:  $\delta$  [ppm] (250 MHz,  $DMSO-d_6$ )

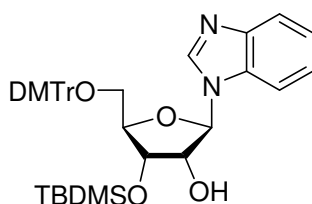
8.35 (s, 1H, 2H); 7.66 (m, 2H,  $H_{ar}$ ); 7.41 – 6.82 (m, 15H,  $H_{ar}$ ); 5.92 (d,  $J = 6.5$  Hz, 1H, 1'H); 5.19 (d,  $J = 5.5$  Hz, 1H, 3'-OH); 4.58 (t,  $J = 5.7$  Hz, 1H, 2'H); 4.18 (m, 1H, 3'H); 4.13 (m, 1H, 4'H); 3.71 (s, 6H,  $OCH_3$ ); 3.29 (m, 2H, 5'H); 0.68 (s, 9H,  $SiC(CH_3)_3$ ); -0.15 ( $SiCH_3$ ); -0.31 ( $SiCH_3$ )

$^{13}C$ -NMR:  $\delta$  [ppm] (100.6 MHz,  $DMSO-d_6$ )

158.10 (DMTr); 144.72 (DMTr); 143.95 (C2); 142.59 (C<sub>ar</sub>); 135.21 (DMTr); 135.11 (DMTr); 132.40 (C<sub>ar</sub>); 129.78 (DMTr); 129.72 (DMTr); 127.79 (DMTr); 127.61 (DMTr); 126.73 (DMTr); 122.37 (C<sub>ar</sub>); 122.12 (C<sub>ar</sub>); 119.65 (C<sub>ar</sub>); 113.16 (DMTr); 111.92 (C<sub>ar</sub>); 88.61 (C1'); 85.82 (DMTr); 83.99 (C4'); 74.51 (C2'); 69.94 (C3'); 63.50 (C5'); 55.00 (OCH<sub>3</sub>); 25.43 (SiC(CH<sub>3</sub>)<sub>3</sub>); 17.69 (SiC(CH<sub>3</sub>)<sub>3</sub>); -5.12 (SiCH<sub>3</sub>); -5.61 (SiCH<sub>3</sub>)

ESI (+): m/z 667.6 ([M+H]<sup>+</sup>);

**5'-O-(4,4'-Dimethoxytriphenylmethyl)-3'-O-*tert.*-butyldimethylsilyl-1'-deoxy-1'-N-benzimidazolyl-β-D-ribofuranose 122**



C<sub>39</sub>H<sub>46</sub>N<sub>2</sub>O<sub>6</sub>Si

666.85 g/mol

5'-O-(4,4'-Dimethoxytriphenylmethyl)-3'-O-*tert.*-butyldimethylsilyl-1'-deoxy-1'-N-benzimidazolyl-β-D ribofuranose 123 was obtained as a side product while preparing 5'-O-(4,4'-Dimethoxytriphenylmethyl)-2'-O-*tert.*-butyldimethylsilyl-1'-deoxy-1'-N-benzimidazolyl-β-D-ribofuranose 120.

Yield: 410 mg (3.0 %)

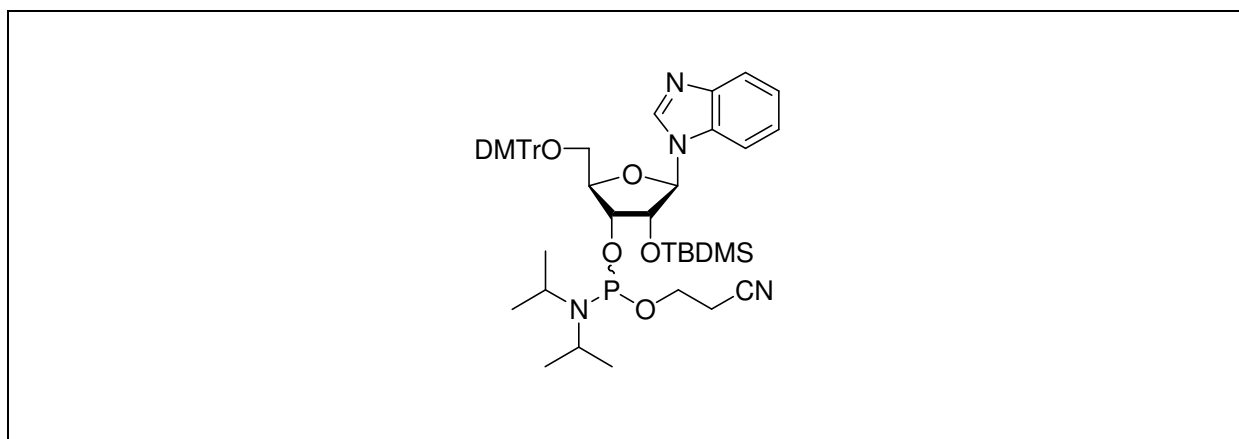
TLC: R<sub>f</sub> = 0.32 (CH<sub>2</sub>Cl<sub>2</sub>/*i*PrOH 98:2)

<sup>1</sup>H-NMR: δ [ppm] (250 MHz, DMSO-*d*<sub>6</sub>)

8.40 (s, 1H, 2H); 7.69 (m, 2H, H<sub>ar</sub>); 7.40 – 6.82 (m, 15H, H<sub>ar</sub>); 5.90 (d, J = 6.1 Hz, 1H, 1'H); 5.50 (d, J = 6.5 Hz, 1H, 2'-OH); 4.52 (q, J = 5.8 Hz, 1H, 2'H); 4.35 (m, 1H, 3'H); 4.07 (m, 1H, 4'H); 3.72 (s, 6H, OCH<sub>3</sub>); 3.24 (m, 2H, 5'H); 0.82 (s, 9H, SiC(CH<sub>3</sub>)<sub>3</sub>); 0.07 (SiCH<sub>3</sub>); 0.02 (SiCH<sub>3</sub>)

$^{13}\text{C}$ -NMR:  $\delta$  [ppm] (100.6 MHz, DMSO- $d_6$ )  
 158.11 (DMTr); 144.58 (DMTr); 143.99 (C<sub>2</sub>); 142.52 (C<sub>ar</sub>); 135.26 (DMTr);  
 135.17 (DMTr); 132.64 (C<sub>ar</sub>); 129.69 (DMTr); 127.81 (DMTr); 127.63  
 (DMTr); 126.74 (DMTr); 122.47 (C<sub>ar</sub>); 122.11 (C<sub>ar</sub>); 119.64 (C<sub>ar</sub>); 113.16  
 (DMTr); 111.85 (C<sub>ar</sub>); 88.87 (C1'); 85.87 (DMTr); 83.82 (C4'); 72.47 (C2');  
 71.92 (C3'); 63.14 (C5'); 55.03 (OCH<sub>3</sub>); 25.73 (SiC(CH<sub>3</sub>)<sub>3</sub>); 17.99  
 (SiC(CH<sub>3</sub>)<sub>3</sub>); -4.50 (SiCH<sub>3</sub>); -5.14 (SiCH<sub>3</sub>)  
 ESI (+): m/z 667.5 ([M+H]<sup>+</sup>);

**3'-O- (2-Cyanethoxydiisopropylphosphin) -1'-deoxy-5'-O- (4,4'-dimethoxy-  
 triphenylmethyl) -1'-N-benzimidazolyl-2'-O- (tert.-butyldimethylsilyl) - $\beta$ -D-  
 ribofuranose 123**



$\text{C}_{48}\text{H}_{63}\text{N}_4\text{O}_7\text{PSi}$

867.05 g/mol

300 mg (0.44 mmol) 5'-O-(4,4'-Dimethoxytriphenylmethyl)-2'-O-tert.-butyldimethylsilyl-1'-deoxy-1'-N-benzimidazolyl- $\beta$ -D-ribofuranose 121 were dissolved in 16 ml abs. acetonitril and 570  $\mu\text{l}$  (4.4 mmol) *sym.* collidine and 18  $\mu\text{l}$  (0.22 mmol) 1-methylimidazole were added. The reaction mixture were cooled in an icebath to 0°C and 145  $\mu\text{l}$  (0.64 mmol) 2-cyanethyldiisopropylchlorphosphoramidite 96 were added. The reaction was stirred for 15min. at 0°C and 45 min. at RT. The reaction was stopped by adding of 10 ml of 0.01 M citric acid and extracted with methylene chloride three times. Combined organic phases were washed twice with 0.01 M citric acid, dried over MgSO<sub>4</sub> and evaporated to dryness.

Purification was done by FC with methylene chloride/methanol 99:1 as eluent. The product (mixture of two diastereomers) was obtained as white foam.

Yield: 210 mg (53.8 %)

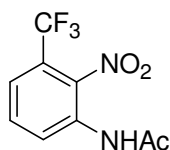
TLC:  $R_f = 0.09$  (*n*-hexan: ethyl acetate 4:1)

$^1\text{H-NMR}$ :  $\delta$  [ppm] (400 MHz,  $\text{CDCl}_3$ )  
 8.12, 8.08 (s, 2H, 2H); 7.79 (d,  $J = 8.0$  Hz, 2H,  $\text{H}_{\text{ar}}$ ); 7.63 (d,  $J = 8.1$  Hz, 2H,  $\text{H}_{\text{ar}}$ ); 7.48 – 6.80 (m, 30H,  $\text{H}_{\text{ar}}$ ); 5.92, 5.86 (d,  $J = 7.5$  Hz,  $J = 7.0$  Hz, 2H, 1'H); 4.76 (m, 2H, 2'H); 4.31 (m, 2H, 3'H); 3.95 (m, 2H, 4'H); 3.79, 3.78 (s, 12H,  $\text{OCH}_3$ ); 3.56 (m, 8H, 5'H,  $\text{CH}_2\text{CN}$ ); 2.68 (m, 4H,  $\text{OCH}_2$ ), 1.20 (m, 12H,  $\text{CH}(\text{CH}_3)_2$ ); 0.81, 0.74 (s, 18H,  $\text{SiC}(\text{CH}_3)_3$ ); -0.14, -0.37, -0.40, -0.49 (s, 12H,  $\text{SiCH}_3$ )

$^{31}\text{P-NMR}$ :  $\delta$  [ppm] (162 MHz,  $\text{CDCl}_3$ )  
 150.58 and 149.99 (ratio 1 : 1.6)

ESI (+):  $m/z$  867.7 ( $[\text{M}+\text{H}]^+$ );

### **2-Nitro-3-trifluoromethyl acetanilide 56**

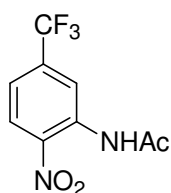


$\text{C}_9\text{H}_7\text{N}_2\text{O}_3\text{F}_3$   
 $248.01\text{g mol}^{-1}$

3-Trifluoromethyl acetanilide (10g, 50mmol) was added over 10 min. (in 1g portions) to 12.5g of mixture of equal parts of  $\text{HNO}_3$  ( $d=1.52$ ) and  $(\text{CH}_3\text{COO})_2\text{O}$  cooled to  $0^\circ\text{C}$  (4.2ml  $\text{HNO}_3$  and 5.8ml  $(\text{CH}_3\text{COO})_2\text{O}$ ). The reaction was continued for 15min. at  $0^\circ\text{C}$  and continued 4h at room temperature. The white precipitate (the wanted product) was filtered and washed with 5 ml of  $(\text{CH}_3\text{COO})_2\text{O}$ .

Yield: 2.9g (24%)  
 TLC: Rf= 0.30 (CH<sub>2</sub>Cl<sub>2</sub>/MeOH, 98:2)  
<sup>1</sup>H NMR: δ [ppm] (250MHz, DMSO- *d*<sub>6</sub>)  
 10.19(s, 1H, N-H), 7.94-7.82 (m, 3H, aromH), 2.05 (s, 3H, CH<sub>3</sub>);  
<sup>13</sup>C NMR: δ [ppm] (62.9MHz, DMSO- *d*<sub>6</sub>)  
 168.73(C=O), 141.54, 131.96, 131.53, 123.72, 123.64, 121.28 (*arom C*), 112.2  
 (CF<sub>3</sub>), 20.1 (CH<sub>3</sub>);  
 ESI(+): m/z 266.0 ([M+NH<sub>4</sub>]<sup>+</sup>);

### 6-Nitro-3-trifluoromethyl acetanilide **57**



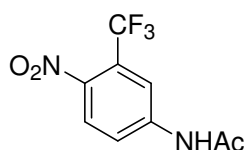
C<sub>9</sub>H<sub>7</sub>N<sub>2</sub>O<sub>3</sub>F<sub>3</sub>  
 248.01gmol<sup>-1</sup>

6-Nitro-3-trifluoromethyl acetanilide **57** was obtained while synthesizing 2-nitro-3-trifluoromethyl acetanilide **56** as a side product. It stays in solution after filtering **56**. Then the solution is extracted with methylene chloride and **57** is obtained by FC (methylene chloride/methanol, 98:2).

Yield: 4.2 g (35%)  
 TLC: Rf= 0.44 (CH<sub>2</sub>Cl<sub>2</sub>/MeOH, 98:2)  
<sup>1</sup>H NMR: δ [ppm] (250MHz, DMSO- *d*<sub>6</sub>)  
 10.50(s, 1H, N-H), 8.10 (d, J=7,2 Hz, 1H, H5), 8.00(s, 1H, H2), 7.90 (d, J=7.32  
 Hz, 1H, H6), 2.05 (s, 3H, CH<sub>3</sub>);

$^{13}\text{C}$  NMR:  $\delta$  [ppm] (62.9MHz, DMSO-  $d_6$ )  
169.73(C=O), 141.64, 131.98, 131.53, 125.72, 123.64, 121.28 (*arom* C), 112.2  
(CF<sub>3</sub>), 20.1 (CH<sub>3</sub>);  
ESI(+): m/z 266.2 ([M+NH<sub>4</sub>]<sup>+</sup>);

### 4-Nitro-3-trifluoromethyl acetanilide **58**



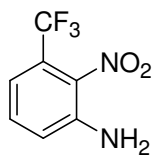
C<sub>9</sub>H<sub>7</sub>N<sub>2</sub>O<sub>3</sub>F<sub>3</sub>  
248.01 gmol<sup>-1</sup>

4-nitro-3-trifluoromethyl acetanilide **58** was obtained while synthesizing 2-nitro-3-trifluoromethyl acetanilide **56** as a side product. It stays in solution after filtering **56**. Then the solution is extracted with methylene chloride and **58** is obtained by FC (methylene chloride/methanol, 98:2).

Yield: 1.2 g (10%)  
TLC: R<sub>f</sub>= 0.68 (CH<sub>2</sub>Cl<sub>2</sub>/MeOH, 98:2)  
 $^1\text{H}$  NMR:  $\delta$  [ppm] (250MHz, DMSO-  $d_6$ )  
10.80(s, 1H, N-H), 8.10 (s, 1H, 2H), 8.00 (d, J=7.8Hz, 1H, 5H), 7.92 (d, J=7.8  
Hz, 1H, 6H), 1.95 (s, 3H, CH<sub>3</sub>);  
 $^{13}\text{C}$  NMR:  $\delta$  [ppm] (62.9MHz, DMSO-  $d_6$ )  
168.73(C=O), 141.54, 131.96, 131.53, 123.72, 123.64, 121.28 (*arom* C), 112.2  
(CF<sub>3</sub>), 20.1 (CH<sub>3</sub>);  
ESI(+): m/z 266.0 ([M+NH<sub>4</sub>]<sup>+</sup>);



## 2-Nitro-3-trifluoromethyl-aniline 59



$C_7H_5N_2O_2F_3$

206.0 g/mol

The solution of **56** (2g, 8.1mmol) in 25 ml of 0.1 M NaOH was refluxed for 90 min (TLC control). The reaction was cooled to room temperature, extracted with methylene chloride, the organic phase was dried over  $MgSO_4$  and evaporated. The product was obtained as yellow crystals.

Yield: 1.40g (84%)

TLC :  $R_f = 0.63$  ( $CH_2Cl_2/MeOH$ , 99/1)

$^1H$  NMR:  $\delta$  [ppm] (250MHz,  $CDCl_3$ ):

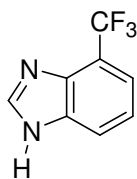
7.37 (m, 1H, 5H); 7.11(m, 2H, 4H, 6H); 5.02 (s, 2H,  $NH_2$ );

$^{13}C$  NMR:  $\delta$  [ppm] (62,9MHz,  $CDCl_3$ ):

145.1, 136.3, 132.3, 125.1, 120.1, 117.2 (arom C), 111.8( $CF_3$ );

ESI(-): m/z 205.6 ( $[M-H]^-$ );

## 4-Trifluoromethyl benzoimidazole 61



$C_8H_5N_2F_3$

186 g/mol

**59** (1.4g, 6,8mmol) was dissolved in abs. ethanol (50ml), 150mg  $PtO_2$  (0,65mmol) were added and reaction was performed in  $H_2$  atmosphere for 2h (TLC control,  $CH_2Cl_2/MeOH$ , 99/1,  $R_f=0,5$ ). The reaction mixture was then filtered over cellite and filtrate was evaporated. The crude product was dissolved in 90%  $HCOOH$  (100ml) and heated under reflux for 3h.  $HCOOH$  was evaporated to obtain crude product, which was purified by FC ( $CH_2Cl_2/MeOH$ , 9:1).

Yield: 1.2g(94%)

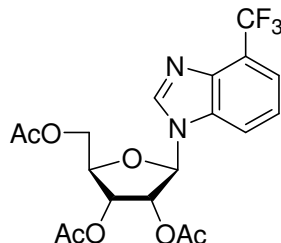
TLC:  $R_f= 0.41$  ( $CH_2Cl_2/MeOH$ , 9/1)

$^1H$  NMR:  $\delta$  [ppm] (250MHz,  $DMSO-d_6$ )  
 8.40 (d, 1H,  $J=3.83Hz$ , 7H); 7.90 (s, 1H, N-H); 7.54 (d, 1H,  $J=4.68Hz$ , 5H);  
 7.36 (m, 1H, 6H);

$^{13}C$  NMR:  $\delta$  [ppm] (62.9MHz,  $DMSO-d_6$ ):  
 163.62, 145.54, 126.00, 123.30, 121.98, 119.60, 119.20 (arom C),  
 114.10( $CF_3$ );

ESI(-):  $m/z$  186.7 ( $[M+H]^+$ );

**2',3,5'-Tri-O-acetyl-1'-deoxy-1'-(4-trifluoromethyl-1-N-benzimidazole-1-yl)-β-D-ribofuranose 71**



$C_{19}H_{19}F_3N_2O_7$

444.33 g/mol

To a suspension of **61** (1.2 g, 6.4 mmol) in acetonitrile (50 ml) *N,O*-bis(trimethylsilyl)acetamide (2.40 ml, 9.90 mmol) was added and heated under reflux for 15 min. After the mixture was cooled to room temperature, 1,2,3,5-Tetra-O-acetyl-β-D-ribofuranose (2.1g, 6.55mmol) in acetonitrile (20ml) and trimethylsilyl trifluoromethanesulfonate (1.5ml, 8.16mmol) were added and heated under reflux for 2.5h. The reaction mixture was after cooling to room temperature treated with 5%  $NaHCO_3$  solution and extracted with methylene chloride. The organic phase was dried (over  $MgSO_4$ ) and evaporated and the residue purified by means of preparative HPLC (*MN Nucleoprep 100-20* from *Macherey-Nagel*, n-hexan: ethyl acetate, 10:25). The product was obtained as *faster* migrating isomer, as white foam.

Yield: 2.0g (70%)

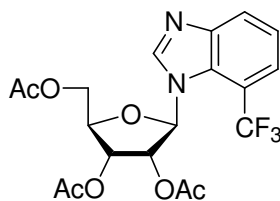
TLC:  $R_f = 0.40$  ( $CH_2Cl_2/MeOH$ , 95:5);

$^1H$  NMR:  $\delta$  [ppm] (400MHz,  $DMSO-d_6$ )  
 8.69 (s, 1H, 2H); 8.10 (d,  $J=8.2Hz$ , 1H, 5H); 7.64 (d,  $J=7.56Hz$ , 1H, 7H); 7.49 (m, 1H, 6H); 6.42 (d,  $J=6.08Hz$ , 1H, 1H'); 5.70 (t,  $J=6.22Hz$ , 1H, 2H'); 5.05 (m, 1H, 3H'); 4.39 (m, 1H, 4H'); 4.20 (m, 2H, 5H'); 2.11 (s, 3H,  $CH_3$ ); 2.08 (s, 3H,  $CH_3$ ); 2.04 (s, 3H,  $CH_3$ );

$^{13}\text{C}$  NMR:  $\delta$  [ppm] (100.6 MHz, DMSO-  $d_6$ )  
 171.5, 169.08, 169.00 (C=O); 144.36 (C2); 142.40, 133.90, 122.70, 120.25,  
 120.20, 120.18 (*arom* C); 114.5 (CF<sub>3</sub>); 86.71 (C1'); 78.21 (C4'); 71.30 (C2');  
 69.18 (C3'); 62.53 (C5'); 20.10, 19.91, 19.58 (CH<sub>3</sub>);

ESI(+):  $m/z$  445.4 ([M+H]<sup>+</sup>);

**2',3',5'-Tri-*O*-acetyl-1'-deoxy-1'-(4-trifluoromethyl-3-*N*-benzoimidazole-1-yl)- $\beta$ -D-ribofuranose 72**



$\text{C}_{19}\text{H}_{19}\text{F}_3\text{N}_2\text{O}_7$

444.33 g/mol

2',3',5'-Tri-*O*-acetyl-1'-deoxy-1'-(4-trifluoromethyl-3-*N*-benzoimidazole-1-yl)- $\beta$ -D-ribofuranose 72 was obtained in the same procedure as 71 but as *slower* migrating isomer during preparative HPLC (*MN Nucleoprep 100-20* from *Macherey-Nagel*, n-hexan: ethyl acetate, 10:25) separation. The product was obtained as white foam.

Yield: 0.77 g (27%)

TLC:  $R_f=0.40$  (CH<sub>2</sub>Cl<sub>2</sub>/MeOH, 95:5)

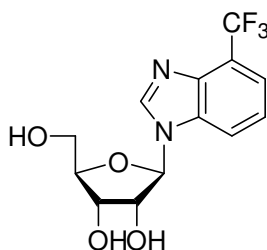
$^1\text{H}$  NMR:  $\delta$  [ppm] (400MHz, DMSO-  $d_6$ )  
 8.67 (s, 1H, 2H); 7.84 (d,  $J=8.3\text{Hz}$ , 1H, 7H); 7.62 (d,  $J=8.20\text{Hz}$ , 1H, 5H); 7.50  
 (m, 1H, 6H); 6.38 (d,  $J=6.10\text{Hz}$ , 1H, 1H'); 5.70 (t,  $J=6.30\text{Hz}$ , 1H, 2H'); 5.10  
 (m, 1H, 3H'); 4.42 (m, 1H, 4H'); 4.18 (m, 2H, 5H'); 2.09 (s, 3H, CH<sub>3</sub>); 2.07 (s,  
 3H, CH<sub>3</sub>); 2.06 (s, 3H, CH<sub>3</sub>);

$^{13}\text{C}$  NMR:  $\delta$  [ppm] (100.6 MHz, DMSO-  $d_6$ )  
 170.5, 169.10, 169.00 (C=O); 145.10 (C2); 142.40, 134.00, 122.70, 120.30,  
 120.20, 120.16 (*arom* C); 113.5 (CF<sub>3</sub>); 87.00 (C1'); 78.41 (C4'); 71.10 (C2');  
 69.20 (C3'); 62.50 (C5'); 20.10, 19.90, 19.70 (CH<sub>3</sub>);

ESI(+):  $m/z$  445.4 ([M+H]<sup>+</sup>);

**1'-Deoxy-1'-(4-trifluoromethyl-1-N-benzoimidazole-1-yl)- $\beta$ -D-ribofuranose**

**33**



$\text{C}_{13}\text{H}_{13}\text{F}_3\text{N}_2\text{O}_4$

318.23 g/mol

2',3,5'-Tri-*O*-acetyl-1'-deoxy-1'-(4-trifluoromethyl-1-*N*-benzoimidazole-1-yl)- $\beta$ -D-ribofuranose **71** (1g, 2.25mmol) was dissolved in methanol (25ml) and 185 $\mu$ l of MeONa/MeOH (5.4M, Fluka) were added at room temperature and the reaction was TLC controlled. The reaction was complete after 60 min. and neutralised with DOWEX 50, filtered and evaporated.

The product was obtained as white foam.

Yield: 0.66g (92%) ;

TLC:  $R_f$ =0.28 (CH<sub>2</sub>Cl<sub>2</sub>/MeOH, 9:1):

$^1\text{H}$  NMR:  $\delta$  [ppm] (400MHz, DMSO-  $d_6$ ):  
 8.64 (s, 1H, 2H); 8.11 (d, J=8.20 Hz, 1H, 7H); 7.60 (d, J=7.56Hz, 1H, 5H);  
 7.42 (m, 1H, 6H); 5.95 (d, J=6.28Hz, 1H, 1H'); 5.51 (d, J=6.44Hz, 1H, 2'OH);

5.26 (d, J=4.68Hz, 1H, 3OH'); 5.15 (t, J=5.12Hz, 1H, 5OH'); 4.38 (q, J= 5.84 Hz, 1H, 2H'); 4.16 (m, 1H, 3H'); 4.01 (m, 1H, 4H'); 3.66 (m, 2H, 5H');

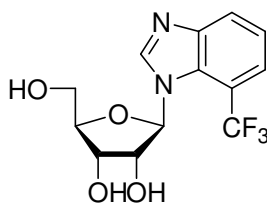
<sup>13</sup>C NMR : δ [ppm] (100.6 MHz, DMSO- *d*<sub>6</sub>):  
143.10 (C2); 136.05, 130.10, 128.10, 125.10, 125.00, 124.10 (*arom C*); 114.10 (CF<sub>3</sub>); 89.00 (C1'); 86.10 (C4'); 74.10 (C2'); 70.00 ( C3'); 62.10 (C5');

<sup>19</sup>F-NMR: δ [ppm] (254,2 MHz, DMSO-*d*<sub>6</sub>)  
-59.45 (s, 3F, CF<sub>3</sub>)

ESI(-): m/z 317.30 ([M-H]<sup>-</sup>);

### 1'-Deoxy-1'-(4-trifluoromethyl-3-*N*-benzimidazole-1-yl)-β-D-ribofuranose

**124**



C<sub>13</sub>H<sub>13</sub>F<sub>3</sub>N<sub>2</sub>O<sub>4</sub>

318.23 g/mol

1'-deoxy-1'-(4-trifluoromethyl-3-*N*-benzimidazole-1-yl)-β-D-ribofuranose **72** (0.5g, 1.12mmol) was dissolved in methanol (25ml) and 185μl of MeONa/ MeOH (5.4M, Fluka) were added at room temperature and the reaction was TLC controlled. The reaction was complete after 60 min. and than neutralized with DOWEX 50, filtered and evaporated. The product was obtained as white foam.

Yield: 0.33g (93%);

TLC: R<sub>f</sub>=0.28 (CH<sub>2</sub>Cl<sub>2</sub>/MeOH, 9:1);

<sup>1</sup>H NMR : δ [ppm] (400MHz, DMSO- *d*<sub>6</sub>)  
8.25 (s, 1H, 2H); 7.80 (d, J=8.00 Hz, 1H, 7H); 7.50 (d, J=7.56Hz,1H, 5H); 7.44 (m, 1H, 6H); 6.00 (d, J=6.30Hz, 1H, 1H'); 5.50 (d, J=6.50Hz, 1H, 2'OH); 5.28

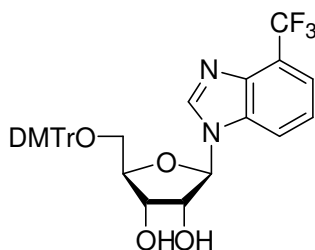
(d, J=4.70Hz, 1H, 3OH'); 5.20 (t, J=5.12Hz, 1H, 5OH'); 4.32 (q, J= 5.86 Hz, 1H, 2H'); 4.10 (m, 1H, 3H'); 4.00 (m, 1H, 4H'); 3.64 (m, 2H, 5H');

<sup>13</sup>C NMR: δ [ppm] (100.6 MHz, DMSO- *d*<sub>6</sub>)  
142.10 (C2); 136.10, 130.10, 128.10, 125.20, 125.05, 124.10 (*arom* C); 114.20 (CF<sub>3</sub>); 89.00 (C1'); 86.20 (C4'); 74.20 (C2'); 70.00 (C3'); 62.10 (C5');

<sup>19</sup>F-NMR: δ [ppm] (254.2 MHz, DMSO-*d*<sub>6</sub>)  
-59.35 (s, 3F, CF<sub>3</sub>)

ESI(-): m/z 316.90 ([M-H]<sup>-</sup>);

**1'-Deoxy-5'-O-(4,4'-dimethoxytriphenylmethyl)-1'-(4-trifluoro-1-N-benzimidazolyl)-β-D-ribofuranose 125**



C<sub>34</sub>H<sub>31</sub>F<sub>3</sub>N<sub>2</sub>O<sub>6</sub>

620.63 g/mol

380 mg (1.2 mmol) 1'-Deoxy-1'-(4-trifluorobenzimidazolyl)-β-D-ribofuranose 33 were dissolved in 10 ml abs. pyridine and 0.25 ml (1.8 mmol) triethylamine and 0.45 g (1.30 mmol) 4,4'-dimethoxytriphenylmethylchloride were added. The reaction mixture was stirred under argon at RT for 20h. The reaction was stopped by adding 3ml of methanol and saturated water solution of NaHCO<sub>3</sub>. It was extracted with methylene chloride three times, the organic phases were collected and dried over. MgSO<sub>4</sub> and than evaporated to dryness. The product was twice co-evaporated with toluoene. Further purification was done by FC with methylenechloride/methanol 95:5, as eluent. The product was obtained as yellow foam.

Yield: 500 mg (68%)

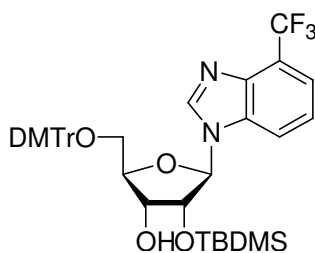
TLC: R<sub>f</sub>=0.18 (CH<sub>2</sub>Cl<sub>2</sub>/CH<sub>3</sub>OH, 95:5)

<sup>1</sup>H NMR: δ [ppm] (250 MHz, DMSO- *d*<sub>6</sub>)  
 8.53 (s, 1H, 2H); 8.05 (d, J=8,2Hz, 1H, 5H); 7. (d, 1H, J=5.45 Hz, 6H); 7.60-6.81(m, 15H, Har, 6H, 7H); 6.01 (d, J=5,44 Hz, 1H, 1H'); 5.68 (d, J=6.00Hz, 1H, 2'OH); 5.30 (d, J=5.44Hz, 1H, 3OH'); 4.52 (m, 1H, 2H'); 4.23(m, 1H, 3H'); 4.23(m, 1H, 3H'); 4.13 (m, 1H, 4H'); 3.66(s, 6H, 2OCH<sub>3</sub>); 3.35 (m, 2H, 5H');

<sup>13</sup>C NMR : δ [ppm] (100.6 MHz, DMSO- *d*<sub>6</sub>)  
 158.10 (DMTr); 144.60 (DMTr); 143.10(C2); 141.10(C5); 135.80(C6);  
 135.40(DMTr); 135.30(DMTr); 132.30(C4); 130.85(DMTr); 128.00(DMTr);  
 127.80(DMTr); 127.10(DMTr); 123.30(C8); 114.310(CF<sub>3</sub>); 113.20(DMTr);  
 109.7(C7); 107.60(C9); 89.60(C1'); 85.80(DMTr); 83.50(C4'); 73.20(C2');  
 70.10(C3'); 63.70(C5'); 55.00(OCH<sub>3</sub>);

ESI(-): m/z 619.5 ([M-H]);

**5'-O-(4,4'-Dimethoxytriphenylmethyl)-2'-O-*tert.*-butyldimethylsilyl-1'-deoxy-1'-(4-trifluoromethyl-1-*N*-benzimidazolyl)-β-D-ribofuranose 126**



C<sub>40</sub>H<sub>42</sub>F<sub>3</sub>N<sub>2</sub>O<sub>6</sub>Si

734.93 g/mol

500 mg (0.82 mmol) 5'-O-(4,4'-Dimethoxytriphenylmethyl)-1'-deoxy-1'-β-D-(4-trifluoromethyl-1-*N*-benzimidazolyl)-ribofuranose 125 were dissolved in 20 ml of 1:1 mixture of THF/pyridine and 180 mg (1.06 mmol) AgNO<sub>3</sub> and 1.2 ml (6.2 mmol) 1 M *tert.*-butyldimethylsilylchloride-solution in THF were added. The reaction mixture was stirred for



20 hours at RT under argon. The reaction was stopped by adding 10ml of saturated water NaHCO<sub>3</sub>-solution. Left AgCl was filtered over celite and the filtrate was extracted with methylenechloride three times. The combined organic phases were dried over MgSO<sub>4</sub> and evaporated to dryness. The crude product was co-evaporated with toluol twice. Further purification of the product was done by. HPLC (MN Nucleoprep 100-20 of Macherey-Nagel, *n*-hexan/ethylacetate 10:3.5]+30% methylenechloride). The product (*slow-Isomer*) was obtained as white foam.

Yield: 216 mg (36%)

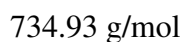
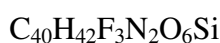
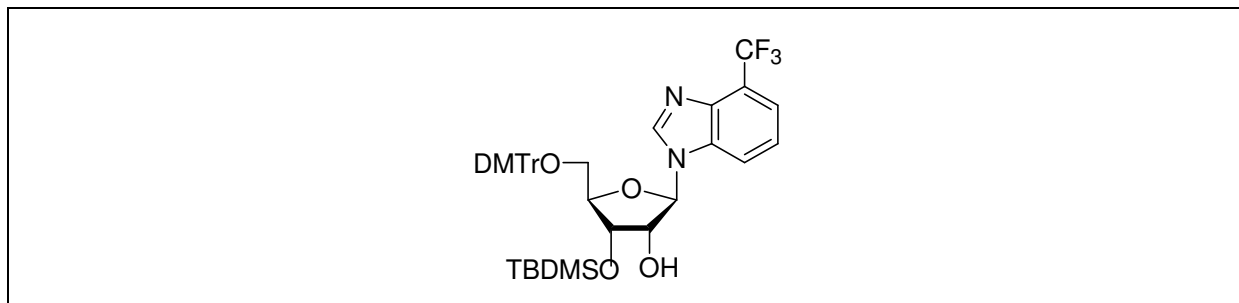
TLC: R<sub>f</sub>=0.48 (*n*-hexane/ethyl acetate, 4:1)

<sup>1</sup>H NMR: δ [ppm] (400 Hz, DMSO- *d*<sub>6</sub>)  
8.31 (s, 1H, 2H); 7.94 (d, J=8.2Hz, 1H, 5H); 7.59-6.80(m, 15H, Har, 6H, 7H);  
5.89 (d, J=4.96Hz, 1H, 1H'); 5.68(d, J=6.0Hz, 1H, 2'OH); 4.30(m, 2H, 2H',  
3H'); 4.35 ( m, 1H, 3H'); 4.11 (m, 1H, 4H'); 3.68 (s, 6H, 2OCH<sub>3</sub>); 3.50(m, 2H,  
5'CH<sub>2</sub>); 0.91( s, 9H, SiC(CH<sub>3</sub>)<sub>3</sub>); 0.09 (s, 3H, SiCH<sub>3</sub>); 0.00( s, 3H, SiCH<sub>3</sub>);

<sup>13</sup>C NMR: δ [ppm] (100.6 MHz, DMSO- *d*<sub>6</sub>)  
158.20 (DMTr); 144.90 (DMTr); 144.10(C2); 141.10(C5); 135.80(C6);  
135.70(DMTr); 135.30(DMTr); 132.40(C4); 130.75(DMTr); 128.10(DMTr);  
127.70(DMTr); 127.00(DMTr); 123.30(C8); 114.10(CF<sub>3</sub>); 113.20(DMTr);  
108.0(C7); 107.75(C9); 89.15(C1'); 85.72(DMTr); 83.50(C4'); 73.25(C2');  
70.20(C3'); 63.60(C5'); 55.05(OCH<sub>3</sub>); 25,60(SiC(CH<sub>3</sub>)<sub>3</sub>), -5,00(SiCH<sub>3</sub>), -  
5,30(SiCH<sub>3</sub>);

ESI(+): m/z 736.1 ([M+H]<sup>+</sup>);

**5'-O-(4,4'-Dimethoxytriphenylmethyl)-3'-O-*tert.*-butyldimethylsilyl-1'-deoxy-1'-(4-trifluoromethyl-1-*N*-benzimidazolyl)- $\beta$ -D-ribofuranose 127**



5'-O-(4,4'-Dimethoxytriphenylmethyl)-3'-O-*tert.*-butyldimethylsilyl-1'-deoxy-1'-(4-trifluoromethyl-1-*N*-benzimidazolyl)- $\beta$ -D-ribofuranose 127 was obtained as a side product (*fast-Isomer*) in the synthesis of 5'-O-(4,4'-Dimethoxytriphenylmethyl)-2'-O-*tert.*-butyldimethylsilyl-1'-deoxy-1'-(4-trifluoromethyl-1-*N*-benzimidazolyl)- $\beta$ -D-ribofuranose 126.

Yield: 198 mg (33%)

TLC:  $R_f=0.48$  (n-hexane:EtOAc, 4:1)

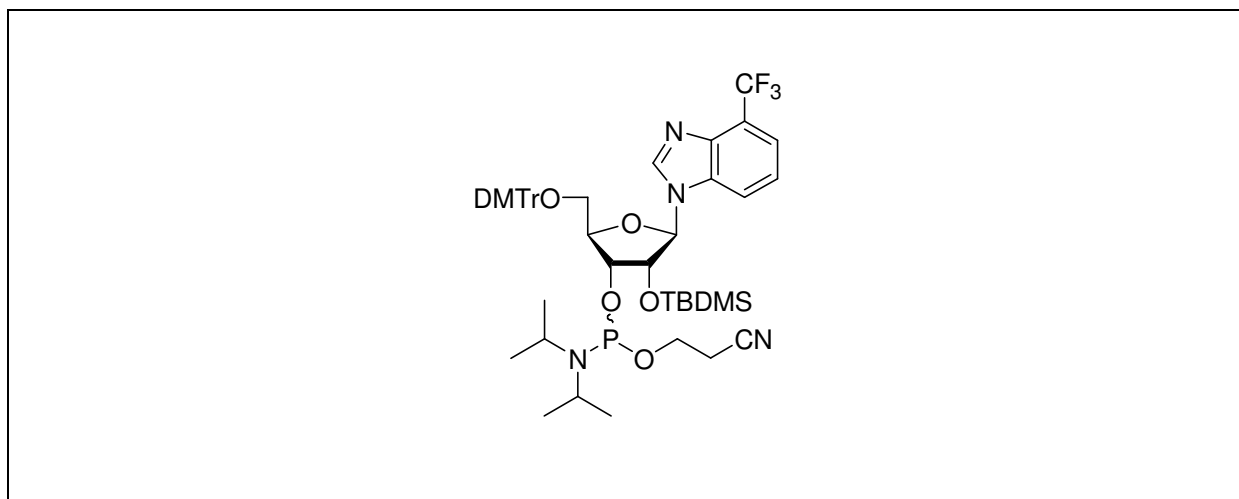
$^1\text{H NMR}$ :  $\delta$  [ppm] (400 MHz, DMSO-  $d_6$ )  
 8.23 (s, 1H, 2H); 7.94 (d,  $J=8.2\text{Hz}$ , 1H, 5H); 7.55-6.81(m, 15H, Har, 6H, 7H);  
 5.89 (d,  $J=47.16\text{Hz}$ , 1H, 1H'); 5.65(d,  $J=6.10\text{Hz}$ , 1H, 3'OH); 4.79(m, 1H,  
 2H'); 4.35 ( m, 2H, 3H', 4H'); 4.11 (m, 1H, 4H'); 3.80 (s, 6H, 2OCH<sub>3</sub>);  
 3.46(m, 2H, 5'CH<sub>2</sub>); 0.82( s, 9H, SiC(CH<sub>3</sub>)<sub>3</sub>); 0.13 (s, 3H, SiCH<sub>3</sub>); -0.36 (s, 3H,  
 SiCH<sub>3</sub>);

$^{13}\text{C NMR}$  :  $\delta$  [ppm] (100.6 MHz, DMSO-  $d_6$ )  
 158.20 (DMTr); 144.90 (DMTr); 144.50(C2); 141.10(C5); 135.80(C6);  
 135.70(DMTr); 135.30(DMTr); 132.40(C4); 131.75(DMTr); 128.10(DMTr);  
 127.70(DMTr); 127.00(DMTr); 123.30(C8); 114.10(CF<sub>3</sub>); 114.20(DMTr);  
 108.0(C7); 107.75(C9); 89.15(C1'); 85.72(DMTr); 83.50(C4'); 73.20(C2');

70.20(C3'); 63.60(C5'); 55.00(OCH<sub>3</sub>); 26,60(SiC(CH<sub>3</sub>)<sub>3</sub>,-5,20(SiCH<sub>3</sub>), -  
5,10(SiCH<sub>3</sub>);

ESI(+): m/z 736.3 ([M+H]<sup>+</sup>);

**3'-O-(2-Cyanethoxydiisopropylphosphin)-1'-deoxy-5'-O-(4,4'-dimethoxy-  
triphenylmethyl)-1'-(4-trifluoromethyl-1-N-benzimidazolyl)-2'-O-(tert.-  
butyl-dimethylsilyl)-β-D-ribofuranose 128**



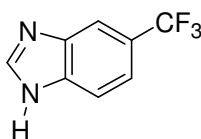
C<sub>49</sub>H<sub>62</sub>F<sub>3</sub>N<sub>4</sub>O<sub>7</sub>PSi

935.04 g/mol

240 mg (0.33 mmol) 5'-O-(4,4'-Dimethoxytriphenylmethyl)-2'-O-tert.-butyldimethylsilyl-1'-deoxy-1'-(4-trifluoromethyl-1-N-benzimidazolyl)-β-D-ribofuranose 126 were dissolved in 10 ml abs. acetonitrile and 420 μl (3.3 mmol) *sym.* collidine and 16 μl (0.16 mmol) 1-methylimidazole were added. The reaction mixture was cooled in an icebath to 0°C and 98 μl (0.48 mmol) 2-cyanethyldiisopropylchlorophosphoramidite 96 were added. The reaction was stirred for 15 min. at 0°C and 45 min. at RT. The reaction was stopped by adding 10 ml of 0.01 M citric acid and three times extracted with methylenechloride. The combined organic phases were washed twice with 0.01 M citric acid, dried over MgSO<sub>4</sub> and evaporated to dryness. Purification was done by FC with methylenechloride/methanol 99:1 as eluent. The product ( mixture of two diastereomers) was obtained as white foam.

Yield: 305 mg (69%)  
 TLC: Rf=0.55; 0.52; (CH<sub>2</sub>Cl<sub>2</sub>/MeOH,99:1);  
<sup>1</sup>H NMR: δ [ppm] (400 MHz, DMSO- *d*<sub>6</sub>)  
 8.44, 8.39 (s, 2H, 2H); 8.00 (d,J=8,1Hz, 2H, 5H); 7.79-6.80(m, 32H, Har, 5H, 6H, 7H); 5.93, 5.86(d, J=5,82Hz, J=7,08Hz, 2H, 1H'), 4.80 (m, 2H, 2H'); 4.38 (m, 2H, 3H'), 3.99 (m, 2H, 4H'), 3.,80, 3,79(s, 12H, 2OCH<sub>3</sub>), 3.56(m, 4H, 5'CH<sub>2</sub>),2.76(mm,4H, OCH<sub>2</sub>), 1,22(m, 12H, CH(CH<sub>3</sub>)<sub>2</sub>), 0,80( s, 18H, Si(CH<sub>3</sub>)<sub>3</sub>) -0,10( s, 6H, SiCH<sub>3</sub>), -0,29( s, 6H, SiCH<sub>3</sub>);  
<sup>31</sup>P NMR: δ [ppm] (162 MHz, CDCl<sub>3</sub>):  
 153.26 and 149.63 (ratio 1:4)  
 ESI(+): m/z 936.1 ([M+H]<sup>+</sup>);

### 5-Trifluoromethyl benzimidazole 63



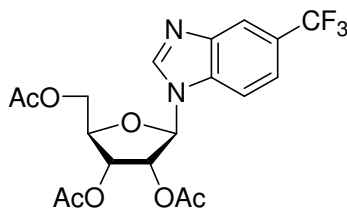
C<sub>8</sub>H<sub>5</sub>N<sub>2</sub>F<sub>3</sub>

186 g/mol

3,4-diaminobenzofluorid (2.2g, 12.5mmol) was heated under reflux with 90% HCOOH for 3h. HCOOH was than evaporated and the crude product purified by FC (CH<sub>2</sub>Cl<sub>2</sub>/MeOH, 9:1).

Yield: 2.10g ( 90%);  
 TLC: Rf=0.57 (CH<sub>2</sub>Cl<sub>2</sub>/MeOH, 9:1):  
<sup>1</sup>H NMR : δ [ppm] (250MHz, DMSO- *d*<sub>6</sub>):  
 12.87 (s,1H, NH); 8.46 (s, 1H, 2H); 8.01 (s, 1H, 4H); 7.78 (d, J=8.42Hz, 1H, 6H); 7.51 (dd, J=8.48Hz, J=1.63Hz, 1H, 7H);  
<sup>13</sup>C NMR : δ [ppm] (60.9 MHz, DMSO- *d*<sub>6</sub>):  
 142.05 (C2); 140.50, 138.10, 121.10, 119.10, 119.70, 119.20 (*arom* C, CF<sub>3</sub>);  
 ESI(+): m/z 187.0 ([M+H]<sup>+</sup>);

**2',3',5'-Tri-O-acetyl-1'-deoxy-1'-(5-trifluoromethyl-1-N-benzoimidazole-1-yl)-β-D-ribofuranose 129**



$C_{19}H_{19}F_3N_2O_7$

444.33 g/mol

To a suspension of 5-trifluoromethyl-1H-benzoimidazole **63** (1.5g, 8.05mmol) in acetonitrile (50ml) N,O-bis(trimethylsilyl)acetamide (3.00ml, 12.00mmol) was added and heated under reflux for 15 min. After the mixture was cooled to room temperature, 1,2,3,5-tetra-O-acetyl-β-D-ribofuranose (2.60g, 8.05mmol) in acetonitrile (20ml) and trimethylsilyl trifluoromethanesulfonate (1.8ml, 10.00mmol) were added and heated under reflux for 2.5h. The reaction mixture was cooled room temperature treated with 5% NaHCO<sub>3</sub> solution and extracted with methylene chloride. The organic phase was dried (over MgSO<sub>4</sub>) and evaporated and the residue purified by means of preparative HPLC (MN Nucleoprep 100-20 from Macherey-Nagel, n-hexan:ethyl acetate, 10:20). The product was obtained as *faster* migrating isomer, as white foam.

Yield: 2.04g (57%)

TLC: R<sub>f</sub>= 0.55 (CH<sub>2</sub>Cl<sub>2</sub>/MeOH, 95:5):

<sup>1</sup>H NMR : δ [ppm] (400MHz, DMSO- *d*<sub>6</sub>):

8.72 (1H, s, 2H), 8.10 (1H, s, 4H), 7.99 (1H, d, J=8.58Hz, 7H), 7.68 (1H, d, J=8.55Hz, 6H), 6.42 (1H, d, J=6.20Hz, 1H'), 5.68 (1H, t, J=6.28Hz, 2H'), 5.44 (1H, m, 3H'), 4.56-4.37 (2H, m, 4H', 5H'), 2.07 (3H, s, CH<sub>3</sub>), 2.06 (3H, s, CH<sub>3</sub>), 2.04 (3H, s, CH<sub>3</sub>);

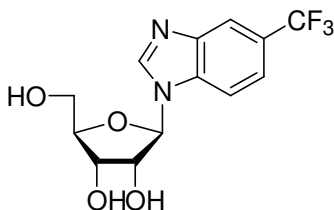
<sup>13</sup>C NMR: δ [ppm] (100.6 MHz, DMSO- *d*<sub>6</sub>):

170.10, 169.70, 169.00 (C=O); 145.10 (C2); 144.40, 134.00, 123.10, 120.30, 120.20, 120.16 (*arom* C); 113.6 (CF<sub>3</sub>); 87.00 (C1'); 78.40 (C4'); 71.20 (C2'); 69.80 (C3'); 62.70 (C5'); 20.20, 19.90, 19.80 (CH<sub>3</sub>);

ESI(+): m/z 445.0 ([M+H]<sup>+</sup>);

**1'-Deoxy-1'-(5-trifluoromethyl-1-N-benzimidazole-1-yl)-β-D-ribofuranose**

**34**



$C_{13}H_{13}F_3N_2O_4$

318.23 g/mol

2',3',5'-Tri-*O*-acetyl-1'-deoxy-1'-(5-trifluoromethyl-1-*N*-benzimidazole-1-yl)-β-D-ribofuranose **129** (0.74g, 1.67mmol) was dissolved in MeOH (15ml) and 111μl of MeONa/MeOH (5.4M, Fluka) were added at room temperature and reaction was TLC controlled. The reaction was complete after 60 min. and neutralized with DOWEX 50, filtered and evaporated. The product was obtained as white foam.

Yield: 0.48g (91%);

TLC:  $R_f=0.36$  ( $CH_2Cl_2/MeOH$ , 9:1)

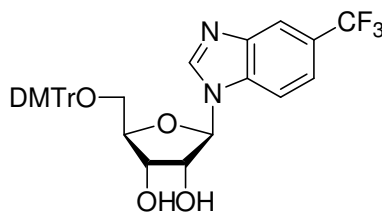
$^1H$  NMR:  $\delta$  [ppm] (250MHz,  $DMSO-d_6$ ):  
 8.68 (s, 1H, 2H); 8.02 (m, 2H, 4H, 7H); 7.58 (d,  $J=8.40Hz$ , 1H, 6H); 5.95 (, d,  $J=6.13Hz$ , 1H, 1H'), 5.51 (d,  $J=7.50Hz$ , 1H, 2'OH); 5.20 (d,  $J=4.68Hz$ , 1H, 3OH'); 5.15 (t,  $J=5.12Hz$ , 1H, 5OH'); 4.37 (q,  $J=5.50Hz$ , 1H, 2H'); 4.13 (m, 1H, 3H'); 4.00 (m, 1H, 4H'); 3.66 (m, 2H, 5H');

$^{13}C$  NMR :  $\delta$  [ppm] (100.6 MHz,  $DMSO-d_6$ ):  
 143.10 (C2), 137.05, 132.10, 128.10, 125.10, 125.00, 124.10 (arom C); 114.10 (CF<sub>3</sub>), 88.90 (C1'); 86.20 (C4'); 74.20 (C2'); 70.20 (C3'); 62.300 (C5');

$^{19}F$ -NMR:  $\delta$  [ppm] (254,2 MHz,  $DMSO-d_6$ )  
 -59.48 (s, 3F, CF<sub>3</sub>)

ESI (-):  $m/z$  316.8([M-H]<sup>-</sup>);

**1'-Deoxy -5'-O-(4,4'-dimethoxytriphenylmethyl)-1'-(5-trifluoromethyl-1-N-benzimidazolyl)- $\beta$ -D-ribofuranose 130**



$C_{34}H_{31}F_3N_2O_6$

620.63 g/mol

400 mg (1.26 mmol) 1'-Deoxy-1'-(5-trifluoromethyl-1-N-benzimidazolyl)- $\beta$ -D-ribofuranose 34 were dissolved in 10 ml abs. pyridine and 0.25 ml (2.0 mmol) triethylamine and 0.50 g (1.67 mmol) 4,4'-dimethoxytriphenylmethylchloride were added. The reaction mixture was stirred under argon at RT for 20h. The reaction was stopped by adding of 3 ml of methanol and saturated water solution of  $NaHCO_3$ . It was three times extracted with methylene chloride, organic phases were collected and dried over  $MgSO_4$  and then evaporated to dryness. The product was twice co-evaporated with toluene. Further purification was done by FC with methylene chloride/methanol 95:5, as eluent. The product was obtained as yellow foam.

Yield: 600 mg(77%)

TLC:  $R_f=0.29$  ( $CH_2Cl_2:MeOH$ , 95:5)

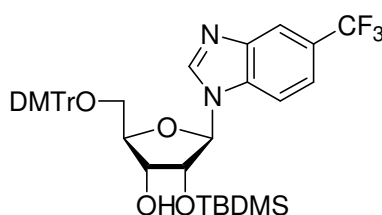
$^1H$  NMR:  $\delta$  [ppm] (250 MHz,  $DMSO-d_6$ )  
 8.57 (s, 1H, 2H); 8.07 (s, 1H, 4H); 7.93 (d,  $J=5.45$  Hz, 1H, 6H); 7.86 (d,  $J=4.7$  Hz, 1H, 7H); 7.40-6.28(m, 13H, Har); 6.00 (d,  $J=6.40$  Hz, 1H, 1H'); 5.65 (d,  $J=6.05$ Hz, 1H, 2'OH); 5.30 (d,  $J=5.43$ Hz, 1H, 3OH'); 4.52 (m, 1H, 2H'); 4.19 (m, 1H, 3H'); 4.26-4.13 (m, 2H, 3'H, 4H'); 3.25 (m, 2H, 5H');

$^{13}C$  NMR :  $\delta$  [ppm] (100.6 MHz,  $DMSO-d_6$ )  
 158.10 (DMTr); 144.80 (DMTr); 143.00(C2); 141.10(C4); 135.80(C6);  
 135.40(DMTr); 135.30(DMTr); 132.30(C5); 130.75(DMTr); 128.00(DMTr);  
 127.70(DMTr); 127.00(DMTr); 123.30(C8); 114.10(CF<sub>3</sub>); 113.20(DMTr);

108.7(C7); 107.60(C9); 89.10(C1'); 85.72(DMTr); 83.50(C4'); 73.25(C2');  
70.10(C3'); 63.60(C5'); 55.05(OCH<sub>3</sub>);

ESI (-): m/z 619.20 ([M-H]);

**5'-O-(4,4'-Dimethoxytriphenylmethyl)-2'-O-*tert.*-butyldimethylsilyl-1'-deoxy-1'-(5-trifluoromethyl-1-N-benzimidazolyl)-β-D-ribofuranose 131**



C<sub>40</sub>H<sub>42</sub>F<sub>3</sub>N<sub>2</sub>O<sub>6</sub>Si

734.93 g/mol

1.80 g (2.90 mmol) 5'-O-(4,4'-Dimethoxytriphenylmethyl)-1'-deoxy-1'-β-D-(5-trifluoromethyl-1-N-benzimidazolyl)-ribofuranose 130 were dissolved in 30 ml of 1:1 mixture of THF/pyridine and 600 mg (3.53 mmol) AgNO<sub>3</sub> and 4.1 ml (4.1 mmol) 1 M *tert.*-butyldimethylsilylchloride-solution in THF were added. The reaction mixture was stirred for 20 hours at RT under argon. The reaction was stopped by adding 10 ml of saturated water NaHCO<sub>3</sub>-solution. Left AgCl was filtered over celite and filtrate was extracted with methylene chloride three times. The combined organic phases were dried over MgSO<sub>4</sub> and evaporated to dryness. The crude product was co-evaporated with toluene twice. Further purification of the product was done by HPLC (MN Nucleoprep 100-20 of Macherey-Nagel, [*n*-hexan/methylacetat 10:20]+30% methylenechloride). The product (*slow-Isomer*) was obtained as white foam.

Yield: 915 mg (43%)

TLC: R<sub>f</sub>=0.45 (hexane/EtOAc,4:1)

<sup>1</sup>H NMR: δ [ppm] (400 MHz, DMSO- *d*<sub>6</sub>)

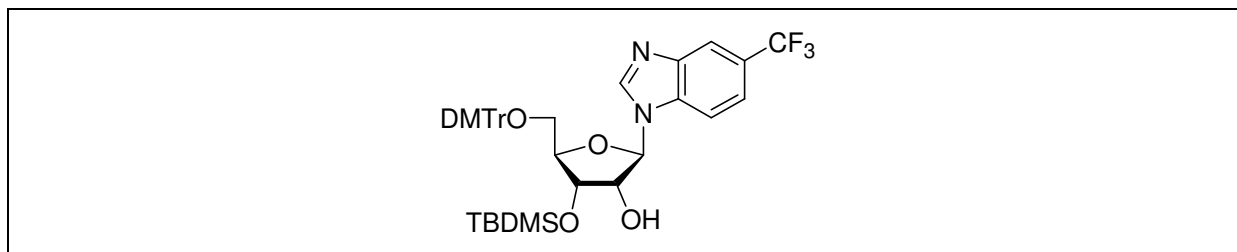


8.59 (s, 1H, 2H); 8.04 (s, 1H, 4H); 7.91 (d, 1H, J=8.56 Hz, 6H); 7.35-6.81(m, 14H, Har+7H); 5.96 (d, J=5.92 Hz, 1H, 1H'); 5.51 (d, J=6.52Hz, 1H, 2'OH); 4.50 (m, 1H, 2H'); 4.34 (m, 1H, 3H'); 4.11 (m, 1H, 4H'); 3.70 (s, 6H, 2OCH<sub>3</sub>); 3.25(m, 2H, 5'CH<sub>2</sub>); 0.90 (s, 9H, Si(CH<sub>3</sub>)<sub>3</sub>); 0.05 (s, 3H, SiCH<sub>3</sub>), -0.05 (s, 3H, SiCH<sub>3</sub>);

<sup>13</sup>C NMR : δ [ppm] (100.6 MHz, DMSO- *d*<sub>6</sub>)  
 158.20 (DMTr); 144.80 (DMTr); 143.10(C2); 141.10(C4); 135.80(C6); 135.40(DMTr); 135.30(DMTr); 132.30(C5); 130.75(DMTr); 128.10(DMTr); 127.70(DMTr); 127.00(DMTr); 123.30(C8); 114.10(CF<sub>3</sub>); 113.20(DMTr); 108.7(C7); 107.60(C9); 89.10(C1'); 85.72(DMTr); 83.50(C4'); 73.25(C2'); 70.10(C3'); 63.60(C5'); 55.05(OCH<sub>3</sub>); 25.60(SiC(CH<sub>3</sub>)<sub>3</sub>); -5.01(SiCH<sub>3</sub>); -5.20(SiCH<sub>3</sub>);

ESI(+): m/z 737.5 ([M+H]<sup>+</sup>);

**5'-O-(4,4'-Dimethoxytriphenylmethyl)-3'-O-*tert.*-butyldimethylsilyl-1'-deoxy-1'-(5-trifluoromethyl-1-*N*-benzimidazolyl)-β-D-ribofuranose 132**



C<sub>40</sub>H<sub>42</sub>F<sub>3</sub>N<sub>2</sub>O<sub>6</sub>Si

734.93 g/mol

5'-O-(4,4'-Dimethoxytriphenylmethyl)-3'-O-*tert.*-butyldimethylsilyl-1'-deoxy-1'-(5-trifluoromethyl-1-*N*-benzimidazolyl)-β-D-ribofuranose 132 was obtained as a side product (*fast-Isomer*) in the synthesis 5'-O-(4,4'-Dimethoxytriphenylmethyl)-2'-O-*tert.*-butyldimethylsilyl-1'-deoxy-1'-(5-trifluoromethyl-1-*N*-benzimidazolyl)-β-D-ribofuranose 131.

Yield: 870 mg (41%)

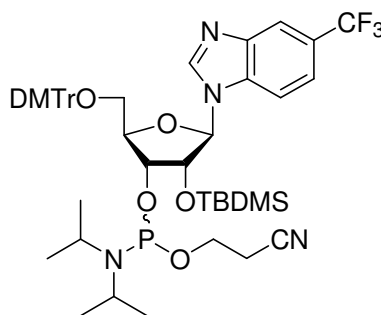
TLC: Rf=0.45 (hexane/EtOAc,4:1)

<sup>1</sup>H NMR: δ [ppm] (400 MHz, DMSO- *d*<sub>6</sub>)  
 8.58(s, 1H, 2H); 8.04 (s, 1H, 4H); 7.91 (d, 1H, J=8.56 Hz, 6H); 7.34-6.80(m, 14H, Har, 7H); 6,01 ( d, J=6,32 Hz, 1H, 1H'); 5.24 (d, J=5,60Hz, 1H, 3'OH); 4.54 (m, 1H, 2H'); 4.17 ( m, 2H, 3H',4H'); 3.70( s, 6H, 2OCH<sub>3</sub>); 3.25(m, 2H, 5'CH<sub>2</sub>); 0,67( s, 9H, Si(CH<sub>3</sub>)<sub>3</sub>); -0.13( s, 3H, SiCH<sub>3</sub>); -0.29( s, 3H, SiCH<sub>3</sub>);

<sup>13</sup>C NMR : δ [ppm] (100.6 MHz, DMSO- *d*<sub>6</sub>)  
 158.30 (DMTr); 144.80 (DMTr); 144.10(C2); 141.10(C4); 136.80(C6); 135.80(DMTr); 135.30(DMTr); 132.30(C5); 130.75(DMTr); 128.60(DMTr); 127.80(DMTr); 127.00(DMTr); 123.30(C8); 114.20(CF<sub>3</sub>); 113.20(DMTr); 109.7(C7); 107.60(C9); 89.10(C1'); 85.72(DMTr); 83.50(C4'); 73.25(C2'); 70.10(C3'); 63.30(C5'); 55.00(CH<sub>3</sub>); 25,80(SiC(CH<sub>3</sub>)<sub>3</sub>,-5,10(SiCH<sub>3</sub>), -5,20(SiCH<sub>3</sub>);

ESI(+): m/z 736.8 ([M+H]<sup>+</sup>);

**3'-O-(2-Cyanethoxydiisopropylphosphin)-1'-deoxy-5'-O-(4,4'-dimethoxy-triphenylmethyl)-1'-(5-trifluoromethyl-1-N-benzimidazolyl)-2'-O-(tert.-butyl-dimethylsilyl)-β-D-ribofuranose 133**



C<sub>49</sub>H<sub>62</sub>F<sub>3</sub>N<sub>4</sub>O<sub>7</sub>PSi

935.04 g/mol

250 mg (0.34 mmol) 5'-*O*-(4,4'-Dimethoxytriphenylmethyl)-2'-*O*-*tert*-butyldimethylsilyl-1'-deoxy-1'-(5-trifluoromethyl-1-*N*-benzimidazolyl)- $\beta$ -D-ribofuranose **131** were dissolved in 10 ml abs. acetonitrile and 450  $\mu$ l (3.4 mmol) *sym*. collidine and 16  $\mu$ l (0.16 mmol) 1-methylimidazole were added. The reaction mixture was cooled in an icebath to 0°C and 113  $\mu$ l (0.50 mmol) 2-cyanethyldiisopropylchlorophosphoramidite **96** was added. The reaction was stirred for 15min. at 0°C and 45 min. at RT. The reaction was stopped by adding 10ml of 0.01 M citric acid and three times extracted with methylene chloride. The combined organic phases were washed twice with 0.01 M citric acid, dried over MgSO<sub>4</sub> and evaporated to dryness. Purification was done by FC with methylene chloride/methanol 99:1 as eluent. The product (mixture of two diastereomers) was obtained as white foam.

Yield: 245 mg (77%)

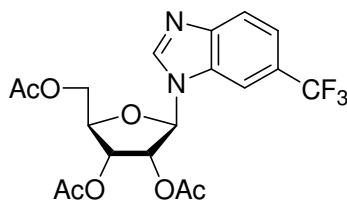
TLC: R<sub>f</sub>=0.50;0.48 (CH<sub>2</sub>Cl<sub>2</sub>/MeOH,99:1)

<sup>1</sup>H NMR:  $\delta$  [ppm] (400 MHz, CDCl<sub>3</sub>)  
 8.22, 8.17 (s, 2H, 2H); 8.05 (s, 2H, 4H); 7.77-6.81(m, 32H, Har, 5H, 6H, 7H);  
 5.93, 5.86 (d, J=5.72Hz, J=7.08Hz, 2H, 1H'); 4.75 (m, 2H, 2H'); 4.40 ( m, 2H,  
 3H'); 3.95 (m, 2H, 4H'); 3.80, 3.79(s, 12H, 2OCH<sub>3</sub>); 3.46(m, 4H, 5'CH<sub>2</sub>);  
 2.66(mm,4H, OCH<sub>2</sub>); 1.20(m, 12H, CH(CH<sub>3</sub>)<sub>2</sub>); 0.75( s, 18H, Si(CH<sub>3</sub>)<sub>3</sub>); -0.14(  
 s, 6H, SiCH<sub>3</sub>); -0.39( s, 6H, SiCH<sub>3</sub>);

<sup>31</sup>P NMR:  $\delta$  [ppm] (162 MHz, CDCl<sub>3</sub>):  
 153.2 and 150.03 (ratio 1:11)

ESI(+): m/z 937.0 ([M+H]<sup>+</sup>);

**2',3',5'-Tri-*O*-acetyl-1'-deoxy-1'-(5-trifluoromethyl-3-*N*-benzimidazole-1-yl)-β-D-ribofuranose 134**



$C_{19}H_{19}F_3N_2O_7$

444.33 g/mol

2',3',5'-Tri-*O*-acetyl-1'-deoxy-1'-(5-trifluoromethyl-3-*N*-benzimidazole-1-yl)-β-D-ribofuranose 134 was obtained in the same procedure as 129 but like *slower* migrating isomer during preparative HPLC separation (*MN Nucleoprep 100-20* from *Macherey-Nagel*, n-hexane:ethyl acetate, 10:20). The product was obtained as white foam .

Yield: 1.43g (40%)

TLC:  $R_f=0.55$  ( $CH_2Cl_2/MeOH$ , 95:5)

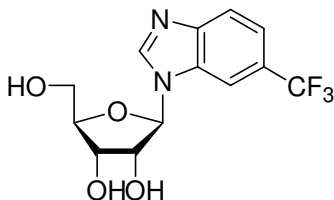
$^1H$  NMR:  $\delta$  [ppm] (400MHz,  $DMSO-d_6$ )  
 8.75 (s, 1H, 2H); 8.21 (s, 1H, 4H); 7.92 (d,  $J=8.48Hz$ , 1H, 7H); 7.61 (d,  $J=8.68Hz$ , 1H, 6H); 6.49 (d,  $J=6.16Hz$ , 1H, 1H'); 5.69 (t,  $J=6.20Hz$ , 1H, 2H'); 5.44 (m, 1H, 3H'); 4.40 (m, 1H, 4H'); 4.37 (m, 2H, 5H'); 2.08 (s, 3H,  $CH_3$ ), 2.06 (s, 3H,  $CH_3$ ); 2.03 (s, 3H,  $CH_3$ );

$^{13}C$  NMR:  $\delta$  [ppm] (100.6 MHz,  $DMSO-d_6$ )  
 170.10, 169.70, 169.00 (C=O); 145.00 (C2); 140.40, 134.00, 123.10, 120.30, 120.20, 120.10 (*arom C*); 114.0 ( $CF_3$ ); 87.00 (C1'); 78.50 (C4'); 71.20 (C2'); 69.90 (C3'); 62.70 (C5'); 20.20, 19.90, 19.80 ( $CH_3$ );

ESI(+):  $m/z$  445.0 ( $[M+H]^+$ );

**1'-Deoxy-1'-(5-trifluoromethyl-3-N-benzoimidazole-1-yl)-β-D-ribofuranose**

**35**



$C_{13}H_{13}F_3N_2O_4$

318.23 g/mol

2',3',5'-Tri-*O*-acetyl-1'-deoxy-1'-(5-trifluoromethyl-3-*N*-benzoimidazole-1-yl)-β-*D*-ribofuranose **134** (0.34g, 0.8mmol) was dissolved in methanol (15ml) and 111μl of MeONa/MeOH (5.4M, Fluka) were added at room temperature and the reaction was TLC controlled. The reaction was complete after 60 min. and neutralized with DOWEX 50, filtered and evaporated. The product was obtained as white foam.

Yield: 0.22g ( 90%);

TLC:  $R_f=0.37$  ( $CH_2Cl_2/MeOH$ , 9:1):

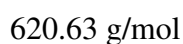
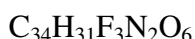
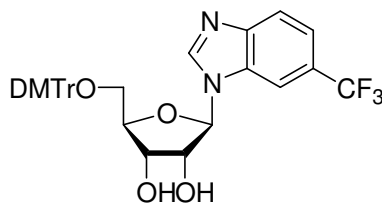
$^1H$  NMR:  $\delta$  [ppm] (250 MHz,  $DMSO-d_6$ )  
 8.68 (s, 1H, 2H); 8.34 (s, 1H, 4H); 7.88 (d,  $J=6.40Hz$ , 1H, 7H); 7.55 (d,  $J=8.55Hz$ , 1H, 6H); 5.99 (d,  $J=6.40Hz$ , 1H, 1H'); 5.52 (d,  $J=6.45Hz$ , 1H, 2'OH); 5.28 (d,  $J=4.70Hz$ , 1H, 3OH'); 5.20 (t,  $J=5.12Hz$ , 1H, 5OH'); 4.36 (q,  $J=5.40 Hz$ , 1H, 2H'); 4.13 (m, 1H, 3H'); 4.02 (q,  $J=2.95Hz$ , 1H, 4H'); 3.51 (m, 2H, 5H');

$^{19}F$ -NMR:  $\delta$  [ppm] (254.2 MHz,  $DMSO-d_6$ )  
 -59.55 (s, 3F,  $CF_3$ );

$^{13}C$  NMR:  $\delta$  [ppm] (100.6 MHz,  $DMSO-d_6$ )  
 141.10 (C2); 136.10, 132.10, 129.10, 125.20, 125.10, 124.10 (arom C); 114.40 ( $CF_3$ ); 88.10 (C1'); 87.20 (C4'); 75.20 (C2'); 71.00 (C3'); 62.20 (C5');

ESI(-):  $m/z$  316.90 ([M-H]);

**1'-Deoxy -5'-O-(4,4'-dimethoxytriphenylmethyl)-1'-(5-trifluoromethyl-3-N-benzimidazolyl)-β-D-ribofuranose 135**



1.80 g (5.65 mmol) 1'-deoxy-1'-(5-trifluoromethyl-3-N-benzimidazolyl)-β-D-ribofuranose **35** were dissolved in 40 ml abs. pyridine and 1.10 ml (8.50 mmol) triethylamine and 2.00 g (6.00 mmol) 4,4'-dimethoxytriphenylmethylchloride were added. The reaction mixture was stirred under argon at RT for 20h. The reaction was stopped by adding 5 ml of methanol and saturated water solution of NaHCO<sub>3</sub>. It was three times extracted with methylene chloride, organic phases were collected and dried over MgSO<sub>4</sub> and then evaporated to dryness. The product was twice co-evaporated with toluene. Further purification was done by FC with methylene chloride/methanol 95:5, as eluent. The product was obtained as yellow foam.

Yield: 2.21 g (63%)

TLC: R<sub>f</sub>=0.29 (CH<sub>2</sub>Cl<sub>2</sub>/MeOH, 95:5)

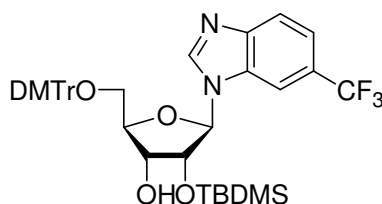
<sup>1</sup>H NMR: δ [ppm] (250 MHz, DMSO- *d*<sub>6</sub>)  
 8.58 (s, 1H, 2H), 8.09 (s, 1H, 4H), 7.86 (m, 2H, 6H, 7H), 7.58-6.76 (m, 13H, Har), 6.08 (d, 1H, J=7.56Hz, 1H'), 5.71 (d, J=9.44Hz, 1H, 2'OH), 5.25 (d, J=8.84Hz, 1H, 3OH'), 4.51 (m, 1H, 2H'), 4.17 (m, 2H, 3H', 4H'), 3.65 (s, 6H, 2OCH<sub>3</sub>), 3.21 (m, 2H, 5H');

<sup>13</sup>C NMR: δ [ppm] (100.6 MHz, DMSO- *d*<sub>6</sub>)  
 158.10 (DMTr); 144.80 (DMTr); 143.00(C2); 141.10(C4); 135.80(C6);  
 135.40(DMTr); 135.30(DMTr); 132.30(C5); 130.75(DMTr); 128.00(DMTr);  
 127.70(DMTr); 127.00(DMTr); 123.30(C8); 114.10(CF<sub>3</sub>); 113.20(DMTr);

108.7(C7); 107.60(C9); 89.10(C1'); 85.72(DMTr); 83.50(C4'); 73.25(C2');  
70.10(C3'); 63.60(C5'); 55.05(OCH<sub>3</sub>);

ESI(-): m/z 619.20 ([M-H]);

**5'-O-(4,4'-Dimethoxytriphenylmethyl)-2'-O-*tert.*-butyldimethylsilyl-1'-deoxy-1'-(5-trifluoromethyl-3-*N*-benzimidazolyl)-β-D-ribofuranose 136**



C<sub>40</sub>H<sub>42</sub>F<sub>3</sub>N<sub>2</sub>O<sub>6</sub>Si

734.93 g/mol

2.00 g (3.22 mmol) 5'-O-(4,4'-Dimethoxytriphenylmethyl)-1'-deoxy-1'-β-D-(5-trifluoromethyl-3-*N*-benzimidazolyl)-ribofuranose 135 were dissolved in 30 ml of 1:1 mixture of THF/pyridine and 660 mg (3.90 mmol) AgNO<sub>3</sub> and 6.00 ml (6.00 mmol) 1 M *tert.*-butyldimethylsilylchloride-solution in THF were added. The reaction mixture was stirred under argon for 20 hours at RT. The reaction was stopped by adding 10 ml of saturated water NaHCO<sub>3</sub>-solution. Left AgCl was filtered over celite and the filtrate was extracted with methylene chloride three times. The combined organic phases were dried over MgSO<sub>4</sub> and evaporated to dryness. The crude product was twice co-evaporated with toluene. Further purification of product was done by. HPLC (*MN Nucleoprep 100-20* of *Macherey-Nagel*, [*n*-hexan/ethylacetat 10:6.67]+30% methylene chloride). The product (*slow-Isomer*) was obtained as white foam.

Yield: 923 mg (39%)

TLC: R<sub>f</sub>=0.45 (hexane/EtOAc,4:1)

<sup>1</sup>H NMR: δ [ppm] (400 MHz, DMSO- *d*<sub>6</sub>)

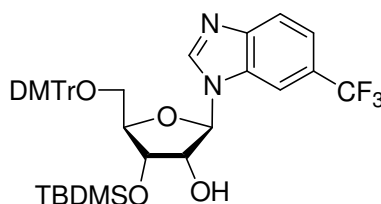
8.63(s, 1H, 2H); 8.07 (s, 1H, 4H); 7.88 (d, 1H, J=8.44 Hz, 7H); 7.32-6.77(m, 14H, Har, 6H); 6,04 ( d, J=5,12 Hz, 1H, 1H'), 5.55 (d, J=6,24Hz, 1H, 2'OH),

4.49 (m, 1H, 2H'); 4.25 (m, 1H, 3H'); 4.03(m, 1H, 4H'); 3.68( s, 6H, 2OCH<sub>3</sub>); 3.23(m, 2H, 5'CH<sub>2</sub>); 0,78( s, 9H, Si(CH<sub>3</sub>)<sub>3</sub>); 0.04( s, 3H, SiCH<sub>3</sub>), -0.03( s, 3H, SiCH<sub>3</sub>);

<sup>13</sup>C NMR : δ [ppm] (100.6 MHz, DMSO- *d*<sub>6</sub>)  
 158.30 (DMTr); 144.80 (DMTr); 144.10(C2); 141.10(C4); 136.80(C6);  
 135.80(DMTr); 135.30(DMTr); 132.30(C5); 130.75(DMTr); 128.60(DMTr);  
 127.80(DMTr); 127.00(DMTr); 123.30(C8); 114.20(CF<sub>3</sub>); 113.20(DMTr);  
 109.7(C7); 107.60(C9); 89.10(C1'); 85.72(DMTr); 83.50(C4'); 73.25(C2');  
 70.10(C3'); 63.30(C5'); 55.00(CH<sub>3</sub>); 25,80(SiC(CH<sub>3</sub>)<sub>3</sub>), -5,10(SiCH<sub>3</sub>), -  
 5,20(SiCH<sub>3</sub>);

ESI(+): m/z 736.6 ([M+H]<sup>+</sup>);

**5'-O-(4,4'-Dimethoxytriphenylmethyl)-3'-O-*tert.*-butyldimethylsilyl-1'-deoxy-1'-(5-trifluoromethyl-3-*N*-benzimidazolyl)-β-D-ribofuranose 137**



C<sub>40</sub>H<sub>42</sub>F<sub>3</sub>N<sub>2</sub>O<sub>6</sub>Si

734.93 g/mol

5'-O-(4,4'-Dimethoxytriphenylmethyl)-3'-O-*tert.*-butyldimethylsilyl-1'-deoxy-1'-(5-trifluoromethyl-3-*N*-benzimidazolyl)-β-D-ribofuranose 137 was obtained as a side product (*fast-Isomer*) in the synthesis of 5'-O-(4,4'-Dimethoxytriphenylmethyl)-2'-O-*tert.*-butyldimethylsilyl-1'-deoxy-1'-(5-trifluoromethyl-3-*N*-benzimidazolyl)-β-D-ribofuranose 136.

Yield: 947 mg (40%)

TLC: R<sub>f</sub>=0.45 (hexane/EtOAc,4:1)

<sup>1</sup>H NMR: δ [ppm] (400 MHz, DMSO- *d*<sub>6</sub>)  
 8.34 (s, 1H, 2H); 7,92 (d, J=7,12Hz, 1H, 7H); 7.80 (s, 1H, 4H); 7.50-6.80(m, 14H, Har, 6H); 5,96 ( d, J=6,76 Hz, 1H, 1H'); 5.60 (d, J=7,10Hz, 1H, 3'OH);

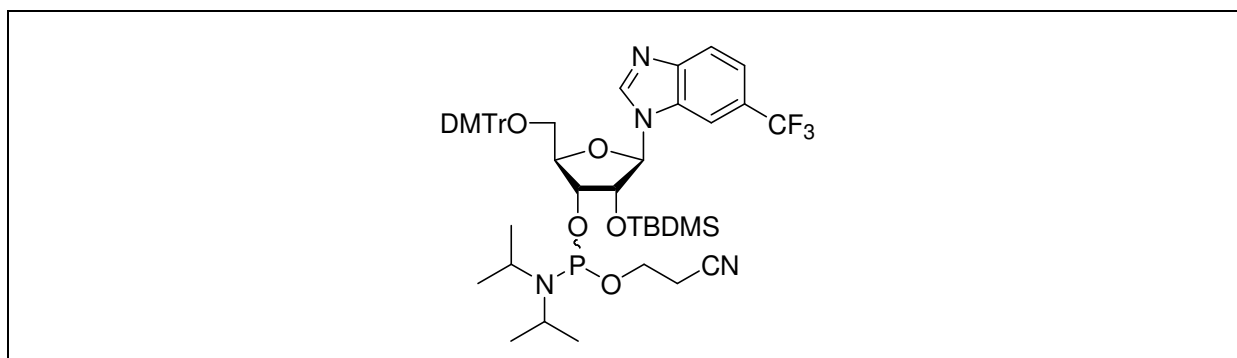


4.62 (m, 1H, 2H'); 4.35 (m, 1H, 3H'); 4.11 (m, 1H, 4H'); 3.70 (s, 6H, 2OCH<sub>3</sub>); 3.52 (m, 2H, 5'CH<sub>2</sub>); 0.80 (s, 9H, Si(CH<sub>3</sub>)<sub>3</sub>); -0.10 (s, 3H, SiCH<sub>3</sub>); -0.36 (s, 3H, SiCH<sub>3</sub>);

<sup>13</sup>C NMR : δ [ppm] (100.6 MHz, DMSO- *d*<sub>6</sub>)  
 158.40 (DMTr); 145.80 (DMTr); 143.20(C2); 141.10(C4); 135.90(C6);  
 135.460(DMTr); 135.30(DMTr); 132.30(C5); 130.80(DMTr); 128.10(DMTr);  
 127.70(DMTr); 127.10(DMTr); 123.40(C8); 114.10(CF<sub>3</sub>); 113.40(DMTr);  
 109.70(C7); 107.70(C9); 89.30(C1'); 85.72(DMTr); 83.60(C4'); 73.25(C2');  
 70.40(C3'); 63.60(C5'); 55.05(OCH<sub>3</sub>); 26.40(SiC(CH<sub>3</sub>)<sub>3</sub>); -5.00(SiCH<sub>3</sub>), -  
 5.40(SiCH<sub>3</sub>);

ESI(+): m/z 737.5 ([M+H]<sup>+</sup>);

**3'-O-(2-Cyanethoxydiisopropylphosphin)-1'-deoxy-5'-O-(4,4'-dimethoxy-triphenylmethyl)-1'-(5-trifluoromethyl-3-N-benzimidazolyl)-2'-O-(tert.-butyl-dimethylsilyl)-β-D-ribofuranose 138**



C<sub>49</sub>H<sub>62</sub>F<sub>3</sub>N<sub>4</sub>O<sub>7</sub>PSi

935.04 g/mol

250 mg (0.34 mmol) 5'-O-(4,4'-Dimethoxytriphenylmethyl)-2'-O-tert.-butyldimethylsilyl-1'-desoxy-1'-(5-trifluoromethyl-1-N-benzimidazolyl)-β-D-ribofuranose 136 were dissolved in 10 ml abs. acetonitrile and 450 μl (3.4 mmol) *sym.* collidine and 16 μl (0.16 mmol) 1-methylimidazole were added. The reaction mixture was cooled in an icebath to 0°C and 113 μl (0.50 mmol) 2-cyanethyldiisopropylchlorophosphoramidite 96 was added. The reaction was stirred for 15min. at 0°C and 45 min. at RT. The reaction was stopped by adding of 10 ml

of 0.01 M citric acid and three times extracted with methylene chloride. Collected organic phases were washed twice with 0.01 M citric acid, dried over  $\text{MgSO}_4$  and evaporated to dryness. The purification was done by FC with methylene chloride/methanol 99:1 as eluent. The product (mixture of two diastereomers) was obtained as white foam.

Yield: 251 mg (79%)

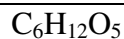
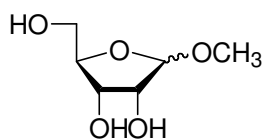
TLC:  $R_f=0.59$ ; 0.49 ( $\text{CH}_2\text{Cl}_2/\text{MeOH}$ , 99:1)

$^1\text{H}$  NMR:  $\delta$  [ppm] (400 MHz,  $\text{CDCl}_3$ )  
8.42, 8.37 (s, 2H, 2H); 8.05 (s, 2H, 4H); 7.77-6.81(m, 32H, Har, 5H, 6H, 7H);  
5.93, 5.86(d,  $J=5.72\text{Hz}$ ,  $J=7.08\text{Hz}$ , 2H, 1H'); 4.75 (m, 2H, 2H'); 4.40 (m, 2H,  
3H'); 3.95 (m, 2H, 4H'); 3.80, 3.79(s, 12H, 2OCH<sub>3</sub>); 3.46(m, 4H, 5'CH<sub>2</sub>);  
2.66(m, 4H, OCH<sub>2</sub>); 1.20(m, 12H, CH(CH<sub>3</sub>)<sub>2</sub>); 0.75( s, 18H, Si(CH<sub>3</sub>)<sub>3</sub>); -0.14( s,  
6H, SiCH<sub>3</sub>); -0.39( s, 6H, SiCH<sub>3</sub>);

$^{31}\text{P}$  NMR :  $\delta$  [ppm] (162 MHz,  $\text{CDCl}_3$ )  
155.2 and 153.03 (ratio 1:5.5)

ESI (+):  $m/z$  937.1 ( $[\text{M}+\text{H}]^+$ );

## 1-Methyl-ribofuranose 80



164.16 g/mol

10 g (66.6 mmol)  $\beta$ -D-Ribofuranose was dissolved in 140 ml abs. methanol and cooled to 0°C. Then 0.6 ml conc.  $\text{H}_2\text{SO}_4$  were added and the reaction was stirred for 24 hours at 4°C. The reaction mixture was neutralized with amberlite IRA-93 filtrated on vacuum and the filtrate was evaporated to dryness. The product was obtained as light yellow oil, which contains both C (1) epimeres and crystallizes upon storage.

Yield: 10.92 g (99.9 %)

TLC:  $R_f = 0.52$  ( $\beta$ );  $0.45$  ( $\alpha$ ) ( $\text{CH}_3\text{CN}/\text{H}_2\text{O}$  4:1)

$^1\text{H-NMR}$ :  $\delta$  [ppm] (250 MHz,  $\text{D}_2\text{O}$ )

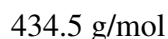
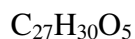
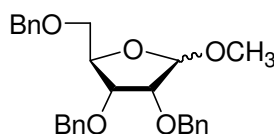
5.03 (d,  $J = 4.3$  Hz, 1H, 1H ( $\alpha$ )); 4.93 (d,  $J = 0.8$  Hz, 1H, 1H ( $\beta$ )); 4.21 – 3.49 (m, 16H, 2H, 3H, 4H, 5H, 2-OH, 3-OH, 5-OH ( $\alpha+\beta$ )); 3.47 (s, 3H,  $\text{OCH}_3$  ( $\alpha$ )), 3.44 (s, 3H,  $\text{OCH}_3$  ( $\beta$ ));

$^{13}\text{C-NMR}$ :  $\delta$  [ppm] (62.9 MHz,  $\text{D}_2\text{O}$ )

107.80 (C1 ( $\beta$ )); 103.04 (C1 ( $\alpha$ )); 84.36 (C4 ( $\alpha$ )); 82.68 (C4 ( $\beta$ )); 74.05 (C2 ( $\beta$ )); 70.95 (C2 ( $\alpha$ )); 70.63 (C3 ( $\beta$ )); 69.55 (C3 ( $\alpha$ )); 62.61 (C5 ( $\beta$ )); 61.38 (C5 ( $\alpha$ )); 55.28 ( $\text{OCH}_3$  ( $\alpha$ )); 55.00 ( $\text{OCH}_3$  ( $\beta$ ))

ESI (-):  $m/z$  163.0 ( $[\text{M-H}]^-$ );

**1-Methyl-2,3,5-tri-*O*-benzyl-ribofuranose 81**



10.9 g (66.4 mmol) 1-Methyl-ribofuranose **80** were dissolved in 100 ml THF and 50 g (891 mmol) of powdered KOH and 70 ml of benzyl chloride were added. The reaction mixture was refluxed for 24 hours. After cooling to room temperature the reaction mixture was filtrated and the filtrate evaporated under reduced pressure. Most side products were removed while heating up to 170°C on the oil bath. Purification of the crude product was done by FC using methylene chloride/methanol 98:2 as eluent. The product was obtained as light yellow oil, which contains both C (1) epimeres.

Yield: 24.7 g (85.7 %)

TLC:  $R_f = 0.55$  ( $\alpha$ );  $0.49$  ( $\beta$ ) ( $\text{CH}_2\text{Cl}_2/\text{MeOH}$  98:2)

$^1\text{H-NMR}$ :  $\delta$  [ppm] (250 MHz,  $\text{CDCl}_3$ )

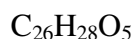
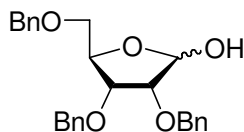
7.38 – 7.24 (m, 30 H,  $\text{H}_{\text{ar}}(\alpha+\beta)$ ); 4.91 (d,  $J = 0.8$  Hz, 1H, 1H( $\beta$ )); 4.87 (d,  $J = 4.0$  Hz, 1H, 1H( $\alpha$ )); 4.64 – 4.42 (m, 12H,  $\text{CH}_2$ -benzyl ( $\alpha+\beta$ )); 4.34 (m, 1H, 4H( $\beta$ )); 4.24 (m, 1H, 4H( $\alpha$ )); 4.01 (dd,  $J = 4.7$  Hz,  $J = 7.0$  Hz, 1H, 3H( $\beta$ )); 3.83 (dd,  $J = 1.0$  Hz,  $J = 4.7$  Hz, 1H, 2H( $\beta$ )); 3.77 (m, 2H, 2H( $\alpha$ ), 3H( $\alpha$ )); 3.55 (m, 2H, 5H( $\beta$ )); 3.46 (s, 3H,  $\text{OCH}_3(\alpha)$ ); 3.37 (m, 2H, 5H( $\alpha$ )); 3.30 (s, 3H,  $\text{OCH}_3(\beta)$ )

$^{13}\text{C-NMR}$ :  $\delta$  [ppm] (62.9 MHz,  $\text{CDCl}_3$ )

138.21 ( $\text{C}_{\text{ar}}$ ); 137.73 ( $\text{C}_{\text{ar}}$ ); 128.25 ( $\text{C}_{\text{ar}}$ ); 128.21 ( $\text{C}_{\text{ar}}$ ); 128.16 ( $\text{C}_{\text{ar}}$ ); 127.80 ( $\text{C}_{\text{ar}}$ ); 127.73 ( $\text{C}_{\text{ar}}$ ); 127.65 ( $\text{C}_{\text{ar}}$ ); 127.63 ( $\text{C}_{\text{ar}}$ ); 127.62 ( $\text{C}_{\text{ar}}$ ); 127.48 ( $\text{C}_{\text{ar}}$ ); 127.43 ( $\text{C}_{\text{ar}}$ ); 127.35 ( $\text{C}_{\text{ar}}$ ); 106.25 (C1); 80.35 (C4); 79.62 ( $\text{CH}_2$ -benzyl); 78.29 ( $\text{CH}_2$ -benzyl); 73.03 ( $\text{CH}_2$ -benzyl); 72.29 (C3); 72.17 (C2); 71.21 (C5); 54.91 ( $\text{OCH}_3$ )

ESI(+):  $m/z$  452.1 ( $[\text{M}+\text{NH}_4]^+$ );

## 2,3,5-Tri-*O*-benzyl-ribofuranose **82**



420.48 g/mol

19.9 g (45.8 mmol) 1-Methyl-2,3,5-tri-*O*-benzyl-ribofuranose **81** were dissolved in 350 ml of dioxane and 150 ml 0,1 N HCl solution and reaction mixture was refluxed for 20 hours. After cooling to room temperature 15 ml of 1 N NaOH were added to neutralise the solution and the reaction was evaporated to dryness. Left oil was extracted with methylene chloride three times, dried over  $\text{MgSO}_4$  and evaporated under reduced pressure. The purification was done by FC with methylene chloride/methanol 98:2 as eluent. The product was obtained as light yellow oil which contains both C (1) epimeres.

Yield: 18.02 g (93.6 %)

TLC:  $R_f = 0.32$  ( $\text{CH}_2\text{Cl}_2/\text{MeOH}$  98:2)

$^1\text{H-NMR}$ :  $\delta$  [ppm] (250 MHz,  $\text{CDCl}_3$ )

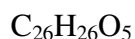
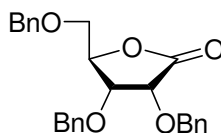
7.36 – 7.19 (m, 15H,  $H_{ar}$ ); 5.28 (m, 1H, 1H); 4.70 – 4.26 (m, 7H,  $\text{CH}_2$ -benzyl, 1-OH); 4.19 (m, 1H, 4H); 3.96 (m, 1H, 3H); 3.73 (m, 1H, 2H); 3.44 (m, 2H, 5H)

$^{13}\text{C-NMR}$ :  $\delta$  [ppm] (62.9 MHz,  $\text{CDCl}_3$ )

137.75 ( $C_{ar}$ ); 137.68 ( $C_{ar}$ ); 137.61 ( $C_{ar}$ ); 137.34 ( $C_{ar}$ ); 137.24 ( $C_{ar}$ ); 128.33 ( $C_{ar}$ ); 128.30 ( $C_{ar}$ ); 128.26 ( $C_{ar}$ ); 127.68 ( $C_{ar}$ ); 127.79 ( $C_{ar}$ ); 127.71 ( $C_{ar}$ ); 127.64 ( $C_{ar}$ ); 127.57 ( $C_{ar}$ ); 127.43 ( $C_{ar}$ ); 100.21, 96.09 ( $C_1$ ); 80.90, 80.67 ( $C_4$ ); 77.64 ( $\text{CH}_2$ -benzyl); 77.58 ( $\text{CH}_2$ -benzyl); 77.16 ( $\text{CH}_2$ -benzyl); 73.35, 72.67 ( $C_3$ ); 72.32, 72.15 ( $C_2$ ); 69.88, 69.42 ( $C_5$ )

ESI (+):  $m/z$  438.3 ( $[\text{M}+\text{NH}_4]^+$ );

**2,3,5-Tri-*O*-benzyl-ribo- $\gamma$ -lacton 83**



418.47 g/mol

17.71 g (42.1 mmol) 2,3,5-Tri-*O*-benzyl-ribofuranose **82** were dissolved in 60 ml of DMSO and 42 ml of acetic anhydride were added. The reaction mixture was stirred at room temperature 24 hours and poured in icewater. It was extracted three times with methylene chloride and with saturated solution of NaHCO<sub>3</sub>. Organic phases were collected and dried over MgSO<sub>4</sub> and evaporated to dryness. Left DMSO was evaporated under reduced pressure (oil pump vacuum). Further purification was done by FC using methylene chloride/methanol 99:1 as eluent. The product was obtained as yellow oil, which crystallizes upon storage.

Yield: 16.84 g (95.5 %)

TLC: R<sub>f</sub> = 0.70 (CH<sub>2</sub>Cl<sub>2</sub>/MeOH 98:2)

<sup>1</sup>H-NMR:  $\delta$  [ppm] (250 MHz, CDCl<sub>3</sub>)

7.29 – 7.07 (m, 15H, H<sub>ar</sub>); 4.87 und 4.66 (AB, J<sub>a,b</sub> = 12.0 Hz, 2H, CH<sub>2</sub>-benzyl)

4.61 und 4.48 (AB, J<sub>a,b</sub> = 9.0 Hz, 2H, CH<sub>2</sub>-benzyl); 4.47 – 4.31 (m, 4H, 2H,

4H, CH<sub>2</sub>-benzyl); 4.02 (dd, J = 2.1 Hz, J = 5.6 Hz, 1H, 3H); 3.50 ( $\psi$ dq, J = 2.8

Hz, J = 11.0 Hz, J = 14.5 Hz, 2H, 5H);

<sup>13</sup>C-NMR:  $\delta$  [ppm] (62.9 MHz, CDCl<sub>3</sub>)

173.52 (C1); 137.12 (C<sub>ar</sub>); 137.00 (C<sub>ar</sub>); 136.83 (C<sub>ar</sub>); 128.39 (C<sub>ar</sub>); 128.35

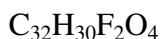
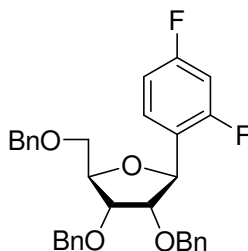
(C<sub>ar</sub>); 128.34 (C<sub>ar</sub>); 128.25 (C<sub>ar</sub>); 128.10 (C<sub>ar</sub>); 127.95 (C<sub>ar</sub>); 127.90 (C<sub>ar</sub>);

127.83 (C<sub>ar</sub>); 127.63 (C<sub>ar</sub>); 127.45 (C<sub>ar</sub>); 81.64 (C4); 75.26 (C3); 73.61 (C2);

73.50 (CH<sub>2</sub>-benzyl); 72.58 (CH<sub>2</sub>-benzyl); 72.25 (CH<sub>2</sub>-benzyl); 68.62 (C5);

ESI(+): m/z 436.4 ([M+NH<sub>4</sub>]<sup>+</sup>);

**2',3',5'-Tri-*O*-benzyl-1'-deoxy-1'-(2,4-difluorophenyl)- $\beta$ -D-ribofuranose 139**



516.56 g/mol

To the solution that contains 150  $\mu\text{l}$  (1.3 mmol) 1-bromo-2, 4-difluorbenzol in 10 ml abs. diethyl ether at  $-78^\circ\text{C}$  under argon over 10 minutes 2.4 ml of 1.6 M solution of *n*-butyl lithium in *n*-hexane were added. After 20 minutes at  $-78^\circ\text{C}$  solution of 2,3,5-tri-*O*-benzyl-ribo- $\gamma$ -lacton **83** (1.0 g, 2.4 mmol) in 5 ml abs. diethyl ether over 30 minutes was added and 1 hour stirred at  $-78^\circ\text{C}$ . Afterwards the reaction mixture was allowed to warm up to  $-20^\circ\text{C}$  over two hours. The reaction was stopped by adding 5 ml of water and three times extracted with etar. The combined organic phases were dried over  $\text{MgSO}_4$  and evaporated to dryness. Left oil was immediately dissolved in 10 ml of methylene chloride, cooled to  $-78^\circ\text{C}$  and 600  $\mu\text{l}$  (4.8 mmol) bortrifluorid -ethyletherat and 760  $\mu\text{l}$  (4.8 mmol) triethylsilane were added. The reaction mixture was left at  $-78^\circ\text{C}$  and allowed to warm up to  $10^\circ\text{C}$  over night. The reaction was stopped by adding 10 ml of saturated water solution of  $\text{NaHCO}_3$  and extracted three times with methylene chloride. The combined organic phases were dried over  $\text{MgSO}_4$  and evaporated under reduced pressure. Further purification was done by FC using *n*-hexane/ethyl acetate 4:1 as eluent. The product was obtained as light orange solid.

Yield: 1.04 g (84.6 %)

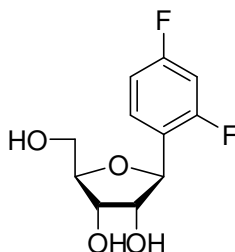
TLC:  $R_f = 0.35$  (*n*-hexane/ethyl acetate 4:1)

$^1\text{H-NMR}$ :  $\delta$  [ppm] (270 MHz,  $\text{DMSO-d}_6$ )

7.59 ( $\Psi_q$ ,  $J = 6.9$  Hz, 1H, 6H); 7.29 (m, 16H,  $\text{H}_{ar}$ , 3H); 6.93 (dt,  $J = 8.4$  Hz,  $J = 2.2$  Hz, 1H, 5H); 5.17 (d,  $J = 4.5$  Hz, 1H, 1'H); 4.55 (m, 6H,  $\text{CH}_2$ -benzyl); 4.22 (q,  $J = 3.9$  Hz, 1H, 4'H); 4.05 (m, 2H, 2'H, 3'H); 3.67 (m, 2H, 5'H);

$^{13}\text{C-NMR}$ :  $\delta$  [ppm] (67.9 MHz, DMSO- $d_6$ )  
 162.51 (C4); 158.87 (C2); 138.18 (C<sub>ar</sub>); 138.10 (C<sub>ar</sub>); 137.96 (C<sub>ar</sub>); 129.36 (C6); 128.22 (C<sub>ar</sub>); 128.09 (C<sub>ar</sub>); 127.70 (C<sub>ar</sub>); 127.50 (C<sub>ar</sub>); 127.42 (C<sub>ar</sub>); 127.11 (C<sub>ar</sub>); 123.61 (C1); 111.30 (C5); 103.62 (C3); 82.10 (C1'); 80.72 (C4'); 76.84 (C2'); 75.96 (C3'); 72.40 (CH<sub>2</sub>-benzyl); 71.04 (CH<sub>2</sub>-benzyl); 69.73 (C5');  
 ESI(+): m/z 534.4 ([M+NH<sub>4</sub>]<sup>+</sup>);

**1'-Deoxy-1'-(2,4-difluorophenyl)- $\beta$ -D-ribofuranose 9**



$\text{C}_{11}\text{H}_{12}\text{F}_2\text{O}_4$

246.2 g/mol

6.5 g (12.6 mmol) 2', 3', 5'-Tri-*O*-benzyl-1'-deoxy-1'-(2,4-difluorophenyl)- $\beta$ -D-ribofuranose **139** was dissolved in 100 ml abs. ethanol and 50 ml cyclohexene and 1 g palladium-hydroxide (20%) on carbon was added. The reaction mixture was refluxed for 3 hours. Then the reaction mixture was filtrated over celite and filtrate was evaporated under reduced pressure. The purification was done by FC with methylene chloride/methanol 9:1, as eluent. Product was obtained as colourless solid. For analytical purposes the product was crystallized from water and methanol.

Yield: 3.08 g (99.3 %)

TLC:  $R_f = 0.42$  (CH<sub>2</sub>Cl<sub>2</sub>/MeOH 9:1)

$^1\text{H-NMR}$ :  $\delta$  [ppm] (270 MHz, DMSO- $d_6$ )



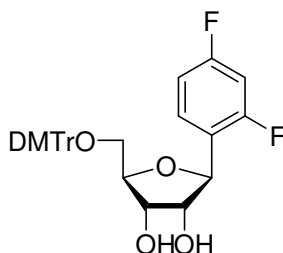
7.65 (Ψq, J = 6.9 Hz, 1H, 6H); 7.18 (m, 1H, 3H); 7.07 (dt, J = 8.6 Hz, J = 2.4 Hz, 1H, 5H); 5.04 (d, J = 6.0 Hz, 1H, 2'-OH); 4.91 (d, J = 5.0 Hz, 3'-OH); 4.84 (m, 2H, 1'H, 5'-OH); 3.85 (m, 3H, 2'H, 3'H, 4'H); 3.57 (m, 2H, 5'H)

<sup>13</sup>C-NMR: δ [ppm] (67.9 MHz, DMSO-d<sub>6</sub>)  
162.58 (C4); 158.94 (C2); 129.67 (C6); 124.40 (C1); 114.74 (C5); 103.42 (C3); 84.59 (C1'); 77.08 (C4'); 76.65 (C2'); 70.94 (C3'); 61.59 (C5')

<sup>19</sup>F-NMR: δ [ppm] (254.2 MHz, DMSO-d<sub>6</sub>)  
-112.0 (1F, 4F); -114.74 (1F, 2F)

ESI(-): m/z 245.0 ([M-H]<sup>-</sup>);

**5'-O-(4,4'-Dimethoxytriphenylmethyl)-1'-deoxy-1'-(2,4-difluorophenyl)-β-D-ribofuranose 140**



C<sub>32</sub>H<sub>30</sub>F<sub>2</sub>O<sub>6</sub>

548.56 g/mol

1.0 g (4.0 mmol) 1'-Deoxy-1'-(2,4-difluorophenyl)-β-D-ribofuranose **9** was dissolved in 25 ml abs. pyridine and 0.84 ml (6.0 mmol) triethylamine and 1.63 g (4.8 mmol) 4,4'-dimethoxytriphenylmethylchloride were added. The reaction mixture was stirred under argon at RT for 2.5 hours. The reaction was stopped by adding of 3 ml of methanol and saturated water solution of NaHCO<sub>3</sub>. It was extracted with methylene chloride three times, organic phases were collected and dried over MgSO<sub>4</sub> and than evaporated to dryness. The product was twice co-evaporated with toluene. Further purification was done by FC with methylene chloride/methanol 98:2 as eluent. The product was obtained as yellow foam.

Yield: 1.86 g (83.4 %)

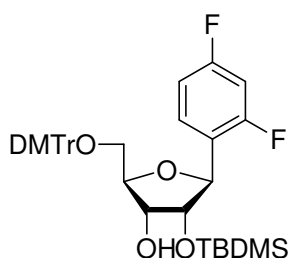
TLC:  $R_f = 0.48$  ( $\text{CH}_2\text{Cl}_2/\text{MeOH}$  95:5)

$^1\text{H-NMR}$ :  $\delta$  [ppm] (270 MHz,  $\text{DMSO-}d_6$ )  
 7.56 ( $\Psi_q$ ,  $J = 6.8$  Hz, 1H, 6H); 7.45 – 6.86 (m, 15H,  $\text{H}_{\text{ar}}$ , 3H, 5H); 5.19 (d,  $J = 5.4$  Hz, 1H, 2'-OH); 4.98 (d,  $J = 5.2$  Hz, 1H, 3'-OH); 4.92 (d,  $J = 4.3$  Hz, 1H, 1'H); 3.98 (q,  $J = 5.2$  Hz, 1H, 2'H); 3.90 (m, 2H, 3'H, 4'H); 3.74 (s, 6H,  $\text{OCH}_3$ ); 3.20 (m, 2H, 5'H)

$^{13}\text{C-NMR}$ :  $\delta$  [ppm] (67.9 MHz,  $\text{DMSO-}d_6$ )  
 161.71 (C4); 161.53 (C2); 158.04 (DMTr); 144.87 (DMTr); 135.63 (DMTr); 135.54 (DMTr); 129.71 (DMTr); 129.11 (C6); 127.76 (DMTr); 127.72 (DMTr); 126.63 (DMTr); 124.28 (C1); 113.13 (DMTr); 111.12 (C5); 103.69 (C3); 85.40 (DMTr); 82.25 (C1'); 78.10 (C4'); 76.36 (C2'); 70.93 (C3'); 63.77 (C5'); 54.98 ( $\text{OCH}_3$ )

ESI(-):  $m/z$  547.2 ( $[\text{M-H}]^-$ );

**5'-O-(4,4'-Dimethoxytriphenylmethyl)-2'-O-*tert.*-butyldimethylsilyl-1'-deoxy-1'-(2,4-difluorophenyl)- $\beta$ -D-ribofuranose 141**



$\text{C}_{38}\text{H}_{44}\text{F}_2\text{O}_6\text{Si}$

668.1 g/mol

2.35 g (4.3 mmol) 5'-O-(4,4'-Dimethoxytriphenylmethyl)-1'-deoxy-1'- $\beta$ -D-(2,4-difluorophenyl)-ribofuranose **140** were dissolved in 40 ml of 1:1 mixture of THF/pyridine and with 870 mg (5.2 mmol)  $\text{AgNO}_3$  and 6.0 ml (6.0 mmol) 1 M *tert.*-butyldimethylsilylchloride-solution in THF were added. The reaction mixture was stirred for 20 hours at RT under argon. Adding 10ml of saturated water  $\text{NaHCO}_3$ -solution stopped the

reaction. Left AgCl was filtered over celite and filtrate was extracted with methylene chloride three times. Collected organic phases were dried over MgSO<sub>4</sub> and evaporated to dryness. The crude product was co-evaporated with toluene twice. Further purification of the product was done by FC with methylene chloride as eluent. The product was obtained as white foam.

Yield: 1.01 g (35.5 %)

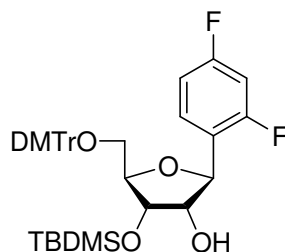
TLC: R<sub>f</sub> = 0.18 (CH<sub>2</sub>Cl<sub>2</sub>)

<sup>1</sup>H-NMR: δ [ppm] (270 MHz, DMSO-*d*<sub>6</sub>)  
7.59 (q, J = 6.7 Hz, 1H, 6H); 7.45 – 6.82 (m, 15H, H<sub>ar</sub>, 3H, 5H); 4.96 (d, J = 5.7 Hz, 1H, 3'-OH); 4.84 (d, J = 5.7 Hz, 1H 1'H); 4.02 (m, 2H, 3'H, 4'H); 3.93 (t, J = 5.2 Hz, 1H, 2'H); 3.74 (s, 6H, OCH<sub>3</sub>); 3.21 (m, 2H, 5'H); 0.79 (s, 9H, SiC(CH<sub>3</sub>)<sub>3</sub>); -0.05 (SiCH<sub>3</sub>); -0.11 (SiCH<sub>3</sub>)

<sup>13</sup>C-NMR: δ [ppm] (67.9 MHz, DMSO-*d*<sub>6</sub>)  
161.69 (C2); 161.51 (C4); 158.04 (DMTr); 144.87 (DMTr); 135.46 (DMTr); 135.41 (DMTr); 129.71 (DMTr); 129.68 (DMTr); 129.07 (dd, J = 11.6 Hz, J = 7.8 Hz, C6); 127.73 (DMTr); 127.62 (DMTr); 123.85 (C1); 113.12 (DMTr); 111.12 (C5); 103.61 (C3); 85.45 (DMTr); 82.94 (C1'); 78.79 (C4'); 77.20 (C2'); 70.20 (C3'); 63.51 (C5'); 54.97 (OCH<sub>3</sub>); 25.50 (SiC(CH<sub>3</sub>)<sub>3</sub>); 17.78 (SiC(CH<sub>3</sub>)<sub>3</sub>); -4.93 (SiCH<sub>3</sub>); -5.47 (SiCH<sub>3</sub>)

ESI(-): m/z 661.6 ([M-H]<sup>-</sup>);

**5'-O-(4,4'-Dimethoxytriphenylmethyl)-3'-*tert.*-butyldimethylsilyl-1'-deoxy-1'-(2,4-difluorophenyl)- $\beta$ -D-ribofuranose 142**



$C_{38}H_{44}F_2O_6Si$

662.81 g/mol

5'-O-(4,4'-Dimethoxytriphenylmethyl)-3'-O-*tert.*-butyldimethylsilyl-1'-deoxy-1'-(2,4-difluorophenyl)- $\beta$ -D-ribofuranose 142 was obtained as a side product while synthesizing 5'-O-(4,4'-Dimethoxytriphenylmethyl)-2'-O-*tert.*-butyldimethylsilyl-1'-deoxy-1'-(2,4-difluorophenyl)- $\beta$ -D-ribofuranose 141.

Yield: 890 mg (31.4 %)

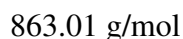
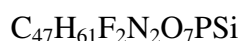
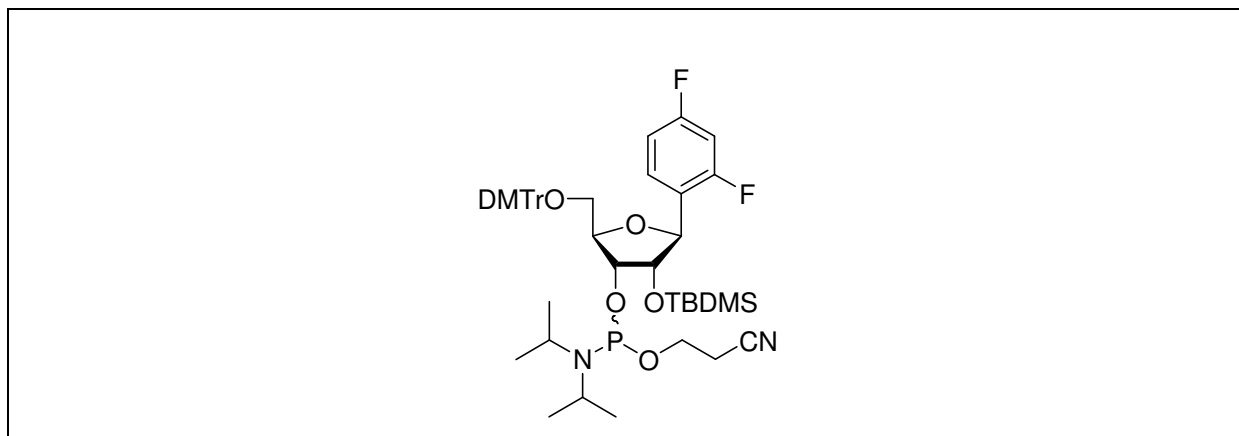
TLC:  $R_f = 0.21$  ( $CH_2Cl_2$ )

$^1H$ -NMR:  $\delta$  [ppm] (270 MHz, DMSO- $d_6$ )  
 7.61 (q,  $J = 8.2$  Hz, 1H, 6H); 7.45 – 6.84 (m, 15H,  $H_{ar}$ , 3H, 5H); 4.96 (d,  $J = 6.6$  Hz, 1H, 2'OH); 4.83 (d,  $J = 5.6$  Hz, 1H, 1'H); 4.02 (m, 1H, 3'H); 3.94 (m, 1H; 2'H); 3.73 (s, 6H, OCH<sub>3</sub>); 3.29 (m, 1H, 4'H); 3.15 (m, 2H, 5'H); 0.76 (SiC(CH<sub>3</sub>)<sub>3</sub>); -0.01 (SiCH<sub>3</sub>); -0.08 (SiCH<sub>3</sub>)

$^{13}C$ -NMR:  $\delta$  [ppm] (67.9 MHz, DMSO- $d_6$ )  
 161.65 (C2); 161.49 (C4); 158.05 (DMTr); 144.67 (DMTr); 135.46 (DMTr); 135.42 (DMTr); 129.67 (DMTr); 129.13 (C6); 127.71 DMTr); 127.63 (DMTr); 126.63 (DMTr); 123.82 (C1); 113.11 (DMTr); 111.30 (C5); 103.59 (C3); 85.46 (DMTr); 82.52 (C1'); 78.29 (C4'); 75.94 (C2'); 72.63 (C3'); 63.21 (C5'); 54.97 (OCH<sub>3</sub>); 25.64 (SiC(CH<sub>3</sub>)<sub>3</sub>); 17.82 (SiC(CH<sub>3</sub>)<sub>3</sub>); -4.59 (SiCH<sub>3</sub>); -5.21 (SiCH<sub>3</sub>)

ESI(-):  $m/z$  661.4 ([M-H]<sup>-</sup>);

**3'-O-(2-Cyanethoxydiisopropylphosphin)-1'-deoxy-5'-O-(4,4'-dimethoxy-triphenylmethyl)-1'-(2,4-difluorophenyl)-2'-O-*tert.*-butyldimethylsilyl- $\beta$ -D-ribofuranose 143**



250 mg (0.38 mmol) 5'-O-(4,4'-Dimethoxytriphenylmethyl)-2'-O-*tert.*-butyldimethylsilyl-1'-deoxy-1'-(4,6-difluorobenzimidazolyl)- $\beta$ -D-ribofuranose 141 were dissolved in 12 ml abs. acetonitrile and 500  $\mu\text{l}$  (3.8 mmol) *sym.* collidine and 15  $\mu\text{l}$  (0.19 mmol) 1-methylimidazole were added. The reaction mixture was cooled in an icebath to 0°C and 128  $\mu\text{l}$  (0.43 mmol) 2-cyanethyldiisopropylchlorphosphoramidit 96 were added. The reaction was stirred for 15 min. at 0°C and for 1 hour. At RT. The reaction was stopped by adding of 10 ml of 0.01 M citric acid and three times extracted with methylene chloride. Combined organic phases were washed twice with 0.01 M citric acid, dried over  $\text{MgSO}_4$  and evaporated to dryness. Purification was done by FC with *n*-hexane/ethyl acetate, 4:1, as eluent. The product (mixture of two diastereomers) was obtained as white foam.

Yield: 250 mg (76.8 %)

TLC:  $R_f = 0.34; 0.36$  (*n*-hexan/ethylacetat 4:1)

$^1\text{H-NMR}$ :  $\delta$  [ppm] (270 MHz,  $\text{DMSO-d}_6$ )

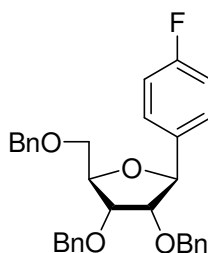
7.67 (m, 2H, 6H); 7.53 – 6.77 (m, 30H,  $H_{ar}$ , 3H, 5H); 5.14, 5.12 (d,  $J = 7.7$  Hz,  $J = 6.8$  Hz, 2H, 1'H); 4.23 (m, 6H, 2'H, 3'H, 4'H); 3.80, 3.79 (s, 12H,  $\text{OCH}_3$ );

3.54 (m, 4H, 5'H); 1.17 (m, 12H, CH(CH<sub>3</sub>)<sub>2</sub>); 0.82 (s, 18H, SiC(CH<sub>3</sub>)<sub>3</sub>); -0.05 (s, 6H, SiCH<sub>3</sub>); -0.17 (s, 6H, SiCH<sub>3</sub>)

<sup>31</sup>P-NMR: δ [ppm] (162 MHz, CDCl<sub>3</sub>)  
150.70 and 148.85 (ratio 1 : 3.8)

ESI(+): m/z 863.6 ([M+H]<sup>+</sup>);

### 2',3',5'-Tri-*O*-benzyl-1'-deoxy-1'-(4-fluorophenyl)-β-D-ribofuranose 144



C<sub>32</sub>H<sub>31</sub>FO<sub>4</sub>

498.57 g/mol

To the solution that contains 2.73 ml (25 mmol) 1-Bromo-4-fluorobenzene in 80 ml THF was stirred at -78°C under argon over 10 minutes and 15.6 ml 1.6 M solution of *n*-butyl lithium in *n*-hexane were added. After 20 minutes at -78°C a solution of 2,3,5-tri-*O*-benzyl-ribo-γ lacton **83** (7.0 g, 16.7 mmol) in 50 ml THF was added over 30 minutes (via cannula) and 1 hour stirred at -78°C. Afterwards the reaction mixture was allowed to warm up to -20°C over two hours. The reaction was stopped by adding 30 ml of water and three times extracted with ether. The collected organic phases were dried over MgSO<sub>4</sub> and evaporated to dryness. Left oil was immediately dissolved in 10 ml of methylene chloride, cooled to -78°C and 4.2 ml (33.4 mmol) boron trifluoride etherate and 5.3 ml (33.4 mmol) triethylsilane were added. The reaction mixture was left at -78°C and over night allowed to warm up to 10°C. The reaction was stopped by adding of 10 ml of saturated water solution of NaHCO<sub>3</sub>, extracted three times with methylene chloride. The combined organic phases were dried over MgSO<sub>4</sub> and evaporated under reduced pressure. Further purification was done by FC using *n*-hexan/ethyl acetate 4:1 as eluent. The product was obtained as light orange solid.

Yield: 6.31 g (75.8 %)

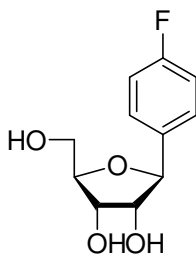
TLC:  $R_f = 0.35$  (*n*-hexane/ethyl acetate 4:1)

$^1\text{H-NMR}$ :  $\delta$  [ppm] (250 MHz, DMSO- $d_6$ )  
 7.44 – 7.08 (m, 19H,  $H_{ar}$ ); 4.87 (d,  $J = 6.8$  Hz, 1H,  $1'H$ ); 4.61 – 4.42 (m, 6H,  $\text{CH}_2$ -benzyl); 4.24 (q,  $J = 3.8$  Hz, 1H,  $4'H$ ); 4.07 (dd,  $J = 4.8$  Hz, 3.8 Hz, 1H,  $3'H$ ); 3.87 (dd,  $J = 5.0$  Hz,  $J = 6.8$  Hz, 1H,  $2'H$ ); 3.64 (m, 2H,  $5'H$ )

$^{13}\text{C-NMR}$ :  $\delta$  [ppm] (67.9 MHz, DMSO- $d_6$ )  
 138.19 ( $C_{ar}$ ); 137.95 ( $C_{ar}$ ); 136.63 ( $C1$ ); 128.18 ( $C_{ar}$ ); 128.11 ( $C_{ar}$ ); 128.05 ( $C_{ar}$ ); 127.74 ( $C_{ar}$ ); 127.43 ( $C_{ar}$ ); 127.36 ( $C_{ar}$ ); 123.99 ( $C5$ ); 114.95 ( $C2$ ); 114.64 ( $C6$ ); 83.41 ( $C1'$ ); 81.23 ( $C4'$ ); 81.08 ( $C2'$ ); 77.27 ( $C3'$ ); 72.41 ( $\text{CH}_2$ -benzyl); 71.10 ( $\text{CH}_2$ -benzyl); 70.96 ( $\text{CH}_2$ -benzyl); 70.27 ( $C5'$ )

ESI(+):  $m/z$  516.2 ( $[\text{M}+\text{H}]^+$ );

### 1'-Deoxy-1'-(4-fluorophenyl)- $\beta$ -D-ribofuranose 36



$\text{C}_{11}\text{H}_{13}\text{FO}_4$

228.21 g/mol

3.0 g (6.0 mmol) 2',3',5'-Tri-*O*-benzyl-1'-deoxy-1'-(4-fluorophenyl)- $\beta$ -D-ribofuranose 144 were dissolved in 60 ml abs. ethanol and 30 ml cyclohexene and 600 mg palladium-hydroxide (20%) on carbon were added. The reaction mixture was refluxed for 5 hours. Then the reaction mixture was filtrated over celite and the filtrate was evaporated under reduced pressure. Purification was done by FC with methylene chloride/methanol 9:1 as eluent. The product was obtained as colourless solid. For analytical purposes it was crystallized from water and methanol.

Yield: 1.36 g (99.5 %)

TLC:  $R_f = 0.39$  ( $\text{CH}_2\text{Cl}_2/\text{MeOH}$  9:1)

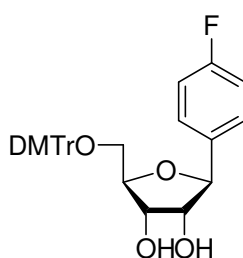
$^1\text{H-NMR}$ :  $\delta$  [ppm] (250 MHz,  $\text{DMSO-}d_6$ )  
 7.42 (m, 2H,  $\text{H}_{\text{ar}}$ ); 7.14 (m, 2H,  $\text{H}_{\text{ar}}$ ); 4.97 (d,  $J = 7.0$  Hz, 1H, 1'H); 4.91 (d,  $J = 4.7$  Hz, 1H, 3'-OH); 4.82 (t,  $J = 5.5$  Hz, 1H, 5'-OH); 4.56 (d,  $J = 7.3$  Hz, 1H, 2'-OH); 3.89 (m, 1H, 3'H); 3.81 (m, 1H, 4'H); 3.66 (m, 1H, 2'H); 3.54 (m, 2H, 5'H)

$^{13}\text{C-NMR}$ :  $\delta$  [ppm] (67.9 MHz,  $\text{DMSO-}d_6$ )  
 137.72 (C1); 128.06 (C3); 114.79 (C2); 114.47 (C6); 85.18 (C1'); 82.21 (C4'); 77.55 (C2'); 71.35 (C3'); 61.97 (C5')

$^{19}\text{F-NMR}$ :  $\delta$  [ppm] (254.2 MHz,  $\text{DMSO-}d_6$ )  
 -115.87 (1F, 4F)

ESI(-):  $m/z$  227.0 ( $[\text{M-H}]^-$ );

**5'-O-(4,4'-Dimethoxytriphenylmethyl)- 1'-deoxy-1'-(4-fluorophenyl)- $\beta$ -D-ribofuranose 145**



$\text{C}_{32}\text{H}_{31}\text{FO}_6$

530.57 g/mol

1.37 g (6.0 mmol) 1'-Deoxy-1'-(4-fluorophenyl)- $\beta$ -D-ribofuranose **36** were dissolved in 30 ml abs. pyridine and 1.25 ml (9.0 mmol) triethylamine and 2.44 g (7.2 mmol) 4,4'-dimethoxytriphenylmethylchloride were added. The reaction mixture was stirred under argon at RT for 4.5 hours. Adding 3 ml of methanol stopped the reaction and the saturated water solution of  $\text{NaHCO}_3$  was added. It was three times extracted with methylene chloride, organic phases were collected and dried over  $\text{MgSO}_4$  and then evaporated to dryness. The product was



twice co-evaporated with toluene. Further purification was done by FC with methylene chloride/methanol 98:2 as eluent. The product was obtained as yellow foam.

Yield: 2.52 g (79.1 %)

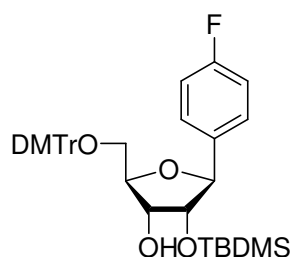
TLC:  $R_f = 0.37$  ( $\text{CH}_2\text{Cl}_2/\text{MeOH}$  98:2)

$^1\text{H-NMR}$ :  $\delta$  [ppm] (250 MHz,  $\text{DMSO-}d_6$ )  
 7.48 – 6.87 (m, 17H,  $\text{H}_{\text{ar}}$ ); 5.13 (d,  $J = 6.7$  Hz, 1H, 1'H); 5.01 (d,  $J = 5.1$  Hz, 1H, 3'-OH); 4.66 (d,  $J = 6.6$  Hz, 1H, 2'-OH); 3.98 (m, 1H, 4'H); 3.89 (q,  $J = 4.9$  Hz, 1H, 3'H); 3.74 (s, 7H, 2'H,  $\text{OCH}_3$ ); 3.18 m, 2H, 5'H)

$^{13}\text{C-NMR}$ :  $\delta$  [ppm] (62.9 MHz,  $\text{DMSO-}d_6$ )  
 158.07 (DMTr); 149.63 (C4); 144.95 (DMTr); 137.44 (C1); 135.63 (DMTr); 129.76 (DMTr); 127.84 (DMTr); 127.78 (DMTr); 126.68 (DMTr); 123.91 (C5); 115.03 (C2); 114.70 (C6); 113.18 (DMTr); 85.40 (DMTr); 83.19 (C1'); 82.69 (C4'); 77.60 (C2'); 71.42 (C3'), 64.14 (C5'); 55.03 ( $\text{OCH}_3$ )

ESI(-):  $m/z$  529.2 ( $[\text{M-H}]^-$ );

**5'-O-(4,4'-Dimethoxytriphenylmethyl)-2'-O-tert.-butyldimethylsilyl-1'-deoxy-1'-(4-fluorophenyl)- $\beta$ -D-ribofuranose 146**



$\text{C}_{38}\text{H}_{45}\text{FO}_6\text{Si}$

644.82 g/mol

530 mg (1.0 mmol) 5'-O-(4,4'-Dimethoxytriphenylmethyl)-1'-deoxy-1'- $\beta$ -D-(4-fluorophenyl)-ribofuranose 145 was dissolved in 10 ml of 1:1 mixture of THF/pyridine and with 204 mg (1.2 mmol)  $\text{AgNO}_3$  and 1.4 ml (1.4 mmol) 1 M *tert.*-Butyldimethylsilylchloride-

solution in THF were added. The reaction mixture was stirred for 20 hours at RT under argon. Adding 10ml of saturated water NaHCO<sub>3</sub>-solution stopped the reaction. Precipitated AgCl was filtered over celite and filtrate was extracted with methylene chloride three times. The combined organic phases were dried over MgSO<sub>4</sub> and evaporated to dryness. The crude product was twice co-evaporated with toluene. Further purification of product was done by FC with methylene chloride as eluent. The product was obtained as white foam.

Yield: 280 mg (43.5 %)

TLC: R<sub>f</sub> = 0.22 (CH<sub>2</sub>Cl<sub>2</sub>)

<sup>1</sup>H-NMR: δ [ppm] (400 MHz, DMSO-*d*<sub>6</sub>)

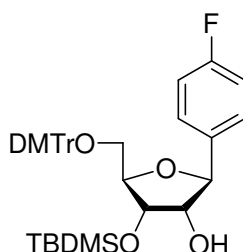
7.49 – 6.83 (m, 17H, H<sub>ar</sub>); 4.77 (d, J = 4.4 Hz, 1H, 3'-OH); 4.67 (d, J = 6.4 Hz, 1H, 1'H); 4.00 (m, 1H, 4'H); 3.93 (m, 2H, 2'H, 4'H); 3.73 (s, 6H, OCH<sub>3</sub>); 3.28 (m, 1H, 5'H); 3.15 (m, 1H, 5'H); 0.78 (s, 9H, SiC(CH<sub>3</sub>)<sub>3</sub>); -0.11 (s, 3H, SiCH<sub>3</sub>); -0.17 (s, 3H; SiCH<sub>3</sub>)

<sup>13</sup>C-NMR: δ [ppm] (100.6 MHz, DMSO-*d*<sub>6</sub>)

158.07 (DMTr); 144.96 (C4); 144.75 (DMTr); 137.22 (C1); 135.52 (DMTr); 135.44 (DMTr); 129.74 (DMTr); 129.71 (DMTr); 129.66 (DMTr); 128.88 (DMTr); 128.19 (DMTr); 127.89 (DMTr); 127.61 (DMTr); 126.67 (C3); 114.94 (C2); 114.73 (C6); 113.14 (DMTr); 85.57 (DMTr); 83.50 (C1'); 82.68 (C4'); 79.59 (C2'); 71.56 (C3'); 63.83 (C5'); 55.00 (OCH<sub>3</sub>); 25.57 (SiC(CH<sub>3</sub>)<sub>3</sub>); 17.85 (SiC(CH<sub>3</sub>)<sub>3</sub>); -5.07 (SiCH<sub>3</sub>); -5.30 (SiCH<sub>3</sub>)

ESI(-): m/z 643.0 ([M-H]<sup>-</sup>);

**5'-O-(4,4'-Dimethoxytriphenylmethyl)-3'-O-*tert.*-butyldimethylsilyl-1'-deoxy-1'-(4-fluorophenyl)- $\beta$ -D-ribofuranose 147**



$C_{38}H_{45}FO_6Si$

644.82 g/mol

5'-O-(4,4'-Dimethoxytriphenylmethyl)-3'-O-*tert.*-butyldimethylsilyl-1'-deoxy-1'-(4-fluorophenyl)- $\beta$ -D-ribofuranose 147 was obtained as a side product in the synthesis of 5'-O-(4,4'-Dimethoxytriphenylmethyl)-2'-O-*tert.*-butyldimethylsilyl-1'-deoxy-1'-(4-fluorophenyl)- $\beta$ -D-ribofuranose 146.

Yield: 270 mg (42.0 %)

TLC:  $R_f = 0.42$  ( $CH_2Cl_2$ )

$^1H$ -NMR:  $\delta$  [ppm] (400 MHz,  $DMSO-d_6$ )

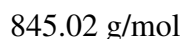
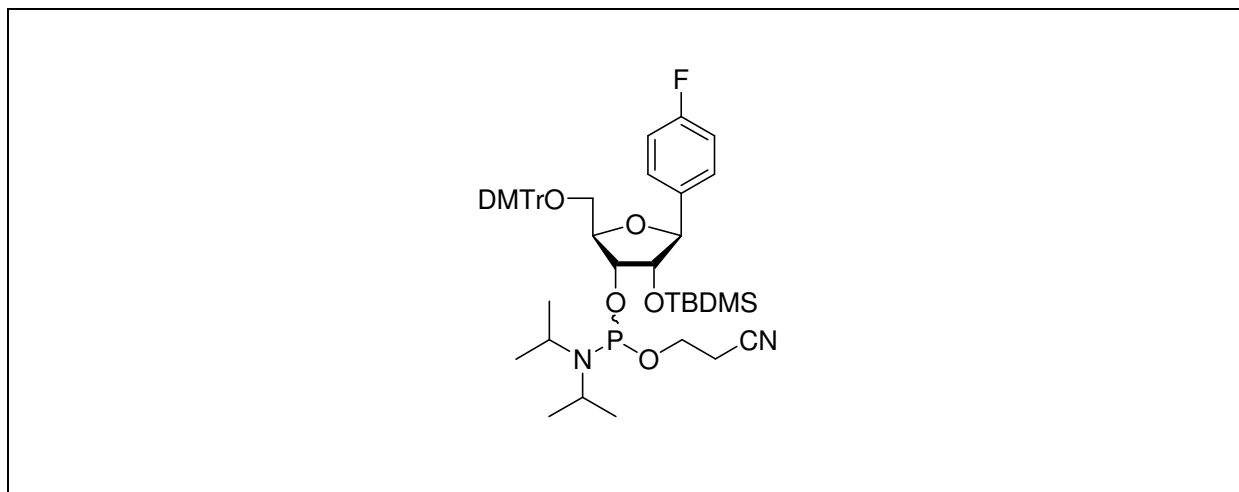
7.49 – 6.87 (m, 17H,  $H_{ar}$ ); 4.89 (d,  $J = 7.2$  Hz, 1H, 2'-OH); 4.66 (d,  $J = 6.7$  Hz, 1H, 1'H); 4.01 (m, 1H, 3'H); 3.94 (m, 1H, 4'H); 3.75 (m, 1H, 2'H); 3.73 (s, 6H,  $OCH_3$ ); 3.29 (m, 1H, 5'H); 3.09 (m, 1H, 5'H); 0.79 (s, 9H,  $SiC(CH_3)_3$ ); 0.01 (s, 3H,  $SiCH_3$ ); -0.05 (s, 3H,  $SiCH_3$ )

$^{13}C$ -NMR:  $\delta$  [ppm] (100.6 MHz,  $DMSO-d_6$ )

158.07 (DMTr); 144.96 (C4); 144.75 (DMTr); 137.21 (C1); 135.51 (DMTr); 135.44 (DMTr); 129.74 (DMTr); 129.70 (DMTr); 129.66 (DMTr); 128.19 (DMTr); 127.77 (DMTr); 127.66 (DMTr); 126.67 (C3); 114.94 (C2); 114.73 (C6); 113.14 (DMTr); 85.46 (DMTr); 83.93 (C1'); 82.27 (C4'); 77.27 (C2'); 73.29 (C3'); 63.49 (C5'); 54.99 ( $OCH_3$ ); 25.74 ( $SiC(CH_3)_3$ ); 17.95 ( $SiC(CH_3)_3$ ); -4.51 ( $SiCH_3$ ); -5.09 ( $SiCH_3$ )

ESI(-):  $m/z$  643.4 ([M-H]);

**3'-O-(2-Cyanoethoxydiisopropylphosphin)-1'-deoxy-5'-O-(4,4'-dimethoxy-triphenylmethyl)-1'-(4-fluorophenyl)-2'-O-*tert.*-butyldimethylsilyl- $\beta$ -D-ribofuranose 148**



200 mg (0.31 mmol) 5'-O-(4,4'-Dimethoxytriphenylmethyl)-2'-O-*tert.*-butyldimethylsilyl-1'-deoxy-1'-(4-fluorophenyl)- $\beta$ -D-ribofuranose 146 were dissolved in 10 ml abs. acetonitrile and 440  $\mu\text{l}$  (3.1 mmol) *sym.* collidine and 14  $\mu\text{l}$  (0.18 mmol) 1-methylimidazole were added. The reaction mixture was cooled in an ice bath to 0°C and 112  $\mu\text{l}$  (0.33 mmol) 2-cyanoethyldiisopropylchlorophosphoramidite 96 were added. The reaction was stirred for 15 min. at 0°C and 15 min. at RT. The reaction was stopped by adding of 10 ml of 0.01 M citric acid and extracted with methylene chloride three times. The combined organic phases were washed with 0.01M citric acid twice, dried over  $\text{MgSO}_4$  and evaporated to dryness. Purification was done by FC with *n*-hexane/ethyl acetate, 4:1 as eluent. The product (mixture of two diastereomers) was obtained as white foam.

Yield: 176 mg (67.22 %)

TLC:  $R_f = 0.42$  (n-Hexan/Ethylacetat 4:1)

$^1\text{H-NMR}$ :  $\delta$  [ppm] (270 MHz,  $\text{CDCl}_3$ )

7.51 – 6.81 (m, 34H,  $\text{H}_{\text{ar}}$ ); 4.75, 4.70 (d,  $J = 8.2 \text{ Hz}$ ,  $J = 8.1 \text{ Hz}$ , 2H, 1'H); 4.17 (m, 2H, 3'H); 4.12 (m, 2H, 2'H); 3.98 (m, 2H, 4'H); 3.79, 3.78 (s, 12H,

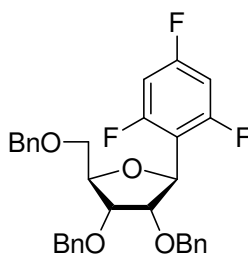
OCH<sub>3</sub>); 3.54 (m, 6H, 5'H, CH<sub>2</sub>CN); 3.19 (m, 2H, 5'H); 2.66 (m, 4H, OCH<sub>2</sub>); 1.17 (m, 12H, CH(CH<sub>3</sub>)<sub>2</sub>); 0.80, 0.79 (m, 18H, SiC(CH<sub>3</sub>)<sub>3</sub>); -0.10, -0.12, -0.20, -0.28 (s, 12H, SiCH<sub>3</sub>)

<sup>31</sup>P-NMR: δ [ppm] (162 MHz, CDCl<sub>3</sub>)  
151.37 and 148.68 (ratio 1 : 3.25)

ESI (+): m/z 845.8 ([M+H]<sup>+</sup>);

## 2',3',5'-Tri-*O*-benzyl-1'-deoxy-1'-(2,4,6-trifluorophenyl)-β-D-ribofuranose

**90**

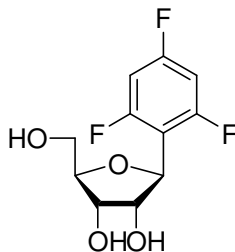


C<sub>32</sub>H<sub>29</sub>F<sub>3</sub>O<sub>4</sub>  
534.54 g/mol

To solution that contains 0.8g (5.8 mmol) 2, 4, 6-trifluorobenzene in 10 ml abs. diethyl ether at -78°C under argon was over 30 minutes 3.90 ml 1.5 M (5.8 mmol) solution of *t*-butyl lithium in *n*-pentane were added. After 30 minutes at -78°C the solution of 2,3,5-Tri-*O*-benzyl-ribo-γ-lacton (2.0 g, 4.8 mmol) **83** in 20 ml abs. diethyl ether over 30 minutes was added and 1 hour stirred at -78°C. Afterwards the reaction mixture was allowed to warm up to -20°C over two hours. The reaction was stopped by adding 5 ml of water and three times extracted with ether. The combined organic phases were dried over MgSO<sub>4</sub> and evaporated to dryness. Left oil was immediately dissolved in 20 ml of methylene chloride, cooled to -78°C and 1.20 ml (9.6 mmol) boron trifluoride etherate and 1.50 μl (9.60 mmol) triethylsilane were added. The reaction mixture was left at -78°C and over night allowed to warm up to 10°C. The reaction was stopped by adding of 10 ml of saturated water solution of NaHCO<sub>3</sub> and extracted three times with methylene chloride. The combined organic phases were dried over MgSO<sub>4</sub> and evaporated under reduced pressure. Further purification was done by FC using *n*-hexane/ethyl acetate 4:1 as eluent. The product was obtained as white solid.

Yield: 1.42g (55%)  
 TLC: R<sub>f</sub>=0.38 (*n*-hexane/EtOAc, 4:1)  
<sup>1</sup>H NMR: δ [ppm] ( 270MHz, DMSO-*d*<sub>6</sub>)  
 7.49-7.23(m, 18H, Har, 3H, 5H); 5.14(d, J=4.6 Hz, 1H, 1'H); 4.60(m, 6H, CH<sub>2</sub>-benzyl); 4.23(q, J=4.0 Hz, 1H, 4'H); 4.06(m, 2H, 2'H, 3'H); 3.70(m, 2H, 5'CH<sub>2</sub>);  
<sup>13</sup>C NMR: δ [ppm] (67.9 MHz, DMSO-*d*<sub>6</sub>)  
 162.51(C4); 158.9(C2); 158.80(C6); 138.20(Car); 138.12(Car) ; 137.8(Car);  
 128.20(Car) ; 128.09(Car); 127.80(Car); 127.50(Car); 127.42(Car);  
 127.10(Car); 123.61(C1); 111.40(C5); 103.55(C3); 82.10(C1'); 80.80(C4');  
 76.84(C2'); 75.96(C3'); 72.40(CH<sub>2</sub>-benzyl); 71.04(CH<sub>2</sub>-benzyl); 62.10(C5');  
 ESI (+): 552.4 ([M+H]<sup>+</sup>);

**1'-Deoxy-1'-(2,4,6-trifluorophenyl)-β-D-ribofuranose 37**



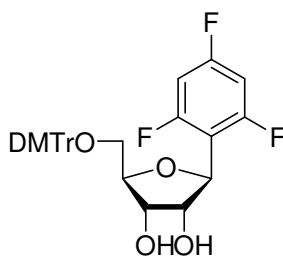
C<sub>11</sub>H<sub>11</sub>F<sub>3</sub>O<sub>4</sub>

264.2 g/mol

2.0 g (3.70 mmol) 2',3',5'-Tri-*O*-benzyl-1'-deoxy-1'-(2,4,6-trifluorophenyl)-β-D-ribofuranose 90 were dissolved in 50 ml abs. ethanol and 25 ml cyclohexene and 400 mg palladium-hydroxide (20%) on carbon were added. The reaction mixture was refluxed for 4 hours. Then the reaction mixture was filtrated over celite and the filtrate was evaporated under reduced pressure. The purification was done by FC with methylene chloride/methanol 9:1, as eluent. The product was obtained as colourless solid. For analytical purposes the product was crystallized from water and from methanol.

Yield: 910 mg (92%)  
 TLC: Rf=0.40 (CH<sub>2</sub>Cl<sub>2</sub>/MeOH, 9:1)  
<sup>1</sup>H NMR: δ [ppm] ( 270MHz, DMSO-*d*<sub>6</sub>)  
 7.20(t, 12H, J=9.72 Hz, 3H, 5H); 5.06(d, J=4.7 Hz, 1H, 1'H); 4.95(d, J=5.0 Hz, 1H, 3'OH); 4.83(d, J=7.8 Hz, 1H, 2'OH); 4.70(t, J=5.6 HZ, 1H, 5'OH); 4.17(m,1H, 2'H); 3.90 (m, 1H, 3'H); 3.74(m, 1H, 4'H); 3.46(m, 2H, 5'CH<sub>2</sub>);  
<sup>13</sup>C NMR: δ [ppm] (67.9 MHz, DMSO-*d*<sub>6</sub>)  
 163.39(C4); 156.90(C2); 156.40(C6); 112.03(C1); 102.20(C3); 99.65(C5); 86.54(C1'); 75.67(C4'); 73.48(C2'); 72.35(C3'); 62.01(C5');  
<sup>19</sup>F NMR: δ [ppm] (235.3 MHz, DMSO-*d*<sub>6</sub>)  
 -107.5(t, 1F, 4F); -110.7(d, 2F, 2F, 6F);  
 ESI (-): 263.0 ([M-H]<sup>-</sup>);

**5'-O- (4,4'-Dimethoxytriphenylmethyl)- 1'-deoxy-1'-(2,4, 6-trifluorophenyl)-β-D-ribofuranose 149**



C<sub>32</sub>H<sub>29</sub>F<sub>3</sub>O<sub>6</sub>

566.56 g/mol

0.75 g (2.84 mmol) 1'-Deoxy-1'-(2,4,6-trifluorophenyl)-β-D-ribofuranose **37** were dissolved in 20 ml abs. pyridine and 0.60 ml (4.25 mmol) triethylamine and 1.20 g (3.50 mmol) 4,4'-dimethoxytriphenylmethylchloride were added. The reaction mixture was stirred under argon at RT for 5 hours. The reaction was stopped by adding 3 ml of methanol and saturated water solution of NaHCO<sub>3</sub>. It was three times extracted with methylene chloride, organic phases

were collected and dried over  $\text{MgSO}_4$  and then evaporated to dryness. The product was twice co-evaporated with toluene. Further purification was done by FC with methylene chloride/methanol 98:2 as eluent. The product was obtained as yellow foam.

Yield: 1.60 g (81.3%)

TLC:  $R_f=0.61$  ( $\text{CH}_2\text{Cl}_2:\text{MeOH}$ , 95:5)

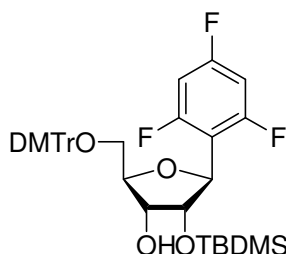
$^1\text{H}$  NMR:  $\delta$  [ppm] (270MHz,  $\text{DMSO}-d_6$ )  
7.42-6.82 (m, 15H, Har, 3H, 5H); 5.26(d,  $J=5.0$  Hz, 1H, 1'H); 5.16(d,  $J=6.2$  Hz, 1H, 2'OH); 5.02(d,  $J=6.3$  Hz, 1H, 3'OH); 4.83(d,  $J=7.8$  Hz, 1H, 2'OH); 4.17(q,  $J=5.75$ Hz, 1H, 2'H); 3.83 (m, 2H, 3'H, 4H); 3.73(s, 6H, 2OCH<sub>3</sub>); 3.17(m, 2H, 5'H);

$^{13}\text{C}$  NMR:  $\delta$  [ppm] (67.9 MHz,  $\text{DMSO}-d_6$ )  
158.07(DMTr); 149.63(C4); 144.95(DMTr); 137.44(C1); 135.63(DMTr); 129.76(DMTr); 127.84(DMTr); 127.78(DMTr); 126.70(DMTr); 123.91(C5); 115.03(C2); 114.70(C6); 113.1 (DMTr); 85.40(DMTr); 83.19(C1'); 82.69(C4'); 77.60(C2'); 71.20(C3'); 64.14(C5'), 55.03 (OCH<sub>3</sub>);

ESI (-): 565.5 ( $[\text{M}-\text{H}]^-$ );



**5'-O-(4,4'-Dimethoxytriphenylmethyl)-2'-O-*tert.*-butyldimethylsilyl-1'-deoxy-1'-(2,4,6-trifluorophenyl)- $\beta$ -D-ribofuranose 150**



$C_{38}H_{43}F_3O_6Si$

680.81 g/mol

1.15 g (2.03 mmol) 5'-O-(4,4'-Dimethoxytriphenylmethyl)-1'-deoxy-1'- $\beta$ -D-(2,4,6-trifluorophenyl)-ribofuranose **149** were dissolved in 20 ml of 1:1 mixture of THF/pyridine and with 410 mg (2.4 mmol)  $AgNO_3$  and 2.80 ml (2.80 mmol) 1 M *tert.*-Butyldimethylsilylchloride-solution in THF were added. The reaction mixture was stirred for 20 hours at RT under argon. Adding 10ml of saturated water  $NaHCO_3$ -solution stopped the reaction. Left  $AgCl$  was filtered over celite and the filtrate was extracted with methylene chloride three times. The combined organic phases were dried over  $MgSO_4$  and evaporated to dryness. The crude product was twice co-evaporated with toluene. Further purification of product was done by HPLC (*MN Nucleoprep 100-20* of Machrey-Nagel, [hexane/ethylacetate10:0.5]+30% methylene chloride). The product was obtained as the *slower*-migrating isomer and as white foam.

Yield: 566 mg (41%)

TLC:  $R_f=0.60$  ( $CH_2Cl_2$ )

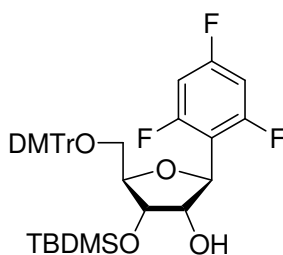
$^1H$  NMR:  $\delta$  [ppm] ( 270MHz,  $DMSO-d_6$ )  
 7.42-6.82 (m, 15H, Har, 3H, 5H); 4.81 (d,  $J=7.60$  Hz, 1H, 1'H); 4.72 (d,  $J=5.96$  Hz, 1H, 3'OH); 4.21 (m, 1H, 2'H); 3.82 (m, 1H, 3'H); 3.61 (s, 6H, 2OCH<sub>3</sub>); 2.98(m, 2H, 5'CH<sub>2</sub>); 0.67 (s, 3H, Si(OCH<sub>3</sub>)<sub>3</sub>); -0.17(s, 3H, SiCH<sub>3</sub>); -0.27 (s, 3H, SiCH<sub>3</sub>);

$^{13}C$  NMR:  $\delta$  [ppm] (67.9 MHz,  $DMSO-d_6$ )

157.48(DMTr); 149.05(Car); 144.35(DMTr); 134.54(Car); 133.13(Car);  
 129.14(DMTr); 127.18(DMTr); 125.04(DMTr); 123.32(Car); 112.96(Car);  
 111.39(Car); 100.90(DMTr); 100.43(DMTr) ; 100.00(DMTr) ; 84.80(C1');  
 82.96(C4') ; 74.67(C2') ; 73.03(C3') ; 63.43(C5') ; 54.46(OCH<sub>3</sub>) ;  
 25.80(Si(CH<sub>3</sub>)<sub>3</sub>); 17.87(Si(CH<sub>3</sub>)<sub>3</sub>); -5.08(SiCH<sub>3</sub>);  
 -5.35(SiCH<sub>3</sub>);

ESI (-): 679.0 ([M-H]<sup>-</sup>);

**5'-O-(4,4'-Dimethoxytriphenylmethyl)-3'-tert.-butyldimethylsilyl-1'-deoxy-1'-(2,4,6-trifluorophenyl)-β-D-ribofuranose 151**



C<sub>38</sub>H<sub>43</sub>F<sub>3</sub>O<sub>6</sub>Si

680.81 g/mol

5'-O-(4,4'-Dimethoxytriphenylmethyl)-3'-O-tert.-butyldimethylsilyl-1'-deoxy-1'-(2,4,6-trifluorophenyl)-β-D-ribofuranose **151** was obtained as a side product (*faster-migrating isomer*) in the synthesis of 5'-O-(4,4'-Dimethoxytriphenylmethyl)-2'-O-tert.-butyldimethylsilyl-1'-deoxy-1'-(2,4,6-trifluorophenyl)-β-D-ribofuranose **150**.

Yield: 590 mg (43 %)

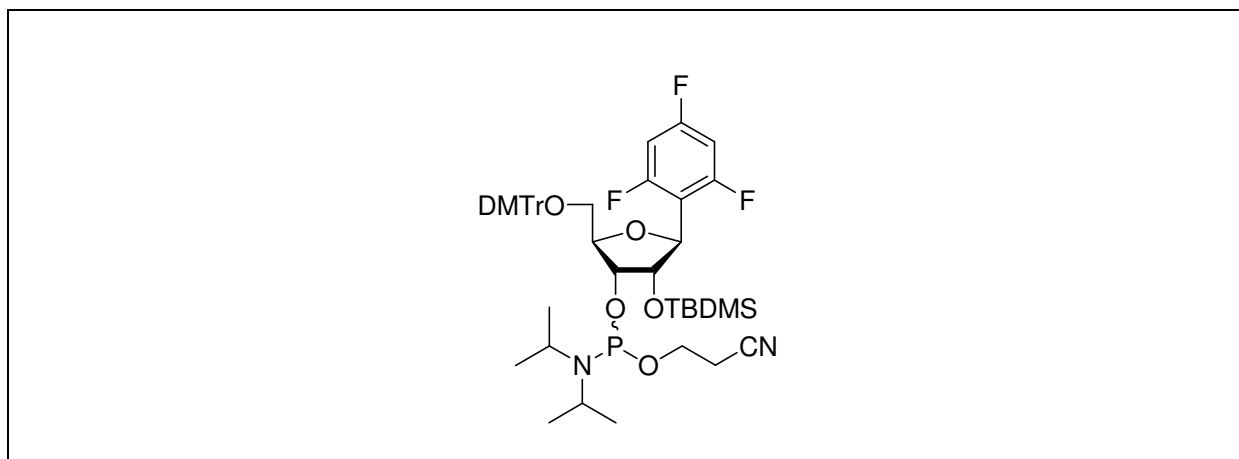
TLC: R<sub>f</sub>=0.60 (CH<sub>2</sub>Cl<sub>2</sub>)

<sup>1</sup>H NMR: δ [ppm] ( 270MHz, DMSO-*d*<sub>6</sub>)

7.41-6.80 (m, 15H, Har, 3H, 5H); 4.97 (d, J= 7.04 Hz, 1H, 1'H); 4.87 (d, J=6.88 Hz, 1H, 2'OH); 4.08(m, 1H, 2'H); 3.92 (m, 1H, 3'H); 3.77(s, 6H, 2OCH<sub>3</sub>); 3.75(m, 2H, 5'H); 3.10(m, 2H, 5'CH<sub>2</sub>); 0.78(s, 3H, Si(OCH<sub>3</sub>)<sub>3</sub>); -0.08(s, 3H, SiCH<sub>3</sub>); -0.18(s, 3H, SiCH<sub>3</sub>);

$^{13}\text{C}$  NMR:  $\delta$  [ppm] (67.9 MHz, DMSO- $d_6$ )  
 157.48(DMTr); 149.05(Car); 144.35(DMTr); 135.54(Car); 135.13(Car);  
 129.14(DMTr); 127.18(DMTr); 126.04(DMTr); 123.32(Car); 112.56(Car);  
 111.38(Car); 100.90(DMTr); 100.43(DMTr) ; 100.01(DMTr) ; 84.75(C1');  
 82.96(C4') ; 74.57(C2') ; 73.03(C3') ; 63.43(C5') ; 54.46(OCH<sub>3</sub>) ;  
 25.60(SiC(CH<sub>3</sub>)<sub>3</sub>); 17.85(SiC(CH<sub>3</sub>)<sub>3</sub>); -5.07(SiCH<sub>3</sub>); -5.30(SiCH<sub>3</sub>);  
 ESI (-): 679.0 ([M-H]<sup>-</sup>);

**3'-O-(2-Cyanethoxydiisopropylphosphin)-1'-desoxy-5'-O-(4,4'-dimethoxy-triphenylmethyl)-1'-(2,4,6-trifluorophenyl)-2'-O-*tert.*-butyldimethylsilyl- $\beta$ -D-ribofuranose 152**



$\text{C}_{47}\text{H}_{60}\text{F}_3\text{N}_2\text{O}_7\text{PSi}$

881.01 g/mol

460 mg (0.68 mmol) 5'-O-(4,4'-Dimethoxytriphenylmethyl)-2'-O-*tert.*-butyldimethylsilyl-1'-desoxy-1'-(2,4,6-trifluorophenyl)- $\beta$ -D-ribofuranose 150 were dissolved in 20 ml abs. acetonitrile and 900  $\mu\text{l}$  (6.80 mmol) *sym.* collidine and 27  $\mu\text{l}$  (0.34 mmol) 1-methylimidazole were added. The reaction mixture was cooled in an icebath to 0°C and 230  $\mu\text{l}$  (1.02 mmol) 2-cyanethyldiisopropylchlorphosphoramidite 96 were added. The reaction was stirred for 15 min. at 0°C and 1 hour at RT. The reaction was stopped by adding of 10 ml of 0.01M citric acid and extracted with methylene chloride three times. The combined organic phases were washed with 0.01M citric acid twice, dried over MgSO<sub>4</sub> and evaporated to dryness. The

purification was done by FC with *n*-hexane/ethyl acetate, 4:1, as eluent. The product (mixture of two diastereomers) was obtained as white foam.

Yield: 477 mg (80%)

TLC: R<sub>f</sub> = 0.37 (hexane/EtOAc, 4:1)

<sup>1</sup>H NMR: δ [ppm] ( 400MHz, CDCl<sub>3</sub>)

7.49-6.64 (m, 15H, Har, 3H, 5H); 5.14 (d, J= 8.84 Hz, 1H, 1'H); 4.52 (m, 1H, 2'H); 4.20 (m, 1H, 3'H); 3.97 (m, 1H, 4'H); 3.78 (s, 6H, 2OCH<sub>3</sub>); 3.55 (m, 2H, CH<sub>2</sub>CN); 3.25 (m, 2H, 5'CH<sub>2</sub>); 2.67 (m, 2H, OCH<sub>2</sub>); 1.10 (m, 6H, CH(CH<sub>3</sub>)<sub>2</sub>); 0.78 (s, 9H, SiC(CH<sub>3</sub>)<sub>3</sub>); -0.04 (s, 3H, SiCH<sub>3</sub>); -0.18 (s, 3H, SiCH<sub>3</sub>);

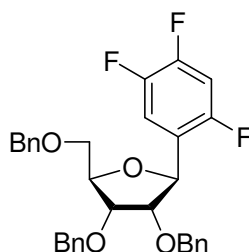
<sup>31</sup>P NMR: δ [ppm] ( 162 MHz, CDCl<sub>3</sub>)

151.93 and 149.24 (ratio 1:19.8)

ESI (+): 903.7 ([M+Na]<sup>+</sup>);

**2',3',5'-Tri-*O*-benzyl-1'-deoxy-1'-(2,4,5-trifluorophenyl)- $\beta$ -D-ribofuranose**

**86**



$C_{32}H_{29}F_3O_4$

534.54 g/mol

To the solution that contains 1.52 g (7.20 mmol) 1-bromo-2, 4, 5-trifluorobenzene in 15 ml abs. diethyl ether at  $-78^{\circ}\text{C}$  under argon over 30 minutes 4.50 ml 1.6 M (7.20 mmol) solution of *n*-Butyl lithium in *n*-hexane were added. After 30 minutes at  $-78^{\circ}\text{C}$  solution of 2,3,5-Tri-*O*-benzyl-ribo- $\gamma$ -lacton (2.0 g, 4.8 mmol) **83** in 20 ml abs. diethyl ether was added over 30 minutes and 1 hour stirred at  $-78^{\circ}\text{C}$ . Afterwards the reaction mixture was allowed to warm up to  $-20^{\circ}\text{C}$  over two hours. The reaction was stopped by adding 5 ml of water and three times extracted with ether. The combined organic phases were dried over  $\text{MgSO}_4$  and evaporated to dryness. Left oil was immediately dissolved in 20 ml of methylene chloride, cooled to  $-78^{\circ}\text{C}$  and 1.90 ml (15.0 mmol) borontrifluorid ethyletherat and 2.40 ml (15.0 mmol) triethylsilan were added. The reaction mixture was left at  $-78^{\circ}\text{C}$  and over night was allowed to warm up to  $10^{\circ}\text{C}$ . The reaction was stopped by adding of 10 ml of saturated water solution of  $\text{NaHCO}_3$  and extracted three times with methylene chloride. The combined organic phases were dried over  $\text{MgSO}_4$  and evaporated under reduced pressure. Further purification was done by FC using *n*-hexane/ethyl acetate 4:1 as eluent. The product was obtained as yellow oil.

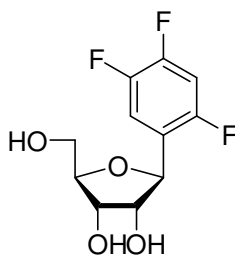
Yield: 2.50 g (65%)

TLC:  $R_f=0.57$  (hexane,EtOAc, 4:1)

$^1\text{H NMR}$ :  $\delta$  [ppm] ( 270MHz,  $\text{DMSO}-d_6$ )  
 7.60-7.21(m, 17H, Har, 3H, 6H); 5.16(d,  $J=4.655\text{Hz}$ , 1H, 1'H); 4.55(m, 6H,  
 $\text{CH}_2$ -benzyl); 4.22( m, 1H, 2'H); 4.07(m, 2H, 3'H, 4'H); 3.70(m, 2H, 5'CH<sub>2</sub>);

$^{13}\text{C}$  NMR:  $\delta$  [ppm] (67.9 MHz,  $\text{DMSO-}d_6$ )  
 162.50(C4); 158.9(C2); 158.80(C5); 138.20(Car); 138.12(Car) ; 137.8(Car);  
 128.20(Car) ; 128.09(Car); 127.80(Car); 127.50(Car); 127.42(Car);  
 127.10(Car); 123.61(C1); 111.40(C6); 103.55(C3); 82.10(C1'); 80.82(C4');  
 76.84(C2'); 75.98(C3'); 72.38( $\text{CH}_2$ -benzyl); 71.06( $\text{CH}_2$ -benzyl); 62.10(C5');  
 ESI(+): 552.4 ( $[\text{M}+\text{NH}_4]^+$ );

**1'-Deoxy-1'-(2,4,5-trifluorophenyl)- $\beta$ -D-ribofuranose 38**



$\text{C}_{11}\text{H}_{11}\text{F}_3\text{O}_4$

264.2 g/mol

2.20 g (4.05 mmol) 2',3',5'-Tri-*O*-benzyl-1'-deoxy-1'-(2,4,5-trifluorophenyl)- $\beta$ -D-ribofuranose **86** were dissolved in 40 ml abs. ethanol and 20 ml cyclohexen and 450 mg palladium-hydroxide (20%) on carbon were added. The reaction mixture was refluxed for 5 hours. Than the reaction mixture was filtrated over celite and the filtrate was evaporated under reduced pressure. The purification was done by FC with methylene chloride/methanol 9:1, as eluent. The product was obtained as colourless solid. For analytical purposes the product was crystallized from water and from methanol.

Yield: 1.02 g (93.6 %)

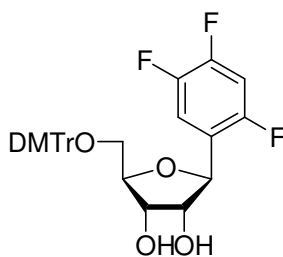
TLC:  $R_f=0.40$  ( $\text{CH}_2\text{Cl}_2/\text{MeOH}$ , 9:1)

<sup>1</sup>H NMR: δ [ppm] ( 400 MHz, DMSO-*d*<sub>6</sub>)  
 7.72(m, 1H, 3H); 7.49(m, 1H, 6H); 5.10 (d, J=6.08 Hz, 1H, 1'H); 4.92(m, 3H, 3'OH, 2'OH, 5'OH); 4.85(m, 1H, 2'H); 3.91 (m, 2H, 3'H, 4'H); 3.82(m, 2H, 5'CH<sub>2</sub>);

<sup>13</sup>C NMR: δ [ppm] (67.9 MHz, DMSO-*d*<sub>6</sub>)  
 163.39(C4); 159.69(C5); 159.5(C2); 112.03(C1); 102.20(C3); 99.65(C6); 86.55(C1'); 75.68(C4'); 73.50(C2'); 72.35(C3'); 62.00(C5');

ESI (-): 262.9 ([M-H]);

**5'-O- (4,4'-Dimethoxytriphenylmethyl)- 1'-deoxy-1'-(2,4,5-trifluorophenyl)-β-D-ribofuranose 153**



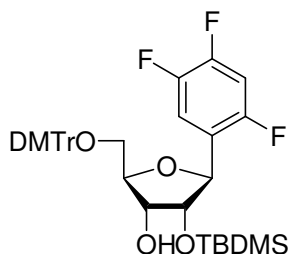
C<sub>32</sub>H<sub>29</sub>F<sub>3</sub>O<sub>6</sub>

566.56 g/mol

1.20g ( 4.54 mmol) 1'-Deoxy-1'-(2,4,5-trifluorophenyl)-β-D-ribofuranose 38 were dissolved in 20 ml abs. pyridine and 0.95 ml (6.80 mmol) triethylamine and 1.90 g (5.58 mmol) 4,4'-Dimethoxytriphenylmethylchloride were added. The reaction mixture was stirred under argon at RT for 5 hours. The reaction was stopped by adding 3 ml of methanol and saturated water solution of NaHCO<sub>3</sub>. It was three times extracted with methylene chloride, organic phases were collected and dried over MgSO<sub>4</sub> and then evaporated to dryness. Product was co-evaporated with toluene. Further purification was done by FC with methylene chloride/methanol 98:2 as eluent. The product was obtained as yellow foam.

Yield: 1.30 g (51%)  
 TLC: R<sub>f</sub>=0.50 (CH<sub>2</sub>Cl<sub>2</sub>/MeOH, 95:5)  
<sup>1</sup>H NMR: δ [ppm] ( 270MHz, DMSO-*d*<sub>6</sub>)  
 7.69-6.76 (m, 15H, Har, 3H, 6H); 5.15(d, J= 5.48 Hz, 1H, 1'H); 4.88(d, J=5.68 Hz, 1H, 2'OH); 4.81(m, 1H, 3'OH); 3.88-3.78 (m, 3H,2'H, 3'H, 4H); 3.73(s, 6H, 2OCH<sub>3</sub>); 3.10(m, 2H, 5'H);  
<sup>13</sup>C NMR: δ [ppm] (67.9 MHz, DMSO-*d*<sub>6</sub>)  
 158.06(DMTr); 150.01(C4); 144.95(DMTr); 137.44(C1); 135.65(DMTr);  
 130.00(DMTr); 128.10(DMTr);127.85(DMTr); 126.80(DMTr); 124.10(C5);  
 115.03(C2); 114.70(C6); 113.18(DMTr); 85.40(DMTr); 83.19(C1');  
 82.70(C4'); 77.60(C2'); 71.10(C3'); 64.20(C5'), 55.00 (OCH<sub>3</sub>);  
 ESI (-): 565.3 ([M-H]<sup>-</sup>);

**5'-O-(4,4'-Dimethoxytriphenylmethyl)-2'-O-*tert.*-butyldimethylsilyl-1'-deoxy-1'-(2, 4, 5-trifluorophenyl)-β-D-ribofuranose 154**



C<sub>38</sub>H<sub>43</sub>F<sub>3</sub>O<sub>6</sub>Si

680.81 g/mol

1.20 g (2.12 mmol) 5'-O-(4,4'-Dimethoxytriphenylmethyl)-1'-deoxy-1'-β-D-(2,4,5-trifluorophenyl)-ribofuranose **153** were dissolved in 20 ml of 1:1 mixture of THF/pyridine and with 450 mg (2.6 mmol) AgNO<sub>3</sub> and 3.20 ml (3.20 mmol) 1 M *tert.*-butyldimethylsilyl chloride-solution in THF were added. The reaction mixture was stirred for 20 hours at RT under argon. Adding 10ml of saturated water NaHCO<sub>3</sub>-solution stopped the reaction. Left AgCl was filtered over celite and the filtrate was extracted with methylene chloride three times. Collected organic phases were dried over MgSO<sub>4</sub> and evaporated to dryness. The crude product was twice co-evaporated with toluene. Further purification of the product was done



by HPLC (*MN Nucleoprep 100-20* of Machrey Nagel, [hexane/ethylacetate, 10:0.6])+30% methylene chloride. The product was obtained as the *slower*-migrating isomer and as white foam.

Yield: 590 mg (41 %)

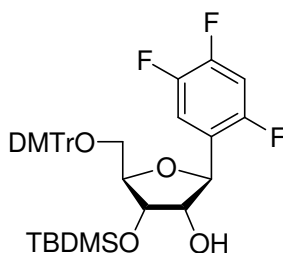
TLC: Rf=0.58 (CH<sub>2</sub>Cl<sub>2</sub>)

<sup>1</sup>H NMR: δ [ppm] ( 400MHz, DMSO-*d*<sub>6</sub>)  
 7.58-6.82 (m, 15H, Har, 3H, 6H); 4.94 (d, J= 5.32 Hz, 1H, 1'H); 4.91 (d, J=5.84 Hz, 1H, 3'OH); 4.03 (m, 2H, 2'H,3'H); 3.98(m, 1H, 4'H); 3.72 (s, 6H, 2OCH<sub>3</sub>);3.21 (m, 2H, 5'H); 0.80 (s, 9H, SiC(CH<sub>3</sub>)<sub>3</sub>); -0.05 (s, 3H, SiCH<sub>3</sub>); -0.10 (s, 3H, SiCH<sub>3</sub>);

<sup>13</sup>C NMR: δ [ppm] (100.6 MHz, DMSO-*d*<sub>6</sub>)  
 158.00 (DMTr); 151.00 (Car), 144.30 (DMTr); 135.50 (Car); 135.13 ( Car);  
 129.15 (DMTr); 127.18 (DMTr); 126.04 (DMTr); 123.32 (Car); 112.56 (Car);  
 111.10 (Car); 100.95 (DMTr); 100.48 (DMTr); 100.08 (DMTr); 84.76 (C1');  
 82.98 (C4'); 74.47 (C2'); 73.00 (C3') ; 63.43 (C5'); 54.50 (OCH<sub>3</sub>) ; 24.8  
 (SiC(CH<sub>3</sub>)<sub>3</sub>); 17.88 (SiC(CH<sub>3</sub>)<sub>3</sub>); -5.12 (SiCH<sub>3</sub>); -5.35 (SiCH<sub>3</sub>);

ESI (-): 680.0 ([M-H]<sup>-</sup>);

**5'-O-(4,4'-Dimethoxytriphenylmethyl)-3'-*tert.*-butyldimethylsilyl-1'-deoxy-1'-(2,4,5-trifluorophenyl)-β-D-ribofuranose 155**



C<sub>38</sub>H<sub>43</sub>F<sub>3</sub>O<sub>6</sub>Si

680.81 g/mol

5'- O- (4,4'-Dimethoxytriphenylmethyl)- 3'-O-*tert.*-butyldimethylsilyl- 1'-deoxy-1'- (2,4,5-trifluorophenyl)-β-D-ribofuranose 155 was obtained as a side product (*faster*-migrating

isomer) while synthesizing 5'-O-(4,4'-Dimethoxytriphenylmethyl)-2'-O-tert.-butyldimethylsilyl-1'-deoxy-1'-(2,4,5-trifluoro-phenyl)- $\beta$ -D-ribofuranose **154**.

Yield: 530 mg (37%)

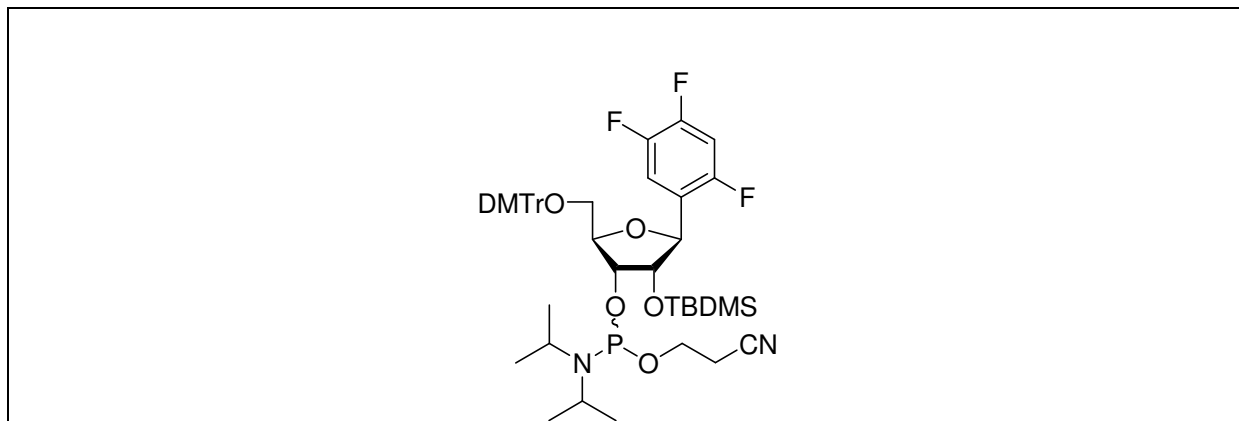
TLC: R<sub>f</sub> = 0.58 (CH<sub>2</sub>Cl<sub>2</sub>)

<sup>1</sup>H NMR:  $\delta$  [ppm] (400 MHz, DMSO-*d*<sub>6</sub>)  
7.54-6.85 (m, 15H, Har, 3H, 6H); 5.06 (d, J= 6.48 Hz, 1H, 1'H); 4.92 (d, J=5.88 Hz, 1H, 2'OH); 4.00 (m, 3H, 2'H,3'H, 4'H); 3.72 (s, 6H, 2OCH<sub>3</sub>); 3.30 (m, 2H, 5'H); 0.80 (s, 9H, Si(OCH<sub>3</sub>)<sub>3</sub>); -0.03 (s, 3H, SiCH<sub>3</sub>); -0.10 (s, 3H, SiCH<sub>3</sub>);

<sup>13</sup>C NMR:  $\delta$  [ppm] (100.6 MHz, DMSO-*d*<sub>6</sub>)  
157.50 (DMTr); 149.05 (Car), 144.35 (DMTr); 135.50 (Car); 135.13 (Car);  
129.14 (DMTr); 127.18 (DMTr); 126.04 (DMTr); 123.32 (Car); 112.56 (Car);  
111.40 (Car); 100.90 (DMTr); 100.43 (DMTr); 100.01 (DMTr); 84.75 (C1');  
82.96 (C4'); 74.57 (C2'); 73.03 (C3'); 63.43 (C5'); 54.46 (OCH<sub>3</sub>); 25.6 (SiC(CH<sub>3</sub>)<sub>3</sub>); 17.85 (SiC(CH<sub>3</sub>)<sub>3</sub>); -5.10 (SiCH<sub>3</sub>); -5.30 (SiCH<sub>3</sub>);

ESI (-): 679.90 ([M-H]<sup>-</sup>);

**3'-O-(2-Cyanoethoxydiisopropylphosphin)-1'-deoxy-5'-O-(4,4'-dimethoxy-triphenylmethyl)-1'-(2,4,5-trifluorophenyl)-2'-O-*tert.*-butyldimethylsilyl- $\beta$ -D-ribofuranose 156**



$C_{47}H_{60}F_3N_2O_7PSi$

881.01 g/mol

230 mg (0.34 mmol) 5'-O-(4,4'-Dimethoxytriphenylmethyl)-2'-O-*tert.*-butyldimethylsilyl-1'-deoxy-1'-(2,4,5-trifluorophenyl)- $\beta$ -D-ribofuranose 154 were dissolved in 10 ml abs. acetonitrile and 450  $\mu$ l (3.40 mmol) *sym.* collidine and 14  $\mu$ l (0.17 mmol) 1-methylimidazole were added. The reaction mixture was cooled in an icebath to 0°C and 115  $\mu$ l (0.51 mmol) 2-cyanoethyldiisopropylchlorophosphoramidite 96 was added. The reaction was stirred for 15min. at 0°C and 1 hour at RT. The reaction was stopped by adding of 10 ml of 0.01 M citric acid and three times extracted with methylene chloride. The combined organic phases were washed with 0.01 M citric acid twice, dried over  $MgSO_4$  and evaporated to dryness. Purification was done by FC with *n*-hexane/ethyl acetate, 4:1, as eluent. The product (mixture of two diastereomers) was obtained as white foam.

Yield: 190 mg (79%)

TLC:  $R_f$  =0.39 (hexane/EtOAc, 4:1)

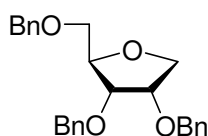
$^1H$  NMR:  $\delta$  [ppm] ( 400MHz,  $DMSO-d_6$ )

7.52-6.80 (m, 15H, Har, 3H, 6H); 5.12 (d,  $J$  = 7.48 Hz, 1H, 1'H); 4.19 (m, 2H, 2'H,3'H); 3.97 (m, 1H, 4'H); 3.74 (s, 6H, 2OCH<sub>3</sub>); 3.55 (m, 4H, CH<sub>2</sub>CN, 5'CH<sub>2</sub>); 2.70 (m, 2H, OCH<sub>2</sub>); 1.16 (m, 6H, 2CHCH<sub>3</sub>); 0.80 (s, 9H, SiC(CH<sub>3</sub>)<sub>3</sub>); -0.13 (s, 3H, SiCH<sub>3</sub>); -0.30 (s, 3H, SiCH<sub>3</sub>);

$^{31}\text{P}$  NMR:  $\delta$  [ppm] ( 162 MHz, DMSO- $d_6$ )  
151.61 and 149.63 (ratio 1:4.6)

ESI (+): 883.0 ( $[\text{M}+\text{H}]^+$ );

### 2,3,5-Tri-*O*-benzyl-1-deoxy-D-ribofuranose 98



$\text{C}_{26}\text{H}_{28}\text{O}_4$

404.48 g/mol

1.0 g (2.4 mmol) 2,3,5-tri-*O*-benzyl-ribofuranose was dissolved in 10 ml of acetonitrile and 0.6 ml (9.6 mmol) triethylsilane and 0.6 ml (4.8 mmol)  $\text{BF}_3 \cdot \text{OEt}_2$  were added. The reaction mixture was refluxed 1.5 hours at room temperature in argon atmosphere. The reaction was stopped by adding 10 ml of saturated water solution of  $\text{NaHCO}_3$ . The mixture was extracted three times with methylene chloride. The combined organic phases were dried over  $\text{MgSO}_4$  and evaporated to dryness. Purification was done by FC, with *n*-hexane/ethylacetate 4:1, as eluent. The product was obtained as colourless oil.

Yield: 850 mg (88.4 %)

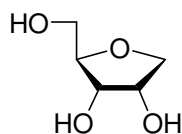
TLC:  $R_f = 0.49$  ( $\text{CH}_2\text{Cl}_2/\text{MeOH}$  99:1)

$^1\text{H}$ -NMR:  $\delta$  [ppm] (270 MHz, DMSO- $d_6$ )  
7.29 – 7.17 (m, 15H,  $\text{H}_{\text{ar}}$ ); 4.58 – 4.41 (m, 6H,  $\text{CH}_2$ -benzyl); 4.09 (m, 1H, 4H);  
3.89 (m, 4H, 1H, 2H, 3H); 3.50 (m, 2H, 5H)

$^{13}\text{C}$ -NMR:  $\delta$  [ppm] (62.9 MHz, DMSO- $d_6$ )  
138.05 ( $\text{C}_{\text{ar}}$ ); 137.88 ( $\text{C}_{\text{ar}}$ ); 137.80 ( $\text{C}_{\text{ar}}$ ); 128.25 ( $\text{C}_{\text{ar}}$ ); 128.21 ( $\text{C}_{\text{ar}}$ ); 128.18 ( $\text{C}_{\text{ar}}$ ); 127.80 ( $\text{C}_{\text{ar}}$ ); 127.72 ( $\text{C}_{\text{ar}}$ ); 127.61 ( $\text{C}_{\text{ar}}$ ); 127.49 ( $\text{C}_{\text{ar}}$ ); 127.42 ( $\text{C}_{\text{ar}}$ ); 80.35 (C4); 78.18 (C1); 76.42 (C2); 73.28 ( $\text{CH}_2$ -benzyl), 72.05 ( $\text{CH}_2$ -benzyl), 71.66 ( $\text{CH}_2$ -benzyl); 70.45 (C3); 69.93 (C5).

ESI(+): 422.2 ( $[\text{M}+\text{NH}_4]^+$ );

## 1-Deoxy-D-ribofuranose 42



134.13 g/mol

3.9 g (9.6 mmol) 2,3,5-Tri-*O*-benzyl-1-deoxy-D-ribofuranose **98** were dissolved in 70 ml of abs. ethanol and 35 ml of cyclohexane and 800 mg palladium hydroxide (20%) on carbon were added. The reaction mixture was refluxed for 4 hours. The palladium catalyst was then filtered over celite and the filtrate was evaporated to dryness. Further purification was done by FC with methylene chloride/methanol 9:1, as eluent. The product was obtained as colourless solid.

Yield: 1.23 g (95.3 %)

TLC:  $R_f = 0.22$  ( $\text{CH}_2\text{Cl}_2/\text{MeOH}$  9:1)

$^1\text{H-NMR}$ :  $\delta$  [ppm] (250 MHz,  $\text{DMSO-}d_6$ )

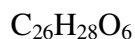
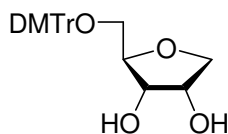
4.69 (m, 2H, 2-OH, 3-OH); 4.57 (t,  $J = 5.7$  Hz, 1H, 5-OH); 3.96 (m, 1H, 4H);  
3.83 (m, 1H, 2H); 3.74 (q,  $J = 5.5$  Hz, 1H, 3H); 3.52 (m, 3H, 1H, 5H); 3.35 (m,  
1H, 5H)

$^{13}\text{C-NMR}$ :  $\delta$  [ppm] (62.9 MHz,  $\text{DMSO-}d_6$ )

83.20 (C4), 71.99 (C1); 71.55 (C2); 70.41 (C3); 61.76 (C5)

ESI(-): 133.0 ( $[\text{M-H}]^-$ );

**5-O-(4,4'-Dimethoxytriphenylmethyl)-1-deoxy-D-ribofuranose 99**



436.49 g/mol

1.22 g (9.1 mmol) 1-Deoxy-D-ribofuranose **42** were dissolved in 40 ml of abs. pyridine and 1.9 ml (19 mmol) of triethylamine and 3.7 g (10.9 mmol) 4,4'-dimethoxytriphenylmethylchloride were added. The reaction was stirred for 4 hours at room temperature in argon atmosphere. The reaction was stopped by adding 3 ml of methanol and saturated  $\text{NaHCO}_3$ -solution was added. It was extracted then three times with methylene chloride. The combined organic phases were dried over  $\text{MgSO}_4$  and evaporated to dryness. The crude product was twice with toluene co-evaporated. Purification was done by FC with methylene chloride/methanol 98:2, as eluent. The product was obtained as white foam.

Yield: 3.41 g (85.9 %)

TLC:  $R_f = 0.13$  ( $\text{CH}_2\text{Cl}_2/\text{MeOH}$  98:2)

$^1\text{H-NMR}$ :  $\delta$  [ppm] (250 MHz,  $\text{DMSO-}d_6$ )

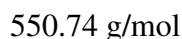
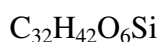
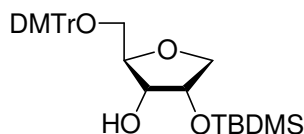
7.42-6.86 (m, 13H,  $\text{H}_{\text{ar}}$ ); 4.77 (d,  $J = 4.5$  Hz, 1H, 2-OH); 4.73 (d,  $J = 6.2$  Hz, 1H, 3-OH); 4.01 (m, 1H, 2H); 3.94 (m, 1H, 1H); 3.77 (m, 2H, 3H, 4H); 3.73 (s, 6H,  $\text{OCH}_3$ ); 3.60 (dd,  $J = 8.9$  Hz,  $J = 3.1$  Hz, 1H, 1H); 3.02 (m, 2H, 5H)

$^{13}\text{C-NMR}$ :  $\delta$  [ppm] (62.9 MHz,  $\text{DMSO-}d_6$ )

158.02 (DMTr); 145.06 (DMTr); 135.79 (DMTr); 129.70 (DMTr); 127.74 (DMTr); 126.58 (DMTr); 113.14 (DMTr); 85.15 (DMTr); 80.97 (C4); 72.50 (C1); 72.24 (C2); 70.30 (C3); 64.45 (C5); 55.01 ( $\text{OCH}_3$ )

ESI(-): 435.2 ( $[\text{M-H}]^-$ );

**5-O-(4,4'-Dimethoxytriphenylmethyl)-2-O-*tert.*-butyldimethylsilyl-1-deoxy-D-ribofuranose 101**



3.2 g (7.3 mmol) 5-O-(4,4'-Dimethoxytriphenylmethyl)-1-deoxy-D-ribofuranose **99** was dissolved in mixture 60 ml of 1:1 of THF/pyridine and 1.5 g (13.3 mmol) silvernitrate and 10.2 ml (10.2 mmol) 1 M *tert.*-butyldimethylsilylchloride solution in THF were added. The reaction mixture was stirred for 20 hours at room temperature in argon atmosphere. The reaction was stopped by adding 10 ml of saturated water NaHCO<sub>3</sub>-solution. Silverchloride was then filtered over celite and the filtrate was extracted with methylene chloride three times. The combined organic phases were dried over MgSO<sub>4</sub> and evaporated to dryness. The crude product was co-evaporated with toluene twice. The purification was done by FC with methylene chloride as eluent. The product was obtained as white foam

Yield: 2.43 g (60.3 %)

TLC: R<sub>f</sub> = 0.43 (CH<sub>2</sub>Cl<sub>2</sub>)

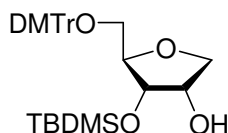
<sup>1</sup>H-NMR: δ [ppm] (250 MHz, DMSO-*d*<sub>6</sub>)  
 7.40 - 6.83 (m, 13H, H<sub>ar</sub>); 4.49 (d, J = 6.0 Hz, 1H, 3-OH); 4.19 (m, 1H, 2H);  
 3.96 (m, 1H, 1H); 3.77 (m, 2H, 3H, 4H); 3.73 (s, 6H, OCH<sub>3</sub>); 3.58 (m, 1H,  
 1H); 3.00 (m, 2H, 5H); 0.88 (s, 9H, SiC(CH<sub>3</sub>)<sub>3</sub>); 0.07 (s, 3H, SiCH<sub>3</sub>); 0.06 (s,  
 3H, SiCH<sub>3</sub>)

<sup>13</sup>C-NMR: δ [ppm] (100.6 MHz, DMSO-*d*<sub>6</sub>)  
 158.05 (DMTr); 145.09 (DMTr); 135.75 (DMTr); 129.73 (DMTr); 127.78  
 (DMTr); 127.73 (DMTr); 127.42 (DMTr); 126.51 (DMTr); 113.16 (DMTr);  
 85.17 (DMTr); 80.92 (C4); 73.56 (C1); 72.57 (C2); 70.24 (C3); 64.33 (C5);

55.05 (OCH<sub>3</sub>); 25.88 (SiC(CH<sub>3</sub>)<sub>3</sub>); 18.11 SiC(CH<sub>3</sub>)<sub>3</sub>; -4.54 (SiCH<sub>3</sub>); -4.87 (SiCH<sub>3</sub>)

ESI(-): 549.4 ([M-H]<sup>-</sup>);

**5-*O*-(4,4'-Dimethoxytriphenylmethyl)-3-*O*-*tert*.-butyldimethylsilyl-1-deoxy-D-ribofuranose 100**



C<sub>32</sub>H<sub>42</sub>O<sub>6</sub>Si

550.74 g/mol

5-*O*-(4,4'-Dimethoxytriphenylmethyl)-3-*O*-*tert*.-butyldimethylsilyl-1-deoxy-D-ribofuranose 100 was obtained as a side product in the synthesis of 5-*O*-(4,4'-Dimethoxytriphenylmethyl)-2-*O*-*tert*.-butyldimethylsilyl-1-deoxy-D-ribofuranose 101.

Yield: 1.1 g (27.3 %)

TLC: R<sub>f</sub> = 0.64 (CH<sub>2</sub>Cl<sub>2</sub>)

<sup>1</sup>H-NMR: δ [ppm] (250 MHz, DMSO-*d*<sub>6</sub>)  
 7.42 - 6.82 (m, 13H, H<sub>ar</sub>); 4.53 (d, J = 4.7 Hz, 1H, 2-OH); 4.17 (q, J = 4.4 Hz, 1H, 2H); 3.95 (m, 1H, 1H); 3.89 (m, 1H, 3H); 3.79 (m, 1H, 4H); 3.72 (s, 6H, OCH<sub>3</sub>); 3.57 (m, 1H, 1H); 3.02 (m, 2H, 5H); 0.72 (s, 9H, SiC(CH<sub>3</sub>)<sub>3</sub>); -0.04 (s, 3H, SiCH<sub>3</sub>); -0.15 (s, 3H, SiCH<sub>3</sub>)

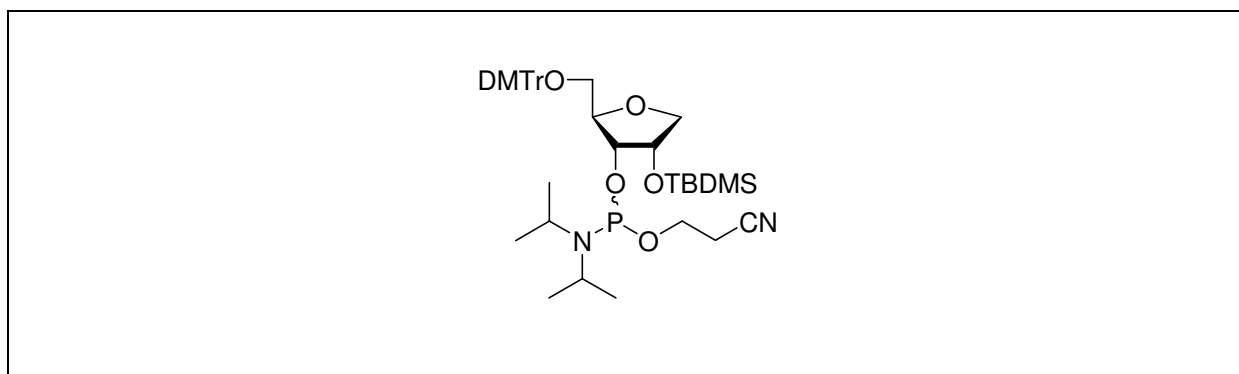
<sup>13</sup>C-NMR: δ [ppm] (62.9 MHz, DMSO-*d*<sub>6</sub>)  
 158.07 (DMTr); 144.94 (DMTr); 135.56 (DMTr); 129.68 (DMTr); 127.76 (DMTr); 127.65 (DMTr); 126.61 (DMTr); 113.82 (DMTr); 85.33 (DMTr);



81.42 (C4); 73.36 (C1); 72.13 (C2); 71.77 (C3); 63.85 (C5); 54.99 (OCH<sub>3</sub>);  
25.61 (SiC(CH<sub>3</sub>)<sub>3</sub>); 17.65 SiC(CH<sub>3</sub>)<sub>3</sub>; -4.71 (SiCH<sub>3</sub>); -5.29 (SiCH<sub>3</sub>)

ESI(-): 549.3 ([M-H]<sup>-</sup>);

**3-O-(2-Cyanethoxydiisopropylphosphin)-1-deoxy-5-O-(4,4'-dimethoxy-triphenylmethyl)-2-O-*tert.*-butyldimethylsilyl-D-ribofuranose 102**



C<sub>41</sub>H<sub>59</sub>N<sub>2</sub>O<sub>7</sub>PSi

750.94 g/mol

200 mg (0.36 mmol) 5-O-(4,4'-Dimethoxytriphenylmethyl)-2-O-*tert.*-butyldimethylsilyl-1-deoxy-D-ribofuranose 101 were dissolved in 11 ml of abs. acetonitrile and 480 μl (3.7 mmol) *sym.* collidine and 15 μl (0.19 mmol) 1-methylimidazole were added. The reaction mixture was cooled on in icebath to 0°C and 122 μl (0.54 mmol) 2-cyanethyl-diisopropylchlorophosphoramidite 96 was added. The reaction was stirred 15 minutes at 0°C and 35 minutes at room temperature. The reaction was stooped by adding 3 ml of saturated water NaHCO<sub>3</sub>-solution. The mixture was three times extracted with methylene chloride and collected organic phasesd were dried over MgSO<sub>4</sub> and evaporated to dryness. The purification was done by FC with methylene chloride/methanol 99:1, as eluent. The product (mixture of two diastereoisomers ) was obtained as white foam.

Yield: 130 mg (47.8 %)

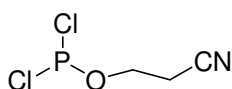
TLC: R<sub>f</sub> = 0.49; 0.55 (CH<sub>2</sub>Cl<sub>2</sub>/MeOH 99:1)

<sup>1</sup>H-NMR: δ [ppm] (400 MHz, CDCl<sub>3</sub>)  
 7.40 – 6.72 (m, 34H, H<sub>ar</sub>); 4.36, 4.30 (q, J = 4.9 Hz, J = 5.3 Hz, 2H, 2H); 4.07 (m, 2H, 1H); 4.00 (m, 4H, 3H, 4H); 3.72, 3.71 (s, 12H, OCH<sub>3</sub>); 3.46 (m, 6H, 1H, CH<sub>2</sub>CN); 3.28 (m, 4H, 5H); 2.53 (m, 4H, OCH<sub>2</sub>); 1.05 (m, 12H, CH(CH<sub>3</sub>)<sub>2</sub>); 0.85, 0.83 (m, 18H, SiC(CH<sub>3</sub>)<sub>3</sub>); 0.05, 0.04, 0.02, 0.01 (s, 12H, SiCH<sub>3</sub>)

<sup>31</sup>P-NMR: δ [ppm] (162 MHz, CDCl<sub>3</sub>)  
 149.67 and 149.15 (ratio 1 : 1.3)

ESI(+): 751.1 ([M+H]<sup>+</sup>);

### 2-Cyanoethoxy-dichlorophosphin 157



C<sub>3</sub>H<sub>4</sub>Cl<sub>2</sub>NOP

171.95 g/mol

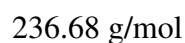
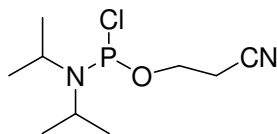
175 ml (2 mol) phosphorustrichloride was mixed with 100 ml of abs. diethylether in a round flask and over 20 minutes a mixture of 19.5 ml (285 mmol) 3-hydroxypropionitrile and 120 ml abs. diethylether was added dropwise. The reaction mixture was stirred 1 hour at room temperature. Ether was evaporated at temperature lower than 40°C and the left oil was separated by fractional distillation in vacuum. The product was obtained as colourless liquid at 68 – 70 °C ( 4\*10<sup>-5</sup> mbar).

Yield: 31.3 g (63.6 %)

<sup>1</sup>H-NMR: δ [ppm] (250 MHz, CDCl<sub>3</sub>)  
 4.36 (q, J = 7.7 Hz, 2H, CH<sub>2</sub>CN); 2.73 (t, J = 6.9 Hz, 2H, OCH<sub>2</sub>)

<sup>31</sup>P-NMR: δ [ppm] (101.2 MHz, CDCl<sub>3</sub>)  
 175.02

## 2-Cyanoethyldiisopropylchlorophosphoamidite 96



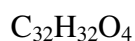
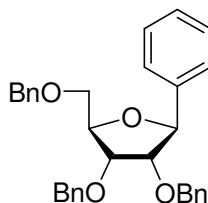
29.7 g (173 mmol) 2-cyanoethoxydichlorophosphine **157** and 150 ml from abs. Ether were mixed in a round flask and a mixture of 47.2 ml (336 mmol) diisopropylamine in 70 ml abs. Diethylether were slowly added over 90 minutes at  $-30^\circ\text{C}$ . The reaction mixture was stirred over night. White precipitate was filtrated and ether was evaporated. Left oil was fractionally distilled in vacuum. The product was obtained as oil boiling at  $78 - 80^\circ\text{C}$  ( $1 \cdot 10^{-5}$  mbar).

Yield: 22.66 g (55.8 %)

$^1\text{H-NMR}$ :  $\delta$  [ppm] (250 MHz,  $\text{CDCl}_3$ )  
 4.05 (qt,  $J = 6.9$  Hz, 2H,  $\text{CH}_2\text{CN}$ ); 3.80 (m, 2H,  $\text{CH}_2$  isopropyl); 2.74 (q,  $J = 6.9$  Hz, 2H,  $\text{OCH}_2$ ); 1.25 (m, 12H,  $\text{CH}_3$  isopropyl)

$^{31}\text{P-NMR}$ :  $\delta$  [ppm] (162 MHz,  $\text{CDCl}_3$ )  
 181.22

**2',3',5'-Tri-*O*-benzyl-1'-deoxy-1'-phenyl- $\beta$ -D-ribofuranose 91**



480.57 g/mol

To solution of 0.76 ml (7.1 mmol) bromobenzene in 20 ml abs. THF at  $-78^\circ\text{C}$  in argon atmosphere within 10 minutes 4.5 ml 1.6 M solution of *n*-butyllithium in *n*-hexane were added dropwise. After 20 minutes at  $-78^\circ\text{C}$  solution of 2,3,5-Tri-*O*-benzyl-ribo- $\gamma$ -lacton **83** (2.0 g, 4.8 mmol) in 20 ml abs. THF was added over 30 minutes dropwise and 1 hour stirred at  $-78^\circ\text{C}$ . Then the reaction mixture was allowed to warm up to  $-30^\circ\text{C}$  over two hours. The reaction was stopped by adding 5 ml of water and extracted three times with diethylether. The combined organic phases were dried over  $\text{MgSO}_4$  and evaporated to dryness. Left oil was dissolved in 20 ml methylene chloride, cooled to  $-78^\circ\text{C}$  and then 1.2 ml (9.5 mmol) boron trifluoride etherate and 1.5 ml (9.5 mmol) triethylsilane were added. The reaction mixture was then stirred 1 hour at  $-78^\circ\text{C}$  and then allowed to warm up over night to  $10^\circ\text{C}$ . Adding of 10 ml of saturated water solution of  $\text{NaHCO}_3$  stopped the reaction. Extraction with methylene chloride was done three times and collected organic phases were dried over  $\text{MgSO}_4$  and evaporated to dryness. Further purification was done by FC with *n*-hexane/ethyl acetate 4:1. The product was obtained as orange solid.

Yield: 1.71 g (74.7 %)

TLC:  $R_f = 0.45$  (*n*-hexane/ethyl acetate 4:1)

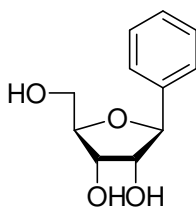
$^1\text{H-NMR}$ :  $\delta$  [ppm] (250 MHz,  $\text{DMSO-}d_6$ )

7.40 – 7.19 (m, 20H,  $\text{H}_{\text{ar}}$ ); 4.88 (d,  $J = 6.5$  Hz, 1H, 1'H); 4.61 – 4.43 (m, 6H,  $\text{CH}_2$ -benzyl); 4.24 (q,  $J = 4.0$  Hz, 1H, 4'H); 4.06 (t,  $J = 4.4$  Hz, 1H, 3'H); 3.90 (m, 1H, 2'H); 3.64 (m, 2H, 5'H)

<sup>13</sup>C-NMR:  $\delta$  [ppm] (62.9 MHz, DMSO-*d*<sub>6</sub>)  
 140.60 (C<sub>ar</sub>); 138.30 (C<sub>ar</sub>); 138.20 (C<sub>ar</sub>); 138.07 (C<sub>ar</sub>); 128.26 (C<sub>ar</sub>); 128.21 (C<sub>ar</sub>); 128.15 (C<sub>ar</sub>); 127.84 (C<sub>ar</sub>); 127.56 (C<sub>ar</sub>); 127.50 (C<sub>ar</sub>); 127.40 (C<sub>ar</sub>); 126.25 (C<sub>ar</sub>); 83.42 (C1'); 81.90 (C4'); 81.07 (C2'); 77.28 (C3'); 72.42 (CH<sub>2</sub>-benzyl); 71.07 (CH<sub>2</sub>-benzyl); 70.98 (CH<sub>2</sub>-benzyl); 70.32 (C5')

ESI(+): 498.4 ([M+NH<sub>4</sub>]<sup>+</sup>);

### 1'-Deoxy-1'-phenyl- $\beta$ -D-ribofuranose 41



C<sub>11</sub>H<sub>14</sub>O<sub>4</sub>

210.2 g/mol

0.2 g (0.42 mmol) 2',3',5'-Tri-*O*-benzyl-1'-deoxy-1'-phenyl- $\beta$ -D-ribofuranose 91 were dissolved in 8 ml. of abs. methylene chloride and cooled to -78°C. Then 1 ml of borontribromide (1M in methylene chloride) was added and for 1.5 hours stirred at -78°C. The reaction was stopped by adding 5 ml of 1:1 mixture methylene chloride/methanol and evaporated to dryness. Left brown oil was twice purified by FC with methylene chloride/methanol 9:1, as eluent. The product was obtained as light yellow solid.

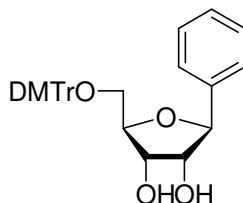
Yield: 60 mg (69.0 %)

TLC: R<sub>f</sub> = 0.24 (CH<sub>2</sub>Cl<sub>2</sub>/MeOH 9:1)

<sup>1</sup>H-NMR:  $\delta$  [ppm] (250 MHz, DMSO-*d*<sub>6</sub>)  
 7.41 – 7.22 (m, 5H, H<sub>ar</sub>); 4.93 (d, J = 6.8 Hz, 1H, 1'H); 4.86 (d, J = 4.7 Hz, 1H, 3'-OH); 4.77 (t, J = 5.5 Hz, 1H, 5'-OH); 4.54 (d, J = 7.1 Hz, 1H, 2'-OH); 3.88 (m, 1H, 4'H); 3.80 (m, 1H, 3'H); 3.68 (q, J = 5.6 Hz, 1H, 2'H); 3.53 (m, 2H, 5'H)

$^{13}\text{C}$ -NMR:  $\delta$  [ppm] (62.9 MHz,  $\text{DMSO-}d_6$ )  
 141.42 ( $\text{C}_{\text{ar}}$ ); 127.96 ( $\text{C}_{\text{ar}}$ ); 127.23 ( $\text{C}_{\text{ar}}$ ); 126.24 ( $\text{C}_{\text{ar}}$ ); 85.06 ( $\text{C1}'$ ); 82.99 ( $\text{C4}'$ );  
 77.63 ( $\text{C2}'$ ); 71.44 ( $\text{C3}'$ ); 62.06 ( $\text{C5}'$ )  
 ESI(-): 209.0 [ $\text{M-H}$ ] $^-$ ;

**5'-O-(4,4'-Dimethoxytriphenylmethyl)- 1'-deoxy-1'-phenyl- $\beta$ -D-ribofuranose 158**



$\text{C}_{32}\text{H}_{32}\text{O}_6$

512.56 g/mol

1.0 g (4.75 mmol) 1'-Deoxy-1'-phenyl- $\beta$ -D-ribofuranose **41** was dissolved in 25 ml abs. pyridine and 1.0 ml (7.2 mmol) triethylamine and 1.93 g (5.7 mmol) 4,4'-dimethoxytriphenylmethylchloride were added. The reaction mixture was stirred under argon at RT for 4 hours. The reaction was stopped by adding 3 ml of methanol and saturated water solution of  $\text{NaHCO}_3$ . It was three times extracted with methylene chloride, organic phases were collected, dried over  $\text{MgSO}_4$  and then evaporated to dryness. The product was twice co-evaporated with toluene. Further purification was done by FC with methylene chloride/methanol 98:2, as eluent. The product was obtained as yellow foam.

Yield: 1.83 g (75.3 %)

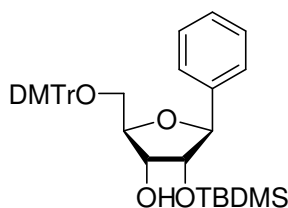
TLC:  $R_f = 0.23$  ( $\text{CH}_2\text{Cl}_2/\text{MeOH}$  98:2)

<sup>1</sup>H-NMR: δ [ppm] (250 MHz, DMSO-*d*<sub>6</sub>)  
 7.47 – 6.86 (m, 18H, H<sub>ar</sub>); 5.07 (d, J = 6.5 Hz, 1H, 1'H); 4.93 (d, J = 5.2 Hz, 1H, 3'-OH); 4.66 (d, J = 6.3 Hz, 1H, 2'-OH); 3.99 (m, 1H, 4'H); 3.88 (q, J = 4.9 Hz, 1H, 3'H); 3.74 (m, 1H, 2'H); 3.73 (s, 6H, OCH<sub>3</sub>); 3.18 (m, 2H, 5'H)

<sup>13</sup>C-NMR: δ [ppm] (62.9 MHz, DMSO-*d*<sub>6</sub>)  
 158.08 (DMTr); 149.62 (C<sub>ar</sub>); 144.98 (DMTr); 141.29 (C<sub>ar</sub>); 136.11 (C<sub>ar</sub>); 135.69 (DMTr); 129.77 (DMTr); 128.06 (DMTr); 127.79 (DMTr); 127.29 (C<sub>ar</sub>); 126.66 (C<sub>ar</sub>); 125.96 (C<sub>ar</sub>); 123.89 (C<sub>ar</sub>); 113.17 (DMTr); 85.40 (DMTr); 83.56 (C1'); 82.99 (C4'); 77.60 (C2'); 71.41 (C3'); 64.18 (C5'); 55.03 (OCH<sub>3</sub>)

ESI(-): 511.4 ([M-H]);

**5'-O-(4,4'-Dimethoxytriphenylmethyl)-2'-O-*tert.*-butyldimethylsilyl-1'-deoxy-1'-phenyl-β-D-ribofuranose 159**



C<sub>38</sub>H<sub>46</sub>O<sub>6</sub>Si

626.82 g/mol

1.09 g (2.1 mmol) 5'-O-(4,4'-Dimethoxytriphenylmethyl)-1'-deoxy-1'-phenyl-β-D-ribofuranose **158** were dissolved in 20 ml of 1:1 mixture of THF/pyridine and with 430 mg (2.5 mmol) AgNO<sub>3</sub> and 2.5 ml (2.5 mmol) 1 M *tert.*-butyldimethylsilylchloride-solution in THF were added. The reaction mixture was stirred for 20 hours at RT under argon. Adding 10ml of saturated water NaHCO<sub>3</sub>-solution stopped the reaction. Left AgCl was filtered over celite and the filtrate was extracted with methylene chloride three times. The combined organic phases were dried over MgSO<sub>4</sub> and evaporated to dryness. The crude product was twice co-evaporated with toluene. Further purification of the product was done FC with methylene chloride/isopropanol 95:5, as eluent. The product was obtained as white foam.

Yield: 390 mg (29.3 %)

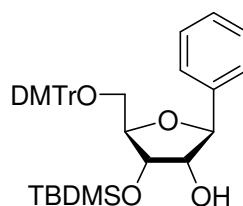
TLC:  $R_f = 0.24$  ( $\text{CH}_2\text{Cl}_2$ )

$^1\text{H-NMR}$ :  $\delta$  [ppm] (250 MHz,  $\text{DMSO-}d_6$ )  
 7.46 – 6.82 (m, 18H,  $\text{H}_{\text{ar}}$ ); 4.74 (d,  $J = 5.2$  Hz, 1H, 3'-OH); 4.67 (d,  $J = 6.4$  Hz, 1H, 1'H); 3.95 (m, 3H, 2'H, 3'H, 4'H); 3.73 (s, 6H,  $\text{OCH}_3$ ); 3.23 (m, 2H, 5'H); 0.78 (s, 9H,  $\text{SiC}(\text{CH}_3)_3$ ); -0.12 ( $\text{SiCH}_3$ ); -0.17 ( $\text{SiCH}_3$ )

$^{13}\text{C-NMR}$ :  $\delta$  [ppm] (100.6 MHz,  $\text{DMSO-}d_6$ )  
 158.06 (DMTr); 145.02 (DMTr); 140.54 ( $\text{C}_{\text{ar}}$ ); 140.21 ( $\text{C}_{\text{ar}}$ ); 135.54 (DMTr); 135.47 (DMTr); 129.75 (DMTr); 128.88 ( $\text{C}_{\text{ar}}$ ); 128.17 ( $\text{C}_{\text{ar}}$ ); 128.03 (DMTr); 127.76 (DMTr); 127.37 ( $\text{C}_{\text{ar}}$ ); 126.65 ( $\text{C}_{\text{ar}}$ ); 126.22 (DMTr); 113.13 (DMTr); 85.43 (DMTr); 83.66 ( $\text{C}1'$ ); 83.13 ( $\text{C}4'$ ); 79.66 ( $\text{C}2'$ ); 71.55 ( $\text{C}3'$ ); 63.88 ( $\text{C}5'$ ); 55.01 ( $\text{OCH}_3$ ); 25.63 ( $\text{SiC}(\text{CH}_3)_3$ ); 17.89 ( $\text{SiC}(\text{CH}_3)_3$ ); -4.98 ( $\text{SiCH}_3$ ); -5.28 ( $\text{SiCH}_3$ )

ESI(-): 625.6 ( $[\text{M-H}]^-$ );

**5'-O-(4,4'-Dimethoxytriphenylmethyl)-3'-O-tert.-butyldimethylsilyl-1'-deoxy-1'-phenyl- $\beta$ -D-ribofuranose 160**



$\text{C}_{38}\text{H}_{46}\text{O}_6\text{Si}$

626.82 g/mol

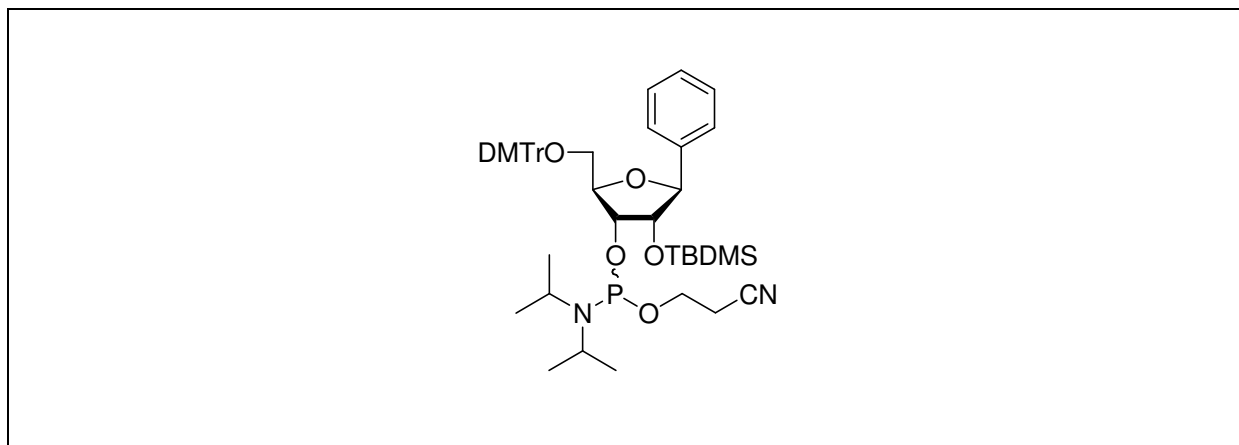
5'-O-(4,4'-Dimethoxytriphenylmethyl)-3'-O-tert.-butyldimethylsilyl-1'-deoxy-1'-phenyl- $\beta$ -D-ribofuranose 160 was obtained as a side product in the synthesis of 5'-O-(4,4'-Dimethoxytriphenylmethyl)-2'-O-tert.-butyldimethylsilyl-1'-deoxy-1'-phenyl- $\beta$ -D-ribofuranose 160.



- Yield: 560 mg (42.1 %)
- TLC:  $R_f = 0.27$  ( $\text{CH}_2\text{Cl}_2$ )
- $^1\text{H-NMR}$ :  $\delta$  [ppm] (250 MHz,  $\text{DMSO-}d_6$ )  
7.42 – 6.82 (m, 18H,  $\text{H}_{\text{ar}}$ ); 4.89 (d,  $J = 7.2$  Hz, 1H, 2'-OH); 4.67 (d,  $J = 6.4$  Hz, 1H, 1'H); 4.01 (m, 1H, 3'H); 3.94 (m, 1H, 2'H); 3.74 (m, 1H, 4'H); 3.72 (s, 6H,  $\text{OCH}_3$ ); 3.22 (m, 2H, 5'H); 0.78 (s, 9H,  $\text{SiC}(\text{CH}_3)_3$ ); -0.01 ( $\text{SiCH}_3$ ); -0.06 ( $\text{SiCH}_3$ )
- $^{13}\text{C-NMR}$ :  $\delta$  [ppm] (62.9 MHz,  $\text{DMSO-}d_6$ )  
157.78 (DMTr); 145.01 (DMTr); 140.54 ( $\text{C}_{\text{ar}}$ ); 140.22 ( $\text{C}_{\text{ar}}$ ); 135.44 (DMTr); 135.48 (DMTr); 129.75 (DMTr); 128.89 ( $\text{C}_{\text{ar}}$ ); 128.04 ( $\text{C}_{\text{ar}}$ ); 127.75 (DMTr); 127.64 (DMTr); 127.37 ( $\text{C}_{\text{ar}}$ ); 126.39 ( $\text{C}_{\text{ar}}$ ); 126.22 (DMTr); 112.73 (DMTr); 85.43 (DMTr); 83.72 ( $\text{C}1'$ ); 83.38 ( $\text{C}4'$ ); 79.88 ( $\text{C}2'$ ); 71.63 ( $\text{C}3'$ ); 63.84 ( $\text{C}5'$ ); 54.98 ( $\text{OCH}_3$ ); 25.73 ( $\text{SiC}(\underline{\text{C}}\text{H}_3)_3$ ); 17.88 ( $\text{Si}\underline{\text{C}}(\text{CH}_3)_3$ ); -5.01 ( $\text{SiCH}_3$ ); -5.25 ( $\text{SiCH}_3$ )
- ESI(-): 625.5 ( $[\text{M-H}]^-$ );

**3'-O-(2-Cyanethoxydiisopropyl-phosphin)-1'-deoxy-5'-O-(4,4'-dimethoxy-triphenylmethyl)-1'-phenyl-2'-O-tert.-butyldimethylsilyl-β-D-ribofuranose**

**161**



$C_{47}H_{63}N_2O_7PSi$

827.02 g/mol

200 mg (0.32 mmol) 5'-O-(4,4'-Dimethoxytriphenylmethyl)-2'-O-tert.-butyldimethylsilyl-1'-deoxy-1'-phenyl-β-D-ribofuranose **159** were dissolved in 10 ml abs. acetonitrile and 430 μl (3.0 mmol) *sym.* collidine and 13 μl (0.17 mmol) 1-methylimidazole were added. The reaction mixture was cooled in an icebath to 0°C and 110 μl (0.50 mmol) 2-cyanethyldiisopropylchlorophosphoramidit **96** were added. The reaction was stirred for 15 min. at 0°C and 1 hour at RT. The reaction was stopped by adding of 5 ml of 0.01 M citric acid and extracted with methylene chloride. The combined organic phases were washed with 0.01 M citric acid twice, dried over MgSO<sub>4</sub> and evaporated to dryness. Purification was done by FC with *n*-hexane/ethyl acetate, 4:1, as eluent. The product (mixture of two diastereomers) was obtained as white foam.

Yield: 152 mg (57.6 %)

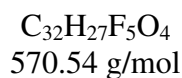
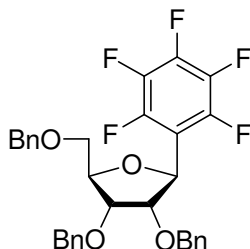
TLC:  $R_f = 0.39$  (*n*-hexan/ethylacetat 4:1)

<sup>1</sup>H-NMR: δ [ppm] (400 MHz, CDCl<sub>3</sub>)

7.56 – 6.83 (m, 36H, H<sub>ar</sub>); 4.77 (m, 2H, 1'H); 4.16 (m, 4H, 2'H, 3'H); 3.95 (m, 2H, 4'H); 3.79, 3.78 (s, 12H, OCH<sub>3</sub>); 3.55 (m, 8H, 5'H, CH<sub>2</sub>CN); 2.66 (m, 4H,

OCH<sub>2</sub>); 1.16 (m, 12H, CH(CH<sub>3</sub>)<sub>2</sub>); 0.80, 0.79 (s, 18H, SiC(CH<sub>3</sub>)<sub>3</sub>); -0.13, -  
0.15, -0.29, -0.30 (SiCH<sub>3</sub>)  
<sup>31</sup>P-NMR: δ [ppm] (162 MHz, CDCl<sub>3</sub>)  
151.88 and 149.35 (ratio 1 : 4.5)  
ESI(+): 827.6 ([M+H]<sup>+</sup>);

**2',3',5'-Tri-*O*-benzyl-1'-deoxy-1'-pentafluorophenyl- $\beta$ -D-ribofuranose 162**



To the solution that contains 5.5 g (22 mmol) pentafluorobromobenzene in 20 ml abs. diethyl ether at  $-78^{\circ}\text{C}$  under argon over 30 minutes 13 ml 1.7 M (22 mmol) solution of *n*-Butyl lithium in *n*-hexane were added. After 30 minutes at  $-78^{\circ}\text{C}$  solution of 2,3,5-Tri-*O*-benzyl-ribo- $\gamma$ -lacton (3.4 g, 8.16 mmol) **83** in 20 ml abs. diethyl ether was added over 20 minutes and 1 hour stirred at  $-78^{\circ}\text{C}$ . Afterwards the reaction mixture was allowed to warm up to  $-20^{\circ}\text{C}$  over two hours. The reaction was stopped by adding 10 ml of water and three times extracted with ether. The combined organic phases were dried over  $\text{MgSO}_4$  and evaporated to dryness. Left oil was immediately dissolved in 20 ml of methylene chloride, cooled to  $-78^{\circ}\text{C}$  and 2.1 ml (16.8 mmol) borontrifluoride ethyletherate and 2.62 (16.8 mmol) triethylsilane were added. The reaction mixture was left at  $-78^{\circ}\text{C}$  and then allowed to warm up to  $10^{\circ}\text{C}$  over night. The reaction was stopped by adding 10 ml of saturated water solution of  $\text{NaHCO}_3$  and extracted with methylene chloride three times. The combined organic phases were dried over  $\text{MgSO}_4$  and evaporated under reduced pressure. Further purification was done by FC using *n*-hexane/ethyl acetate 4:1 as eluent. The product was obtained as white solid.

Yield: 2.30 g (50 %)

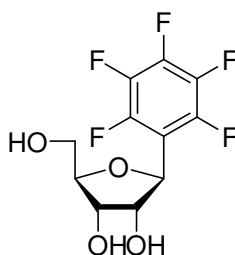
TLC:  $R_f=0.60$  (*n*-hexane/EtOAc, 4:1)

$^1\text{H NMR}$ :  $\delta$  [ppm] (400 MHz,  $\text{DMSO}-d_6$ )

7.38-7.27(m, 15H, Har); 5.04(d,  $J=7.92$  Hz, 1H, 1'H); 4.69-4.12(m, 9H,  $\text{CH}_2$ -benzyl, 4'H, 3'H, 2'H); 3.55(m, 2H, 5' $\text{CH}_2$ );

$^{13}\text{C}$  NMR:  $\delta$  [ppm] (67.9 MHz, DMSO- $d_6$ )  
 138.36(Car); 138.19(Car); 137.76(C6); 135.70(Car); 135.70(Car) ; 129.86  
 (Car); 128.80(Car) ; 128.09(Car); 128.24(Car); 128.21(Car); 128.18(Car);  
 127.0(Car); 113.66(C1); 113.65(C5); 112.39(C2), 112.28 (C4),  
 112.10(C3);112.00(C1) ; 82.10(C1'); 80.80(C4'); 76.84(C2'); 75.96(C3');  
 72.46(CH<sub>2</sub>-benzyl); 71.07(CH<sub>2</sub>-benzyl); 62.12(C5');  
 ESI (+): 593.10 ([M+Na]<sup>+</sup>);

### 1'-Deoxy-1'-pentafluorophenyl- $\beta$ -D-ribofuranose **39**



300.2 g/mol

1.4 g (2.45 mmol) 2',3',5'-Tri-*O*-benzyl-1'-deoxy-1'-pentafluorophenyl- $\beta$ -D-ribofuranose **162** were dissolved in 40 ml of abs. ethanol and 20 ml cyclohexene and 400 mg palladium-hydroxide (20%) on carbon were added. The reaction mixture was refluxed for 4 hours. Then the reaction mixture was filtrated over celite and the filtrate was evaporated under reduced pressure. The purification was done by FC with methylene chloride/methanol 9:1, as eluent. The product was obtained as colourless solid. For analytical purposes the product was crystallised from water and methanol.

Yield: 669 mg (91%)

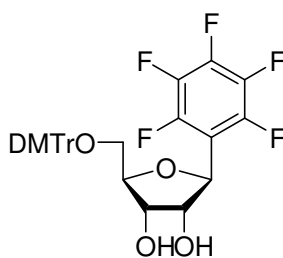
TLC: R<sub>f</sub>=0.40 (CH<sub>2</sub>Cl<sub>2</sub>/MeOH, 9:1)

$^1\text{H}$  NMR:  $\delta$  [ppm] ( 400 MHz,  $\text{DMSO-}d_6$ )  
 5.19(d,  $J=6.56$  Hz, 1H, 1'H); 5.08 (d,  $J=5.24$  Hz, 1H, 3'OH); 4.89(d,  $J=7.5$  Hz, 1H, 2'OH); 4.76(t,  $J=5.6$  HZ, 1H, 5'OH); 4.20(m,1H, 4'H); 3.94 (m, 1H, 3'H); 3.80 (m, 1H, 2'H); 3.50 (m, 2H, 5'CH<sub>2</sub>);

$^{19}\text{F}$  NMR:  $\delta$  [ppm] (235.3 MHz,  $\text{DMSO-}d_6$ )  
 -142.89 (m, 2F, 1F, 5F); -155.35 (t, 1F,  $J=23,5$  Hz, 3F); -163.21 (m, 2F, 2F, 4F);

ESI (-): 298.9 ([M-H]<sup>-</sup>);

**5'-O- (4,4'-Dimethoxytriphenylmethyl)- 1'-deoxy-1'-pentafluorophenyl- $\beta$ -D-ribofuranose 163**



$\text{C}_{32}\text{H}_{27}\text{F}_5\text{O}_6$

602.56 g/mol

0.50 g (1.66 mmol) 1'-Deoxy-1'-pentafluorophenyl- $\beta$ -D-ribofuranose **39** were dissolved in 15 ml abs. pyridine and 0.60 ml (4.25 mmol) triethylamine and 1.00 g (2.90 mmol) 4,4'-dimethoxytriphenylmethyl chloride were added. The reaction mixture was stirred under argon at RT for 24 hours. The reaction was stopped by adding 3 ml of methanol and saturated water solution of  $\text{NaHCO}_3$ . It was extracted with methylene chloride three times, organic phases were collected and dried over  $\text{MgSO}_4$  and then evaporated to dryness. Product was twice co-evaporated with toluene. Further purification was done by FC with methylene chloride/methanol 98:2 as eluent. The product was obtained as yellow foam.

Yield: 830 mg (83 %)

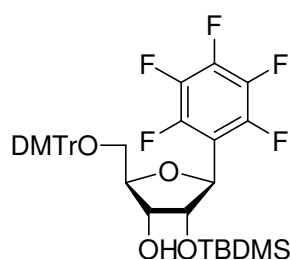
TLC: Rf=0.30 (CH<sub>2</sub>Cl<sub>2</sub>:MeOH, 95:5)

<sup>1</sup>H NMR: δ [ppm] ( 270MHz, DMSO-*d*<sub>6</sub>)  
 7.41-6.89 (m, 13H, Har); 5.26(d, J= 5.8 Hz, 1H, 1'H); 5.13(d, J=5.28 Hz, 1H, 2'OH); 4.93 (d, J=6.92 Hz, 1H, 3'OH); 4.17(m, 1H, 2'H); 3.91 (m, 2H, 3'H, 4H); 3.73(s, 6H, 2OCH<sub>3</sub>);3.14(m, 2H, 5'H);

<sup>13</sup>C NMR: δ [ppm] (67.9 MHz, DMSO-*d*<sub>6</sub>)  
 158.03(DMTr); 149.60(C4); 149.30(C3); 149.10(C5); 135.59(DMTr);  
 129.67(DMTr); 127.73(DMTr);127.66(DMTr); 127.60(C2);  
 1127.69(C2);127.50(C6); 127.00(C1); 113.11 (DMTr); 85.40(DMTr);  
 83.20(C1'); 82.70 (C4'); 77.65 (C2'); 71.10 (C3') ; 64.15 (C5'); 54.99 (OCH<sub>3</sub>) ;

ESI (-): 601.2 ([M-H]<sup>-</sup>);

**5'-O-(4,4'-Dimethoxytriphenylmethyl)-2'-O-*tert.*-butyldimethylsilyl-1'-deoxy-1'-(pentafluorophenyl)-β-D-ribofuranose 164**



C<sub>38</sub>F<sub>5</sub>O<sub>6</sub>Si

716.81 g/mol

750 mg (1.24 mmol) 5'-O-(4,4'-Dimethoxytriphenylmethyl)-1'-deoxy-1'-(pentafluorophenyl)-β-D ribofuranose **163** were dissolved in 20 ml of 1:1 mixture of THF/pyridine and with 250 mg (1.46 mmol) AgNO<sub>3</sub> and 1.80 ml (1.80 mmol) 1 M *tert.*-butyldimethylsilyl chloride-solution in THF were added. The reaction mixture was stirred for 20 hours at RT under argon. Adding 10 ml saturated water NaHCO<sub>3</sub>-solution stopped the reaction. Left AgCl

was filtered over celite and the filtrate was extracted with methylene chloride three times. The combined organic phases were dried over  $\text{MgSO}_4$  and evaporated to dryness. The crude product was twice co-evaporated with toluene. Further purification of product was done by HPLC (*MN Nucleoprep 100-20* of *Machrey-Nagel*, hexane/methyl acetate, 10:1). The product was obtained as the *slower*-migrating isomer and as white foam.

Yield: 347 mg (39%)

TLC:  $R_f=0.50$  ( $\text{CH}_2\text{Cl}_2$ )

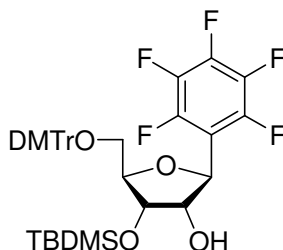
$^1\text{H}$  NMR:  $\delta$  [ppm] (270MHz,  $\text{DMSO}-d_6$ )  
7.41-6.85 (m, 13H, Har); 5.15 (d,  $J=7.04$  Hz, 1H, 3'OH); 4.94 (d,  $J=6.96$  Hz, 1H, 1'H); 4.17 (m, 1H, 2'H); 4.10 (m, 1H, 3'H); 3.93 (s, 6H, 2OCH<sub>3</sub>); 3.08(m, 2H, 5'CH<sub>2</sub>); 0.80 (s, 3H, Si(OCH<sub>3</sub>)<sub>3</sub>); 0.03(s, 3H, SiCH<sub>3</sub>); -0.02 (s, 3H, SiCH<sub>3</sub>);

$^{13}\text{C}$  NMR:  $\delta$  [ppm] (67.9 MHz,  $\text{DMSO}-d_6$ )  
158.03(DMTr); 149.60(C4); 149.30(C3); 149.10(C5); 135.59(DMTr);  
129.67(DMTr); 127.73(DMTr);127.66(DMTr); 127.60(C2);  
1127.69(C2);127.50(C6); 127.00(C1); 113.11 (DMTr); 85.40(DMTr);  
83.20(C1'); 82.70 (C4'); 77.65 (C2'); 71.10 (C3') ; 64.15 (C5'); 54.99  
(OCH<sub>3</sub>) ; 25.80(SiC(CH<sub>3</sub>)<sub>3</sub>); 17.87(SiC(CH<sub>3</sub>)<sub>3</sub>); -5.08(SiCH<sub>3</sub>);-5.35(SiCH<sub>3</sub>);

ESI (-): 715.50 ([M-H]<sup>-</sup>);



**5'-O-(4,4'-Dimethoxytriphenylmethyl)-3'-*tert.*-butyldimethylsilyl-1'-deoxy-1'-(pentafluorophenyl)- $\beta$ -D-ribofuranose 165**



$C_{38}H_{41}F_5O_6Si$

716.81 g/mol

5'-O-(4,4'-Dimethoxytriphenylmethyl)-3'-O-*tert.*-butyldimethylsilyl-1'-deoxy-1'-(pentafluorophenyl)- $\beta$ -D-ribofuranose 165 were obtained as a side product (*faster*-migrating isomer) while synthesising 5'-O-(4,4'-Dimethoxytriphenylmethyl)-2'-O-*tert.*-butyldimethylsilyl-1'-deoxy-1'-(pentafluorophenyl)- $\beta$ -D-ribofuranose 164.

Yield: 320 mg (36 %)

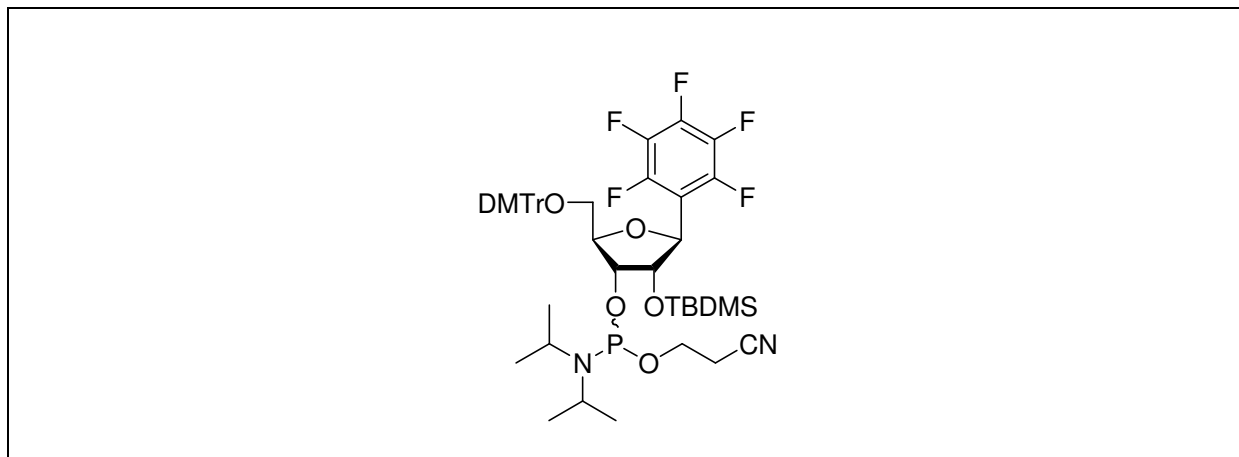
TLC:  $R_f=0.50$  ( $CH_2Cl_2$ )

$^1H$  NMR:  $\delta$  [ppm] (270MHz,  $DMSO-d_6$ )  
 7.41-6.80 (m, 13H, Har); 5.12 (d,  $J=7.04$  Hz, 1H, 1'H); 4.90 (d,  $J=6.88$  Hz, 1H, 2'OH); 4.12(m, 1H, 2'H); 3.92 (m, 1H, 3'H); 3.77(s, 6H, 2OCH<sub>3</sub>); 3.75(m, 2H, 5'H); 3.10(m, 2H, 5'CH<sub>2</sub>); 0.81(s, 3H, Si(OCH<sub>3</sub>)<sub>3</sub>); 0.02(s, 3H, SiCH<sub>3</sub>); -0.04(s, 3H, SiCH<sub>3</sub>);

$^{13}C$  NMR:  $\delta$  [ppm] (67.9 MHz,  $DMSO-d_6$ )  
 158.03(DMTr); 149.60(C4); 149.30(C3); 149.10(C5); 135.59(DMTr); 129.67(DMTr); 127.73(DMTr); 127.66(DMTr); 127.60(C2); 1127.69(C2); 127.50(C6); 127.00(C1); 113.11 (DMTr); 85.40(DMTr); 83.20(C1'); 82.70 (C4'); 77.65 (C2'); 71.10 (C3') ; 64.15 (C5'); 54.99 (OCH<sub>3</sub>) ; 25.60(SiC(CH<sub>3</sub>)<sub>3</sub>); 17.85(SiC(CH<sub>3</sub>)<sub>3</sub>); -5.07(SiCH<sub>3</sub>); -5.30(SiCH<sub>3</sub>);

ESI (-): 715.60 ([M-H]<sup>-</sup>);

**3'-O-(2-Cyanethoxydiisopropylphosphin)-1'-deoxy-5'-O-(4,4'-dimethoxy-triphenylmethyl)-1'-(pentafluorophenyl)-2'-O-*tert.*-butyldimethylsilyl- $\beta$ -D-ribofuranose 166**



$C_{47}H_{58}F_5N_2O_7PSi$

917.01 g/mol

200 mg (0.22 mmol) 5'-O-(4,4'-Dimethoxytriphenylmethyl)-2'-O-*tert.*-butyldimethylsilyl-1'-desoxy-1'-(pentafluorophenyl)- $\beta$ -D-ribofuranose 164 were dissolved in 10 ml abs. acetonitrile and 290  $\mu$ l (2.2 mmol) *sym.* collidine and 9  $\mu$ l (0.12 mmol) 1-methylimidazole were added. The reaction mixture was cooled in an icebath to 0°C and 75  $\mu$ l (0.33 mmol) 2-cyanethyldiisopropylchloro phosphoramidite 96 was added. The reaction was stirred for 15min. at 0°C and 1 hour at RT. The reaction was stopped by adding 10 ml of 0.01 M citric acid and three times extracted with methylene chloride. The combined organic phases were washed twice with 0.01 M citric acid, dried over  $MgSO_4$  and evaporated to dryness. Purification was done by FC with *n*-hexane/ethyl acetate, 4:1, as eluent. The product (mixture of two diastereomers) was obtained as white foam.

Yield: 125 mg (62 %)

TLC:  $R_f$  =0.33 (hexane/EtOAc, 4:1)

$^1H$  NMR:  $\delta$  [ppm] ( 400MHz,  $CDCl_3$ )

7.49-6.68 (m, 15H, Har); 5.12 (d,  $J$ = 7.54 Hz, 1H, 1'H); 4.52 (m, 1H, 2'H);

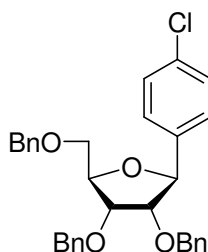
4.20 (m, 1H, 3'H); 3.96 (m, 1H, 4'H); 3.78 (s, 6H, 2OCH<sub>3</sub>); 3.60 (m, 2H,

CH<sub>2</sub>CN); 3.28 (m, 2H, 5'CH<sub>2</sub>); 2.68 (m, 2H, OCH<sub>2</sub>); 1.12 (m, 6H, CH(CH<sub>3</sub>)<sub>2</sub>);  
0.78 (s, 9H, SiC(CH<sub>3</sub>)<sub>3</sub>); 0.05 (s, 3H, SiCH<sub>3</sub>); -0.04 (s, 3H, SiCH<sub>3</sub>);

<sup>31</sup>P NMR: δ [ppm] ( 162 MHz, CDCl<sub>3</sub>)  
155.93 and 152.24 (ratio 1:4.2)

ESI (+): 941.7 ([M+Na]<sup>+</sup>);

### 2',3',5'-Tri-*O*-benzyl-1'-deoxy-1'-(4-chlorophenyl)-β-D-ribofuranose 167



C<sub>32</sub>H<sub>31</sub>ClO<sub>4</sub>

515.02 g/mol

To the solution that contains 1.5 g (7.8 mmol) 1-Bromo-4-chloro benzene in 40 ml THF at -78°C under argon over 10 minutes 4.9 ml 1.6 M (7.84 mmol) solution of *n*-butyl lithium in *n*-hexane were added. After 20 minutes at -78°C solution of 2,3,5-tri-*O*-benzyl-ribo- $\gamma$ -lacton **83** (2.81g, 6.7 mmol) in 20 ml THF was added over 30 minutes (via cannula) and 1 hour stirred at -78°C. Afterwards the reaction mixture was allowed to warm up to -20°C over two hours. The reaction was stopped by adding of 30 ml of water and three times extracted with ether. The combined organic phases were dried over MgSO<sub>4</sub> and evaporated to dryness. Left oil was immediately dissolved in 50 ml of methylene chloride, cooled to -78°C and 1.7 ml (13.4 mmol) borontrifluoride ethyletherat and 2.10 ml (13.4 mmol) triethylsilane were added. The reaction mixture was left at -78°C and than over night allowed to warm up to 10°C. The reaction was stopped by adding 10 ml of saturated water solution of NaHCO<sub>3</sub>, extracted three times with methylene chloride. The combined organic phases were dried over MgSO<sub>4</sub> and evaporated under reduced pressure. Further purification was done by FC using *n*-hexane/ethyl acetate 4:1 as eluent. The product was obtained as light orange solid.

Yield: 2.4 g (73 %)

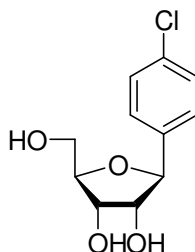
TLC:  $R_f = 0.50$  (*n*-hexan/ethyl acetate 4:1)

$^1\text{H-NMR}$ :  $\delta$  [ppm] (250 MHz,  $\text{DMSO-}d_6$ )  
 7.44 – 7.08 (m, 19H,  $\text{H}_{\text{ar}}$ ); 4.87 (d,  $J = 6.8$  Hz, 1H,  $1'\text{H}$ ); 4.61 – 4.42 (m, 6H,  $\text{CH}_2\text{-benzyl}$ ); 4.24 (q,  $J = 3.8$  Hz, 1H,  $4'\text{H}$ ); 4.07 (dd,  $J = 4.8$  Hz, 3.8 Hz, 1H,  $3'\text{H}$ ); 3.87 (dd,  $J = 5.0$  Hz,  $J = 6.8$  Hz, 1H,  $2'\text{H}$ ); 3.64 (m, 2H,  $5'\text{H}$ )

$^{13}\text{C-NMR}$ :  $\delta$  [ppm] (67.9 MHz,  $\text{DMSO-}d_6$ )  
 138.19 ( $\text{C}_{\text{ar}}$ ); 137.95 ( $\text{C}_{\text{ar}}$ ); 136.63 ( $\text{C1}$ ); 128.18 ( $\text{C}_{\text{ar}}$ ); 128.11 ( $\text{C}_{\text{ar}}$ ); 128.05 ( $\text{C}_{\text{ar}}$ ); 127.74 ( $\text{C}_{\text{ar}}$ ); 127.43 ( $\text{C}_{\text{ar}}$ ); 127.36 ( $\text{C}_{\text{ar}}$ ); 123.99 ( $\text{C5}$ ); 114.95 ( $\text{C2}$ ); 114.64 ( $\text{C6}$ ); 83.41 ( $\text{C1}'$ ); 81.23 ( $\text{C4}'$ ); 81.08 ( $\text{C2}'$ ); 77.27 ( $\text{C3}'$ ); 72.41 ( $\text{CH}_2\text{-benzyl}$ ); 71.10 ( $\text{CH}_2\text{-benzyl}$ ); 70.96 ( $\text{CH}_2\text{-benzyl}$ ); 70.27 ( $\text{C5}'$ )

ESI(+):  $m/z$  515.5 ( $[\text{M}+\text{H}]^+$ );

### 1'-Deoxy-1'-(4-chlorophenyl)- $\beta$ -D-ribofuranose 43



$\text{C}_{11}\text{H}_{13}\text{ClO}_4$

244.45 g/mol

2.0 g (3.9 mmol) 2',3',5'-Tri-*O*-benzyl-1'-deoxy-1'-(4-chlorophenyl)- $\beta$ -D-ribofuranose 167 were dissolved in 40 ml abs. ethanol and 20 ml cyclohexene and 300 mg palladium-hydroxide (20%) on carbon were added. The reaction mixture was refluxed for 3 hours. Then the reaction mixture was filtrated over celite and the filtrate was evaporated under reduced pressure. The purification was done by FC with methylene chloride/methanol 9:1 as eluent. The product was obtained as colourless solid. For analytical purposes it was crystallized from water and methanol.

Yield: 0.92 g (95 %)

TLC:  $R_f = 0.42$  ( $\text{CH}_2\text{Cl}_2/\text{MeOH}$  9:1)

$^1\text{H-NMR}$ :  $\delta$  [ppm] (250 MHz,  $\text{DMSO-}d_6$ )

7.42 (m, 4H,  $\text{H}_{\text{ar}}$ ); 4.91 (d,  $J = 4.7$  Hz, 1H, 3'-OH); 4.82 (t,  $J = 5.5$  Hz, 1H, 5'-OH); 4.67 (d,  $J = 7.0$  Hz, 1H, 1'H); 4.56 (d,  $J = 7.3$  Hz, 1H, 2'-OH); 3.89 (m, 1H, 3'H); 3.81 (m, 1H, 4'H); 3.66 (m, 1H, 2'H); 3.24 (m, 2H, 5'H)

$^{13}\text{C-NMR}$ :  $\delta$  [ppm] (67.9 MHz,  $\text{DMSO-}d_6$ )

137.72 (C1); 128.06 (C3); 114.79 (C2); 114.47 (C6); 85.18 (C1'); 82.21 (C4'); 77.55 (C2'); 71.35 (C3'); 61.97 (C5')

ESI(-):  $m/z$  242.7 ([M-H]);

## 10.6 Synthesis of Oligonucleotides

RNA Synthesis was done on 1 $\mu$ mol scale on the Synthesizer from company PerSeptive Biosystems (Model Expedite 8905). We used 500 Å CPG solid phase from PerSeptive Biosystems. Standard coupling times of 10 minutes were used for all RNA nucleosides. Coupling yields were similar in-between all synthesised oligonucleotides. The RNA amidites were used for synthesis in 0.01M concentration. After the synthesis DMTr-group was cleaved. Oligonucleotides were kept at 55°C over night after treatment with ammonia/methanol mixture (3:1). The mixture was then filtrated through 0,2 $\mu$ mol sterile filter with cellulose membrane and filtrate was evaporated in a Speed Vac concentrator. To left solid was added 1 ml of triethylaminetrihydrofluoride and after 24h at room temperature the 2'TBDMS groups were cleaved. Than 3ml of n-butanol, cooled to -20°C, was added and the mixture was left at -20°C for three hours. At the end the mixture was centrifuged for 15 minutes at 12000 at 4 °C. Afterwards the solution was decanted and left solid dissolved in 150  $\mu$ l of DEPC water and 150  $\mu$ l 1-methyl-2-pyrrolidinone dissolved. The dissolved oligonucleotide was purified with ion exchange-HPLC.

## 10.7 Purification and Analytics of Oligonucleotides

### 10.7.1 HPLC-purification

The RNA oligonucleotides were synthesised in "Trityl off" modus and with ion-exchange-HPLC purified. We used HPLC machine from JASCO, which has PU-980 pump, LG-980-02 mixer, UV-970 detector, column heating oven and computer. As analytical column was used Dionex NucleoPac<sup>TM</sup>PA100 column ( 250\*4mm). With the flow of 5ml/min. As preparative column was used Dionex NucleoPac<sup>TM</sup>PA100 column ( 250\*9mm). The linear gradient from 0% to 70% of B in A (in 40 min.) was used (Puffer A: DEPC-water (pH=8,00), puffer B: 1M LiCl (pH=8,00)). The UV-detection was preformed at 260 nm. After separation the oligo was over Sephadex PD 10 column with G25 material desalted. Than the amount of synthesised oligonucleotide was determined through measuring of OD<sub>260</sub>. The purity of product was controlled with MALDI.

### 10.7.2 The amounts of synthesised oligonucleotides

Purified and desalted oligonucleotide was dissolved in 1,00 ml of DEPC water. Then 10 µl of the solution was taken and added into the 10mm quartz cuvette with DEPC water filled up to 1000 µl. Absorbance or optical density at 260 nm was measured. The value read at the machine was multiplied with 100. The result is the yield in OD<sub>260</sub> that is in 1ml dissolved. This leaves us with the possibility to count the extinction coefficient  $\epsilon$  and the concentration.

### 10.7.3 The Extinction coefficient of Oligonucleotides

The molar extinction coefficient of oligonucleotides could be calculated from the sum of known extinction coefficients for natural nucleosides. According to Eckstein (Eckstein, 1991) the following is known:

$$\epsilon = ( 8,8 \cdot nT + 7,3 \cdot nC + 11,7 \cdot nG + 15,4 \cdot nA ) \cdot 0,9 [1000 \text{ cm}^2 \text{ mol}^{-1}]$$

The n is the number of each nucleoside in oligonucleotide. The factor 0,9 corrects the UV absorbance concerning the influence of the bases in single strand oligonucleotide.

The exact method for determination of molar extinction coefficient is given from Puglisi and Tinoco (Tinoco, 1989) and also Gray (Gray et al., 1995). In the determination is also calculated the influence of chromophores with neighbours. This tells us that the extinction coefficient of dinucleotide is not sum of extinction coefficients of nucleosides. The values are given in table .The extinction coefficient is determined through following:

$$\epsilon(\text{ACGU}...) = 2 [\epsilon(\text{AC}) + \epsilon(\text{CG}) + \epsilon(\text{GU}) + \dots] - [\epsilon(\text{C}) + \epsilon(\text{G}) + \epsilon(\text{U}) + \dots]$$

<b>Building block</b>	<b>RNA</b>	<b>Building block</b>	<b>RNA</b>
A	15,34	CG	9,39
C	7,60	CU	8,37
G	12,16	GA	12,92
U	10,21	GC	9,19
AA	13,65	GG	11,43
AC	10,67	GU	10,96
AG	12,79	UA	12,52
AU	12,14	UC	8,90
CA	10,67	UG	10,40
CC	7,52	UU	10,11

*Figure 10.1. The extinction coefficients of monomer and dimers at 260 nm after Puglisi and Tinoco ( 1989) also Gray et al. (1995). The values are given at 25 °C, pH7, 00 and ion strength of 0.1.*

The extinction coefficients of analogues that are not known, in this case are calculated as the values for U or G.

The concentration of oligonucleotide solution in mol dm<sup>-3</sup> and d, in cm, is in connection with OD<sub>260</sub>, absorbance at 260 nm, in the following sense:

$$OD_{260} = \epsilon \cdot c \cdot d$$

$$c = OD_{260} / \epsilon \cdot d$$

## 10.8 UV-Melting Curves

The UV- melting curves were measured using UV-/VIS-Spectrophotometer Cary 1, from Varian company. As a puffer was used phosphate puffer 140 mM NaCl, 10 mM Na<sub>2</sub>HPO<sub>4</sub> and 10 mM NaH<sub>2</sub>PO<sub>4</sub>. The solution's pH value was with solution of HCl fixed to pH=7,00. The used water was DEPC water. For DEPC water was made 0,1% solution of DEPC in water, left over night and than 30 min. autoclaved.

For performing a measurement as a reference was used 1ml of puffer in a reference civet. The sample cuvette, with the same d, was fulfilled with a same puffer and the 0 was set up at



machine. Then the concentration of 2 μmol of each strain that together make duplex was measured in cuvette. The oligonucleotides are dissolved in known volume of DEPC water . Before we begin to measure we close teflon cover. The measurement begins with denaturation. Therefore we heat the cuvettes 10 min up to 80°C and afterwards at 5°C for a min. we renature them. Then the system was cooled up to the starting temperature (5 or 10°C) and kept on starting temperature for 10 minutes. The measurement is done with heating rate from 0,5°C/min at 260 nm and 274 nm. Every 30 seconds data are registered. This is considered precise enough (Varian, 1998). After measurement is finished the data are automatically shown in a graph and the sample cooled to 25°C. All measurements were done at least twice. Comparing measurements at 260 nm and 274 nm no significant differences were registered. The  $T_m$  value was from  $\alpha = f(T)$  curve calculated. For all the measurements below 20°C the cuvettes were purged with N<sub>2</sub>, to put way the influence of condensation of air water on the walls of cuvettes.

For the better comparing the OD values are normalized in the following way:

$$OD_{norm} = (OD(T) - OD_B) / (OD_E - OD_B)$$

were OD<sub>B</sub> is the beginning value of absorbance and OD<sub>E</sub> the end value of absorbance.

## **10.9 CD-Spectroscopy of Oligonucleotides**

The CD spectra were measured with JASCO J-170 Spectropolarimeter, with thermostatic cuvette ( Neslab RTE-100) holder. The same samples that were used for UV measurements were used. For each measurement five measurements were accumulated from 350 nm to 200 nm. Following conditions were used: 0,2 nm, scan speed 50 nm/min., response 1 sec. And band at 1 nm. In this way measured spectra at each temperature of measurement the spectra of buffer was leaved off.

## **10.10 Determination of Partition Coefficient**

For determination of partition coefficients the nucleosides were dissolved in water, using the concentrations that have absorbance between 0,8-1,2. From this solution 2 ml were mixed with the same volume of 1-octanol over 10 minutes. Than the samples were centrifuged over 10 min. with 10 000 rpm and two faces were separated. The absorbance of water and 1-

octanol phase were measured. The partition coefficient was calculated from the following equation:

$$\log P = A_{\text{octanol}}/A_{\text{water}}$$

### **10.11 Determination of HPLC Retention Times**

For determination of retention times were used solutions that were also used for determination of partition coefficients of unprotected nucleosides. The retention times were measured on HPLC machine designed by JASCO, with PU-980 pump, LG-980-02-mixer, UV-970 detector, heating oven for column and computer. As analytic column was used RP-18 (5 $\mu$ m) from Merck company (lichrosphere EcoCART 125-3, Nr. 647318) with flow of 0,6 ml/min. As eluent was used a 5% solution of acetonitrile in water. Identification was done at 260 nm.



# 11 References

Adamson, A. G.; Rees, W. C.; Towards the Total Synthesis of cyclo[n]carbons and the generation of cyclo[6]carbon, *J. Chem. Soc. Perkin Trans 1*, **1996**, 1535-1543

Albright, J.D.; Goldman, L.; Dimethyl sulfoxid-acid anhydride mixtures for the oxidation of alcohols, *J. Am. Chem. Soc.*, **1967**, 89, 2416-2423

Bahr, U.; Karas, M.; Hillenkamp, F.; Analysis of biopolymers by matrix-assisted laser desorption/ionization (MALDI) mass spectrometry, *Fres. J. Anal. Chem.*, **1994**, 348, 783-791

Balzarini, J.; Baba, M.; Pauwels, R.; Herdewijn, P.; De Clercq, E.; Anti-retrovirus activity of 3'-fluoro- and 3'-azido-substituted pyrimidine 2',3'-dideoxynucleoside analogues, *Biochem. Pharmacol.*, **1988**, 37, 2847-2856

Balzarini, J.; Cools, M.; Herdewijn, P.; De Clercq, E.; Estimation of the Lipophilicity of anti-HIV Nucleoside Analogues by Determination of the Partition coefficient and Retention Time on Lichrospher 60 RP-8 HPLC column, *Biochem. Biophys. Res. Com.*, **1989**, 158, 413-422

Barker, R.; Fletcher, H.G. Jr.; 2,3,5-Tri-*O*-benzyl-D-ribosyl and -L-arabinosyl bromides, *J. Org. Chem.*, **1969**, 34, 384-389

Batey, R. T.; Rambo, R. T.; Doudna, J. A.; Tertiäre Motive bei Struktur und Faltung von RNA, *Angew. Chemie*, **1999**, 2472-2491

Bats, J.W.; Parsch, J.; Engels, J.W.; 1-Deoxy-1-(3-fluorophenyl)- $\beta$ -D-ribofuranose, *Acta Cryst. C*, **1999**, 55, IUC9900070

Bats, J.W.; Parsch, J.; Engels, J.W.; 1-Deoxy-1-(2-fluorophenyl)- $\beta$ -D-ribofuranose, *Acta Cryst. C*, **1999a**, 55, IUC9900069

Bats, J.W.; Parsch, J.; Engels, J.W.; 1-Deoxy-1-(4-fluorophenyl)- $\beta$ -D-ribofuranose, its hemihydrate, and 1-deoxy-1-(2,4-difluorophenyl)- $\beta$ -D-ribofuranose: Structural evidence for intermolecular C-H $\cdots$ F-C interactions, *Acta Cryst. C*, **2000**, 56, 201-205

Beaucage, S.L.; Caruthers, M.H.; Deoxynucleoside phosphoramidites – a new class of key intermediates for deoxypolynucleotide synthesis, *Tetrahedron Lett.*, **1981**, 22, 1859-1862

Beaucage, S.L.; Iyer, R.P.; Advances in the synthesis of oligonucleotides by the phosphoramidite approach, *Tetrahedron*, **1992**, 48, 2223-2311

Beaucage, S.L.; Iyer, R.P.; The synthesis of modified oligonucleotides by phosphoramidite approach and their applications, *Tetrahedron*, **1993**, 49, 6123-6194

Berger, M.; Wu, Y.; Ogawa, A.K.; McMinn, D.L.; Schultz, P.G.; Romesberg, F.E.; Universal bases for hybridisation, replication and chain termination, *Nucleic Acids Res.*, **2000**, 28, 2911-2914

Bergstrom, D.E.; Ruth, J.L.; Reddy, P.A.; De Clercq, E.; Synthesis of (E)-5-(3,3,3-trifluoro-1-propenyl)-2'-deoxyuridine and related analogues: Potent and unusually selective antiviral activity of (E)-5-(3,3,3-trifluoro-1-propenyl)-2'-deoxyuridine against herpes simplex virus type 1, *J. Med. Chem.*, **1984**, 27, 279-284

Bergstrom, D.E.; Zhang, P.M.; Toma, P.H.; Andrews, P.C.; Nichols, R.; Synthesis, structure and deoxyribonucleic acid sequencing with a universal base: 1-(2'-deoxy- $\beta$ -D-ribofuranosyl)-3-nitropyrrole, *J. Am. Chem. Soc.*, **1995**, 117, 1201-1209

Berner, S.; Mühlegger, K.; Seliger, H.; Studies on the role of tetrazole in the activation of phosphoramidites, *Nucleic Acids Res.*, **1989**, 17, 853-864

Blackburn, G.M.; Phosphonates as analogs of biological phosphates, *Chem. Ind. (London)*, **1981**, 134-138

Blackburn, G.M.; Perrée, T.D.; Rashid, A.; Bisbal, C.; Lebleu, B.; Isosteric and isopolar analogs of nucleotides, *Chemica Scripta*, **1986**, 26, 21-24

Blackburn, G.M.; Gait, M.J.; Nucleic acids in chemistry and biology, 2<sup>nd</sup> edition, Oxford University Press, Oxford New York Tokyo, **1996**

Boenigk, D.; Mootz, D.; Fluorides and fluoro acids. Part 18. The system pyridine-hydrogen fluoride at low temperatures. Formation and crystal structures of solid complexes with very strong NHF and FHF hydrogen bonding, *J. Am. Chem. Soc.*, **1988**, *110*, 2135-2139

Bragg, W.H.; Bragg, W.C.; The reflection of X-rays by crystals, *Proc. Roy. Soc. London*, **1913**, (A) 88, 428-438

Brahms, J.; Optical activity and the conformation of polynucleotides, *J. Am. Chem. Soc.*, **1963**, *85*, 3298-3300

Brahms, J.; Circular dichroism investigations of the two conformations of polyriboadenylic acid, *Nature*, **1964**, *202*, 797-798

Brahms, J.; Mommaerts, W.F.H.M.; A study of conformation of nucleic acids in solution by means of circular dichroism, *J. Mol. Biol.*, **1964**, *10*, 73-88

Brahms, J.; Optical activity and the conformation of polynucleotide models of nucleic acids, *J. Mol. Biol.*, **1965**, *11*, 785-801

Brahms, J.; Maurizot, J.C.; Michelson, A.M.; Conformation and thermodynamic properties of oligocytidylic acids, *J. Mol. Biol.*, **1967**, *25*, 456-480

Bridges, J. A.; Patt, C. W.; Stickney M.T.; A Dramatic solvent effect during Aromatic Halogen-Methyl Exchanges. Different products from Lithiation of Polyfluorobenzenes in Etar and THF, *J. Org. Chem.*, **1990**, *55*, 773-775

Brown, D.M.; Todd, A.R.; Nucleotides, part X. Some observations on structure and chemical behaviour of nucleic acids, *J. Chem. Soc.*, **1952**, 52-58

Brückner, C.; Holzinger, H.; Reissig, H.U.; Diastereoselective syntheses of highly substituted methyl tetrahydrofuran-3-carboxylates by reactions of  $\gamma$ -lactols with silylated nucleophiles, *J. Org. Chem.*, **1988**, *53*, 2450-2456

Bush, C.A.; Brahms, J.; Optical activity of single-strand oligonucleotides, *J. Chem. Phys.*, **1967**, *46*, 79-88

Caruthers, M.D.; Gene synthesis machines: DNA chemistry and its uses, *Science*, **1985**, *230*, 281-285

Caruthers, M.H.; Barone, A.D.; Beaucage, S.L.; Dodds, D.L.; Fisher, E.F.; McBride, L.J.; Matteucci, M.; Stabinski, Z.; Tang, J.-Y.; Chemical synthesis of deoxynucleotides by the phosphoramidite method, *Methods Enzymol.*, **1987**, *154*, 287-313

Clark, L.C.; Cecil, K.P.; Singh, D.; Gray, M.D.; CD Absorption and Thermodynamic Analysis of Repeating Dinucleotides DNA, RNA and Hybrid Duplexes [d/r(AC)]<sub>12</sub>\*[d/r(GT/U)]<sub>12</sub> and the Influence of Phosphotioate Substitution, *Nucleic Acids Res.*, **1997**, *25*, 4098-4105

Chargaff, E.; Structure and function of nucleic acids as cell constituents, *Fed. Proc.*, **1951**, *10*, 654-659

Chen, C.; Russu, M.I.; Sequence dependence of the Energetics of Opening of AT Basepairs in DNA, *Biophysical Journal*, **2004**, *87*, 2545-2551

Cheng, D.M.; Kan, L.S.; Ts'ó, P.O.P.; Uesugi, S.; Takatsuka, Y.; Ikehara, M.; Multinuclear magnetic resonance studies of monomers and dimers containing 2'-fluoro-2'-deoxyadenosine, *Biopolymers*, **1983**, *22*, 1427-1444

Chidgeavadze, Z.G.; Scamrov, A.V.; Beabealashvilli, R.S.; Kvasnyuk, E.I.; Zaitseva, G.V.; Mikhailopulo, I.A.; Kowollik, G.; Langen, P.; 3'-Fluoro-2',3'-dideoxyribonucleoside-5'-triphosphates: terminators of DNA synthesis, *FEBS Lett.*, **1985**, *183*, 275-278

Coe, P.L.; Waring, A.J.; Yarwood, T.D.; The lithiation of fluorinated benzenes and its dependence on solvent and temperature, *J. Chem. Soc. Perkin Trans. 1*, **1995**, 2729-2737

Csizmadia, F.; Tsantili- Kakoulidou, A.; Panderi, I.; Darvas, F.; Prediction of Distribution Coefficient from Structure.!. Estimation Method, *J. of Pharm. Sci.*, **1997**, *86*, 865-871

Desiraju, R.G.; Hydrogen Bridges in Crystall Engineering: Interactions without Borders, *Acc. Chem. Res.*, **2002**, *35*, 565-573

Dahl, B.H.; Nielsen, J.; Dahl, O.; Mechanistic studies on the phosphoramidite coupling reaction in oligonucleotide synthesis. I. Evidence for nucleophilic catalysis by tetrazole and rate variations with the phosphorus substituents, *Nucleic Acids Res.*, **1987**, *15*, 1729-1743

Dickerson, R.E. et al.; Definitions and nomenclature of nucleic acid structure components, *Nucleic Acids Res.*, **1989**, *17*, 1797-1803

Dixon, A.J.; Fischman, H.D.; Dudinyan, S.R.; Nucleophilic Attack Leading to Addition of Alkylolithium Reagents to Aromatic Hydrocarbons, *Tetrahedron Lett.*, **1964**, *12*, 613-616

Dole, M.; Mack, L.L.; Hines, L.R.; Molecular Beams of Macroins, *The Journal of Chem. Physic.*, **1968**, *49*, 2240-2249

Dole, M.; Mack, L.L.; Kralik, P.; Rheude, A.; Molecular Beams of Macroins II, *The Journal of Chem. Physic.*, **1970**, *52*, 4977-4986

Dunitz, J.D.; Perspectives in Supramolecular Chemistry: The Crystals as a Supramolecular Entity, *Wiley, Chichester*, **1996**, 1-30

Dunitz, J.D.; Taylor, R.; Organic fluorine hardly ever accepts hydrogen bonds, *Chem. Eur. J.*, **1997**, *3*, 89-98

Dunitz, J.D.; Organic Fluorine: Odd Man Out, *ChemBioChem*, **2004**, *5*, 614-621

Dunitz, J.D.; Gavezzoti, A.; Schweitzer, B.W.; Molecular Shape and Intermolecular Laison: Hydrocarbons and Fluorocarbons, *Helv. Chim. Acta*, **2003**, *86*, 4073-4092

Eckstein, F. (Hrsg.); Oligonucleotides and Analogues: A Practical Approach, IRL Press, Oxford, **1991**



Edelhoch, H.; Osborne, J.C. Jr.; The thermodynaminc basis of the stability of proteins, nucleic acids, and membranes, *Adv. Protein Chem.*, **1976**, *30*, 183-250

Engels, J.W.; Eckstein, F.; Encyclopedia of Molecular Cell Biology, Ed. Meyers, **2003**

Etzold, G.; Hintsche, R.; Kowollik, G.; Langen, P.; Nucleoside von Fluorzucker-VI. Synthese und Reaktivität von 3'-Fluor- und 3'-Chlor-3-Desoxythymidin, *Tetrahedron*, **1971**, *27*, 2463-2472

*Falk, M.; Hartman, K.A. Jr.; Lord, R.C.; Hydration of deoxyribonucleic acid. II. An infrared study, J. Am. Chem. Soc.*, **1963**, *85*, 387-391

Fauvet, G.; Masseur, M.; Chevalier, R.; Study of the crystal structure of benzonitrile at 198 K, *Acta Cryst.*, **1978**, *B34*, 1376-1378

Felsenfeld, G.; Hirschman, S.Z.; A neighbor-interaction analysis of the hypochromism and spectra of DNA, *J. Mol. Biol.*, **1965**, *13*, 407-427

Finger, G.C.; Reed, F.H.; Finnerty, J.L.; Aromatic fluorine compounds. V. 1,3,5-Trifluorobenzene, *J. Am. Chem. Soc.*, **1951**, *73*, 153-155

Fisher, E.F.; Caruthers, M.H.; Color coded triarylmethylprotecting groups useful for deoxypolynucleotide synthesis, *Nucleic Acids Res.*, **1983**, *11*, 1589-1599

Fitzgerald, M.C.; Smith, L.M.; Mass spectrometry of nucleic acids: the promise of matrix-assisted laser desorption-ionization (MALDI) mass spectrometry, *Annu. Rev. Biophys. Biomol. Struct.*, **1995**, *24*, 117-140

Gait, M.J.; (Hrsg.) Oligonucleotide Synthesis: A Practical Approach, IRL Press, Oxford **1984**

Gallicchio, E.; Kubo, M.M.; Levy, R.M.; Entropy-enthalpy compensation in solvation and ligand binding revisited, *J. Am. Chem. Soc.*, **1998**, *120*, 4526-4527

Gandhi, V.; Mineishi, S.; Huang, P.; Chapman, A.J.; Young, Y.; Chen, F.; Nowak, B.; Chubb, S.; Hertel, L.W.; Plunkett, W.; Cytotoxicity, metabolism, and mechanisms of action of 2',2'-difluorodideoxyguanosine in chinese hamster ovary cells, *Cancer Res.*, **1995**, *55*, 1517-1524

Garegg, P.J.; Lindh, I.; Regberg, T.; Stawinski, J.; Strömberg, R.; Nucleoside-H-phosphonates, *Tetrahedron Lett.*, **1986**, *27*, 4055-4058

Gasparutto, D.; Livache, T.; Bazin, H.; Dupla, A.M.; Guy, A.; Khorlin, A.; Molko, D.; Roget, A.; Teoule, R.; Chemical synthesis of a biologically active natural t-RNA with its minor bases, *Nucleic Acids Res.*, **1992**, *20*, 5152-5166

Gewirtz, A.M.; Souol, D.L.; Rataczak, M.Z.; Nucleic Acid Therapeutics state of the Art and future prospects, *Blood*, **1998**, *92*, 712-736

Goodman, A.J.; Breinlinger, E.C.; McIntosh, C.M.; Grimaldi, L.N.; Rotello, V.M.; Model system for Flavoenzyme Activity. Control of Flavin Recognition via Specific Electrostatic Interactions, *Organic Lett.*, **2001**, *3*, 1531-1534

Gray, D.M.; Ratliff, R.L.; Vaughan, M.R.; Circular dichroism spectroscopy of DNA, *Methods Enzymol.*, **1992**, *211*, 389-406

Gray, D.M.; Hung, S.-H.; Johnson, K.H.; Absorption and circular dichroism spectroscopy of nucleic acid duplexes and triplexes, *Methods Enzymol.*, **1995**, *246*, 19-34

Guckian, K.M.; Schweitzer, B.A.; Ren, R.X.F.; Sheils, C.J.; Paris, P.L.; Tahmassebi, D.C.; Kool, E.T.; Experimental measurement of aromatic stacking affinities in the context of duplex DNA, *J. Am. Chem. Soc.*, **1996**, *118*, 8182-8183

Guckian, K.M.; Schweitzer, A.B., Ren, F.X.R.; Sheils, J.C.; Talmassite, C.D.; Kool, E.T.; Factors Contributing to Aromatic Stacking in Water: Evaluation in the Contest of DNA, *J. Am. Chem. Soc.*, **2000**, *122*, 2213-2222

Haiduc, J.; Gilman, H.; Polyhalo-organometallic and-organometaloidal Compounds, *Journal of Organomet. Chem.*, **1967**, 394-395

Haasnoot, C.A.G.; Altona, C.; A conformational study of nucleic acid phosphate ester bonds using phosphorus-31 nuclear magnetic resonance, *Nucleic Acids Res.* **1979**, *6*, 1135-1149

Haeberlein, M.; Brinck, T.; Prediction of Water-Octanol Partition Coefficients using Theoretical Descriptors derived from the Molecular Surface Area and the Electrostatic Potential, *J. Chem. Soc., Perkin. Trans. 2*, **1997**, 289-297

Hakimelahi, G.H.; Proba, Z.A.; Ogilvie, K.K.; Nitrate ions as catalyst for selective silylations of nucleosides, *Tetrahedron Lett.*, **1981**, *22*, 4775-4778

Hakimelahi, G.H.; Proba, Z.A.; Ogilvie, K.K.; New catalysts and procedures for the dimethoxytritylation and selective silylation of ribonucleosides, *Can. J. Chem.*, **1982**, *60*, 1106-1113

Hanessian, S.; Liak, T.J.; Vanasse, B.; Facile cleavage of benzyl ethers by catalytic transfer hydrogenation, *Synthesis*, **1981**, 396-397

Hannon, G.J.; RNA Interference, *Nature*, **2002**, *418*, 244-251

Hansske, F.; Madej, D.; Robins, M.J.; 2'- und 3'-Ketonucleosides and their arabino and xylo reduction products, *Tetrahedron*, **1984**, *40*, 125-135

Harada, K.; Matulic-Adamic, J.; Price, R.W.; Schinazi, R.F.; Watanabe, K.A.; Nucleosides. 139. Synthesis of anticyclomegalovirus and antiherpes simplex virus activity of 5'-modified analogues of 2'-fluoro-arabinosylpyrimidine nucleosides, *J. Med. Chem.*, **1987**, *30*, 226-230

Harrell, S.A.; McDaniel, D.H.; Strong hydrogen bonds II. The hydrogen difluoride ion, *J. Am. Chem. Soc.*, **1964**, *86*, 4497

Hashizme, T.H.; Synthesis in Nucleoside Antibiotics II Facile synthesis of Nebularine and its Analogues by Modified Fusion Procedure, *J. Org. Chem.*, **1968**, *33*, 1796-1799

Heath, P.; Mann, J.; Walsh, E.B.; Wadsworth, A.H.; The preparation of dioxaprostacyclin analogues from D-(-)-ribose, *J. Chem. Soc. Perkin Trans. 1*, **1983**, 2675-2679

Henry, A.A.; Olsen, G.A.; Matsuda, S.; Yu, C.; Geierstanger, H.B.; Romesberg, E.F.; Efforts To Expand the Genetic Alphabet: Identification of a Replicable Unnatural DNA Self-Pair, *J. Am. Chem. Soc.*, **2004**, *126*, 6923-6931

Hoogsteen, K.; The structure of crystals containing a hydrogen-bonded complex of 1-methylthymine and 9-methyladenine, *Acta Cryst.*, **1959**, *12*, 822-823

Hossain, N.; van Halbeek, H.; De Clercq, E.; Herdewijn, P.; Synthesis of 3'-C-branched 1'-5'-anhydromannitol nucleosides as new antiherpes agents, *Tetrahedron*, **1998**, *54*, 2209-2226

Howard, J.A.K.; Hoy, V.J.; O'Hagan, D.; Smith, G.T.; How good is fluorine as a hydrogen bond acceptor?, *Tetrahedron*, **1996**, *52*, 12613-12622

Howels, D.R.; Gilman, H.; A Pronounced Temperature Effect in the Reaction of 1,3,5-trifluorobenzene with t-BuLi, *Tetrahedron*, **1974**, 1319-1320

Hunter, C.A.; Sequence-dependent DNA structure, the role of base stacking interactions, *J. Mol. Biol.*, **1993**, *230*, 1025-1054

Ikehara, M.; 2'-Substituted 2'-deoxypurinenucleotides, their conformation and properties, *Heterocycles*, **1984**, *21*, 75-90

IUPAC-IUB Joint Commission on Biochemical Nomenclature (JCBN), Abbreviations and symbols for the description of conformations of polynucleotide chains, *Eur. J. Biochem.*, **1983**, *131*, 9-15

Jenkins, I.D.; Verheyden, J.P.H.; Moffatt, J.G.; 4'-Substituted nucleosides. 2. Synthesis of the nucleoside antibiotic nucleocidin, *J. Am. Chem. Soc.*, **1976**, *98*, 3346-3357

Joecks, A.; Koppel, H.; Schleinitz, K.D.; Cech, D.; NMR- spectroscopic studies of the conformational behavior of some 2' and 3'- halogeno-substituted pyrimidine nucleosides, *J. Prakt. Chem.*, **1983**, *325*, 881-892

Jones, S.R.; Reese, C.B.; Migration of t-butyldimethylsilyl protecting groups, *J. Chem. Soc. Perkin Trans.I*, **1979**, 2762-2764

Karas, M.; Hillenkamp, F.; Laser desorption ionization of proteins with molecular masses exceeding 10000 daltons, *Anal. Chem.*, **1988**, *60*, 2299-2301

Kinckaid, K.; Beckman, J.; Zivkovic, A; Halcomb, L.M.; Engels, J.W.; Kuchta, R.D.; Exploration of Factors Driving Incorporation of Unnatural dNTPs into DNA by Klenow Fragment (DNA polymerase I) and DNA polymerase  $\alpha$ , *submitted to Nucleic Acid Res.*, **2005**

Kirk, K.L.; Cohen, L.A.; The synthesis of some fluoronitrobenzimidazoles and their reactivities toward peptide nucleophiles, *J. Org. Chem.*, **1969**, *34*, 384-389

Kloepffer, A.E.; Die Synthese von 2'-aminoalkyl substituierter, fluorierter Nucleosidanaloga und ihr Einfluß auf die katalitische Aktivität von anti-HIV Hammerhead Ribozymen, *Dissertation*, **2004**, J. W. Goethe-Universität, Frankfurt am Main

Kirpekar, F.; Nordhoff, E.; Kristiansen, K.; Roepstorff, P.; Lezius, A.; Hahner, S.; Karas, M.; Hillenkamp, F.; Matrix assisted laser desorption/ionization mass spectrometry of enzymatically synthesized RNA up to 150 kDa, *Nucleic Acids Res.*, **1994**, *22*, 3866-3870

Kobayashi, Y.; Kumadaki, I.; Yamamoto, K.; Simple synthesis of trifluoromethylated pyrimidine nucleosides, *J. Chem. Soc. Chem. Comm.*, **1977**, 536-537

Kool, E.T.; Synthetically modified DNAs as substrates for polymerases, *Curr. Opin. Chem. Biol.*, **2000a**, *4*, 602-608

Kool, E.T.; Preorganization of DNA: Design Principles for Improving Nucleic Acid Recognition by Synthetic Oligonucleotides, *Chem. Rev.*, **1997**, *97*, 1473-1487

Kraus, A.G.; Molina, T.M.; A Direct Synthesis of C-Glycosylic Compounds, *J. Org. Chem.*, **1988**, *53*, 752-753

Krohn, K.; Heins, H.; Wielcknes, K.; Synthesis and cytotoxic activity of C-glycosidic nicotinamide riboside analogues, *J. Med. Chem.*, **1992**, *35*, 511-517

Lai, J.S.; Kool, E.T.; Selective pairing of Polyfluorinated DNA Bases, *J. Of Am. Chem. Soc.*, **2004**, *126*, 3040-3041

Lehmann, W.D.; Massenspektrometrie in der Biochemie, Spektrum Akademischer Verlag, Heidelberg Berlin Oxford, **1996**

Letsinger, R.L.; Finnan, J.L.; Heaver, G.A.; Lunsford, W.B.; Phosphite coupling procedure for generating internucleotide links, *J. Am. Chem. Soc.*, **1975**, *97*, 3278-3279

Letsinger, R.L.; Lunsford, W.B.; Synthesis of thymidine oligonucleotides by phosphite triester intermediates, *J. Am. Chem. Soc.*, **1976**, *98*, 3655-3661

Lien, E.J.; Gao, H.; Prabhakar, H.; Physical Factors Contributing to the Partition Coefficient and Retention time of 2',3'-dideoxynucleoside Analogues, *J. Pharm. Sci.*, **1991**, *80*, 517-521

Loakes, D.; Brown, D.M.; 5-Nitroindole as an universal base analogue, *Nucleic Acids Res.*, **1994**, *22*, 4039-4043

Loakes, D.; Brown, D.M.; Linde, S.; Hill, F.; 3-Nitropyrrole and 5-nitroindole as universal bases in primers for DNA sequencing and PCR, *Nucleic Acids Res.*, **1995**, *23*, 2361-2366

Loakes, D.; Hill, F.; Brown, D.M.; Salisbury, S.A.; Stability and structure of DNA oligonucleotides containing non-specific base analogues, *J. Mol. Biol.*, **1997**, *270*, 426-435

Loakes, D.; The Applications of Universal DNA Base Analogues; *Nucl. Acids Res.*, **2001**, *29*(12), 2437-2447

Makochekanwa, C.; Sueoka, O.; Kimura, M.; Experimental Investigation of Electron and positron Interactions with Monosubstituted and Disubstituted Benzene derivatives: Fluorobenzene, 1,3-Difluorobenzene and 1,4-Difluorobenzene Molecules, *J. Phys. B: At. Mol. Opt. Phys.*, **2004**, *37*, 1841-1857

Marky, L.A.; Breslauer, K.J.; Calculating thermodynamic data for transitions of any molecularity from equilibrium melting curves, *Biopolymers*, **1987**, *26*, 1601-1620

Mathias, G.; Hunziker, J.; Towards a DNA-like Duplex without Hydrogen-Bonded Base Pairs, *Angew. Chem. Int. Ed.*, **2002**, *41* (17), 3203-3204

Matulic-Adamic, J.; Watanabe, K.A.; Price, R.W.; Nucleosides. 138. Synthesis and biological activity of  $\alpha$ -monofluoro- and  $\alpha,\alpha$ -difluoro-thymine, *Chimica Scripta*, **1986**, *26*, 127-134

Matulic-Adamic, J.; Beigelman, L.; Portmann, S.; Egli, M.; Usman, N.; Synthesis and Structure of 1-Deoxy-1-phenyl- $\beta$ -D-ribofuranose and its incorporation into oligonucleotides, *J. Org. Chem.* **1996**, *61*, 3909-3911

Matulic-Adamic, J.; Karpeisky, A.M.; Gonzales, C.; Burgin Jr., A.B.; Usman, N.; McSwiggen, J.A.; Beigelman, L.; Modified nucleosides for ribozyme structure-activity studies, *Collect. Czech. Chem. Commun.*, **1996a**, *61*, 271-275

Matulic-Adamic, J.; Beigelman, L.; Synthesis of 3-( $\beta$ -D-ribofuranosyl)-2-fluoropyridine and 3-( $\beta$ -D-ribofuranosyl)-pyridin-2-one, *Tetrahedron Lett.*, **1997**, *38*, 203-206

McBride, L.J.; Caruthers, M.H.; An investigation of several deoxynucleoside phosphoramidites useful for synthesizing deoxyoligonucleotides, *Tetrahedron Lett.*, **1983**, *24*, 245-248

McNamara, D. J.; Cook, P.D.; Synthesis and antitumor activity of fluorine-substituted 4-amino-2(1H)-pyrimidinones and their nucleosides. 3-Deazacytosines, *J. Med. Chem.*, **1987**, *30*, 340-347

Merrifield, R.B.; Solid phase peptide synthesis. I. The synthesis of a tetrapeptide, *J. Am. Chem. Soc.*, **1963**, *85*, 2149-2154

Montgomery, J.A.; Hewson, K.; Synthesis of potential anticancer agents. XXXIV. Fluorobenzimidazoles and fluorobenzotriazoles, *J. Med. Chem.*, **1965**, *8*, 737-740

Moore, L.C.; Zivkovic, A.; Engels, J.W.; Kuchta, D.; Human DNA Primase Uses Watson-Crick Hydrogen Bonds To Distinguish between Correct and Incorrect Nucleoside Triphosphates, *Biochemistry*, **2004**, *43*, 12367-12374

Moran, S.; Ren, R.X.F.; Rumney IV, S.; Kool, E.T.; Difluorotoluene, a nonpolar isostere for thymine, codes specifically and efficiently for adenine in DNA replication, *J. Am. Chem. Soc.*, **1997**, *119*, 2056-2057

Moran, S.; Ren, R.X.F.; Kool, E.T.; A thymidine triphosphate shape analog lacking Watson-Crick pairing ability is replicated with high sequence selectivity, *Proc. Natl. Acad. Sci. USA*, **1997a**, *94*, 10506-10511

Mountford, J.A.; Hughes, L.D.; Lancaster, J.S.; Intra- and Inter- molecular C-H...F-C and N-H...F-C Hydrogen Bonding in Secondary Amine Adducts of B(C<sub>6</sub>F<sub>5</sub>)<sub>3</sub> Relevance to Key Interactions in Alkene Polymerisation Catalysis, *Chem. Commun.*, **2003**, 2148-2149

Narang, S.A.; Brousseau, R.; Hsiung, H.M.; Michniewicz, J.J.; Chemical synthesis of deoxynucleotides by the modified triester method, *Methods Enzymol.*, **1980**, *65*, 610-628

Neilson, T.; Werstiuk, E.S.; Oligoribonucleotide synthesis. II. Preparation of 2'-O-tetrahydropyranyl derivatives of adenosine and cytidine necessary for insertion in stepwise synthesis, *Can. J. Chem.*, **1971**, *49*, 493-499

Newcomb, L.F.; Gellman, S.H.; Aromatic stacking Interactions in Aqueous Solution: Evidence That neither Classical Hydrophobic Effects nor Dispersion Forces are Important, *J. Am. Chem. Soc.*, **1994**, *116*, 4993-4994

Ogilvie, K.K.; Sadana, K.L.; Thompson, E.A.; The use of silyl groups in protecting the hydroxyl functions of ribonucleosides, *Tetrahedron Lett.*, **1974**, 2861-63

Ogilvie, K.K.; Beaucage, S.L.; Schifman, A.L.; Theriault, N.Y.; Sadana, K.L.; The synthesis of oligoribonucleotides. II. The use of silyl protecting groups in nucleoside and nucleotide chemistry, *Can. J. Chem.*, **1978**, *56*, 2768-2780



O'Hagan D.; Rzepa, S.H.; Some Influences of Fluorine in Bioorganic Chemistry, *Chem. Commun.*, **1997**, 645-652

Pankiewicz, K.W.; Fluorinated nucleosides, *Carbohydr. Res.*, **2000**, 327, 87-105

Parsch, J.; Engels, J.W.; C-F...H-C Hydrogen Bonds in Crystals of Fluorobenzene Ribonucleosides, *Collection Symposium Series*, Vol. 2, Ed. A. Holy and M. Hocek, Institute of Organic Chemistry and Biochemistry, Academy of Sciences of the Czech Republic, Prague, **1999**, 11-14.

Parsch, J.; Engels, J.W.; Synthesis of Fluorobenzene and Benzimidazole Nucleic-Acid Analogues and Their Influence on Stability of RNA Duplexes, *Helv. Chim. Acta*, **2000**, 83, 1791-1808

Parsch, J.; Synthese von Fluorobenzol- und Fluorobenzimidazol-Nucleosiden und ihr Einfluß auf die Stabilität von RNA Duplexen, *Dissertation*, **2001**, J. W. Goethe-Universität, Frankfurt am Main

Parsch, J.; Engels, J.W.; C-F...H-C Hydrogen Bonds in Ribonucleic Acids, *J. Am. Chem. Soc.*, **2002**, 124, 5664-5672

Patani, A.G.; La Voie, J.E.; Bioisosterism: A Rational Approach in Drug Design, *Chem. Rev.*, **1996**, 96, 3147-3176

Pauling, L.; „The nature of the chemical bond“, 2<sup>nd</sup> Edition, Cornell University Press, Ithaca New York, **1940**

Pauling, L.; „The nature of the chemical bond“, 3<sup>rd</sup> Edition, Cornell University Press, Ithaca New York, **1960**

Pearlman, W.M.; Noble metal hydroxides on carbon nonpyrophoric dry catalysts, *Tetrahedron Lett.*, **1967**, 1663-1664

Pein, C.D.; Cech, D.; Zur Synthese von Difluormethylethern verschieden substituierter Pyrimidinnucleoside durch Reaktion mit Difluorcarben, *Tetrahedron Lett.*, **1985**, 26, 4915-4918

Pfizzner, K.E.; Moffatt, J.G.; Sulfoxide-carbodiimide reactions. I. A facile oxidation of alcohols, *J. Am. Chem. Soc.*, **1965**, 87, 5661-5678

Pieles, U.; Zürcher, W.; Schär, M.; Moser, H.E.; Matrix-assisted laser desorption ionization time-of-flight mass spectrometry: a powerful tool for the mass and sequence analysis of natural and modified oligonucleotides, *Nucleic Acids Res.*, **1993**, 21, 3191-3196

Pitsch, S.; Weiss, P.A.; Jenny, L.; Ribonucleoside-derivative and methode for preparing the same, Patent, **1999**, International publication number WO99/09044

Pochet, S.; Dugue, L.; Oligodeoxynucleotides embodying the ambiguous base-Z, 5-aminoimidazole-4-carboxamide, *Nucleosides Nucleotides*, **1995**, 14, 1195-1210

Pouterman, E.; Girardet, A.; Synthese de la 6- et de la 8- trifluoromethyl quonoleine, *Helv. Chim. Acta*, **1947**, 30, 107-112

Puglisi, J.D.; Tinoco, I.; Absorbance melting curves of RNA, *Methods Enzymol.*, **1989**, 180, 304-325

Purdy, D.F.; Zintek, L.B.; Nair, V.; Synthesis of isonucleosides related to AZT and AZU, *Nucleosides Nucleotides*, **1994**, 13, 109-126

Rashkin, J.M., waters, L.M.; Unexpected Sustituent Effects in Offset  $\pi$ - $\pi$  Stacked Interactions in Water, *J. Am. Chem. Soc.*, **2002**, 124(9), 1860-1861

Reichenbacher, K.; Süß, H.I.; Hullier, J.; Fluorine in Crystal engineering-,the Little Atom that could', *Chem. Rev. Soc.*, **2005**, 34, 22-30

Saenger, W.; Principles of nucleic acid structure, Springer Verlag, New York Berlin, **1984**

Scaringe, A.S.; Kitchen, D.; Kaiser, R.; Marshall, S.W.; Preparation of 5'-Silyl-2'-orthoester Ribonucleosides for use in Oligoribonucleoside Synthesis, *Curr. Prot. In Nucl. Acids Chem.*, **2004**, 2.10.1-2.20.15

Sanger, F.; Nicklen, S.; Coulson, A.R.; DNA sequencing with chain-terminating inhibitors, *Proc. Natl. Acad. Sci. USA*, **1977**, 74, 5463-5467

Schaller, H.; Weimann, G.; Lerch, B.; Khorana, H.G.; Studies on polynucleotides. XXIV. The stepwise synthesis of specific deoxyribonucleotides (4). Protected derivatives of deoxyribonucleosides and new syntheses of deoxyribonucleoside-3'-phosphates, *J. Am. Chem. Soc.*, **1963**, 85, 3821-3827

Schirley, A.D.; Hendrix, P.J.; Steric Effects in the Metalation of Some Aromatic Substrates with Alkylolithium Reagents, *J. Organometal. Chem.*, **1968**, 11, 217-226

Schwarz, D.S.; Hutraggar, G.; Du, T.; Xu, Z.; Aromn, U.; Zamore, P.D.; Assymetry in the Assembly of RNAi Enzyme Complex, *Cell*, **2003**, 115, 199-208

Schweitzer, B.A.; Kool, E.T.; Aromatic nonpolar nucleosides as hydrophobic isosteres of pyrimidine and purine nucleosides, *J. Org. Chem.*, **1994**, 59, 7238-7242

Schweitzer, B.A.; Kool, E.T.; Hydrophobic, non-hydrogen-bonding bases and base pairs in DNA, *J. Am. Chem. Soc.*, **1995**, 117, 1863-1872

Searle, M.S.; Williams, D.H.; On the stability of nucleic acid structures in solution: enthalpy-entropy compensations, internal rotations and reversibility, *Nucleic Acids Res.*, **1993**, 21, 2051-2056

Seela, F.; Bourgeois, W.; Rosemeyer, H.; Wenzel, T.; Synthesis of 4-substituted 1H benzimidazole 2'-deoxyribonucleosides and utility of the 4-nitro compound as universal base, *Helv. Chim. Acta*, **1996**, 79, 488-498

Seiin, T.L.Jr.; Yen, W.; Jansen, A.S.; Halogen Trapped Aniline Trimers. A Way from Polyaniline Paradigm by Isosterism Replacement of Aminogroups:A Theoretical Study, *J. Phys. Chem.*, **2000**, 104, 11371-11374

Sinha, N.D.; Biernat, J.; Köster, H.;  $\beta$ -Cyanoethyl *N,N*-dialkylamino/*N*-morpholinomonochloro phosphoamidites, new phosphitylating agents facilitating ease of deprotection and work-up of synthesized oligonucleotides, *Tetrahedron. Lett.*, **1983**, *24*, 5843-5846

Smart, B.E.; „Characteristics of C-F Systems“ in „Organofluorine Chemistry: Principals and Commercial Applications“ Ed Banks, R.E. Plenum Press, New York, **1994**

Smart, B.E.; Fluorine Substituent Effects ( on bioactivity), *J. Of Fluorine Chem.*, **2001**, *109*, 3-11

Smith, M.; Rammler, D.H.; Goldberg, I.H.; Khorana, H.G.; Studies on polynucleotides. XIV. Specific synthesis of the C-3'- C-5'-interribonucleotide linkage. Synthesis of uridylyl-(3'- 5')-uridine and uridylyl-(3'- 5')-adenosine, *J. Am. Chem. Soc.*, **1962**, *84*, 430-440

Sprang, S.; Sundaralingam, M.; Crystal Structure of 2-chloro-1-( $\beta$ -D-ribofuranose)benzimidazole, *Acta Cryst.*, **1973**, *B29*, 1910-1916

Stawinski, J.; Strömberg, R.; Thelin, M.; Westman, E.; Studies on the *t*-butyldimethylsilyl groups as 2'-*O* protection in oligonucleotide synthesis via H-phosphonate approach, *Nucleic Acids Res.*, **1988**, *16*, 9285-9298

Still, W.C.; Kahn, M.; Mitra, A.; Rapid chromatographic technique for preparative separations with moderate resolution, *J. Org. Chem.*, **1978**, *43*, 2923-2925

Strähle, J.; Untersuchungsmethoden in der Chemie: Einführung in die moderne Analytik, Herausgegeben von H. Naumer und W. Heller, 2. Auflage, Thieme Verlag Stuttgart New York, **1990**

Stryer, L.; Biochemie, Spektrum Akademischer Verlag, Heidelberg, Berlin, New York, **1991**

Stults, J.T.; Marsters, J.C.; Improved electrospray ionization of oligodeoxynucleotides, *Rapid Commun. Mass Spectrom.*, **1991**, *5*, 359-363

Tanaka, K.; Waki, H.; Iod, Y.; Akita, S.; Yoshida, Y.; Yoshida, T.; Protein and polymer analyses up to  $m/z$  100000 by laser ionization time-of-flight mass spectrometry, *Rapid Commun. Mass. Spectrom.*, **1988**, 2, 151-153

Thalladi, V.R.; Weiss, H.C.; Bläser, D.; Boese, R.; Nangia, A.; Desiraju, G.R.; C-H...F interactions in the crystal structures of some fluorobenzenes, *J. Am. Chem. Soc.*, **1998**, 120, 8702-8710

Thiellier, H.P.M.; Koomen, G.J.; Pandit, U.K.; Unconventional nucleotide analogues – XVIII. Ring expansion of uridine halocarbene adducts. Synthesis of diazepine nucleosides, *Tetrahedron*, **1977**, 33, 2609-2612

Timpe, W.; Dax, K.; Wolf, N.; Weidmann, H.; 3-Desoxyhex-2-enono-1,4-lactone aus D-Hexofuran(osid)-urono-6,3-lactonen, *Carbohydr. Res.*, **1975**, 39, 53-60

Tuschl, T.; RNA Sets the Standards, *Nature*, **2003**, 421, 220-221

Uesugi, S.; Miki, H.; Ikehara, M.; Iwahashi, H.; Kyogoku, Y.; A linear relationship between electronegativity of 2'-substituents and conformation of adenine nucleosides, *Tetrahedron Lett.* **1979**, 42, 4073-4076

Uesugi, S.; Kaneyusa, T.; Imura, J.; Ikehara, M.; Cheng, D.M.; Kan, L.S.; Ts'ó, P.O.P.; <sup>1</sup>H-NMR studies on the dinucleoside monophosphates containing 2'-halogeno-2'-deoxypurine nucleosides: Effects of 2'-substitutes on conformation, *Biopolymers*, **1983**, 22, 1189-1202

Ulku, D.; Huddle, B.P.; Morrow, J.C.; Crystal structure of pyridine-1-oxide, *Acta Cryst.*, **1971**, B27, 432-436

Varian; Mitteilung der technischen Abteilung, Varian Darmstadt, **1998**

Veliz, E.A.; Stephens, O.M.; Beal, P.A.; Synthesis and Analysis of RNA Containing 6-Trifluoromethylpurine Ribonucleoside, *Org. Lett.*, **2001**, 3(19), 2969-2972

Vogel, H.J.; Bridger, W.A.; Phosphorus-31 nuclear magnetic resonance studies of the methylene and fluoro analogues of adenine nucleotides. Effects of pH and Magnesium ion binding, *Biochemistry*, **1982**, *21*, 394-401

Vorbrüggen, H.; Krolkiewicz, K.; Bennua, B.; Nucleoside synthesis with trimethylsilyl triflate and perchlorate as catalysts, *Chem. Ber.*, **1981**, *114*, 1234-1255

Vorbrüggen, H.; Höfle, G.; On the mechanism of nucleoside synthesis, *Chem. Ber.*, **1981a**, *114*, 1256-1268

Waehnert, U.; Langen, P.; Incorporation of 3'-deoxy-3'-fluorothymidylat into DNA in vitro, *Proc. Hung. Annu. Meet. Biochem.*, **1979**, *19*, 27-28

Wang, S.; Friedman, A.E.; Kool, E.T.; Origins of high sequence selectivity: a stopped flow kinetics study of DNA/RNA hybridization by duplex- and triplex-forming oligonucleotides, *Biochemistry*, **1995**, *34*, 9774-9784

Watanabe, K.A.; Reichman, U.; Hirota, K.; Lopez, C.; Fox, J.J.; Nucleosides 110. Synthesis and antiherpes virus activity of some 2'-fluoro-2'-deoxyarabinosylpyrimidine nucleosides, *J. Med. Chem.*, **1979**, *22*, 21-24

Watanabe, K.A.; Su, T.L.; Klein, R.S.; Chu, C.K.; Matsuda, A.; Chun, M.W.; Lopez, C.; Fox, J.J.; Nucleosides. 123. Synthesis of antiviral nucleosides: 5-substituted 1-(2-deoxy-2-halogeno- $\beta$ -D-arabinofuranosyl)cytosines and -uracils. Some structure-activity relationships, *J. Med. Chem.*, **1983**, *26*, 152-156

Watanabe, K.A.; Su, T.L.; Reichman, U.; Greenberg, N.; Lopez, C.; Fox, J.J.; Nucleosides. 129. Synthesis of antiviral nucleosides: 5-alkenyl-1-(2-deoxy-2-fluoro- $\beta$ -D-arabinofuranosyl)uracils, *J. Med. Chem.*, **1984**, *27*, 91-94

Waters, L.M.; Aromatic Interactions in Model Systems, *Curr. Opinion in Chem. Biol.*, **2002**, *6*, 736-741

Watson, J.D.; Crick, F.H.C.; Molecular structure of nucleic acids: a structure for deoxyribose nucleic acid, *Nature*, **1953**, *171*, 737-738

Watson, J.D.; Crick, F.H.C.; Genetic implications of the structure of deoxyribonucleic acid, *Nature*, **1953a**, *171*, 964-967

Wepster, B.M.; Verkade, P.E.; Steric effects on mesomerism. III. Estimation of the direct influence of substituents on the rate of deacylation of *ortho*- and *para*-nitro-acetanilide, *Rec. Trav. Chim. Pays-Bas*, **1949**, *68*, 77-87

Westman, E.; Strömberg, R.; Removal of *t*-butyldimethylsilyl protection in RNA-synthesis. Triethylamine trihydrofluoride (TEA·3HF) is a more reliable alternative to tetrabutylammonium fluoride (TBAF), *Nucleic Acids Res.*, **1994**, *22*, 2430-2431

Williams, H.J.; The Molecular Electric Quadrupole Moment and Solid State architecture, *Acc. Chem. Res.*, **1993**, *26*, 593-598

Witt, O.N.; Utermann, A.; Ein neues Nitrierungsverfahren, *Ber.*, **1906**, *39*, 3901-3905

Wolfrom, M.L.; McWain, P.; Nucleosides of D-Glucuronic Acid and of D-Glucofuranose and D-Galactofuranose, *J. Org. Chem.*, **1965**, *30*, 1099-1101

Wörner, K.; Strube, T.; Engels, J.W.; Synthesis and stability of GNRA-loop analogs, *Helv. Chim. Acta*, **1999**, *82*, 2094-2104

Yoshikawa, M.; Kato, T.; Takenishi, T.; A novel method for phosphorylation of nucleosides to 5'-nucleotides, *Tetrahedron Lett.*, **1967**, *50*, 5065-5068

Zacharias, M.; Engels, J.W.; Influence of a fluorobenzene nucleobase analogue on the conformational flexibility of RNA studied by molecular dynamics simulation, *Nucleic Acids Res.*, **2004**, *32* (21), 6304-6311

Zaman, R.J.G.; Michiels, A.J.P.; Coeckel, A.A.C.; targeting RNA New Opportunities to Address Drugless targets, *Drug. Desc. Tod.*, **2003**, *8*, 297-306

## *References*

---

Zamecnick, P.C.; Stephenson, M.L.; Inhibition of rous sarcoma virus RNA Replication and Cell Transformation by a Specific Oligonucleotide, *Proc. Natl. Acad. Sci. USA*, **1978**, *75*(1), 280-284





## 12 Attachment

### 12.1 Crystal Data of Crystallized Compounds

#### 12.1.1 Crystal data of 1'-deoxy-1'-(2,4,6-trifluorophenyl)- $\beta$ -D-ribofuranose

A single crystal ( colorless rod with dimensions 0.14 x 0.30 x 0.55 mm ) was measured on a SIEMENS SMART diffractometer at a temperature of about -131 °C. Repeatedly measured reflections remained stable. A numerical absorption correction using six indexed crystal faces gave a transmission factor between 0.930 and 0.980 . Equivalent reflections were averaged. Friedel opposites were not averaged.  $R(I)_{\text{internal}} = 0.032$  . The structure was determined by direct methods using program SHELXS. The H atoms were taken from a difference synthesis and were refined with isotropic thermal parameters. The non-H atoms were refined with anisotropic thermal parameters. The structure was refined on  $F^2$  values using program SHELXL-97. The final difference density was between -0.18 and +0.31  $e/\text{\AA}$  .

The five-membered furanose ring approximately has a C2-endo-envelope conformation. The hydroxyl group attached to C2 is in an equatorial position, the hydroxyl group attached to C3 is in a pseudo-axial position and the phenyl group attached to C1 is in a pseudo-equatorial position with respect to the furanose ring. The trifluorophenyl group adopts a position with an almost syn-periplanar orientation of the C11-F3 bond and the C1-H1 bond. The intramolecular H1...F3 distance of 2.34  $\text{\AA}$  is slightly shorter than the van der Waals contact distance. The phenyl group shows a small deviation from planarity: substituent atoms C1 and F1 deviate 0.11  $\text{\AA}$  in opposite directions from the phenyl plane. This deviation from planarity may result from a steric interaction between atoms F1 and O4. The observed F1...O4 distance of 2.819  $\text{\AA}$  is slightly shorter than the van der Waals contact distance. The ribofuranose groups are connected by intermolecular O-H...O hydrogen bonds to a two-dimensional network parallel to the a,b - plane. These molecular layers are connected in the c - direction

by an intermolecular C-H...O interaction with a H...O distance of 2.48 Å and two intermolecular C-H...F interactions (involving the para-F atom) with H...F distances of 2.54 and 2.63 Å.

#### Intermolecular hydrogen bonds

O - H ... O	O - H	H...O	O...O	O-H-O	symmetry
[Å]	[Å]	[Å]	[deg]		
O2 - H02 ... O5	0.79	2.04	2.816	167	2-x, y-1/2, 3/2-z
O3 - H03 ... O4	0.82	1.99	2.815	175	2-x, y-1/2, 3/2-z
O5 - H05 ... O2	0.82	1.95	2.772	173	1-x, 1/2+y, 3/2-

Table 1. Crystal data and structure refinement for 1'-deoxy-1'-(2,4,6-trifluorophenyl)-β-D-ribofuranose

Identification code	engels
Empirical formula	C11 H11 F3 O4
Formula weight	264.20
Temperature	142(2) K
Wavelength	0.71073 Å
Crystal system, space group	Orthorhombic, P22121
Unit cell dimensions	a = 4.9699(12) Å alpha = 90 deg. b = 11.209(3) Å beta = 90 deg. c = 20.221(5) Å gamma = 90 deg.
Volume	1126.4(5) Å <sup>3</sup>
Z, Calculated density	4, 1.558 Mg/m <sup>3</sup>
Absorption coefficient	0.148 mm <sup>-1</sup>
F(000)	544
Crystal size	0.55 x 0.30 x 0.14 mm
Theta range for data collection	2.01 to 32.45 deg.
Limiting indices	-7<=h<=7, -16<=k<=16, -30<=l<=29

Reflections collected / unique	19923 / 3826 [R(int) = 0.0320]
Completeness to theta = 32.45	96.0 %
Absorption correction	Numerical (SHELXTL, Sheldrick, 1996)
Max. and min. transmission	0.980 and 0.930
Refinement method	Full-matrix least-squares on F <sup>2</sup>
Data / restraints / parameters	3826 / 0 / 207
Goodness-of-fit on F <sup>2</sup>	1.169
Final R indices [I > 2sigma(I)]	R1 = 0.0325, wR2 = 0.0810
R indices (all data)	R1 = 0.0361, wR2 = 0.0839
Absolute structure parameter	0.2(5)
Largest diff. peak and hole	0.306 and -0.182 e.A <sup>-3</sup>

Table 2. Atomic coordinates ( $\times 10^5$ ) and equivalent isotropic displacement parameters ( $\text{Å}^2 \times 10^4$ ) for engels.  $U(\text{eq})$  is defined as one third of the trace of the orthogonalized  $U_{ij}$  tensor.

	x	y	z	U(eq)
O(2)	80656(18)	38745(7)	84091(4)	191(2)
O(5)	68850(18)	77417(7)	65235(4)	196(2)
F(1)	52333(15)	74945(7)	83724(4)	227(2)
O(4)	97123(17)	67038(7)	76383(4)	154(2)
F(3)	127271(17)	56800(8)	93713(4)	287(2)
O(3)	110565(19)	41761(8)	72085(4)	223(2)
F(2)	78260(30)	86047(11)	105099(5)	538(3)
C(7)	69780(20)	73966(10)	88818(6)	192(2)
C(1)	97380(20)	59148(9)	82027(5)	134(2)
C(6)	90970(20)	65953(10)	88245(5)	161(2)
C(4)	88710(20)	60369(9)	70531(5)	140(2)
C(5)	63230(20)	65688(10)	67670(6)	183(2)
C(3)	85220(20)	47456(9)	72776(5)	162(2)
C(8)	65130(30)	80962(12)	94334(7)	283(3)
C(2)	78110(20)	49061(9)	80115(5)	145(2)
C(9)	82250(30)	79270(14)	99623(7)	333(3)
C(10)	102980(30)	71130(15)	99673(7)	319(3)
C(11)	106740(20)	64720(11)	93888(6)	219(2)

Table 3. Bond lengths [ $\text{\AA}$ ] and angles [deg] for 1'-deoxy-1'-(2,4,6-trifluorophenyl)- $\beta$ -D-ribofuranose

O(2)-C(2)	1.4140(13)
O(5)-C(5)	1.4313(14)
F(1)-C(7)	1.3508(14)
O(4)-C(1)	1.4438(12)
O(4)-C(4)	1.4606(13)
F(3)-C(11)	1.3531(15)
O(3)-C(3)	1.4191(14)
F(2)-C(9)	1.3574(15)
C(7)-C(8)	1.3829(17)
C(7)-C(6)	1.3890(16)
C(1)-C(6)	1.5048(15)
C(1)-C(2)	1.5313(15)
C(6)-C(11)	1.3913(16)
C(4)-C(5)	1.5146(15)
C(4)-C(3)	1.5269(15)
C(3)-C(2)	1.5360(15)
C(8)-C(9)	1.380(2)
C(9)-C(10)	1.376(2)
C(10)-C(11)	1.3855(18)
C(1)-O(4)-C(4)	109.23(8)
F(1)-C(7)-C(8)	117.51(11)
F(1)-C(7)-C(6)	118.39(10)
C(8)-C(7)-C(6)	124.09(12)
O(4)-C(1)-C(6)	110.37(8)
O(4)-C(1)-C(2)	104.31(8)
C(6)-C(1)-C(2)	116.92(9)
C(7)-C(6)-C(11)	115.02(10)
C(7)-C(6)-C(1)	123.92(10)
C(11)-C(6)-C(1)	121.05(10)
O(4)-C(4)-C(5)	110.32(9)
O(4)-C(4)-C(3)	106.07(8)
C(5)-C(4)-C(3)	113.05(9)

O(5)-C(5)-C(4)	109.26(9)
O(3)-C(3)-C(4)	107.22(9)
O(3)-C(3)-C(2)	110.61(9)
C(4)-C(3)-C(2)	101.67(8)
C(9)-C(8)-C(7)	116.39(13)
O(2)-C(2)-C(1)	113.84(9)
O(2)-C(2)-C(3)	115.65(9)
C(1)-C(2)-C(3)	100.75(8)
F(2)-C(9)-C(10)	118.33(14)
F(2)-C(9)-C(8)	117.72(14)
C(10)-C(9)-C(8)	123.95(12)
C(9)-C(10)-C(11)	116.01(13)
F(3)-C(11)-C(10)	117.64(11)
F(3)-C(11)-C(6)	117.94(11)
C(10)-C(11)-C(6)	124.41(12)

Symmetry transformations used to generate equivalent atoms

*Table 4. Anisotropic displacement parameters ( $\text{Å}^2 \times 10^4$ ) for engelsI'-deoxy-I'-(2,4,6-trifluorophenyl)- $\beta$ -D-ribofuranose. The anisotropic displacement factor exponent takes the form  $-2 \pi^2 [ h^2 a^{*2} U11 + \dots + 2 h k a^* b^* U12 ]$*

	U11	U22	U33	U23	U13	U12
O(2)	190(4)	130(3)	255(4)	59(3)	35(3)	-5(3)
O(5)	181(4)	150(4)	257(4)	31(3)	-10(3)	26(3)
F(1)	187(3)	219(3)	273(3)	12(3)	-4(3)	39(3)
O(4)	207(4)	114(3)	143(3)	6(2)	-14(3)	-37(3)
F(3)	253(4)	348(4)	260(3)	76(3)	-74(3)	21(3)
O(3)	267(4)	130(4)	272(4)	11(3)	74(3)	62(3)
F(2)	606(7)	712(7)	297(4)	-301(5)	140(5)	-82(6)
C(7)	193(5)	182(5)	200(5)	-3(4)	39(4)	-21(4)
C(1)	135(4)	120(4)	149(4)	15(3)	-2(3)	-13(3)
C(6)	181(5)	153(5)	149(4)	6(3)	11(3)	-28(4)
C(4)	156(4)	121(4)	143(4)	-8(3)	-16(3)	-7(3)
C(5)	175(4)	149(4)	224(5)	17(4)	-49(4)	-15(4)
C(3)	188(5)	110(4)	187(4)	-13(3)	-6(4)	-5(4)
C(8)	286(6)	262(6)	302(6)	-86(5)	116(5)	-22(5)
C(2)	134(4)	105(4)	197(4)	19(3)	14(4)	-13(3)
C(9)	386(7)	413(8)	201(5)	-121(5)	108(5)	-109(6)
C(10)	344(7)	446(8)	165(5)	-21(5)	2(5)	-104(6)
C(11)	215(5)	257(6)	184(5)	32(4)	-6(4)	-39(4)

Table 5. Hydrogen coordinates ( $x 10^4$ ) and isotropic displacement parameters ( $\text{Å}^2 \times 10^3$ ) for 1'-deoxy-1'-(2,4,6-trifluorophenyl)- $\beta$ -D-ribofuranose

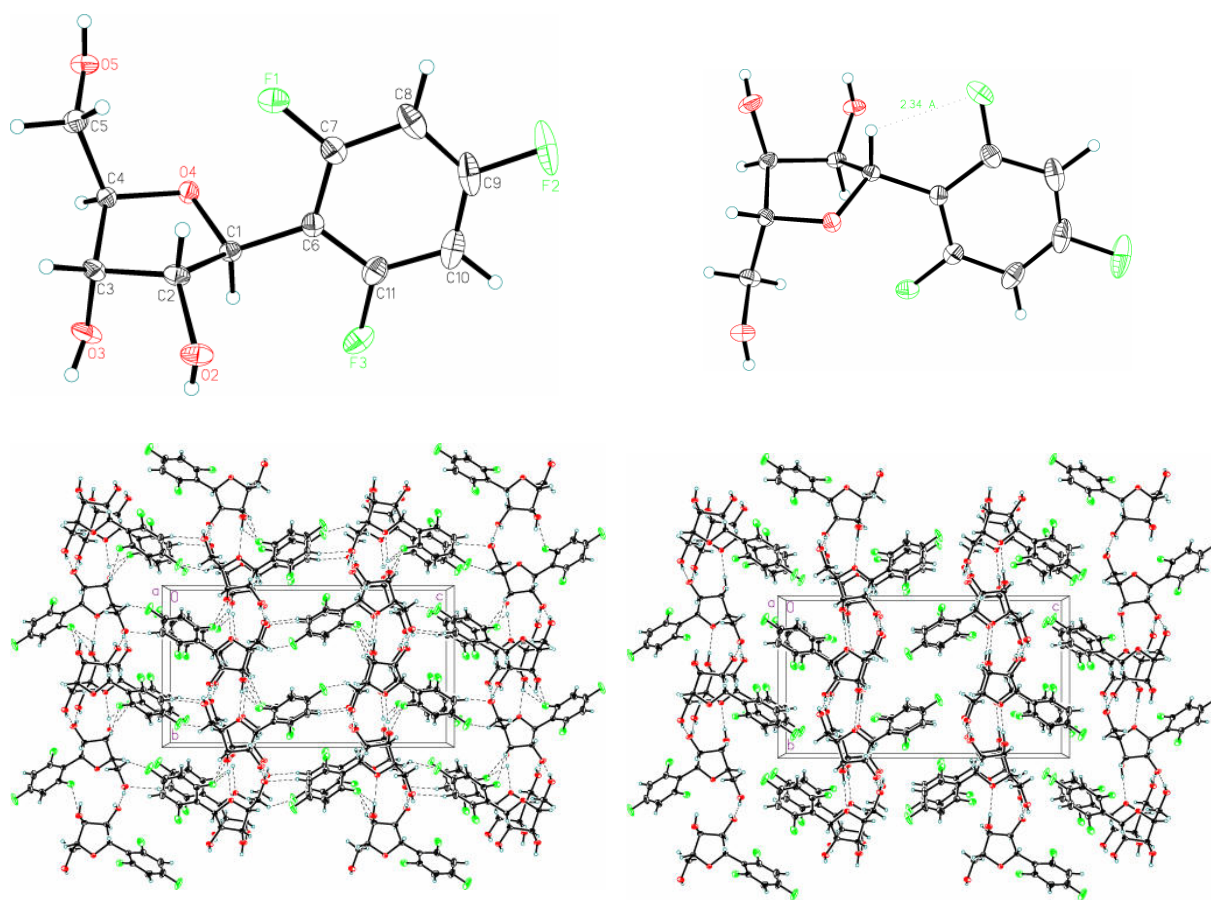
	x	y	z	U(eq)
H(5B)	4940(40)	6565(16)	7088(9)	23(4)
H(4)	10250(30)	6126(14)	6713(7)	14(3)
H(2)	5940(30)	5231(15)	8059(8)	18(4)
H(1)	11560(30)	5542(12)	8252(7)	13(3)
H(3)	7160(30)	4331(14)	7032(8)	19(4)
H(5A)	5770(40)	6088(16)	6389(8)	23(4)
H(8)	5050(50)	8649(19)	9460(11)	46(6)
H(10)	11520(40)	7037(18)	10369(10)	41(5)
H(02)	9520(40)	3605(18)	8371(10)	31(5)
H(05)	5440(40)	8097(18)	6512(9)	32(5)
H(03)	10940(40)	3450(20)	7260(10)	34(5)

Table 6. Torsion angles [deg] for 1'-deoxy-1'-(2,4,6-trifluorophenyl)- $\beta$ -D-ribofuranose

C(4)-O(4)-C(1)-C(6)	-149.30(8)
C(4)-O(4)-C(1)-C(2)	-22.92(10)
F(1)-C(7)-C(6)-C(11)	-174.89(10)
C(8)-C(7)-C(6)-C(11)	4.30(17)
F(1)-C(7)-C(6)-C(1)	6.37(16)
C(8)-C(7)-C(6)-C(1)	-174.44(11)
O(4)-C(1)-C(6)-C(7)	46.94(14)
C(2)-C(1)-C(6)-C(7)	-72.02(14)
O(4)-C(1)-C(6)-C(11)	-131.73(11)

C(2)-C(1)-C(6)-C(11)	109.31(12)
C(1)-O(4)-C(4)-C(5)	119.51(9)
C(1)-O(4)-C(4)-C(3)	-3.26(11)
O(4)-C(4)-C(5)-O(5)	65.88(11)
C(3)-C(4)-C(5)-O(5)	-175.54(9)
O(4)-C(4)-C(3)-O(3)	-88.38(10)
C(5)-C(4)-C(3)-O(3)	150.60(9)
O(4)-C(4)-C(3)-C(2)	27.75(11)
C(5)-C(4)-C(3)-C(2)	-93.27(10)
F(1)-C(7)-C(8)-C(9)	176.16(12)
C(6)-C(7)-C(8)-C(9)	-3.04(19)
O(4)-C(1)-C(2)-O(2)	163.82(9)
C(6)-C(1)-C(2)-O(2)	-74.01(12)
O(4)-C(1)-C(2)-C(3)	39.37(9)
C(6)-C(1)-C(2)-C(3)	161.54(9)
O(3)-C(3)-C(2)-O(2)	-49.88(12)
C(4)-C(3)-C(2)-O(2)	-163.51(9)
O(3)-C(3)-C(2)-C(1)	73.32(10)
C(4)-C(3)-C(2)-C(1)	-40.30(10)
C(7)-C(8)-C(9)-F(2)	179.73(12)
C(7)-C(8)-C(9)-C(10)	-0.5(2)
F(2)-C(9)-C(10)-C(11)	-177.97(13)
C(8)-C(9)-C(10)-C(11)	2.2(2)
C(9)-C(10)-C(11)-F(3)	178.73(12)
C(9)-C(10)-C(11)-C(6)	-0.7(2)
C(7)-C(6)-C(11)-F(3)	178.21(10)
C(1)-C(6)-C(11)-F(3)	-3.01(16)
C(7)-C(6)-C(11)-C(10)	-2.32(18)
C(1)-C(6)-C(11)-C(10)	176.46(11)





*Crystal structure of 1'-deoxy-1'-(2,4,6-trifluorophenyl)-β-D-ribofuranose*

### 12.1.2 Crystal data of 1'-deoxy-1'-(2,4,5-trifluorophenyl)- $\beta$ -D-ribofuranose

A single crystal ( colorless plate with dimensions 0.10 x 0.38 x 0.60 mm ) was measured on a SIEMENS SMART diffractometer at a temperature of about -130 °C. Repeatedly measured reflections remained stable. An empirical absorption correction with program SADABS (Sheldrick, 2000) gave a correction factor between 0.867 and 1.000 . Equivalent reflections were averaged. Friedel opposites were not averaged.  $R(I)_{\text{internal}} = 0.033$  . The structure was determined by direct methods using program SHELXS. The H atoms were taken from a difference synthesis and were treated as riding atoms. The non-H atoms were refined with anisotropic thermal parameters. The structure was refined on  $F^2$  values using program SHELXL-97. The final difference density was between -0.21 and +0.35 e/Å . The crystal structure of the title compound is isomorphous with the structure of 1-deoxy-1-(2-fluorophenyl)- $\beta$ -D-ribofuranose (Bats, Parsch & Engels, Acta Cryst., C55, 1999, IUC9900069). The five-membered furanose ring approximately has a C2-endo-envelope conformation. The phenyl group attached to C1 and the hydroxyl group attached to C2 are in pseudo-equatorial positions, the hydroxyl group attached to C3 is in a pseudo-axial position with respect to the furanose ring. The phenyl group is planar within experimental uncertainty. The ribofuranose groups are connected by intermolecular O-H...O hydrogen bonds to a two-dimensional network parallel to the a,b - plane. The molecules are further stabilized in the a,b -direction by a number of weak C-H...F interactions (involving F1 and F3) with H...F distances between 2.60 and 2.75 Å. Neighboring molecules are connected in the b - direction by a rather short intermolecular C-H...O interaction with a H...O distance of 2.32 Å. No significant intermolecular interactions are observed in the crystallographic c - direction: the shortest intermolecular C8-H8...F2 interactions have a H...F distance of 2.90 Å which is too long to be significant. Surprisingly the C-H... $\pi$ (phenyl) interaction which was observed in the isomorphous 2-fluoro-phenyl compound is replaced in the title compound by an intermolecular C10-F3...C9 interaction with a F...C distance of 3.05 Å, which is slightly shorter than the van der Waals contact distance. The nature of this interaction is unclear. Similar C-H...C interactions with F...C distances between 2.96 and 3.15 Å are found in the crystal structure of hexafluorobenzene (Boden et al., Mol. Phys., 25, 1973, 81).

## Intermolecular hydrogen bonds

O - H ... O	O - H	H...O	O...O	O-H-O	symmetry
	[Å]	[Å]	[Å]	[deg]	
O2 - H02 ... O5	0.84	2.07	2.890	165	x-1/2, y-1/2, z
O3 - H03 ... O5	0.84	1.96	2.775	164	1/2-x, y-1/2, -z
O5 - H05 ... O2	0.84	1.95	2.779	168	1/2+x, y-1/2, z

Table 1. Crystal data and structure refinement for 1-deoxy-1-(2,4,5-trifluorophenyl)- $\beta$ -D-ribofuranose

Identification code	M2
Empirical formula	C11 H11 F3 O4
Formula weight	264.20
Temperature	143(2) K
Wavelength	0.71073 Å
Crystal system, space group	Monoclinic, C2
Unit cell dimensions	a = 13.248(2) Å    alpha = 90 deg. b = 4.9913(10) Å    beta = 100.18(2) deg. c = 16.312(6) Å    gamma = 90 deg.
Volume	1061.6(5) Å <sup>3</sup>
Z, Calculated density	4, 1.653 Mg/m <sup>3</sup>
Absorption coefficient	0.157 mm <sup>-1</sup>
F(000)	544
Crystal size	0.60 x 0.38 x 0.10 mm
Theta range for data collection	2.54 to 34.23 deg.
Limiting indices	-19<=h<=20, -7<=k<=7, -24<=l<=24
Reflections collected / unique	11905 / 3784 [R(int) = 0.0334]
Completeness to theta = 34.23	91.0 %
Absorption correction	Empirical (SADABS, Sheldrick, 2000)

Max. and min. transmission	1.000 and 0.867
Refinement method	Full-matrix least-squares on F <sup>2</sup>
Data / restraints / parameters	3784 / 1 / 166
Goodness-of-fit on F <sup>2</sup>	1.052
Final R indices [I > 2σ(I)]	R1 = 0.0343, wR2 = 0.0794
R indices (all data)	R1 = 0.0429, wR2 = 0.0834
Absolute structure parameter	-0.1(5)
Largest diff. peak and hole	0.352 and -0.212 e.Å <sup>-3</sup>

Table 2. Atomic coordinates ( $\times 10^5$ ) and equivalent isotropic displacement parameters ( $\text{Å}^2 \times 10^4$ ) for 1'-deoxy-1'-(2,4,5-trifluorophenyl)-β-D-ribofuranose  
*U*(eq) is defined as one third of the trace of the orthogonalized *U*<sub>ij</sub> tensor.

	x	y	z	U(eq)
O(2)	3841(6)	3212(19)	10938(6)	204(2)
O(4)	27508(6)	-17160(20)	24102(5)	209(2)
O(5)	43563(6)	1953(19)	8896(6)	212(2)
F(3)	28907(7)	61530(20)	43079(6)	334(2)
F(1)	-1654(6)	-5748(18)	29416(5)	294(2)
O(3)	16453(7)	-38751(19)	7283(6)	207(2)
F(2)	10539(7)	64010(20)	47908(6)	363(2)
C(6)	15410(8)	9050(20)	30039(7)	173(2)
C(4)	30677(8)	-18140(20)	16080(7)	159(2)
C(11)	23190(10)	26440(30)	33690(8)	207(2)
C(5)	39003(8)	2790(30)	16231(8)	186(2)
C(2)	14428(8)	2950(20)	14487(7)	154(2)
C(7)	6073(9)	11060(30)	32755(8)	205(2)
C(1)	16895(8)	-9900(20)	23188(7)	165(2)
C(3)	21090(8)	-13440(20)	9547(7)	158(2)
C(8)	4069(10)	29200(30)	38678(9)	248(3)
C(10)	21410(10)	44690(30)	39564(8)	229(2)
C(9)	11941(11)	46080(30)	42058(8)	244(3)

Table 3. Bond lengths [Å] and angles [deg] for 1'-deoxy-1'-(2,4,5-trifluorophenyl)-β-D-ribofuranose

O(2)-C(2)	1.4198(13)
O(4)-C(1)	1.4340(13)
O(4)-C(4)	1.4440(15)
O(5)-C(5)	1.4331(15)
F(3)-C(10)	1.3494(15)
F(1)-C(7)	1.3605(14)
O(3)-C(3)	1.4245(14)
F(2)-C(9)	1.3449(16)
C(6)-C(7)	1.3893(15)
C(6)-C(11)	1.3975(17)
C(6)-C(1)	1.5034(17)
C(4)-C(5)	1.5164(15)
C(4)-C(3)	1.5249(16)
C(11)-C(10)	1.3720(19)
C(2)-C(3)	1.5326(16)
C(2)-C(1)	1.5391(16)
C(7)-C(8)	1.3839(18)
C(8)-C(9)	1.378(2)
C(10)-C(9)	1.3873(19)
C(1)-O(4)-C(4)	110.56(9)
C(7)-C(6)-C(11)	116.79(11)
C(7)-C(6)-C(1)	121.54(10)
C(11)-C(6)-C(1)	121.60(10)
O(4)-C(4)-C(5)	106.81(9)
O(4)-C(4)-C(3)	106.76(9)
C(5)-C(4)-C(3)	114.77(10)
C(10)-C(11)-C(6)	120.32(11)
O(5)-C(5)-C(4)	112.28(10)
O(2)-C(2)-C(3)	114.19(10)
O(2)-C(2)-C(1)	114.42(9)
C(3)-C(2)-C(1)	102.37(9)
F(1)-C(7)-C(8)	117.35(10)
F(1)-C(7)-C(6)	118.52(11)
C(8)-C(7)-C(6)	124.13(12)
O(4)-C(1)-C(6)	109.66(9)
O(4)-C(1)-C(2)	104.22(9)
C(6)-C(1)-C(2)	112.89(10)
O(3)-C(3)-C(4)	108.22(9)
O(3)-C(3)-C(2)	110.34(9)
C(4)-C(3)-C(2)	101.58(9)
C(9)-C(8)-C(7)	117.03(11)
F(3)-C(10)-C(11)	120.39(12)
F(3)-C(10)-C(9)	118.69(12)
C(11)-C(10)-C(9)	120.92(12)
F(2)-C(9)-C(8)	120.07(12)
F(2)-C(9)-C(10)	119.13(12)
C(8)-C(9)-C(10)	120.79(12)

Table 4. Anisotropic displacement parameters ( $\text{Å}^2 \times 10^4$ ) for 1'-deoxy-1'-(2,4,5-trifluorophenyl)- $\beta$ -D-ribofuranose. The anisotropic displacement factor exponent takes the form:  $-2 \pi^2 [h^2 a^{*2} U11 + \dots + 2 h k a^* b^* U12]$

	U11	U22	U33	U23	U13	U12
O(2)	144(3)	223(4)	241(4)	17(4)	23(3)	23(3)
O(4)	161(3)	287(5)	186(4)	56(4)	52(3)	58(3)
O(5)	154(3)	239(4)	258(5)	69(4)	77(3)	14(3)
F(3)	363(4)	333(4)	293(4)	-82(4)	23(3)	-148(4)
F(1)	199(3)	348(4)	354(5)	-121(4)	99(3)	-76(3)
O(3)	241(4)	176(4)	206(4)	-22(3)	45(3)	-56(3)
F(2)	460(5)	346(5)	304(5)	-145(4)	121(4)	-15(4)
C(6)	187(5)	174(5)	162(5)	23(4)	37(4)	0(4)
C(4)	151(4)	141(5)	194(5)	12(4)	51(4)	9(4)
C(11)	203(5)	232(6)	186(6)	21(4)	32(4)	-33(4)
C(5)	164(4)	171(5)	230(6)	3(5)	50(4)	-20(4)
C(2)	135(4)	147(4)	183(5)	19(4)	31(4)	12(4)
C(7)	184(5)	230(5)	204(6)	-14(5)	44(4)	-15(4)
C(1)	137(4)	176(5)	187(6)	20(4)	43(4)	6(4)
C(3)	162(4)	146(5)	175(5)	18(4)	54(4)	-17(4)
C(8)	234(6)	291(6)	237(6)	-34(5)	90(5)	19(5)
C(10)	269(6)	213(5)	192(6)	2(5)	9(5)	-60(5)
C(9)	329(6)	236(6)	171(6)	-23(5)	51(5)	20(5)

Table 5. Hydrogen coordinates ( $\times 10^4$ ) and isotropic displacement parameters ( $\text{Å}^2 \times 10^3$ ) for M2.

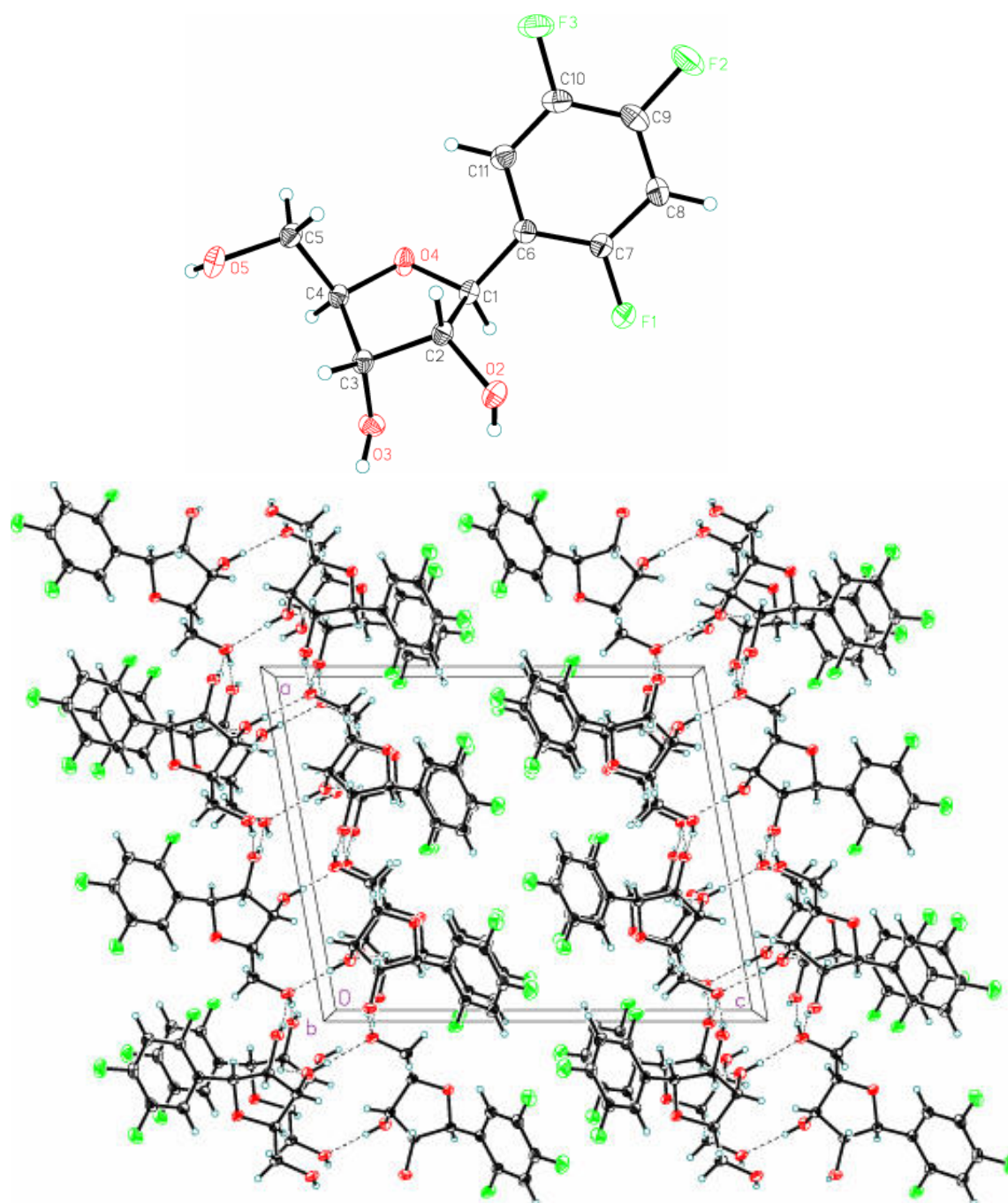
	x	y	z	U(eq)
H(02)	180	-1256	991	31
H(05)	4704	-1212	892	32
H(03)	1340	-3820	231	31
H(4)	3354	-3627	1524	19
H(11)	2974	2563	3210	25
H(5A)	3603	2079	1673	22
H(5B)	4439	-16	2119	22
H(2)	1699	2183	1489	19
H(1)	1261	-2630	2339	20
H(3)	2264	-342	461	19
H(8)	-245	2999	4034	30

Table 6. Torsion angles [deg] for M2

---

C(1)-O(4)-C(4)-C(5)	118.16(10)
C(1)-O(4)-C(4)-C(3)	-5.07(12)
C(7)-C(6)-C(11)-C(10)	-0.98(18)
C(1)-C(6)-C(11)-C(10)	175.91(12)
O(4)-C(4)-C(5)-O(5)	173.98(9)
C(3)-C(4)-C(5)-O(5)	-67.92(13)
C(11)-C(6)-C(7)-F(1)	-179.26(11)
C(1)-C(6)-C(7)-F(1)	3.84(17)
C(11)-C(6)-C(7)-C(8)	0.86(19)
C(1)-C(6)-C(7)-C(8)	-176.04(13)
C(4)-O(4)-C(1)-C(6)	-139.85(10)
C(4)-O(4)-C(1)-C(2)	-18.74(12)
C(7)-C(6)-C(1)-O(4)	-153.93(11)
C(11)-C(6)-C(1)-O(4)	29.32(15)
C(7)-C(6)-C(1)-C(2)	90.34(13)
C(11)-C(6)-C(1)-C(2)	-86.41(13)
O(2)-C(2)-C(1)-O(4)	158.82(10)
C(3)-C(2)-C(1)-O(4)	34.74(11)
O(2)-C(2)-C(1)-C(6)	-82.24(12)
C(3)-C(2)-C(1)-C(6)	153.67(9)
O(4)-C(4)-C(3)-O(3)	-89.61(10)
C(5)-C(4)-C(3)-O(3)	152.26(9)
O(4)-C(4)-C(3)-C(2)	26.56(11)
C(5)-C(4)-C(3)-C(2)	-91.57(11)
O(2)-C(2)-C(3)-O(3)	-46.41(13)
C(1)-C(2)-C(3)-O(3)	77.82(10)
O(2)-C(2)-C(3)-C(4)	-161.01(9)
C(1)-C(2)-C(3)-C(4)	-36.78(10)
F(1)-C(7)-C(8)-C(9)	179.73(12)
C(6)-C(7)-C(8)-C(9)	-0.4(2)
C(6)-C(11)-C(10)-F(3)	-179.83(12)
C(6)-C(11)-C(10)-C(9)	0.68(19)
C(7)-C(8)-C(9)-F(2)	-179.32(13)
C(7)-C(8)-C(9)-C(10)	0.0(2)
F(3)-C(10)-C(9)-F(2)	-0.33(19)
C(11)-C(10)-C(9)-F(2)	179.17(13)
F(3)-C(10)-C(9)-C(8)	-179.68(13)
C(11)-C(10)-C(9)-C(8)	-0.2(2)

---



*Crystal structure of 1'-deoxy-1'-(2,4,5-trifluorophenyl)-β-D-ribofuranose*



### 12.1.3 Crystal data of 1'-deoxy-1'-(4-chlorophenyl)- $\beta$ -D-ribofuranose

A single crystal ( colorless transparent rod with dimensions 0.14 x 0.20 x 0.50 mm ) was measured on a SIEMENS SMART diffractometer at a temperature of about -128 °C. Repeatedly measured reflections remained stable. A numerical absorption correction using six indexed crystal faces gave a transmission factor from 0.872 to 0.955 . Equivalent reflections were averaged. Friedel opposites were not averaged.  $R(I)_{\text{internal}} = 0.041$  . The structure was determined by direct methods using program SHELXS. The H atoms were geometrically positioned and were treated as riding atoms. The structure was refined on  $F^2$  values using program SHELXL-97. The final difference density was between -0.45 and +0.31 e/Å . The absolute configuration of the compound was confirmed by the value of the Flack  $x$  - parameter [  $x = 0.00(6)$  ]. The crystal structure of the title compound is isomorphous with the crystal structure of one of the two modifications of 1-deoxy-1-(4-fluorophenyl)- $\beta$ -D-ribofuranose reported by Bats, Parsch and Engels (Acta Cryst., C56, 2000,201-205. The ribofuranose ring has a conformation which is intermediate between a C2'-endo,C3'-exo twist and a C2'-endo envelope. The conformation of the molecule is rather similar to the conformation observed in 1-deoxy-1-(3-fluorophenyl)- $\beta$ -D-ribofuranose ( Bats, Parsch and Engels, 1999, Acta Cryst., C55, IUC9900070) and the conformation observed in 1-deoxy-1-phenyl- $\beta$ -D-ribofuranose ( Matulic-Adamic et al., 1996, J. Org. Chem., 61, 3909 ). The phenyl group attached to C1 and the hydroxyl group attached to C2 are in pseudo-equatorial positions, the hydroxyl group attached to C3 and the methanol group attached to C4 are in a pseudo-axial positions with respect to the five-membered ring. The shortest intramolecular contact distance is 2.43 Å between O4 and H11.

The crystal packing shows three intermolecular hydrogen bonds:

O - H ... O	O - H	H ... O	O ... O	O - H - O	symmetry
[Å]	[Å]	[Å]	[deg]		
O2 - H02 ... O5	0.84	1.91	2.718(1)	160	x-1, y, z
O3 - H03 ... O2	0.84	1.89	2.720(1)	169	-x, y-0.5, 1.5-z
O5 - H05 ... O3	0.84	1.97	2.807(1)	175	1-x, y-0.5, 1.5-z

In this way each molecule is connected by hydrogen bonding to six different neighboring molecules leading to a two-dimensional network in the a,b - direction. The bonding in the c - direction consists of weak intermolecular C8-H8...Cl interactions with a H...Cl distance of 2.74 Å and a C-H-Cl angle of 150° .

A search of the Cambridge Data Base for structures containing intermolecular C(phenyl)-Cl...H-C(phenyl) interactions with a Cl...H distance shorter than 2.8 Å revealed 149 possible crystal structures. Intermolecular C-H...Cl contacts with a H...Cl distance of 2.78 Å very similar to those in the title compound occur in the crystal structure of N-(4-chlorophenyl) -mannopyranosylamine (Ojala, Ostman & Ojala, Carbohydr. Res., 326, 2000, 104-112).

*Table 1. Crystal data and structure refinement for 1'-deoxy-1'-(4-chlorophenyl)-β-D-ribofuranose*

Identification code	Engels5
Empirical formula	C11 H13 Cl O4
Formula weight	244.66
Temperature	145(2) K
Wavelength	0.71073 Å
Crystal system, space group	Orthorhombic, P 212121
Unit cell dimensions	a = 6.7097(9) Å    alpha = 90 deg. b = 6.8447(9) Å    beta = 90 deg. c = 23.948(4) Å    gamma = 90 deg.
Volume	1099.9(3) Å <sup>3</sup>
Z, Calculated density	4, 1.478 Mg/m <sup>3</sup>
Absorption coefficient	0.343 mm <sup>-1</sup>
F(000)	512
Crystal size	0.50 x 0.20 x 0.14 mm
Theta range for data collection	1.70 to 34.25 deg.
Limiting indices	-10 ≤ h ≤ 10, -10 ≤ k ≤ 10, -35 ≤ l ≤ 37
Reflections collected / unique	24403 / 4226 [R(int) = 0.0407]

Completeness to theta = 34.25	95.2 %
Absorption correction	Numerical (SHELXTL, Sheldrick, 1996)
Max. and min. transmission	0.955 and 0.872
Refinement method	Full-matrix least-squares on F <sup>2</sup>
Data / restraints / parameters	4226 / 0 / 145
Goodness-of-fit on F <sup>2</sup>	1.072
Final R indices [I > 2σ(I)]	R1 = 0.0407, wR2 = 0.0885
R indices (all data)	R1 = 0.0572, wR2 = 0.0952
Absolute structure parameter	0.00(6)
Largest diff. peak and hole	0.305 and -0.452 e.Å <sup>-3</sup>

Table 2. Atomic coordinates ( $\times 10^5$ ) and equivalent isotropic displacement parameters ( $\text{Å}^2 \times 10^4$ ) for 1'-deoxy-1'-(4-chlorophenyl)-β-D-ribofuranose.  $U(\text{eq})$  is defined as one third of the trace of the orthogonalized  $U_{ij}$  tensor.

	x	y	z	U(eq)
Cl	33380(9)	60913(7)	46291(2)	515(2)
O(2)	-6742(13)	4113(14)	67754(4)	202(2)
O(3)	13676(15)	-11775(15)	76751(4)	218(2)
O(4)	46391(14)	3337(14)	68726(5)	241(2)
O(5)	72925(13)	-30075(15)	66828(5)	231(2)
C(1)	28080(18)	12872(18)	67318(6)	177(2)
C(2)	12591(18)	-3539(18)	66912(6)	165(2)
C(3)	19915(18)	-17979(19)	71342(6)	174(2)
C(4)	42583(18)	-16278(18)	70706(6)	171(2)
C(5)	51633(18)	-31020(20)	66742(6)	217(3)
C(6)	30090(20)	24940(20)	62077(6)	205(2)
C(7)	13830(20)	35970(20)	60277(6)	257(3)
C(8)	14880(30)	47130(20)	55444(7)	318(3)
C(9)	32610(30)	47300(20)	52455(6)	324(4)
C(10)	48960(30)	37010(30)	54194(7)	351(4)
C(11)	47710(20)	25640(20)	59031(7)	292(3)

Table 3. Bond lengths [ $\text{\AA}$ ] and angles [deg] for Engels5.

---

Cl-C(9)	1.7465(16)
O(2)-C(2)	1.4134(15)
O(2)-H(02)	0.8400
O(3)-C(3)	1.4260(16)
O(3)-H(03)	0.8400
O(4)-C(1)	1.4315(16)
O(4)-C(4)	1.4466(16)
O(5)-C(5)	1.4303(15)
O(5)-H(05)	0.8400
C(1)-C(6)	1.5088(19)
C(1)-C(2)	1.5334(18)
C(1)-H(1)	1.0000
C(2)-C(3)	1.5310(18)
C(2)-H(2)	1.0000
C(3)-C(4)	1.5331(17)
C(3)-H(3)	1.0000
C(4)-C(5)	1.5126(18)
C(4)-H(4)	1.0000
C(5)-H(5A)	0.9900
C(5)-H(5B)	0.9900
C(6)-C(11)	1.390(2)
C(6)-C(7)	1.395(2)
C(7)-C(8)	1.389(2)
C(7)-H(7)	0.9500
C(8)-C(9)	1.388(2)
C(8)-H(8)	0.9500
C(9)-C(10)	1.369(3)
C(10)-C(11)	1.398(2)
C(10)-H(10)	0.9500
C(11)-H(11)	0.9500
C(2)-O(2)-H(02)	109.5
C(3)-O(3)-H(03)	109.5
C(1)-O(4)-C(4)	110.41(9)
C(5)-O(5)-H(05)	109.5
O(4)-C(1)-C(6)	111.64(11)
O(4)-C(1)-C(2)	105.23(10)
C(6)-C(1)-C(2)	114.15(11)
O(4)-C(1)-H(1)	108.5
C(6)-C(1)-H(1)	108.5
C(2)-C(1)-H(1)	108.5
O(2)-C(2)-C(3)	115.78(11)
O(2)-C(2)-C(1)	109.97(10)
C(3)-C(2)-C(1)	102.21(10)
O(2)-C(2)-H(2)	109.5
C(3)-C(2)-H(2)	109.5
C(1)-C(2)-H(2)	109.5
O(3)-C(3)-C(2)	110.06(10)
O(3)-C(3)-C(4)	111.04(11)

---

C(2)-C(3)-C(4)	101.56(10)
O(3)-C(3)-H(3)	111.3
C(2)-C(3)-H(3)	111.3
C(4)-C(3)-H(3)	111.3
O(4)-C(4)-C(5)	110.04(11)
O(4)-C(4)-C(3)	106.16(10)
C(5)-C(4)-C(3)	114.21(11)
O(4)-C(4)-H(4)	108.8
C(5)-C(4)-H(4)	108.8
C(3)-C(4)-H(4)	108.8
O(5)-C(5)-C(4)	111.20(11)
O(5)-C(5)-H(5A)	109.4
C(4)-C(5)-H(5A)	109.4
O(5)-C(5)-H(5B)	109.4
C(4)-C(5)-H(5B)	109.4
H(5A)-C(5)-H(5B)	108.0
C(11)-C(6)-C(7)	118.99(14)
C(11)-C(6)-C(1)	122.11(13)
C(7)-C(6)-C(1)	118.90(12)
C(8)-C(7)-C(6)	121.03(15)
C(8)-C(7)-H(7)	119.5
C(6)-C(7)-H(7)	119.5
C(9)-C(8)-C(7)	118.54(16)
C(9)-C(8)-H(8)	120.7
C(7)-C(8)-H(8)	120.7
C(10)-C(9)-C(8)	121.73(15)
C(10)-C(9)-Cl	120.52(13)
C(8)-C(9)-Cl	117.74(14)
C(9)-C(10)-C(11)	119.35(15)
C(9)-C(10)-H(10)	120.3
C(11)-C(10)-H(10)	120.3
C(6)-C(11)-C(10)	120.34(15)
C(6)-C(11)-H(11)	119.8
C(10)-C(11)-H(11)	119.8

---

Symmetry transformations used to generate equivalent atoms:

*Table 4. Anisotropic displacement parameters ( $A^2 \times 10^4$ ) for 1'-deoxy-1'-(4-chlorophenyl)- $\beta$ -D-ribofuranose. The anisotropic displacement factor exponent takes the form:  $-2 \pi^2 [h^2 a^{*2} U11 + \dots + 2 h k a^* b^* U12]$*

---

	U11	U22	U33	U23	U13	U12
Cl	827(4)	446(2)	272(2)	76(2)	63(2)	-268(3)
O(2)	120(4)	180(4)	306(5)	-19(4)	-4(4)	-3(3)
O(3)	242(5)	195(4)	217(4)	12(4)	56(4)	-11(4)

---

O(4)	126(4)	153(4)	445(6)	23(4)	-31(4)	-14(3)
O(5)	133(4)	195(4)	364(6)	2(4)	3(4)	11(3)
C(1)	145(5)	138(5)	247(6)	-14(5)	-14(5)	0(4)
C(2)	121(4)	155(5)	218(6)	-13(5)	-3(4)	-6(4)
C(3)	151(5)	154(5)	217(6)	-7(5)	14(5)	-12(4)
C(4)	150(5)	141(6)	221(6)	-11(4)	-17(4)	-7(4)
C(5)	150(5)	190(6)	310(7)	-61(5)	-9(5)	-8(4)
C(6)	218(6)	158(5)	239(6)	-23(5)	32(5)	-26(5)
C(7)	261(6)	244(7)	266(6)	37(5)	40(6)	-3(5)
C(8)	392(8)	265(7)	296(7)	57(6)	7(7)	-32(7)
C(9)	508(10)	248(7)	217(6)	-10(6)	73(7)	-158(7)
C(10)	406(9)	304(8)	342(8)	-55(7)	182(7)	-93(7)
C(11)	260(7)	236(6)	380(8)	-47(6)	104(6)	-29(6)

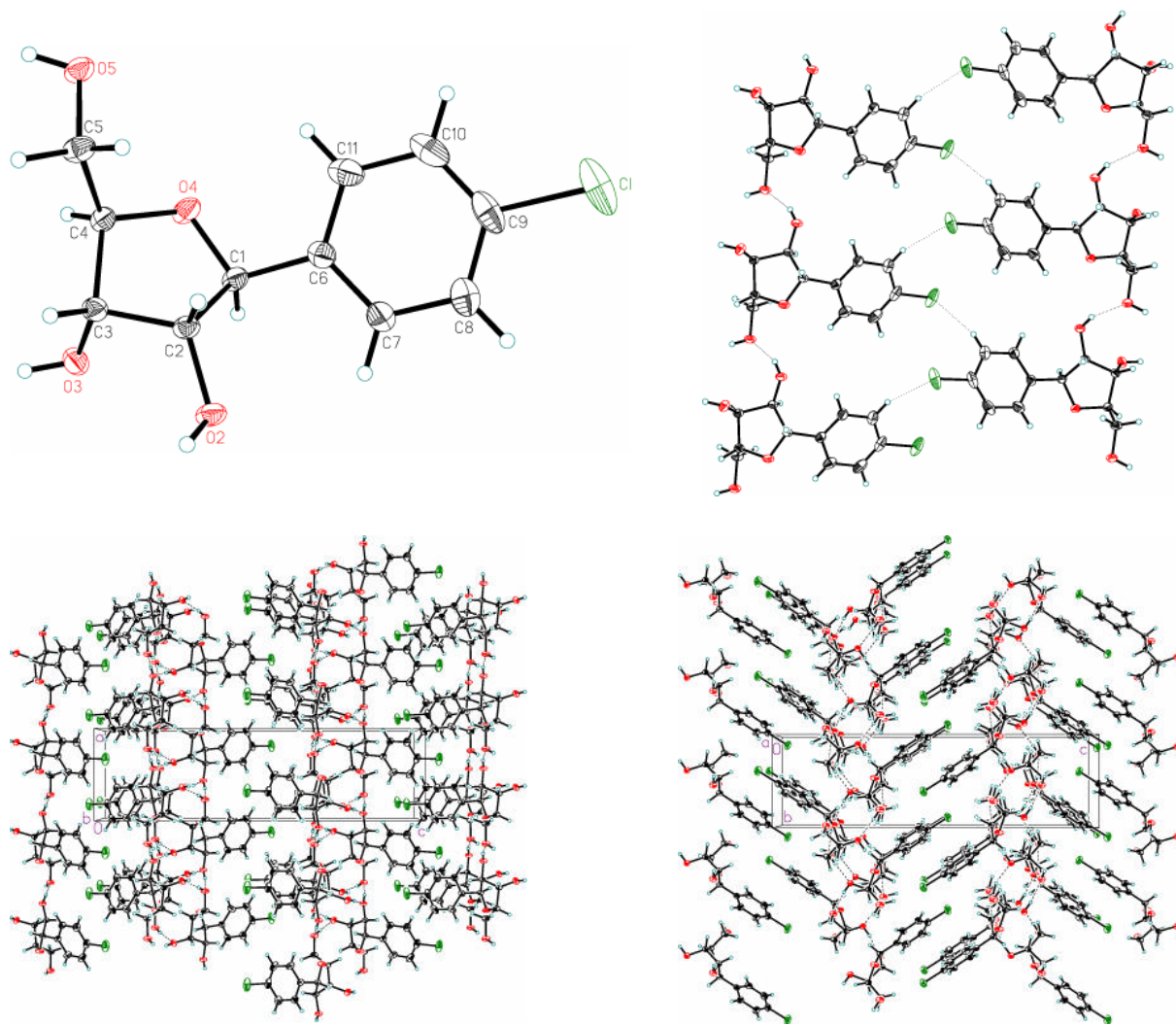
Table 5. Hydrogen coordinates ( $\times 10^4$ ) and isotropic displacement parameters ( $\text{Å}^2 \times 10^3$ ) for 1'-deoxy-1'-(4-chlorophenyl)- $\beta$ -D-ribofuranose

	x	y	z	U(eq)
H(02)	-1523	-466	6716	30
H(03)	1211	-2158	7882	33
H(05)	7746	-3966	6861	35
H(1)	2427	2172	7046	21
H(2)	1336	-976	6314	20
H(3)	1523	-3155	7052	21
H(4)	4889	-1788	7446	21
H(5A)	4729	-4432	6782	26
H(5B)	4681	-2844	6291	26
H(7)	185	3584	6239	31
H(8)	372	5449	5421	38
H(10)	6105	3758	5213	42
H(11)	5895	1835	6024	35

Table 6. Torsion angles [deg] for 1'-deoxy-1'-(4-chlorophenyl)- $\beta$ -D-ribofuranose

C(4)-O(4)-C(1)-C(6)	-140.08(11)
C(4)-O(4)-C(1)-C(2)	-15.74(14)
O(4)-C(1)-C(2)-O(2)	156.78(11)
C(6)-C(1)-C(2)-O(2)	-80.48(14)
O(4)-C(1)-C(2)-C(3)	33.26(13)
C(6)-C(1)-C(2)-C(3)	156.01(11)

O(2)-C(2)-C(3)-O(3)	-38.87(14)
C(1)-C(2)-C(3)-O(3)	80.64(12)
O(2)-C(2)-C(3)-C(4)	-156.57(10)
C(1)-C(2)-C(3)-C(4)	-37.06(12)
C(1)-O(4)-C(4)-C(5)	115.67(12)
C(1)-O(4)-C(4)-C(3)	-8.39(14)
O(3)-C(3)-C(4)-O(4)	-88.29(13)
C(2)-C(3)-C(4)-O(4)	28.70(13)
O(3)-C(3)-C(4)-C(5)	150.28(11)
C(2)-C(3)-C(4)-C(5)	-92.72(13)
O(4)-C(4)-C(5)-O(5)	67.33(14)
C(3)-C(4)-C(5)-O(5)	-173.42(12)
O(4)-C(1)-C(6)-C(11)	2.20(18)
C(2)-C(1)-C(6)-C(11)	-116.98(15)
O(4)-C(1)-C(6)-C(7)	-176.90(12)
C(2)-C(1)-C(6)-C(7)	63.92(16)
C(11)-C(6)-C(7)-C(8)	1.6(2)
C(1)-C(6)-C(7)-C(8)	-179.25(14)
C(6)-C(7)-C(8)-C(9)	-0.8(2)
C(7)-C(8)-C(9)-C(10)	-0.9(2)
C(7)-C(8)-C(9)-Cl	178.31(12)
C(8)-C(9)-C(10)-C(11)	1.6(2)
Cl-C(9)-C(10)-C(11)	-177.59(13)
C(7)-C(6)-C(11)-C(10)	-0.9(2)
C(1)-C(6)-C(11)-C(10)	179.99(14)
C(9)-C(10)-C(11)-C(6)	-0.7(2)



Crystal structure of 1'-deoxy-1'-(4-chlorophenyl)-β-D-ribofuranose



### 12.1.4 Crystal data of 5'-O-(4,4'-Dimethoxytriphenylmethyl)-2'-O-tert.-butyldimethylsilyl-1'-deoxy-1'-(4,6-difluoro-1-N-benzimidazolyl)- $\beta$ -D-ribofuranose 106 at -123 C

A single crystal ( colorless rod with dimensions 0.04 x 0.08 x 1.0 mm ) was measured on a SIEMENS SMART diffractometer at a temperature of about -123 °C. Repeatedly measured reflections remained stable. An empirical absorption correction with program SADABS (Sheldrick, 2000) gave a correction factor between 0.799 and 1.000 . Equivalent reflections were averaged. Friedel opposites were not averaged.  $R(I)_{\text{internal}} = 0.087$  . The structure was determined by direct methods using program SHELXS. The two methoxy groups were found to be statistically distributed over three possible positions. The occupancy factors of the methoxy groups were refined: O6-C26 0.572(8), O7-C33 0.800(9) and O8-C40 0.663(7). The H atoms were geometrically positioned and were treated as riding atoms. The non-H atoms were refined with anisotropic thermal parameters. The structure was refined on  $F^2$  values using program SHELXL-97. The final difference density was between -0.52 and +0.75 e/Å .

The five-membered furanose ring has a twisted O4-endo, C1-exo conformation. The C1-N1, C2-O2 and C4-C5 bonds are in pseudo-equatorial positions, the C3-O3 bond is in a bisecting position with respect to the furanose ring. A different conformation (C2-endo) has been reported for the related 2-chloro-( $\beta$ -D-ribofuranosyl)-benzimidazole (Sprang & Sundaralingam, ActaCryst., B29, 1973, 1910). The bond distances in the ribofuranosyl group are very similar in the title compound and in the 2-chloro-( $\beta$ -D-ribofuranosyl)-benzimidazole structure with rather short O4-C1 and C4-C5 bonds and a long O4-C4 bond. The benzimidazole group adopts a syn orientation about the glycosyl bond with a torsion angle O4-C1-N1-C12 of 62.5° . The benzimidazole group is planar (mean deviation from plane: 0.008 Å). The orientation about the exocyclic C4-C5 bond is +sc(gauche,gauche). The shortest intramolecular contacts are O5...H3 2.40, O5...H32 2.42 and O5...H35 2.41 Å. The angles between the planes of the three phenyl groups attached to C19 are 64.5, 74.5 and 85.2. The molecules are connected by intermolecular hydrogen bonds between the hydroxyl group and the imidazole group to chains running in the crystallographic b-direction, which also corresponds to the long macroscopic dimension of the crystal. The hydrogen bonded chains are also stabilized by intermolecular C3-H3...F1 contacts with a H...F distance of 2.43 Å and a C-H..F angle of 150 . The crystal packing also shows an additional intermolecular C-H...F contact, an intermolecular C-H...O contact and three intermolecular C-H... $\pi$ (phenyl) contacts.

hydrogen bond

O - H ... N	O-H	H...N	O...N	O-H-N	symmetry
	[Å]	[Å]	[Å]	[deg]	
O3 -H03 ... N2	0.84	1.98	2.805	167	x, y-1, z

Table 1. Crystal data and structure refinement for 5'-O- (4,4'-Dimethoxytriphenylmethyl) - 2'-O-tert.-butyldimethylsilyl-1'-deoxy-1' - (4,6-difluoro-1-N-benzimidazolyl) - $\beta$ -D-ribofuranose

Identification code	zivkovic1
Empirical formula	C <sub>39</sub> H <sub>44</sub> F <sub>2</sub> N <sub>2</sub> O <sub>6</sub> Si
Formula weight	702.85
Temperature	150(2) K
Wavelength	0.71073 Å
Crystal system, space group	Monoclinic, C 2
Unit cell dimensions	a = 30.832(3) Å    alpha = 90 deg. b = 9.1318(9) Å    beta = 91.296(5) deg. c = 13.2625(15) Å    gamma = 90 deg.
Volume	3733.1(7) Å <sup>3</sup>
Z, Calculated density	4, 1.251 Mg/m <sup>3</sup>
Absorption coefficient	0.120 mm <sup>-1</sup>
F(000)	1488
Crystal size	1.0 x 0.08 x 0.04 mm
Theta range for data collection	1.54 to 28.51 deg.
Limiting indices	-39<=h<=40, -12<=k<=12, -17<=l<=17
Reflections collected / unique	22479 / 8294 [R(int) = 0.0866]
Completeness to theta = 28.51	91.0 %
Absorption correction	Empirical, SADABS (Sheldrick, 2000)
Max. and min. transmission	1.000 and 0.799
Refinement method	Full-matrix least-squares on F <sup>2</sup>

Data / restraints / parameters 8294 / 1 / 476

Goodness-of-fit on  $F^2$  1.010

Final R indices [ $I > 2\sigma(I)$ ]  $R_1 = 0.0749$ ,  $wR_2 = 0.1443$

R indices (all data)  $R_1 = 0.1696$ ,  $wR_2 = 0.1766$

Absolute structure parameter 0.1(2)

Largest diff. peak and hole 0.744 and -0.519 e. $\text{\AA}^{-3}$

Table 2. Atomic coordinates ( $\times 10^5$ ) and equivalent isotropic displacement parameters ( $\text{\AA}^2 \times 10^4$ ) for zivkovic1.  $U(\text{eq})$  is defined as one third of the trace of the orthogonalized  $U_{ij}$  tensor

	x	y	z	U(eq)
Si	83137(5)	48975(17)	83006(11)	518(4)
O(2)	80665(9)	53770(30)	93531(19)	330(7)
O(5)	87593(9)	37690(30)	126780(20)	339(7)
O(4)	81889(10)	62030(30)	119670(20)	318(7)
F(1)	90485(10)	121600(30)	101890(20)	597(9)
N(1)	82470(12)	80680(40)	107770(30)	301(9)
N(2)	82376(13)	104270(40)	103550(30)	359(9)
C(29)	95381(13)	50470(50)	157930(30)	351(11)
O(3)	78343(11)	31530(30)	106040(20)	420(8)
C(1)	80742(15)	65990(40)	109650(30)	278(10)
C(12)	86821(15)	84960(50)	107930(30)	341(11)
F(2)	98233(10)	79310(40)	110180(30)	925(12)
C(20)	87834(14)	18160(50)	139200(30)	330(11)
C(6)	80027(15)	92490(50)	105190(30)	339(11)
C(27)	91477(14)	43310(50)	142610(30)	307(11)
C(22)	84442(15)	-5330(50)	135990(40)	404(12)
C(34)	94514(15)	26790(50)	130090(30)	329(11)
C(3)	81864(14)	40070(50)	109720(30)	349(11)
C(8)	90510(19)	107280(50)	104380(40)	453(13)
C(4)	80842(14)	46520(40)	120160(30)	298(10)
C(11)	90680(16)	77590(60)	109960(40)	489(14)
C(19)	90274(14)	31560(50)	134880(30)	320(11)
O(7)	96124(15)	76370(40)	161360(30)	560(17)
C(7)	86623(16)	99820(50)	105060(30)	356(11)
C(28)	93802(15)	39930(50)	151380(30)	389(12)
C(39)	97079(15)	16060(50)	134260(40)	390(12)
C(30)	94616(16)	65210(50)	155720(40)	435(12)

---

C(31)	92286(16)	68870(50)	147250(40)	461(13)
C(36)	100075(17)	30620(60)	117970(40)	479(14)
C(37)	102634(17)	19520(60)	122450(40)	509(14)
C(35)	96101(16)	34130(50)	121760(30)	394(12)
C(32)	90714(15)	58250(50)	140540(40)	375(12)
C(5)	83104(14)	39510(50)	128840(30)	328(11)
O(6)	79260(19)	-13540(60)	148330(40)	440(20)
C(21)	87160(15)	6100(50)	133080(30)	370(12)
C(2)	82635(14)	53860(40)	103090(30)	306(10)
C(13)	89069(17)	50730(80)	84760(40)	780(20)
C(25)	85846(15)	18540(50)	148540(40)	401(12)
C(24)	83156(16)	7330(50)	151510(40)	440(13)
C(38)	101090(17)	12390(60)	130680(40)	438(13)
C(23)	82442(16)	-4650(60)	145110(40)	455(13)
O(8)	106439(16)	15960(60)	118340(40)	511(19)
C(9)	94393(19)	100580(60)	106220(40)	570(15)
C(10)	94300(18)	85810(70)	108820(50)	619(16)
C(14)	81770(20)	29650(70)	79890(50)	820(20)
C(26)	78130(30)	-25350(100)	142210(70)	610(30)
C(15)	80940(20)	61110(70)	72890(40)	694(18)
C(17)	82610(30)	55380(90)	62490(40)	1070(30)
C(33)	98790(20)	73050(80)	169820(50)	580(20)
C(18)	76140(20)	61310(80)	72290(50)	840(20)
C(16)	82460(30)	77220(80)	75510(70)	1400(40)
C(40)	108900(30)	3680(90)	122380(60)	600(30)

---

Table 3. Bond lengths [Å] and angles [deg] for zivkovic1.

---

Si-O(2)	1.664(3)
Si-C(13)	1.845(6)
Si-C(15)	1.856(6)
Si-C(14)	1.859(6)
O(2)-C(2)	1.394(5)
O(5)-C(5)	1.427(5)
O(5)-C(19)	1.453(5)
O(4)-C(1)	1.415(5)
O(4)-C(4)	1.454(5)
F(1)-C(8)	1.349(5)
N(1)-C(6)	1.355(5)
N(1)-C(12)	1.397(6)
N(1)-C(1)	1.467(5)
N(2)-C(6)	1.318(6)
N(2)-C(7)	1.381(6)
C(29)-C(28)	1.379(6)
C(29)-C(30)	1.396(6)
O(3)-C(3)	1.415(5)
C(1)-C(2)	1.532(6)
C(12)-C(11)	1.388(7)
C(12)-C(7)	1.410(6)

---

F(2)-C(10)	1.358(6)
C(20)-C(21)	1.381(6)
C(20)-C(25)	1.395(6)
C(20)-C(19)	1.553(6)
C(27)-C(28)	1.386(6)
C(27)-C(32)	1.410(6)
C(27)-C(19)	1.524(6)
C(22)-C(23)	1.372(7)
C(22)-C(21)	1.398(6)
C(34)-C(39)	1.369(6)
C(34)-C(35)	1.390(6)
C(34)-C(19)	1.529(6)
C(3)-C(4)	1.545(6)
C(3)-C(2)	1.557(6)
C(8)-C(9)	1.362(7)
C(8)-C(7)	1.383(7)
C(4)-C(5)	1.478(6)
C(11)-C(10)	1.356(7)
O(7)-C(30)	1.341(6)
O(7)-C(33)	1.410(7)
C(39)-C(38)	1.376(7)
C(30)-C(31)	1.361(6)
C(31)-C(32)	1.396(6)
C(36)-C(35)	1.373(7)
C(36)-C(37)	1.408(7)
C(37)-O(8)	1.345(7)
C(37)-C(38)	1.365(7)
O(6)-C(23)	1.350(7)
O(6)-C(26)	1.390(10)
C(25)-C(24)	1.381(6)
C(24)-C(23)	1.399(7)
O(8)-C(40)	1.450(9)
C(9)-C(10)	1.393(8)
C(15)-C(18)	1.479(8)
C(15)-C(17)	1.574(8)
C(15)-C(16)	1.580(10)
O(2)-Si-C(13)	110.1(2)
O(2)-Si-C(15)	106.4(2)
C(13)-Si-C(15)	112.6(3)
O(2)-Si-C(14)	109.3(2)
C(13)-Si-C(14)	109.3(3)
C(15)-Si-C(14)	109.2(3)
C(2)-O(2)-Si	124.5(3)
C(5)-O(5)-C(19)	116.2(3)
C(1)-O(4)-C(4)	103.9(3)
C(6)-N(1)-C(12)	108.0(3)
C(6)-N(1)-C(1)	124.7(4)
C(12)-N(1)-C(1)	127.3(4)
C(6)-N(2)-C(7)	105.0(4)
C(28)-C(29)-C(30)	119.1(4)
O(4)-C(1)-N(1)	108.0(3)

O(4)-C(1)-C(2)	105.0(3)
N(1)-C(1)-C(2)	114.8(3)
C(11)-C(12)-N(1)	133.3(4)
C(11)-C(12)-C(7)	123.4(5)
N(1)-C(12)-C(7)	103.3(4)
C(21)-C(20)-C(25)	118.6(4)
C(21)-C(20)-C(19)	118.6(4)
C(25)-C(20)-C(19)	122.3(4)
N(2)-C(6)-N(1)	112.8(4)
C(28)-C(27)-C(32)	117.3(4)
C(28)-C(27)-C(19)	121.4(4)
C(32)-C(27)-C(19)	120.8(4)
C(23)-C(22)-C(21)	119.6(5)
C(39)-C(34)-C(35)	117.1(5)
C(39)-C(34)-C(19)	121.8(4)
C(35)-C(34)-C(19)	120.8(4)
O(3)-C(3)-C(4)	110.4(4)
O(3)-C(3)-C(2)	112.2(3)
C(4)-C(3)-C(2)	103.6(3)
F(1)-C(8)-C(9)	118.7(5)
F(1)-C(8)-C(7)	119.6(5)
C(9)-C(8)-C(7)	121.8(5)
O(4)-C(4)-C(5)	110.8(3)
O(4)-C(4)-C(3)	106.3(3)
C(5)-C(4)-C(3)	115.5(4)
C(10)-C(11)-C(12)	114.4(5)
O(5)-C(19)-C(27)	110.6(3)
O(5)-C(19)-C(34)	106.3(3)
C(27)-C(19)-C(34)	106.4(3)
O(5)-C(19)-C(20)	107.7(3)
C(27)-C(19)-C(20)	114.7(3)
C(34)-C(19)-C(20)	110.8(3)
C(30)-O(7)-C(33)	118.0(5)
N(2)-C(7)-C(8)	131.7(4)
N(2)-C(7)-C(12)	110.9(4)
C(8)-C(7)-C(12)	117.3(5)
C(29)-C(28)-C(27)	122.8(4)
C(34)-C(39)-C(38)	123.4(5)
O(7)-C(30)-C(31)	116.3(5)
O(7)-C(30)-C(29)	124.1(4)
C(31)-C(30)-C(29)	119.5(4)
C(30)-C(31)-C(32)	121.7(5)
C(35)-C(36)-C(37)	120.6(5)
O(8)-C(37)-C(38)	122.1(5)
O(8)-C(37)-C(36)	119.2(6)
C(38)-C(37)-C(36)	118.6(5)
C(36)-C(35)-C(34)	120.8(5)
C(31)-C(32)-C(27)	119.6(4)
O(5)-C(5)-C(4)	110.1(3)
C(23)-O(6)-C(26)	117.1(6)
C(20)-C(21)-C(22)	121.1(4)

O(2)-C(2)-C(1)	110.9(3)
O(2)-C(2)-C(3)	116.1(3)
C(1)-C(2)-C(3)	101.5(3)
C(24)-C(25)-C(20)	120.9(5)
C(25)-C(24)-C(23)	119.6(4)
C(37)-C(38)-C(39)	119.5(5)
O(6)-C(23)-C(22)	126.6(5)
O(6)-C(23)-C(24)	112.6(5)
C(22)-C(23)-C(24)	120.2(5)
C(37)-O(8)-C(40)	119.4(5)
C(8)-C(9)-C(10)	117.2(5)
C(11)-C(10)-F(2)	118.5(5)
C(11)-C(10)-C(9)	125.8(5)
F(2)-C(10)-C(9)	115.6(5)
C(18)-C(15)-C(17)	107.7(6)
C(18)-C(15)-C(16)	107.0(6)
C(17)-C(15)-C(16)	113.6(6)
C(18)-C(15)-Si	113.3(5)
C(17)-C(15)-Si	108.2(4)
C(16)-C(15)-Si	107.1(5)

Symmetry transformations used to generate equivalent atoms:

Table 4. Anisotropic displacement parameters ( $A^2 \times 10^4$ ) for zivkovic1. The anisotropic displacement factor exponent takes the form:  $-2 \pi^2 [h^2 a^{*2} U11 + \dots + 2 h k a^* b^* U12]$

	U11	U22	U33	U23	U13	U12
Si	601(10)	503(10)	455(8)	55(7)	135(7)	90(8)
O(2)	411(18)	258(17)	320(16)	21(13)	22(14)	15(14)
O(5)	347(19)	272(17)	396(18)	58(14)	-19(14)	-7(14)
O(4)	470(20)	128(15)	356(17)	-17(13)	-55(14)	-28(14)
F(1)	780(20)	240(15)	780(20)	-16(14)	169(18)	-222(15)
N(1)	410(20)	117(19)	380(20)	41(16)	-24(17)	-59(17)
N(2)	480(30)	160(20)	450(20)	55(17)	19(19)	-34(19)
C(29)	340(30)	350(30)	360(20)	-30(20)	-80(20)	80(20)
O(3)	570(20)	110(16)	570(20)	-6(15)	-167(17)	-43(15)
C(1)	390(30)	130(20)	320(20)	21(18)	50(20)	0(20)
C(12)	450(30)	220(20)	350(30)	-60(20)	20(20)	-50(20)
F(2)	430(20)	710(20)	1630(40)	20(30)	-210(20)	-28(19)
C(20)	360(30)	300(30)	330(30)	90(20)	-20(20)	10(20)
C(6)	400(30)	190(20)	430(30)	0(20)	-70(20)	50(20)
C(27)	320(30)	230(20)	370(30)	13(19)	60(20)	60(20)
C(22)	440(30)	310(30)	450(30)	50(20)	-110(20)	-40(20)
C(34)	380(30)	180(20)	410(30)	-10(20)	-110(20)	-50(20)
C(3)	320(30)	240(30)	490(30)	10(20)	-100(20)	20(20)

---

C(8)	630(40)	230(30)	510(30)	-30(20)	110(30)	-110(30)
C(4)	350(30)	110(20)	440(30)	-5(19)	-30(20)	-25(19)
C(11)	450(30)	260(30)	750(40)	30(30)	-80(30)	30(30)
C(19)	360(30)	210(20)	390(30)	0(20)	-70(20)	-30(20)
O(7)	740(30)	320(30)	610(30)	-150(20)	-260(20)	10(20)
C(7)	490(30)	230(30)	350(20)	-20(20)	50(20)	-90(20)
C(28)	450(30)	290(30)	430(30)	-20(20)	-10(20)	50(20)
C(39)	370(30)	330(30)	470(30)	-40(20)	-60(20)	-20(20)
C(30)	410(30)	320(30)	570(30)	-80(30)	-70(30)	-10(20)
C(31)	500(30)	250(30)	630(30)	-10(30)	-90(30)	0(20)
C(36)	520(30)	450(30)	470(30)	-70(30)	80(30)	-210(30)
C(37)	420(30)	440(30)	660(40)	-260(30)	-10(30)	30(30)
C(35)	380(30)	310(30)	490(30)	10(20)	-20(20)	-20(20)
C(32)	380(30)	220(30)	520(30)	50(20)	-20(20)	20(20)
C(5)	330(30)	270(30)	380(30)	70(20)	-60(20)	-50(20)
O(6)	510(40)	270(30)	530(40)	40(30)	80(30)	-120(30)
C(21)	470(30)	310(30)	340(30)	20(20)	20(20)	0(20)
C(2)	350(30)	160(20)	410(30)	-30(20)	40(20)	0(20)
C(13)	660(40)	1000(50)	690(40)	170(40)	280(30)	210(40)
C(25)	420(30)	290(30)	500(30)	-10(20)	50(20)	-30(20)
C(24)	510(30)	400(30)	410(30)	0(20)	80(20)	-50(30)
C(38)	430(30)	400(30)	480(30)	-80(30)	-70(30)	0(30)
C(23)	480(30)	430(30)	450(30)	70(20)	10(20)	-110(30)
O(8)	470(40)	390(30)	670(40)	50(30)	200(30)	70(30)
C(9)	520(40)	340(30)	860(40)	-100(30)	70(30)	-190(30)
C(10)	330(30)	650(40)	880(40)	-70(30)	-30(30)	-60(30)
C(14)	1380(60)	420(40)	670(40)	-150(30)	240(40)	10(40)
C(26)	800(80)	490(60)	540(60)	20(50)	-20(50)	-390(60)
C(15)	740(40)	840(50)	510(30)	200(30)	200(30)	300(40)
C(17)	1520(70)	1140(60)	560(40)	240(40)	520(40)	580(60)
C(33)	750(50)	440(40)	550(40)	-80(30)	-170(40)	-50(40)
C(18)	860(50)	960(50)	690(40)	-140(40)	-130(30)	490(40)
C(16)	1590(80)	660(50)	1940(100)	790(60)	-270(70)	-300(60)
C(40)	490(50)	490(50)	810(60)	0(50)	120(40)	80(50)

---

Table 5. Hydrogen coordinates ( $\times 10^4$ ) and isotropic displacement parameters ( $\text{Å}^2 \times 10^3$ ) for zivkovic1.

---

	x	y	z	U(eq)	
H(29A)	9697		4775	16386	42
H(03)	7923		2312	10457	63
H(1A)	7751		6611	10881	33
H(6A)	7695		9229	10462	41
H(22A)	8398		-1352	13167	48
H(3A)	8456		3400	11016	42
H(4A)	7765		4560	12116	36

---



---

H(11A)	9078	6762	11199	59
H(28A)	9433	2992	15293	47
H(39A)	9604	1087	13992	47
H(31A)	9171	7890	14588	55
H(36A)	10111	3573	11226	57
H(35A)	9442	4166	11866	47
H(32A)	8914	6107	13462	45
H(5A)	8279	4565	13493	39
H(5B)	8178	2984	13017	39
H(21A)	8857	557	12679	44
H(2A)	8582	5547	10244	37
H(13A)	8980	6093	8634	117
H(13B)	9050	4780	7854	117
H(13C)	9006	4439	9031	117
H(25A)	8635	2663	15292	48
H(24A)	8180	775	15786	53
H(38A)	10277	496	13390	53
H(9A)	9705	10576	10575	68
H(14A)	7862	2870	7887	123
H(14B)	8273	2327	8544	123
H(14C)	8323	2679	7370	123
H(26A)	8062	-3194	14166	92
H(26B)	7727	-2179	13549	92
H(26C)	7570	-3065	14516	92
H(17A)	8152	6174	5705	160
H(17B)	8158	4536	6135	160
H(17C)	8579	5548	6259	160
H(33A)	10148	6844	16758	87
H(33B)	9726	6631	17426	87
H(33C)	9950	8208	17350	87
H(18A)	7518	6795	6688	126
H(18B)	7500	6469	7872	126
H(18C)	7506	5141	7086	126
H(16A)	8137	8396	7030	210
H(16B)	8564	7759	7579	210
H(16C)	8133	8008	8207	210
H(40A)	10739	-547	12065	89
H(40B)	10916	459	12973	89
H(40C)	11179	361	11949	89

---

Table 6. Torsion angles [deg] for zivkovic1.

---

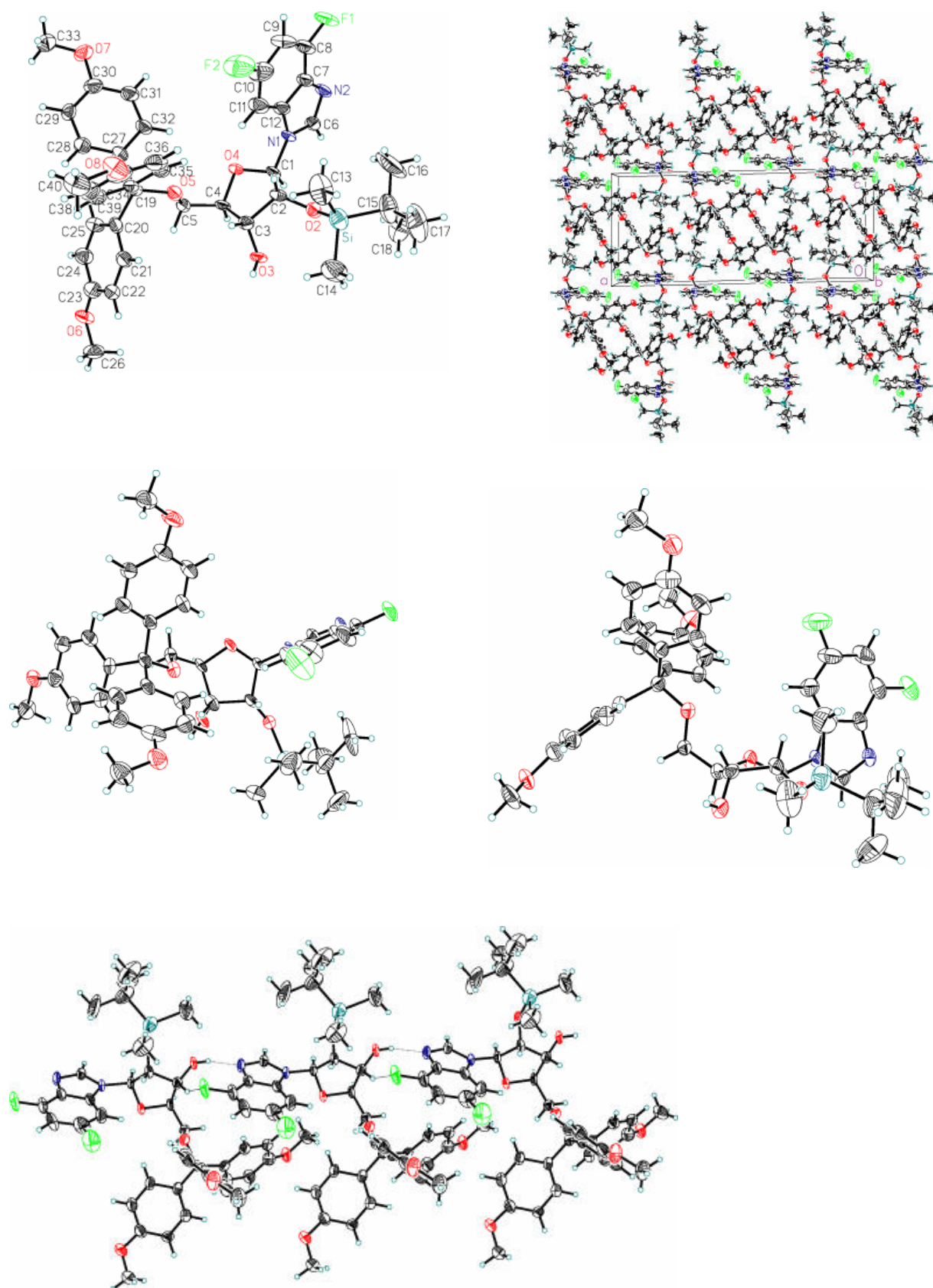
C(13)-Si-O(2)-C(2)	-21.6(4)
C(15)-Si-O(2)-C(2)	-143.9(4)
C(14)-Si-O(2)-C(2)	98.4(4)
C(4)-O(4)-C(1)-N(1)	-168.9(3)
C(4)-O(4)-C(1)-C(2)	-45.9(4)
C(6)-N(1)-C(1)-O(4)	-119.9(4)
C(12)-N(1)-C(1)-O(4)	62.5(5)

C(6)-N(1)-C(1)-C(2)	123.3(4)
C(12)-N(1)-C(1)-C(2)	-54.3(6)
C(6)-N(1)-C(12)-C(11)	-179.6(5)
C(1)-N(1)-C(12)-C(11)	-1.6(8)
C(6)-N(1)-C(12)-C(7)	-1.2(4)
C(1)-N(1)-C(12)-C(7)	176.8(4)
C(7)-N(2)-C(6)-N(1)	0.6(5)
C(12)-N(1)-C(6)-N(2)	0.4(5)
C(1)-N(1)-C(6)-N(2)	-177.6(4)
C(1)-O(4)-C(4)-C(5)	161.5(3)
C(1)-O(4)-C(4)-C(3)	35.2(4)
O(3)-C(3)-C(4)-O(4)	-131.2(3)
C(2)-C(3)-C(4)-O(4)	-11.0(4)
O(3)-C(3)-C(4)-C(5)	105.4(4)
C(2)-C(3)-C(4)-C(5)	-134.4(4)
N(1)-C(12)-C(11)-C(10)	177.1(5)
C(7)-C(12)-C(11)-C(10)	-1.0(7)
C(5)-O(5)-C(19)-C(27)	-80.1(4)
C(5)-O(5)-C(19)-C(34)	164.8(3)
C(5)-O(5)-C(19)-C(20)	46.0(4)
C(28)-C(27)-C(19)-O(5)	176.0(4)
C(32)-C(27)-C(19)-O(5)	-11.7(6)
C(28)-C(27)-C(19)-C(34)	-69.0(5)
C(32)-C(27)-C(19)-C(34)	103.3(5)
C(28)-C(27)-C(19)-C(20)	53.9(5)
C(32)-C(27)-C(19)-C(20)	-133.8(4)
C(39)-C(34)-C(19)-O(5)	-155.4(4)
C(35)-C(34)-C(19)-O(5)	30.3(5)
C(39)-C(34)-C(19)-C(27)	86.7(5)
C(35)-C(34)-C(19)-C(27)	-87.6(5)
C(39)-C(34)-C(19)-C(20)	-38.6(5)
C(35)-C(34)-C(19)-C(20)	147.0(4)
C(21)-C(20)-C(19)-O(5)	65.4(5)
C(25)-C(20)-C(19)-O(5)	-106.6(4)
C(21)-C(20)-C(19)-C(27)	-171.0(4)
C(25)-C(20)-C(19)-C(27)	17.0(6)
C(21)-C(20)-C(19)-C(34)	-50.5(5)
C(25)-C(20)-C(19)-C(34)	137.6(4)
C(6)-N(2)-C(7)-C(8)	179.6(5)
C(6)-N(2)-C(7)-C(12)	-1.4(5)
F(1)-C(8)-C(7)-N(2)	0.4(7)
C(9)-C(8)-C(7)-N(2)	-179.9(5)
F(1)-C(8)-C(7)-C(12)	-178.6(4)
C(9)-C(8)-C(7)-C(12)	1.1(7)
C(11)-C(12)-C(7)-N(2)	-179.8(4)
N(1)-C(12)-C(7)-N(2)	1.6(5)
C(11)-C(12)-C(7)-C(8)	-0.6(7)
N(1)-C(12)-C(7)-C(8)	-179.2(4)
C(30)-C(29)-C(28)-C(27)	0.1(7)
C(32)-C(27)-C(28)-C(29)	-0.5(7)
C(19)-C(27)-C(28)-C(29)	172.1(4)

C(35)-C(34)-C(39)-C(38)	0.5(7)
C(19)-C(34)-C(39)-C(38)	-174.0(4)
C(33)-O(7)-C(30)-C(31)	-175.9(5)
C(33)-O(7)-C(30)-C(29)	2.7(8)
C(28)-C(29)-C(30)-O(7)	-177.6(5)
C(28)-C(29)-C(30)-C(31)	0.9(7)
O(7)-C(30)-C(31)-C(32)	177.1(5)
C(29)-C(30)-C(31)-C(32)	-1.5(8)
C(35)-C(36)-C(37)-O(8)	177.6(5)
C(35)-C(36)-C(37)-C(38)	-0.3(7)
C(37)-C(36)-C(35)-C(34)	-0.2(7)
C(39)-C(34)-C(35)-C(36)	0.1(6)
C(19)-C(34)-C(35)-C(36)	174.7(4)
C(30)-C(31)-C(32)-C(27)	1.1(8)
C(28)-C(27)-C(32)-C(31)	-0.1(7)
C(19)-C(27)-C(32)-C(31)	-172.8(4)
C(19)-O(5)-C(5)-C(4)	177.1(3)
O(4)-C(4)-C(5)-O(5)	-74.5(4)
C(3)-C(4)-C(5)-O(5)	46.5(5)
C(25)-C(20)-C(21)-C(22)	1.9(7)
C(19)-C(20)-C(21)-C(22)	-170.4(4)
C(23)-C(22)-C(21)-C(20)	-0.6(7)
Si-O(2)-C(2)-C(1)	147.9(3)
Si-O(2)-C(2)-C(3)	-97.0(4)
O(4)-C(1)-C(2)-O(2)	161.5(3)
N(1)-C(1)-C(2)-O(2)	-80.0(5)
O(4)-C(1)-C(2)-C(3)	37.6(4)
N(1)-C(1)-C(2)-C(3)	156.1(3)
O(3)-C(3)-C(2)-O(2)	-16.3(5)
C(4)-C(3)-C(2)-O(2)	-135.4(4)
O(3)-C(3)-C(2)-C(1)	104.0(4)
C(4)-C(3)-C(2)-C(1)	-15.1(4)
C(21)-C(20)-C(25)-C(24)	-1.9(7)
C(19)-C(20)-C(25)-C(24)	170.1(4)
C(20)-C(25)-C(24)-C(23)	0.6(7)
O(8)-C(37)-C(38)-C(39)	-176.9(5)
C(36)-C(37)-C(38)-C(39)	0.9(7)
C(34)-C(39)-C(38)-C(37)	-1.0(7)
C(26)-O(6)-C(23)-C(22)	5.8(10)
C(26)-O(6)-C(23)-C(24)	176.6(6)
C(21)-C(22)-C(23)-O(6)	169.4(5)
C(21)-C(22)-C(23)-C(24)	-0.7(7)
C(25)-C(24)-C(23)-O(6)	-170.6(5)
C(25)-C(24)-C(23)-C(22)	0.8(8)
C(38)-C(37)-O(8)-C(40)	3.4(8)
C(36)-C(37)-O(8)-C(40)	-174.5(6)
F(1)-C(8)-C(9)-C(10)	179.8(5)
C(7)-C(8)-C(9)-C(10)	0.1(8)
C(12)-C(11)-C(10)-F(2)	-176.9(5)
C(12)-C(11)-C(10)-C(9)	2.4(9)
C(8)-C(9)-C(10)-C(11)	-2.0(9)

C(8)-C(9)-C(10)-F(2)	177.3(5)
O(2)-Si-C(15)-C(18)	-51.8(5)
C(13)-Si-C(15)-C(18)	-172.4(5)
C(14)-Si-C(15)-C(18)	66.1(5)
O(2)-Si-C(15)-C(17)	-171.1(5)
C(13)-Si-C(15)-C(17)	68.2(6)
C(14)-Si-C(15)-C(17)	-53.3(6)
O(2)-Si-C(15)-C(16)	66.0(5)
C(13)-Si-C(15)-C(16)	-54.6(6)
C(14)-Si-C(15)-C(16)	-176.1(5)

---



*Crystal data of 5'-O-(4,4'-Dimethoxytriphenylmethyl)-2'-O-tert.-butyldimethylsilyl-1'-deoxy-1'-(4,6-difluoro-1-N-benzimidazolyl)- $\beta$ -D-ribofuranose 106 at -123 C*

## 12.2 Abbreviations

### A

A	Adenosine
Å	Ångstrom
abs.	absolute
Ac	acetyl
ACN	acetonitrile
ATP	adenosine-5'-triphosphate

### B

Bp	base pair
BSA	<i>N,O</i> -Bis(trimethylsilyl)acetamide

### C

C	active carbon
C	cytosine
<i>C. elegans</i>	<i>Caenorhabditis elegans</i>
CD	Circular dichroismus
conc.	concentrated

### D

d	dublett
<i>D. melano gaster</i>	- <i>Drosiphila melanogaster</i>
dest.	Distilled
DMAP	<i>N,N'</i> -dimethylaminopyridine
DMTr	4,4'-dimethoxytriphenylmethyl
DNA	deoxyribonucleic acid
dNTP	natural 2'-deoxynucleoside-5'-triphosphate
dsRNA	doblestranded RNA

### E

<i>E.coli</i>	<i>Escherichia coli</i>
ESI(-)-MS	Electronspray-Ionisation in negative modus
ESI(+)-MS	Electronspray-Ionisation in positive modus
<i>et al.</i>	et alii

### F

FC	Flash chromatography
----	----------------------

**G**

G Guanosine

**H**

HCV *Hepatitis C Virus*

HIV *Human Immunodeficiency Virus*

HPLC high performance liquid chromatography

h hour

**I**

*i* iso-

**J**

J[Hz] Coupling constant in NMR spectroscopy (in Herz)

**L**

LDA Lithiumdiisopropylamide

**M**

Me methyl

MeOH methanol

min. minutes

mRNA messenger RNA

**N**

nt nucleotide

**P**

p.a. pro analysi

pH potentia hydrogenii

polyA poly adenosine

PP<sub>i</sub> inorganic pyrophosphate

Py pyridine

**Q**

q quartett

**R**

Rf retention factor

RNA ribonucleic acid

RNAi RNA interference

RNAse ribonuclease

RT room temperature

**S**

s	singlett
siRNA	small interfering RNA

**T**

T	Thymidine
T	Temperature
t	triplett
TBAF	tetrabutylammoniumfluoride
TBDMS	<i>tert.</i> -butyldimethylsilyl
TCA	trichloroacetic acid
techn.	technical
<i>tert.</i>	Tertiary
THF	tetrahydrofurane
T <sub>m</sub>	melting point of oligonucleotide doble helix
TOM	<u>Triisopropyloxymethyl</u>
tRNA	transfer RNA
TLC	thin layer chromatography

**U**

U	Uridine
---	---------





---

## *Curriculum vitae*

Name	<b>Aleksandra Živković</b>
Date\place of birth	*4 <sup>th</sup> of January 1976 in Niš, Serbia and Montenegro
	<b>School</b>
1982-1990	Primory school "Ivan Goran Kovacic", Niška Banja, Serbia and Montenegro;
1990-1994	Gymnasium "Stevan Sremac", Niš, Serbia and Montenegro;
27 <sup>th</sup> of June 1994	abitur
	<b>University</b>
1994-1998	Chemistry, University of Niš, Serbia and Montenegro; 29 <sup>th</sup> of September 1998 diploma exam Thema of diploma work: "Intermolecular transfers in Bicyclic Systems of Carbohydrates" average note: 9,81 ( excellent) and diploma note : 10,0 (excellent)
December 1998	Prize "Povelja" as the best student of Chemistry at University of Niš
	<b>Work experience</b>
1.8.1999.-29.9.1999.	Department of research and new technologies in Textile industry "NITEX", Niš, Serbia and Montenegro
1.12.1999-31.01.2001	teaching assistant at University of Niš, Serbia and Montenegro
from 1 <sup>st</sup> of June 2001	Doctor dissertation at University of Frankfurt in group of Prof. Dr. J. W. Engels



---

## Publications

- [1] Živković A., Bats J.W., Engels J. W. ; Crystal Structures of Fluoro- and Chloro-Modified Benzene Nucleosides, *Coll.Symp. Ser.*, **2002**, Vol. 5, 396-398
- [2] Živković A., Engels J. W.; Synthesis of Modified RNA-Oligonucleotides for Structural Investigations, *Nucl. Nucl. &Nucl.Acids* , **2003**, 22(5-8), 1167-1170
- [3] Moore C. L. , Živković A., Engels J. W., Kuchta R. D.; Human DNA Primase Uses Watson-Crick Hydrogen Bonds to Distinguish between Correct and Incorrect Nucleoside Triphosphates, **2004**, *Biochemistry*, *43*, 12367-12374
- [4] Živković A., Engels J. W.; RNA-recognition by fluoro-aromatic substituted nucleic acid analogues, *Nucl. Nucl. &Nucl.Acids* , **2004**, submitted
- [5] Kinckaid K., Beckman J., Živković A., Halcomb L. H., Engels J. W. and Kucta D. R.; Exploration of Factors Driving Incorporation of Unnatural dNTPS into DNA by Klenow Fragment ( DNA Polymerase I) and DNA Polymerase  $\alpha$ , *Nucleic Acids Res.*, submitted
- [6] Živković A.and Engels J. W.;Fluorinated Benzenes and Benzimidazoles as RNA analogues, *in preparation*

## Oral Presentations

- [1] `` Fluorinated substituted RNA nucleosides``, Minisymposium of foreign Ph. D. students in biology, biological chemistry and medicine at the Göthe University , Frankfurt, 11-12.10.2002.
- [2] ``Synthesis of zwitterionic and lipophilic siRNA molecules for evaluation of RNAi activity``, 1<sup>st</sup> RIGHT meeting (RNAi), 13-14.10.2004, Paris, France

---

## Poster Presentations

- [1] Živković A., Engels J. W.; RNA-recognition by fluoro-aromatic substituted nucleic acid analogues, XVIth International Roundtable conference, 12-16.09.2004, Minneapolis, USA
- [2] Živković A., Engels J. W.; New RNA Analogues, Conference of the SFB 30.10-1.11.2003, Frankfurt am Main, Germany
- [3] Živković A., Klöpffer, A. E., Parsch, J., Engels, J. W. `` Synthesis of Fluoro Substituted Nucleic Acids Analogues and Their Influence on the Structure and Stability of RNA Duplexes``, 5<sup>th</sup> Cambridge symposium on Nucleic Acids Chemistry and Biology, 31.8-3.9.2003, Cambridge, UK
- [4] Klöpffer, A. E., Zivkovic, A., Parsch, J., Engels, J. W. `` Fluorobenzene and benzimidazoles as Universal Bases and Base Pairs in RNA``, Symposium `` Fluorine in Life Sciences`` 6-10.07.2003, Bürgenstock, Schweiz
- [5] Živković A., Bats J.W., Engels J. W. ; Crystal Structures of Fluoro- and Chloro- Modified Benzene Nucleosides, XII Symposium on the Chemistry of Nucleic Acid Components, 03-08.09.2002, Spindleruv Mlyn, Czech Republik
- [6] Živković A., Engels J. W.; Synthesis of Modified RNA-Oligonucleotides for Structural Investigations, **XVth** International Round Table ``Nucleosides, Nucleotides and their Biological Investigations``, 10-14.09.2002, Leuven, Belgien
- [7] ] Živković A., Engels J. W.; Synthesis of Fluoro-modified Nucleosides for Structural Investigation of RNA , Conference of the SFB 579, 21-22.03.2002, Frankfurt a.M., Germany

---

## **Eidesstattliche Erklärung**

Hiermit erkläre ich an Eides statt, dass ich die vorliegende Doktorarbeit selbstständig und nur unter Zuhilfenahme der genannten Literatur und der angegebenen Hilfsmittel angefertigt habe.

Frankfurt am Main, 10. März 2005

-----  
Aleksandra Živković